Mathematics of the Holographic Principle

Thesis by
Elliott Gesteau

In Partial Fulfillment of the Requirements for the
Degree of
Doctor of Philosophy

Caltech

CALIFORNIA INSTITUTE OF TECHNOLOGY
Pasadena, California

2025
Defended May 27, 2025

© 2025

Elliott Gesteau
ORCID: 0000-0002-3189-0953

ACKNOWLEDGEMENTS

I am incredibly grateful to my phenomenal advisor, Matilde Marcolli. Matilde took me on as a student back in 2018, as I was beginning a master's degree in Canada and knew very little mathematics or physics. During the last seven years and the two degrees I completed under her supervision, Matilde has never failed me once as an advisor. Even when going through a global pandemic, a country move, and many other circumstances that would have largely justified for her to be less present, Matilde was always there for me. She was extremely generous with her time, gave me complete freedom to explore the topics I wanted to, shared so much knowledge with me, and perhaps most importantly, was always there to help during the most difficult parts of my academic and personal lives. Having an advisor who is not only an immense scientist to learn from, but also an exceptional human being to look up to, is a rare privilege. Matilde, I am so proud to have been your student.

I would also like to address my deepest gratitude to Hong Liu, who has been an incredible mentor to me during the second half of my doctoral studies. It is very rare for such an established scientist to agree to work with a graduate student from another institution, and I feel very fortunate for his trust, his time, and all the knowledge he has passed onto me. Hong is a wonderful collaborator, and our joint work has led to what I consider to be some of the most important results presented in this thesis. Thank you so much, Hong, and I look forward to doing a lot more physics together when I move to Boston.

There are many other wonderful collaborators without whom this work would have never happened. Many thanks to Wissam Chemissany, Netta Engelhardt, Alexander Jahn, Jake McNamara, Daniel Murphy, Sridip Pal, Sarthak Parikh, Leonardo Santilli, Leo Shaposhnik, David Simmons–Duffin, and Yixin Xu for teaching me so much science! Also many thanks to Anton Kapustin and Hirosi Ooguri for agreeing to be part of my thesis committee, and making themselves available during my years at Caltech.

My years as a graduate student at Caltech were made so much easier thanks to the hard work of all the administrative staff of the mathematics and physics departments. I would like to thank in particular Michelle Vine for being so reliable and helpful with administrative duties.

I am so happy to have met so many wonderful people during my time at Caltech.

Thank you to Adam and Thorgal for our beautiful trips, for making our office a place where we could always have a laugh, and for listening to all my drama. Thank you to Sita for all the good mood and the interesting math discussions. To Yixin for being such a fun friend, an amazing physicist I could learn from, and also a great teammate in adverse situations. To Allic for all the physics and arts conversations, and for being such a supportive friend. Thank you so much to Clara and Sam for all the SEC adventures, from WeHo to Silverlake, which were the most fun I had during the last few years. Finally, thank you to Ismail for making Caltech feel like home from the first day we met.

Another great thing about academic life is that it gives a great opportunity for making friends all over the world. From Canada to Japan, I feel so lucky to now count people from all over the world in my friends. I would especially like to thank Suzanne, for all the fun we had from to Santa Barbara to Amsterdam, Alex for being a great host in San Francisco and for her emotional support, Bibi and Goncalo for so many laughs and for being the best hosts in Okinawa, Shounak for being such a great roommate during my time in Santa Barbara, Aiden for all the movie fun, Kasia for all the moral support and scientific help she has given me throughout my PhD, Felipe, who was a great support to me over the course of many years, and Amalia, for all the adventures we went on togehter.

A special thank you goes with love to Tobi, who is the most special person I was gifted to meet during my graduate years.

Finally, I cannot end this acknowledgement section without thanking my life-long friends and my family. Thank you to my big sister at heart Ariane, for all the support she has given me since we met in Paris, and for being my LA family together with Chase. To my oldest friend Emilie for always keeping in touch throughout more than twenty years. To my high school family: Nico, Héloïse, FX, Gaia, Gautier, Cécile, and Marie. Growing up together has been one of the biggest joys of my life. To the Carteau family, for always taking such good care of me. To Nathalie, for teaching me many of the values I hold dearest. To my grandparents Annie and Philippe for being such an appeasing presence in my life, and always offering me the safe haven I need. To my father Thierry, for always listening to me, never judging me, and always doing everything in his power to help. To my mother Valérie, for all her love, her care, and for teaching me that success does not come without hard work and determination. And to my little sister Juliette, whose talent and moral strength are a great inspiration to me.

ABSTRACT

The holographic principle, which states that quantum gravity in a given spacetime region admits an equivalent description in terms of a quantum system without gravity on its boundary, is a very promising candidate to lay the foundations of our understanding of quantum gravity. However, a precise general formulation of this principle, as well as its domain of applicability, are yet to be understood. This thesis explores the foundations of holography from a mathematical point of view. In particular, the theory of von Neumann algebras is exploited to understand features of the emergence of spacetime in holography, leveraging tools from quantum error correction in infinite dimensions as well as results on harmonic analysis. Some connections between hyperbolic geometry and recent developments in holography are also elucidated, an approach to the factorization of holographic theories based on Hopf algebras is developed, and a puzzle regarding the description of a closed universe within the context of the AdS/CFT correspondence is put forward.

PUBLISHED CONTENT AND CONTRIBUTIONS

[1]   Wissam Chemissany et al. "On Infinite Tensor Networks, Complementary Recovery and Type II Factors". In: (Mar. 2025). arXiv: 2504.00096 [hep-th].
E.G. participated in the conception of the project, the derivation of the proofs and the writing of the manuscript.

[2]   Netta Engelhardt and Elliott Gesteau. "Further Evidence Against a Semiclassical Baby Universe in AdS/CFT". In: (Apr. 2025). arXiv: 2504.14586 [hep-th].
E.G. participated in the conception of the project, the derivation of the proofs and the writing of the manuscript.

[3]   Elliott Gesteau et al. "Bounds on spectral gaps of Hyperbolic spin surfaces". In: *J. Assoc. Math. Res.* 3.1 (2025), pp. 72–139. DOI: 10.56994/JAMR.003.001.003. arXiv: 2311.13330 [math.SP].
E.G. participated in the conception of the project, the derivation of the proofs and the writing of the manuscript.

[4]   Elliott Gesteau and Hong Liu. "Toward stringy horizons". In: (Aug. 2024). arXiv: 2408.12642 [hep-th].
E.G. participated in the conception of the project, the derivation of the proofs and the writing of the manuscript.

[5]   Elliott Gesteau, Matilde Marcolli, and Jacob McNamara. "Wormhole Renormalization: The gravitational path integral, holography, and a gauge group for topology change". In: (July 2024). arXiv: 2407.20324 [hep-th].
E.G. participated in the conception of the project, the derivation of the proofs and the writing of the manuscript.

[6]   Elliott Gesteau and Leonardo Santilli. "Explicit large N von Neumann algebras from matrix models". In: (Feb. 2024). arXiv: 2402.10262 [hep-th].

[7]   Elliott Gesteau. "Emergent spacetime and the ergodic hierarchy". In: (Oct. 2023). arXiv: 2310.13733 [hep-th].

[8]   Elliott Gesteau. "Large N von Neumann algebras and the renormalization of Newton's constant". In: (Feb. 2023). arXiv: 2302.01938 [hep-th].

[9]   Elliott Gesteau, Matilde Marcolli, and Sarthak Parikh. "Holographic tensor networks from hyperbolic buildings". In: *JHEP* 10.169 (2022). DOI: 10.1007/JHEP10(2022)169. arXiv: 2202.01788 [hep-th].

[10] Elliott Gesteau and Monica Jinwoo Kang. "Nonperturbative gravity corrections to bulk reconstruction". In: (Dec. 2021). arXiv: 2112.12789 [hep-th].

TABLE OF CONTENTS

LIST OF ILLUSTRATIONS

LIST OF TABLES

C h a p t e r   1

INTRODUCTION

"Il en est qui, face à cela, se contentent de hausser les épaules d'un air désabusé et de parier qu'il n'y a rien à tirer de tout cela, sauf des rêves. Ils oublient, ou ignorent, que notre science, et toute science, serait bien peu de chose, si depuis ses origines elle n'avait été nourrie des rêves et des visions de ceux qui s'y adonnent avec passion."

– Alexandre Grothendieck

Theoretical physics aims at understanding the laws of nature from simple principles. For example, the principle of least action allows to unify classical mechanics into one, united framework. Similarly, the equivalence principle lies at the core of Einstein's theory of general relativity, and Heisenberg's uncertainty principle is the foundational pillar of quantum mechanics.

One of the deepest contemporary questions in theoretical physics is to unify quantum mechanics and general relativity into one fully coherent framework. These two theories are extremely different: for example, time is a variable in quantum mechanics, whereas it is a gauge symmetry in general relativity. Such a unification is therefore a formidable challenge, and it is likely that in order to make progress, we will need a new principle, which supersedes the ones mentioned above.

A leading candidate for such a principle is the holographic principle, which was first proposed by 't Hooft and Susskind [1, 429]. In a physicist's words, it could be stated as follows:

A quantum theory of gravity in a region R of spacetime is equivalent to a somewhat local theory without gravity on its boundary ∂R, whose total number of degrees of freedom is equal, in Planck units, to

$$S = \frac{A(\partial R)}{4},$$ (1.1)

where A denotes the area.

Very compelling theoretical evidence for such a principle has been found. First, the equations of general relativity can be recast into a form that mimics thermodynamics [43], in particular, in this reformulation, the area of the horizon of a black hole

behaves like an entropy functional, suggesting a statistical interpretation. Later, Bekenstein and Hawking obtained the formula (1.1) for the entropy of a quantum black hole using a path integral over spacetime metrics. Strominger and Vafa [425] were later able to show that for some supersymmetric black holes in string theory, a microscopic counting of degrees of freedom was able to recover (1.1).

The first full-fledged realization of holography, which not only shows an area scaling of microstates but also proposes a description of quantum gravity in a region of spacetime in terms of a dual theory on its boundary, was given by Maldacena [319] a few years later, through the discovery of the Anti-deSitter/Conformal Field Theory (AdS/CFT) correspondence. The original version of AdS/CFT used open-closed string duality to show that type IIB superstring theory on an $AdS_5 \times S^5$ background admits an equivalent description in terms of the $\mathcal{N} = 4$ Super-Yang–Mills (SYM) theory on $\mathbb{R}^4$, which is a superconformal field theory on the conformal boundary of AdS_5. This dual description in terms of $\mathcal{N} = 4$ SYM theory therefore provides a concrete realization of the holographic principle: it is a non-gravitational, local theory on the boundary of the spacetime region of interest – here, AdS_5.

The holographic principle goes against intuition: naively, semiclassical field theory on a region of spacetime has a number of degrees of freedom that scales like volume rather than area. This begs two questions:

1. If we start from effective field theory in a region of spacetime, new quantum gravity effects must drastically reduce its number of degrees of freedom. In other words, there must exist many states in the Hilbert space of of this region which look different from the point of view of effective field theory, but which only differ by a "null" state of zero norm in the non-perturbative description of quantum gravity, so that the Hilbert space matches with the one of a local theory in a reduced number of dimensions of spacetime. What is the nature of these new null states from the point of view of the gravity theory?

2. Conversely, if we consider the Hilbert space of the boundary theory, we must explain how the physics of effective field theory in a higher-dimensional spacetime emerge in the limit where quantum gravity effects are turned off in the bulk, which corresponds to the limit in which the number N of degrees of freedom of the boundary theory goes to infinity. Which properties of this large N limit are responsible for this emergent phenomenon?

The conceptual tension raised by Questions 1 and 2 is illustrated on Figure 1.1.

Null States

Semiclassical physics
on bulk spacetime

Boundary quantum theory with
N degrees of freedom

Large N limit
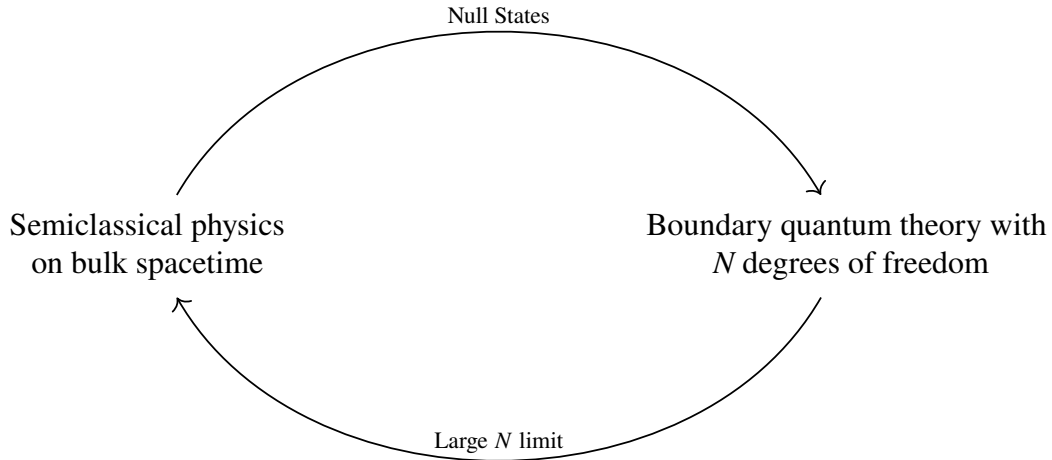
Figure 1.1: The conceptual tension of holography. The top arrow describes Question 1: how can the Hilbert space of a semiclassical field theory be modified so that so many states become null in the nonperturbative quantum gravity regime that it becomes the Hilbert space of a boundary theory? The bottom arrow describes Question 2: how can semiclassical physics on a higher-dimensional spacetime background emerge from a lower-dimensional quantum theory when its number of degrees of freedom is taken to infinity?

The work undertaken in this thesis aims at approaching these two questions from the perspective of a mathematician. As it is often the case in mathematical physics, it will be necessary to invoke very different parts of mathematics to make progress. In particular, Question 1 is about *structure*. In order to answer it, we must understand the precise patterns of equivalences that lead to a drastic dimensional reduction of the Hilbert space of effective field theory. In mathematics, *algebra* is the science of structure. Therefore, in order to make progress on Question 1, we will need to make use of mathematical fields pertaining to the world of algebra - Hopf algebras will for example play an important role in the chapter of this thesis which is mainly dedicated to this question. On the other hand, Question 2 is about the emergent behavior that appears in a very intricate *limit*: the large N limit of a quantum many-body system. In mathematics, *analysis* is the science of limits. Therefore, in order to study Question 2, we will need to use fields from *analysis*. In particular, the theory of von Neumann algebras, which is a noncommutative analog of measure theory, as well as harmonic analysis, will be prominently featured in this thesis.

Before moving on to describing the different chapters of this thesis in more detail,

the following subsections introduce some of the main themes studied in this thesis, and in particular how they fit into the larger goal of answering Questions 1 and 2.

Von Neumann algebras in holography

The first recurring mathematical subject in this thesis is the theory of von Neumann algebras, which can be seen as a quantum analog of measure theory. The analogy goes as follows. in measure theory, the basic object of study is the some measurable space X, equipped with some measure μ and some σ-algebra $\mathcal{A}$ of measurable sets. Then the usual observables one considers are the bounded, measurable functions $f \in L^\infty(X)$, whose expectation values are given by

$$\langle f \rangle_\mu := \int_X f \, d\mu. \tag{1.2}$$

Constructing a quantum analog of classical measure theory is not completely straightforward. In particular, in quantum mechanics the algebra of observables becomes noncommutative, and therefore has no chance of being expressible as $L^\infty(X)$ for some measurable space X, as this algebra is commutative for the pointwise product of functions. The theory of von Neumann algebras axiomatizes properties of noncommutative algebras that give them enough features in common with $L^\infty(X)$ that a quantum analog of measure theory can be developed in these algebras. A possible definition is:

Definition 1.0.1. A von Neumann algebra M acting on a Hilbert space $\mathcal{H}$ is an algebra of bounded operators on $\mathcal{H}$ which is stable under Hermitian conjugation, contains the identity, and is closed for the weak operator topology.

The lesson to draw from this analogy with measure theory, in the context of holography that we are interested in, is that von Neumann algebras are a field of analysis that becomes relevant when one needs to deal with questions about quantum systems whose classical analog involves measure theory. In particular, we saw above that Question 2 requires the understanding of a very subtle limit: the one where the number of degrees of freedom of a quantum dynamical system goes to infinity. This question obviously requires a resort to analysis, and is about the properties of a dynamical system: the holographic quantum theory. Since the theory of classical dynamical systems makes extensive use of measure theory, it is therefore legitimate to expect that the correct mathematical language to explore this question is that of von Neumann algebras.

We will see that many subtle properties of the large N limit of a holographic system can be related to the change of *type* of von Neumann algebra that describes this system. For example, as first discussed in [294, 295], at high temperature the type of the von Neumann algebra of operators describing $\mathcal{N} = 4$ SYM theory on a compact space goes from I to III_1. This has deep consequences for the emergence of a black hole struture in the bulk.

The chapters of this thesis where von Neumann algebras are featured attempt to shed light on the answer to Question 2, mainly by understanding the mathematical properties of the large N limit. In particular:

- Chapters 2 and 9 are concerned with studying the error-correcting structure underlying the emergence of spacetime, which was long conjectured by physicists in toy models, by using the language of von Neumann algebras.

- Chapter 3 takes the analogy between von Neumann algebras and measure theory outlined in this introduction one step further, in order to draw a precise parallel between various notions of emergent spacetime and the *ergodic* properties of the large N limit.

- Chapter 4 uses the theory of von Neumann algebras to define a general notion of emergent causal structure in string theory. The basic idea is to use some algebraic constructions as well as results from harmonic analysis to understand the inclusion structure of time band algebras in the holographic dual.

- Chapter 5 explicitly constructs von Neumann algebras for matrix models whose large N limit share some, but not all, of the properties required to obtain an emergent spacetime.

- Finally, Chapter 8 studies the continuum limit of holographic tensor networks, and shows that the local algebras obtained are type II rather than III, which precisely distinguishes the limit of these networks form a *bona fide* quantum field theory. No notion of large N limit is present there, and this chapter illustrates that von Neumann algebras are also relevant to understand the short-scale behavior of quantum systems.

Hyperbolic geometry, from tensor networks to conformal field theory

Another mathematical theme in this thesis is that of hyperbolic geometry. This theme inevitably shows up in holography, as the AdS/CFT correspondence, which has so

far been our main theoretical laboratory to understand the holographic principle, involves a spacetime with negative curvature.

- Chapter 6 uses some insight from conformal field theory, whose structure is instrumental to the AdS/CFT correspondence, to provide new bounds on spectral gaps of various hyperbolic surfaces with spin. The reason why techniques from CFT, and more precisely from the conformal bootstrap, are relevant is because the harmonic analysis of the group $SO(2, d)$ is involved both in the conformal bootstrap and in the study of hyperbolic surfaces.

- Chapter 7 constructs holographic error-correcting codes on exotic hyperbolic geometries known as hyperbolic buildings. These discrete objects satisfy many properties that are similar to those of tilings of the hyperbolic plane, but are allowed to be more general – in particular their boundary at infinity is allowed to have a non-integer dimension. These structures allow to shed light on the answer to question 2 by studying the emergence of spacetime from an exotic hologram which lives on a fractal, and to relate some features of holography, like the Ryu–Takayanagi formula, to the Hausdorff dimension of this fractal.

Implications of holography for spatially closed spacetimes

One last strand of ideas which permeates the later chapters of this thesis concerns how one may be able to apply the lessons of holography to a universe without a boundary at spatial infinity. Indeed in this case, the implications seem radical: since the holographic principle states that the dimension of the Hilbert space of a subregion scales like the area of its boundary, it seems that the only Hilbert space which can describe a universe without boundary is a Hilbert space of dimension one! Of course this is a strange puzzle, and it can be understood as a much stronger version of the conceptual tension of Figure 1.1: while we were asking about the emergence of a spacetime with more degrees of freedom from a quantum system with fewer degrees of freedom, we now need to ask for all of spacetime to emerge from seemingly zero degrees of freedom! While the full resolution of this puzzle, which will probably involve explicitly taking into account the presence of an observer, is beyond the scope of this thesis, Chapters 10 and 11 sharpen it in the following way.

- Chapter 10 gives a sketch, in a very simple toy model, of how string theory may be able to collapse a naively large Hilbert space of states for a closed uni-

verse into a one-dimensional Hilbert space of states, through an analogy with perturbative renormalization. In the gravitational path integral, it appears that the analog of the counterterms that cancel divergences in perturbative QFT become nonlocal stringy contributions which drastically collapse the dimension of the semiclassical Hilbert space. The underlying mathematical structure is that of a combinatorial Hopf algebra, and can be seen as a realization of a structure of null states similar to the one relevant to Question 1.

- Chapter 11 gives an argument that closed spacetimes cannot be reconstructed within the context of the AdS/CFT correspondence, therefore suggesting that a new paradigm which goes beyond AdS/CFT (and likely explicitly takes into account the presence of gravitating observers), is necessary to describe physics in a closed universe.

Contents of the thesis

Each chapter of this thesis corresponds to a paper written during my time at as a Caltech student, and can be understood as attempts to make progress on Questions 1 and 2, or both at the same time.

Chapter 2 is a single-authored chapter from 2023, published in *Communications in Mathematical Physics*. It derives an area/entropy formula from the error-correcting properties of the large N limit of holographic theories using the language of von Neumann algebras, and interprets an ambiguity between area and bulk entropy in the entropy formula in terms of the renormalization of Newton's constant of gravitation. It can be understood as making progress on Question 2, as it explains the emergence of a geometric quantity in the bulk (the area) in terms of the large N limit. The technical assumptions of the paper also include the presence of the null states relevant to Question 1.

Chapter 3 is a single-authored paper from 2023, published in *Physical Review D*. It puts forward a close parallel between the emergence of a holographic spacetime in the large N limit and the ergodic hierarchy of classical dynamical systems. It provides a conceptual framework to think about Question 2.

Chapter 4 is a recent paper in collaboration with Hong Liu, submitted for publication. In this paper, by making use of the language of von Neumann algebras, we provide a *definition* of an emergent holographic causal structure from a general quantum many-body system which satisfies large N factorization. This includes, for example $\mathcal{N} = 4$ SYM theory at all values of the 't Hooft coupling λ. What this

definition does in the light of Question 2 is that it allows to make sense of the causal structure of an emergent spacetime even when it is not fully local. For example, at finite λ, $\mathcal{N} = 4$ SYM has been thought to give rise to an emergent "stringy geometry," but it has been difficult to precisely define what this geometry is. Our work ascribes a well-defined causal structure to this geometry.

Chapter 5 is a paper from 2024 in collaboration with Leonardo Santilli, published in *Advances in Theoretical and Mathematical Physics*, where we completely explicitly construct the large N von Neumann algebras of a large class of matrix quantum mechanical theories. These algebras have type III_1, but do not carry any emergent causal structure. They are placed at an interesting location in the ergodic hierarchy presented in Chapter 2.

Chapter 6 is a paper from 2023 in collaboration with Sridip Pal, David Simmons-Duffin and Yixin Xu, published in the *Journal of the Association for Mathematical Research*. This paper makes an analogy between the conformal bootstrap, which is instrumental to understanding the CFT side of AdS/CFT, and the hyperbolic geometry of surfaces, to derive new bounds on their spectral gap. It can be understood as an application of the structures that constrain the nonperturbative description of the bulk theory in Question 1 to some problems in pure mathematics.

Chapter 7 is a paper from 2021 in collaboration with Matilde Marcolli and Sarthak Parikh, published in the *Journal of High Energy Physics*. It constructs a general mathematical theory of the geometries which can support tensor network toy models of quantum gravity. The most well-known tensor networks simulating holographic dualities are tilings of the hyperbolic plane, but in this paper we construct more general geometries which can support holographic tensor networks which cannot be embedded in the plane, and whose boundary is the fractal. We find that the entanglement structure of the networks and its gravity interpretation are directly related to the Hausdorff dimension of the boundary theory. This paper informs Question 2 in that it provides emergent holographic geometries for exotic theories on a space of non-integer dimension.

Chapter 8 is a paper from 2025 in collaboration with Wissam Chemissany, Alexander Jahn, Daniel Murphy, and Leo Shaposhnik. It investigates the type of the locals von Neumann algebras of various kinds of tensor networks when their size is taken to infinity. We find that the type of the algebras at the boundary of the most standard holographic codes is II_∞, which is inconsistent with the type III_1 local structure of quantum field theory, making them incomplete models to give a full answer to study

Questions 1 and 2.

Chapter 9 is a paper from 2021 in collaboration with Monica Jinwoo Kang, published in *Journal of Physics A: Mathematical and Theoretical*. It derives a proof that the entanglement wedge can be reconstructed for approximate holographic codes in infinite dimensions. It explains some of the mechanisms underlying the emergence of semiclassical physics in the large N limit, therefore providing a contribution to the resolution of Question 2.

Chapter 10 is a recent paper in collaboration with Matilde Marcolli and Jacob McNamara, submitted for publication. It makes an analogy between the gravitational path integral and perturbative renormalization in quantum field theory to find a Hopf algebra structure which gives a systematic way of UV-completing a gravitational path integral into a "stringy" theory compatible with the holographic principle. This Hopf algebra can be seen as organizing the null states relevant to Question 1.

Chapter 11 is a recent paper in collaboration with Netta Engelhardt, submitted for publication, which shows that the physics of a large class of closed cosmologies *cannot* emerge from the large N limit of a conformal field theory without violating the most basics principles of the AdS/CFT correspondence. There is a clear relevance to Questions 1 and 2, in that the failure of the emergence of a closed universe in AdS/CFT can be traced to the fact described above that the UV-complete description of this closed universe is a one-dimensional Hilbert space. Therefore the outcome is that the null states of Question 1 become too numerous to use the conventional tools of AdS/CFT, and describing the emergence of a closed cosmology from this fundamental description, which is what Question 2 is concernd with, seems to require a new formulation of the holographic principle.

C h a p t e r 2

LARGE *N* VON NEUMANN ALGEBRAS AND THE RENORMALIZATION OF NEWTON'S CONSTANT

This chapter is based on the work [192].

2.1 Introduction

The quantum extremal surface (QES) formula [401, 242, 296, 162, 225, 143] is one of the most important results in holography. It is a powerful probe of the emergent geometry of spacetime, as it relates the area of a surface in the bulk to the entanglement entropy of the boundary dual region. More precisely, if ρ is the state of the boundary theory, it holds that

$$S(\rho) = \frac{A(\Sigma)}{4G_N} + S_{bulk}(\rho), \tag{2.1}$$

where $S(\rho)$ is the UV-complete entanglement entropy of the boundary state, $A(\Sigma)$ is the area of the *quantum extremal surface* associated to ρ, G_N is Newton's gravitation constant, and $S_{bulk}(\rho)$ is the entanglement entropy of ρ *in the bulk effective theory*.

As crucial as this result is, the precise definitions of the terms in the QES formula remain elusive, and some paradoxes seem to arise. Namely:

- $S_{bulk}(\rho)$ is divergent in the bulk effective theory. Indeed, it is a general property of quantum field theory that the entanglement entropy of bulk subregions diverges, and one needs to regulate it with a UV cutoff. A more abstract formulation of this fact is that the von Neumann algebra of the bulk effective theory has type III_1, or II_∞ if one includes perturbative corrections and quantizes the ADM mass [294, 293, 457].[1]

- The smooth spacetime description of the bulk is only valid in the $G_N = 0$ limit. In this limit, the area term also blows up and it is not clear what approximations need to be made in the bulk to consider G_N small but nonzero.

---

[1]Technically, the same kind of issue arises for the boundary entropy associated to a nontrivial subregion. However, when considering two boundary theories in the thermofield double state, or in a large class of more general entangled states, this kind of divergence does not occur, and this is less of a serious problem in one wants to get to a conceptual understanding of holography. As a result, I will mostly consider boundary regions that are dual to one side of a black hole, and ignore this extra complication here.

- The bulk effective theory seems to perform a calculation at $G_N = 0$, or at least perturbatively in G_N. However, on the boundary, the calculation of $S(\rho)$ corresponds to a calculation in a conformal field theory at *large but finite N*, so at *small but finite G_N*, as $G_N \sim \frac{1}{N^2}$ from the holographic dictionary. At $N = \infty$, the left hand side actually also blows up, and the QES formula loses its meaning.

In order to solve these puzzles, it seems that the crucial issue is to understand how to deal with the finiteness of Newton's constant on the boundary, as well as with the UV cutoff of the bulk fields. An interesting proposal in the case of the exterior region of a black hole, originally due to Susskind–Uglum [430], and developed in an important body of work (see for example [267, 136, 252, 289, 181]), is that these two issues are actually related. More precisely, the proposal is the following:

Conjecture 2.1.1 (Susskind–Uglum, [430])**.** *The renormalization of the bulk entropy due to the bulk UV cutoff exactly cancels out the renormalization of Newton's constant in the area term.*

In other words, the choice of UV cutoff for the fields in the bulk is not independent of the running of Newton's constant, and the renormalization of one term of the QES formula in the bulk exactly cancels out the renormalization of the other term, making the right hand side of the QES formula only dependent on the value of Newton's constant (i.e., N) on the boundary, and not on the choice of UV cutoff in the bulk EFT. For N large enough, the effective description is then approximately valid below the bulk cutoff, making it possible to obtain a well-defined, and cutoff-independent, QES formula. The way that Susskind–Uglum originally argued for this proposal is by resorting to string theory arguments and to the Euclidean path integral. These arguments are not fully rigorous and only valid in specific cases.

A more modern way to understand the QES formula, which reduces to the formula for black hole entropy considered by Susskind–Uglum in the case of a two-sided black hole, is through the lens of quantum error correction in AdS/CFT [10, 225]. In this context, the bulk term of the QES formula is reinterpreted as the entanglement entropy of a state in a *code subspace* of the full UV-complete Hilbert space. The area term then captures the entropy of the state which is *not* associated with encoded observables, but instead, with other degrees of freedom in the CFT that do not appear in the bulk fields. The interpretation is that it is the entanglement of these

UV degrees of freedom that conspires to create a geometry in the bulk and make spacetime emerge.

The early breakthroughs in holographic quantum error correction [372, 225, 130, 231] were mainly achieved in the context of toy models, that approximate the full-fledged holographic situation in terms of qubits and finite-dimensional Hilbert spaces. While these models already retain a lot of the important properties of holography, their discreteness makes it difficult to tackle the continuous nature of spacetime in the bulk EFT, the notion of large N limit, and the infinite-dimensional nature of the boundary Hilbert space. However, recent progress [270, 196, 164, 194, 168] has allowed to move past the finite-dimensional case by recasting holographic quantum error correction in the language of infinite-dimensional von Neumann algebras. In this more general language, it is now possible to precisely define the aforementioned notions. The goal of this chapter is to show that this new language is enough to construct a framework in which the Susskind–Uglum conjecture can be formulated and proven.

The first task will be to understand how to obtain a formulation of holographic quantum error correction in the context of the large N limit of AdS/CFT, in a way in which it is possible to derive an entropy formula. A first step towards this goal has been taken by Faulkner and Li [168], and in particular, it has been shown that it is possible to derive the JLMS formula and the correspondence between bulk and boundary modular flows [254] in the large N limit.

The new input of this work will be to note that while the notions of convergence introduced in [168] allow to derive results like the JLMS formula in the large N limit, they are too loose to define a notion of code subspace that is robust enough to satisfy a formula that involves von Neumann entropies in the bulk, like the Ryu–Takayanagi formula. For this latter purpose, the large N bulk von Neumann algebra instead needs to be regulated in order to isolate observables that contribute to the bulk entropy in the large N limit. More precisely, I will construct a family of type I von Neumann algebras which retain a finite amount of large N bulk entropy. These algebras will be nested inside one another and related through conditional expectations, which will implement a renormalization group flow of code subspaces.

Once this new setup based on conditional expectations is introduced at the level of the bulk theory at large N, the next step will be to introduce the bulk-to-boundary maps, which, along the same lines as [8], relate the semiclassical bulk theory to finite N boundary theories. Under physically motivated assumptions, I will show

that this newly introduced family of codes satisfies an asymptotic entropy formula when $N \to \infty$ on the boundary. An important ingredient will be the definition of the area term for an approximate quantum error-correcting code proposed in [8], in terms of the entropy of the Choi–Jamiolkowski state associated to the code. Thanks to the regulation of the code subspace, each individual term of the formula will be well-defined. The conditional expectations in the bulk will concretely implement the renormalization group flow for bulk entropy, and the invariance of the entropy formula under this flow will yield a rigorous proof of the Susskind–Uglum conjecture.

For clarity, the main findings of the chapter are summarized below:

- This work provides a construction of a setup in which holographic entropy formulae as well as a renormalization scheme for the code subspace can be rigorously defined in the large N limit of holography, and the Susskind–Uglum conjecture can be proven.

- It clarifies some subtleties about the type of the bulk von Neumann algebras at large N. While the full, unregulated bulk algebra has type II_∞ or III_1, the pertinent algebras contributing to the bulk entropy in QES-like formulas have type I as long as this entropy is $O(1)$ in the large N limit.

- The role of conditional expectations in holography will be clarified and further extended. In particular, it will be shown that they can implement the renormalization group flow for bulk degrees of freedom. This role is somewhat related to the original proposal of [164] that the boundary-to-bulk map should be modelled by a conditional expectation. Here, I will argue that while this original picture breaks down at finite N because reconstruction becomes approximate, it can still be made sense of at large N, and that the possible code subalgebras are related to each other inside the large N algebra by conditional expectations that implement a renormalization group flow.

- This work also puts forward an intimate relationship between the Susskind–Uglum conjecture and the ER=EPR paradigm. In particular, the fact that the entropy formula is invariant under RG flow can be interpreted as the fact that depending on the choice of code subalgebra, some boundary entanglement can be seen either as entanglement in the code subspace or as a contribution to the area term without changing any of the physics. This shows a com-

plete equivalence between entanglement and geometric contributions in this context.

The exposition is organized as follows: in Section 2.2, the Hilbert space of large N effective field theory in the bulk is introduced. After summarizing recent constructions related to large N von Neumann algebras [294, 293, 457] and asymptotically isometric codes [168], it is argued that the large N von Neumann algebras need to be further regulated if one wants to be able to make sense of holographic entropy formulae. In Section 2.3, a precise notion of code subspace renormalization is constructed. UV-regulated bulk algebras and code subspaces at large N are defined. The renormalization group flow between the algebras is implemented by conditional expectations. In Section 2.4, this RG flow of code subspaces is mapped into the boundary theory in the case of finite-dimensional regulated algebras. It is shown that under physically relevant assumptions for the bulk-to-boundary map, an entropy formula is true for this family of codes, regardless of the choice of renormalization scale in the bulk. This provides an explicit proof of the Susskind–Uglum conjecture, and aligns with the ER=EPR proposal. In Section 2.5, the results of the previous section are generalized to various more general cases, that amount to relaxing some conditions on the dimensions of the various algebras considered. Section 2.6 comments on various potential extensions of this work and further directions. Finally, Appendix 2.7 gives infers the type I of a von Neumann factor from a boundedness condition on the entropy of some finite-dimensional subalgebras.

Technical warning: Unless specified otherwise, all von Neumann algebras introduced here are hyperfinite and all Hilbert spaces are separable.

2.2 The Hilbert space of effective field theory

Much of the work on the error-correcting structure of holography has been focusing on the subtle way in which the low-energy effective field theory in the bulk is encoded in the unitary boundary CFT. The increasingly precise interpretation based on quantum codes has proven to be very fruitful to understand delicate issues about the semiclassical limit of gravity, such as the consistency between black hole evaporation and unitarity [379, 7]. This section will review how bulk effective theory emerges in the large N limit of AdS/CFT, and the error-correcting properties of the mappings of the $N = \infty$ theory (or perturbation theory around it) into large but finite N theories. It will largely be based on the recent developments [294, 293, 457, 168].

Large N algebras and the crossed product

It has recently been argued by Leutheusser and Liu [294, 293] (see also [295] for a more general version of this proposal) that in order to study the emergence of spacetime in the large N limit of AdS/CFT, one needs to consider the von Neumann algebra generated by the single-trace operators of the gauge theory. More precisely, at large N, these operators behave like generalized free fields (i.e., their correlation functions factorize but they do not satisfy any equation of motion). One can then consider the GNS representation of the C^*-algebra of fields in a thermal state (i.e., the thermofield double Hilbert space), and define the corresponding large N algebra as the bicommutant of the GNS representation.

The main conjecture of [294, 293] is that the large N von Neumann algebra changes type across the Hawking–Page transition: if T_{HP} is the Hawking–Page temperature, for $T < T_{HP}$, it has type I, and for $T > T_{HP}$, it has type III_1. The change of type of the large N algebra is associated to the presence of a continuous Källén–Lehmann density, which, in turn, can be related to the emergence of a black hole horizon, the connectedness of the thermofield double state, and the lack of factorizability of the large N Hilbert space.

It is possible to take this idea one step further. The issue with type III_1 algebras is that they do not admit any faithful normal semifinite trace, so it is not possible to define a good notion of entropy on them. It is therefore difficult to express the usual holographic statements that involve entanglement entropy in the bulk. What was shown in [457] is that adding perturbative $\frac{1}{N}$ corrections and quantizing an extra mode corresponding to the ADM mass of spacetime amounts to deforming the bulk algebra from a type III_1 factor to a type II_∞ factor through a standard construction known as the crossed product with the modular automorphism group. Such a construction has proven to be very important in pure mathematics, in the context of the classification of type III factors [120].

In a type II_∞ factor, it is possible to define a one-parameter family of traces, but there is no canonical choice of normalization. Instead, the traces are related to one another by a scaling automorphism. The consequence is that in these algebras, von Neumann entropy is only defined up to an overall constant [457]. The physical meaning of this is that entropy in a type II_∞ factor is a renormalized version of entropy, where an infinite amount of entanglement has been thrown away. How much entanglement needs to be thrown away is arbitrary and cannot be fixed simply by looking at the type II_∞ factor. This is in sharp contrast with the situation in a

type *I* algebra, which corresponds to the UV-complete description of the algebra on one side of the thermofield double (in AdS/CFT, at finite *N* any CFT algebra has type *I*). In a type *I* algebra, the trace is uniquely defined and there is only one way to define entropy, because no infinity needs to be subtracted. What this tells us is that entropy in the crossed product is a coarse-grained quantity that can only be calculated up to an overall constant, whereas entropy in the UV-finite theory is of course uniquely defined.

In [99], it was shown that entropy in the large *N* crossed product algebra can be identified with the generalized entropy of a quantum extremal surface, up to an overall constant. The argument requires a formula [450] relating the generalized entropy at late times to the one on a given time slice. This approach gives a justification for the quantum extremal surface formula directly at the level of the bulk theory in the large *N* limit (including an extra mode corresponding to the ADM mass). The focus of this chapter is different, as it will derive the holographic entropy formula from the perspective of quantum error correction in the large *N* limit of holographic codes.

Embedding into UV-complete theories and quantum error correction

The perspective here will be to derive a family of Ryu–Takayanagi formulae in the large *N* limit of holography within the framework of quantum error-correction. A quantum code is essentially the data of a code Hilbert space $\mathcal{H}_{code}$, a boundary Hilbert space $\mathcal{H}_{phys}$, and a bulk-to-boundary map $V : \mathcal{H}_{code} \longrightarrow \mathcal{H}_{phys}$.

Recently, Faulkner and Li [168] observed that in order to study the large *N* limit of holography, one does not need to consider a single code, but rather, a sequence of codes. More precisely, if $\mathcal{H}_{code}$ is the bulk Hilbert space at large *N* (i.e., the Hilbert space on which the large *N* algebra is represented), then there exist an infinity of boundary Hilbert spaces $\mathcal{H}_N$ and bulk to boundary maps V_N: one for each choice of *N*. These maps are required to be "asymptotically isometric": they are required to approach the properties of an isometry, so that an exact quantum error-correcting structure is recovered as *N* goes to infinity. In particular, Faulkner and Li impose the following conditions:

$$V_N^{\dagger} V_N - Id \underset{N \to \infty, \, w.o.t.}{\longrightarrow} 0, \tag{2.2}$$

and for all $A \in M_{code}$, where M_{code} is the algebra to reconstruct,

$$\gamma_N(A) V_N - V_N A \underset{N \to \infty, \, s.o.t.}{\longrightarrow} 0, \tag{2.3}$$

where γ_N is the reconstruction map and the subscripts w.o.t. and s.o.t. indicate that the limits are respectively taken for the *weak* and *strong* operator topologies.

The weak and strong operator topologies does not coincide with the topology induced by the operator norm in infinite dimensions. While this might seem like a technical subtlety, this choice of topology actually carries a lot of physical meaning. The two convergences described above mean that if one *fixes* two states $|\psi\rangle$ and $|\varphi\rangle$ in $\mathcal{H}_{code}$, then the matrix elements $\langle\psi| V_N^\dagger V_N |\varphi\rangle$ converge towards $\langle\psi|\varphi\rangle$, and the vectors $(\gamma_N(A)V_N - V_N A) |\psi\rangle$ converge to zero. However, this convergence is *not* required to be uniform in the choice of $|\psi\rangle$ and $|\varphi\rangle$, or A.

This means that for each value of N, no matter how large, there may (and do!) exist states for which reconstruction fails dramatically. This makes sense physically: if N is very large but fixed, the effective field theory picture will break down for some operators that scale parametrically with N, and the reconstruction map should not be trusted anymore for such high energy excitations.

This is a first hint that if one wants to relate the entropy of a large but finite N boundary theory to that of the bulk effective theory at large N like the Ryu–Takayanagi formula does, the full bulk von Neumann algebra may not be considered as a code subalgebra. Rather, this algebra needs to be *regulated*, and only a subset of observables for which one can require stronger reconstruction properties, must be singled out. In other words, *the large N algebra must be renormalized.* This introduces an arbitrary choice of regularization. The next step is therefore to introduce a general method to regulate the code subspace of a large N code, and to introduce a renormalization group flow between different choices of regulations.

2.3   Code subspace renormalization

It is now clear that no matter how large N is chosen in the UV-complete boundary theory, the mapping of the bulk effective theory into the boundary theory will dramatically fail for some operators. It is then useful to define UV-regulated algebras of observables in the bulk, that can be mapped into the boundary theory with good precision for large enough, but fixed, values of N. In this section, I introduce a new notion of *code subspace renormalization*, that allows to define such algebras and compare their respective cutoff scales.

What should a consistent renormalization procedure be?

The first goal is to study which possible von Neumann subalgebras of the large N algebra of observables can be chosen to match the bulk entropy term of the Ryu–Takayanagi formula. At least as a first step, I will assume the standard scaling for bulk entropy

$$S_{bulk} = O(1), \tag{2.4}$$

in the large N limit. It turns out that the fact that a normal state on a von Neumann algebra carries a finite amount of entropy strongly constrains its possible type. Actually, it will be shown in Appendix 2.7 that a very mild finiteness of entropy condition implies that the associated von Neumann algebra must have type I. This can already be noticed from an intuitive point of view: in the type II and type III cases, divergences of entropies imply that von Neumann entropy is either not possible to define at all, or that the only possible equivalent throws away an infinite amount of entanglement. Hence, it is natural, at least in the case in which one requires the bulk entropy term to be uniformly bounded in N, to associate it to a type I von Neumann subalgebra of the large N observables. Note that this is a somewhat more abstract argument that shows that it is not right to consider the whole large N algebra of observables in order to show something like a Ryu–Takayanagi formula.[2]

The crucial point of this chapter is that such a choice of algebra, and Hilbert subspace on which it acts, is highly nonunique. There is a large amount of arbitrariness in how one chooses the subalgebra of the effective bulk theory that will be considered as the "code subalgebra" of the holographic code.

However, one cannot choose the reconstructible subalgebra and Hilbert subspace completely arbitrarily. In order to show Ryu–Takayanagi formulae, it is indispensable that a good notion of complementary recovery remains. This implies that the Hilbert subspaces of the large N Hilbert space, and the von Neumann subalgebras, must be chosen so that the commutant structures are compatible with the one of the full large N Hilbert space, and with one another.

The goal of the rest of this section will be to introduce a setup that defines such possible choices of type I subalgebras and relates them with each other in a way that preserves complementarity. The idea is to construct a renormalization scheme by considering a nested family of type I factors that can be projected onto one another by

---

[2]If the bulk entropy were to diverge at large N, one would still expect to be able to single out a family of type I subalgebras that carry an N-dependent amount of entropy.

"integrating out some entanglement." These successive coarse-graining operations can be interpreted as implementing a renormalization group flow. In an operator-algebraic setting, projections of norm one are called conditional expectations. More precisely:[3]

Definition 2.3.1. Let $N \subset M$ be an inclusion of von Neumann algebras. A conditional expectation $E : M \rightarrow N$ is a linear map such that $E(Id) = Id$, and for $n_1, n_2 \in N$ and $m \in M$,

$$E(n_1 m n_2) = n_1 E(m) n_2. \tag{2.5}$$

Hence, the right structure to look at is a family of conditional expectations $\mathcal{E}_\lambda$, that project the observables of the large N theory M onto some type I subalgebra M_λ, for λ with values in a partially ordered set. The order in this set should be understood as a fine graining direction, so I will assume that for every $\mu \leq \lambda$, there exists a faithful normal conditional expectation $E_{\lambda\mu} : M_\lambda \rightarrow M_\mu$. This family of conditional expectations implements the renormalization group flow of the holographic code. It then turns out that conditional expectations react very well with commutant structures. This is essentially the content of Takesaki's theorem [435]. The idea will be to construct Hilbert spaces of states that are invariant under the successive conditional expectations, and Takesaki's theorem will guarantee that these subspaces are compatible with the commutant structure.

Interestingly, the structure of conditional expectation has already been introduced as a model of exact holographic codes in the past [164]. In retrospect, this is not surprising, and reflects the fact that exact entanglement wedge reconstruction is recovered (under this reinterpretation in terms of renormalization) in the large N theory. Note that the link between conditional expectations and renormalization group flow has also already been mentioned in [182].

Formal setup

More formally, the ideas presented above can be captured by the following definition of a code subspace renormalization scheme:[4]

Definition 2.3.2. Let M be a von Neumann factor. A *code subspace renormalization scheme* for M is a datum $(\Lambda, (M_\lambda)_{\lambda \in \Lambda}, (\mathcal{E}_\lambda)_{\lambda \in \Lambda}, (E_{\lambda\mu})_{\lambda,\mu \in \Lambda, \lambda \geq \mu}, \omega)$, where:

---

[3] In some simple cases which will turn out to be relevant here, conditional expectations can be expressed in a more explicit manner, see for example the discussion below Proposition 2.3.5.

[4] Assumptions relative to faithfulness made throughout the chapter are here essentially for convenience. The von Neumann algebras considered here are also all taken to be factors for simplicity.

- Λ is a partially ordered set,

- The M_λ are type I subfactors of M,

- The $\mathcal{E}_\lambda$ are faithful normal conditional expectations from M onto M_λ,

- The $E_{\lambda\mu}$ are faithful normal conditional expectations from M_λ onto M_μ.

- For $\lambda \geq \mu \geq \nu$, the following compatibility relations hold:

$$\mathcal{E}_\mu = E_{\lambda\mu} \circ \mathcal{E}_\lambda, \tag{2.6}$$

$$E_{\lambda\nu} = E_{\mu\nu} \circ E_{\lambda\mu}. \tag{2.7}$$

- ω is a faithful normal state on M that is invariant under all the $\mathcal{E}_\lambda$.

The next step is to introduce a Hilbert space of states on which M acts. A natural choice, if one wants to think of a situation in which there are two boundary CFT's with a black hole in the center, is to think of the GNS representation of M in the state ω, which carries a nontrivial commutant structure for M:

Definition 2.3.3. Let $(\Lambda, (M_\lambda)_{\lambda\in\Lambda}, (\mathcal{E}_\lambda)_{\lambda\in\Lambda}, (E_{\lambda\mu})_{\lambda,\mu\in\Lambda,\,\lambda\geq\mu}, \omega)$ be a code subspace renormalization scheme. The *unregulated code subspace* associated to this scheme is the GNS Hilbert space $\mathcal{H}$ of M in the state ω.

Note that as an alternative to constructing the Hilbert space directly from the GNS procedure, one could also have defined the a code subspace renormalization scheme directly from the action of a von Neumann algebra on a Hilbert space that contains a cyclic separating vector whose restriction to the von Neumann algebra is invariant under the conditional expectations. By uniqueness of the GNS representation, such a construction is isomorphic to the one described above. The next step is to introduce Hilbert subspaces associated to the regulated subalgebras M_λ.[5]

Definition 2.3.4. Let $(\Lambda, (M_\lambda)_{\lambda\in\Lambda}, (\mathcal{E}_\lambda)_{\lambda\in\Lambda}, (E_{\lambda\mu})_{\lambda,\mu\in\Lambda,\,\lambda\geq\mu}, \omega)$ be a code subspace renormalization scheme. The *regulated code subspaces* $\mathcal{H}_\lambda \subset \mathcal{H}$ associated to the von Neumann subalgebra M_λ are the Hilbert spaces spanned by the $M_\lambda |\Omega\rangle$, where $|\Omega\rangle$ is the GNS vector associated to ω in $\mathcal{H}$.

---

[5]Related Hilbert subspaces were introduced in [168] in the context of the proof of an asymptotic information-disturbance tradeoff, although compatibility with a conditional expectation structure was not assumed. For these subspaces, reconstruction assumptions involving finer than weak or strong operator topologies can be assumed, in the same spirit as what will be done in the next section of this chapter.

The following proposition makes it explicit why the structure just introduced is well-adapted to describe a renormalization scheme for entropy. In particular, it identifies Hilbert spaces associated to states that are invariant under the conditional expectations.

Proposition 2.3.5. *Let $(\Lambda, (M_\lambda)_{\lambda\in\Lambda}, (\mathcal{E}_\lambda)_{\lambda\in\Lambda}, (E_{\lambda\mu})_{\lambda,\mu\in\Lambda,\ \lambda\geq\mu}, \omega)$ be a code subspace renormalization scheme, and let $\lambda \geq \mu$. There exist decompositions of the form*

$$M = M_\lambda \otimes M_\lambda^c, \tag{2.8}$$

and

$$M = M_\mu \otimes M_{\lambda\mu} \otimes M_\lambda^c, \tag{2.9}$$

where M_μ and $M_{\lambda\mu}$ are type I factors. Moreover, the Hilbert spaces $\mathcal{H}_\lambda$ and $\mathcal{H}_\mu$ are isomorphic to the GNS Hilbert spaces of M_λ and M_μ in the state ω, and there exist Hilbert spaces $\mathcal{H}_\lambda^0$, $\mathcal{H}_\mu^0$, $\mathcal{H}_\lambda^{0c}$, $\mathcal{H}_\mu^{0c}$ such that

$$\mathcal{H} = \mathcal{H}_\lambda^0 \otimes \mathcal{H}_\lambda^{0c}, \tag{2.10}$$

and

$$\mathcal{H} = \mathcal{H}_\mu^0 \otimes \mathcal{H}_\mu^{0c} \tag{2.11}$$

and states $|\chi_\mu\rangle \in \mathcal{H}_\mu^{0c}$, $|\chi_\lambda\rangle \in \mathcal{H}_\lambda^{0c}$ such that

$$\mathcal{H}_\lambda = \mathcal{H}_\lambda^0 \otimes |\chi_\lambda\rangle, \tag{2.12}$$

and

$$\mathcal{H}_\mu = \mathcal{H}_\mu^0 \otimes |\chi_\mu\rangle. \tag{2.13}$$

Moreover there exists a further decomposition

$$\mathcal{H}_\mu^{0c} = \mathcal{H}_{\lambda\mu}^0 \otimes \mathcal{H}_\lambda^{0c}, \tag{2.14}$$

and a state $|\chi_{\lambda\mu}\rangle \in \mathcal{H}_{\lambda\mu}^0$ under which

$$|\chi_\mu\rangle = |\chi_{\lambda\mu}\rangle \otimes |\chi_\lambda\rangle. \tag{2.15}$$

Further, note that under the decomposition described by the above proposition, the conditional expectations take a very simple form

$$\mathcal{E}_\lambda = Id_{\mathcal{B}(\mathcal{H}_\lambda)} \otimes \chi_\lambda, \qquad E_{\lambda\mu} = Id_{\mathcal{B}(\mathcal{H}_\mu)} \otimes \chi_{\lambda\mu}, \qquad (2.16)$$

where the linear functionals χ_λ, $\chi_{\lambda\mu}$ are the expectation value functionals induced by the states $|\chi_\lambda\rangle$, $|\chi_{\lambda\mu}\rangle$.

Proof. The first two factorizations follow from the fact that the M_λ are type I factors, for a proof see paragraph 9.15 of [424]. With these factorizations in hand, Equation 4.10 of [164] guarantees that ω, which is an invariant state under both $\mathcal{E}_\lambda$ and $E_{\lambda\mu}$ must have the form $\omega_\mu \otimes \omega_{\lambda\mu} \otimes \omega_\lambda^c$. Hence its GNS vector has the form

$$|\Omega\rangle = |\chi_\mu\rangle \otimes |\chi_{\lambda\mu}\rangle \otimes |\chi_\lambda^c\rangle. \qquad (2.17)$$

The result straightforwardly follows. $\qquad\qquad\qquad\qquad\qquad\qquad\qquad\quad$ □

The above factorizations make it possible to calculate von Neumann entropy very explicitly for invariant states under the conditional expectations.

In the most explicit case in which it is possible to define a good additive notion of von Neumann entropy on M, for any state of the form $|\psi_\lambda\rangle \otimes |\chi_\lambda^c\rangle$, we have

$$S(|\psi_\lambda\rangle \otimes |\chi_\lambda\rangle, M) = S(|\chi_\lambda\rangle, M_\lambda^c) + S(|\psi_\lambda\rangle, M_\lambda). \qquad (2.18)$$

The entanglement entropy therefore splits into two pieces: a UV piece, $S(|\chi_\lambda\rangle, M_\lambda^c)$, which is generically divergent, and a (potentially) finite piece corresponding to the regulated type I algebra M_λ.

Moreover, under the renormalization group flow, we have the further decomposition

$$S(|\psi_\mu\rangle \otimes |\chi_{\lambda\mu}\rangle \otimes |\chi_\lambda\rangle) = S(|\chi_\lambda\rangle, M_\lambda^c) + S(|\chi_{\lambda\mu}\rangle, M_{\lambda\mu}) + S(|\psi_\mu\rangle, M_\mu). \quad (2.19)$$

The interpretation of the new term in the middle, $S(|\psi_{\lambda\mu}\rangle, M_{\lambda\mu})$, is that it integrates out some of the entropy associated to observables that are in M_λ but not in M_μ, and throws it into the UV piece of the entanglement of the state. This extra term will be reinterpreted as a renormalization term for Newton's constant in the next section. Note, however, that importantly, even in the case in which it is no longer possible to define the divergent term $S(|\chi_\lambda\rangle, M_\lambda^c)$ (or to give it a state counting interpretation), it is still possible to talk about the entropy of the type I subalgebras involved, so that code subspace renormalization yields

$$S(|\psi_\lambda\rangle, M_\lambda) = S(|\chi_{\lambda\mu}\rangle, M_{\lambda\mu}) + S(|\psi_\mu\rangle, M_\mu). \qquad (2.20)$$

Crucially, it is only this latter equality that will be necessary to prove an entropy formula.

The other nice feature of the structure of code subspace renormalization scheme is that it respects the commutant structures. More precisely, by Takesaki's theorem, the modular structures of M, M_λ and M_μ are compatible. This implies:

Proposition 2.3.6. *Let* $(\Lambda, (M_\lambda)_{\lambda\in\Lambda}, (\mathcal{E}_\lambda)_{\lambda\in\Lambda}, (E_{\lambda\mu})_{\lambda,\mu\in\Lambda,\ \lambda\geq\mu}, \omega)$ *be a code subspace renormalization scheme. For* $\lambda, \mu \in \Lambda$, *in* $\mathcal{H}_\lambda$ *and* $\mathcal{H}_\mu$,

$$M'_\lambda = JM_\lambda J, \quad M'_\mu = JM_\mu J, \tag{2.21}$$

where J is the modular conjugation of $|\Omega\rangle$ *with respect to M.*

Proof. This is a direct consequence of Takesaki's theorem, given that states in $\mathcal{H}_\lambda$ and $\mathcal{H}_\mu$ are invariant under the corresponding conditional expectations. $\square$

This fact guarantees the compatibility of the commutant structures along the renormalization group flow, and a nice nesting of all subspaces and subalgebras at hand. In particular, then, there also exist faithful normal conditional expectations $\mathcal{E}'_\lambda$, $\mathcal{E}'_\mu$ and $E'_{\lambda\mu}$, defined on M' and M'_λ, respectively, by

$$\mathcal{E}'_\lambda(X) := J\mathcal{E}_\lambda(JXJ)J, \tag{2.22}$$

$$\mathcal{E}'_\mu(X) := J\mathcal{E}_\mu(JXJ)J, \tag{2.23}$$

$$E'_{\lambda\mu}(X) := JE_{\lambda\mu}(JXJ)J. \tag{2.24}$$

Note that the compatibility condition

$$\mathcal{E}'_\mu = E'_{\lambda\mu} \circ \mathcal{E}'_\lambda \tag{2.25}$$

is satisfied.

Figure 2.1 summarizes the structure of code subspace renormalization scheme, and how the compatibility between conditional expectations and commutant structures is realized, thanks to a commutative diagram.

It follows from the previous analysis that the structure of code subspace renormalization scheme proposed here, and based upon nested type I factors and Hilbert

$$
\begin{array}{ccc}
M \xrightarrow{\quad ' \quad} M' & \mathcal{H} \\[2em]
\mathcal{E}_\lambda \downarrow \qquad \mathcal{E}'_\lambda \downarrow & \downarrow \\[2em]
\mathcal{E}_\mu \left(M_\lambda \xrightarrow{\quad ' \quad} M'_\lambda \right) \mathcal{E}'_\mu & \mathcal{H}_\lambda \\[2em]
E_{\lambda\mu} \downarrow \qquad E'_{\lambda\mu} \downarrow & \downarrow \\[2em]
M_\mu \xrightarrow{\quad ' \quad} M'_\mu & \mathcal{H}_\mu
\end{array}
$$
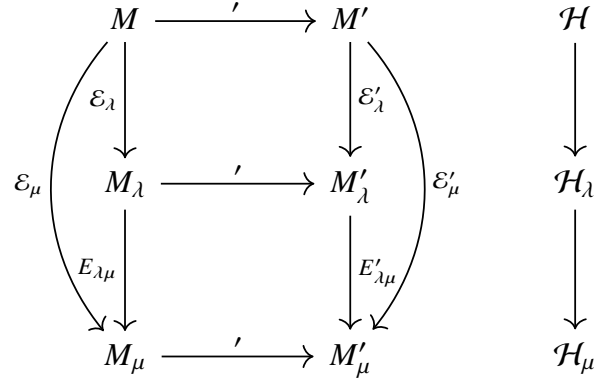
Figure 2.1: A commutative diagram summarizing the structure of code subspace renormalization. Here the full bulk von Neumann algebras M and M', which are commutants of each other, are mapped to the subalgebras M_λ and M_μ and their commutants, corresponding to different cutoff scales, through the conditional expectations $\mathcal{E}_\lambda$, $\mathcal{E}_\mu$ and $\mathcal{E}'_\lambda$, $\mathcal{E}'_\mu$. The prime on the horizontal arrows denotes the commutant structure implemented by modular conjugation. Given that the states in $\mathcal{H}_\lambda$ and $\mathcal{H}_\mu$ are invariant under the conditional expectations, Takesaki's theorem guarantees that the commutant structure is respected, and that the diagram commutes.

spaces related to each other by conditional expectations, is a good choice in the sense that it allows to completely decouple the contribution to the bulk entropy of different subalgebras of the large N theory, and most importantly, to preserve complementarity. However, it does not provide a constructive way of defining these algebras – the most naive attempt of considering low energy products of single trace operators fails because such spaces are not closed under multiplication.

Instead, one should think of the type I factors introduced here as something closer to the type I factors arising for subregions in theories that satisfy the split property. It has been argued in the past (see for example [149]) that such algebras can be thought of as UV-regulators for a quantum field theory. It is quite tempting to observe that restricting observables to a type I factor can be thought of as imposing a "brick wall" cutoff in the bulk QFT in the spirit of [430], and it would be very interesting to understand this better.

2.4   A proof of the Susskind–Uglum conjecture

Now that a renormalization scheme for the bulk effective theory has been defined, one can ask how the UV-regulated algebras map into the boundary theory. In this section,
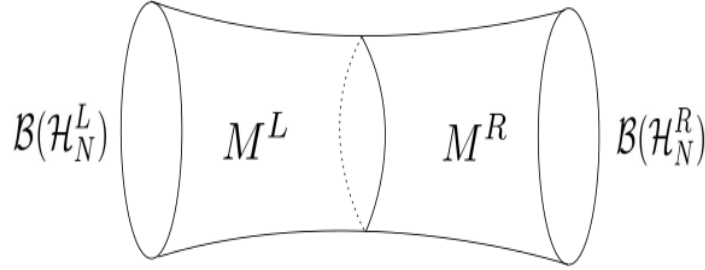
Figure 2.2: The code in the case of two entangled CFT's on a compact space. The large N algebras M^L and M^R need to be regulated in order for the map to the finite N algebras $\mathcal{B}(\mathcal{H}_N^L)$ and $\mathcal{B}(\mathcal{H}_N^R)$ to allow the derivation of an entropy formula.

I show that for suitable values of N and of the UV cutoff, the reconstruction map is good enough that the code satisfies a Ryu–Takayanagi formula. The value of the UV cutoff corresponds to a renormalization scale, and its choice is entirely arbitrary as long as it remains within a suitable range. I show that the Ryu–Takayanagi formula is invariant under the renormalization group flow. This provides an explicit proof of the Susskind–Uglum conjecture.

The bulk to boundary map

The next step in this work is to map the effective theory at large N in the bulk to a finite N theory on the boundary. In order to do this, one needs to introduce one more object: the bulk-to-boundary map. This motivates the following definition of a renormalizable large N quantum error-correcting code, see Figure 2.2.[6]

Definition 2.4.1. A *renormalizable large-N holographic quantum error correcting code* is defined by the data of a sequence of Hilbert spaces $(\mathcal{H}_N)_{N\in\mathbb{N}}$, and a sequence of contractive maps $V_N : \mathcal{H} \longrightarrow \mathcal{H}_N \otimes \mathcal{H}_N$, where $\mathcal{H}$ corresponds to the unregulated Hilbert space of a code subspace renormalization scheme
$(\Lambda, (M_\lambda)_{\lambda\in\Lambda}, (\mathcal{E}_\lambda)_{\lambda\in\Lambda}, (E_{\lambda\mu})_{\lambda,\mu\in\Lambda,\,\lambda\geq\mu}, \omega)$.

In order to explicitly differentiate between the two sides of the code, the algebras M_λ will often be denoted M_λ^L, and their commutants M_λ^R, and similarly for the Hilbert spaces $\mathcal{H}_N^L$ and $\mathcal{H}_N^R$ on the boundary.

---

[6]Once again note that here I will be mainly focusing on the case of two entangled CFT's, rather than the case of subregions of one CFT. This is because the latter case would require an extra regulation procedure due to the infiniteness of the Ryu–Takayanagi surface, but this regulation procedure would not teach us anything meaningful about the physics described here.

It was argued above that for each finite value of N, the holographic code drastically fails to map some of the bulk states to the boundary with good precision. Hence, one needs to renormalize the code subspace. The idea of this section will be to use the framework of code subspace renormalization put forward above to define UV-regulated subalgebras for which strong enough reconstruction properties can be imposed. A Ryu–Takayanagi formula will then be proven. Moreover, under the renormalization group flow, I will explicitly show that the corrections to the area term and the bulk entropy term of the formula exactly compensate each other.

A technical remark is that in order to be able to control the von Neumann entropy of states on the boundary, it will be necessary to impose strong reconstruction assumptions on the states in regularized code subspaces (typically, a nonperturbatively small error in the $1/N$ expansion, or at least, small enough that the polynomially divergent factor in Fannes' inequality does not spoil the conclusions). In order to be able to impose such an assumption, one needs to include backreaction effects in the code subspace that go beyond the strict large-N limit of Leutheusser–Liu, and may introduce some N-dependence not only at the level of the boundary theory, but also of the code subspace and its renormalization scheme. Different ideas exist to construct code subalgebras allowing for perturbation theory in $1/N$ [457, 168]. While it is beyond the scope of this chapter to attempt such a construction, I emphasize that the results introduced here are still valid if the code subspace and its renormalization scheme depend perturbatively on N (and it would be interesting to find a systematic way to interpolate between schemes with different values of N). For convenience, the rest of this section (and of this chapter) will not make it explicit in its notations that the code subspace renormalization scheme and its Hilbert spaces themselves might depend on N.

A Ryu–Takayanagi formula

This section will cover the simplest case in which the chosen bulk algebra M_λ, as well as the boundary algebra, are taken to be finite-dimensional. In this case, the Ryu–Takayanagi formula can be derived by adapting the proof of a result of [8], which introduces a framework in which it is possible to talk about area terms for approximate and non-isometric codes. It generalizes to the approximate case the notion of area term for quantum codes introduced in [225].

Let us first briefly recall the setup of [8], and especially, how one defines a good notion of area term from the structure of the code in this context. The idea is to

consider a map

$$V : \mathcal{K}_L \otimes \mathcal{K}_R \longrightarrow \mathcal{H}_L \otimes \mathcal{H}_R, \tag{2.26}$$

where $\mathcal{K}_{L,R}$ are left and right bulk Hilbert spaces (in the context considered here where the bulk regions are associated to different sides of the black hole) and are finite-dimensional, and introduce a reference Hilbert space

$$\mathcal{K}^{ref} := \mathcal{K}_L^{ref} \otimes \mathcal{K}_R^{ref}, \tag{2.27}$$

where $\mathcal{K}_L^{ref}$ and $\mathcal{K}_R^{ref}$ have the same dimensions as $\mathcal{K}_L$ and $\mathcal{K}_R$ and are identified with dual Hilbert spaces. One can then introduce the canonical maximally entangled state

$$|MAX\rangle \in \mathcal{K}_L \otimes \mathcal{K}_R \otimes \mathcal{K}^{ref}, \tag{2.28}$$

which maximally entangles $\mathcal{K}_{L,R}$ and $\mathcal{K}_{L,R}^{ref}$ together in a basis-independent manner. The Choi–Jamiolkowski state is then

$$|CJ\rangle := (V \otimes Id)\,|MAX\rangle \in \mathcal{H}_L \otimes \mathcal{H}_R \otimes \mathcal{K}^{ref}. \tag{2.29}$$

The definition of area term for a subregion proposed in [8] (for example, associated to $\mathcal{H}_L$) is then given by:

Definition 2.4.2. In the code defined by the map V, the area term of the region L is defined by

$$A(\mathcal{K}_L) := S(|CJ\rangle, \mathcal{B}(\mathcal{H}_L) \otimes \mathcal{B}(\mathcal{K}_L^{ref})). \tag{2.30}$$

Note that this definition is independent of the choice of state in $\mathcal{K}_L \otimes \mathcal{K}_R$.[7] However, it *does* depend on the choice of code subspace $\mathcal{K}_L \otimes \mathcal{K}_R$. This point was not made explicit in [8] as in their context, only one code subspace is considered. Here however, in the novel framework of code subspace renormalization, the choice of code subspace and code subalgebras becomes highly nonunique, and it will turn out to be very important that the value of the area term does depend on the choice of code subspace, even though it does not depend on the choice of a particular state inside it.

The proof of the Ryu–Takayanagi formula in [8] heavily relies on the Fannes inequality, which turns out to become vacuous in the case of an infinite-dimensional

---

[7]In the context of this chapter, $\mathcal{K}_L$ and $\mathcal{K}_R$ are the regulated Hilbert spaces, and this independence reflects the fact that the regulated algebras are assumed to not have a center.

boundary Hilbert space. In conformal field theory, even at finite N, the Hilbert space is infinite-dimensional, and the boundary algebra is a type I_∞ factor. However it is usual to assume, as a first approximation, that the logarithm of the dimension of $\mathcal{H}_N$ grows polynomially in N in order to obtain a proof of the Ryu–Takayanagi formula. This is usually justified due to the fact that the boundary entropy grows polynomially in N. In Section 2.5, I will introduce an alternative to this assumption, thanks to the use of an alternative to Fannes' inequality due to Winter [454]. However I will simply make a finite-dimensional assumption in this section, as the proof will be less technical and easier to follow for the reader who is content with such a simplification.

Before stating and proving the theorem, let us introduce the statement of Fannes' inequality for convenience (see for example [8]).

Proposition 2.4.3. *Let ρ and σ be subnormalized density matrices on a Hilbert space $\mathcal{H}$ of finite dimension d. Suppose that for $0 < \varepsilon < e^{-1}$, $\|\rho - \sigma\|_1 \le \varepsilon$. Then,*

$$|S(\rho) - S(\sigma)| \le \varepsilon \log\left(\frac{d}{\varepsilon}\right). \tag{2.31}$$

The theorem then reads:

Theorem 2.4.4. *Let $(\Lambda, (M_\lambda)_{\lambda\in\Lambda}, (\mathcal{E}_\lambda)_{\lambda\in\Lambda}, (E_{\lambda\mu})_{\lambda,\mu\in\Lambda,\,\lambda\ge\mu}, \omega, V_N)$ be a large N quantum error-correcting code. Suppose that for some choice of λ, M_λ is finite-dimensional of dimension d_λ^2 constant in N. Suppose that there exists a polynomial P in N such that the dimension d_N of $\mathcal{H}_N$ satisfies*

$$\log d_N \le P(N). \tag{2.32}$$

Let $|\Psi\rangle \in \mathcal{H}_\lambda$ (normalized). Suppose that for all unitary operators $U_\lambda^L, \hat{U}_\lambda^L$ and $U_\lambda^R, \hat{U}_\lambda^R$ in M_λ^L and M_λ^R, there exist unitary operators $\tilde{U}_\lambda^L$ and $\tilde{U}_\lambda^R$ (chosen in a measurable way) in $\mathcal{B}(\mathcal{H}_N^L)$ and $\mathcal{B}(\mathcal{H}_N^R)$ such that[8]

$$\|V_N U_\lambda^R U_\lambda^L |\Psi\rangle - \tilde{U}_\lambda^R \tilde{U}_\lambda^L V_N \hat{U}_\lambda^R \hat{U}_\lambda^L |\Psi\rangle\| \le \delta_N, \tag{2.33}$$

where δ_N decays faster than any polynomial in N. Then,

$$|S(|\Psi\rangle, M_\lambda^L) + A(\mathcal{H}_{L,\lambda}) - S(V_N \hat{U}_\lambda^R \hat{U}_\lambda^L |\Psi\rangle, \mathcal{B}(\mathcal{H}_N^L))| \xrightarrow[N\to\infty]{} 0. \tag{2.34}$$

---

[8]The $\hat{U}$'s are introduced essentially to match with the notations of [8]. The result shown here implies that the choice of $\hat{U}$'s only changes boundary entropy by an amount that goes to 0 as $N \to \infty$. Also note that δ_N only needs to be smaller than all polynomials appearing in the proof.

Proof. This theorem is essentially a translation of Theorem 5.5 of [8] in the present setup, and this proof will closely follow the strategy used there.

The Hilbert space $\mathcal{H}_\lambda$ (once identified with the $\mathcal{H}_\lambda^0$ of the previous section) can be written as $\mathcal{H}_\lambda^L \otimes \mathcal{H}_\lambda^R$, where the decomposition is consistent with $\mathcal{B}(\mathcal{H}_\lambda) = \mathcal{B}(\mathcal{H}_\lambda^L) \otimes \mathcal{B}(\mathcal{H}_\lambda^R) = M_\lambda^L \otimes M_\lambda^R$. Construct an isometry

$$W_\lambda^L : \mathcal{H}_\lambda \longrightarrow L^2(U(\mathcal{H}_\lambda^L)) \otimes \mathcal{H}_\lambda \tag{2.35}$$

$$|\Psi\rangle \longmapsto \int dU_L \, |U_L\rangle_{U_L} \otimes U_L \, |\Psi\rangle . \tag{2.36}$$

One can use the Peter–Weyl theorem (see [8], Lemma 4.4) to show that

$$W_\lambda^L \, |\Psi\rangle = |\Psi\rangle_{aR} \otimes |MAX\rangle_{Lr} , \tag{2.37}$$

where a, r are reference systems of dimensions equal to that of $\mathcal{H}_\lambda^R$ and $\mathcal{H}_\lambda^L$ and correspond to the fundamental and antifundamental representations of the unitary group. One defines the isometry W_λ^R in an exactly similar way. Then (see Equation 4.32 of [8]),

$$S(V_N W_\lambda^L W_\lambda^R \, |\Psi\rangle , \, \mathcal{B}(\mathcal{H}_N^L \otimes \mathcal{H}_f \otimes \mathcal{H}_f^*)) = A_L(\mathcal{H}_\lambda^L) + S(|\Psi\rangle , \, \mathcal{B}(\mathcal{H}_\lambda^L)), \quad (2.38)$$

where $\mathcal{H}_f$ and $\mathcal{H}_f^*$ are the fundamental and antifundamental Hilbert spaces. Now, introduce the operators $W_N^{L,R}$, defined by

$$W_N^{L,R} := \int dU_\lambda^{L,R} \, |U_\lambda^{L,R}\rangle \otimes \tilde{U}_\lambda^{L,R}. \tag{2.39}$$

Substituting inequality (2.33), one then obtains

$$\|W_N^L W_N^R V_N \hat{U}_\lambda^L \hat{U}_\lambda^R \, |\Psi\rangle - V_N W_\lambda^L W_\lambda^R \, |\Psi\rangle \| \le \delta_N. \tag{2.40}$$

From this inequality, one can deduce a bound on the difference of entropies thanks to Fannes' inequality.[9] First, recall that by the Peter–Weyl theorem,

$$L^2(U(\mathcal{H}_\lambda^L)) = \bigoplus_\mu \mathcal{H}_\mu \otimes \mathcal{H}_\mu^*, \tag{2.41}$$

where μ runs over the finite-dimensional irreducible representations of $U(\mathcal{H}_\lambda^L)$. What is shown in Lemma 4.4 of [8] is that the maps W_λ^L, W_λ^R only have range on

---

[9]The bound derived in [8] misses some terms, and a few extra steps need to be taken care of in order to get a consistent bound. I am grateful to Chris Akers and Geoff Penington for clarifying this point.

the component of the direct sum corresponding to the fundamental representation of $U(\mathcal{H}_\lambda^L)$. Similarly, the image of $\mathcal{H}_N^L$ by W_N^L sits inside $\mathcal{H}_N^L \otimes L^2(U(\mathcal{H}_\lambda^L))$. This fact makes it natural to introduce the Hilbert space

$$\tilde{\mathcal{H}}_N^L := \mathcal{H}_f \otimes \mathcal{H}_f^* \otimes \mathcal{H}_N^L + W_N^L \mathcal{H}_N^L, \tag{2.42}$$

where the subscript f denotes the fundamental representation (the sum need not be direct), and similarly the Hilbert space

$$\tilde{\mathcal{H}}_N^R := \mathcal{H}_f \otimes \mathcal{H}_f^* \otimes \mathcal{H}_N^R + W_N^R \mathcal{H}_N^R. \tag{2.43}$$

Note that

$$\dim(\tilde{\mathcal{H}}_N^L) \leq d_N(d_\lambda^2 + 1). \tag{2.44}$$

Moreover, states of both forms $W_N^L W_N^R V_N \hat{U}_\lambda^L \hat{U}_\lambda^R |\Psi\rangle$ and $V_N W_\lambda^L W_\lambda^R |\Psi\rangle$ are in $\tilde{\mathcal{H}}_N^L \otimes \tilde{\mathcal{H}}_N^R$. As the W's are isometries, one can also deduce:

$$S(V_N \hat{U}_\lambda^L \hat{U}_\lambda^R |\Psi\rangle, \mathcal{B}(\mathcal{H}_N^L)) = S(W_N^L W_N^R V_N \hat{U}_\lambda^L \hat{U}_\lambda^R |\Psi\rangle, \mathcal{B}(W_N^L \mathcal{H}_N^L)) \tag{2.45}$$

$$= S(W_N^L W_N^R V_N \hat{U}_\lambda^L \hat{U}_\lambda^R |\Psi\rangle, \mathcal{B}(\tilde{\mathcal{H}}_N^L)). \tag{2.46}$$

On the other hand,

$$S(V_N W_\lambda^L W_\lambda^R |\Psi\rangle, \mathcal{B}(\mathcal{H}_N^L \otimes \mathcal{H}_f \otimes \mathcal{H}_f^*)) = S(V_N W_\lambda^L W_\lambda^R |\Psi\rangle, \mathcal{B}(\tilde{\mathcal{H}}_N^L)). \tag{2.47}$$

Hence one can apply Fannes' inequality the density matrices associated to these two subnormalized states on $\mathcal{B}(\tilde{\mathcal{H}}_N^L)$, whose 1-norm distance is smaller than $2\delta_N$ by Lemma C.1 of [8]. This implies (for N large enough):

$$|S(|\Psi\rangle, M_\lambda^L) + A(\mathcal{H}_{L,\lambda}) - S(V_N \hat{U}_\lambda^R \hat{U}_\lambda^L |\Psi\rangle, \mathcal{B}(\mathcal{H}_N^L))| \leq 2\delta_N \log\left(\frac{d_N(d_\lambda^2 + 1)}{2\delta_N}\right). \tag{2.48}$$

As $\log d_N$ grows at most polynomially, d_λ is fixed here (see Section 2.5 for a setup in which this assumption is relaxed), and δ_N decays faster than polynomially, this expression goes to zero at large N. $\qquad\square$

Note that although the dimension of the code subspace was kept fixed here, it can also be made to grow with N as long as it grows slowly enough that issues related to state-dependence and entanglement wedge jumps do not arise. In this more complicated case, a setup more akin to the product unitary reconstruction assumption proposed

in [8] must be used instead, as the entanglement wedge could then change depending on the action of certain unitaries in the code subspace. These cases will be further discussed in the next section.

Another remark can be made at this stage: it has been pointed out [457, 100] that in the case where the bulk algebra is a type II_∞ factor, an entanglement entropy associated to the entire, unregulated bulk algebra can be defined but only up to an overall constant, which captures the fact that an infinite amount of entanglement needs to be thrown out in order to obtain a finite answer, and that the part that remains is arbitrary. Here, it is tempting to choose this constant in an N-dependent fashion so that the entropy of the bulk state in the unregulated algebra matches $S(V_N \hat{U}_\lambda^R \hat{U}_\lambda^L |\Psi\rangle, \mathcal{B}(\mathcal{H}_N^L))$. Then, the resulting statement can be seen as another instance of the fact that bulk generalized entropy equals boundary entropy [100].

Invariance under renormalization group flow

Now that it has been shown that the Ryu–Takayanagi formula is true for *any* choice of finite-dimensional M_λ, the previous result, coupled to the framework of code subspace renormalization introduced above, allows to very explicitly demonstrate the validity of the Susskind–Uglum conjecture, and to isolate the counterterm that gets reabsorbed into the area term under the renormalization group flow.

Theorem 2.4.5. *Consider two choices of code subspace regularization M_λ and M_μ, such that $\lambda \geq \mu$, and $|\Psi\rangle \in \mathcal{H}_\mu$ (normalized). Then, under the assumptions of Theorem 2.4.4 on M_λ, for all unitaries $\hat{U}_\mu^L$, $\hat{U}_\mu^R$,*

$$|S(|\Psi\rangle, M_\mu) + A(\mathcal{H}_{L,\mu}) - S(V_N \hat{U}_\mu^L \hat{U}_\mu^R |\Psi\rangle, \mathcal{B}(\mathcal{H}_N))| \xrightarrow[N\to\infty]{} 0, \qquad (2.49)$$

and

$$|S(|\Psi\rangle, M_\mu) + S(|\Psi\rangle, M_{\lambda\mu}) + A(\mathcal{H}_{L,\lambda}) - S(V_N \hat{U}_\mu^L \hat{U}_\mu^R |\Psi\rangle, \mathcal{B}(\mathcal{H}_N))| \xrightarrow[N\to\infty]{} 0. \qquad (2.50)$$

In particular,

$$|A(\mathcal{H}_{L,\mu}) - (S(|\Psi\rangle, M_{\lambda\mu}) + A(\mathcal{H}_{L,\lambda}))| \xrightarrow[N\to\infty]{} 0. \qquad (2.51)$$

Proof. The proof is straightforward. From the previous result,

$$|S(|\Psi\rangle, M_\mu) + A(\mathcal{H}_{L,\mu}) - S(V_N \hat{U}_\mu^L \hat{U}_\mu^R |\Psi\rangle, \mathcal{B}(\mathcal{H}_N))| \xrightarrow[N\to\infty]{} 0, \qquad (2.52)$$

and

$$|S(|\Psi\rangle, M_\lambda) + A(\mathcal{H}_{L,\lambda}) - S(V_N \hat{U}_\mu^L \hat{U}_\mu^R |\Psi\rangle, \mathcal{B}(\mathcal{H}_N))| \underset{N\to\infty}{\longrightarrow} 0. \qquad (2.53)$$

The properties of code subspace renormalization (in particular, Equation (2.20)) imply the identity

$$S(|\Psi\rangle, M_\lambda) = S(|\Psi\rangle, M_\mu) + S(|\Psi\rangle, M_{\lambda\mu}), \qquad (2.54)$$

which immediately yields the result. $\qquad\qquad\square$

The physical meaning of (2.54) is that the sum of the area term associated to M_λ and of the entanglement entropy contained in $M_{\lambda\mu}$ gives the area term associated to M_μ. In other words, under code subspace renormalization, what was previously accounted for in the bulk entropy term now becomes part of the area term associated to M_λ. This is exactly the Susskind–Uglum prediction! Therefore, Theorem 2.4.5 can be seen as a rigorous statement of the Susskind–Uglum conjecture for the above choice of code subspace renormalization scheme.

Susskind–Uglum as ER=EPR

It is now established that Theorem 2.4.5 provides a rigorous proof of the Susskind–Uglum conjecture. I will now argue that, on top of providing a proof, it also implies a *reinterpretation* of this conjecture in terms of the ER=EPR proposal.

The crucial point is that Theorem 2.4.4 is valid for *all* values of λ. This implies that when λ increases, the amount of information contained in the area term decreases, whereas the amount of information contained in M_λ increases. This is possible because the Choi–Jamiolkowski state depends on the choice of code subspace. In particular, the Choi–Jamiolkowski state associated to a larger code subspace will be associated to a smaller area term than the one associated to a smaller code subspace, and will not correspond to a state on the smaller code subspace.

What does this mean physically? Recall that in this chapter's approach (just like in that of [8]), the entanglement structure of the Choi–Jamiolkowski state *defines* the area term (including its quotienting by $4G_N$). The arbitrariness in the choice of λ means that some amount of entropy contained in the area term of the Ryu–Takayanagi formula for a given choice of cutoff λ can equivalently be seen as being part of the code subspace entropy for another choice of λ. This means that some of the entanglement of the boundary state can equivalently be interpreted as bulk

entanglement, or as a contribution to the area term. This concretely equates an entanglement quantity to a contribution to a geometric term.

This type of equivalence between entanglement and geometry falls into the general paradigm of ER=EPR [314]. Here, it is the choice of renormalization scale, which is completely arbitrary, that underlies this equivalence. As a result, the theorem proven in this chapter can be seen as extra evidence for the fact that entanglement and geometry are two sides of the same coin in quantum gravity.

2.5   Generalizations

The proof of the previous section already carries all the essential physical ideas of this chapter, and already demonstrates how all the salient features of the Susskind–Uglum conjecture can be derived from the structure of large N quantum error correcting codes thanks to the notion of code subspace renormalization. However, some technical simplifications were made that it would be nice to lift. It turns out that trying to do so involves interesting mathematics. The goal of this rather technical section is to generalize theorems 2.4.4 and 2.4.5 to more involved setups. I start by introducing an infinite-dimensional analog of Fannes' inequality due to Winter [454], for which the dimension of the Hilbert space gets replaced by an energy condition on the states, and use it to lift the finite-dimensional assumption on the boundary Hilbert space (which was motivated above by the finiteness of black hole entropy at finite N, but is still a simplification). Also, Theorem 2.4.4 assumes that one is picking a finite-dimensional renormalized code subspace, of constant dimension that does not grow with N. However, there are some contexts in which one would like to be able to make the dimension of the renormalized code subspace grow with N. In this section, I also describe possible generalizations of the result to these more complicated cases. These generalizations require interesting assumptions about the way in which the bulk theory is regulated, and it is an important problem to understand better how they can be implemented directly at the level of the large N von Neumann algebras, along the lines of [168].

Infinite-dimensional boundary at finite N

In the finite-dimensional context of [8], it was necessary to suppose that the logarithm of the dimension of $\mathcal{H}_N$ was polynomial in N in order to obtain a proof of the Ryu–Takayanagi formula. This is because the proof requires an application of Fannes' inequality for the boundary Hilbert space, which explicitly involves its dimension. Resorting to dimension arguments is not fully valid for CFT Hilbert spaces, which

are infinite-dimensional even for finite values of N. However, the energy of a thermal state of a CFT does not grow too fast in N, and I will show that this fact can be used as an alternative to the finite-dimensional argument of [8]. The key technical tool will be the machinery introduced in [454], which states an analog of Fannes' inequality that involves an energy bound on the states rather than a dimension bound on the Hilbert space. More precisely, one can define:

Definition 2.5.1. Let $\mathcal{B}(\mathcal{H})$ be a type I factor. Let H be a self-adjoint operator on $\mathcal{H}$ such that for all $\beta > 0$, $e^{-\beta H}$ is trace-class. For $E > 0$, let

$$\gamma(E) := \frac{e^{-\beta(E)H}}{\mathrm{Tr}\left(e^{-\beta(E)H}\right)}, \tag{2.55}$$

where $\beta(E)$ is the solution of the equation

$$\mathrm{Tr}\left(e^{-\beta H}(H - E)\right) = 0. \tag{2.56}$$

The inequality of [454], which I will refer to as Winter's inequality, then stipulates:

Proposition 2.5.2 ([454])**.** *Let $\mathcal{B}(\mathcal{H})$ be a type I factor, let H be a self-adjoint operator on $\mathcal{H}$ such that for all $\beta > 0$, $e^{-\beta H}$ is trace-class. Let $E > 0$, let ρ and σ be two normal states on $\mathcal{B}(\mathcal{H})$ such that*

$$\mathrm{Tr}(\rho H) \le E, \quad \mathrm{Tr}(\sigma H) \le E, \tag{2.57}$$

where the normal states are identified with their density operators. Let $\varepsilon > 0$ and suppose that

$$\frac{1}{2}\|\rho - \sigma\|_1 \le \varepsilon \le 1. \tag{2.58}$$

Then,

$$|S(\rho) - S(\sigma)| \le 2\varepsilon S(\gamma(E/\varepsilon)) + h(\varepsilon), \tag{2.59}$$

where

$$h(\varepsilon) = -\varepsilon \log \varepsilon - (1 - \varepsilon)\log(1 - \varepsilon). \tag{2.60}$$

The idea here is to use Winter's inequality to replace the assumption on the finite-dimensional nature of the boundary Hilbert space, and to adapt the proof of [8]. One then obtains the following result:

Theorem 2.5.3. *Let* $(\Lambda, (M_\lambda)_{\lambda\in\Lambda}, (\mathcal{E}_\lambda)_{\lambda\in\Lambda}, (E_{\lambda\mu})_{\lambda,\mu\in\Lambda, \lambda\geq\mu}, \omega, V_N)$ *be a large N quantum error-correcting code. Suppose that for some choice of* λ, M_λ *is finite-dimensional of dimension* d_λ^2 *constant in N. Suppose that*

$$\|V_N^\dagger V_N|_{\mathcal{H}_\lambda} - Id|_{\mathcal{H}_\lambda}\| \leq \mu_N, \tag{2.61}$$

where μ_N *decays faster than any polynomial in N. Let* $|\Psi\rangle \in \mathcal{H}_\lambda$ *(normalized). Suppose that for every unitary operator* $U_\lambda^L, \hat{U}_\lambda^L$ *and* $U_\lambda^R, \hat{U}_\lambda^R$ *in* M_λ^L *and* M_λ^R, *there exist unitary operators* $\tilde{U}_\lambda^L$ *and* $\tilde{U}_\lambda^R$ *(chosen in a measurable way) in* $\mathcal{B}(\mathcal{H}_N^L)$ *and* $\mathcal{B}(\mathcal{H}_N^R)$ *such that*

$$\|V_N U_\lambda^R U_\lambda^L |\Psi\rangle - \tilde{U}_\lambda^L \tilde{U}_\lambda^R V_N \hat{U}_\lambda^R \hat{U}_\lambda^L |\Psi\rangle\| \leq \delta_N, \tag{2.62}$$

where δ_N *decays faster than any polynomial in N. Also suppose that there exists a self-adjoint operator* $\tilde{H}_N$ *on* $\tilde{\mathcal{H}}_N^L := \mathcal{H}_f \otimes \mathcal{H}_f^* \otimes \mathcal{H}_N^L + W_N^L \mathcal{H}_N^L$ *(with* W_N^L *defined as in (2.39)) such that* $e^{-\beta\tilde{H}_N}$ *is trace class for all* $\beta > 0$, *and for all polynomials Q and all sequences* (ξ_N) *decaying faster than polynomially:*

$$\xi_N S(\gamma(Q(N)/\xi_N)) \xrightarrow[N\to\infty]{} 0, \tag{2.63}$$

and that there exists a polynomial P such that for the unitaries and isometries introduced before, the density matrices ρ *of* $W_N^L W_N^R V_N \hat{U}_\lambda^R \hat{U}_\lambda^L |\Psi\rangle$ *and* $V_N W_\lambda^R W_\lambda^L |\Psi\rangle$ *restricted to* $\mathcal{B}(\tilde{\mathcal{H}}_N^L)$ *satisfy*

$$\text{Tr}(\rho\tilde{H}_N) \leq P(N), \tag{2.64}$$

and that the entropies of these density matrices are polynomially bounded in N. Then, for all $|\Psi\rangle \in \mathcal{H}_\lambda$,

$$|S(|\Psi\rangle, M_\lambda^L) + A(\mathcal{H}_{L,\lambda}) - S(V_N \hat{U}_\lambda^R \hat{U}_\lambda^L |\Psi\rangle, \mathcal{B}(\mathcal{H}_N^L))| \xrightarrow[N\to\infty]{} 0. \tag{2.65}$$

Before turning to the proof of this theorem, first note that the trace-class nature of $e^{-\beta\tilde{H}_N}$ and condition (2.63) deserve a bit more justification as they may look a bit abstract at first sight. However, it seems reasonable to assume them in the case of a nonabelian gauge theory at high temperature and of a code with good reconstruction properties. What should at least be true is that there exists an H_N satisfying such a condition on $\mathcal{H}_N^L$: the Hamiltonian of the gauge theory. A heuristic justification goes as follows: the trace-class condition follows from the fact that the finite N algebras all have type I, and the quantity introduced in (2.63) can be estimated by dimensional analysis. Specifically, in the high temperature limit of a d-dimensional

holographic CFT on a sphere with $O(N^2)$ degrees of freedom, the temperature of the Gibbs state of energy E scales (see for example [271]) like[10]

$$T \sim \left(\frac{E}{N^2}\right)^{\frac{1}{d}},$$

(2.66)

and the entropy scales like

$$S \sim \frac{E}{T} \sim N^{\frac{2}{d}} E^{1-\frac{1}{d}}.$$

(2.67)

This means that

$$\xi_N S(\gamma(Q(N)/\xi_N)) \sim N^{\frac{2}{d}} Q(N)^{1-\frac{1}{d}} \xi_N^{\frac{1}{d}}.$$

(2.68)

As ξ_N decays faster than any polynomial, this gives a heuristic justification for assumption (2.63). Now arguably $\tilde{\mathcal{H}}_N$ is a bit larger than $\mathcal{H}_N$, so this condition on $\tilde{\mathcal{H}}_N$ can be seen as requiring an extra strength of the code. It would be interesting to see if this assumption can be improved. However, if one did not need to introduce an extra reference system of square integrable functions on the unitary group, this argument would provide a full justification of why of Fannes' inequality can be replaced by Winter's inequality in the infinite-dimensional case, in the case of a high temperature CFT.

Another remark is that one now needs to introduce the extra assumption (2.61) compared to the previous case. The reason is that it does not seem trivial that Winter's inequality is still valid for non-normalized states, so one needs the norm of the different states introduced to be very close to 1. It would be interesting to find out whether there exists an analog of Winter's inequality for non-normalized states.

Let us now see how under such an assumption, the previous proof can be adapted.

Proof. The proof of 2.4.4 can be adapted identically until Fannes' inequality comes into play. In the latter part of the proof, one needs to replace Fannes' inequality with Winter's inequality.

Now denote by $V_N \hat{U}_\lambda^L \hat{U}_\lambda^R |\Psi\rangle^{norm}$ the normalized state associated to $V_N \hat{U}_\lambda^L \hat{U}_\lambda^R |\Psi\rangle$, and by $V_N W_\lambda^L W_\lambda^R |\Psi\rangle^{norm}$ the normalized state associated to $V_N W_\lambda^L W_\lambda^R |\Psi\rangle$. By the triangle inequality and assumption (2.61), there exists δ'_N decaying faster than polynomially such that

$$\| W_N^L W_N^R V_N \hat{U}_\lambda^L \hat{U}_\lambda^R |\Psi\rangle^{norm} - V_N W_\lambda^L W_\lambda^R |\Psi\rangle^{norm} \| \leq \delta'_N.$$

(2.69)

---

[10]I am grateful to David Simmons-Duffin for suggesting a reasoning based on dimensional analysis.

It is straightforward that the normalized states also have polynomially bounded energy (by say a polynomial $P_{norm}(N)$). Therefore applying Winter's inequality (and Lemma C.1 of [8]) yields

$$|S(W_N^L W_N^R V_N \hat{U}_\lambda^L \hat{U}_\lambda^R |\Psi\rangle^{norm}, \mathcal{B}(\tilde{\mathcal{H}}_N^L)) - S(V_N W_\lambda^L W_\lambda^R |\Psi\rangle^{norm}, \mathcal{B}(\tilde{\mathcal{H}}_N^L))|$$
$$\leq 2\delta_N' S(\gamma(P_{norm}(N)/\delta_N')) + h(\delta_N'). \quad (2.70)$$

Since the norm differences $\|V_N \hat{U}_\lambda^L \hat{U}_\lambda^R |\Psi\rangle^{norm} - V_N \hat{U}_\lambda^L \hat{U}_\lambda^R |\Psi\rangle\|$ and $\|V_N W_\lambda^L W_\lambda^R |\Psi\rangle^{norm} - V_N W_\lambda^L W_\lambda^R |\Psi\rangle\|$ decay faster than any polynomial in N, the triangle inequality and Winter's inequality allow to obtain the result: indeed

$$|S(V_N \hat{U}_\lambda^L \hat{U}_\lambda^R |\Psi\rangle, \mathcal{B}(\mathcal{H}_N^L)) - S(V_N W_\lambda^L W_\lambda^R |\Psi\rangle, \mathcal{B}(\tilde{\mathcal{H}}_N^L))|$$
$$\leq |S(V_N \hat{U}_\lambda^L \hat{U}_\lambda^R |\Psi\rangle, \mathcal{B}(\mathcal{H}_N^L)) - S(V_N \hat{U}_\lambda^L \hat{U}_\lambda^R |\Psi\rangle^{norm}, \mathcal{B}(\mathcal{H}_N^L))|$$
$$+ |S(W_N^L W_N^R V_N \hat{U}_\lambda^L \hat{U}_\lambda^R |\Psi\rangle^{norm}, \mathcal{B}(\tilde{\mathcal{H}}_N^L)) - S(V_N W_\lambda^L W_\lambda^R |\Psi\rangle^{norm}, \mathcal{B}(\tilde{\mathcal{H}}_N^L))|$$
$$+ |S(V_N W_\lambda^L W_\lambda^R |\Psi\rangle^{norm}, \mathcal{B}(\tilde{\mathcal{H}}_N^L)) - S(V_N W_\lambda^L W_\lambda^R |\Psi\rangle, \mathcal{B}(\tilde{\mathcal{H}}_N^L))| \quad .$$
$$(2.71)$$

The first and last term decay to zero, as μ_N decays faster than polynomially whereas all involved entropies grow at most polynomially, while the middle term decays due to Winter's inequality coupled to the assumption on the dynamics. □

Type I_∞ factors in the bulk

Another possible generalization of the previous result corresponds to the case where the bulk algebra is infinite-dimensional. Of course, an infinite-dimensional code subspace cannot be encoded well in the boundary theory at finite N, but if one allows the code subspace dimension to grow with N, one can imagine a situation in which this infinite-dimensional algebra is approximated increasingly well by bigger and bigger subalgebras for each value of N. The mildest possible case is that in which the entropy associated to the bulk state is still $O(1)$ at large N, but is carried by an *infinite-dimensional* factor. As shown in Appendix 2.7, boundedness of entropy for a finite-dimensional resolution of the bulk algebra implies that algebra in question must have type I - since it is here supposed to be infinite-dimensional, type I_∞. This is an important case as a potential choice of regulator for entanglement entropy in the bulk effective theory could be provided by the split property [149], which famously involves type I_∞ factors. Type I_∞ factors can be identified with $\mathcal{B}(\mathcal{H})$ for $\mathcal{H}$ a separable Hilbert space, which means that in this case normal states can be identified with density operators. In particular, they have a Schmidt decomposition.

This allows to approximate states by finite-dimensional density matrices in a very explicit way, and to define a set of "admissible states" for which these approximations are strong enough that the Ryu–Takayanagi formula is still valid independently of the choice of approximation.

The first step in this investigation of recovery for infinite-dimensional type I factors is to introduce a general approximation procedure for a type I_∞ factor in terms of a given faithful normal state and its Schmidt coefficients.

Definition 2.5.4. For M a type I_∞ factor standardly represented on a Hilbert space $\mathcal{K}$ and $|\Psi\rangle$ a cyclic separating vector, write $M = \mathcal{B}(\mathcal{H})$ for some infinite-dimensional Hilbert space $\mathcal{H}$. The restriction of $|\Psi\rangle$ to M is a trace-class density operator ρ on $\mathcal{H}$, as it is a normal state on a type I factor. Arrange the eigenvalues $(\lambda_1, \ldots, \lambda_i, \ldots)$ in decreasing order, and find a corresponding eigenbasis $(e_1, \ldots, e_i, \ldots)$. Now for $d \in \mathbb{N}$, decompose $(e_1, \ldots, e_i, \ldots)$ into d families of the form $(e_{md+k})_{m\in\mathbb{N}}$, with k running from 1 to d. This induces a tensor product factorization of the form

$$\mathcal{H} = \mathcal{H}_d \otimes \mathcal{H}'_d, \tag{2.72}$$

with $\mathcal{H}_d$ finite-dimensional. For this decomposition, define

$$M_d := \mathcal{B}(\mathcal{H}_d) \otimes Id, \tag{2.73}$$

and the conditional expectation onto M_d

$$E_{\Psi,d}(X \otimes Y) := \Psi(Id \otimes Y)(X \otimes Id). \tag{2.74}$$

Note that

$$\Psi \circ E_{\Psi,d} = \Psi|_{M_d} \otimes \Psi|_{M'_d}. \tag{2.75}$$

It is easy to show that $\Psi \circ E_{\Psi,d}$ and Ψ become arbitrarily close in norm (and so do their von Neumann entropies) for a state with finite entropy as d goes to infinity. However, the goal of approximating the boundary entropy of Ψ with that of some $\Psi \circ E_{\Psi,d}$ cannot in general be achieved by keeping d fixed as N grows. Indeed, as N goes to infinity Fannes' inequality (or Winter's inequality) introduces a divergent factor that needs to be cancelled by an N-dependent improvement of the approximation. I now introduce a class of states for which such a regulation is possible.

Definition 2.5.5. Let $|\Psi\rangle \in \mathcal{H}_\lambda$, cyclic separating with respect to M_λ. Let (e_i, λ_i) be a Schmidt basis and the Schmidt coefficients associated to $|\Psi\rangle$, with Schmidt coefficients in decreasing order. Let $\eta > 0$, and let $k(\eta)$ be the smallest integer such that

$$\sum_{i=k(\eta)+1}^{\infty} \lambda_i \leq \eta. \tag{2.76}$$

Let $\mathcal{H}_{\Psi,\eta}$ be the vector space spanned by the action of $M_\lambda^{k(\eta)}$ on the vector representative $|\Psi_0^\eta\rangle$ of $\Psi \circ E_{\Psi,k(\eta)}$ in the natural cone of $|\Psi\rangle$. Denote by $M_\lambda^{L,R,k(\eta)}$ the algebra $M_\lambda^{k(\eta)}$ and its commutant represented on $\mathcal{H}_{\Psi,\eta}$. The state $|\Psi\rangle$ is said to be *admissible* for the family of maps (V_N) if it has finite entropy, and there exists a sequence of thresholds $(\eta_N)_{N\in\mathbb{N}}$ such that $\sqrt{\eta_N}$ decays faster than $(\log d_N)^{-1}$, where d_N is the dimension of $\mathcal{H}_N$, $\log k(\eta_N)$ grows at most polynomially, and for every unitary operator $U_\lambda^L, \hat{U}_\lambda^L$ and $U_\lambda^R, \hat{U}_\lambda^R$ in $M_\lambda^{L,k(\eta_N)}$ and $M_\lambda^{R,k(\eta_N)}$, there exist unitary operators $\tilde{U}_\lambda^L$ and $\tilde{U}_\lambda^R$ in $\mathcal{B}(\mathcal{H}_N^L)$ and $\mathcal{B}(\mathcal{H}_N^R)$ such that

$$\| V_N U_\lambda^R U_\lambda^L |\Psi_0^{\eta_N}\rangle - \tilde{U}_\lambda^L \tilde{U}_\lambda^R V_N \hat{U}_\lambda^R \hat{U}_\lambda^L |\Psi_0^{\eta_N}\rangle \| \leq \delta_N, \tag{2.77}$$

where δ_N decays faster than any polynomial in N.

Here, a few comments are in order. First, the bound given in Equation (2.99) of the appendix of this chapter shows that if one allows for the dimension of $\mathcal{H}_{\Psi,\eta_N}$ to scale like the exponential of a polynomial in N (assuming this is the scaling of the dimension of $\mathcal{H}_N$), the restriction on the decay of η_N is vacuous for states of bounded entropy. However, allowing the code space to be exponentially large comes with its own sets of problems, and requires new assumptions, as will soon be discussed. It would be interesting to see if the bound (2.99) can be made more constraining by imposing some kind of physical condition on the state. Without trying to do this, one can however imagine an intermediate class of states, that are not invariant under any conditional expectation onto a finite-dimensional subalgebra, but for which the threshold η_N is still saturated quickly enough (for example, polynomially in N). For these states, it is reasonable to keep the same assumptions as before and prove a closely related Ryu–Takayanagi formula, thanks to the following lemma.

Lemma 2.5.6. *If ρ is a density matrix on M, for the previous factorization and for $d > 0$,*

$$\| \rho - \rho_1 \otimes \rho_2 \|_1 \leq 4 \sum_{l=d+1}^{\infty} \lambda_l. \tag{2.78}$$

Proof. If $\lambda_1, \ldots, \lambda_n, \ldots$ are the Schmidt coefficients of ρ, for $d > 0$, $1 \leq k \leq d$:

$$(\rho_1 \otimes \rho_2)_{id+k} = \left(\sum_{j=0}^{\infty} \lambda_{jd+k} \right) \left(\sum_{l=1}^{d} \lambda_{id+l} \right). \tag{2.79}$$

Hence, for $1 \leq k \leq d$,

$$(\rho_1 \otimes \rho_2)_k = \left(\sum_{j=0}^{\infty} \lambda_{jd+k} \right) \left(\sum_{l=1}^{d} \lambda_l \right). \tag{2.80}$$

We deduce,

$$|(\rho_1 \otimes \rho_2)_k - \rho_k| = \left| \left(\sum_{j=0}^{\infty} \lambda_{jd+k} \right) \left(\sum_{l=1}^{d} \lambda_l \right) - \lambda_k \right| \tag{2.81}$$

$$= \left| \left(\sum_{j=1}^{\infty} \lambda_{jd+k} \right) \left(\sum_{l=1}^{d} \lambda_l \right) - \lambda_k \sum_{l=d+1}^{\infty} \lambda_l \right| \tag{2.82}$$

$$\leq \sum_{j=1}^{\infty} \lambda_{jd+k} + \lambda_k \sum_{l=d+1}^{\infty} \lambda_l. \tag{2.83}$$

Similarly, for $i \geq 1$:

$$|(\rho_1 \otimes \rho_2)_{id+k} - \rho_{id+k}| \leq \left(\sum_{j=0}^{\infty} \lambda_{jd+k} \right) \left(\sum_{l=1}^{d} \lambda_{id+l} \right) + \lambda_{id+k}. \tag{2.84}$$

Hence,

$$\|\rho - \rho_1 \otimes \rho_2\|_1 \leq \sum_{k=1}^{d} \sum_{j=1}^{\infty} \lambda_{jd+k} + \sum_{k=1}^{d} \lambda_k \sum_{l=d+1}^{\infty} \lambda_l + \sum_{k=1}^{d} \sum_{i=1}^{\infty} \left(\left(\sum_{j=0}^{\infty} \lambda_{jd+k} \right) \left(\sum_{l=1}^{d} \lambda_{id+l} \right) + \lambda_{id+k} \right) \tag{2.85}$$

$$\leq 4 \sum_{l=d+1}^{\infty} \lambda_l. \tag{2.86}$$

□

The Ryu–Takayanagi formula for admissible states can then be formulated as follows:

Theorem 2.5.7. *Let* $(\Lambda, (M_\lambda), (\mathcal{E}_\lambda), (E_{\lambda\mu}), \omega, V_N)$ *be a renormalizable large-N quantum error-correcting code. Let* $|\Psi\rangle$ *be a (normalized) state in* $\mathcal{H}_{\lambda_0}$. *Then, for all* $\lambda \geq \lambda_0$ *such that* $|\Psi\rangle$ *is admissible for* M_λ, *and for all* $\varepsilon > 0$, *there exists a sequence of finite-dimensional Hilbert subspaces* $\mathcal{H}_{\lambda,N}^{fin}$ *of* $\mathcal{H}_\lambda$ *such that*

$$|S(|\Psi\rangle, M_\lambda) + A(\mathcal{H}_{\lambda,N}^{fin}) - S(V_N |\Psi\rangle, \mathcal{B}(\mathcal{H}_N))| \xrightarrow[N \to \infty]{} 0. \tag{2.87}$$

Proof. If $\Psi_0^{\eta_N}$ denotes $\Psi \circ E_{\Psi, k(\eta_N)}$, by the standard continuity bound for the mapping of this state onto the natural cone,

$$\| \, |\Psi\rangle - |\Psi_0^{\eta_N}\rangle \, \| \leq 2\sqrt{\sum_{l=k(\eta_N)+1}^{\infty} \lambda_l}. \tag{2.88}$$

Now, as V_N is a contraction,

$$\|V_N \, |\Psi\rangle - V_N \, |\Psi_0^{\eta_N}\rangle \, \| \leq 2\sqrt{\sum_{l=k(\eta_N)+1}^{\infty} \lambda_l}. \tag{2.89}$$

By Fannes' inequality and Lemma C.1 of [8], it follows that

$$|S(V_N \, |\Psi\rangle \,, \mathcal{B}(\mathcal{H}_N)) - S(V_N \, |\Psi_0^{\eta_N}\rangle \,, \mathcal{B}(\mathcal{H}_N))| \leq 4\sqrt{\eta_N}\log\left(\frac{d_N}{4\sqrt{\eta_N}}\right). \tag{2.90}$$

for N large enough, and this goes to zero at infinity. Then the entropy of $V_N \, |\Psi_0^{\eta_N}\rangle$ is controlled by exactly the same technique as in the proof of Theorem 2.4.4. The only places where one should worry are the ones where the dimension $k(\eta_N)$ appears because it now grows with N, but since $\log k(\eta_N)$ grows at most polynomially, the obtained bounds are still strong enough. Moreover the difference in entropy of $|\Psi_0^{\eta_N}\rangle$ on $M_\lambda^{k(\eta_N)}$ and of $|\Psi\rangle$ on M_λ goes to zero, which concludes the proof. $\square$

Also note that an analogous result could have been formulated for admissible states for the case of an infinite-dimensional boundary Hilbert space, by introducing a condition allowing to apply Winter's inequality like in the previous subsection. Another remark is that as noted earlier, the code subspace renormalization scheme itself can depend on N. In that case, the whole proof goes through, except the last step in which it is assumed that the entropies of the regulated subalgebras get asymptotically close to the one of the type I_∞ factor, because now this I_∞ factor and the corresponding Schmidt coefficients are also N-dependent. One then needs to add this condition by hand in the definition of admissible state.

Large codes and minimality

It is natural to try to generalize the methods developed in this chapter to codes subspaces with faster, exponential growth in N. This regime is also of great interest in order to study black holes and their evaporation [231, 8, 7]. However, in this case, some assumptions made before are no longer reasonable. In particular, supposing that the map V_N is very close in norm to an isometry (which was necessary in order to

use Winter's inequality) no longer makes sense, because the code subspace becomes too big and V_N can get a kernel. Also, unitary reconstruction in the entanglement wedge for all unitaries can no longer be true, as the code subspace can now carry enough entropy to compete with the area term and macroscopically shift the position of the Ryu–Takayanagi surface. The Ryu–Takayanagi formula then really needs to become a quantum extremal surface formula.

Fortunately, the setup of [8] allows for such a generalization, by subdividing the code subspace into a tensor product of further finite-dimensional subspaces, that are then interpreted as local degrees of freedom, and only asking for the reconstruction of product unitaries. It would be very interesting to understand how such a factorization, or a similar regulation procedure, can be systematically implemented in the large N theory. Assuming such a refined structure for the renormalized code subspace, that the boundary Hilbert space is finite-dimensional, and that the logarithm of its dimension is polynomial in N, the results of [8] can be applied in this setup without any modification, including the result about minimality of generalized entropy in the entanglement wedge.

A technical detail is that it is important that Fannes' inequality also holds for subnormalized states for the proof of [8] to work, as it is no longer an option to assume that V_N is very close to an isometry for a very large code subspace. It would be interesting to figure out whether an analog of Winter's inequality holds for subnormalized states, and some result of this kind would become important in this regime in order to drop the finite-dimension assumption on $\mathcal{H}_N$.

At any rate, large codes seem to require even more work than the ones discussed before in order to concretely implement regularizations and a code subspace renormalization scheme that allow to formulate a family of quantum extremal surface formulae that satisfy the Susskind–Uglum prescription. It is an important question to understand how to implement such regularizations explicitly, first for small codes and then for larger codes. Understanding perturbative G_N corrections and the split property in the framework of [168] seems to be a very promising first step in this direction.

2.6 Discussion

In this chapter, I introduced a new derivation of the Ryu–Takayanagi formula in the large N limit of holography. This new setup makes it manifest that not all of the large N von Neumann algebra can be reconstructed satisfactorily at fixed N on the

boundary. Instead, it must be regulated (into a type *I* algebra if one wants to retain a finite amount of code subspace entropy in the large *N* limit), and with this regulation comes an arbitrary choice of UV cutoff.

I then argued that an appropriate way to define the renormalization group flow between the different code subspaces (or subalgebras) is through conditional expectations that integrate out some of the degrees of freedom. From such a family of conditional expectations, one can then construct a nested family of code subspaces, each of which contributes a different amount of entropy, that decreases when high energy modes are integrated out. This nested structure reacts well with the commutant structure, so that a good notion of complementary recovery can be defined in a consistent way. It is interesting to note that the use of conditional expectations, which was previously proposed as a model of exact holography, finds a new interpretation as a renormalization group flow in the limit where the code becomes exact.

The next and last step was to prove a Ryu–Takayanagi formula: it was shown that for a state in a regulated code subspace with admissible properties with respect to the bulk-to-boundary map, the Ryu–Takayanagi formula is satisfied, with the area term associated to the code space being identified with the entropy of a Choi–Jamiolkowski state, along the lines of [8]. Then, as the bulk cutoff is changed, the variation of the area term was proven to exactly compensate that of the bulk entropy, therefore providing a full proof of the Susskind–Uglum proposal. In this new framework of quantum error correction, this proposal can be reinterpreted as a precise instance of the ER=EPR paradigm.

A few possible extensions of the result would be nice to obtain:

- It is not clear how to easily single out a UV-regulated type *I* algebra at large *N*. The most naive guess, which is to take products of single trace operators capped off at some finite number of factors, fails because these operators do not form an algebra. It would be nice to understand better how to extract type *I* algebras carrying a finite amount of entropy from a large *N* algebra. More generally, it would be very interesting to embed the results of this chapter into the framework of asymptotically isometric codes initiated in [168].

- It also seems important to extend the reasonings provided here to code subspaces that are not made out of states that are invariant under a conditional expectation, or that only are in some approximate way. This would probably

be useful to better understand how area laws work in the examples of large N sectors introduced in [168].

- Perhaps more ambitiously, one could try to generalize the results presented here to the case of linear spaces of operators with no product structure. Some preliminary attempts [202, 305] have been made in this direction in the literature.

- In the proofs appearing in this chapter, either Fannes' or Winter's inequalities provided bounds on the entropies of the boundary states. It would be interesting to understand the assumptions required for the application of Winter's inequality better, and to derive them in explicit examples. It would also be nice to understand to what extent Winter's inequality generalizes to the case of subnormalized states.

- This proof most closely mimics the case of one side of a two-sided holographic black hole. It is also necessary to tackle the extra regularizations needed for the case where one considers a subregion of a CFT, and the area of the quantum extremal surface become infinite. Perhaps the canonical purification of [149] can be used to define such regulations more precisely.

- One can also allow the code subspace entropy to diverge as N becomes large. Maybe one can identify some N-dependent regularizations of the code subspace that asymptote to von Neumann algebras that have type II or III, and it would be nice to understand this better.

- More generally, in the case of a large code, this chapter only scratched the surface of the problem, by directly applying the setup of [8]. It is an interesting problem to understand how to subdivide a large N algebra into (N-dependent) local degrees of freedom in the bulk, so that conditions on product unitaries, or an analog of them, can be formulated in a meaningful way. The case of large codes is especially important to describe state-dependent black hole reconstruction and black hole evaporation [231, 379, 194, 7], which makes it a particularly interesting avenue of research.

- It also seems very important to see how the equivalence between large N entanglement and areas contributions arises in explicit models of quantum gravity. The SYK model [98], matrix quantum mechanics [340], or maybe

some supersymmetric field theories seem to be cases in which one could try to implement a renormalization scheme akin to the one identified in this chapter.

2.7 Appendix: Bounded entropy implies type I

This work mainly considers the case in which the code subspace of the holographic code contains a *finite $O(1)$* amount of entropy in the large N limit. Of course, this is impossible if the full algebra of observables in a region is taken into account due to UV divergences, but as was stressed above, this calculation would not be physical anyway because the code would break at a scale that is parametrically large in N. However, if one regulates the algebra of the EFT by simply considering one of its subalgebras that carries finite entropy, it is possible to make sense of bulk entropy in the large N limit. The goal of this appendix is to characterize those algebras that can carry a finite amount of entropy. The answer turns out to be that these algebras must have type I. This can already be guessed at an intuitive level from the trace structure of von Neumann algebras: the only algebras that have a non-renormalized trace are type I algebras.

A more precise result can be shown by adapting an argument formulated by Matsui [331] in the context of the mathematical study of spin chains: if there is a cyclic separating state on the Hilbert space whose entropy for a finite-dimensional resolution of M is bounded, then M has type I. The rest of this appendix is dedicated to the proof of the following theorem:

Theorem 2.7.1. *Let M be a von Neumann factor acting on a Hilbert space $\mathcal{H}$, and let $|\Psi\rangle \in \mathcal{H}$ be cyclic separating with respect to M. Suppose that there exists an increasing sequence of finite-dimensional unital simple subalgebras $(M_n)_{n\in\mathbb{N}}$ of M such that*

$$\sup_{n\in\mathbb{N}} S(|\Psi\rangle, M_n) < \infty, \tag{2.91}$$

and M is the closure of the union of the M_n for the weak operator topology. Then, M has type I.

Proof. For this proof, it will be easier to recast the problem at the level of C^*-algebras and norm closures, which is the goal of this first lemma.

Lemma 2.7.2. *Let $\mathcal{A}$ be the norm closure of the union of the M_n. Then, $\mathcal{H}$ is isomorphic to the GNS representation of $\mathcal{A} \otimes \mathcal{A}^{op}$[11] in the state defined by $\psi(X \otimes JYJ) := \langle\Psi| XJYJ |\Psi\rangle$.*

---

[11]The opposite algebra is isomorphic to $J\mathcal{A}J$.

Proof. The vector $|\Psi\rangle$ is cyclic separating with respect to M, so one can apply Tomita–Takesaki theory to obtain the characterization of the commutant

$$M' = JMJ, \tag{2.92}$$

where J is the modular conjugation associated to $|\Psi\rangle$.

Now let $\mathcal{A}$ be the be the norm closure of the union of the M_n. The (nuclear) C^*-algebra $\mathcal{A} \otimes \mathcal{A}^{op}$ has a representation on $\mathcal{H}$ sending the operator $A \otimes JBJ$ to $AJBJ$. This representation coincides with the GNS representation of the state defined by the composition of ψ and this representation. The Hilbert space is isomorphic to $\mathcal{H}$, and the respective images of $\mathcal{A} \otimes Id$ and $Id \otimes \mathcal{A}^{op}$ are strong operator dense in M and its commutant, respectively, which makes the proof of the lemma straightforward. $\quad\square$

Now, the goal is to show that the state ψ is quasiequivalent to a tensor product of the form $\psi_R \otimes \psi_L$ on $\mathcal{A} \otimes \mathcal{A}^{op}$. In order to do this, I will adapt a proof due to Matsui [331] in the context of spin chains to the present case.

For $n \in \mathbb{N}$, M_n is a type I factor acting on $\mathcal{H}$, so one can write (see [424], paragraph 9.15)

$$\mathcal{H} = \mathcal{H}_n \otimes \mathcal{H}_n^c, \tag{2.93}$$

where

$$M_n = \mathcal{B}(\mathcal{H}_n) \otimes Id. \tag{2.94}$$

With respect to this factorization, the state $|\Psi\rangle$ admits a Schmidt decomposition

$$|\Psi\rangle = \sum_{j=1}^{d_n} \sqrt{\lambda_j^{(n)}} \, \xi_j^{(n)} \otimes \eta_j^{(n)}, \tag{2.95}$$

with $\xi_j^{(n)} \in \mathcal{H}_n$ and $\eta_j^{(n)} \in \mathcal{H}_n^c$, $1 \geq \lambda_1^{(n)} \geq \cdots \geq \lambda_{d_n}^{(n)} \geq 0$, and $\sum_{j=1}^{d_n} \lambda_j^{(n)} = 1$.

Let

$$S := \sup_{n \in \mathbb{N}} S(|\Psi\rangle, M_n). \tag{2.96}$$

Lemma 2.7.3. *Let* $1 > \varepsilon > 0$. *If* k *is the integer defined by*

$$\sum_{j=k}^{d_n} \lambda_j^{(n)} \geq \varepsilon \tag{2.97}$$

and

$$\sum_{j=k+1}^{d_n} \lambda_j^{(n)} < \varepsilon, \tag{2.98}$$

then

$$k \leq \exp\left(\frac{S}{\varepsilon}\right), \tag{2.99}$$

and

$$\lambda_1^{(n)} \geq \exp\left(-\frac{S}{\varepsilon}\right). \tag{2.100}$$

Proof. As the logarithm is an increasing function,

$$-\varepsilon \log \lambda_k^{(n)} \leq -\sum_{j=k}^{d_n} \lambda_j^{(n)} \log \lambda_k^{(n)} \leq S. \tag{2.101}$$

This already proves (2.100). Then it suffices to note that

$$k \lambda_k^{(n)} \leq \sum_{j=1}^{k} \lambda_j^{(n)} \leq 1 \tag{2.102}$$

to obtain the other bound (2.99). □

Now, let us relabel the two tensor factors in $\mathcal{A} \otimes \mathcal{A}^{op}$ by $\mathcal{A}_R$ and $\mathcal{A}_L$. We have:

Lemma 2.7.4. *Let $\psi_j^{(n)}$ be an extension of $\xi_j^{(n)}$ to $\mathcal{A}_R$, and let $\varphi_j^{(n)}$ be an extension of $\eta_j^{(n)}$ to $\mathcal{A}_L$. Consider $\psi_{R,j}$ and $\varphi_{L,j}$, two weak-* limits of the sequences $\psi_j^{(n)}$ and $\varphi_j^{(n)}$. Up to passing to a subsequence one can also assume convergence of the $\lambda_j^{(n)}$. If $\lim_{n\to\infty} \lambda_j^{(n)}$ is nonzero (which is the case for λ_1), then $\psi_{R,j}$ is quasi-equivalent to Ψ_R, and $\varphi_{L,j}$ is quasi-equivalent to Ψ_L, where Ψ_R and Ψ_L are the restrictions of the state $|\Psi\rangle$ to the algebras $\mathcal{A}_R$ and $\mathcal{A}_L$, respectively.*

Proof. It suffices to note that on any M_n,

$$\Psi_R = \sum \lambda_j^{(n)} \psi_j^{(n)} \geq \lambda_{j_0}^{(n)} \psi_{j_0}^{(n)} \tag{2.103}$$

for all j_0. By going to the limit,

$$\left(\lim_{n\to\infty} \lambda_{j_0}^{(n)}\right) \psi_{R,j_0} \leq \Psi_R. \tag{2.104}$$

This inequality applied to $\lim_{n\to\infty} \lambda_1^{(n)} \neq 0$, together with the fact that the GNS representation associated to Ψ_R is a factor by assumption, shows that the two representations are quasi-equivalent. The same reasoning can be applied to $\mathcal{A}_L$. □

We are now ready to show that Ψ is quasi-equivalent to $\Psi_L \otimes \Psi_R$. Lemma 2.7.4 shows that it is enough to demonstrate that it is quasi-equivalent to $\Psi_{L,1} \otimes \Psi_{R,1}$. For this last part of the proof, I will closely follow the notations of [331].

Let $1 > \varepsilon > 0$, and let K be defined as the largest integer smaller or equal to $\exp\left(\frac{S}{\varepsilon}\right)$. Define the vectors (for notational simplicity, bra-ket notation is not explicitly used for these)

$$\tilde{\Omega}(n) := \sum_{j=1}^{K} \sqrt{\lambda_j^{(n)}} \xi_j^{(n)} \otimes \eta_j^{(n)}, \tag{2.105}$$

and

$$\Omega(n) := \frac{\tilde{\Omega}(n)}{\|\tilde{\Omega}(n)\|}. \tag{2.106}$$

We then have that

$$0 < 1 - \|\tilde{\Omega}(n)\|^2 < \varepsilon, \tag{2.107}$$

$$1 - \|\tilde{\Omega}(n)\| < \frac{\varepsilon}{1 + \|\tilde{\Omega}(n)\|} < \varepsilon, \tag{2.108}$$

and

$$\|\tilde{\Omega}(n) - |\Psi\rangle\|^2 < \varepsilon. \tag{2.109}$$

$$\|\Omega(n) - |\Psi\rangle\|^2 = \left(\frac{1}{\|\tilde{\Omega}(n)\|} - 1\right)^2 \left(\sum_{j=1}^{K} \lambda_j^{(n)}\right) + \sum_{j=K+1}^{d_n} \lambda_j^{(n)} = (\|\tilde{\Omega}(n)\| - 1)^2 + \sum_{j=K+1}^{d_n} \lambda_j^{(n)} \leq 2\varepsilon. \tag{2.110}$$

Now consider ω_∞, a weak-* accumulation point of the ω_n, linear functionals associated to the $\Omega(n)$. It follows that

$$\|\omega_n - \Psi\| \leq 2\sqrt{2\varepsilon}, \tag{2.111}$$

and going to the limit,

$$\|\omega_\infty - \Psi\| \leq 2\sqrt{2\varepsilon}. \tag{2.112}$$

Now, the Cauchy–Schwarz inequality gives on any $M_{n_0} \otimes \mathcal{A}_L$, for $n \geq n_0$,

$$\omega_n \leq \frac{K}{1 - \varepsilon} \sum_{j=1}^{K} \lambda_j^{(n)} \psi_j^{(n)} \otimes \varphi_j^{(n)}. \tag{2.113}$$

Going once again to the limit (one can suppose that all the $\lambda_j^{(n)}$ converge), we get, on a dense set and hence on the full $\mathcal{A}_R \otimes \mathcal{A}_L$,

$$\omega_\infty \le \frac{K}{1-\varepsilon} \sum_{j=1}^{K_0} \bar{\lambda}_j \psi_{j,R} \otimes \varphi_{j,L}, \tag{2.114}$$

where the $\bar{\lambda}_j$ are the $K_0 \le K$ nonzero limits of the $\lambda_j^{(n)}$. If one defines a state $\check{\Psi}$ such that

$$C\check{\Psi} = \frac{K}{1-\varepsilon} \sum_{j=1}^{K_0} \bar{\lambda}_j \psi_{j,R} \otimes \varphi_{j,L}, \tag{2.115}$$

for some constant C, then $\check{\Psi}$ is a linear combination of the $\psi_{j,R} \otimes \varphi_{j,L}$ with nonzero coefficients, so it is quasi-equivalent to $\Psi_R \otimes \Psi_L$, by Lemma 2.7.4. As a consequence, it is a factor state, and ω_∞ is quasiequivalent to it by Equation (2.114). Equation (2.112), combined with Theorem 2.7 of [391], then implies by the triangle inequality that Ψ is quasiequivalent to $\Psi_R \otimes \Psi_L$.

From this last fact, one can deduce that the von Neumann algebra M has type I. Indeed, Ψ is pure so it is type I. It is quasiequivalent to the tensor product of Ψ_R and Ψ_L, which means that both must also be type I (as a tensor product is type I if and only if both factors are type I). Now M corresponds to a factor representation, so every one of its subrepresentations is quasiequivalent to it. In particular, this is true for the GNS representation of Ψ_R, which shows that M has type I (see Lemma 4.3 of [353]). $\qquad\qquad\square$

C h a p t e r   3

EMERGENT SPACETIME AND THE ERGODIC HIERARCHY

This chapter is based on the work [191].

3.1 Introduction

One of the main goals of quantum gravity is to understand the emergence of space-time. While there exists a wide range of holographic theories, very few of them have a semiclassical limit that recovers weakly coupled quantum fields on a classical, smooth, gravitational spacetime in the dual description. It is therefore of central importance to understand the conditions required for a holographic theory to possess a "good" semiclassical limit of this kind. In the context of AdS/CFT [319], theories with such a semiclassical limit in the bulk are the ones in which the 't Hooft coupling is strong and the gauge rank N is taken to infinity. It makes sense to ask what is special about these theories. It has long been realized that a diagnostic of bulk locality is quantum chaos [413], but coming up with a fully satisfactory definition of quantum chaos is still an open problem. While various diagnostics [59] exist and capture different chaotic features of quantum systems, there is no clear overarching picture.

On the other hand, the theory of chaos for classical dynamical systems is under much better control. Thanks to pioneering work from the second part of the twentieth century, various diagnostics of classical chaos have been firmly established. One of the main upshots is that there is not a single way of diagnosing chaos in a classical dynamical system, but instead, a full *hierarchy* of them [52]. Near the top of this hierarchy sits the notion of Kolomogorov system (K-system) [451], which is a system with complete memory loss.

It turns out that the ergodic theory of classical dynamical systems has a quantum counterpart, although it does not capture all quantum chaotic phenomena. The goal of this letter is to show that the quantum analog of the classical ergodic hierarchy is surprisingly relevant to the emergence of time in holography. In this hierarchy, the looser properties known as mixing properties encode the late time decay of correlation functions, while stronger properties like the K-property and the closely related Anosov property are closely tied to the emergence of horizons

and information loss. Some "intrinsically quantum" diagnostics, like the type of emergent von Neumann algebras [294, 293, 295, 457, 100, 183, 168, 192], also fit nicely into this hierarchy. By better understanding the parallels between the quantum ergodic hierarchy and the emergence of semiclassical physics, we may discover new ways to characterize how to interpolate between quantum gravity and its semiclassical limit.

A theme of central importance will be that of von Neumann algebras, as it is the natural setting to formulate the quantum analog of measure theory, which lies at the heart of the theory of dynamical systems. Interestingly, the emergence of nontrivial types of von Neumann algebras has recently been identified as a diagnostic of the appearance of a somewhat semiclassical bulk [293, 294, 295], and one of the goals of this letter is to sharpen this connection.

Note added: The material presented here has been expanded upon in [367], after the author explained it to one of the authors of [367] during a conference this summer. We decided to coordinate our releases.

3.2   Ergodic classical systems and their hierarchy

The mathematical investigation of chaos in classical dynamical systems is well-developed, and known as ergodic theory. It was realized in the second half of the twentieth century that chaotic systems can be organized into a *hierarchy* of systems satisfying stronger and stronger properties [180]. This section briefly recalls these properties and gives some intuition on them.

Definition 3.2.1. A dynamical system is a triple (X, μ, σ_t), where X is a measurable space, μ is a probability measure on X, and σ_t is a measure-preserving flow on X.[1]

Here, we want to find a way to quantify how chaotic a dynamical system is. It turns out that there is a *hierarchy* of chaos in the theory of classical dynamical systems, which consists of five increasingly strong levels of chaos. More precisely, there is the chain of implications

Ergodic $\Longleftarrow$ **Weakly Mixing** $\Longleftarrow$ **Strongly Mixing** $\Longleftarrow$ **Kolmogorov** $\Longleftarrow$ **Bernoulli**.

---

[1]The general discussion assumes that we are looking at systems with continuous time, but discrete time can be defined completely analogously.

Ergodicity and mixing

The weakest characterization of chaos is given by the notion of *ergodicity*. The intuition behind this notion is that on average, the dynamics decorrelates events A and B and turns them into independent events. It is given by the following definition:

Definition 3.2.2. A classical dynamical system (X, μ, σ_t) is *ergodic* if for all measurable sets $A, B \subset X$,

$$\lim_{T \to \infty} \frac{1}{2T} \int_{-T}^{T} \mu(\sigma_t(B) \cap A) dt = \mu(B)\mu(A). \tag{3.1}$$

The first way in which one can strengthen the property of ergodicity is by imposing convergence to zero of the *difference* between the measure of the interesection of the two events and their product, either on average or pointwise:

Definition 3.2.3. A classical dynamical system (X, μ, σ_t) is *weakly mixing* if for all measurable sets $A, B \subset X$,

$$\lim_{T \to \infty} \frac{1}{2T} \int_{-T}^{T} |\mu(\sigma_t(B) \cap A) - \mu(B)\mu(A)| dt = 0. \tag{3.2}$$

Definition 3.2.4. A classical dynamical system (X, μ, σ_t) is *strongly mixing* if for all measurable sets $A, B \subset X$,

$$\lim_{t \to \infty} \mu(\sigma_t(B) \cap A) = \mu(B)\mu(A). \tag{3.3}$$

Kolmogorov systems

So far, the characterizations of chaos in dynamical systems have been fairly simple and quantitative: they simply are a matter of limits. However, one can ask for stronger properties of chaos, that are more algebraic in nature. In particular, another way of thinking about chaos is that dynamics should make an observer lose all possible information about the initial data. This is formalized by asking that there are less and less measurable sets left in the σ-algebra as time passes. The most extreme version of the idea leads to the notion of K-system (Kolmogorov system) [451], which asks for complete memory loss at infinite time.

Definition 3.2.5. Let (X, μ, σ_t) be a classical dynamical system, and let Σ be the σ-algebra of measurable subsets of X. (X, μ, σ_t) is a Kolmogorov system (K-system) if there exists a σ-algebra $\Sigma_0 \subset \Sigma$ such that:

- For $t > 0$, $\sigma_t(\Sigma_0) \subset \Sigma_0$,

- $\bigvee_{t \in \mathbb{R}} \sigma_t(\Sigma_0) = \Sigma,$

- $\bigwedge_{t \in \mathbb{R}} \sigma_t(\Sigma_0) = \{\emptyset, X\}.$

Bernoulli systems

The notion of Bernoulli shift sits at the very top of the ergodic hierarchy. The idea of such a system is that at each step, it completely forgets the previous one. A typical example of such a system is a repeated coin toss. More formally:

Definition 3.2.6. Let $(X, \mathcal{A}, \mu)$ be a probability space. Then a Bernoulli scheme is $(X, \mathcal{A}, \mu)^{\mathbb{Z}}$. A Bernoulli scheme equipped with its shift automorphism is called a Bernoulli dynamical system.

The Bernoulli property is the strongest property of chaos one can ask for in a dynamical system, however, only few systems possess it. It will not be directly relevant in our case.

Anosov systems

Although not part of the canonical ergodic hierarchy, the notion of Anosov system is very important in the study of dynamical systems. The idea of an Anosov flow requires a bit more structure, and it can be seen as a useful special case that often displays a lot of the properties described in this letter. In the case of an Anosov system, the underlying measured space is actually a manifold (at least in the most basic case). The idea is then to split the tangent bundle of this manifold into contracting and expanding directions under the flow under consideration. More formally [382]:

Definition 3.2.7. Let M be a smooth compact connected oriented manifold. Let ϕ_t be a nonsingular flow of class C^r on M. ϕ_t is an Anosov flow of class C^r if there exists a ϕ_t-invariant continuous splitting of the tangent bundle of M, given by $TM = E^u \oplus E^s \oplus E^T$, where E^T is the line bundle tangent to ϕ_t and E^u and E^s satisfy:

- There exist constants $A > 0$, $\mu > 1$ such that for $t \in \mathbb{R}$ and $v \in E^u$:

$$\|\phi_{t*}(v)\| \geq A\mu^t \|v\|, \tag{3.4}$$

- There exist constants $B > 0$, $\lambda < 1$ such that for $t \in \mathbb{R}$ and $v \in E^s$:

$$\|\phi_{t*}(v)\| \leq B\lambda^t \|v\|. \tag{3.5}$$

The splitting elements E^u and E^s can be interpreted as expanding and contracting directions for the flow ϕ_t. The presence of these expansions and contractions is related to chaotic properties of the flow. This can be seen very explicitly in the case of geodesic flow on a Riemann surface, as it will be explained in Section 3.2.

Under reasonable conditions, the Anosov property implies the K-property. In particular,

Theorem 3.2.8 ([93]). *Any C^2 topologically mixing volume preserving Anosov flow is a K-system (and even Bernoulli).*

It will turn out that in the case of quantum modular automorphisms, one obtains an even stronger link between the Anosov and K-properties, where to each K-system can be associated an Anosov flow.

Example: Geodesic flow on a hyperbolic Riemann surface

The prototypical example of an Anosov system is geodesic flow on a compact orientable Riemann surface of constant negative curvature. Any such surface can be written as a quotient $\Sigma = \Gamma \backslash \mathbb{H}$, where Γ is a cocompact Fuchsian group. Consider $Q \cong PSL(2, \mathbb{R})$, the unit tangent bundle to the upper half-plane $\mathbb{H}$. The geodesic flow $\phi_t = \begin{pmatrix} e^{t/2} & 0 \\ 0 & e^{-t/2} \end{pmatrix}$, as well as the horocycle flows $h_t^* = \begin{pmatrix} 1 & t \\ 0 & 1 \end{pmatrix}$, $h_t = \begin{pmatrix} 1 & 0 \\ t & 1 \end{pmatrix}$ define invariant flows on Q, which descend to invariant flows on P, the unit tangent bundle of Σ. Then one can decompose the tangent space $TP = E^+ \oplus E^0 \oplus E^-$, where E^+ and E^- are the expanding and contracting directions along the horocycle flows, and E^0 is the geodesic flow direction. One can show that this decomposition satisfies the axioms of an Anosov system.

An important fact about this example is that the geodesic and horocycle flows satisfy the commutation relations

$$g_t h_s^* = h_{se^{-t}}^* g_t, \qquad g_t h_s = h_{se^t} g_t. \tag{3.6}$$

These commutation relations will be the starting point of the definition of quantum Anosov systems. Note that they are the same as the ones between boosts and null translations in Rindler space, as will be explored in more detail in the next section.

3.3 Quantum chaotic dynamics: von Neumann algebras

One would like to define a similar hierarchy of chaos for the case of quantum systems. Of course, this implies resorting to a quantum notion of dynamical system

on which measure theory can be used. The language of von Neumann algebras shows up naturally when one attempts to formulate a quantum analog of the notion of classical dynamical system. The reason is the following.

In a quantum system, observables cannot be expressed as functions on a classical phase space, and the best one can do is to consider such a noncommutative algebra of observables more abstractly. However in order to have a suitable notion of quantum dynamical system, one needs to find a quantum analog of the notion of measure on phase space. Once again, since there no longer are any "points" on a noncommutative configuration space, a measure itself cannot be defined. However, a related notion still makes sense: that of taking the expectation value of a function against a probability measure thanks to the formula

$$\langle f \rangle_\nu = \int_X f \, d\nu. \tag{3.7}$$

If ν is a probability measure, this is a linear functional of norm one on the space of functions. Thus it is natural to encode the notion of probability measure into that of expectation value functional in the noncommutative case - and an expectation value functional is nothing else than a quantum state. Hence, the quantum counterpart of the measure in a classical dynamical system is simply a quantum state.

Finally dynamics is trivially generalized as a (strongly continuous) one-parameter group of automorphisms of the von Neumann algebra M. This leads to the definition of quantum dynamical systems that will be used in this letter:

Definition 3.3.1. A quantum dynamical system is a triple (M, ω, τ_t), where M is a von Neumann algebra, ω is a normal state on M, and τ_t is a strongly continuous one-parameter group of automorphisms of M.

It is common to assume that $\omega \circ \tau_t = \omega$.

In the quantum case, a new situation of interest appears that used to be trivial in the classical case: if ω is also faithful then τ_t can be the modular automorphism group of ω. This is of particular interest given the central role played by modular flow in the emergence of spacetime. It is then useful to define:

Definition 3.3.2. If the quantum dynamical system (M, ω, τ_t), with ω faithful, is defined so that τ_t is the modular automorphism group of ω, then (M, ω, τ_t) is said to be a modular quantum dynamical system.

One can summarize the relationship between von Neumann algebras and measured spaces as indicated in Table 3.1.

Classical case	Quantum case
$C^0(X)$	C^*-algebra
$L^\infty(X, \mu)$	von Neumann algebra
Measure $\nu \ll \mu$	Normal state ω
σ-algebra automorphism σ_t	von Neumann algebra automorphism τ_t
Dynamical system (X, μ, σ_t)	Dynamical system (M, ω, τ_t)

Table 3.1: The parallel between classical and quantum dynamical systems.

Ergodicity and mixing

The generalization of ergodicity and mixing to the quantum case is completely straightforward now that we have a good definition of a quantum dynamical system. We simply define:

Definition 3.3.3. The quantum dynamical system (M, ω, τ_t) is:

- Ergodic if for all $A, B \in M$,

$$\lim_{T \to \infty} \frac{1}{2T} \int_{-T}^{T} \omega(\tau_t(B)A) = \omega(B)\omega(A), \tag{3.8}$$

- Weakly mixing if for all $A, B \in M$,

$$\lim_{T \to \infty} \frac{1}{2T} \int_{-T}^{T} |\omega(\tau_t(B)A) - \omega(B)\omega(A)| dt = 0, \tag{3.9}$$

- Strongly mixing if for all $A, B \in M$,

$$\lim_{t \to \infty} \omega(\tau_t(B)A) = \omega(B)\omega(A). \tag{3.10}$$

Quantum Kolmogorov systems

It is also quite straightforward to transfer the notion of K-system to the quantum case.

Definition 3.3.4 ([357])**.** Let (M, τ_t) be a quantum dynamical system. M is *refining* if there exists a von Neumann subalgebra $N \subsetneq M$ such that for $t > 0$, $\tau_t(N) \subset N$. It is a *K-system* if in addition, $\bigvee_{t \in \mathbb{R}} \tau_t(N) = M$, and $\bigcap_{t \in \mathbb{R}} \tau_t(N) = \mathbb{C}$.

Quantum Anosov systems

There is also a good notion of Anosov flow for quantum systems, although one needs to relax it appropriately to allow for the contracting and expanding transformations to be non-invertible (only endomorphisms rather than automorphisms).

Definition 3.3.5 ([356])**.** Let (M, τ_t) be a quantum dynamical system, ω be an invariant faithful normal state on M, and $\mathcal{H}_\omega$ be its GNS representation. The system (M, τ_t) is *Anosov* if there exists a strongly continuous one-parameter group of automorphisms $\sigma_s \in \text{Aut}\mathcal{B}(\mathcal{H}_\omega)$ such that for $s > 0$, $\sigma_s(M) \subsetneq M$, and for all $s, t \in \mathbb{R}$,

$$\tau_t \circ \sigma_s = \sigma_{se^{-t}} \circ \tau_t. \tag{3.11}$$

In the case of a modular quantum dynamical system, the Anosov and K-properties are very closely related:

Proposition 3.3.6 ([356])**.** *Let (M, τ_t, ω) be a modular quantum dynamical system. Then (M, τ_t, ω) is refining if and only if it is Anosov.*

Much more can be proven about Anosov/K-systems, see [356, 355, 358, 206].

Analogy with Rindler space

As it was hinted above, Rindler space is the stereotypical example of a modular quantum K-system with continuous evolution. By the Bisognano–Wichmann theorem [60], modular flow of the algebra of observables in the Rindler wedge coincides with boosts along the Rindler horizon. If τ_t denotes modular flow and $\sigma_s^\pm$ denote the two null translations along the horizon, they then satisfy the relation

$$\tau_t \circ \sigma_s^\pm \circ \tau_{-t} = \sigma_{se^{\pm t}}^\pm, \tag{3.12}$$

which matches with the Anosov relation (3.11), and is part of the relations corresponding to the local Poincaré symmetry.

Moreover, one can note that denoting by $\mathcal{M}$ the algebra of the Rindler wedge, and by $\mathcal{N}^\pm := \sigma_1^\pm(\mathcal{M})$, $\bigcap_{t \in \mathbb{R}} \tau_t(\mathcal{N}^\pm) = \mathbb{C}$ [290]. In other words:

Proposition 3.3.7 ([152]). *The Rindler wedge is a quantum K-system with continuous dynamics.*

What we learn from this example is that the structure of half-sided modular inclusion exactly fits into the definition of a modular K-system! Therefore there is an interpretation of the nesting of algebras along the horizon in terms of chaos: as one moves along the horizon there are less and less observables until there are none, which is a signature of complete memory loss. It is also interesting to note that the generators of null translations $G^{\pm}$ satisfy the commutation relations

$$[H, G^{\pm}] = \pm i G^{\pm}, \tag{3.13}$$

which were already related to some notion of maximal chaos in [134], where the $G^{\pm}$ referred to as "modular scrambling modes."

Table 3.2 compares the properties of the Rindler wedge to those of geodesic flow on Riemann surfaces.

Geodesic flow on hyperbolic surfaces	QFT in Rindler space
Geodesic flow	Modular flow/boost
Horocycle flow	Null translation
Refining property	Half-sided modular inclusion
K-property	Complete information loss

Table 3.2: The parallel between geodesic flow on hyperbolic surfaces and QFT in Rindler spacetime.

3.4 Application to holography

This section uses the previously introduced formalism to summarize how the different elements of the ergodic hierarchy can be seen as various diagnostics of the emergence of semiclassical features of the bulk of a holographic theory.

Mixing and information loss

The weakest properties of the ergodic hierarchy have to do with mixing, i.e. decay of two-point functions. In holography, the late-time decay of the two-point function at high temperature has been related to information loss at large N [318, 171, 172,

183]. It is also expected that the analytical properties of the large N real time two-point functions give information on the black hole interior and the singularity. Therefore, one can interpret mixing as a signature of the emergence of at least some stringy notion of spacetime. On the other hand, the late time decay of two-point functions at high temperature is expected in weakly coupled gauge theories [171, 172], or even in vector models [246, 247], whose holographic duals are very far from a usual local theory.

Emergent half-sided modular inclusions

In [294, 293, 295], it was pointed out that the emergence of a half-sided modular inclusion in the large N limit of a high temperature thermofield double state in AdS/CFT is related to the emergence of a black hole horizon and of time in the black hole interior, see Figure 3.1. The commutation relation between null translations and boosts along the horizon in a half-sided modular inclusion is exactly (3.12), which corresponds to a modular Anosov structure, and allows to recover some of the Poincaré symmetry, following [134].

These emergent half-sided modular inclusions relate to the emergence of a thermodynamic arrow of time in the bulk. Recalling the interpretation of the nesting of the algebras inside a K/refining system, the fact that the algebra of observables becomes smaller and smaller can be interpreted as some emergent form of information loss.

Remark on the role of type III$_1$

In [294, 293, 295], it was pointed out that the emergence of type III$_1$ factors in the semiclassical limit of holography is a crucial feature in order to allow for the emergence of spacetime. What is now easy to note is that while type III$_1$ is necessary (mixing can only happen in a type III$_1$ factor [183]), it may not be sufficient on its own to guarantee the emergence of a good notion of "horizon" physics. Indeed, properties attached to half-sided modular inclusions, like the Anosov property and the K-property, are analogs of strictly stronger properties from the ergodic hierarchy.

Some open questions

It would be very interesting to reverse the logic of this letter, and to ask whether given a holographic theory the $G_N \to 0$ limit, some notions of horizons, emergent times and local Poincaré symmetry appear in the bulk. It has been shown here that it may be possible to make progress on such a question by studying where the $G_N \to 0$ limit of the theory sits in the ergodic hierarchy.
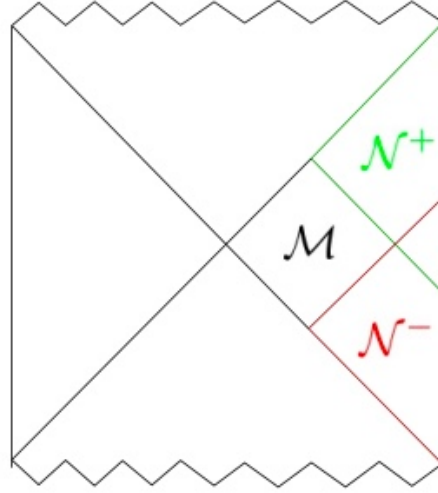
Figure 3.1: The half-sided modular inclusions of Leutheusser–Liu, which are reinterpreted here as quantum Anosov systems. The algebras $\mathcal{N}^+$ and $\mathcal{N}^-$ represent the strict algebras of the right wedge algebra $\mathcal{M}$ of the thermofield double. They can be obtained from null translations along the horizon which, together with modular flow, give rise to an Anosov structure.

In the case of AdS/CFT, the relevant case is that of the large N theory, which corresponds to generalized free fields. It was shown in [236] and reinterpreted in modern language in [183] that the absolute continuity of the spectral density of these fields with respect to the Lebesgue measure guarantees that at finite temperature, the dynamics is strongly mixing at the level of the von Neumann algebra. In particular, this implies that the corresponding von Neumann algebra has type III_1. But what about the higher levels of the ergodic hierarchy introduced here? In particular:

- When is the K-property satisfied for generalized free fields at finite temperature?

- To what extent can the K-property characterize the semiclassical nature of a bulk theory?

- Can the K-property be leveraged to obtain a notion of arrow of time, horizon physics and black hole interiors even when the bulk theory is subject to strong stringy effects? See [197].

Chapter 4

TOWARD STRINGY HORIZONS

This chapter is based on the work [197], in collaboration with Hong Liu.

4.1 Introduction

In the semiclassical gravity description,[1] an event horizon is a boundary beyond which events cannot affect an asymptotic observer. While originally defined in terms of the causal structure of a spacetime, event horizons have also played crucial roles in many other aspects of black hole physics, including the discovery of Hawking radiation and black hole thermodynamics.

In string theory, the semiclassical gravity description serves as a low-energy effective theory, arising in the limit where Newton's constant G_N and the string length ℓ_s (or $\alpha' = \ell_s^2$) both approach zero. At finite G_N, spacetime fluctuations prevent sharp definitions of geometric concepts such as event horizons, causal structure, and spacetime subregions. It is natural to ask whether these concepts can still be precisely formulated in the so-called "stringy regime," where G_N approaches zero while α' remains finite. In this regime, while there are no quantum gravitational fluctuations, fundamental objects are one-dimensional strings, which probe spacetime very differently from point particles. In particular, sharp locality used in the current formulations of these concepts may not be compatible with the intrinsic non-locality brought by the finite size of these strings. Despite much progress in our understanding of string theory, there have been very limited tools for approaching this question.

In this chapter, we propose a definition of event horizons for holographic gravitational systems in the stringy regime in terms of their boundary duals. As a prototypical example, consider $\mathcal{N} = 4$ Super-Yang-Mills (SYM) theory with gauge group $SU(N)$, which is dual to IIB string theory on $\text{AdS}_5 \times S_5$. The semi-classical regime of the bulk gravity theory corresponds to the $N \to \infty$ and $\lambda \to \infty$ (λ is the 't Hooft coupling) limit of the SYM theory, while the stringy regime corresponds to $N \to \infty$ with λ kept finite. Suppose the SYM theory is in the thermofield double state above the Hawking-Page temperature [230], which in the $N \to \infty$ and $\lambda \to \infty$

---

[1]By semiclassical gravity, we mean classical Einstein gravity (with possible higher derivative corrections) and quantum field theory in a curved spacetime.

limit is dual to an eternal black hole in AdS$_5$ [455, 318]. Now consider the system at finite λ. We will argue that the bulk is described by a stringy black hole and provide tools to explore the corresponding stringy horizon.

The starting point of our proposal is the subregion-subalgebra duality introduced in [294, 295], which provides a new framework for understanding the emergence of bulk spacetime from the boundary theory in the semi-classical regime. The duality states that a bulk subregion $\mathfrak{o}$ can be described by a subalgebra $\mathcal{M}_{\mathfrak{o}}$ of the boundary theory.

$\mathcal{M}_{\mathfrak{o}}$ includes all physical operations that can be performed by bulk observers in the region $\mathfrak{o}$, and encodes its geometric, causal, and entanglement structures. For example, the inclusion of one bulk spacetime region $\mathfrak{o}_1$ in another region $\mathfrak{o}_2$ is described by inclusion of the corresponding dual boundary subalgebras $\mathcal{M}_{\mathfrak{o}_1} \subset \mathcal{M}_{\mathfrak{o}_2}$. That $\mathfrak{o}_1$ and $\mathfrak{o}_2$ are causally disconnected corresponds to the fact that $\mathcal{M}_{\mathfrak{o}_1}$ and $\mathcal{M}_{\mathfrak{o}_2}$ commute. The entanglement structure of a region $\mathfrak{o}$ is reflected in that $\mathcal{M}_{\mathfrak{o}}$ is a type III$_1$ von Neumann algebra and associated algebraic properties.

Philosophically, subregion-subalgebra duality is reminiscent of Gelfand duality in mathematics, where a topological space can be equivalently described by the algebras of functions on that space. Here the collection of boundary subalgebras $\{\mathcal{M}_{\mathfrak{o}}\}$ captures not only the geometric information on the bulk spacetime, but also all the physics defined on it.

Now suppose the boundary subalgebra $\mathcal{M}_{\mathfrak{o}}$ for a bulk subregion $\mathfrak{o}$ can be extended to finite λ. We can consider using $\mathcal{M}_{\mathfrak{o}}$ as a *definition* of the bulk region $\mathfrak{o}$ in the stringy regime. If that can be shown to be sensible, the commutation relations among different algebras can then be used to define the causal structure of the emergent bulk spacetime in the stringy regime, which should in turn enable the definition of an event horizon.

As an illustration, consider the algebra $\mathcal{S}_I$ generated by single-trace operators localized within a time band $I = (-t_0, t_0)$ in the vacuum sector of the boundary theory[2]. In the large λ limit, it has been argued [294, 295] to be dual to a spherical Rindler region $\mathfrak{a}$ in empty AdS (see Fig. 4.1). The bulk diamond region $\mathfrak{b}$, which is the causal complement of $\mathfrak{a}$ in the bulk, can be described by the boundary subalgebra $\mathcal{S}'_I$, the commutant of $\mathcal{S}_I$. It is then natural to use $\mathcal{S}_I$ and $\mathcal{S}'_I$ at finite λ to define the corresponding subregions $\mathfrak{a}$ and $\mathfrak{b}$ in the stringy regime.

---

[2]In the $N \to \infty$ limit, boundary operators at different times are independent, and the space of states in the boundary theory splits into disjoint sectors associated with semi-classical states.
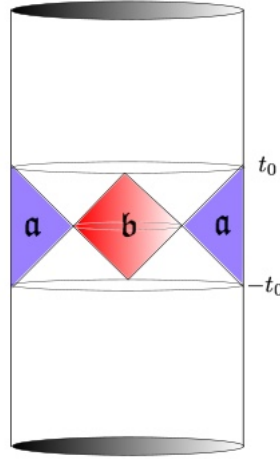
Figure 4.1: A simple illustration of subregion/subalgebra duality in the vacuum state of strongly coupled $\mathcal{N} = 4$ Super-Yang–Mills theory. The region $\mathfrak{a}$, a spherical Rindler region in the bulk, is dual to the algebra $\mathcal{S}_I$ of large N boundary observables in the time band $I = (-t_0, t_0)$. The bulk diamond $\mathfrak{b}$, which does not touch the boundary, can be identified with the commutant of the algebra $\mathcal{S}_I$.

In the large N limit, the bulk theory is free, and the boundary theory is a generalized free field theory. The algebra $\mathcal{M}_{\mathfrak{o}}$ dual to a bulk region $\mathfrak{o}$ is then recovered from all the algebras generated by individual single-trace operators. This feature extends to finite λ. In particular, if we consider a specific spacetime field corresponding to a stringy excitation, it should still be described by a free quantum field theory in a curved spacetime. Similarly, on the boundary each single-trace operator is still described by a generalized free field, and the discussion of operator algebras associated with each single-trace operator goes exactly as that in the $\lambda \to \infty$ limit.

There are, however, two possible complications in using $\mathcal{M}_{\mathfrak{o}}$ as a definition of $\mathfrak{o}$ in the stringy regime:

1. In the semiclassical limit, all bulk fields in the Einstein gravity "see" the same geometry, which is the statement of the "equivalence principle." In the stringy regime, the equivalence principle may be broken, indications of which can already be seen perturbatively in α' by including higher derivative corrections. Due to such corrections, different bulk fields may "see" different effective spacetime metrics[3].

---

[3]An explicit example was given in [86], where adding the Gauss-Bonnet term to the Einstein
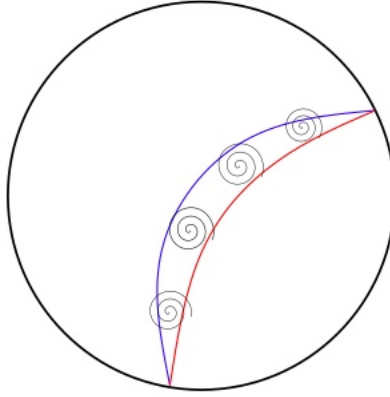
Figure 4.2: A cartoon of how the notion of spacetime may break down in the stringy regime. The bulk region "seen" by a boundary field or another from a given boundary subregion may differ depending on the field - two such regions are represented in blue and red. If these two fields interact, the difference between these two spacetime geometries may become blurry.

Thus it can be that in the stringy regime, sharp definitions of subregions or horizons can be given for each bulk free field, but the definitions differ for different fields. That is, a universal definition that is common to all fields may not exist. In particular, interactions among the fields may lead to a nonlocal smearing of the boundaries or horizons of subregions, see Fig. 4.2 for a cartoon.

It may also happen in certain stringy spacetimes, sharp subregions in general cannot be defined, but an event horizon universal to all stringy fields may still be sharply defined.

In terms of boundary subalgebras, in the $\lambda \to \infty$ limit, the equivalence principle implies that properties of different factors in $\mathcal{M}_{\mathfrak{o}}$ associated with different single-trace operators should "conspire" to describe the same bulk region $\mathfrak{o}$.

action leads to different effective metrics for different components of metric perturbations.

Non-existence of a definition universal to all fields should then be reflected in the breaking of this "conspiracy" among factors of $\mathcal{M}_0$ by finite λ effects.

2. There is a Hagedorn growth in the number of single-trace operators in $\mathcal{M}_0$, dual to stringy modes in the bulk. Given that the Hagedorn growth is what distinguishes a string theory from a field theory with an infinite number of fields[4], it may be expected to have fundamental implications for the structure of $\mathcal{M}_0$.

Despite the above possible complications, $\mathcal{M}_0$ provides a framework and powerful new tools where questions about bulk stringy geometry can be explored. For example, identifying sharp signatures that algebras of different single-trace operators "reconstruct" different bulk spacetime geometries may give insight into the nature of stringy nonlocality, and lead to clues on how to characterize stringy geometry.

Motivated by the above considerations, we will use the structure of boundary algebras to explore geometric aspects of the bulk in the stringy regime, and propose a diagnostic for existence of stringy horizons. Here is a summary of the main results of the chapter:

1. A causal depth parameter, which is also well-defined in the stringy regime, is introduced to quantify the "depth" of the emergent radial direction.

   In the large N limit, the causal depth parameter can be calculated for each single-trace operator by using its boundary spectral function. It measures the depth of the bulk as probed by the bulk field dual to the single-trace operator. Different values of the causal depth parameter for different single-trace operators would be a direct signature that in the stringy regime different fields "see" different bulk geometries.

   We show that for a CFT in the vacuum state (dual to empty AdS), all bulk fields have the same causal depth parameter. The same statement applies to the thermofield double state below the Hawking-Page temperature.

   The computation of the causal depth parameter exactly maps to a well-studied problem from harmonic analysis, which is known as the *exponential type problem*. In many physically relevant situations, this connection makes it

---

[4]IIB supergravity on $AdS_5 \times S_5$ already has an infinite number of fields in AdS_5 from the Kaluza-Klein reduction on S_5.

possible to gain information about the causal depth parameter, in particular whether it is finite or not, without knowing the specific form of the spectral function.

2. We give a boundary diagnostic for the existence of stringy horizons using the causal depth parameter and the existence of half-sided modular inclusions.

   As an example, we argue that the thermofield double state of the $\mathcal{N} = 4$ SYM theory above the Hawking-Page temperature should have a stringy horizon at finite (nonzero) λ. In contrast, the IOP model [246] does not, despite exhibiting information loss and type III$_1$ algebras.

3. We introduce an algebra to characterize the structure of a stringy horizon (or a stringy entangling surface), and discuss how to calculate the $O(N^0)$ part of its generalized entropy.

4. We introduce a modular depth parameter which can be used quantify the "depth" of the emergent radial direction using modular flows of boundary subalgebras.

   This makes it possible to explore an extension of entanglement wedge reconstruction to the stringy regime, and gives a diagnostic for the corresponding RT surfaces/QES [401, 242, 162]. Using the same techniques as the ones developed in the case of event horizons, we define a QES algebra associated to such stringy quantum extremal surfaces.

   We also discuss to what extent the algebraic ER = EPR proposal [155] can be extended to the stringy regime, and propose a possible resolution of a question raised in [155] about spacetime connectivity for an evaporating black hole before and after the Page time.

The plan of the chapter is as follows. In Sec. 4.2 we introduce the causal depth parameter and give a criterion for the existence of a stringy horizon. We also discuss some examples. In Sec. 4.3 we introduce the modular depth parameter and discuss a diagnostic of stringy RT surface/QES. In Sec. 4.4 we conclude with some implications of our results and future perspectives.

Notations and conventions:

- Single-trace operator algebras associated to a field ϕ are denoted $\mathcal{S}_\phi$.

- Unless mentioned otherwise, in this chapter an algebra always means a von Neumann algebra of operators acting explicitly on a Hilbert space.

- The Fourier transform of a function $f(t)$ is by default denoted by $f(\omega)$.

- Without indication, $\int dt \equiv \int_{-\infty}^{\infty} dt$.

- $\theta(\omega)$ is the Heaviside step function.

- In this chapter, all Hilbert spaces are separable.

- $\mathcal{B}(\mathcal{H})$ denotes the algebra of bounded operators on the Hilbert space $\mathcal{H}$

- Throughout the text, we assume that all manipulated distributions satisfy the conditions to be tempered. This allows us to take Fourier transforms without ambiguity in our proofs.

4.2 Causal depth parameter and stringy horizons

In this section we motivate and define a new quantity, which we call *causal depth parameter*, and use it to diagnose the emergence of a causal structure, a radial direction, and horizons in the bulk. We also introduce a horizon algebra to characterize stringy horizons. We use $\mathcal{N} = 4$ SYM theory on S^3 as the prototypical example, and work in the large N limit throughout. For convenience we take the radius of the boundary sphere to be 1.

Causal depth parameter and stringy horizons: the TFD state

Consider two copies of the boundary CFT in the thermofield double (TFD) state. In the large N limit (for all λ), the system is believed to have a Hawking-Page transition at some temperature T_{HP} [5]. For $T < T_{\mathrm{HP}}$, the free energy is of order $O(N^0)$. Furthermore, thermal Euclidean two-point functions of single-trace operators are given from the vacuum ones by summing over images in the Euclidean time circle [85], which implies the thermal spectral function has a discrete spectrum. For $T > T_{\mathrm{HP}}$, the free energy is of order $O(N^2)$, and thermal spectral functions for general single-trace operators are believed to have a complete spectrum [172]. If we further take the large λ limit, then the boundary system is dual to thermal AdS which consists of
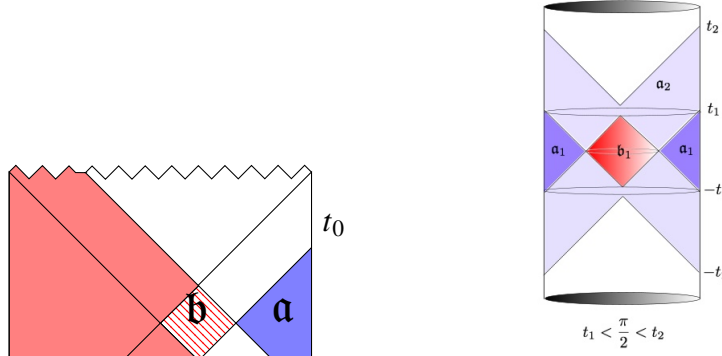
(a) The Penrose diagram of an AdS-Schwarzschild two-sided black hole. For all times t_0, the bulk algebra $\mathfrak{a}$ dual to the single trace algebra $\mathcal{S}_{(-t_0,t_0)}$ has a nontrivial relative commutant $\mathfrak{b}$ in $\mathcal{S}_R$. Topologically, this means that the bulk never fills up and there is a bifurcate horizon.

(b) A depiction of thermal AdS (right copy). The left copy in the thermofield double state is disconnected and not shown. Contrary to the AdS-Schwarzschild case, the region $\mathfrak{a}_1$ dual to $\mathcal{S}_{(-t_1,t_1)}$ for $t_1 < \frac{\pi}{2}$ has a nonempty relative commutant $\mathfrak{b}_1$ inside $\mathcal{S}_R$, but for $t_2 > \frac{\pi}{2}$, $\mathcal{S}_{(-t_2,t_2)}$ is equivalent to the full right copy, is equal to $\mathcal{S}_R$. This means that the bulk "fills up" for $t_1 > \frac{\pi}{2}$, and there is no bifurcate horizon.

Figure 4.3: Diagnosing the presence of a bifurcate horizon from the algebraic structure of boundary time bands.

two copies of AdS (in an entangled state) for $T < T_{\mathrm{HP}}$, and for $T > T_{\mathrm{HP}}$ to an eternal black hole [318]. See Fig. 4.3.

The obvious geometric difference between thermal AdS and the eternal black hole is that the black hole geometry is connected, with a bifurcate horizon separating the R and L regions of the black hole, whereas two copies of thermal AdS are disconnected. We now would like to generalize the notions of connectedness and horizon to the corresponding bulk dual at finite λ where we no longer have a geometric description. In order to do so, we will first provide an algebraic characterization of these geometric features, after which the generalization to finite λ is immediate.

We denote the single-trace operator algebras for the $\mathrm{CFT}_{R,L}$ in the large N limit respectively by $\mathcal{S}_R$ and $\mathcal{S}_L$. They are respectively dual to the bulk regions R and L. In particular, in the case of thermal AdS, the bulk R-region is simply the right copy of AdS.

Consider an open time interval $I = (-t_0, t_0)$ on the right boundary and the associated

single-trace time band operator algebra $\mathcal{S}_I$. By definition we have $\mathcal{S}_I \subseteq \mathcal{S}_R$. For the bulk dual given by the black hole geometry, it has been argued that $\mathcal{S}_I$ is equivalent to the bulk algebra in the spherical Rindler region $\mathfrak{a}$ represented on Fig. 4.3 (a) [294, 295]. The existence of a horizon (or more coarsely, the fact that both sides of the black hole are connected) implies the geometric statement that for any choice of t_0, $\mathfrak{a}$ only covers a proper subset of the $t = 0$ Cauchy slice of the R-region of the black hole. In other words, when the two sides of the thermofield double are connected, the R-region can never be "filled up" by spherical Rindler regions, no matter how large t_0 is. In contrast, consider the copy of thermal AdS represented on Fig. 4.3 (b). There, $\mathfrak{a}$ covers a full Cauchy slice of the R-region for $t_0 \geq \frac{\pi}{2}$.

The above geometric statement can be rephrased algebraically by saying that for the black hole geometry, the algebra $\mathcal{S}_I$ is a strict subalgebra of $\mathcal{S}_R$ for any t_0. More explicitly, the commutant $\mathcal{S}_I'$ is equivalent to the bulk causal complement of $\mathfrak{a}$, which includes the red shaded region and the striped region $\mathfrak{b}$. The relative commutant of $\mathcal{S}_I$ in $\mathcal{S}_R$ is given by $\mathcal{S}_I' \cap \mathcal{S}_R$ and is equivalent to the striped bulk region $\mathfrak{b}$. This is to be contrasted with the thermal AdS case, where we have $\mathcal{S}_I' \cap \mathcal{S}_R = \emptyset$ (or equivalently $\mathcal{S}_I = \mathcal{S}_R$) for $t_0 \geq \frac{\pi}{2}$. Such algebraic statements are powerful, as they do not refer to any geometry, and thus can immediately be generalized to diagnostics of the presence or absence of a horizon in the stringy regime at finite λ.

The above discussion motivates the following definition:

Definition 4.2.1. The two sides of the thermofield double are *stringy-connected* if the algebra $\mathcal{S}_{(-t_0,t_0)}$ is a strict subalgebra of $\mathcal{S}_R$ for any finite value of t_0.

In the case where the two sides of the thermofield double are not stringy-connected, we can also probe the depth of the emergent radial direction thanks to the following:

Definition 4.2.2. The causal depth parameter $\mathcal{T}$ of a large N thermofield double state is the largest value of $2t_0$ for which the algebra $\mathcal{S}_{(-t_0,t_0)}$ is a strict subalgebra of $\mathcal{S}_R$.

From Definition 4.2.2, bulk geometry gives that in the $\lambda \to \infty$ limit

$$\mathcal{T} = \begin{cases} \pi & T < T_{\mathrm{HP}} \\ \infty & T > T_{\mathrm{HP}} \end{cases}. \tag{4.1}$$

In Sec. 4.2, we will give a purely boundary argument for (4.1), and show that it generalizes to finite λ. Using Definition 4.2.2, Definition 4.2.1 can also be stated by
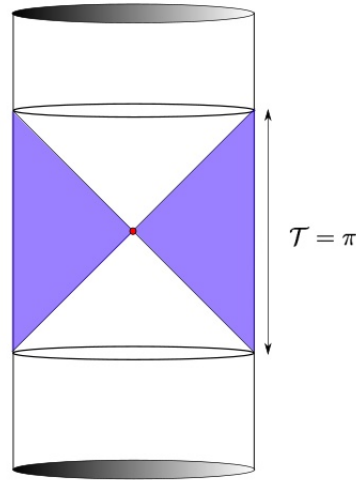
Figure 4.4: A heuristic picture of the depth parameter in thermal AdS. In this case, there is a point, depicted in red, which sits at the "center" of the bulk. The depth parameter $\mathcal{T}$ can be seen as the boundary time interval that can be reached by shooting light rays from this point. Here, $\mathcal{T} = \pi$.

requiring that

$$\mathcal{T} = \infty .\tag{4.2}$$

Intuitively, in the semi-classical limit, the depth parameter quantifies the depth of the bulk R-region, by relating this depth to the time width of the boundary region obtained by sending light rays from a bulk point. See Fig. 4.4. Note that when there is a horizon, clearly by definition, $\mathcal{T}$ is infinite. In [153], such considerations were in fact used to characterize the depth of the bulk geometry using the bulk causal structure, and in [359], a quantum circuit model following the same line of thought was constructed. Here we have given an intrinsic boundary definition in terms of the commutant structure, which can in turn be used to characterize the bulk causal structure in the stringy regime.

The depth parameter also has an interesting boundary interpretation. It is the minimal width of a time interval such that the knowledge of the algebra of observables localized in the interval is enough to determine the full algebra of the R-system. For example, in the case of thermal AdS, $\mathcal{S}_I = \mathcal{S}_R$ for $t_0 > \frac{\pi}{2}$, i.e., we already have access to all the operations in the R-system given such an $\mathcal{S}_I$. But in the case of a black hole, it is not possible to have access to the full $\mathcal{S}_R$ for any t_0. For the theory at finite N, access to the operator algebra on a single Cauchy slice suffices to

determine its future evolution. But the large N limit, such a property breaks down as there are no equations of motion. This is related to the loss of determinism on the boundary in the large N limit. Hence there is a sense that the large N limit leads to information loss even in the vacuum sector, although in the end all the information can be recovered by having access to the operator algebra for a time band with finite $t_0 > \frac{\pi}{2}$. In the black hole sector, information loss is more drastic: one can never recover all the information even with access to operator algebras of finite time bands of arbitrary width. The causal depth parameter $\mathcal{T}$ can thus also be viewed as quantifying the amount of information loss there is in the system. Whenever it is nonzero, there is a loss of determinism. Under this interpretation, it is not only the formation of black holes, but also the emergence of the whole radial direction, that is related to information loss. It should also be mentioned that even systems with $\mathcal{T} = 0$ can have information loss, as we will see in an example later.

In the semiclassical regime, while an event horizon is defined through the causal structure, it also has many other properties. For example, it is also a hypersurface of infinite redshift, a property that plays an essential role for the existence of Hawking radiation. In particular, it implies that quantum fields living outside the black hole must have spectral support for arbitrarily small frequencies (in terms of the Schwarzschild time). We would like to have a definition for a stringy black hole that still retains this property. As we will discuss later in Sec. 4.2, Definition 4.2.1 does not by itself imply that quantum fields living outside such a "horizon" have spectral support for arbitrarily small frequencies. We will now formulate an additional condition to ensure that.

An important property associated with a horizon in the semi-classical regime is the existence of not only a bifurcation surface, but also half-sided modular inclusions along the future or past horizon (see Fig. 4.5). In the TFD state, modular flow coincides with time translation. The existence of a half-sided modular inclusion then requires that the algebra of a semi-infinite time band is a strict subalgebra of $\mathcal{S}_R$. This a strictly stronger condition than Definition 4.2.1, as it involves semi-infinite intervals and not only finite intervals. While it may not be immediately intuitive, we will show in Sec. 4.2 that the emergence of a half-sided inclusion ensures that the spectral support of bulk quantum fields includes arbitrarily small frequencies. While Condition 1 captures some form of connectivity, it is only Condition 2 that guarantees all the properties of horizons. We therefore propose the definition:

Definition 4.2.3. There is a stringy horizon in the thermofield double state if the subalgebra $\mathcal{S}_{(0,\infty)}$ is a strict subalgebra of $\mathcal{S}_R$.

Note that by invariance under time translation and time reversal, this definition implies that $\mathcal{S}_{(t_0,\infty)}$ is a strict subalgebra of $\mathcal{S}_R$, and similarly for $\mathcal{S}_{(-\infty,t_0)}$, for all values of t_0.

Instead of imposing the condition of half-sided inclusion, we could imagine defining the existence a stringy horizon by imposing the requirement that the system is "chaotic." There are various possible levels of chaos in a system [191, 367]. For example, one possible requirement is that two-point functions cluster in time, i.e., decay with time. In particular, if $\rho(t)$ clusters exponentially fast, i.e., for some constants $C > 0$ and $\alpha > 0$,

$$|\rho(t)| \leq Ce^{-\alpha t}, \tag{4.3}$$

then $\rho(\omega)$ is analytic on a strip, therefore it can only vanish on isolated points. We will see in Sec. 4.2 that under mild assumptions, if $\rho(\omega)$ vanishes only at the origin, we can show that there is an emergent half-sided modular inclusion in the system. The condition (4.3) gives the weaker condition that $\rho(\omega)$ vanishes at an at most countable number of points on the real axis. It would be interesting to see to what extent a half-sided inclusion also emerges under this weaker assumption.

We also note that by definition $\bigvee_{t_0>0} \mathcal{S}_I = \mathcal{S}_R$, and thus even in the case $\mathcal{T} = \infty$, we have $\bigcap_{t_0>0} (\mathcal{S}'_I \cap \mathcal{S}_R) = \mathbb{C}$. In particular if we want to define an algebra of operators associated with the bifurcate horizon, it is not enough to consider $\bigcap_{t_0>0} (\mathcal{S}'_I \cap \mathcal{S}_R)$. One instead needs to perform a sequential construction which will be described in Section 4.2.

We can similarly define a depth parameter and horizons using time band subalgebras of $\mathcal{S}_L$. For the thermofield double state, there is an antiunitary operator J that takes $\mathcal{S}_R$ to $\mathcal{S}_L$ and vice versa. As a result, all the results presented here follow in an exactly analogous manner for $\mathcal{S}_L$. In particular, as we will see in Sec. 4.2, there is a precise sense in which the horizon defined using $\mathcal{S}_L$ coincides with the one defined using $\mathcal{S}_R$.

Causal depth parameter and stringy horizons for general states

The definitions of causal depth parameter and stringy horizon in the thermofield double state, as discussed above, can be readily generalized to general semi-classical
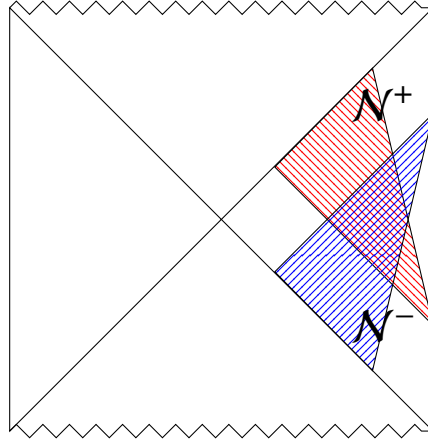
Figure 4.5: Half-sided inclusions for future and past horizons. In the thermofield double state at strong coupling and high temperature, the algebras $\mathcal{N}^+$ and $\mathcal{N}^-$, which supported on future and past semi-infinite time intervals, are dual to the red and blue wedges in the bulk, respectively. In particular, it is the fact that they are inequivalent to the full algebra of right boundary observables that allows for the emergence of nontrivial future and past half-sided modular inclusions, which we will promote to a definition of a horizon in the TFD state in the stringy regime.

two-sided and single-sided states. Note, however, that we defer the generalization of the notion of stringy connectivity until Section 4.3.

We refer to a state in the boundary theory as semi-classical if it has a semi-classical bulk dual in the large N and large λ limit. We would like to probe the corresponding bulk dual in the stringy regime with a finite λ.

First consider a general semi-classical two-sided state $|\Psi\rangle$ in the $\lambda \to \infty$ limit. See Fig. 4.6 for some cartoon examples. Denote by $\mathcal{M}_R$ the algebra of operators of the R-system in the large N limit. In the case of TFD state we have $\mathcal{S}_R = \mathcal{M}_R$, and time translations coincide with modular flows. But in general we have $\mathcal{S}_R \subset \mathcal{M}_R$ and the state is not time translation invariant.[5] Nevertheless, the definition of causal depth parameter and the diagnostic of a horizon are largely not affected except that there is no symmetry between left and right, and the depth parameter can be time-dependent.

Definition 4.2.4. The right causal depth parameter $\mathcal{T}_R(t)$ of a large N two-sided state is the largest value of $2t_0$ for which the algebra $\mathcal{S}_{(t-t_0, t+t_0)}$ is a strict subalgebra of $\mathcal{S}_R$.

---

[5]As we will discuss further in Sec. 4.3, there may be additional operators generated by modular flows. Due to these complications that we will introduce a more general definition of stringy connectivity in Sec. 4.3.

(a) The "long black hole," a connected two-sided geometry.

(b) A disconnected two-sided geometry with bifurcate horizons.

(c) A disconnected two-sided geometry without horizons.

(d) A disconnected two-sided geometry with future horizons.
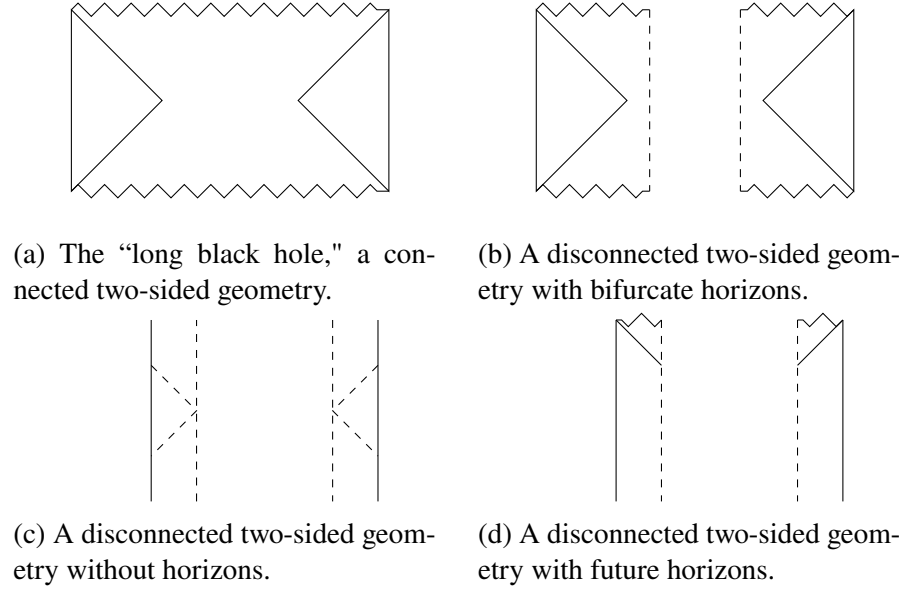
Figure 4.6: Cartoons for various types of two-sided states. These examples also illustrate that the causal depth parameter does not allow to predict spacetime connectivity in a general state. The cases (a) and (b) both have infinite causal depth parameter, but (a) is connected whereas (b) is disconnected. Similarly, (b) and (c) are both disconnected but (b) has infinite causal depth parameter while (c) has finite causal depth parameter. Finally case (d) is disconnected but has a future horizon.

Definition 4.2.5. A large N two-sided state has a right bifurcate horizon if semi-infinite future and past time band algebras are proper subalgebras of $\mathcal{S}_R$.

In fact, it is enough to show that the causal depth parameter $\mathcal{T}_R(t)$ is infinite for one value of t, since then it is infinite for all values of t. Indeed, fix $t' \in \mathbb{R}$. For all values of t_0, the interval $(t' - t_0, t' + t_0)$ is included in some interval of the form $(t + T, t - T)$ where we have chosen T large enough. The algebra of that interval is a strict subalgebra since $\mathcal{T}_R(t) = \infty$, therefore, so is the algebra of $(t' - t_0, t' + t_0)$.

We can also diagnose the future and past horizons as

Definition 4.2.6. A large N two-sided state has a nontrivial right future horizon after time τ if the algebra $\mathcal{S}_{(\tau,\infty)}$ is a strict subalgebra of $\mathcal{S}_R$.

Definition 4.2.7. A large N two-sided state has a nontrivial right past horizon before time τ if the algebra $\mathcal{S}_{(-\infty,\tau)}$ is a strict subalgebra of $\mathcal{S}_R$.

There are parallel definitions for the L-system. Note that in the case of a state that is

invariant under time translations such as the thermofield double, all three definitions coincide.

When $\mathcal{T}_R(t)$ is finite, i.e., the R-region has a finite depth, the bulk geometry should necessarily be disconnected. But as indicated in Fig. 4.6, $\mathcal{T}_R(t)$ being infinite does not say anything whether the bulk geometry is connected or disconnected. To diagnose whether the bulk geometry is connected requires the further developments of Sec. 4.3 and will be discussed in Sec. 4.3.

The above definitions can also be straightforwardly adapted for a single-sided semi-classical state (i.e., with only one boundary). We just need to change two-sided state to single-sided state and remove the word "right" in various places. For example,

Definition 4.2.8. The causal depth parameter $\mathcal{T}(t)$ of a large N single-sided state is the largest value of $2t_0$ for which the algebra $\mathcal{S}_{(t-t_0,t+t_0)}$ is a strict subalgebra of $\mathcal{S}$.

Here $\mathcal{S}$ is the single-trace operator algebra for the full boundary.

The causal depth parameter from the spectral function

In this subsection we show that the causal depth parameter can be determined by the spectral function of the boundary theory. In fact, it is equal[6] to an invariant known in harmonic analysis as the *exponential type*.

In the large N limit, in a semi-classical state, correlation functions of single-trace operators factorize into sums of products of two-point functions. Consequently, there is a generalized free field theory around the state for each single-trace operator. We can diagonalize two-point functions such that different operators do not mix, and thus each generalized free field generates its own algebra. The full algebra is then recovered from all the algebras associated to individual fields.

In this subsection, we will consider only *one* (Hermitian) generalized free field ϕ acting on the GNS Hilbert space of some semi-classical state $|\Psi\rangle$, which can be the TFD state, the vacuum or other two-sided/single-sided states. We will return to the problem of assembling the results obtained for each individual field later in this section. In the case of a two-sided state, ϕ should be understood as ϕ_R, i.e., a generalized free field in the CFT$_R$. For details on the setup, see Appendix 4.6. For convenience we will assume $|\Psi\rangle$ is time translation invariant and suppress possible spatial directions for notational simplicity.

---

[6]Up to a technicality.

Consider the commutator

$$\rho(t - t') \equiv \langle \Psi | [\phi(t), \phi(t')] | \Psi \rangle \tag{4.4}$$

which satisfies $\rho^*(t) = \rho(-t) = -\rho(t)$. The Fourier transform of $\rho(t)$ is called the spectral function and satisfies the properties

$$\rho(-\omega) = -\rho(\omega), \quad \epsilon(\omega)\rho(\omega) \geq 0 . \tag{4.5}$$

In the TFD state $\rho(\omega)$ is related to the Wightman function as

$$G_+(\omega) = \frac{\rho(\omega)}{1 - e^{-\beta\omega}}, \tag{4.6}$$

while in the vacuum state we have

$$G_+(\omega) = \theta(\omega)\rho(\omega) . \tag{4.7}$$

The algebra $\mathcal{S}_\phi$ associated with the field ϕ is generated by the

$$\phi(f) = \int dt \, f(t)\phi(t) \tag{4.8}$$

with $f(t)$ real and normalizable in terms of the inner product

$$\langle f_1, f_2 \rangle_\beta = \int \frac{d\omega}{2\pi} f_1^*(\omega) \, \theta(\omega)\rho(\omega) \, f_2(\omega) . \tag{4.9}$$

In the above equation, $f_1(\omega)$ is the Fourier transform of $f_1(t)$, with $f_1(-\omega) = f_1^*(\omega)$.

For a general state (not equal to vacuum), normalizability for the inner product (4.9) is too weak. On top of this normalizability, we need to impose the extra condition that f is in the domain of the operator of multiplication by $\mathfrak{b}_-$ defined in Eq. (4.70). In the case of a thermal state which will be of most interest to us, this is equivalent to the stronger normalizability condition

$$\langle f_1, f_2 \rangle_\beta = \int \frac{d\omega}{2\pi} f_1^*(\omega) \, \theta(\omega) \frac{\rho(\omega)}{1 - e^{-\beta\omega}} f_2(\omega) . \tag{4.10}$$

Note that in order to make these inner products positive definite in the case in which the support of $\rho(\omega)$ is not the full real line, the set of the admissible $f(t)$ should also be quotiented out by the functions that are supported only outside the support of ρ.

The subalgebra $\mathcal{S}_I \subseteq \mathcal{S}_\phi$ for the time band $I = (-t_0, t_0)$ is generated by $\phi(f_I)$ with the support supp $f_I(t) \subset I$. We are interested in whether this inclusion is strict. For a

generalized free field, this question can be shown to be equivalent to asking whether the relative commutant of $\mathcal{S}_I$ in $\mathcal{S}_R$, i.e., $\mathcal{S}_I' \cap \mathcal{S}_R$, is nonempty (see Appendix 4.6). The presence of a nontrivial relative commutant indicates the existence of a region in the emergent dual stringy spacetime that is spacelike to the operators in the causal wedge of I.

The (relative) commutant of $\mathcal{S}_I$ can be shown to be generated by $\phi(g)$, for g real-valued, satisfying

$$[\phi(g), \phi(f_I)] = 0 \quad \rightarrow \quad (g, f_I) \equiv \int dt dt'\, g(t)\rho(t - t')f_I(t') = 0 . \quad (4.11)$$

Equation (4.11) by itself only says that the subalgebra generated by $\phi(g)$ belongs to the (relative) commutant of $\mathcal{S}_I$. That it in fact generates the full relative commutant follows from a theorem by Araki, which we review in Appendix 4.6. Equation (4.11) can also be stated as the fact that $\phi(g)$ lies in the symplectic complement of the subspace spanned by f_I, since (g, f), as defined by (4.11), is a symplectic product.

Condition (4.11) can also be phrased as the requirement that the support of the convolution

$$(g * \rho)(t') = \int dt\, g(t)\rho(t' - t), \quad (4.12)$$

lies in the complement of I. It is convenient to write (4.11) and (4.12) in frequency space

$$\int \frac{d\omega}{2\pi} g^*(\omega)\rho(\omega)f_I(\omega) = 0, \quad (g * \rho)(\omega) = g(\omega)\rho(\omega) . \quad (4.13)$$

Thus the relative commutant is fully determined by the spectral function $\rho(\omega)$.

It turns out that our question maps to a well-studied problem in harmonic analysis, known as the *exponential type problem*. The exponential type problem is at the core of some very deep recent results in mathematics and can be formulated as follows:

Exponential type problem: Given a measure $\rho(\omega)$, what is the smallest value of $\mathcal{T}$ for which the Fourier transforms of compactly supported distributions on $(-\mathcal{T}/2, \mathcal{T}/2)$ become dense in $L^2(\rho)$?

The answer to the exponential type problem applied to the spectral density is exactly[7] the depth parameter $\mathcal{T}$. In Appendix 4.7, we review the state of the art on the exponential type problem. While the general case is difficult, it turns out to be quite

---

[7]Assuming that in the finite temperature case, the extra constraint of normalizability with respect to the inner product (4.9) for β finite instead of infinite does not change the answer.

simple to obtain $\mathcal{T}$ for various cases of interest for holographic applications, which we will discuss in Sec. 4.2.

It is amusing to note that the exponential type problem was first introduced in the work of Kolmogorov and others on chaos in classical dynamical systems (see for example [284]), where they asked how much time is necessary to observe a system for in order to be able to predict its whole evolution. Our discussion provides a holographic interpretation of such a question. In particular, this relationship to dynamical systems is closely related to the notion of information loss in a large N system, which we commented on earlier in Sec. 4.2.

General statements on $\mathcal{T}$ and half-sided inclusions

In Sec. 4.2, we introduced two different notions:

(i) the notion of stringy connectivity in the thermofield double (for which $\mathcal{T} = \infty$);

(ii) stringy horizons, in terms of half-sided inclusions of semi-infinite time band algebras.

We saw that (ii) implies (i). Here we further clarify the different physics behind these two conditions. We will see that (i) is only concerned with large frequency behavior of the boundary generalized free field theory, while (ii) is concerned with both large and small frequency behavior.

The value of the causal depth parameter $\mathcal{T}$ can be obtained from the largest value of a for which an *a-uniform, or a-regular*, sequence can be embedded into the spectral density of the generalized free field under consideration. While we refer the reader to Appendix 4.7 for a detailed explanation of these notions, here we give an intuitive account of their physical meaning.

Roughly speaking, an a-uniform or a-regular sequence can be seen as a sequence of points that are embedded in the support of the spectral function, and that become equally spaced with spacing $1/a$ as $\omega \to \pm\infty$. In other words, it is a sequence (λ_n) such that

$$\rho(\lambda_n) \neq 0, \quad \lambda_n \approx \frac{n}{a} + c_{\pm}, \quad n \to \pm\infty, \tag{4.14}$$

where the precise meaning of the symbol $\approx$ is clarified in Appendix 4.7. In particular, only the behavior at large frequencies matters when deciding whether a sequence is a-uniform or not.

Since the depth parameter $\mathcal{T}$ is encoded in the largest value of a for which an a-uniform sequence can be embedded in the spectral density, we deduce that the value of $\mathcal{T}$ (and whether or not it is infinite) is solely encoded in the large-frequency behavior of the boundary spectral function. However, we stress that it is not how $\rho(\omega)$ grows or decays with a large ω—usually characterized as the UV behavior— that is important here. Rather, it is the average spacing between the points in the support of ρ that is required to determine $\mathcal{T}$.

In the semi-classical regime, while an event horizon is defined by the causal structure, it is also a hypersurface of infinite shift. This implies that spectral functions of matter fields outside it are supported at arbitrarily small frequencies, which is in turn important for the thermal interpretation. The condition $\mathcal{T} = \infty$ can be viewed as the algebraic counterpart of the causal definition for an event horizon. The above discussion tells us that whether $\mathcal{T} = \infty$ or not is not sensitive to the behavior of $\rho(\omega)$ at small ω. For example, $\rho(\omega)$ can have a gap near $\omega = 0$ and still give $\mathcal{T} = \infty$. This may be interpreted as an indication that, in the stringy regime, the causal condition no longer warrants the desired spectral behavior needed for interpreting the horizon as being "thermal." Thus a stronger condition is needed.

We now show that the condition of half-sided inclusion does require that $\rho(\omega)$ is supported at all frequencies. To see it, we can prove the following proposition:

Proposition 4.2.9. *In a (0+1)-D generalized free field theory at finite temperature carrying a half-sided modular inclusion, the spectral function cannot vanish on any open interval.*

Proof. Suppose that there exists a nonzero function f, normalizable for the inner product (4.9), in the relative commutant of a half-infinite interval. Then, the Fourier transform of $f(\omega)\rho(\omega)$ must vanish on a half-infinite interval (without loss of generality, say the positive reals). Now we can invoke Beurling's uniqueness theorem [57], for example the version given in Theorem 4 of [48], which we recall here:

Theorem 4.2.10 ([48]). *Suppose that T is a tempered distribution on $\mathbb{R}$ and that the complement of the support of T contains the disjoint union of closed intervals*

$$\bigcup_{n=1}^{\infty}[l_n - a_n, l_n + a_n],$$

$$0 < l_1 < l_2 < \cdots < l_n < \cdots \to \infty,$$

that

$$\sum_{n=1}^{\infty}\left(\frac{a_n}{l_n}\right)^2 = \infty,$$

and that the Fourier transform $\hat{T}$ vanishes on an open interval. Then, $T = 0$.

In our case we can choose the times $l_n = e^n$ and $a_n = e^{n-1}/2$, to deduce that $f(\omega)\rho(\omega)$ does not vanish on any open interval. In particular, this implies that $\rho(\omega)$ does not vanish on any open interval. $\qquad\square$

We now give two physical examples where the depth parameter may be infinite but there is no half-sided modular inclusion.

The spectral function $\rho(\omega, \vec{k})$ of a free scalar field of mass m at zero temperature has the form

$$\rho(\omega, \vec{k}) = f(-k^2)\theta(-k^2 - m^2)(\theta(\omega) - \theta(-\omega)), \quad k^2 \equiv -\omega^2 + \vec{k}^2. \qquad (4.15)$$

The spectral function has a spectral gap at $\omega = 0$ for any $\vec{k}$, but has a continuous spectrum beyond the gap. The depth parameter is infinite, but there is no half-sided inclusion, as expected of a system at zero temperature.

Another interesting example is the one of the so-called "primon gas" or "Riemannium," whose spectral function is supported at the logarithms of the prime numbers [265]. We have:

Proposition 4.2.11. *The depth parameter of the Riemannium satisfies $\mathcal{T} = \infty$, but there is no stringy horizon in the Riemannium at any temperature.*

Proof. Denote the nth prime number by p_n. We construct a subsequence of the $(\ln p_n)$ that is d-uniform in the sense of Appendix 4.7 in the following way: consider the sequence $I_n = [n(n + 1)/2, (n + 1)(n + 2)/2]$. The energy condition (4.87) is

automatically satisfied. Moreover we can always find $|n|d$ logs of prime numbers in this interval for $|n|$ large enough, as the number of logs of prime numbers in an interval of the form I_n grows exponentially with n. Picking such $|n|d$ representatives furnishes a d-uniform subsequence. This being true for all d, we deduce from Proposition 4.7.7 that $\mathcal{T} = \infty$. However the support of the spectral density is discrete which makes it impossible for there to be a half-sided modular inclusion according to Proposition 4.2.9. $\square$

In contrast to the zero-temperature example (4.15), the Riemannium example shows that finite temperature systems can have $\mathcal{T} = \infty$, but no half-sided inclusion. This exemplifies well the point that $\mathcal{T} = \infty$ is only concerned with the large-frequency behavior. In particular, the Riemannium does not exhibit enough chaos for there to be a half-sided inclusion. Indeed, it can be seen as an infinite noninteracting superposition of oscillatory modes, with frequencies $\ln p$ for all prime numbers p. For each of these modes there is no late time decay of the thermal two point function.

Examples

Finding the depth parameter in a generalized free field theory amounts to solving the exponential type problem for the spectral density. While this is difficult in general, in various cases relevant to holography it is possible to deduce whether it is infinite or finite from the qualitative behavior of the spectral function without the need of knowing its explicit form.

Various results are summarized in Table 4.1:

Theory	Depth parameter
$\mathcal{N} = 4$ SYM, $0 \leq T < T_{HP}$	$\mathcal{T} = \pi$
$\mathcal{N} = 4$ SYM at $\lambda > 0, T > T_{HP}$	$\mathcal{T} = \infty$
IOP model and its generalizations at $T > 0$	$\mathcal{T} = 0$

Table 4.1: The depth parameter in the thermofield double state for various theories.

Evenly spaced spectral density

We first consider the vacuum state of a d-dimensional CFT on S^{d-1}. For general λ, the spectral function of a single-trace operator with given angular quantum numbers on S^{d-1} has the form

$$\rho_0(\omega) = \sum_{n=0}^{\infty} a_n \left[\delta(\omega - 2n - \omega_0) - \delta(\omega + 2n + \omega_0) \right], \tag{4.16}$$

for some $\omega_0 \in \mathbb{R}$. The above form is determined by the conformal symmetry which also completely fixes all the coefficients a_n.

If ω_0 is equal to zero or an integer multiple of 2, it is be fairly straightforward to show that $\mathcal{T} = \pi$: the Fourier transform of any function multiplied by $\rho(\omega)$ is periodic of period π, so if it vanishes on an interval of width π then it vanishes everywhere, which establishes $\mathcal{T} \leq \pi$. If we further assume the a_n do not decay faster than polynomially, we can further construct explicit multiples of $\rho(\omega)$ whose Fourier transforms vanish on an interval of the form $\left(-\frac{\pi}{2} + \varepsilon, \frac{\pi}{2} - \varepsilon \right)$ for all $\varepsilon > 0$, which establishes $\mathcal{T} = \pi$. This construction is detailed in Appendix 4.7.

The general case, however, is more complicated, but the basic idea is that a shift by ω_0 of the spectral function should not alter the result too much, as indicated by our discussion of Sec. 4.2. This is formalized by a result due to Poltoratski [387], see Appendix 4.7 for more details and intuition on this result. Since ρ is separated (i.e., there is a minimal spacing between its peaks), and

$$\sum_n \frac{|\ln a_n|}{1 + n^2} < \infty, \tag{4.17}$$

we can apply Theorem 4 of [387]. The only value of a for which the counting function n_ρ of $\rho(\omega)$ satisfies

$$\int \frac{n_\rho(x) - ax}{1 + x^2} dx < \infty \tag{4.18}$$

is $a = \frac{1}{2}$, so that by Theorem 4 of [387],

$$\mathcal{T} = \frac{2\pi}{2} = \pi. \tag{4.19}$$

Here the conclusion applies to all single-trace operators, and thus all bulk stringy fields have the same causal depth.

Theorem 4 of [387] is stated in a way that only considers summable spectral functions, however, they still hold for our spectral functions, which have polynomial growth [388].

Note that technically, the results of [387] only guarantee the existence of a *complex-valued* test function φ such that $\varphi * \rho$ vanishes on an interval of width π, whereas we need a real-valued one. However, since ρ takes imaginary values, we also have that $\varphi^* * \rho$ vanishes on an interval of width π, so $(\varphi + \varphi^*)/2$, which is real-valued also vanishes on an interval of width π.

The above discussion also applies to the TFD state below the Hawking–Page temperature since there the spectral density has the same form [85] as well, and the normalizability condition (4.9) is equivalent to normalizability with respect to ρ (without the temperature-dependent factor) for discretely supported spectral densities. From the above, we deduce that in the vacuum state or in the TFD state below the Hawking-Page transition, the depth parameter is independent of λ. That is, the geometric picture of empty AdS may extend to finite λ. The statement may not be surprising as empty AdS is the only geometry that is invariant under all the conformal symmetries.

Compact spectral density

As our next case, suppose the spectral function $\rho(\omega)$ has compact support on the frequency axis.

Proposition 4.2.12. *If the spectral density is compactly supported, then $\mathcal{T} = 0$.*

Proof. From our discussion of last subsection, to find the (relative) commutant of $\mathcal{S}_{(-t_0, t_0)}$ we need to identify $g(t)$ such that (4.12) does not have support in $(-t_0, t_0)$.

Since $\rho(\omega)$ is compactly supported, so is $g(\omega)\rho(\omega)$. By Fourier inversion for tempered distributions and the Schwartz–Paley–Wiener theorem, $(g * \rho)(t)$ is an entire function of t. If it vanishes on an open interval, then it has to be identically zero. We thus conclude the (relative) commutant of $\mathcal{S}_{(-t_0, t_0)}$ is trivial for any t_0. That is, $\mathcal{T} = 0$. $\square$

An explicit example of a compact supported spectral function is the IOP model [246], which was proposed as a toy model of black hole information loss. It describes an interacting N-dimensional vector a_i coupled to a free $N \times N$ matrix. The dynamics

of the vector is nontrivial, and exhibit information loss in the sense that thermal two-point functions of a_i decay to zero at late times. The corresponding spectral function has a continuous spectrum, but is compactly supported. The continuous spectrum means that the von Neumann algebra generated by a_i (of the R system) is type III$_1$ [137, 206, 183, 200].

$\mathcal{T} = 0$ appears to indicate that there no stringy horizon, nor a sharply defined emergent smooth radial direction. However, we should caution that in the IOP model, vector a_i is only a sector of the full system, in fact a subleading sector. So it may make sense that this sector does not have a direct bulk geometric interpretation by itself.

There are other matrix quantum mechanical systems in which a probe sector has a spectral function which can be expressed in terms of a semicircle law like in [200], and thus have a compact spectrum. For these systems, we again have $\mathcal{T} = 0$, which means no stringy black hole. Results suggestive of a same picture for non-singlets in the $c = 1$ matrix quantum mechanics were found in [55].

Spectral density with full support

Now consider the case of a spectral density $\rho(\omega)$ that has a complete support on the real frequency axis. This case was long conjectured [171, 172] to be closely related to the emergence of a stringy bifurcate horizon, here we make this idea precise by showing that a spectral density with full support implies that it allows half-sided modular inclusions in both directions (and hence that the depth parameter is infinite).

Proposition 4.2.13. *If the spectral density $\rho(\omega)$ is a continuous function that vanishes only at zero, is differentiable at* 0 *with continuous nonzero first derivative, and decays at most polynomially, then $\mathcal{T} = \infty$ and there is a stringy horizon.*

Proof. We need to show that for any t_0, it is possible to find $g(t)$ such that $(g * \rho)(t)$ does not have support in $I = (-\infty, t_0)$ or $I = (t_0, \infty)$. For this purpose, take a function $\varphi(t)$ that is supported outside I. Let

$$g(\omega) = \frac{\varphi(\omega)}{\rho(\omega)}, \tag{4.20}$$

which by construction $g * \rho = \varphi$ has support outside I. To make $g(t)$ real we need

$$g^*(\omega) = g(-\omega) \quad \rightarrow \quad \varphi^*(\omega) = -\varphi(-\omega) \tag{4.21}$$

where we have used that $\rho(\omega)$ is a real, odd function of ω. Since $\rho(0) = 0$, we also need $\varphi(0) = 0$ such that the ratio (4.11) is well defined at $\omega = 0$. Normalizability of $g(\omega)$ requires that

$$\int_0^\infty \frac{d\omega}{2\pi} \frac{\varphi^*(\omega)\varphi(\omega)}{\rho(\omega)} < \infty \ . \tag{4.22}$$

It is a classical result of Fourier analysis [250] that given a time band, one can always choose a φ with support outside this time band (actually it can even be chosen to have a compact support) such that

$$\tilde{\varphi}(\omega) = O(e^{-|\omega|^{1-\alpha}}) \tag{4.23}$$

for $\alpha > 0$. This establishes the normalizability of $g(\omega)$ as long as ρ decays at most polynomially. $\qquad\square$

It is curious to note that the symplectic complement of the union of two disjoint half-infinite intervals may also be nontrivial. Consider, e.g., $I = (-\infty, t_0) \cup (t_1, +\infty)$ with $t_1 > t_0$. We can then choose $\varphi(t)$ in the above discussion to have support in (t_0, t_1).

In [172], it was argued that for a gauged quantum mechanical system with multiple matrices (which includes $\mathcal{N} = 4$ SYM theory on $\mathbb{R} \times S^3$) in the large N limit, the spectral function of a generic single-trace operator exhibits a complete spectrum for any nonzero 't Hooft coupling above the Hawking-Page transition temperature.

For large q SYK something more interesting happens: the spectral function has complete spectrum but exponential decay [316],[8] so equation (4.22) is generically violated for a test function with asymptotics of the form (4.23). In order to construct a nontrivial relative commutant for a half-infinite time band, we would need to find stronger asymptotic bounds on the decay of $\tilde{\varphi}(\omega)$. The easiest would be for it to have exponential decay, but this is never possible for a test function vanishing on a half-infinite interval (because it is not holomorphic on any strip). Therefore it is not clear whether a relative commutant exists in that case, and if it does its structure is quite different from the one of a spectral density with decay slower than exponential. We leave a more thorough analysis of that case to future work. More generally we believe that our framework could be useful to investigate the SYK model away from the maximally chaotic regime, for example it would be interesting to relate our techniques to the recent results of [140].

---

[8]We thank Vladimir Narovlansky for communications on this point.

Systems with uncompact spatial directions

We now consider some examples of the boundary theory on $\mathbb{R}^{1,d-1}$.

A simplest example is a free massive field with mass m in the vacuum, whose spectral function was given in (4.15). In this case, the spectral function has a gap in the region $|\omega| < m$ for all $\vec{k}$. This means that the spectral function has a gap around $\omega = 0$. By Proposition 4.2.9, this implies that there is no stringy horizon (in particular, the infinite redshift property is not satisfied). However, the results of [387] (extended to polynomially growing spectral spectral density [388]), still imply that the depth parameter $\mathcal{T}$ is infinite.

For a CFT in the vacuum state, the spectral function of a single-trace operator has the form

$$\rho(\omega, \vec{k}) = C(-k^2)^{\nu}\theta(-k^2)(\theta(\omega) - \theta(-\omega)), \quad k^2 \equiv -\omega^2 + \vec{k}^2 . \qquad (4.24)$$

For each given $\vec{k}$, there is a gap in the spectrum for $\omega^2 < \vec{k}^2$. The gap vanishes in the limit $\vec{k} \to 0$. In the case, the bulk is given by the Poincare patch of empty AdS. There is a Poincare horizon there related to the vanishing of the gap in the $\vec{k} \to 0$ limit.

In AdS-Rindler, the spectral function at fixed momentum has the same form as the one of BTZ, except now there is a continuum of momenta. Therefore the depth parameter is infinite, as expected because the bulk is semiclassical.

Consider the spectral function of a scalar glueball in free Yang–Mills theory at finite temperature. It is found in [229] that the spectral function is continuous and does not vanish outside of an interval. Therefore, following [387], the depth parameter should be infinite and there is a half-sided inclusion.

Another interesting case is the one of the large N limit of symmetric product orbifolds. The bulk theory is thought to be far from regular general relativity on a fixed spacetime, however we were made aware of the work [46], which shows that at least for some specific probes, spectral densities are the ones of the BTZ black hole, suggesting an infinite depth parameter and an emergent stringy horizon. We believe understanding this case in more detail could be particularly insightful.

Characterization of stringy connectivity: Einstein–Rosen algebra

We now focus the case of the thermofield double when $\mathcal{T} = \infty$. In that case, there is stringy connectivity between two sides. As we discussed earlier, with $\mathcal{T} = \infty$ alone,

what connects the left and right systems may not qualify as a bifurcate horizon. We will thus refer to it as a stringy "Einstein-Rosen bridge." In this section, we will construct an algebra of observables associated with an Einstein-Rosen bridge.

We will need the extra assumption that to each open interval I of $\mathbb{R}$ one can associate not only a von Neumann algebra M_I, but also a weak operator dense C^*-algebra $\mathcal{A}_I$ (this is clearly true in the case of generalized free fields, where one can simply consider the Weyl C^*-algebra of operators constructed out of the real symplectic structure on the one particle Hilbert space). Denoting $\mathcal{A} = \mathcal{A}_\mathbb{R}$, we also assume that $\bigcup_t \mathcal{A}_{(-t,t)}$ is norm-dense in $\mathcal{A}$. We now define a notion of *Einstein–Rosen sequence* (ER sequence), which will allow us to define an algebra attached to a stringy Einstein-Rosen bridge. We will call this algebra an Einstein-Rosen algebra (ER algebra) or with a slight abuse of language, horizon algebra.

Definition 4.2.14. Let $\mathcal{A}$ be the C^*-algebra generated by single-trace operators of one boundary and let (A_n) be a sequence of operators in $\mathcal{A}$. (A_n) is said to be an *ER sequence* if it is bounded in norm, and for all $t \in \mathbb{R}$, $A_n \in \mathcal{A}'_{(-t,t)}$ except for a finite number of terms.

In order to define a good notion of ER algebra, we first need to introduce one piece of machinery known as ultrapowers and central sequences.

Definition 4.2.15. The ultrapower algebra $\mathcal{A}^\omega$ of a C^*-algebra $\mathcal{A}$ at a free ultrafilter ω is defined to be the quotient of the space of bounded sequences valued in $\mathcal{A}$ by the space of sequences valued in $\mathcal{A}$ that converge towards a central element (in norm).

Definition 4.2.16. A central sequence (X_n) in a C^*-algebra $\mathcal{A}$ is a bounded sequence of operators (X_n) satisfying, for all $A \in \mathcal{A}$,

$$\| [X_n, A] \| \underset{n \to \infty}{\longrightarrow} 0. \tag{4.25}$$

We can now first show:

Proposition 4.2.17. *ER sequences are central sequences.*

Proof. Let $A \in \mathcal{A}$, let $\varepsilon > 0$. There exists $T \in \mathbb{R}$ and $A_T \in \mathcal{A}_{(-T,T)}$ such that

$$\| A - A_T \| < \varepsilon. \tag{4.26}$$

Moreover for n large enough A_n commutes with A_T, so that

$$\|[A_n, A]\| \leq 2\varepsilon \|A_n\|. \tag{4.27}$$

Since (A_n) is bounded in norm we conclude that (A_n) is a central sequence. $\qquad \square$

Of course, not all central sequences are ER sequences! For example, a sequence of modular flowed operators in a strongly coupled large N CFT would be central, but not an ER sequence.

We now define the ER algebra as

Definition 4.2.18. Let ω be a free ultrafilter. The ER algebra is the (C^*-closure of) the algebra of ER sequences inside $\mathcal{A}^\omega$, up to trivial ones.

By the above proposition, the ER algebra is a C^*-subalgebra of the C^*-algebra of central sequences $\mathcal{A}_\omega = \mathcal{A}' \cap \mathcal{A}^\omega$. In principle, it depends on a choice of free ultrafilter.

The reader can reasonably wonder at this stage why we chose to define the ER algebra at the C^*-level rather than at the von Neumann algebra level. The reason is that the analogous notion of central sequence at the von Neumann level which is known as the *asymptotic centralizer*, is not compatible with the physics of our setup. More precisely, given a normal state φ on a von Neumann algebra M, a sequence (X_n) of observables in a M is said to be part of the asymptotic centralizer of φ if

$$\|\varphi(X_n \cdot) - \varphi(\cdot X_n)\|_{M_*} \underset{n \to \infty}{\to} 0. \tag{4.28}$$

The convergence in (4.28) must happen for the norm topology in the Banach space of linear functionals on M. What this means is that the rate of convergence of $\varphi(X_n A) - \varphi(A X_n)$ towards zero must be *independent* of the choice of A. But this is clearly not the case for a sequence X_n of operators whose support approaches ER bridge: the closer A is to it, the longer it will take for $\varphi(X_n A) - \varphi(A X_n)$ to converge towards zero. Therefore we need a notion of central sequence that allows for dependence on the operator A, and this is provided by the definition at the C^*-level. The price to pay is that the ER algebra is only made of sequences of operators that are in the C^*-closure of the space of local observables, rather than the von Neumann closure which is larger.

Another question is whether the left and right ER algebras detect "the same geometric object." One way to check this is to ask whether the commutant of the algebra
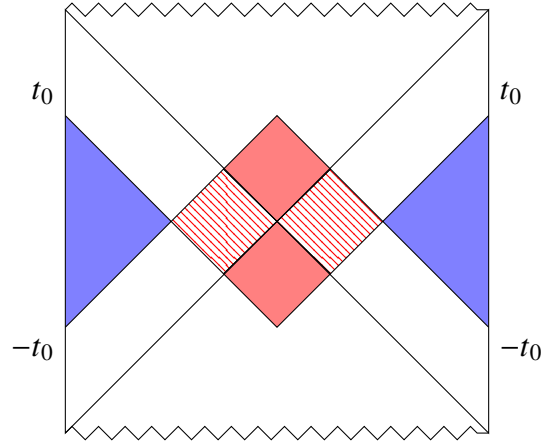
Figure 4.7: Equivalence between the right and left definitions of the ER algebra in the thermofield double state. The holographic duals of the left and right time bands, represented in blue, are related to each other by modular conjugation. The relative commutants of each time band inside the left and right algebras, each carrying red dashed lines, generate the commutant of the two algebras, filled in red. As $t_0 \to \infty$, the three diamonds all collapse onto the bifurcate horizon.

generated by two boundary time bands shrinks to a trivial algebra as the width of the time bands goes to infinity. If it does, then there are no observables between the right and left ER bridges and they coincide. See Figure 4.7. We expect this to be generically true in the thermofield double state, where the full algebra of a single boundary in the large N limit is generated by single-trace operators. In the next section, we will see that in more general states however, there may be more large N operators, such as modular flowed ones, and that the presence of these large N operators can alter the definition of stringy connectivity.

Generalized entropy of a stringy horizon

So far, our framework allows to detect whether or not there is an emergent stringy bifurcate horizon in the bulk, but it does not allow yet to talk about the "area" of this horizon, or any related measure that it could be equipped with. A full resolution of this problem is beyond the scope of this chapter, but here we make the remark that it is at least possible to define the difference between the generalized entropy of an excited state of the CFT and the general entropy of the thermofield double. Indeed, by Wall's proof of the generalized second law [450], we know that at strong coupling, if $|\psi\rangle$ is an excitation of the TFD state $|\text{TFD}\rangle$, the difference in generalized entropies between the entropy of the full bulk subregion and the entropy at infinity

is given by

$$S_{gen}(\infty) - S_{gen}(b) = S(\psi|\text{TFD}), \tag{4.29}$$

where the right hand side is the relative entropy. It is therefore natural to promote this formula to a *definition* of the difference between the generalized entropy of our state for the full subregion and its generalized entropy at infinity.

In the case in which the state $|\psi\rangle$ is a coherent excitation of $|\text{TFD}\rangle$ of the form $W(f)|\text{TFD}\rangle$ in a $(0+1)$-D GFF theory, where f is in the one particle Hilbert space and $W(f)$ is the corresponding Weyl operator, there is an explicit formula due to [108, 75], which gives:

$$S(\psi|\text{TFD}) = \int d\omega \theta(\omega) \frac{\omega}{1 - e^{-\beta\omega}} |f(\omega)|^2. \tag{4.30}$$

Violations of the equivalence principle in the stringy regime?

As discussed in the Introduction section, in the stringy regime, different bulk fields may "see" different bulk geometries. The causal depth parameter $\mathcal{T}$ can be used to probe this phenomenon.

In a large N gauge theory like $\mathcal{N} = 4$ SYM, there are infinitely many generalized free fields. To each of these fields, one can associate a depth parameter. If there is an emergent semiclassical bulk geometry, the large N spectral densities must somehow conspire so that the depth parameter associated to each large N field is the same. Any pair of fields whose depth parameters $\mathcal{T}_1$ and $\mathcal{T}_2$ are not equal cannot be seen as living on the same bulk geometry, as the corresponding depths are different. Therefore such a pair of fields can be seen as giving an obstruction to the validity of the equivalence principle in the bulk.

In the case of empty AdS or thermal AdS, there is a quite general argument ensuring that $\mathcal{T}$ is the same for all fields, as we have seen in Sec. 4.2. This means that there is a somehow universal notion of "bulk depth" at large N in the vacuum and a low temperature thermofield double state, even at finite 't Hooft coupling. However, going away from the vacuum or the thermofield double, one can imagine more general backgrounds in which the equivalence principle may be violated.

For the thermofield double state above the Hawking-Page temperature, we have argued a bifurcate horizon exists for all generalized fields. However, do horizons for different fields coincide? At the moment, we do not have a direct way to answer this question, and will just make some general remarks. The thermofield double

state has a left-right reflection symmetry, which enables us to establish in Sec. 4.2 that the left and right horizons for each field coincide. Therefore, if there is a notion of stringy geometry for all fields (although the effective metric may be different for different fields), then the horizons should sit in the middle of that spacetime, and thus coincide.

Another possible avenue for probing the coincidence of the horizons is to examine how the notion of a common horizon for all fields may become blurry due to potential failures of the split property for algebras describing all bulk fields at finite string length. Indeed, the presence of higher spin fields in the bulk theory leads to nonlocalities that may be related to the failure of the split property [168], or of the closely related modular nuclearity condition [90]. Perhaps relatedly, it is known that when introducing interactions between the large N fields, the notion of entanglement wedge becomes blurry in the stringy regime where the out-of-time-ordered correlator gets a submaximal Lyapunov exponent [97].

Finally, as it will be discussed more in the last section, given a spectral function, we can in principle reconstruct the bulk geometry using methods from inverse scattering theory. That may enable a direct comparison.

4.3 Algebraic diagnostic of QES

The definition of causal depth parameter and the algebraic diagnostic of an event horizon discussed in the last section were motivated from the bulk causal structure in the semi-classical gravity regime. We then used that data as inspiration to probe/define the bulk causal structure in the stringy regime. In this section we would like to generalize the discussion of the previous section by introducing an algebraic diagnostic for the existence of Ryu-Takayanagi (RT) surfaces [401, 242] or more generally quantum extremal surfaces (QES) [162].

The question becomes more difficult as QES are not directly related to the bulk causal structure, which makes them harder to probe. However, the case of the thermofield double, where the bifurcate horizon coincides with the RT surface for the R system, suggests a path forward.

For the thermofield double, the procedure discussed in Sec. 4.2 can also be viewed as diagnosing the possible existence of a particular asymptotically invariant sub-manifold under the modular flows of the boundary algebra $\mathcal{M}_R = \mathcal{S}_R$ for the CFT$_R$, represented with a red dot on Fig. 4.8.[9] This manifold has the following properties

---

[9]It is an asymptotically fixed submanifold as operators localized on the bifurcate horizon do not

in terms of modular data:

1. The Schwarzschild time flow becomes a boost near the bifurcation surface, which leaves the surface invariant.

2. The Schwarzschild time flow is identified with the boundary time flow, which is in turn identified with the modular flows.

3. While both the red and blue dots of Fig. 4.8 are asymptotically invariant submanifolds of the boundary time flows, the ER sequences defined in Sec. 4.2 from the relative commutants of time bands only approach the red dot. Recall that given any finite time band, except for a finite number of terms, an ER sequence $\{A_n\}$ lies in its commutant. In contrast, this is not the case for any sequence approaching the blue dots.

This perspective can now be used to diagnose the possible existence of a QES by *defining* a QES as an asymptotically invariant submanifold under the modular flows of the corresponding boundary algebra, in the sense captured by the three properties above.

We can thus apply the constructions of Sec. 4.2 to construct a good notion of QES in the stringy regime by simply replacing time bands by *modular time* bands. Below we first review aspects of the algebraic formulation of entanglement wedge reconstruction of [295] that will be used in our discussion. We then present our proposal for an algebraic diagnostic of QES that can also be applied to the stringy regime, and discuss some examples. In particular, the proposal gives a possible solution to a question raised in [155] concerning evaporating black holes. We also make comments on a possible generalization of the algebraic notion of ER=EPR discussed in [155] to the stringy regime.

Modular depth parameter and QES from modular time bands

Before stating our proposal for diagnosing the presence of a QES for a boundary subregion algebraically, we first review some elements of the algebraic formulation of entanglement wedge reconstruction that are essential for our discussion.

For a system in a semi-classical state $|\Psi\rangle$ describing some bulk geometry, entanglement wedge reconstruction says that physics in the entanglement wedge of a

---

belong to the boundary algebra $\mathcal{M}_R = \mathcal{S}_R$ for the CFT_R. In fact, since operators always need to be smeared in the time direction, there are no well defined operators localized on the bifurcate horizon.
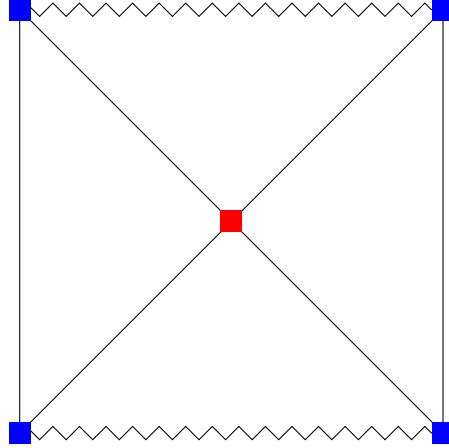
Figure 4.8: Fixed points of modular flow in the Penrose diagram of an AdS-Schwarzschild two-sided black hole. The red dot denotes the QES and the blue dots denote timelike infinity on the boundary. The algebraic difference between the red dot and the blue dots is that the red dot is inside the commutant of all double-sided time band algebras, which is not the case for the blue dots.

boundary *spatial* subregion A can be fully described by observables in A. The entanglement wedge is given by the domain of dependence $\hat{\mathfrak{b}}_A$ of a bulk co-dimension one region $\mathfrak{b}_A$ satisfying $\phi \mathfrak{b}_A = \gamma_A \cup A$ where γ_A denotes the QES for A. On the boundary, denote the large N limit of the local operator algebra $\mathcal{B}_A$ in A by $\mathcal{X}_A$. Entanglement wedge reconstruction can be stated algebraically as

$$\widetilde{\mathcal{M}}_{\mathfrak{b}_A} = \mathcal{X}_A \tag{4.31}$$

where $\widetilde{\mathcal{M}}_{\mathfrak{b}_A}$ is the bulk operator algebra for $\mathfrak{b}_A$. Equation (4.31) means that any bulk operations in $\hat{\mathfrak{b}}_A$ can be expressed in terms of those in $\mathcal{X}_A$. We assume that $|\Psi\rangle$ is cyclic and separating with respect to $\mathcal{B}_A$, and denote the corresponding modular operator by Δ.

Some of our statements will be conditioned on the following assumptions, which all hold in the semiclassical gravity regime:

1. The QES γ_A is an asymptotically invariant submanifold under modular flows generated by Δ.

   This statement comes from the expectation that near γ_A modular flows generated by Δ should act as local boosts.

2. $\mathcal{X}_A$ can be generated by single-trace operators in A via modular flows. More explicitly, $\mathcal{X}_A$ is generated by large N limits of operators of the form

$$\phi(s, \vec{x}) = \Delta^{-is} \phi(\vec{x}) \Delta^{is}, \quad s \in \mathbb{R}, \ \vec{x} \in A \tag{4.32}$$

where ϕ is a single-trace operator. This statement follows from the arguments of [254, 166] in the strongly coupled regime.

3. Haag duality survives the large N limit, i.e.,

$$\mathcal{X}'_A = \mathcal{X}_{\bar{A}}. \tag{4.33}$$

This is guaranteed in the strongly coupled regime by entanglement wedge reconstruction/complementary recovery [142].

Note that while we will use assumption 1 essentially as a definition for our notion of stringy QES, assumptions 2 and 3 are not guaranteed to hold true in the stringy regime. In particular, assumption 2 not being true would signal the existence of more exotic large N observables than large N modular flows, while a breakdown of assumption 3 would signal a breakdown of complementary recovery. We leave a more thorough analysis of these assumptions to the future.

Consider an open *modular* time interval $I = (-s_0, s_0)$, and denote the subalgebra generated by $\phi(s, \vec{x})$ of (4.32) with $s \in I$ as $\mathcal{X}_I$. By definition, $\mathcal{X}_I \subseteq \mathcal{X}_A$. We can then define the modular depth parameter associated with A as follows.

Definition 4.3.1. The modular depth parameter $\mathcal{T}_m(A)$ associated with a boundary region A is the largest value of s_0 for which the algebra $\mathcal{X}_{(-s_0, s_0)}$ has a nontrivial relative commutant inside $\mathcal{X}_A$.

We now would like to characterize the existence of a nonempty QES at the boundary of the entanglement wedge. The existence of such a nonempty QES can be understood as a statement of connectivity between the entanglement wedge and its complement. Therefore it makes sense to reproduce the definition of stringy connectivity proposed in Section 4.2:

Definition 4.3.2. Suppose R and L systems are in an entangled pure state with a large N limit. We say that R and L are share a non-empty QES, or are stringy-connected, if the corresponding modular depth parameters are infinite.

Note that although this definition guarantees that the R and L systems have a QES, it is not clear whether this QES is the same by only making assumption 1 above. However, by adding assumptions 2 and 3 (i.e., that entanglement wedges can be generated by large N limits of modular flows and that Haag duality holds at large N in the bulk), one can show that there are no operators localized in between the right and the left QES, which means that they "coincide" in this sense. More formally:

Proposition 4.3.3. *If R and L systems have a non-empty QES, and assumptions 1, 2 and 3 are satisfied, then*

$$\bigcap_I (\mathcal{X}_I^L \vee \mathcal{X}_I^R)' = \mathbb{C}. \tag{4.34}$$

Proof.

$$\bigvee_I \left(\mathcal{X}_I^L \vee \mathcal{X}_I^R \right) = \mathcal{X}^L \vee \mathcal{X}^R = \mathcal{B}(\mathcal{H}), \tag{4.35}$$

so by going to the complement,

$$\bigcap_I (\mathcal{X}_I^L \vee \mathcal{X}_I^R)' = \mathbb{C}. \tag{4.36}$$

□

The discussion of Sec. 4.2 can also be directly carried over by replacing $\phi(t)$ there by $\phi(s)$ of (4.32). The modular depth parameter and possible existence of a nontrivial QES can then be deduced from the behavior of the modular spectral function in a similar manner to the previous discussion. Note that just as before, this definition staightforwardly extends to the stringy regime, where potentially, different fields can see different entanglement wedges and quantum extremal surfaces. This could lead to at best, field-dependence, and at worst, an inconsistency in the definition of the entanglement wedge, and would be somewhat in line with hints [97] suggesting difficulties in defining the entanglement wedge universally in the stringy regime. We look forward to investigating the potential field-dependence of stringy entanglement wedges in future work.

Now consider some simple examples.

Suppose A is a proper subregion on a boundary Cauchy slice. The entanglement wedge is a proper subregion in the bulk and has a nontrivial QES γ_A. Given that modular flows are expected to act as local boosts near γ_A, we deduce that the "single-particle" modular spectral function should have a complete spectrum, and from the

discussion of Sec. 4.2, the modular depth parameter is ∞. We can generalize this discussion to the stringy regime. Suppose the modular depth parameter for A remains infinite at finite λ, we can then say the QES survives finite α' corrections.

Now consider a two-sided semi-classical state corresponding to the long wormhole shown on Figure 4.6 (a). For simplicity, we will suppose that the bulk spacetime is time-reflection symmetric, and consider A to be the full right boundary on the time-reflection symmetric Cauchy slice. By using nested time bands of single-trace operator algebras defined in Sec. 4.2, we can probe the existence of the causal horizon. In this case there is a nontrivial QES lying outside the horizon, which can be probed by nested modular time bands. So in this case both the causal depth parameter $\mathcal{T}_c$ and the modular depth parameter $\mathcal{T}_m$ are infinite. The fact that the QES lies outside the horizon is reflected in the fact that $\mathcal{S}_R$ has a nontrivial relative commutant inside $\mathcal{X}_R$. Thus the larger the algebra, the deeper we can probe into the bulk, even though we cannot directly compare $\mathcal{T}_c$ and $\mathcal{T}_m$, and both are infinite. At finite λ, we can also use the time bands of $\mathcal{S}_R$ and modular time bands of $\mathcal{X}_R$ to define the stringy horizons and QES. That one probes "deeper" than the other again follows from the proper inclusion of one algebra into the other.

Algebraic ER=EPR in the stringy regime?

In [155], an algebraic version of ER=EPR was proposed in the semiclassical regime to characterize spacetime connectivity with the algebras of the boundary theory. Here we consider the possible extension of this proposal to the stringy regime. In particular, we discuss the subtle relationship between the value of the modular depth parameter and the type of the underlying von Neumann algebra.

Consider first the $\lambda \rightarrow \infty$ limit, and a two-sided pure state with a *classical* dual spacetime M. Suppose $\mathcal{X}_R, \mathcal{X}_L$ are respectively operator algebras of CFT_R and CFT_L in the large N limit. Then the algebraic ER=EPR proposal says that M is:

1. is disconnected iff $\mathcal{X}_R$ and $\mathcal{X}_L$ are both type I. $\hspace{2em}$ (4.37)

2. has a classical wormhole connecting R to L iff $\mathcal{X}_R$ and $\mathcal{X}_L$ are both type III. (4.38)

It would be desirable to generalize the proposal to the stringy regime.

In establishing (4.37)–(4.38) in the algebraic ER=EPR proposal for a classical spacetime [155], it was assumed that the entanglement wedges of the R and L systems are themselves classical spacetime manifolds. Such an assumption can no longer be made in the stringy regime. For example, in the case of the IOP model,

we see that despite the boundary algebra being type III_1, the depth parameter[10] vanishes. While the IOP model may not be dual to a string theory,[11] this example highlights that in general type III_1 by itself does not imply $\mathcal{T}_m = \infty$. Additional physical inputs may be needed to specify what kind of boundary systems are dual to a string theory.

We may also ask the converse mathematical question: does $\mathcal{T}_m = \infty$ imply type III_1?

Again, the answer is no. The reason is that there are some exotic forms of the modular spectral density that lead to an infinite depth parameter while the von Neumann algebra still has type I. In the thermofield double state at inverse temperature β, a necessary and sufficient condition for the large N algebra to be type I is that the operator γ_β on $L^2(\mathbb{R}, \Theta(\omega)\rho(\omega)d\omega)$ defined by

$$\gamma_\beta f(\omega) := e^{-\beta\omega} f(\omega) \tag{4.39}$$

is trace-class [137, 200], i.e., that the support $\{\omega_i\}$ of ρ is discrete and

$$\sum_i e^{-\beta|\omega_i|} < \infty. \tag{4.40}$$

Theorem 3 of [387] shows that it is possible to have Equation (4.40) hold true while having $\mathcal{T} = \infty$. For an explicit example, we can again consider the "primon gas" or "Riemannium" at low temperature, which we saw in 4.2 has depth parameter $\mathcal{T} = \infty$. It has an exponentially growing spectral support but still gives rise to a type I von Neumann algebra at low enough temperature [74]. In this case,

$$\mathrm{Tr}\,\gamma_\beta = \sum_n e^{-\beta \ln p_n} = \sum_n p_n^{-\beta}, \tag{4.41}$$

where p_n denote the nth prime number. This series is convergent at low enough temperature, for $\beta > 1$. So at low enough temperature, we are in a case in which even though the von Neumann algebra is type I, we have $\mathcal{T} = \infty$.

Evaporating black holes: differentiating type III_1 algebras before and after the Page time

In this subsection we give another application of the modular depth parameter by showing how a question raised in [155] about spacetime connectivity for an

---

[10] In that example, modular and causal depth parameters coincide.

[11] In particular it does not have the analogous $\lambda \to \infty$ limit that is dual to the semi-classical gravity regime.
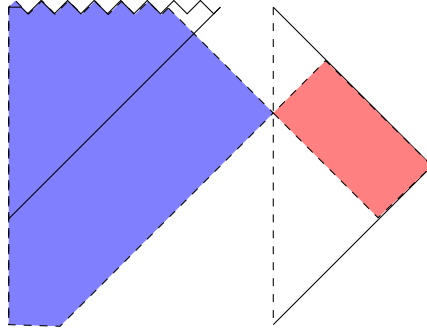
(a) An evaporating black hole shortly before the Page time. The entanglement wedge of the bath of radiation, denoted in red, is disconnected from the entanglement wedge of the black hole denoted in blue: they do not share any nontrivial quantum extremal surface.
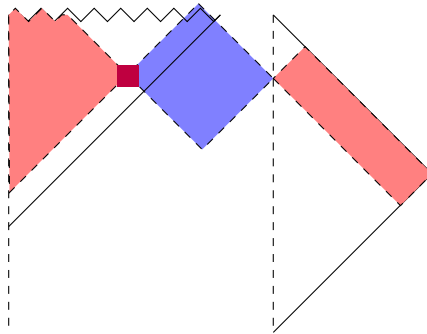
(b) An evaporating black hole shortly after the Page time. The entanglement wedge of the bath of radiation, denoted in red, is now connected to the entanglement wedge of the black hole denoted in blue: they do share a quantum extremal surface represented by the purple dot.

Figure 4.9: An evaporating black hole shortly before and shortly after the Page time. In both cases, the algebra of observables describing the interior has type III_1, however it is only after the Page time that a QES creates connectivity between the entanglement wedge of the radiation and the entanglement wedge of the black hole.

evaporating black hole system can in principle be addressed using the techniques developed in this chapter.

Consider an evaporating black hole system in AdS as discussed in [155]. Shortly before the Page time, the QES for the boundary CFT (i.e., taking A to be a full boundary Cauchy slice) is empty and the black hole (B) is seemingly disconnected from the radiation (R), whereas shortly after the Page time, the QES is nontrivial and the black hole is classically connected with the radiation. See Fig. 4.9.

On both sides of the Page time, the corresponding boundary algebra $\mathcal{X}_B$ for the black hole subsystem has been argued to be type III$_1$. Thus it appears to provide a counterexample to (4.38).

It is not a counterexample, as in this case the dual bulk spacetime is not classical, but quantum volatile[12]—the volume of the black hole interior grows to infinity in the $G_N \rightarrow 0$ limit. It was accordingly argued in [155] that, before the Page time, B and R are quantum connected. However, it was not clear how to distinguish directly the classical connectivity after the Page time from the quantum connectivity before the Page time intrinsically from the structure of the boundary algebra $\mathcal{X}_B$.

We propose that the modular depth parameter can diagnose this change of connectivity, with $\mathcal{T}_m < \infty$ before the Page time, and $\mathcal{T}_m = \infty$ after the Page time. That $\mathcal{T}_m = \infty$ after the Page time follows simply from existence of a non-empty QES. We now outline an argument for $\mathcal{T}_m < \infty$ before the Page time. Since currently we cannot calculate the modular spectral function for $\mathcal{X}_B$ explicitly, the argument we present below should be only viewed as a plausibility argument.

Before the Page time, the entanglement wedge of the boundary includes the interior of the black hole which has an infinite proper length in the $G_N \rightarrow 0$ limit. If it were possible to probe this region using light rays, we would have concluded that the depth parameter should be infinite. We now argue that in terms of the modular depth parameter, it can in fact be finite.

To illustrate the main idea, we will use a simple model. Consider a $(1 + 1)$-dimensional (nonrelativistic) free field theory of a scalar field Φ defined on an infinite half line with boundary at $x = 0$. Consider a localized excitation of the bulk, say by a bump function f_0 localized on a small interval of a one-dimensional time slice $t = 0$ (at infinite volume), of the form

$$\Phi(f) = \int_{-\infty}^{0} dx \, f(x)\Phi(x), \quad f \in L^2(\mathbb{R}_-) . \tag{4.42}$$

Importantly, we allow f to be complex-valued, so that $\phi(f)$ is in general a linear combination of two selfadjoint fields that can be interpreted as position and momentum. We have the commutation relation

$$[\phi(f), \phi(g)] = i \, \text{Im} \, \langle f, g \rangle \, Id. \tag{4.43}$$

---

[12] In a quantum volatile spacetime, one or both of the following are violated in the $G_N \rightarrow 0$ limit: (i) fluctuations of diffeomorphism invariants go to zero as $O(G_N^a)$ for some $a > 0$; (ii) spacetime diffeomorphism invariants such as volumes, areas, and lengths do not scale as $O(G_N^{-a})$ with $a > 0$.

As a toy model, suppose that the bulk modular Hamiltonian can be modelled on the one particle Hilbert space $L^2(\mathbb{R}_-)$ by some selfadjoint operator H. Then in the second quantized picture, the operator $\phi(f)$ is evolved at time t into the operator $\phi(f_t)$, where $f_t(x)$ is the value of the solution $f(x, t)$ to the Schrödinger equation

$$i\partial_t f = Hf, \tag{4.44}$$

with initial condition

$$f(x, 0) = f_0(x). \tag{4.45}$$

Out of this data, we can construct a generalized free field theory in $0+1$ dimensions, as follows. First, define an antisymmetric function of time

$$\rho(t) := \langle [\phi(f_t), \phi(f_0)] \rangle_\beta = i \operatorname{Im} \langle f_t, f_0 \rangle. \tag{4.46}$$

Then construct a generalized free field theory at finite temperature in the same way as in Section 4.2, from this spectral function. We want to show that for a physically reasonable choice of Hamiltonian H, $\mathcal{T} < \infty$.

As a toy example, we can choose H to be the Hamiltonian of a one-dimensional quantum harmonic oscillator. Since the odd eigenfunctions of the harmonic oscillator form a basis of $L^2(\mathbb{R}_-)$, for any choice of $f_0 \in L^2(\mathbb{R}_-)$, we can decompose

$$f_0 = \sum_{n \in 2\mathbb{N}+1} \lambda_n \psi_n, \tag{4.47}$$

where the ψ_n are the harmonic oscillator eigenfunctions of energy $(n + \frac{1}{2})\omega_0$. As a result, $\rho(t)$ is of the form

$$\rho(t) = \sum_{n \in \mathbb{Z}} \mu_n e^{i\left(n+\frac{1}{2}\right)t}, \tag{4.48}$$

which means that in frequency space it is an evenly spaced linear combination of Dirac deltas. Therefore it is periodic up to a phase, and we deduce that the depth parameter $\mathcal{T}$ for this generalized free field is finite (and smaller than 2π).

While modular flows are nonlocal, it may still sound surprising that it can give a finite modular depth for an infinite proper length.

Heuristically, we do not expect the structure of modular flow outside the black hole to significantly differ from the one of the thermofield double state. In the exterior region, we expect that operators can be reconstructed from "simple" single trace

operators on the boundary with good accuracy, and in particular that at least for reasonably small time scales, the modular flows of these operators can be approximated by boundary time evolution of these single trace operators. But modular flow on operators in the interior significantly differs from a thermofield double. These operators are complex and cannot be reconstructed solely from boundary single traces: we also need large N limits of boundary modular flows. On these operators, modular flow can potentially act very differently from boundary time evolution. Hence, outside the black hole we expect operators to propagate under modular flow following (approximately) relativistic laws (in particular, with finite speed), but close enough to the interior, modular flow is so different from any geometric transformation that it could in principle allow for a modular Hamiltonian that is nonlocal enough that it guarantees that the value of $\mathcal{T}$ is finite.

4.4 Discussion

In this chapter, we have taken a first step towards developing a new language to describe causal structure, event horizons, and quantum extremal surfaces (QES) for the bulk duals of boundary systems that extend beyond the standard Einstein gravity regime. Here we comment on some future directions.

1. **Connections between geometric concepts and the ergodic hierarchy/quantum chaos**

   In this chapter we introduced the depth parameter $\mathcal{T}$ by considering the inclusion structure of time band algebras on the boundary. We commented earlier that the depth parameter has an interpretation in terms of ergodicity, in the sense that it encodes how long one needs to wait in order to obtain full information about the large N theory.

   We also defined horizons in terms of half-sided inclusion, which is related to a stronger notion of ergodic or quantum chaotic behavior.

   As recently discussed in [191, 367], there are various other possible levels of ergodicity and chaos in a system, beyond those corresponding to the depth parameter and half-sided modular inclusion. It would be interesting to understand whether they can be associated with emergent bulk geometric structure. Conversely, bulk geometric structures could give inspirations for formulating a mathematical theory of quantum chaos, which is still at early stages.

2. **Structure of higher-point functions**

The structures discussed in this chapter can be deduced with the knowledge of boundary two-point functions. Exploring the structure of higher-point functions could lead to new insights into the non-locality brought by possible violation of equivalence principle mentioned earlier.

Furthermore, at the level of Einstein gravity, the presence of a black hole event horizon leads to universal behavior in out-of-time-ordered correlators (OTOCs) [413], and maximal value of the quantum Lyapunov exponent [315]. Going to the stringy regime, OTOCs involve exchanges of an infinite tower of higher-spin stringy excitations, which gives rise to non-maximal chaos [414]. It would be interesting to understand whether such behavior can still be attributed to a stringy horizon.

3. **Connection to the inverse spectral problem**

The question we are asking here is closely related to the so-called inverse spectral problem. The basic idea is the following. In an asymptotically AdS spacetime, the equation of motion for a free field reduces to a Schrödinger equation in the radial variable, with some potential $V(r)$ dictated by the geometry. The standard formulation of the inverse scattering problem is to ask, given the scattering data for the solutions of the Schrödinger equation, how one may reconstruct the potential $V(r)$.

In our context, the scattering data corresponds to the correlation functions of the boundary generalized free fields, while the potential $V(r)$ would correspond to a "stringy geometry" in the bulk. There is a general approach to the inverse spectral problem, due to Gelfand and Levitan [188], which allows to recover quite explicit results on $V(r)$ given the scattering data. Interestingly, Gelfand–Levitan theory is intimately related to the exponential type problem in harmonic analysis, which we saw that in our context, maps to the determination of the depth parameter $\mathcal{T}$. Therefore it is likely that the ideas introduced here could find a very natural place within Gelfand–Levitan theory, and that understanding how these ideas fit together could teach us more about emergent stringy geometries, especially about modular Hamiltonians of time bands, quasi-normal modes of stringy black holes, and maybe even a description of stringy singularities. We hope to report on this connection in the near future.

4. **Towards a stringy QES formula**

In this work, we were able to construct an algebra of sequences to describe stringy bifurcate horizons. What we are still lacking is some notion of measure on this algebra that could give us information on a stringy notion of "area" of the bifurcate horizon. Coming up with such a notion would open a path towards a possible derivation of a Ryu–Takayanagi/QES formula at nonzero string length.

The operator algebraic language has already proven to be useful in order to understand gravitational entropy, in particular the works [457, 100, 101, 261, 286] on the crossed product have allowed to define a type II entropy that agrees with the semiclassical notion of generalized entropy up to an overall constant. However, this semiclassical notion does not provide any meaningful way of constructing an area term, as the type II entropy is only defined up to a constant. So far, the only meaningful notion of area term in the operator algebraic context have been formulated by mapping the large N theory to the finite N theory through an approximate quantum error correcting code [168, 192]. It is our hope that the methods introduced here may be relevant to define a notion of area term directly at large N, for arbitrary values of the string length, that contributes to gravitational entropy together with the entropy of bulk fields. We expect that such a setup could also provide new insight into the exchange ambiguity between the bulk entropy term and the area term [430, 192].

5. **A new language for stringy spacetime?**

Our results suggest that the algebraic framework is capable of retaining properties that one expects from an emergent spacetime even in a potentially very stringy regime where this spacetime is not described by the usual notion of smooth differentiable Lorentzian manifold. In particular, it appears that the algebraic structure allows to describe the causal structure of this stringy spacetime through the observables that live on some of its subregions.

The idea of describing geometric spaces through the objects that live on their subregions has been extremely fruitful in mathematics, and is at the core of most of modern geometry. In topology, this is exemplified by Gelfand duality, which describes a space by its algebra of functions, while in algebraic geometry this is for example achieved by the notion of sheaf (and actually one can see many of the constructions in algebraic quantum field theory through this lens). It would be very interesting to see how far this idea can

be pushed in our context, and find whether one can *define* the subregions of a stringy spacetime only through the algebras of observables that live on its subregions and their embeddings. This way of defining a space directly through the algebras that characterize its subspaces is somewhat reminiscent of the notion of topos, due to Grothendieck. A hint that such an approach to stringy geometry may be possible is that von Neumann algebras and their commutants on a Fock space already come equipped with a structure: that of a complemented complete lattice [137], which is reviewed in Appendix 4.6. In particular we can construct a set of real symplectic subspaces $\mathcal{V}_i$ of the large N one particle Hilbert space, stable generation, intersection and symplectic complement, and associated von Neumann algebras $\mathcal{M}(\mathcal{V}_i)$, such that

Theorem 4.4.1.

$$\mathcal{M}(\mathcal{V}_1) = \mathcal{M}(\mathcal{V}_2) \text{ iff } \mathcal{V}_1 = \mathcal{V}_2, \tag{4.49}$$

$$\mathcal{V}_1 \subset \mathcal{V}_2 \Rightarrow \mathcal{M}(\mathcal{V}_1) \subset \mathcal{M}(\mathcal{V}_2), \tag{4.50}$$

$$\mathcal{M}\left(\bigvee_i \mathcal{V}_i\right) = \bigvee_i \mathcal{M}(\mathcal{V}_i), \tag{4.51}$$

$$\mathcal{M}\left(\bigcap_i \mathcal{V}_i\right) = \bigcap_i \mathcal{M}(\mathcal{V}_i), \tag{4.52}$$

$$\mathcal{M}(\mathcal{V})' = \mathcal{M}(\mathcal{V}'), \tag{4.53}$$

and $\mathcal{M}(\mathcal{V})$ is a factor iff $\mathcal{V} \cap \mathcal{V}' = \{0\}$.

This structure is ideal in order to retain a notion of causality, since the commutant operation (or the symplectic complement at the one particle level) can be understood as an operation mapping a region to its causal complement. What now remains to be seen is how much geometric structure can be put on top of this causal structure in the stringy regime – how close to a full-fledged Lorentzian manifold can we get?

4.5 Appendix: Elements of distribution theory

In this first appendix, we recall the basic points of distribution theory that are being used throughout the chapter. We particularly emphasize how one can take the Fourier transform of a distribution, as Fourier theory is the central element of our discussion.

Distributions and tempered distributions

Informally, distributions are a generalized notion of function that only makes sense *dually*. Consider the example of the real line. A natural space of functions on $\mathbb{R}$ would be the space of square-integrable functions $L^2(\mathbb{R})$. However, in some contexts one would like to be able to consider more general kinds of "functions" on $\mathbb{R}$, for example, discrete measures such as Dirac's delta, or oscillatory functions like $e^{i\omega t}$.

The issue is that such oscillatory functions, if defined at all, are definitely not square-integrable. This issue is often encountered in quantum mechanics, for example when considering a free particle in one dimension. One would like to diagonalize the Hamiltonian in a "basis of Dirac deltas," but they are not part of the Hilbert space of $L^2(\mathbb{R})$. The well-known solution to this problem, which is sometimes referred to as "rigging" the Hilbert space, amounts to allow more general notions of wavefunctions by passing to a space of distributions.

The idea is the following. By the Riesz representation theorem, the Hilbert space $\mathcal{H} = L^2(\mathbb{R})$ is *reflexive*, which means that it is isomorphic to its topological dual. Therefore there are exactly as many continuous linear functionals on $\mathcal{H} = L^2(\mathbb{R})$ as there are elements of $\mathcal{H} = L^2(\mathbb{R})$. Therefore, if one wants to find a space of generalized functions that is larger than $L^2(\mathbb{R})$, a natural thing to do is to look at a *subspace* of $L^2(\mathbb{R})$, so that there are more continuous linear functionals on it than on $L^2(\mathbb{R})$.

The choice of such a subspace is nonunique, and leads to different notions of distributions. The most obvious choice of dense subspace of $L^2(\mathbb{R})$ is the space of compactly supported test functions $\mathcal{D}(\mathbb{R})$. It turns out that this space can be equipped with a topology, called the *inductive limit topology*, such that for this topology, the topological dual $\mathcal{D}'(\mathbb{R})$ of $\mathcal{D}(\mathbb{R})$ is strictly larger than $\mathcal{D}(\mathbb{R})$. In particular it contains Dirac deltas, and a large family of continuous functions. The space $\mathcal{D}'(\mathbb{R})$ is known as the space of *distributions* on $\mathbb{R}$.

Another interesting choice of dense subspace of $L^2(\mathbb{R})$ is the so-called *Schwartz space $\mathcal{S}(\mathbb{R})$*, of functions whose derivatives all decay faster than polynomially at infinity. There also exists a way to equip $\mathcal{S}(\mathbb{R})$ with a natural topology for which $L^2(\mathbb{R}) \subset \mathcal{S}'(\mathbb{R})$. In fact, we even have a stronger statement: as

$$\mathcal{D}(\mathbb{R}) \subset \mathcal{S}(\mathbb{R}) \subset L^2(\mathbb{R}), \tag{4.54}$$

we have

$$L^2(\mathbb{R}) \subset \mathcal{S}'(\mathbb{R}) \subset \mathcal{D}'(\mathbb{R}). \tag{4.55}$$

Therefore one can see the notion of tempered distribution as a refined notion of distribution, that is continuous on a larger space of test functions (all of Schwartz space). One of the main reasons why tempered distributions are useful is because they are the right kind of distribution to consider in order to take Fourier transforms, as we now review.

Fourier transforms of distributions

The classical formula for the Fourier transform,

$$\tilde{f}(\omega) := \int_{\mathbb{R}} f(t) e^{-i\omega t} dt, \tag{4.56}$$

is only well-defined on $L^1(\mathbb{R})$. However tempered distributions can be much more general. For example any continuous function with subexponential growth defines a tempered distribution. The point, however, is that the dual picture allows to define a notion of Fourier transform for any tempered distribution. The reason why we need the distributions to be tempered is because we need the space of test functions we choose to be stable under Fourier transform. As we point out now, this is obviously not true for compactly supported functions, but it is true for Schwartz space:

Proposition 4.5.1. *The Schwartz space $\mathcal{S}(\mathbb{R})$ is stable under Fourier transform.*

This result allows to write a definition for the Fourier transform of a general tempered distribution.

Definition 4.5.2. Let T be a tempered distribution on $\mathbb{R}$. We define the Fourier transform $\tilde{T}$ of the tempered distribution T as follows. For $f \in \mathcal{S}(\mathbb{R})$,

$$\tilde{T}(f) := T(\tilde{f}). \tag{4.57}$$

In general, the Fourier transform of a tempered distribution is a general tempered distribution, however, under some extra assumption on the tempered distribution, one can say additional things about the regularity of the Fourier transform. There are many results along this line, going from very easy ones to highly nontrivial results in harmonic analysis like the Beurling–Malliavin theorem or solutions to the type problem we will discuss in the next appendix. Here we give one of the most useful "easier" results of this type, namely an important part of the Schwartz–Paley–Wiener theorem:

Proposition 4.5.3. *The Fourier transform of a compactly supported distribution extends to an entire function on the complex plane.*

Pointwise product and convolution of distributions

Most of the time in this work, we reason in Fourier space on tempered distributions whose Fourier transforms are square integrable functions against a suitable measure, hence, it is usually not a problem to pointwise multiply the Fourier transforms. Nevertheless, it is worth pointing out that in general there is an obstruction to performing a pointwise product of distributions. For example, two Dirac deltas cannot be pointwise multiplied because they are all singular at the same point. It is therefore useful to ask when, in general, it is possible to define the pointwise product of distributions. It turns out that the answer relies on the notion of wavefront set, which we now define.

Definition 4.5.4. Let Ω be an open set in $\mathbb{R}^n$. Given a distribution $T \in \mathcal{D}'(\mathbb{R}^n)$, the wavefront set $WF(T)$ of T is defined to be the complement of the union of all conic subsets of T^*U on which T is smooth.

This definition extends straightforwardly to the case of manifolds. We then have the crucial property:

Proposition 4.5.5. *The pointwise product of two distributions T_1 and T_2 is well-defined unless there exists $(x, k) \in T^*U$ such that $(x, k) \in WF(T_1)$ and $(x, -k) \in WF(T_2)$.*

Similarly, since the convolution of two distributions requires mutiplying them pointwise, the notion of wavefront set is also relevant in order to define the convolution product of two general distributions.

4.6 Appendix: Generalized free field theory and review of a theorem of Araki

In this Appendix, we review the construction of the Hilbert space associated with a generalized free field theory around a semi-classical state, and then discuss a theorem of Araki [23] that is used in the main text.

Construction of a generalized free field theory

Consider a single-trace Hermitian operator $\phi(t)$ (again we suppress spatial dependence for notational simplicity), with spectral function

$$\rho(t - t') = \langle \Psi | [\phi(t), \phi(t')] | \Psi \rangle, \tag{4.58}$$

in a semi-classical state $|\Psi\rangle$. For simplicity we will assume that $|\Psi\rangle$ is time translation invariant. $\rho(t)$ and its Fourier transform $\rho(\omega)$ have the properties

$$\rho^*(t) = \rho(-t) = -\rho(t), \quad \rho^*(\omega) = \rho(\omega) = -\rho(-\omega), \quad \theta(\omega)\rho(\omega) \geq 0 . \tag{4.59}$$

Denote the Fourier transform of $\phi(t)$ as ϕ_ω, we have from (4.58) the commutation relations

$$[\phi_\omega, \phi_{\omega'}] = \rho(\omega) 2\pi \delta(\omega + \omega'), \quad \phi_{-\omega} = \phi_\omega^\dagger . \tag{4.60}$$

Introduce smeared operators

$$\phi(f) = \int dt\, f(t)\phi(t) \equiv \int \frac{d\omega}{2\pi} f(-\omega)\phi_\omega, \quad f(-\omega) = f^*(\omega), \tag{4.61}$$

where $f(t)$ is real such that $\phi(f)$ is Hermitian. $\rho(t)$ can be used to define a symplectic product (i.e., anti-symmetric between $f(t)$ and $g(t)$) in the space $\{f(t)\}$

$$(f, g) = -i\langle \Psi | [\phi(f), \phi(g)] | \Psi \rangle = -i \int dt dt'\, f(t)\rho(t-t')g(t') = -i \int \frac{d\omega}{2\pi} f(-\omega)\rho(\omega)g(\omega) . \tag{4.62}$$

We can also associate a complex vector $|f\rangle$ with $(f(\omega), \omega > 0)$ and introduce an inner product

$$\langle f, g \rangle = 2 \int \frac{d\omega}{2\pi} f^*(\omega)\, \theta(\omega)\rho(\omega)\, g(\omega) . \tag{4.63}$$

Upon completion, the set of normalizable vectors then form a Hilbert space $\mathcal{Z}$, which is often referred to as the single-particle Hilbert space. Depending on the state, we will need to restrict admissible test functions to the ones that sit in the domain of a certain operator to be defined below. The space $\mathcal{V}$ of f (i.e., the space of $f(\omega), \forall \omega$) is a closed real subspace of $\mathcal{Z}$, and the symplectic product (4.62) is defined on this real subspace, with

$$(f, g) = \text{Im}\langle f, g \rangle . \tag{4.64}$$

We now consider several explicit examples.

Vacuum state

For $|\Psi\rangle$ to be vacuum state $|\Omega\rangle$, ϕ_ω with $\omega > 0$ is taken to be the annihilation operators, i.e.,

$$\phi_\omega |\Omega\rangle = 0, \quad \omega > 0 . \tag{4.65}$$

The Fock space, usually denoted as $\Gamma(\mathcal{Z})$, can then be obtained acting creation operators $\phi_\omega, \omega < 0$ on the vacuum.

TFD state

For $|\Psi\rangle$ given by the TFD state, we take ϕ to be the operator ϕ^R in the CFT_R. There is also a corresponding ϕ^L with the corresponding single-particle Hilbert space denoted as $\bar{\mathcal{Z}}$. In this case no linear combinations of ϕ^R can annihilate the TFD state. Instead, we have

$$\phi_\omega^{(R)} |\text{TFD}\rangle = e^{-\frac{\beta\omega}{2}} \phi_{-\omega}^{(L)} |\text{TFD}\rangle . \tag{4.66}$$

We can then introduce

$$c_\omega^{(R)} = \mathfrak{b}_+ \phi_\omega^{(R)} - \mathfrak{b}_- \phi_{-\omega}^{(L)}, \quad c_\omega^{(L)} = \mathfrak{b}_+ \phi_\omega^{(L)} - \mathfrak{b}_- \phi_{-\omega}^{(R)}, \quad \mathfrak{b}_\pm \equiv \left(\frac{e^{\pm\frac{\beta|\omega|}{2}}}{2\sinh\frac{\beta|\omega|}{2}} \right)^{\frac{1}{2}}, \tag{4.67}$$

with

$$c_\omega^{(R)} |\text{TFD}\rangle = c_\omega^{(L)} |\text{TFD}\rangle = 0, \quad \omega > 0 . \tag{4.68}$$

The Fock space $\Gamma(\mathcal{Z} \oplus \bar{\mathcal{Z}})$ can be generated by acting $c_\omega^{(R,L)}, \omega < 0$ on $|\text{TFD}\rangle$.

In order to define creation operators associated to a function in $\mathcal{Z}$, we also must require f to be in the domain of the operator of multiplication by $\mathfrak{b}_-$.

A quasi-free state

A quasi-free state $|\Psi_\gamma\rangle$ is a two-sided state defined as

$$\phi_\omega^{(R)} |\Psi_\gamma\rangle = \gamma^{\frac{1}{2}}(\omega)\phi_{-\omega}^{(L)} |\Psi_\gamma\rangle . \tag{4.69}$$

We can then introduce

$$c_\omega^{(R)} = \mathfrak{b}_+ \phi_\omega^{(R)} - \mathfrak{b}_- \phi_{-\omega}^{(L)}, \qquad c_\omega^{(L)} = \mathfrak{b}_+ \phi_\omega^{(L)} - \mathfrak{b}_- \phi_{-\omega}^{(R)}, \tag{4.70}$$

$$\mathfrak{b}_+ \equiv \left(\frac{\gamma^{-\frac{1}{2}}}{\gamma^{-\frac{1}{2}} - \gamma^{\frac{1}{2}}} \right)^{\frac{1}{2}} = (1 + \hat{\rho}_\gamma)^{\frac{1}{2}}, \quad \mathfrak{b}_- \equiv \left(\frac{\gamma^{\frac{1}{2}}(\omega)}{\gamma^{-\frac{1}{2}}(\omega) - \gamma^{\frac{1}{2}}(\omega)} \right)^{\frac{1}{2}} = \hat{\rho}_\gamma^{\frac{1}{2}}, \quad \hat{\rho}_\gamma \equiv \frac{\gamma}{1 - \gamma}, \tag{4.71}$$

with

$$c_\omega^{(R)} |\Psi_\gamma\rangle = c_\omega^{(L)} |\Psi_\gamma\rangle = 0, \quad \omega > 0 . \tag{4.72}$$

The Fock space $\Gamma(\mathcal{Z} \oplus \bar{\mathcal{Z}})$ can be generated by acting $c_\omega^{(R,L)}, \omega < 0$ on $|\Psi_\gamma\rangle$.

In order to define creation operators associated to a function in $\mathcal{Z}$, we also must require f to be in the domain of the operator of multiplication by $\mathfrak{b}_-$.

Symplectic complement and commutant

Consider a single particle Hilbert space $\mathcal{W}$ and the corresponding Fock space $\Gamma(\mathcal{W})$. For the examples discussed earlier, for the vacuum we have $\mathcal{W} = \mathcal{Z}$, while for the TFD and a general quasi-free state we have $\mathcal{W} = \mathcal{Z} \oplus \bar{\mathcal{Z}}$.

Introduce Weyl operators

$$W(f) \equiv e^{i\phi(f)}, \quad f \in \mathcal{W} \tag{4.73}$$

and define a von Neumann algebra

$$\mathcal{M}(\mathcal{W}) \equiv \{W(f), f \in \mathcal{W}\}''. \tag{4.74}$$

It can be shown that

$$\mathcal{M}(\mathcal{W}) = \mathcal{B}(\Gamma(\mathcal{W})) . \tag{4.75}$$

That is, the algebra of bounded operators on $\Gamma(\mathcal{W})$ is the Weyl algebra of operators on the single-particle Hilbert space.

Now suppose $\mathcal{V}$ is closed real subspace of $\mathcal{W}$.

Definition 4.6.1. We define the *symplectic complement* of $\mathcal{V}$ as

$$\mathcal{V}' = \{z \in \mathcal{W}, \forall v \in \mathcal{V}, \operatorname{Im} \langle z, v \rangle = 0\}. \tag{4.76}$$

Definition 4.6.2. We define the von Neumann algebra $\mathcal{M}(\mathcal{V})$ associated with $\mathcal{V}$ as

$$\mathcal{M}(\mathcal{V}) \equiv \{W(v), v \in \mathcal{V}\}''. \tag{4.77}$$

The following theorem due to Araki [23] says that the commutant operation of the von Neumann algebra and the symplectic complement operation are mapped to each other.

Theorem 4.6.3.

$$\mathcal{M}(\mathcal{V}_1) = \mathcal{M}(\mathcal{V}_2) \text{ iff } \mathcal{V}_1 = \mathcal{V}_2, \tag{4.78}$$

$$\mathcal{V}_1 \subset \mathcal{V}_2 \Rightarrow \mathcal{M}(\mathcal{V}_1) \subset \mathcal{M}(\mathcal{V}_2), \tag{4.79}$$

$$\mathcal{M}\left(\bigvee_i \mathcal{V}_i\right) = \bigvee_i \mathcal{M}(\mathcal{V}_i), \tag{4.80}$$

$$\mathcal{M}\left(\bigcap_i \mathcal{V}_i\right) = \bigcap_i \mathcal{M}(\mathcal{V}_i), \tag{4.81}$$

$$\mathcal{M}(\mathcal{V})' = \mathcal{M}(\mathcal{V}'), \tag{4.82}$$

and $\mathcal{M}(\mathcal{V})$ is a factor iff $\mathcal{V} \cap \mathcal{V}' = \{0\}$.

This theorem is very useful, as it allows to translate algebraic statements on the full Fock space to to statements about the one particle Hilbert space.

No nontrivial singular inclusions in a generalized free field theory

If we call a proper inclusion $\mathcal{S}_{(-t_0,t_0)}$ in $\mathcal{S}_R$ with empty relative commutant as a singular inclusion, then for a generalized free field, singular inclusions do not exist. This result seems standard in the algebraic QFT literature, in which significant effort has been made to construct singular inclusions that do *not* come from generalized free fields. For more discussion around this point see for example [128, 304].

4.7 Appendix: A review of the exponential type problem

We saw in the main text that for a generalized free field theory at finite temperature, the value of the depth parameter was equal to the exponential type of the Kallen-Lehmann measure. In general, it is difficult to compute the exponential type of a measure, and there is a large body of mathematical work on this topic. The goal of this appendix is to summarize this mathematical work. If one follows the general intuition given by Heisenberg's uncertainty principle, one expects that the more porous the support of the spectral density, the least porous the support of the Fourier transform of any function supported there can be. In particular, for porous enough support of the spectral density, we expect there to be a maximal gap for any distribution of the form $f * E$ with f admissible.

Therefore, studying the triviality of large enough relative commutants of time bands is closely related to the following analysis problem, which as we saw before, is known as the *exponential type problem.*

A review of the main results

The mathematical results on the exponential type problem (and a close relative known as the gap problem), seem to culminate with the work of Poltoratski in 2012 [387], which gives an explicit answer to the gap problem for finite measures on the real line. Earlier work includes important theorems due to Benedicks [47, 48], Beurling and de Branges [82].

We start by stating the definition of the exponential type:

Definition 4.7.1. Let μ be a measure on $\mathbb{R}$. We define the *exponential type* of μ as

$$T_\mu := \sup_{t \in \mathbb{R}} \{ t \in \mathbb{R}, \exists f \in L^2(\mu), \text{supp}(\widetilde{f\mu}) \cap (0, t) = \emptyset \}. \tag{4.83}$$

The exponential type problem consists in computing the value of T_μ for a measure μ.

The type problem has been solved in various cases. In the examples given in the main text, we showed that

- If μ is evenly spaced with spacing l then $T_\mu \leq 2\pi/l$.

- If μ is compactly supported, then $T_\mu = 0$.

- If μ is a continuous function with complete support (with a few extra technical assumptions), then $T_\mu = \infty$.

The most general solutions to the exponential type problem to date have been provided by Poltoratski in [387], where he introduced. The work of [387] is formulated in the case where the measure μ has *finite* mass, or in the case of Poisson-summable measures, i.e. measures for which

$$\int_{\mathbb{R}} \frac{d|\mu|(x)}{1 + x^2} dx < \infty. \tag{4.84}$$

However it can be straightforwardly extended to the polynomially growing case [388].

The key ingredient of these results is the notion of d-uniform sequence. This notion allows to capture "how concentrated" the support of a sequence is. The definition is a bit technical, we recall it here:

Definition 4.7.2. We say that the discrete sequence of real numbers $\Lambda = (\lambda_n)$ is *d-uniform* if there exists a sequence of disjoint intervals $I_n = (a_n, b_n]$, whose centers go to $\pm\infty$ and widths go to ∞ as $n \to \pm\infty$, such that:

$$\sum_n \frac{|I_n|^2}{1 + \text{dist}(0, I_n)^2} < \infty, \tag{4.85}$$

$$\#(\Lambda \cap I_n) = d|I_n| + o(|I_n|), \tag{4.86}$$

and

$$\sum_n \frac{(\#(\Lambda \cap I_n))^2 \log|I_n| - E_n}{1 + \text{dist}(0, I_n)^2} < \infty, \tag{4.87}$$

where

$$E_n := \sum_{\lambda_k \neq \lambda_l \in I_n} \log|\lambda_k - \lambda_l|. \tag{4.88}$$

Roughly speaking, Equation (4.85) means that the sequence of sampling intervals I_n cannot cover too much of the real line. Equation (4.86) controls the density of the elements of Λ inside the I_n, while Equation (4.87) ensures that the λ_n are reasonably equally spaced inside the I_n, by introducing the term E_n, which can be thought of as a repulsion term between the λ_n, which looks similar to the ones that appear in fermionic statistics.

The most general theorem of [387] is then:

Theorem 4.7.3. *Let μ be a finite positive measure on $\mathbb{R}$. Let $a > 0$. Then $T_\mu \geq a$ if and only if for all lower semi-continuous $W \in L^1(\mu)$ with limit ∞ at $\pm\infty$, and any $0 < d < a$, there exists a d-uniform sequence $(\lambda_n)_{n \in \mathbb{N}}$ in the support of μ such that*

$$\sum_n \frac{\log W(\lambda_n)}{1 + \lambda_n^2} < \infty. \tag{4.89}$$

In practise, this theorem is not always easy to apply, in large part due to the fact that the characterization it introduces needs to be verified for *all* weights W. However, there are some situations in which W can be removed from the statement. For example, in the case where the measure μ is discrete, we have a much more explicit criterion. We first define the notion of *a*-regular and strongly *a*-regular sequence, which is a sequence whose overall density in the reals is approximately a:

Definition 4.7.4. A sequence $\Lambda = (\lambda_n)$ is *a*-regular if for all $\varepsilon > 0$, if there is a sequence I_n of intervals such that for all n,

$$\left| \frac{\#(\Lambda \cap I_n)}{|I_n|} - a \right| \geq \varepsilon, \tag{4.90}$$

then

$$\sum_n \frac{|I_n|^2}{1 + \text{dist}(0, I_n)^2} < \infty. \tag{4.91}$$

Definition 4.7.5. A sequence $\Lambda = (\lambda_n)$ is strongly *a*-regular if

$$\int \frac{n_\lambda(x) - ax}{1 + x^2} dx < \infty, \tag{4.92}$$

where $n_\lambda(x)$ is the counting function of the support of Λ.

The characterization of the exponential type is then:

Proposition 4.7.6. *Let*

$$\mu := \sum_n w(n)\delta_{\lambda_n} \tag{4.93}$$

be a finite measure, where $\Lambda = (\lambda_n)$ is a sequence of points such that for some $c > 0$, $|\lambda_i - \lambda_j| > c$. Let

$$D := \sup \left\{ D_*(\Lambda'), \Lambda' \subset \Lambda, \sum_{\lambda_n \in \Lambda'} \frac{\log w(n)}{1 + n^2} > -\infty \right\}, \tag{4.94}$$

where

$$D_*(\Lambda') = \sup \{a \geq 0, \Lambda \text{ has a strongly } a\text{-regular subsequence}\}. \tag{4.95}$$

Then,

$$T_\mu = 2\pi D. \tag{4.96}$$

It is this characterization that we used to show that below the Hawking–Page temperature, the depth parameter is equal to π. In cases where the sequence is not separated, i.e., where there is no minimal distance separating its points, we have an alternative result:

Proposition 4.7.7. *Let*

$$\mu := \sum_n w(n)\delta_{\lambda_n} \tag{4.97}$$

be a finite measure.

$$D := \sup\left\{d,\, \exists\, d - uniform\, \Lambda' \subset \Lambda,\, \sum_{\lambda_n \in \Lambda'} \frac{\log w(n)}{1 + n^2} > -\infty\right\}. \tag{4.98}$$

Then,

$$T_\mu \geq 2\pi D, \tag{4.99}$$

and there is equality if

$$\int dx \frac{\log(|n_\Lambda| + 1)(x)}{1 + x^2} < \infty. \tag{4.100}$$

There is also another useful result on the exponential type problem in the case of some polynomially growing measures called Frostman measures [386]. These are positive measures μ for which there exist $C, \alpha > 0$ such that for all intervals $I \subset \mathbb{R}$,

$$\mu(I) < C|I|^\alpha. \tag{4.101}$$

In particular, Frostman measures include bounded continuous functions. We then have the following result:

Theorem 4.7.8. *Frostman measures have exponential type* 0 *or* ∞.

In our language this means that if the spectral density of our theories at large N is a bounded continuous function in the TFD state, then either there is no emergent radial direction at all, or there is stringy connectivity between both sides!

The techniques used to prove the results described above are far from elementary, and make use of advanced theories in harmonic analysis, such as the theory of Toeplitz operators. They are also related to other deep areas of mathematical analysis, such as Beurling–Malliavin theory and the Gelfand–Levitan method, which we believe should also play a role in the definition of stringy geometries. The relation between these results and our physical setup shows that our depth parameter contains highly nontrivial information. We also hope that the new physical relevance of the exponential type found in this chapter encourages further developments in the mathematical study of exponential type problems.

An explicit computation in a simple case

Although the arguments of [387] to establish the results above are very involved mathematically, in this appendix we offer an elementary argument to compute the exponential type for a simple choice of spectral function $\rho(\omega)$. Namely we assume

$$\rho(\omega) = \sum_{n=0}^{\infty} a_n \left[\delta(\omega - 2n) - \delta(\omega + 2n) \right], \tag{4.102}$$

which corresponds to the case (4.16) of the vacuum state of a d-dimensional CFT on S^{d-1} in the particular case $\omega_0 = 0$. In this case it can be readily seen that the depth parameter $\mathcal{T}$ is equal to π. More formally:

Proposition 4.7.9. *If the a_n are nonzero and decay at most polynomially, the exponential type of the measure $\rho(\omega)$ is $\mathcal{T} = \pi$.*

Proof. We first establish that $\mathcal{T} \leq \pi$, and then establish that $\mathcal{T} \geq \pi$. First, $\mathcal{T} \leq \pi$. Indeed, suppose that there exists a function f with real-valued Fourier transform such that the Fourier transform of $f(\omega)\rho(\omega)$ (or $\rho_0(\omega)$) vanishes on an interval of size larger than π. Introducing $c_n := f_n a_n$ and noticing that

$$f(\omega)\rho(\omega) = \sum_{n=0}^{\infty} c_n \delta(\omega - 2n) - \sum_{n=0}^{\infty} c_n^* \delta(\omega + 2n), \tag{4.103}$$

we obtain that $(f * \rho)(t)$ is periodic of period π. So if it vanishes on an interval of size larger than π, then it identically vanishes and $f = 0$. Hence we have established that

$$\mathcal{T} \leq \pi. \tag{4.104}$$

Now, we show that $\mathcal{T} \geq \pi$ by explicitly exhibiting, for all $\varepsilon > 0$, test functions in $L^2(\rho)$ such that the Fourier transform of $f(\omega)\rho(\omega)$ vanishes on intervals of size $\pi - \varepsilon$. More precisely, suppose that $\mathcal{T} = \pi - \varepsilon$ for some $\varepsilon > 0$. Then this means that there is no function $f(\omega) \in L^2(\rho)$ such that

$$(f * \rho)(t) = i \left(\Pi * K \right)(t), \tag{4.105}$$

where Π is the Dirac comb and K is a compactly supported smooth function of support inside $(-\frac{\pi}{2}, \frac{\pi}{2})$ but outside $(-\frac{\pi}{2} + \frac{\varepsilon}{2}, \frac{\pi}{2} - \frac{\varepsilon}{2})$) (otherwise integration against such a function would vanish for functions supported on $(-\frac{\pi}{2} + \frac{\varepsilon}{2}, \frac{\pi}{2} - \frac{\varepsilon}{2})$). So in Fourier space this means there are no functions K and f as defined before such that

$$\sum a_{\pm n} f_{\pm n} \delta_{\pm 2n} = \sum K_{\pm n} \delta_{\pm 2n}. \tag{4.106}$$

But for any K compactly supported in t, one can always find such an f: simply define $f_{\pm n} = K_{\pm n}/a_{\pm n}$. Since the $K_{\pm n}$ decay faster than polynomially (as K is in Schwartz space), this implies

$$\sum \frac{|K_{\pm n}|^2}{a_{\pm n}} < \infty, \tag{4.107}$$

so such an f is in $L^2(\rho)$, which is a contradiction. Therefore, in that case,

$$\mathcal{T} = \pi. \tag{4.108}$$

$\square$

Chapter 5

EXPLICIT LARGE *N* VON NEUMANN ALGEBRAS FROM MATRIX MODELS

This chapter is based on the work [200], in collaboration with Leonardo Santilli.

5.1 Introduction

In the past two decades, our understanding of the emergence of spacetime in quantum gravity has immensely improved, in particular in the controlled setting of the AdS/CFT correspondence. This progress is in large part due to the study of the interplay between the emergent geometry of spacetime in the bulk and the entanglement structure of the boundary theory. Important developments include the discovery of the Ryu–Takayanagi formula [401] and its covariant generalization [242], of the quantum extremal surface formula [296, 162], of the quantum error-correcting properties of holography [10, 225], of the "island" prescription [13], and of the replica wormhole configurations [377, 11]. Perhaps most famously, these developments culminated in a derivation of the Page curve for black hole evaporation [379, 12].

This plethora of results clarifies the emergence of *space* in the bulk, as they relate the entanglement entropy of subregions of the boundary theory to the area of surfaces in the bulk. In contrast, the emergence of *time* in the bulk is much less explored, especially inside the black hole interior. While time outside the black hole can be directly mapped to the boundary time [254], interior time is much more mysterious, and faces all sorts of paradoxes, including puzzles related to diffeomorphism invariance [138] and an apparent incompatibility with the axioms of conformal field theory [329]. Importantly, signatures of the black hole singularity remain largely elusive.

A new approach to the emergence of time in the AdS/CFT correspondence was recently put forward by Leutheusser and Liu [293, 294], where they argued that the interior time could only be sharply understood in the large N limit of the boundary theory. After defining a von Neumann algebra of single trace operators at $N = \infty$ in the thermofield double state $|\Psi_\beta\rangle$, they argued that above the Hawking–Page temperature, this algebra becomes type III_1, and that this highly nontrivial entanglement property between the two sides of the thermofield double is related to

the emergence of a new interior time.

It was conjectured in [293, 294] that the sudden transition to type III_1 can be diagnosed by the real-time two-point function of single trace operators in the boundary theory. More precisely, given a single trace operator ϕ:

$$G_+(t) = \langle \Psi_\beta | \phi(t)\phi(0) | \Psi_\beta \rangle. \tag{5.1}$$

The Fourier transform of (5.1) satisfies

$$\widetilde{G}_+(\omega) = \frac{\rho(\omega)}{1 - e^{-\beta\omega}}, \tag{5.2}$$

where $\rho(\omega)$ is the finite temperature Källén–Lehmann spectral function at inverse temperature β. The conjecture of Leutheusser–Liu is then that the type of the von Neumann algebra of each single trace operator at finite temperature is related to the structure of the spectral density $\rho(\omega)$: if it consists in delta-functions, then the von Neumann algebra is type I, whereas if it consists in a continuum,[1] then the von Neumann algebra is type III_1 (and so is the von Neumann algebra of the full theory). This conjecture therefore proposes to use each single trace operator as a "probe", which, through its interactions with the whole system, will help diagnose the emergence of spacetime. We will take a similar viewpoint in this chapter.

The presence of a phase transition with this sort of structural change in the spectral function is expected in holographic theories, and it is associated to the emergence of a black hole horizon in the bulk. In particular, the mixing properties associated to the presence of a sharp horizon require that the two-point functions of single trace operators must vanish at late times [171, 172]. This is related to apparent information loss at large N (see [171, 172]), and is only possible if the spectral function is not discrete, and hence if there is an emergent type III_1 algebra in the large N limit. The relation between the chaotic properties of the two-point function and the type of the underlying von Neumann algebra was recently explored in [183], which in particular used these methods to obtain the type III_1 property from the continuity (or measurability) of the spectral density of generalized free fields. Note that type III_1 is only a necessary condition for this horizon structure, but that it is not obvious it is sufficient, in particular, there exists a whole hierarchy of chaotic properties that are expected for black hole horizons and that are strictly stronger than type III_1 [191, 367].

---

[1] Originally the support was required to be the whole real axis, but we will show that this is not necessary.

In the phase in which the large N gauge theory is characterized by a type III_1 algebra, it is argued in [293, 294] that there can exist a new, emergent notion of time defined from the extension of a *half-sided modular inclusion*, which is the algebraic structure encoding the presence of a horizon in the bulk at large N. This extension allows to take operators outside the horizon to operators in the black hole interior, and allows to potentially ask sharp questions about the emergence of the interior and of the singularity. It also gives yet another clue that interior time should be intrinsically related to the large N limit of the boundary theory.

The proposal in [293, 294] for the emergence of type III_1 factors at large N is holographic in essence, and relies on subregion dualities as well as on the assumption of smoothness of the dual bulk spacetime in the large N limit. In particular, the type III_1 nature of the von Neumann algebras is argued for in a rather indirect way, by resorting to results from algebraic quantum field theory. In this way an algebraic structure of *half-sided modular inclusion* emerges, and it can be shown that this structure only exists for type III_1 von Neumann algebras. However, it is less clear how the emergence of nontrivial algebras arises directly at the level of the string/gauge theory of interest, and how the type of the algebra can be directly inferred from a gauge theory calculation.

The purpose of this chapter is threefold:

- First, to explain how to explicitly construct large N algebras from explicit quantum mechanical theories and rigorously derive their type from considerations related to the spectral function. In particular, a statement similar to, but slightly different from, the conjectures of [293, 294], and that agrees with the relevant results in [183] in the type III_1 case, will be rigorously shown and applied to our examples.

- Second, to propose a broad class of toy models inspired from gauge/string duality, of which [246] constitutes a particularly simple instance, and apply our formalism to them to show they give rise to an emergent type III_1 von Neumann algebra. This part, which is the most prominent both in terms of length and of technical developments, involves mathematics related to random matrix theory and combinatorial representation theory.

- In addition, we further elaborate on these examples and construct a family of models that undergo a first order phase transition in the large N limit. This is

SYMMETRIES AND $\longrightarrow$ QUANTUM $\longrightarrow$ SPECTRAL $\longrightarrow$ VON NEUMANN
REPRESENTATIONS MECHANICS DENSITIES ALGEBRAS
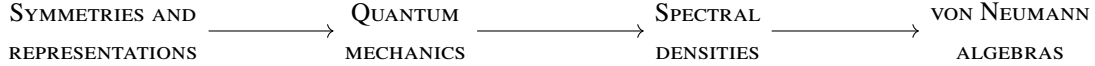
Figure 5.1: In this work we explore the implications of writing the finite temperature partition function of a theory in terms of representations of the global symmetries. We construct a quantum mechanics from these representations and determine the large N von Neumann algebra of operators.

> a general result based on the study of the partition functions of the systems, and the prescription we provide is independent of the considerations on von Neumann algebras. Combining this with the analysis of the spectral density, we show that these modified models carry an associated type III_1 algebra only above the critical temperature.

Our strategy for the first goal will be to apply standard techniques from algebraic quantum field theory to associate a special kind of von Neumann algebra to any quantum dynamical system of harmonic oscillators, under the assumption that correlation functions factorize in the large N limit. The von Neumann algebras describe a generalized free field theory, can be systematically studied, and their type turns out to be classified by the spectrum of an operator closely related to the spectral density (these techniques should be compared to [183]).

The second goal will be met thanks to a general construction of quantum mechanical systems whose partition function can be computed from matrix integrals of a kind that often appears in the string theory literature. In this simple setup, we will be able to calculate thermal correlation functions entirely explicitly. In particular, the large N value of these correlation functions can be expressed in terms of the saddle point eigenvalue density of a discrete matrix ensemble. From this, we will be able to rigorously derive the type of the von Neumann algebra describing these systems at large N. Figure 5.1 sketches the basic ideas.

Finally, we will meet the third goal by enlarging our quantum systems into a direct sum of sectors that transform under different flavor symmetry groups. This will have the effect of promoting the third order phase transition present in our initial examples to a first order one, which will be sharp enough to induce a change at the level of the large N algebra depending on the temperature. This procedure interestingly parallels and revisits early calculations in gauge theory [302].

Effective descriptions of gauge/string dualities in terms of matrix models have a long history, and the incarnation we consider was pioneered in [427, 5]. A particularly

appealing feature of such descriptions is that matrix models often admit character expansions, which can be useful to carry calculations explicitly in a setup more akin to bulk variables. The most precise statements along these lines have been made in $\mathcal{N} = 4$ super-Yang–Mills theory, in the case of half-BPS states [301], as well as in the more recent giant graviton expansion [184, 291]. In our case, the states of the systems we will study will be packaged into such character expansions.
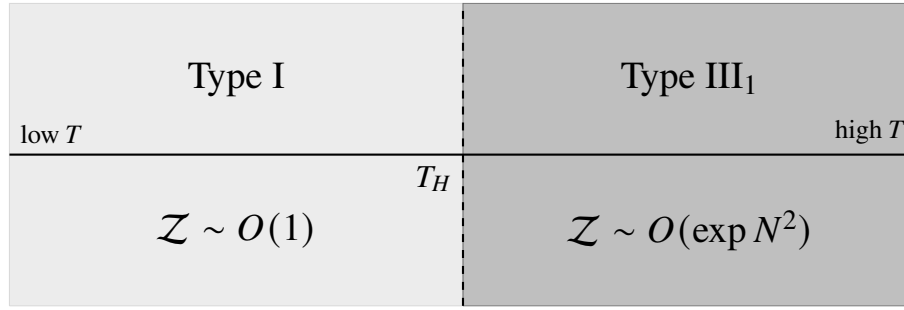
Figure 5.2: Below the Hagedorn temperature ($T < T_H$) the partition function is finite and the algebra of single-trace operators is a type I von Neumann algebra. Above the Hagedorn temperature ($T > T_H$), the partition function diverges and the von Neumann algebra becomes type III$_1$.

The main results of this work can be summarized as follows:

- Building on the foundational work on operator algebras [25, 27] summarized in [137] and its relation to algebraic quantum field theory (see for example [173]), we give a completely general and rigorous procedure to construct large N von Neumann algebras from quantum systems satisfying large N factorization, and to determine their types. In particular, we show that a more precise and entirely rigorous version of the conjecture of [293, 294] relating the type of the von Neumann algebras to the support of the large N spectral function directly follows from these results (see also [183]).

- We put forward a general procedure to construct quantum systems with a third order phase transition in the large N limit, and an extension of these systems to systems with a first order Hagedorn-like transition. An alternative description of these systems is given in terms of unitary matrix models, which often have a more direct gauge theory interpretation. This is ultimately a matrix model result, potentially of independent interest.

- For our class of models, we introduce a general notion of probe operator, analogous to a detector interacting with the gauge theory. We derive a *univer-*

sal relation between the Källén–Lehmann spectral density associated to the real-time two point functions of such probes, and the eigenvalue density of an underlying matrix model.

- From this Källén–Lehmann density, we apply our general method to construct an associated large N von Neumann algebra. This algebra can be constructed from the correlation functions of the probe only. We exploit the relation between spectral density and eigenvalue density to understand the types of our algebras (Figure 5.2).

- We illustrate our results by computing the partition functions and Källén–Lehmann densities entirely explicitly in selected examples inspired by various physical theories.

Organization

The contents of the chapter are organized in two main parts plus appendices. Part 5.1, which is more formal in nature, contains all general constructions, both of large N algebras associated to quantum systems with large N factorization, and of the quantum systems of interest in this chapter. We introduce all the main theoretical results in this part. Part 5.5 is dedicated to explicit examples, where the machinery of Part 5.1 finds explicit realization. We tried to keep the two parts as independent as possible, so that the busy reader interested only in concrete calculations can directly jump to Part 5.5, while the more mathematically minded reader can content themselves with the general and formal constructions of Part 5.1. Figure 5.3 contains a sketch of the main concepts and ideas discussed in the text.

In Section 5.2, we begin with a brief review of the salient features of von Neumann algebras and their relevance for the emergence of interior time in holography. Our construction and results on von Neumann algebras are in Section 5.3. We explain how to construct general von Neumann algebras associated to large N factorizing quantum systems, with a key role played by the Källén–Lehmann spectral density. In Section 5.4 we change gears and introduce the class of systems we aim to study. The operators required as input for the machinery developed in Section 5.3 are explicitly constructed in Subsection 5.4. In Subsection 5.4 we calculate the real-time two-point function of these operators using matrix models, and obtain the spectral density $\rho(\omega)$. This allows us to deduce the type of the associated von Neumann algebra.

GAUGE THEORY
INTERPRETATION

SIMPLE
QUANTUM
MECHANICS

TYPE III$_1$
VON NEUMANN
ALGEBRA

EXTENDED
SYSTEM

TYPE III$_1$
ABOVE
HAGEDORN

(5.55)

(5.362)

(5.109)

(5.59)

(5.23)

(5.127)

(5.23)

DISCRETE MATRIX
MODEL

SPECTRAL
DENSITY

HAGEDORN
TRANSITION

SPECTRAL
DENSITY

(5.107)

(5.135)
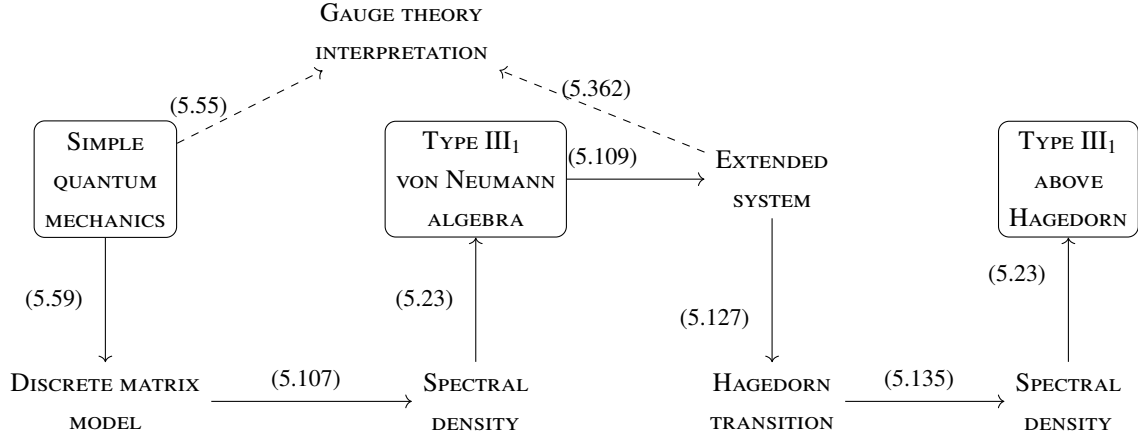
Figure 5.3: The steps through which this work associates von Neumann algebras to quantum mechanical systems with large N factorization.

Then, in Section 5.5, we extend the quantum systems by including a weighted sum over the flavor rank. In Subsection 5.5 we investigate the asymptotic growth of the partition function of these extended models and argue for the presence of a large N, first order phase transition with Hagedorn behavior. Subsection 5.5 replicates the analysis of the spectral density, and shows its different behavior on the two sides of the Hagedorn transition. Combining the three steps therein leads to a jump in the type of von Neumann algebra across the Hagedorn phase transition, which becomes type III$_1$, as indicated in Figure 5.2.

We then proceed to apply our construction to different examples of systems inspired by gauge/string duality, and perform explicit calculations. This is the content of Part 5.5, consisting of Sections 5.6 to 5.9. In Section 5.6 we consider a generalization of a model from [246] (see also [247, 337]) and unveil its connection with supersymmetric QCD in 4d (SQCD$_4$) as well as with Calabi–Yau varieties. We consider a newly introduced ensemble based on a toy model of lattice QCD in 2d (QCD$_2$) [218] in Section 5.7. The third example, in Section 5.8, is the generating function of Donaldson–Thomas invariants of the resolved conifold, and we comment on the geometric meaning of our construction along the way. The final example is based on the partition function of pure Yang–Mills theory in two dimensions, which also recently appeared in the description of generic holographic systems with global symmetry [272, 271], as reported in Section 5.9.

Section 5.10 contains a summary of our results and presents future research directions. The text is complemented by extensive appendices, of which 5.11 and 5.13 may be of independent interest. Appendix 5.11 formally generalizes the construc-

tion of Section 5.3 to any bosonic or fermionic system made of free oscillators. We discuss an effective matrix model for four-dimensional $\mathcal{N} = 4$ super-Yang–Mills theory [302, 150] in Appendix 5.12, which is amenable to be analyzed by the same means as the examples in Part 5.5, even though we lack a quantum mechanical interpretation. The scope of Appendix 5.12 is to showcase our techniques in a familiar matrix model, without attempting any claim concerning $\mathcal{N} = 4$ super-Yang–Mills theory. Appendix 5.13 discusses unitary matrix models at large N and puts forward a general procedure to promote the characteristic third order phase transitions to first order ones. Certain long proofs are gathered in Appendix 5.14.

Disclaimer on notation

In order to facilitate the reading and the retrieval of the main ingredients, the fundamental steps in the derivation are framed as Theorems and Propositions. We will also informally summarize the main achievements as Statements, referring to the accompanying theorem for a precise version. Previously known results are accompanied by citation of the original works or other standard references, while propositions without citations are new. Besides, while aiming at a broad picture in Part 5.1, we highlight with a symbol $\diamond$ caveats that may obstruct the direct application of certain steps to more involved physical models.

In order to make this work self-contained and easily reproducible for the black hole inclined audience, we sketch the proofs of a handful of statements that are likely known to the matrix model practitioner.

The speed-reader's guide to the contents

Given the length of the chapter, we now point at some important parts that can be looked at independently. We also emphasize that the two parts of this work can be read largely independently, and that our examples can be understood without the general theory.

- The reader interested in von Neumann algebras for systems with large N factorization can directly look into Subsection 5.3. The classification result is given in Subsection 5.3.

- For a hands-on definition of our quantum systems, we suggest looking at (5.43), whose reinterpretation as a Hilbert space trace is explained in Subsection 5.4. Our definition of a probe and its interaction with the systems is in

Subsection 5.4 — or one may jump to Corollary 5.4 and Statement 5.4.20 for the properties of the large N spectral density.

- The main technique to promote a third order transition to a first order one is explained in Subsections 5.5 and 5.5. The results about the corresponding new systems are summarized in Subsection 5.5.

- The reader interested in concrete examples may directly look at Part 5.5. Example 1 in Section 5.6 displays all the features discussed abstractly in Part 5.1.

General theory

The goal of this first part is to introduce all our main results in the most general language possible. We will begin with a brief review of the increasingly important role von Neumann algebras have been playing in holography in recent years. We will then provide a general construction of von Neumann algebras capturing the finite temperature correlations of systems with large N factorization, as well as an entirely explicit criterion to determine the type of these algebras based on the support of the spectral function. Then, we will introduce our family of toy models, their relationship to matrix integrals akin to those appearing in string theory, and a general prescription to determine the support of the spectral function of our models in terms of the asymptotic behavior of the underlying matrix integral. In particular, this formula will be enough to determine the types of the large N algebras of our systems.

5.2 Von Neumann algebras in holography

The role of von Neumann algebras in holography is ubiquitous, and has become increasingly important in the recent years (see also the earlier works [370, 371]). They are especially relevant to make sense of statements related to quantum error correction in AdS/CFT [270, 269, 196, 164, 194, 100, 168, 192], which are the backbone of the quantum extremal surface formula [225]. They also appear in the study of the emergence of the bulk radial direction, through the notion of modular chaos [169, 134].

In this preliminary section, we will focus on one particular aspect of the appearance of von Neumann algebras in holography, that is related to the emergence of time in the black hole interior above the Hawking–Page temperature. We hence first review the particular aspects of the theory of von Neumann algebras that are relevant to this topic. Then, in Subsection 5.2, we summarize the construction of emergent times due to Leutheusser–Liu [293, 294].

Classification of factors

Let us first recall the definition of a von Neumann algebra and of a factor on a Hilbert space.

Definition 5.2.1. Let $\mathcal{H}$ be a Hilbert space. The commutant M' of an algebra of bounded operators M on $\mathcal{H}$ is the algebra of bounded operators on $\mathcal{H}$ that commute with all elements of M. The bicommutant $M'' := (M')'$ of M is the commutant of the commutant of M.

Definition 5.2.2. Let $\mathscr{H}$ be a Hilbert space. An algebra of bounded operators M on $\mathscr{H}$ is said to be a von Neumann algebra if it is closed under Hermitian conjugation and is equal to its bicommutant. If the center of M is reduced to multiples of the identity, one says that M is a factor.

It is an important problem to classify all von Neumann algebras up to isomorphism. As any von Neumann algebra can be written as a direct integral of factors, this problem reduces to the easier problem of classifying all *factors*.

In general, this problem is very hard, and still wide open. However, it has been solved in a particular case by Connes [120] and Haagerup [215] in the 1970s, namely, the case of *hyperfinite factors*, which can be approximated by finite-dimensional algebras.

Definition 5.2.3. A von Neumann algebra M is hyperfinite if there exists an increasing sequence of finite-dimensional algebras $(M_n)_{n\in\mathbb{N}}$, such that M is the weak operator closure of $\bigcup\limits_{n\in\mathbb{N}} M_n$.

It turns out that hyperfinite von Neumann algebras are most often the ones that appear in physics. In particular, under reasonable assumptions, one can show that in quantum field theory, local algebras are hyperfinite [212].

The classification of von Neumann algebras relies on the structure of the set of projections inside the algebras [435]. This structure does not necessarily give a lot of physical insight for our purposes, and rather than studying it here, we will simply enumerate the possible types of factors and their main properties.

I) Type I factors are isomorphic to the algebra of operators $\mathcal{B}(\mathscr{H})$, where $\mathscr{H}$ is a separable Hilbert space. There is of course exactly one type I factor for each dimension $\dim(\mathscr{H}) = n \in \mathbb{N} \cup \{\infty\}$. This unique factor is said to have type I_n.

II) Type II factors can no longer be written in the form $\mathcal{B}(\mathscr{H})$, but they still possess a *tracial weight*, namely a (potentially infinite) functional τ that satisfies

$$\tau(xy) = \tau(yx). \tag{5.3}$$

This trace is *not* the same as the trace in $\mathcal{B}(\mathscr{H})$, and can be thought of as a rescaled version of the trace, where an "infinite amount of entanglement"

between the algebra and the rest of the system is subtracted [457]. Type II factors come in two types: type II_1 factors for which the trace is finite on all the algebra, and type II_∞ factors, isomorphic to the tensor product of a type II_1 and a type I_∞ factor, for which the trace is infinite on the identity. Both types are unique up to isomorphism.

III) Type III factors are all those that remain.

The breakthrough of the work of Connes and Haagerup [120, 215] is the classification of type III factors in the hyperfinite case, which seemed completely out of reach beforehand. This classification was made possible by the modular theory of Tomita and Takesaki [437], whose main result we now briefly recall.

Type III factors

Let M be a type III factor. To any faithful, normal state φ on M (weak-* continuous linear functional of norm one which is nonzero on nonzero positive elements), Tomita–Takesaki theory [437] associates an unbounded self-adjoint operator[2] Δ_φ such that for all $t \in \mathbb{R}$,

$$\Delta_\varphi^{-it} M \Delta_\varphi^{it} = M. \tag{5.4}$$

This means that conjugation by imaginary powers of Δ_φ gives rise to a one-parameter automorphism group of M, called the *modular automorphism group*. The state φ satisfies the KMS condition with respect to that group, which is an infinite-dimensional version of a thermal equilibrium condition.

One fundamental difference between type III factors and the other factors is that in the former case, there is no way of implementing modular automorphisms of the algebra by conjugating by a unitary that pertains to the algebra. This means that modular flow is an *outer* automorphism for type III factors, whereas it is inner in the other cases.

The way type III factors are classified then is the following: introduce the *Connes invariant*

$$S(M) := \bigcap_\varphi \operatorname{Sp} \Delta_\varphi, \tag{5.5}$$

---

[2]In the physics literature, Δ_φ corresponds to the exponential of the (full) modular Hamiltonian of the system.

where the intersection is taken over all faithful normal states φ on M, and Sp denotes the spectrum of an unbounded operator.

It turns out that the Connes invariant can take just a few values for type III factors. Let M be a type III factor,

- If $S(M) = \{0, 1\}$, then M is said to have type III_0.

- If for $0 < \lambda < 1$, $S(M) = \{0\} \cup \{\lambda^n, n \in \mathbb{Z}\}$, then M is said to have type III_λ.

- If $S(M) = [0, \infty)$, then M is said to have type III_1.

From this, it is clear that the modular operator Δ_φ of the system has continuous spectrum for all faithful normal states on M if and only if M has type III_1. This is a property that is expected from the modular Hamiltonian of black hole states on one side of the horizon. It turns out that in the hyperfinite case, type is enough to completely classify type III factors. More precisely, there is a unique hyperfinite type III_λ factor for $0 < \lambda \leq 1$. The type III_0 case is more subtle.

In quantum field theory, one of the main applications of Tomita–Takesaki theory is the Bisognano–Wichmann theorem [212], which asserts that the modular automorphisms of local algebras associated to Rindler wedges implement Lorentz boosts along the Rindler horizon. This can be seen as a statement of the Unruh effect, which asserts that the QFT vacuum is thermal with respect to Lorentz boosts.

In fact, due to the horizon structure, the generator of null translations along a Rindler horizon can also be reconstructed from modular theory. Null translations of magnitude a around the horizon are implemented by a semigroup of unitaries $U(a)$. If we denote by $\mathcal{M}$ the algebra of the wedge, and by $\mathcal{N}$ the translated algebra $\mathcal{N} := U(1)\mathcal{M}U^\dagger(1)$, the following relations are satisfied in the vacuum state, for all $t \geq 0$:

$$\begin{aligned}
\Delta_\mathcal{M}^{it} \mathcal{N} \Delta_\mathcal{M}^{-it} &\subset \mathcal{N}, \\
\Delta_\mathcal{M}^{it} U(a) \Delta_\mathcal{M}^{-it} = \Delta_\mathcal{N}^{it} U(a) \Delta_\mathcal{N}^{-it} &= U(e^{-2\pi t} a), \\
J_\mathcal{N} J_\mathcal{M} &= U(2), \\
\Delta_\mathcal{N}^{it} &= U(1) \Delta_\mathcal{M}^{it} U^\dagger(1).
\end{aligned} \tag{5.6}$$

This structure is known in algebraic quantum field theory under the name of *half-sided modular inclusion* [453], and it is necessary to get a well-defined causal structure in the emergent spacetime. It turns out that under reasonable conditions

on the vacuum state, the only von Neumann algebras that are consistent with the half-sided modular inclusion structure are hyperfinite factors of type III_1. This implies that in quantum field theory, local von Neumann algebras must have type III_1. This leads to the following result:

Theorem 5.2.4 ([212])**.** *In a quantum field theory, the von Neumann algebras associated to Rindler wedges are type III_1 factors.*

The Leutheusser–Liu half-sided modular inclusion

The recent, key insight of Leutheusser and Liu [293, 294] is that a von Neumann algebra associated to a spacetime region outside of a *general* horizon should also have type III_1, even in the case of a black hole. The reason is that there is also a half-sided modular inclusion along the black hole horizon.

This fact has strong consequences in holography. Consider two copies of strongly interacting $\mathcal{N} = 4$ super-Yang–Mills theory at large N, in the thermofield double state [318]. The AdS/CFT dictionary tells us that the bulk effective description of the theory is a theory of fields on an asymptotically AdS spacetime. The boundary theory admits a deconfinement phase transition at large N [5], which is dual in the bulk to the Hawking–Page phase transition [455], with the emergence of a wormhole and a horizon on both sides of the thermofield double [318]. For extensive discussion on Hagedorn, deconfinement and Hawking–Page transitions, see [5, 14].

The operator algebraic interpretation put forward in [293, 294] is the following: the algebra of generalized free fields at large N in the bulk is dual to the algebra generated by (appropriately normalized) single-trace operators at $N = \infty$. The emergence of a black hole horizon then implies that the type of this algebra goes from type I to type III_1 at the Hawking–Page temperature.

Actually, even more can be said. What is shown in [293, 294] is that in the case where the large N algebra corresponds to a generalized free field, this half-sided modular inclusion can be extended to positive values of the coordinate on the horizon. It is this extension that allows to cross the horizon and construct a new, emergent time inside the black hole. Therefore, the emergence of time in the black hole interior is very closely related to the type III_1 nature of the algebra of the exterior. This emergent time should furthermore break down at a finite value of the parameter, which would be a signature of the black hole singularity.

Let us note that these observations do not, in principle, rely on the strength of the 't

Hooft coupling on the boundary. While bulk physics is no longer approximated by a supergravity theory in the weakly coupled regime, it has been argued [171, 172] that the Källén–Lehmann spectral density is still continuous at weak (but nonzero) coupling, which implies that the boundary algebra should still become type III_1 above the Hawking–Page temperature. If one could still make sense of the notion of half-sided modular inclusion in this regime, this would imply that there is a precise notion of "stringy horizon" for holographic duals of weakly coupled gauge theories.

5.3 Von Neumann algebras for systems with large N factorization

In this rather formal section, we describe a general procedure that allows to construct a von Neumann algebra describing the correlation functions of any system satisfying large N factorization. In particular, this method would apply to $\mathcal{N} = 4$ super-Yang–Mills if we were able to compute the large N two-point functions of single trace operators rigorously. In order not to clutter the main body of the chapter too much, and also because this will be the case in all our examples, we restrict the discussion here to the case of bosonic systems, however, the fermionic counterpart of the statements presented here can be derived in a completely analogous way thanks to the fermionic algebras introduced in Appendix 5.11. More generally, Appendix 5.11 systematically introduces all the mathematical objects involved here in the language of [137]. On top of this reference, this section also inspires itself from standard techniques of algebraic quantum field theory, see for example [185, 173], as well as [303] and [168, App.C] for recent discussions and comments.

The construction

Consider a sequence of quantum systems indexed by an integer N, at finite inverse temperature β. Let A be an operator defined at each N. We start by defining what we mean by large N factorization.

Definition 5.3.1. A self-adjoint operator $\phi(t)$ is said to satisfy (bosonic) large N factorization if all its large N, finite temperature correlation functions have a limit, and these limits satisfy:

$$\langle \phi(t_1) \ldots \phi(t_{2m-1}) \rangle = 0,$$

$$\langle \phi(t_1) \ldots \phi(t_{2m}) \rangle = \sum_{\text{Wick pairing } \varpi} \prod_{j=1}^{m} \langle \phi(t_{\varpi(2j-1)}) \phi(t_{\varpi(2j)}) \rangle, \tag{5.7}$$

where the sum runs over pairings of operators that respect the ordering, with the corresponding permutations of $2m$ objects denoted ϖ.

A quantum field theory at finite temperature is completely determined by its correlation functions. In what follows, we shall be interested in quantum systems containing some observables that satisfy large N factorization. Equation (5.7) then teaches us that for these observables, all-point functions can be recovered from the datum of two-point functions. The question is now: how does one construct a net of von Neumann algebras and an expectation value functional (i.e., a state on this algebra) whose values reproduce the correlation functions of such a form (5.7), and determine its type? It turns out that this problem can be answered by a standard construction of operator algebra theory, namely, a representation of the *canonical commutation relations* (CCR). Note that the algebra we construct here has no direct definition in terms of the finite N observables of the quantum mechanical theory. The idea is to directly engineer it from the data of the correlation functions at large N, in such a way that it recovers them.

CCR and Araki–Woods theory

More formally, we wish to construct an algebra of quantum fields in 0+1 dimensions, and a state on this algebra, such that this state captures the correlation functions of observables satisfying large N factorization. There is a generic operator algebraic construction that allows to describe the correlations of bosonic creation and annihilation operators in states that factorize (often dubbed *quasi-free states*). This construction is widely used in algebraic quantum field theory, and is precise enough to know about the type of von Neumann algebra when the correlation functions factorize, see for example [173] for a review. Here we will adapt the method of algebraic quantum field theory to the format of [137], which is well-adapted to compute the types of the algebras under consideration.

The algebra we will consider is given by a representation of the canonical commutation relations (CCR algebra) over a one-particle Hilbert space. This Hilbert space is a space of functions of spacetime: here we are in $0 + 1$ dimensions, so it simply is a space of functions of $\mathbb{R}$, interpreted as the time direction. In this manner, the one-particle Hilbert space knows about the creation of individual particles at different times. Equivalently, it will be more convenient to think of the Hilbert space as a space of functions indexed by the frequency ω. More formally, recall the definition of the Wightman function

$$G_+(t) = \langle \phi(t)\phi(0) \rangle_\beta \,, \tag{5.8}$$

and of the Källén–Lehmann spectral density

$$\rho(\omega) := (1 - e^{-\beta\omega})\widetilde{G}_+(\omega). \tag{5.9}$$

Throughout the chapter, to make contact with the sign conventions in [172], the definition used for the Fourier transform is

$$\widetilde{f}(\omega) := \frac{1}{2\pi} \int_{\mathbb{R}} f(t)e^{+i\omega t}dt. \tag{5.10}$$

One can now introduce the following definition.[3]

Definition 5.3.2. The real Hilbert space $L^2(\mathbb{R}, \rho)$ is the completion of the space of rapidly decaying real-valued functions $\mathcal{S}(\mathbb{R})$ on $\mathbb{R}$ whose Fourier transform is square-integrable against ρ, endowed with the inner product defined by

$$(f_1, f_2) := \int_{\mathbb{R}} d\omega \tilde{f}_1^*(\omega) \tilde{f}_2(\omega) \mathrm{sgn}(\omega)\rho(\omega). \tag{5.11}$$

This is a real inner product because it can be checked that $\rho(\omega)$ is an odd function of ω, positive for positive ω. Out of this Hilbert space and our inner product, we now construct a representation of the CCR (see Appendix 5.11 for more details) through a standard procedure known as the *Araki–Woods construction*. The first step is to introduce the operation

$$\widetilde{\mathsf{j}f}(\omega) := -i\,\mathrm{sgn}(\omega)\tilde{f}^*(-\omega). \tag{5.12}$$

This operation endows $L^2(\mathbb{R}, \rho)$ with the structure of a real symplectic space, with symplectic structure given by

$$\sigma(f_1, f_2) := \int_{\mathbb{R}} d\omega \tilde{f}_1^*(\omega) \widetilde{\mathsf{j}f}_2(\omega)\mathrm{sgn}(\omega)\rho(\omega). \tag{5.13}$$

Moreover, note that j squares to -1 (minus the identity operator) and $\mathsf{j}^* = -\mathsf{j}$. This implies that one can promote the structure of $L^2(\mathbb{R}, \rho)$ to that of a complex Hilbert space Z [173], on which $-\mathsf{j}$ implements the imaginary unit, with a sesquilinear inner product given by

$$\langle f_1, f_2 \rangle := \int_{\mathbb{R}} d\omega \tilde{f}_1^*(\omega) \widetilde{f}_2(\omega)\mathrm{sgn}(\omega)\rho(\omega) + \int_{\mathbb{R}} d\omega \tilde{f}_1^*(\omega) \tilde{f}_2^*(-\omega)\rho(\omega) = (f_1, f_2) + i(f_1, \mathsf{j}f_2). \tag{5.14}$$

---

[3]We will assume $\rho(\omega)d\omega$ is a measure on $\mathbb{R}$ that induces a tempered distribution. If ρ is not supported on the whole real axis, then one needs to quotient by the null space of the inner product: functions whose support is included in the space where ρ is zero.

The construction is then given by the following procedure. Let Z be defined as before, and let Γ be the bosonic Fock space over $Z \oplus \bar{Z}$. For f_1, f_2 in the image of $\mathcal{S}(\mathbb{R})$ inside $L^2(\mathbb{R}, \rho)$, we introduce the operators

$$W(f_1, \bar{f}_2) := e^{i\phi(f_1, \bar{f}_2)}, \tag{5.15}$$

where

$$\phi(f_1, \bar{f}_2) = \frac{1}{\sqrt{2}}(a^\dagger(f_1, \bar{f}_2) + a(f_1, \bar{f}_2)), \tag{5.16}$$

a and $a^\dagger$ being the usual raising and lowering operators on the Fock space Γ.

We then introduce the operator ρ_β (not to be confused with the spectral density $\rho(\omega)$ — we chose this notation for consistency with [137]), defined by

$$\rho_\beta := \gamma_\beta(1 - \gamma_\beta)^{-1}, \tag{5.17}$$

where

$$\widetilde{(\gamma_\beta f)}(\omega) := e^{-\beta|\omega|}\tilde{f}(\omega). \tag{5.18}$$

Note that γ_β is a self-adjoint operator satisfying $0 \le \gamma_\beta \le 1$. Then, for $f \in \mathrm{Dom}(\rho_\beta^{\frac{1}{2}})$, we can define two unitary operators $W_{\gamma,l}$ and $W_{\gamma,r}$ on Γ by

$$W_{\beta,l}(f) := W((\rho_\beta + 1)^{\frac{1}{2}}f, \bar{\rho}_\beta^{\frac{1}{2}}\bar{f}), \tag{5.19}$$

$$W_{\beta,r}(\bar{f}) := W(\rho_\beta^{\frac{1}{2}}f, (\bar{\rho}_\beta + 1)^{\frac{1}{2}}\bar{f}). \tag{5.20}$$

It can then be shown that

Proposition 5.3.3 ([137]). *The operators $W_{\beta,l}(f)$ satisfy the canonical commutation relations*

$$W_{\beta,l}(f_1)W_{\beta,l}(f_2) = e^{-\frac{i}{2}\mathrm{Im}\langle f_1, f_2 \rangle}W_{\beta,l}(f_1 + f_2). \tag{5.21}$$

Importantly, the algebra of operators generated by the $W_{\beta,l}(f)$ is not yet a von Neumann algebra: it is only a formal algebra generated by unitary operators, with no extra topological structure. The missing ingredient in order to obtain a von Neumann algebra is to take its *bicommutant* on the Fock space Γ.

Definition 5.3.4. The large N von Neumann algebra M associated to the large N spectral density ρ is the bicommutant of the algebra generated by the operators $W_{\beta,l}$ on the Fock space Γ.

Although this last step of taking the bicommutant might seem like a mere technicality, it is a crucial one: without it, the $W_{\beta,l}(f)$ do not know anything about the underlying entanglement structure of the vacuum state. It is this last step that "teaches" the algebra of the $W_{\beta,l}(f)$ about the entanglement structure of the underlying Hilbert space. In particular, the different types that the von Neumann algebra M can have arise due to this bicommutant operation.

The interest of the construction above is that the correlation functions in the vacuum state $|\Omega_\beta\rangle$ of Γ exactly reproduce those of the system of interest. In particular, while Dirac deltas are not necessarily in $L^2(\mathbb{R}, \rho)$, one can still formally write down the correlation functions of the operators associated to $\delta(\cdot - t)$ and $\delta(\cdot)$. Then, using [137, Proposition 40, 1st point of item 4], one finds:

$$
\begin{aligned}
\langle\Omega_\beta|\,\phi(t)\phi(0)\,|\Omega_\beta\rangle &= \text{Re}\,\langle(\rho_\beta)\delta(\cdot-t),\delta(\cdot)\rangle + \frac{1}{2}\,\langle\delta(\cdot-t),\delta(\cdot)\rangle \\
&= \int_{\mathbb{R}} d\omega\; e^{-i\omega t}\text{sgn}(\omega)\rho(\omega)\left(\frac{e^{-\beta|\omega|}}{1-e^{-\beta|\omega|}}+\frac{1}{2}\right) + \frac{1}{2}\int_{\mathbb{R}} d\omega\; e^{-i\omega t}\rho(\omega) \\
&= \int_{\mathbb{R}} d\omega\; e^{-i\omega t}\rho(\omega)\left(\frac{1}{2}\coth\left(\frac{\beta\omega}{2}\right)+\frac{1}{2}\right) \\
&= \int_{\mathbb{R}} d\omega e^{-i\omega t}\frac{\rho(\omega)}{1-e^{-\beta\omega}},
\end{aligned}
\tag{5.22}
$$

which matches with the Wightman function $G_+(t)$ by Fourier inversion. Similar results can be found for correlations of two creation and/or annihilation operators. Moreover, the correlation functions factorize (this is a consequence of the Araki–Woods construction that directly follows from [137]), which shows that the algebra M satisfies the requirement of describing all correlation functions at finite temperature.

Type of large N algebras

With this construction at hand, we can study the type of the von Neumann algebra generated by the $W_{\gamma_\beta,l}(f)$ thanks to the following result summarized by Dereziński [137]:

Theorem 5.3.5 ([137]). *Let M be the bicommutant of the Araki–Woods representation of the CCR defined above. If γ_β is trace-class, then M has type I. If γ_β has some continuous spectrum, then M has type III_1.*

A more detailed justification of the type III_1 part of this result based on the triviality of the centralizer can for example be found in [206, 183]. Using (5.17), this theorem implies in the context considered by Leutheusser–Liu (which will be enough for our

cases as well):

$$
\begin{array}{ll}
\text{Type I} & \text{if } \operatorname{supp}\rho = \bigsqcup \{ \text{ isolated pts } \} \text{ and } \sum_{\omega \in \operatorname{supp}\rho} e^{-\beta|\omega|} < \infty \ . \\[2mm]
\text{Type III}_1 & \text{if } \operatorname{supp}\rho \subseteq \mathbb{R} \text{ continuous } .
\end{array}
$$

$$(5.23)$$

This follows because if ρ is a continuous function (non-constant equal to zero), then γ_β is just the multiplication operator that multiplies admissible functions by $e^{-\beta|\omega|}$, and has continuous spectrum by continuity of ρ. For the type III$_1$ case we are assuming ρ is a nonzero continuous function, so the preimage of every interval around a point in the image of $e^{-\beta|\omega|}$, which contains an interval, has nonzero measure.

The theory lurking behind the scenes here is that of *quasi-free states* on CCR/CAR algebras. It is a very well-developed theory and an important tool in the proof of many results of algebraic quantum field theory. Appendix 5.11 of this chapter summarizes the main properties of quasi-free states, following [137].

Intermezzo: Comparison with Leutheusser–Liu

At this stage, it is useful to make a remark on the difference between our findings and the conjecture of Leutheusser–Liu [294, 293]. This discrepancy was also recently identified in [183]. The initial conjecture was that a type III$_1$ algebra emerges in the large N limit if and only if the spectral density not only gets a continuous support, but also gets a continuous support *on the full real line*. This is in slight contradiction with our findings: as long as we are looking at a thermal state and the spectral function of the theory has *some* continuous support, we find that the type III$_1$ property will be satisfied. The subtlety that explains this discrepancy is that the argument given in [294, 293] for their conjecture was based on the fact that the modular Hamiltonian of the thermal state needs to have support on the whole real line in order for the algebra to have type III$_1$. This is certainly true. However, the spectral density considered here does not encode the spectrum of the (full) modular Hamiltonian itself, but rather, the spectrum of its counterpart on the one-particle Hilbert space. This means that there is no contradiction between the modular spectrum having to be supported on the whole real line and our result as long as the additive group generated by the one-particle spectrum is dense in $\mathbb{R}$.

This is clearly true if the one-particle spectrum has any continuous component.[4]

5.4 Quantum mechanical systems from matrix models

Now that a general construction of large N algebras has been presented, we are ready to introduce and investigate the basic properties of a large class of quantum mechanical models, which will be the object of study in the rest of the work. These models have the very convenient property of having a partition function which is a unitary matrix integral, which matches the form of effective descriptions of gauge theories on $\mathbb{S}^{d-1} \times \mathbb{S}^1_{\beta_g}$, where β_g is the inverse temperature of the gauge theory. It is the character expansion of the matrix integral that recasts it as a manifest finite temperature partition function of a quantum system.

Alongside with the definition of our models, we introduce the main ingredients that will play a part in our analysis. Our novel construction of a quantum mechanical system from the representations of the flavor symmetry of the theory under consideration, is laid out in Subsection 5.4. We then introduce a formal notion of probe and its associated Hilbert space in Subsection 5.4, and use it to compute the spectral densities in the quantum mechanics of interest in Subsection 5.4.

These ideas are the technical core of this work, and will be exploited at length in the rest of the chapter. They will also be concretely realized in the examples we will discuss in Part 5.5.

Gauge theories, flavor symmetries, representations

Before moving on to the construction of our models, we briefly review some important features of matrix integrals appearing in gauge theory, which will be instrumental in the rest of our analysis.

Gauge theories as unitary matrix models

Our starting point is the family of unitary one-matrix models:

$$\mathcal{Z}_{\text{UMM}}(Y, \tilde{Y}) := \oint_{SU(N+1)} [\mathrm{d}U] \, f(U, U^\dagger; Y, \tilde{Y}). \qquad (5.24)$$

In this expression, $[\mathrm{d}U]$ is the normalized Haar measure on the compact Lie group $SU(N+1)$, and $Y, \tilde{Y} \in SU(L+1)$ or $Y, \tilde{Y} \in U(L)$ are matrices of parameters, whose eigenvalues will play the role of fugacities for the flavor symmetry. Besides, f is

---

[4]Similar arguments about the additive group generated by the one-particle spectrum can be found in the algebraic QFT literature, see for example [174].

some class function, whose details depend on the specifics of the model of interest. Finally, the integration $\oint_{SU(N+1)}$ projects the integrand onto its gauge-invariant part, assuming the interpretation of $SU(N + 1)$ as a gauge group holds. It is sometimes referred to as Molien–Weyl projector.

An important aspect of (5.24) is that the above integral depends on two integer parameters:

- N, which is the rank of the gauge group of the theory, and

- L, which is (or scales with) the rank of the flavor symmetry group of the theory.

In this section, we will be interested in the limit of this model when L and N both become large with fixed ratio, cf. Definition 5.4.15 below.

⋄ For practical convenience, we will often assume that

$$(5.24) \text{ is invariant under } \quad (U, Y) \longleftrightarrow (U^\dagger, \tilde{Y}). \tag{5.25}$$

In a motivating example in Section 5.6, this assumption will have the physical meaning of requiring the theory to be free of chiral anomalies.

Models of the generic form (5.24) have a long history in gauge theory, and include the prototypical Gross–Witten–Wadia model [211, 448, 449]. In some instances, (5.24) is derived directly from a quantum gauge theory placed on the d-dimensional cylinder geometry $\mathbb{S}^{d-1} \times \mathbb{S}^1$ [427, 5]. Denoting r_{d-1} and β_{g} the radii of $\mathbb{S}^{d-1}$ and $\mathbb{S}^1$, respectively, in the limit $r_{d-1}/\beta_{\mathrm{g}} \ll 1$ all the fields are heavy and can be integrated out, except for the holonomy of the gauge field around the thermal $\mathbb{S}^1$. The model reduces to an effective (0+1)-dimensional QFT, i.e., a Euclidean quantum mechanics theory on $\mathbb{S}^1$. Denoting the gauge connection A and

$$\exp \oint_{\mathbb{S}^1} A = U \in SU(N + 1), \tag{5.26}$$

one is left with a (fairly complicated) effective action depending on $U, U^\dagger$ and the external parameters $Y, \tilde{Y}$ [5]. Taking a further simplifying limit of very weak gauge coupling, in which the contributions from massive modes attain a tractable form, one arrives at the expression (5.24). It is in this class of the examples that (5.25) will be related to a condition on the fields participating in the gauge theory.

One well known feature of gauge theories is that their states come arranged into irreducible representations of the global symmetry. This information can be naturally extracted from the unitary matrix models (5.24), through their character expansion. We now proceed to explain this procedure. This picture will become very explicit in the concrete examples we will consider in Part 5.5.

We begin by stating useful generalities about $SU(N + 1)$ representations (see, e.g., [312]) that we will use, and then move on to stating the result. The expert reader can skip this brief review and move on to Subsection 5.4.

Intermezzo: Properties of irreducible representations

Irreducible representations of $SU(N + 1)$ are in one-to-one correspondence with Young diagrams of length at most N. For example, the fundamental and adjoint representations of $SU(5)$ correspond to the Young diagrams:

$$\text{fund} : \square, \qquad \text{adj} : \ \ . \tag{5.27}$$

The diagrams, in turn, are in one-to-one correspondence with partitions of length at most N:

$$R = (R_1, R_2, \ldots, R_N), \qquad R_1 \geq R_2 \geq \cdots \geq R_N \geq 0. \tag{5.28}$$

The non-negative integers R_i in the partition specify the rows of the diagram.

Definition 5.4.1. Let R be an irreducible representation of $SU(N + 1)$ and identify it with a Young diagram R. The length of R is the positive integer $\ell(R)$ such that

$$R_{\ell(R)} > 0, \quad R_{\ell(R)+1} = 0. \tag{5.29}$$

If $R = \emptyset$ is trivial, $\ell(\emptyset) := 0$.

We will also use the notation

$$|R| := \sum_{i=1}^{\infty} R_i. \tag{5.30}$$

The Lie group $SU(N + 1)$ is endowed with an involution

$$\mathsf{C} : U \mapsto U^\dagger \tag{5.31}$$

which has the physical meaning of charge conjugation. It acts on the irreducible representations as $\mathsf{C}(R) = \overline{R}$, with $\overline{R}$ the complex conjugate representation. The

Young diagram for $\overline{R}$ is the complement to R inside a rectangle of edge lengths $(R_1, N+1)$, rotated by $180°$. For example, the anti-fundamental of $SU(5)$ is

$$\overline{\text{fund}} \; : \; \overline{\square} = \begin{array}{|c|} \hline \\ \hline \\ \hline \\ \hline \\ \hline \end{array} . \tag{5.32}$$

Another example is, in $SU(4)$

$$R = (5, 3, 1) \qquad \Longrightarrow \quad \overline{R} = (5, 4, 2) \tag{5.33}$$

whereas the same diagram $R = (5, 3, 1)$ seen as an $SU(5)$ representation of length 3 gives

$$R = (5, 3, 1) \qquad \Longrightarrow \quad \overline{R} = (5, 5, 4, 2). \tag{5.34}$$

The Young diagram consisting of a column with $N + 1$ boxes corresponds to the determinant representation, which is isomorphic to the trivial representation of $SU(N + 1)$.

Proposition 5.4.2 ([87]). *The set of equivalence classes of $SU(N+1)$ representations up to isomorphism, endowed with the direct sum $\oplus$ and tensor product $\otimes$, is a commutative ring, called the* representation ring *of $SU(N + 1)$. It is generated by the set $\Re^{SU(N+1)}$ of isomorphism classes of irreducible representations.*

Unitary matrix models as ensembles of representations: Preliminaries

Character expansions are a widely used tool.[5] We prove a general character expansion formula here in an abstract context, which encompasses the case-by-case studies present in the literature. While the outcome will certainly be familiar to the practitioners, to our knowledge a formulation of the character expansion at such a level of generality has not appeared previously.

We list our setup and working assumptions and then derive Lemma 5.4.3. Let the notation be as in (5.24), with f a class function for both U and $U^\dagger$ separately. The reason why this should be the case in a matrix model derived from a gauge theory was explained in Subsection 5.4. The same reasoning applied to connections in the flavor bundle tells us that f should also be a class function with respect to

---

[5]Implications of characters expansions in 2d gravity have been explored in [275], and more recently in [277, 56].

$Y, \tilde{Y}$. Physically, this is to require that the partition function of the theory does not transform under flavor symmetry transformations (possibly up to an anomalous phase, which plays no role in our discussion thus we neglect it).

Being f a class function by hypothesis it admits a character expansion, that is, an expansion in the basis of functions on $SU(N+1)$ invariant under the adjoint action of the group. With the hypothesis just stated we write f in the character basis as

$$f(U, U^\dagger; Y, \tilde{Y}) = \sum_{R \in \mathfrak{R}^{SU(N+1)}} c_R \chi_R(U) \chi_{\varphi(R)}(Y) \sum_{\tilde{R} \in \mathfrak{R}^{SU(N+1)}} \tilde{c}_{\tilde{R}} \chi_{\tilde{R}}(U^\dagger) \chi_{\tilde{\varphi}(\tilde{R})}(\tilde{Y})$$

(5.35)

(we allow the coefficients $c, \tilde{c}$ to be different in general). Let us unpack the notation. The sums run over isomorphism classes of irreducible representations of $SU(N+1)$. The functions χ_R are the characters of the Lie group, in the representation R. $\varphi(R)$ is a $U(L)$ or $SU(L+1)$ representation, uniquely fixed by R via an map $\varphi : \mathfrak{R}^{SU(N+1)} \to \mathfrak{R}^{U(L)}$ (or $\to \mathfrak{R}^{SU(L+1)}$). The concrete form of φ depends on f, hence on the specifics of the gauge theory under consideration. In many cases, φ is just the pullback of a map $U(L) \to SU(N+1)$, seen as the natural embedding if $L \leq N$ and as a projection if $L > N$. Likewise, $\tilde{\varphi}(\tilde{R})$ is a representation uniquely determined by $\tilde{R}$ via a map $\tilde{\varphi}$. These maps will have very explicit realizations in the examples.

The examples in Part 5.5 will manifestly satisfy these hypothesis. One may think of (5.35) either as

- our working assumption on the matrix models (5.24); or

- as a physics-motivated requirement for (5.24) to be a valid approximation of the gauge theory on $\mathbb{S}^{d-1} \times \mathbb{S}^1$.

Unitary matrix models as ensembles of representations: Character expansion

Lemma 5.4.3. *Consider the setup of Subsection 5.4. There exist a subset $\mathfrak{R}_L^{(N)} \subseteq \mathfrak{R}^{U(L)}$ (respectively $\subseteq \mathfrak{R}^{SU(L+1)}$) of irreducible $U(L)$ (resp. $SU(L+1)$) representations, a bijection $\phi : \mathfrak{R}_L^{(N)} \to \mathfrak{R}_L^{(N)}$ and numbers $\mathfrak{d}_R, \tilde{\mathfrak{d}}_R \in \mathbb{R}$ labelled by elements $R \in \mathfrak{R}_L^{(N)}$, such that*

$$\mathcal{Z}_{\text{UMM}}(Y, \tilde{Y}) = \sum_{R \in \mathfrak{R}_L^{(N)}} \mathfrak{d}_R \tilde{\mathfrak{d}}_R \chi_R(Y) \chi_{\phi(R)}(\tilde{Y}).$$

(5.36)

Proof. The function f in (5.24) is a class function for both U and $U^\dagger$ separately, by hypothesis, and we take its character expansion (5.35).

The character $\chi_{\varphi(R)}(Y)$ in (5.35) vanishes if $\ell(\varphi(R)) > L$. This imposes a constraint on the representations R that contribute non-trivially to (5.24), which intertwines the N- and L-dependence. Moreover, it may happen that the function f is such that some of the coefficients c_R or $\tilde{c}_R$ vanish for certain representations R. We will denote by $\mathfrak{R}_L^{(N)} \subseteq \mathfrak{R}^{U(L)}$ (or $\subseteq \mathfrak{R}^{SU(L+1)}$) the subset of irreducible representations that survive these selection rules.

Plugging (5.35) back into (5.24) and using the orthogonality of characters:

$$\oint_{SU(N+1)} [dU] \chi_R(U) \chi_{\tilde{R}}(U^\dagger) = \delta_{R\tilde{R}}, \tag{5.37}$$

we arrive at

$$\mathcal{Z}_{\text{UMM}}(Y, \tilde{Y}) = \sum_{R \in \varphi^{-1}\left(\mathfrak{R}_L^{(N)}\right)} c_R \tilde{c}_R \chi_{\varphi(R)}(Y) \chi_{\tilde{\varphi}(R)}(\tilde{Y}). \tag{5.38}$$

The sum has been restricted to those R that yield a non-trivial contribution. Changing variables $\hat{R} = \varphi(R)$, this is precisely (5.36), after the identification

$$\mathfrak{d}_{\hat{R}} := c_{\varphi^{-1}(\hat{R})}, \qquad \tilde{\mathfrak{d}}_{\hat{R}} := \tilde{c}_{\varphi^{-1}(\hat{R})}, \qquad \phi := \tilde{\varphi} \circ \varphi^{-1} \tag{5.39}$$

(and eventually renaming $\hat{R} \mapsto R$). $\qquad\qquad\qquad\qquad\qquad\qquad\qquad\qquad\square$

Below we list side remarks concerning formula (5.36):

- In practice, we will discuss models such that f is invariant under the involutions (5.25) and (5.31). This implies $\tilde{c}_R = c_R$, and hence $\tilde{\mathfrak{d}}_{\hat{R}} = \mathfrak{d}_{\hat{R}}$.

- Moreover, applying (5.25) followed by (5.31), we have that the model remains unchanged under the exchange $Y \leftrightarrow \tilde{Y}$, which also implies that

$$\tilde{\varphi} = \varphi \qquad \text{or} \qquad \tilde{\varphi} = \mathsf{C} \circ \varphi. \tag{5.40}$$

  The partition function is insensitive to which of the two options is actually realized.

- Note that, assuming invariance under the charge conjugation involution,

$$\phi(R) = R \quad \forall R \qquad \text{or} \qquad \phi(R) = \overline{R} \quad \forall R. \tag{5.41}$$

- By construction, ϕ is the restriction to $\mathfrak{R}_L^{(N)}$ of an isomorphism of the Grothendieck ring $\mathfrak{R}^{U(L)}$ (or $\mathfrak{R}^{SU(L+1)}$).

- The character expansion extends to other choices of classical gauge group. For integration over $SO(N+1)$ in (5.24), only representations of $Sp(L+1)$ will enter in (5.36), and conversely for integration over $Sp(N+1)$ one gets irreducible $SO(L+1)$ representations. The corresponding Young diagrammatic techniques were pioneered in [281].

Before moving on, we introduce the unrefined version of the partition function (5.24),

$$\mathcal{Z}_L^{(N)}(y) := \oint_{SU(N+1)} [dU] f(U, U^\dagger; \mathrm{diag}(\underbrace{\sqrt{y}, \ldots, \sqrt{y}}_{L}), \mathrm{diag}(\underbrace{\sqrt{y}, \ldots, \sqrt{y}}_{L})).$$

(5.42)

We now apply the character expansion to (5.42).

cor. *Let* $\mathcal{Z}_L^{(N)}$ *be as in* (5.42). *With the notation of Lemma 5.4.3, it holds that*

$$\mathcal{Z}_L^{(N)}(y) = \sum_{R \in \mathfrak{R}_L^{(N)}} y^{|R|} \, \mathfrak{d}_R \tilde{\mathfrak{d}}_R \, (\dim R)(\dim \phi(R)).$$

(5.43)

If moreover the initial unitary matrix model is invariant under the involution (5.31), *then*

$$\mathcal{Z}_L^{(N)}(y) = \sum_{R \in \mathfrak{R}_L^{(N)}} y^{|R|} \, \mathfrak{d}_R^2 (\dim R)^2.$$

(5.44)

The gauge-invariant content of a gauge theory must be assembled into representations of the global symmetries, and one can restrict to irreducible ones without loss of generality. The character expansion does the job, and provides us with an ensemble directly in terms of representations, in which the requirement of gauge invariance only appears through the constraint $R \in \mathfrak{R}_L^{(N)}$.

Expression (5.43) is then interpreted as an ensemble of gauge-invariant operators. These are grouped into superselection sectors labelled by the pair $(R, \phi(R))$ of irreducible representations of the flavor symmetry. The elementary gauge-invariant operators of the theory are the generators of the pair $(R, \phi(R))$. We now proceed to give an explicit construction of quantum mechanical systems based on this character expansion.

Quantum mechanics of flavor symmetry

Inspired from the general results above, we now construct quantum mechanical systems whose partition functions are given by the character expansions of the matrix models described above. We will very explicitly construct the Hilbert space of these systems as well as their Hamiltonian.

Ensembles of representations as quantum systems

Let us now revisit and push forward the previous analysis. We set $y = e^{-\beta}$ in (5.43), so that $y^{|R|} = e^{-\beta|R|}$ is formally written as a Boltzmann factor. We give this hint credit.

In this way, we are led to interpret (5.43) as the partition function of a quantum mechanical system involving the elementary gauge-invariant states, organized into irreducible representations, with Hamiltonian H diagonalized in the representation basis, with eigenvalues $|R|$. The flavor symmetry imposes that all the states belonging to the same pair $(R, \phi(R))$ carry the same energy $|R|$. The degeneracy of all these elementary states of equal energy is already resummed and is accounted for by $(\dim R)(\dim \phi(R))$ in (5.43).

It is important to note here that β will be the inverse temperature of the effective quantum mechanics describing the gauge-invariant states, which may be distinct from the inverse temperature β_g of the gauge theory from which the matrix integral is derived. The two will be related, but possibly in non-trivial ways.

⋄ We henceforth assume $\mathfrak{d}_R, \tilde{\mathfrak{d}}_R \in \mathbb{N}$. This allows us to think of them as additional degeneracy, due to quantum numbers that we are not taking into account. This assumption holds in a vast list of examples of character expansions (even well beyond the current scope, see, e.g., [408, 344, 343]), but we do not know of a deeper mathematical justification.

Following this intuition, we now write down a quantum mechanical system whose Hilbert space $\mathscr{H}_L$ is graded by (isomorphism classes of) irreducible representations R of the flavor symmetry,

$$\mathscr{H}_L = \bigoplus_{R \in \mathfrak{R}^{U(L)}} \mathscr{H}_L(R) \otimes \mathscr{H}_L(\phi(R)). \tag{5.45}$$

The vector space for given R is spanned by

$$|R, v_{\mathsf{a}}, \lambda_{\mathsf{s}}\rangle \otimes |\phi(R), \tilde{v}_{\dot{\mathsf{a}}}, \tilde{\lambda}_{\dot{\mathsf{s}}}\rangle,$$

$$\text{for } \mathsf{a} = 1, \dots, \dim R, \ \dot{\mathsf{a}} = 1, \dots, \dim \phi(R), \ \mathsf{s} = 1, \dots, \eth_R, \ \dot{\mathsf{s}} = 1, \dots, \tilde{\eth}_R.$$
$$(5.46)$$

Throughout, we use undotted and dotted indices, respectively, to refer to the R and $\phi(R)$ part of (5.45).

- The vectors $|R, v_{\mathsf{a}}\rangle$ are in one-to-one correspondence with the generators of R, and likewise for $|\phi(R), \tilde{v}_{\dot{\mathsf{a}}}\rangle$ with the generators of $\phi(R)$.

- The additional quantum numbers λ_{s} and $\tilde{\lambda}_{\dot{\mathsf{s}}}$ account for the additional degeneracy. We interpret them as associated to additional global symmetries that have remained spectators in the character expansion, but which impose additional selection rules.

The states (5.46) are in the canonical normalization

$$\langle R', v_{\mathsf{b}}, \lambda_{\mathsf{r}}| \otimes \langle \phi(R'), \tilde{v}_{\dot{\mathsf{b}}}, \lambda_{\dot{\mathsf{b}}}|R, v_{\mathsf{a}}, \lambda_{\mathsf{s}}\rangle \otimes |\phi(R), \tilde{v}_{\dot{\mathsf{a}}}\lambda_{\dot{\mathsf{s}}}\rangle$$
$$= \langle \phi(R'), \tilde{v}_{\dot{\mathsf{b}}}, \lambda_{\dot{\mathsf{r}}}|\phi(R), \tilde{v}_{\dot{\mathsf{a}}}, \lambda_{\dot{\mathsf{s}}}\rangle \langle R', v_{\mathsf{b}}, \lambda_{\mathsf{r}}|R, v_{\mathsf{a}}, \lambda_{\mathsf{s}}\rangle = \left(\delta_{RR'}\delta_{\mathsf{ab}}\delta_{\lambda_{\mathsf{s}}\lambda_{\mathsf{r}}}\right)\left(\delta_{\phi(R)\phi(R')}\delta_{\dot{\mathsf{a}}\dot{\mathsf{b}}}\delta_{\lambda_{\dot{\mathsf{s}}}\lambda_{\dot{\mathsf{r}}}}\right).$$
$$(5.47)$$

To reduce clutter, we introduce the notation

$$|R, \mathsf{a}, \mathsf{s}; \ \phi(R), \dot{\mathsf{a}}, \dot{\mathsf{s}}\rangle := |R, v_{\mathsf{a}}, \lambda_{\mathsf{s}}\rangle \otimes |\phi(R), \tilde{v}_{\dot{\mathsf{a}}}, \tilde{\lambda}_{\dot{\mathsf{s}}}\rangle \qquad (5.48)$$

and $\sum_{\mathsf{a},\mathsf{s},\dot{\mathsf{a}},\dot{\mathsf{s}}}$ to indicate the sum over the elements of the basis (5.46) at given R.

The Hamiltonian acts as

$$H|R, \mathsf{a}, \mathsf{s}; \ \phi(R), \dot{\mathsf{a}}, \dot{\mathsf{s}}\rangle = |R| \ |R, \mathsf{a}, \mathsf{s}; \ \phi(R), \dot{\mathsf{a}}, \dot{\mathsf{s}}\rangle \qquad (5.49)$$

where we recall that $|R| = \sum_{i \geq 1} R_i$. The fact that the eigenvalues are independent of the generators of the representation R, producing degeneracy in the spectrum, is imposed by the assumption of the existence of global symmetries in the gauge theory.

Definition 5.4.4. Let $\mathfrak{R}_L^{(N)}$ be as in Subsection 5.4 and $\mathscr{H}_L$ as in (5.45). We define the *gauge-invariant Hilbert space* to be

$$\mathscr{H}_L^{(N)} := \bigoplus_{R \in \mathfrak{R}_L^{(N)}} \mathscr{H}_L(R) \otimes \mathscr{H}_L(\phi(R)). \qquad (5.50)$$

The definition is motivated as follows.

- Note that $\mathscr{H}_L^{(N)}$ is not simply a vector space, but inherits a Hilbert space structure from $\mathscr{H}_L$, where the completeness is a consequence of the discreteness of the representation spectrum.

- The restriction to $R \in \mathfrak{R}_L^{(N)}$ stems from having a finite gauge rank N in the gauge theory with start with. We loosely refer to this constraint as stemming from gauge invariance, with a slight abuse of notation.

Putting the pieces together, we have the following.

Theorem 5.4.5. *Under the notation above, it holds that*

$$\mathcal{Z}_L^{(N)}(e^{-\beta}) = \mathrm{Tr}_{\mathscr{H}_L^{(N)}}\left(e^{-\beta H}\right). \tag{5.51}$$

Proof. At any fixed L, we use (5.50) and take the trace in the energy eigenbasis (5.46). This gives

$$\begin{aligned}
\mathrm{Tr}_{\mathscr{H}_L^{(N)}}\left(e^{-\beta H}\right) &= \sum_{R \in \mathfrak{R}_L^{(N)}} \sum_{\mathsf{a},\mathsf{s},\dot{\mathsf{a}},\dot{\mathsf{s}}} \langle R, \mathsf{a}, \mathsf{s};\ \phi(R), \dot{\mathsf{a}}, \dot{\mathsf{s}}|e^{-\beta H}|R, \mathsf{a}, \mathsf{s};\ \phi(R), \dot{\mathsf{a}}, \dot{\mathsf{s}}\rangle \\
&= \sum_{R \in \mathfrak{R}_L^{(N)}} \sum_{\mathsf{a}=1}^{\dim R} \sum_{\mathsf{s}=1}^{\mathfrak{d}_R} \sum_{\dot{\mathsf{a}}=1}^{\dim \phi(R)} \sum_{\dot{\mathsf{s}}=1}^{\tilde{\mathfrak{d}}_R} e^{-\beta|R|} \\
&= \sum_{R \in \mathfrak{R}_L^{(N)}} \mathfrak{d}_R \dim(R)\tilde{\mathfrak{d}}_R \dim(\phi(R))\, e^{-\beta|R|}.
\end{aligned}$$

$$(5.52)$$

$\square$

We emphasize that, despite the apparent simplicity of the Hamiltonian H, these systems behave very differently from free systems. One major distinction is the degeneracy factor $\dim R$, which grows fast with the energy $|R|$.

Definition 5.4.6. Let[6] $\mathscr{H}_L^{\mathrm{E}}, \mathscr{H}_L^{\mathrm{W}} \cong \mathscr{H}_L$ be two copies of $\mathscr{H}_L$, and consider the tensor product space $\mathscr{H}_L^{\mathrm{E}} \otimes \mathscr{H}_L^{\mathrm{W}}$. We endow it with the canonical tensor product basis and

---

[6]We adopt the notation E (east) and W (west), instead of the more customary left and right, to avoid confusion with the symbols L, R.

promote the Hamiltonian H on $\mathcal{H}_L$ to $H \otimes 1$ on $\mathcal{H}_L^{\mathrm{E}} \otimes \mathcal{H}_L^{\mathrm{W}}$. The *thermofield double state* of the system, at inverse temperature β, is

$$|\Psi_\beta\rangle_L := \frac{1}{\sqrt{\mathcal{Z}_L^{(N)}}} \sum_{R \in \mathfrak{R}_L^{(N)}} \sum_{\mathsf{a},\mathsf{s},\dot{\mathsf{a}},\dot{\mathsf{s}}} e^{-\frac{\beta}{2}|R|} |R, \mathsf{a}, \mathsf{s}; \, \phi(R), \dot{\mathsf{a}}, \dot{\mathsf{s}}\rangle^{\mathrm{E}} \otimes |R, \mathsf{a}, \mathsf{s}; \, \phi(R), \dot{\mathsf{a}}, \dot{\mathsf{s}}\rangle^{\mathrm{W}}.$$

(5.53)

Of course, this definition only makes sense if $\mathcal{Z}_L^{(N)}$ is finite, which is expected at finite N but not at large N. The usefulness of the thermofield double state is to compute the thermal expectation values of any operator $\hat{O}$, through the identity

$$_L\langle\Psi_\beta|\hat{O}|\Psi_\beta\rangle_L = \frac{1}{\mathcal{Z}_L^{(N)}} \mathrm{Tr}_{\mathcal{H}_L^{(N)}} \left(e^{-\beta H} \, \hat{O} \right). \qquad (5.54)$$

The construction so far is summarized as:

Gauge + flavor symmetry		Quantum mechanics	
flavor rank L	$\longleftrightarrow$	choice of Hilbert space	
flavor symmetry generators	$\longleftrightarrow$	microscopic states	(5.55)
gauge rank N	$\longleftrightarrow$	constraint on allowed states	
objects in representation ring	$\longleftrightarrow$	superselection sectors	

Global symmetry representations and meson-like formulation

In preparation for Subsection 5.4, we now proceed to reformulate the quantum system in terms of more standard physical operators. This is an insightful rewriting, although not strictly necessary for the construction.

We start with the trivial representation, which provides us with the vacuum $|\emptyset; \emptyset\rangle$. We then identify the number $|R|$ with the number of particles created on top of the vacuum. On the other hand, $|R|$ is total the number of boxes in the Young diagram R, thus

$$\# \text{ of particles } = |R| = \# \text{ of boxes}. \qquad (5.56)$$

All the one-particle states are obtained tensoring the vacuum with the representation $(\square, \phi(\square))$. In this way we identify the state

$$|\square, \mathsf{a}; \phi(\square), \dot{\mathsf{a}}\rangle, \qquad \mathsf{a} = 1, \ldots, \dim \square, \; \dot{\mathsf{a}} = 1, \ldots, \dim \phi(\square) \qquad (5.57)$$

with a *meson-like* state. We emphasize that, when $\phi(R) = \overline{R}$, $|\square, \mathsf{a}; \overline{\square}, \dot{\mathsf{a}}\rangle$ resembles the standard meson, with one index a in the fundamental and the other index $\dot{\mathsf{a}}$ in the anti-fundamental, combined in a gauge-invariant fashion.

Iterating this procedure and tensoring with arbitrary symmetric powers of $(\square, \phi(\square))$ one ends up constructing all the necessary states, which is a consequence of the isomorphism

$$\bigoplus_{n=0}^{\infty} \mathrm{Sym}^n(\square, \phi(\square)) \cong \bigoplus_{R \in \mathfrak{R}^{SU(L+1)}} (R, \phi(R)), \tag{5.58}$$

which holds as well replacing $R \in \mathfrak{R}^{SU(L+1)}$ with $R \in \mathfrak{R}^{U(L)}$ on the right-hand side and interpreting $\square$ on the left-hand side as the fundamental representation of $U(L)$.

The partition function as a discrete matrix model

In Subsection 5.4, the character expansion has been used to repackage the gauge-invariant operators into an ensemble of irreducible representations, or of Young diagrams. We now proceed to rewrite this system as a matrix model in which the eigenvalues live on the lattice $\mathbb{N}^L$, called *discrete matrix models*. This presentation is more suitable for computations.

Proposition 5.4.7 ([397, 148]). *For every $L \in \mathbb{N}$, there exists an injective map $\iota : \mathfrak{R}_L^{(N)} \to \mathbb{N}^{L+1}$ such that the equality holds:*

$$\mathcal{Z}_L^{(N)}(y) = y^{-\frac{L^2}{2}} \sum_{\vec{h} \in \mathfrak{H}_L^{(N)}} \frac{y^{\sum_{i=1}^{L}\left(h_i+\frac{1}{2}\right)}}{L!\, G(L+2)^2}\, \mathfrak{d}_{\vec{h}}^2 \prod_{1 \le i < j \le L+1} (h_i - h_j)^2, \tag{5.59}$$

where $G(\cdot)$ is Barnes's G-function [38], $\mathfrak{H}_L^{(N)} := \iota\left(\mathfrak{R}_L^{(N)}\right) \subseteq \mathbb{N}^L$, $\vec{h} = (h_1, \ldots, h_L, -1) \in \mathbb{N}^{L+1}$, and $\mathfrak{d}_{\vec{h}}$ denotes the image of $\mathfrak{d}_R$ under ι.

We have restricted to the case $\phi(R) = R$ or $\phi(R) = \overline{R}$, but the argument can be easily adapted to a more general situation. In that case, the discrete matrix model is non-standard, because the squared Vandermonde factor gets modified.

Besides, (5.59) is stated for $SU(L+1)$, but the adaptation to $U(L)$ is straightforward, the only difference residing in the value of $\dim R$.

Proof. The equivalence passes through the change of variables

$$h_i = R_i - i + L, \tag{5.60}$$

with the new variables h_i satisfying

$$h_1 > h_2 > \cdots > h_L \ge 0. \tag{5.61}$$

The map ι is thus specified by (5.60). Direct computation gives $\frac{L^2}{2}+|R| = \frac{L}{2}+\sum_{i=1}^{L} h_i$. It remains to express $\dim R$ as [312]

$$\dim R = \prod_{1 \le i < j \le L+1} \left(\frac{R_i - R_j - i + j}{j - i} \right). \tag{5.62}$$

The standard substitution (5.60) casts $\dim R$ in terms of the Vandermonde determinant:

$$\dim R = \frac{1}{G(L+2)} \prod_{1 \le i < j \le L+1} (h_i - h_j), \tag{5.63}$$

where the Barnes's G-function at integer argument satisfies $G(L+2) = \prod_{n=1}^{L}(n!)$, and with the understanding $h_{j>L} = 0$. For $U(L)$ representations we have

$$\dim R = \frac{1}{G(L+1)} \prod_{1 \le i < j \le L} (h_i - h_j). \tag{5.64}$$

The last step of the proof is to notice that the summand is totally symmetric in the variables h_i, and vanishes whenever two are equal, due to the Vandermonde determinant. Therefore, one can lift the restriction (5.61) and divide by the order of the symmetric group of L elements, i.e., $L!$, to remove the over-counting.

The proof we have given here is a generalization of the one in [148]. The result was certainly known in the matrix model community, and our only contribution it to cast it in a very general form. □

The discreteness of the matrix ensemble (5.59) and the presence of additional constraints will generically induce large N third order phase transitions. This is a recurrent theme, initiated in [148]. This property is nothing but the mirror of the ubiquitous third order phase transitions in the unitary one-matrix models we have started with. We will see that, in several cases, passing to a larger ensemble will promote the phase transition from third to first order, with Hagedorn-like behavior. We elaborate on this comment in Subsection 5.5, and in Appendix 5.13 from the point of view of the unitary matrix model.

The two-step dictionary that emerges, in going from the gauge theory to the discrete matrix model passing through the ensemble of representations, is:

GAUGE + FLAVOR SYMMETRY		DISCRETE MATRIX MODEL
gauge rank N	$\longleftrightarrow$	constraint on allowed configurations
flavor rank L	$\longleftrightarrow$	# of eigenvalues L
gauge-invariant state	$\longleftrightarrow$	eigenvalue configuration

$$\tag{5.65}$$

Coupling to a probe

Now that the Hilbert space of our system and a Hamiltonian have been specified, we recall our main objective: constructing a large N von Neumann algebra of type III_1. As we have proven earlier in Section 5.3, one can do so by constructing observables satisfying large N factorization such that the spectral density has continuous support. This is the goal of this subsection. The strategy will be to couple a probe operator to the system and to explicitly calculate its real-time correlation functions. The correlation functions of the probe will then be described by a large N von Neumann algebra of type III_1. Importantly, constructing this large N von Neumann algebra will only require the correlation functions of the probe. The idea is that just like in $\mathcal{N} = 4$ super-Yang–Mills, the correlation functions of one single trace operator allow to probe the emergence of spacetime, here the correlation functions of our probe will give information on the emergent properties of the full quantum system in the large N limit.

Probe operators

Very schematically, the idea is to define an auxiliary object that creates a probe excitation at time 0 and let it propagate until it is annihilated at a later time $t > 0$. The probe particle is a bosonic particle in the representation $(\square, \emptyset)$. Of course, the alternative choice $(\emptyset, \overline{\square})$ is equally valid and can be dealt with in exactly the same manner. The probe is coupled to the system by tensoring the corresponding Hilbert spaces.

Definition 5.4.8. Let

$$\Gamma_{\mathrm{probe}} := \bigoplus_{n=0}^{\infty} \mathrm{Sym}^n(\square, \emptyset) \tag{5.66}$$

denote the bosonic Fock space of a probe in the fundamental representation. The $n = 0$ component is the trivial vector space, consisting only of the vacuum. The probe is said to be coupled to the system if $\mathscr{H}_L^{(N)}$ is replaced with the total Hilbert space

$$\begin{aligned} \mathscr{H}_L^{\mathrm{tot}} &:= \mathscr{H}_L^{(N)} \otimes \Gamma_{\mathrm{probe}} \\ &\cong \left[\mathscr{H}_L^{(N)} \otimes (\emptyset, \emptyset)_{\mathrm{probe}} \right] \oplus \left[\mathscr{H}_L^{(N)} \otimes (\square, \emptyset)_{\mathrm{probe}} \right] \oplus \cdots \end{aligned} \tag{5.67}$$

Definition 5.4.9. The *probe approximation* consists in neglecting all terms in (5.67) other than the one giving the first non-trivial contribution to the correlation functions.

In practice, the probe approximation can be enforced by modifying the Hamiltonian adding a large mass term on Γ_{probe}. We will provide a more formal definition below, in Definition 5.4.10.

The $n = 0$ component of Γ_{probe} consists only of the vacuum

$$|\emptyset; \emptyset\rangle_{\text{probe}} \cong |\underbrace{0, \ldots, 0}_{L}; \underbrace{0, \ldots, 0}_{L}\rangle_{\text{probe}}. \tag{5.68}$$

Here and in what follows, the semicolon denotes the tensor product between the left and the right for the probe, while the commas separate the occupation numbers of the different modes in the one-particle Hilbert space. We define the creation and annihilation operators $c_p^{\dagger}, c_p$ acting on the probe sector Γ_{probe}. The lowest non-trivial probe sector is the $n = 1$ term in Γ_{probe}, consisting of

$$\left\{ \left(c_p^{\dagger} \otimes 1 \right) |0, \ldots, 0; 0, \ldots, 0\rangle_{\text{probe}}, \ \forall p = 1, \ldots, L \right\}. \tag{5.69}$$

The full Γ_{probe} is built acting with $c_p^{\dagger} \otimes 1$ on the Fock vacuum of the probe. We emphasize that $c_p^{\dagger}, c_p$ act on the probe sector rather than $\mathscr{H}_L^{(N)}$. We therefore indicate them with a different letter. Nevertheless, the two sets of operators behave in the same way when expressed in terms of $SU(L + 1)$ representations.

In the composite system, in which the probe is coupled to the rest, the push-forward of the creation operator is

$$(1 \otimes 1) \otimes \left(c_p^{\dagger} \otimes 1 \right)_{\text{probe}} \tag{5.70}$$

where the first parenthesis is the identity operator on $\mathscr{H}_L$ (or its restriction to the subspace $\mathscr{H}_L^{(N)}$), that decomposes into $1 \otimes 1$ on the R-graded terms $\mathscr{H}_L(R) \otimes \mathscr{H}_L(\phi(R))$ in (5.45).

Hamiltonian and interactions

The next step is to promote the Hamiltonian H on $\mathscr{H}_L$ to a Hamiltonian H' on the combined Hilbert space $\mathscr{H}_L \otimes \Gamma_{\text{probe}}$ of the system coupled to the probe. This Hamiltonian must necessarily contain a term $H \otimes 1_{\text{probe}}$. We would also like to add the tensor product of the identity on $\mathscr{H}_L$ and a large mass term acting only on Γ_{probe}, and add an interaction term between the probe and the rest of the system. In order to be able to discuss possible interaction terms more precisely, we will make the following assumption:

◇ In what follows, we assume (5.25), and moreover take $\phi(R) = R$. The situation with $\phi(R) = \overline{R}$ can easily be retrieved from the ensuing discussion, with minor variations. The generic situation for arbitrary $\phi(R)$ can also be worked out along the same lines, but is not immediate, as it requires a more careful analysis of allowed interaction terms.

Recall the Hilbert space of the composite system of the probe and our quantum theory in (5.67), given by

$$\mathscr{H}_L^{\text{tot}} = \mathscr{H}_L^{(N)} \otimes \Gamma_{\text{probe}}, \tag{5.71}$$

where Γ_{probe} is the Fock space of the probe. Define the free Hamiltonian operator on Γ_{probe}:

$$H_{0,\text{probe}} := \mu \sum_{p=1}^{L} \left(c_p^\dagger c_p \otimes 1 \right)_{\text{probe}}, \tag{5.72}$$

where $\mu > 0$ has the meaning of a mass for the probe, and we will later assume $\mu \gg 1$ (and also larger than all other relevant scales in the problem), which enforces the probe approximation.

Then, without coupling the probe to the gauge theory, one can define the Hamiltonian associated to the two systems as an operator on $\mathscr{H}_L^{\text{tot}}$:

$$H_{\text{decoupled}} := 1 \otimes H_{0,\text{probe}} + H \otimes 1, \tag{5.73}$$

where H is the Hamiltonian of our quantum mechanical theory from Subsection 5.4, which satisfies $H(R, \phi(R)) = |R|$, where $H(R, \phi(R))$ denotes the restriction of H to $\mathscr{H}_L(R) \otimes \mathscr{H}_L(\phi(R))$.

Clearly, letting the system in $\mathscr{H}_L^{\text{tot}}$ evolve with $H_{\text{decoupled}}$ is a trivial operation, as the probe and the system do not talk to each other. In order to witness a non-trivial behavior and the ensuing appearance of a large N type III$_1$ algebra, the probe must interact with our quantum system. Hence the full Hamiltonian reads:

$$H' := 1 \otimes H_{0,\text{probe}} + H \otimes 1 + H_{\text{int}}, \tag{5.74}$$

where H_{int} is an interaction Hamiltonian that we now define directly inside the tensor product Hilbert space $\mathscr{H}_L^{\text{tot}}$. If our models were derived top down in string theory, H_{int} would be determined by the action on the probe brane. Instead, our construction

of the quantum mechanics is bottom up, and we will introduce the interaction by hand, selecting a tractable sample of all the possible interactions H_{int}.

The idea is that in the original quantum Hilbert space (without adding the probe), all pairs of representations appearing are of the form $(R, \phi(R))$. However, once one tensors these with the symmetric powers of the fundamental representation of $SU(L+1)$, which corresponds to the one-particle Hilbert space of the probe, more generic pairs of representations start appearing in the Hilbert space. This motivates the definition of H_{int} as an operator that is zero on pairs of the form $(R, \phi(R))$, and nonzero on other pairs (R_1, R_2) (upon identifying $\mathscr{H}_L^{\text{tot}}$ with a Hilbert space spanned by representations of the form (R_1, R_2), where R_2 is some $\phi(R)$, and R_1 is an irreducible representation that appears in the decomposition of the tensor product of some symmetric power of the fundamental representation with R). It should also respect $SU(L+1)$ symmetry.

With this in mind, one possible interaction term is

$$H_{\text{int}}(R_1, R_2) = \frac{g}{2} \left[Q(R_1) - Q(R_2) \right], \qquad Q(R) := C_2(R) + (L+1)|R|, \quad (5.75)$$

where C_2 is the quadratic Casimir. We will work with (5.75) in the rest of this part. Of course, other similar choices can be made, for example by switching R with $\phi(R)$, or by switching signs. For example, to ease the comparison with [246], we will make a slightly different choice of interaction Hamiltonian in Section 5.6, see (5.181).

The coupling g sets the strength of the interaction. Coming from a matrix model, it will be natural to consider a 't Hooft limit with $g \propto 1/L$ in the large N and large L limit. The choice of the factor $L|R|$ is merely to avoid some cumbersome shifts in the ensuing expressions. Dropping it, or changing its coefficient, would not alter the conclusions.

> ⋄ Higher Casimir invariants may be included in H_{int}, as well as more sophisticated interactions. We restrict ourselves to the simplest non-trivial interaction. The choice is motivated by the sake of tractability and an analogy with [246].

Now that we have introduced the Hamiltonian, we can write down a more precise version of Definition 5.4.9.

Definition 5.4.10. Consider the $\mathbb{C}$-valued map

$$\hat{O} \mapsto \operatorname{tr}_{\mathscr{H}_L^{\mathrm{tot}}} \left(e^{-\beta H'} \hat{O} \right), \qquad \hat{O} \in \mathcal{L} \left(\mathscr{H}_L^{\mathrm{tot}} \right) \tag{5.76}$$

and write the right-hand side in the form

$$\operatorname{tr}_{\mathscr{H}_L^{\mathrm{tot}}} \left(e^{-\beta H'} \hat{O} \right) = \sum_{\vec{n} \in \mathbb{N}^{L+1}} e^{-\beta \mu |\vec{n}|} \operatorname{tr}_{\mathscr{H}_L^{(N)}} \left({}_{\mathrm{probe}}\langle \vec{n}; \emptyset | e^{-\beta(H+H_{\mathrm{int}})} \hat{O} |\vec{n}; \emptyset \rangle_{\mathrm{probe}} \right) \tag{5.77}$$

where we have used $\dim \square = L + 1$ for $SU(L+1)$ and introduced the shorthand notations

$$\vec{n} = (n_1, \dots, n_{L+1}), \qquad |\vec{n}; \emptyset\rangle_{\mathrm{probe}} := |n_1, \dots, n_{L+1}; 0, \dots, 0\rangle_{\mathrm{probe}}, \qquad |\vec{n}| := \sum_{i=1}^{L+1} n_i \tag{5.78}$$

and the Hamiltonian (5.74). The outer sum runs over all states in the probe sector. The partition functions (5.77) and the ensuing correlation functions are treated as series expansions in the parameter $e^{-\beta \mu}$. The *probe approximation* consists in discarding all contributions except the lowest order one.

This definition based on the series expansion in the parameter $e^{-\beta \mu}$ formalizes the physical intuition that a probe is an object with a large mass $\mu \gg 1$, so that the excited states are not accessible. Note that the order of limits will be important later. We first take $\beta \mu \gg 1$ with every other parameter fixed. Then, when considering the large N limit, we will take $N, L \gg 1$ but assuming μ is still large enough with respect to L. In the continuation we make two remarks on this definition.

- Notice that the probe approximation is a different concept than a cutoff at energy scales $O(\mu)$, and when the probe is decoupled from the system, the latter is not affected.

- Retaining only the lowest order contribution to the correlation functions, as per Definition 5.4.10, *is not* the same as setting $\vec{n} = (0, \dots, 0)$ in (5.77). While this latter prescription will often work, it may happen that one needs to compute correlation functions of the form

$$e^{\beta \mu} \operatorname{tr}_{\mathscr{H}_L^{\mathrm{tot}}} \left(e^{-\beta H'} \hat{O} \right) \tag{5.79}$$

  for some operator $\hat{O}$ that annihilates the probe vacuum. In such a scenario, the contribution from $\vec{n} = (0, \dots, 0)$ trivializes, whereas the first excited states

with $|\vec{n}| = 1$ will yield the first non-trivial contribution,

$$
e^{\beta\mu} \ \mathrm{tr}_{\mathscr{H}_L^{\mathrm{tot}}} \left(e^{-\beta H'} \ \hat{O} \right)
$$

$$
= e^{\beta\mu} \cdot \left\{ 0 \ + \ e^{-\beta\mu} \sum_{\substack{\vec{n}\in\mathbb{N}^{L+1} \\ |\vec{n}|=1}} \mathrm{tr}_{\mathscr{H}_L^{(N)}} \left({}_{\mathrm{probe}}\langle\vec{n};\emptyset|e^{-\beta(H+H_{\mathrm{int}})} \ \hat{O} |\vec{n};\emptyset\rangle_{\mathrm{probe}} \right) \ + \ O(e^{-2\beta\mu}) \right\}
$$

$$
= \sum_{\substack{\vec{n}\in\mathbb{N}^{L+1} \\ |\vec{n}|=1}} \mathrm{tr}_{\mathscr{H}_L^{(N)}} \left({}_{\mathrm{probe}}\langle\vec{n};\emptyset|e^{-\beta(H+H_{\mathrm{int}})} \ \hat{O} |\vec{n};\emptyset\rangle_{\mathrm{probe}} \right) \ + \ O(e^{-\beta\mu}).
$$

$$(5.80)$$

Correlation functions

We wish to calculate real-time two-point correlation functions of the probe. We now introduce new operators whose correlations can be computed easily. They are related to the c_p's by a $U(L)$ rotation, and consequently, by flavor symmetry, the correlations of these operators will be the same as the ones of any creation or annihilation operator of the probe in a given basis. However it will be useful for computations to write operators down in a form that treats all basis vectors democratically. With the ingredients defined insofar, we hence introduce the operator

$$
O_L := \frac{1}{\sqrt{L+1}} \sum_{p=1}^{L+1} (1 \otimes 1) \otimes \left(c_p^\dagger \otimes 1 \right)_{\mathrm{probe}} \tag{5.81}
$$

on $\mathscr{H}_L^{\mathrm{tot}}$. Likewise, the annihilation operator is $O_L^\dagger = \frac{1}{\sqrt{L+1}} \sum_{p=1}^{L+1} (1\otimes1)\otimes\left(c_p \otimes 1 \right)_{\mathrm{probe}}$.

As the Hamiltonian of the systems respects the flavor symmetry, it is clear that these operators have correlation functions equal to the ones of any $c_p^\dagger$. They also satisfy the commutation relations:

$$
[c_p, c_q^\dagger] = \delta_{p,q} \quad \Longrightarrow \quad \left[O_L^\dagger, O_L \right] = 1. \tag{5.82}
$$

The normalization by $1/\sqrt{L+1}$ in (5.81) ensures that the correlation functions are properly normalized. The reason why we introduced the $O_L^\dagger$ instead of calculating correlation functions directly at the level of the $c_p^\dagger$ is because it will be useful to have explicit sums over flavor indices in our calculations.

In order to lighten the notation, we will omit the subscript on the probe part, and identify $c_p^\dagger$ with $(c_p^\dagger \otimes 1)_{\mathrm{probe}}$, so to write

$$
O_L = \frac{1}{\sqrt{L+1}} \sum_{p=1}^{L+1} 1 \otimes c_p^\dagger. \tag{5.83}
$$

The left operator in the tensor product acts on $\mathscr{H}_L^{(N)}$ and the right acts on Γ_{probe}.

Equipped with the Hamiltonian H' from (5.74), we generate the time evolution in the Heisenberg picture of the operators in

$$\text{End}\left(\mathscr{H}_L^{\text{tot}}\right) \cong \text{End}\left(\mathscr{H}_L^{(N)} \otimes \Gamma_{\text{probe}}\right). \tag{5.84}$$

What we will require is the time-evolved annihilation operator at time t:

$$O_L^\dagger(t) = e^{itH'} \left(\frac{1}{\sqrt{L+1}} \sum_{p=1}^{L+1} 1 \otimes c_p\right) e^{-itH'}. \tag{5.85}$$

The correlation functions of time-ordered products of operators $O_L, O_L^\dagger$ inserted at different times provide well-posed observables of the quantum system. Observe that

- Correlation functions will be non-vanishing only if an equal number of O_L and $O_L^\dagger$ is taken. This is of course a consequence of the simplicity of the probe operators, and differs from the more sophisticated models of, e.g., [457, 100].

- In the two-point functions, i.e. in the expectation values of operators

$$O_L^\dagger(t)O_L(0) = \frac{1}{L+1} \sum_{p,q=1}^{L+1} e^{itH'} \left(1 \otimes c_q\right) e^{-itH'} \left(1 \otimes c_p^\dagger\right) \tag{5.86}$$

  only terms with $q = p$ will yield a non-vanishing contribution, by flavor symmetry.

- We also notice the normalization by $\dim \square = L + 1$, that keeps the correlation functions properly normalized. To work with $U(L)$ instead of $SU(L+1)$, one lets p run from 1 to L and normalizes O_L by $1/\sqrt{L}$.

We arrive at the following statement.

Lemma 5.4.11. *The two-point function of a probe is computed by the finite temperature expectation value of* $O_L^\dagger(t)O_L(0) \in \mathcal{L}\left(\mathscr{H}_L^{\text{tot}}\right)$, *evolved with Hamiltonian* (5.74). *Explicitly:*

$$O_L^\dagger(t)O_L(0) \qquad \text{and} \qquad \frac{1}{L+1} \sum_{p=1}^{L+1} e^{itH'} \left(1 \otimes c_p\right) e^{-itH'} \left(1 \otimes c_p^\dagger\right) \tag{5.87}$$

have the same correlation functions.

⬦ In the present discussion, we are neglecting the additional quantum numbers $\lambda_s, \lambda_{\dot{s}}$ in the probe sector. They can be reinstated replacing $c_p^\dagger$ and c_p with the appropriate creation and annihilation operators that create a state decorated with additional quantum numbers, but we do not sum over them.

Finally, to make contact with the conventions used in the study of von Neumann algebras, we introduce the self-adjoint operator

$$\phi_L := \frac{1}{\sqrt{2}} \left(O_L^\dagger + O_L \right). \tag{5.88}$$

In terms of the probe creation and annihilation operators, ϕ_L reads

$$\phi_L = \sum_{p=1}^{L+1} \frac{c_p + c_p^\dagger}{\sqrt{2(L+1)}}. \tag{5.89}$$

Intermezzo: On creation and annihilation operators

Let us clarify a subtlety about the creation and annihilation operators from the get go. In the concrete models we have constructed, there are creation and annihilation operators associated to a probe particle coupled to our quantum systems. It is important to note that these operators, although closely related, are formally *not* the same as the ones appearing in Section 5.3.

Indeed, in the case of Section 5.3, the one-particle Hilbert space is $L^2(\mathbb{R}, \rho)$ and corresponds to functions of the time variable (or equivalently, their Fourier transforms), whereas in our quantum systems the one-particle Hilbert space will be indexed by the number of degrees of freedom of the theory. As this number goes to infinity, we will see momentarily that the real-time correlation functions of the system will factorize according to Wick's theorem. What Section 5.3 tells us is that then, the same correlation functions can be recovered by a quasi-free state on the CCR algebra over $L^2(\mathbb{R}, \rho)$. It is in that sense that the two sets of creation and annihilation operators are related, and that one will be able to identify the von Neumann algebras constructed in Section 5.3 and Appendix 5.11 with the large N von Neumann algebras of our quantum systems.

Spectral densities

We have shown in Subsection 5.3 that, in order to determine the type of the von Neumann algebras, one needs to calculate the real-time Wightman function at finite temperature, as well as its associated Källén–Lehmann spectral density $\rho(\omega)$. Here,

we introduce appropriate Wightman functions for the class of models of Subsection 5.4, and derive general properties of the associated spectral density. These properties will allow us to determine the type of the large N von Neumann algebras constructed in Section 5.3.

Definitions

We begin introducing the notation, and then proceed with the main statements. Recall the quantum system of Subsection 5.4 and the correlation function of creation and annihilation operators from Subsection 5.4. With these ingredients at hand, we introduce the Wightman functions of the systems. Our conventions follow [172, App.B].

Definition 5.4.12. The real-time, finite temperature Wightman function is

$$G_{L,+}(t) := \frac{1}{\mathcal{Z}_L^{(N)}} \, \mathrm{tr}_{\mathcal{H}_L^{\mathrm{tot}}} \left(e^{-\beta H'} \, \phi_L(t)\phi_L(0) \right). \tag{5.90}$$

The dependence on the parameter N and β is left implicit in the notation $G_{L,+}(t)$.

The importance of this quantity lies in its appearance in the right-hand side of (5.22). Let $\widetilde{G}_{L,+}(\omega)$ be the Fourier transform of $G_{L,+}(t)$. From (5.9), $\widetilde{G}_{L,+}(\omega)$ is simply related to the Källén–Lehmann spectral density $\rho(\omega)$, or *spectral density* for short, through

$$\widetilde{G}_{L,+}(\omega) = \frac{\rho(\omega)}{1 - e^{-\beta\omega}}. \tag{5.91}$$

There are related types of Wightman functions that are useful in practice for certain computations [172, App.B].

Definition 5.4.13. With the definitions and prescription of Subsection 5.4, the real-time, finite temperature, retarded and advanced Wightman functions are, respectively,

$$G_{L,\mathrm{R}}(t) := \quad i\theta(t) \ \frac{1}{\mathcal{Z}_L^{(N)}} \mathrm{Tr}_{\mathcal{H}_L^{\mathrm{tot}}} \left(e^{-\beta H'} \, [\phi_L(t), \phi_L(0)] \right), \tag{5.92}$$

$$G_{L,\mathrm{A}}(t) := -i\theta(-t) \frac{1}{\mathcal{Z}_L^{(N)}} \mathrm{Tr}_{\mathcal{H}_L^{\mathrm{tot}}} \left(e^{-\beta H'} \, [\phi_L(t), \phi_L(0)] \right), \tag{5.93}$$

with $\theta(t)$ the Heaviside step function.

Definition 5.4.14. With the notation as in Subsection 5.4, let H_{int} be as in (5.75) and $|\Psi_\beta\rangle_L$ be the thermofield double state (5.53). Besides, for every $R \in \mathfrak{R}_L^{(N)}$ let

$$\mathcal{J}_R := \{J = 1\} \cup \{J \in \{2, \ldots, L+1\} \; : \; R_{J-1} > R_J\} \qquad (5.94)$$

and, $\forall J \in \mathcal{J}_R$, denote by $R \sqcup \square_J$ the Young diagram obtained adding a box at the end of the Jth row of R. Let also

$$E_J^{\text{int}} := H_{\text{int}}(R \sqcup \square_J, \phi(R)), \qquad (5.95)$$

$$E_J(\mu) := E_J^{\text{int}} + \mu. \qquad (5.96)$$

For the specific H_{int} in (5.75) one gets

$$E_J^{\text{int}} := g(R_J - J + L + 1). \qquad (5.97)$$

For every $\omega \in \mathbb{R}$, introduce the shifted variable ω_{r} defined as

$$\omega_{\text{r}} := |\omega| - \mu. \qquad (5.98)$$

Moreover, for $\phi(R) = R$ or $\phi(R) = \overline{R}$, define $\mathsf{G}(\omega)$ through

$$\langle R, \mathsf{a}, \mathsf{s}; \phi(R), \dot{\mathsf{a}}, \dot{\mathsf{s}}|\mathsf{G}(\omega)|R, \mathsf{a}, \mathsf{s}; \phi(R), \dot{\mathsf{a}}, \dot{\mathsf{s}}\rangle := \frac{1}{L} \sum_{J \in \mathcal{J}_R} \delta\left(\omega - E_J(\mu)\right) \left(\frac{\dim(R \sqcup \square_J)}{\dim R}\right)$$

$$(5.99)$$

and $\Omega(\omega)$ through

$$\langle R, \mathsf{a}, \mathsf{s}; \phi(R), \dot{\mathsf{a}}, \dot{\mathsf{s}}|\Omega(\omega)|R, \mathsf{a}, \mathsf{s}; \phi(R), \dot{\mathsf{a}}, \dot{\mathsf{s}}\rangle = \frac{1}{L} \sum_{J \in \mathcal{J}_R} \frac{1}{\omega - E_J(\mu)} \frac{\dim(R \sqcup \square_J)}{\dim R}.$$

$$(5.100)$$

For later reference, we introduce here the notion of Veneziano limit. It will have a prominent role in the study of the planar limit of the unitary matrix models (5.42).

Definition 5.4.15. Consider a gauge theory with gauge rank N and flavor rank L. The *Veneziano parameter* is the ratio

$$\gamma = \frac{L}{N}. \qquad (5.101)$$

The *Veneziano limit* is a large N planar limit in which γ is kept finite.

Main results on the spectral density

The following results are the linchpin of the subsequent derivation. For a cleaner presentation, we have collected the proofs in Appendix 5.14. We encourage the reader to consult that appendix to gain familiarity with the very explicit computations in these models.

Theorem 5.4.16. *With the notation as in Definition 5.4.14 and $\theta(\omega)$ the Heaviside step function, the identity*

$$\rho(\omega) = \frac{1}{2} \, {}_L\langle \Psi_\beta | \theta(\omega) \mathsf{G}(\omega) - \theta(-\omega) \mathsf{G}(-\omega) | \Psi_\beta \rangle_L \tag{5.102}$$

holds in the probe approximation.

Proof. The proof is instructive but lengthy, thus it is spelled out in detail in Appendix 5.14. It is based on writing $\rho(\omega) = (1 - e^{-\beta\omega})\widetilde{G}_{L,+}(\omega)$, explicitly computing the right-hand side and retaining the lowest order in $e^{-\beta\mu}$. □

A few remarks on the theorem are in order.

- First, $\rho(\omega)$ is manifestly odd, as it should be.

- Second, notice that $\rho(\omega)$ really depends on ω_r in (5.98). Recall that the variable ω measure differences in the energy levels. Due to the probe mass term, the correlation functions are centered around μ; that is, there is a uniform shift by μ for every R. The physically meaningful variable, that probes the interaction of the non-trivial quantum mechanics with the probe, is (5.98).

- Third, we are not including the additional quantum numbers λ_s in our probe for simplicity. They can be reinstated by replacing $c_p^\dagger$ appropriately in the definition of $\mathcal{O}_L$ in Subsection 5.4. With an appropriate normalization, this modification inserts a ratio $\frac{\eth_{R \sqcup J}}{\eth_R}$ in the right-hand side of (5.99).

- Fourth, an interesting aspect of the proof of (5.102), given below, is that the degeneracy factors remain spectators. As a consequence, several extensions are automatically built-in in our formula, including: the replacement $(\dim R)^2 \mapsto (\dim R)^{2-2\mathsf{g}}$ for an arbitrary integer $\mathsf{g} \in \mathbb{N}$, and refining $(\dim R)^2$ into a q-deformed or Macdonald measure [72].

Next, we give an equivalent characterization of (5.102). In practice we will use Theorem 5.4.17 for the computations in Part 5.5.

Theorem 5.4.17. *With the notation as in Definition 5.4.14, it holds that*

$$\widetilde{G}_{L,R}(\omega + i\varepsilon) = -\frac{1}{2} {}_L\langle\Psi_\beta|\Omega(\omega + i\varepsilon) + \Omega(-\omega - i\varepsilon)|\Psi_\beta\rangle_L, \tag{5.103}$$

$$\widetilde{G}_{L,A}(\omega - i\varepsilon) = -\frac{1}{2} {}_L\langle\Psi_\beta|\Omega(\omega - i\varepsilon) + \Omega(-\omega + i\varepsilon)|\Psi_\beta\rangle_L. \tag{5.104}$$

Proof. The proof is done in Appendix 5.14 by direct calculation. □

The crucial aspect of Theorem 5.4.17 is that, thanks to (5.22), we can equivalently compute $\rho(\omega)$ via the discontinuity equation [172, Eq.(B.7)]

$$\rho(\omega) = -i \lim_{\varepsilon\to0^+} \left[\widetilde{G}_{L,R}(\omega + i\varepsilon) - \widetilde{G}_{L,A}(\omega - i\varepsilon)\right]. \tag{5.105}$$

This expression relates the support of $\rho(\omega)$ to the branch cuts of $\widetilde{G}_{L,R}$ and $\widetilde{G}_{L,A}$.

cor.

$$\rho(\omega) = \frac{i}{2} \lim_{\varepsilon\to0^+} \left\{\theta(\omega)\left[{}_L\langle\Psi_\beta|\Omega(\omega + i\varepsilon) - \Omega(\omega - i\varepsilon)|\Psi_\beta\rangle_L\right]\right.$$
$$\left. -\theta(-\omega)\left[{}_L\langle\Psi_\beta|\Omega(-\omega + i\varepsilon) - \Omega(-\omega - i\varepsilon)|\Psi_\beta\rangle_L\right]\right\}. \tag{5.106}$$

Proof. It follows immediately from Theorem 5.4.17 and some rewriting. Noting that the singularities of $\Omega(\omega)$ are located on $\mathbb{R}_{>0}$, only the terms with $+\omega$ will contribute to the discontinuity if $\omega > 0$ and only the terms with $-\omega$ will contribute if $\omega < 0$. □

- We will crucially resort to Corollary 5.4 for the explicit calculation of the eigenvalue density in all the examples.

- The relation between $\rho(\omega)$ and ${}_L\langle\Psi_\beta|\Omega(\omega)|\Psi_\beta\rangle_L$ provided by Corollary 5.4 for each fixed sign(ω) is (up to a normalization by π) exactly the relation between any density $\rho(\omega)$ and its Stieltjes transform. That is, $\pi\Omega(\cdot)$ is the resolvent for the spectral density $\rho(\omega)$.

We are now interested in the large N limit. With the change of variables (5.60), $\widetilde{G}_{L,R}(\omega)$, and similarly $\widetilde{G}_{L,A}(\omega)$, are in turn related via (5.103) to the planar resolvent of the matrix model (5.59) in the Veneziano limit (Definition 5.4.15). It is a standard fact that the branch cuts of the latter quantity determine the eigenvalue density of the matrix ensemble. This chain of identities intertwines the two key quantities, the spectral density $\rho(\omega)$ and the eigenvalue density, and implies the following result.

cor. *Consider the planar Veneziano limit $N \rightarrow \infty$ with $\gamma = L/N$ and $\lambda = gL$ fixed. If the discrete matrix model $\mathcal{Z}_L^{(N)}$ in (5.59) has a continuous eigenvalue density, $\lim_{N \rightarrow \infty} \text{supp}\, \rho \subseteq \mathbb{R}$ is continuous.*

From the perspective of the quantum mechanics of Subsection 5.4, and especially of the matrix model (5.59), it is natural to consider a planar limit in which g scales as $1/L$, rather than $1/N$. Insisting on the gauge theory origin of these models, one may prefer to take N as the reference scale. For the current section, our choice will result in a more convenient normalization, but the other choice would have worked equally well, simply differing by $\lambda \mapsto \gamma \lambda$.

The discontinuity equation (5.105) establishes a direct correspondence between the support of $\rho(\omega)$ to the branch cuts of $\widetilde{G}_{L,R}$ and $\widetilde{G}_{L,A}$. The next Lemma expresses these quantities using the eigenvalue densities of the matrix models (5.59). Combining these two facts will lead to a proof of Corollary 5.4.

Lemma 5.4.18. *Consider the discrete matrix model (5.59) in the Veneziano large N limit. Assume it admits a non-trivial saddle point configuration and denote $\varrho_*(x)$ the corresponding saddle point eigenvalue density. Then, at leading order in the planar limit,*

$$_L\langle\Psi_\beta|\Omega(\omega)|\Psi_\beta\rangle_L = \frac{1}{\lambda}\left[-1 + \exp\left(\int dx \frac{\varrho_*(x)}{\frac{\omega-\mu}{\lambda} - x}\right)\right]. \qquad (5.107)$$

A different definition of planar limit in which $\lambda = gN$ is kept fixed, instead of our choice $\lambda = gL$, would simply result is a redefinition $\lambda \mapsto \gamma\lambda$ in the formula.

Proof. The idea behind the proof of this lemma is to exploit Theorem 5.4.17 and then use Cauchy's theorem to write the Wightman function as a contour integral. In the Veneziano limit, the integral can be evaluated by a saddle point approximation, yielding (5.107). The reader can consult all the details in Appendix 5.14. □

Proof of Corollary 5.4. Let us start assuming that the matrix model $\mathcal{Z}_L^{(N)}$ in (5.59) admits a non-trivial saddle point, which means that $\ln \mathcal{Z}_L^{(N)}$ shows the usual $O(N^2)$ growth. Lemma 5.4.18 relates the Wightman functions $\widetilde{G}_{L,R}(\omega), \widetilde{G}_{L,A}(\omega)$ to the saddle point eigenvalue density. The formula has logarithmic branch cuts if $\frac{\omega_r}{\lambda} \in$

supp ϱ_*. Expressing $\varrho(\omega)$ through the discontinuity equation (5.105), these branch cuts will contribute to supp ρ with a continuous interval in $\mathbb{R}$, proving the claim.

$$\square$$

If the matrix model does not possess a large N scaling for the chosen values of the parameters, the large N argument that led to Lemma 5.4.18 does not apply. The lack of a large N scaling prevents the coalescence of the eigenvalues of the matrix model, which do not form a continuum. It is certainly possible to take the inductive limit over N of the sequence of eigenvalue densities as $N \to \infty$, but in this case the limiting eigenvalue density $\varrho_*(x)$ will be a distribution, i.e., an infinite sum of Dirac deltas. Taking the inductive $N \to \infty$ limit of Theorem 5.4.16 still *formally* relates the eigenvalue density ϱ_* to ρ, whenever the limit of the latter exists. This would formally imply the discreteness of supp ρ in the phase(s) in which the eigenvalues do not coalesce in the planar limit, with the caveat that we are not proving existence of the limit in this case.

Stated differently, we have shown that

$$\text{supp } \varrho_* \text{ continuous} \quad \Longrightarrow \quad \text{supp } \rho \text{ continuous}, \qquad (5.108)$$

and heuristically we expect the same implication for discrete support, but there may be potential obstructions in taking the limit of Theorem 5.4.16 in the phase(s) that do not satisfy the assumptions of Lemma 5.4.18.

In any case, discrete random matrix ensembles such as the ones considered throughout this section typically have a continuous density of eigenvalues in the large N limit. This is an extremely widespread property of these models, so that Corollary 5.4 generically applies. In Section 5.5 we will have to work harder and add extra ingredients to get the situation without continuous eigenvalue density, at low temperature. In particular, the third order transitions that typically appear in the discrete ensembles, separate two phases both with continuous eigenvalue density.

Intermezzo: Comparison with IOP

We ought to stress that (5.103) is closely related to [246, Eq.(5.13)], which in fact was a source of inspiration for the present analysis, especially in the choice of H_{int}. We have also chosen conventions for the probe vacuum energy that agree with [246]. Nevertheless, (5.103) remains valid for a wide class of models, and also incorporates

the N-dependent constraint, which enriches the dynamics of the toy models. A more detailed comparison is in Section 5.6.

Another difference with the treatment in [246] is that, while the probe approximation works essentially in the same way, the shift $\omega \mapsto \omega - \mu$ due to the probe mass is removed in [246] by adding a counterterm by hand. For consistency with the probe approximation, we keep the shift by μ. This has turned out to be important for $\rho(\omega)$ and the derivation of the von Neumann algebra, while this subtlety would not be appreciated in the correlation functions of $O_L^\dagger(t)O_L(0)$, which generalize the computation of [246].

Large N algebras

In order to make statements about large N algebras, we need our systems to satisfy large N factorization, as defined in Subsection 5.3. In this short subsection, we argue that it is the case and deduce the types of the large N algebras.

Lemma 5.4.19. *Consider the discrete matrix model* (5.59) *in the large N Veneziano limit, and assume it admits a non-trivial saddle point configuration. At leading order, the n-point functions of $\phi_L(t)$ satisfy the large N factorization property of Definition 5.3.1.*

Proof. The proof is done explicitly for the four-point function and then by induction on n. We relegate the lengthy details to Appendix 5.14. The basic idea goes as follows.

(1) We first expand ϕ_L in terms of $O_L, O_L^\dagger$, so that we reduce to study n-point functions of these operators. Only combinations with an equal number of O_L and $O_L^\dagger$ give a non-vanishing contribution.

(2) We study the various non-trivial combinations by direct computation.

(3) We approximate the thermal ensemble of representations by its saddle point approximation.

(4) We match the resulting terms with the ones predicted by the factorization property (cf. Proposition 5.14.1), thus showing the lemma.

A few remarks on this proof:

- A technical assumption in this factorization lemma is that the number n of operator insertions is given from the onset and kept fixed in the large N limit. This is a standard requirement, see for instance [370] for a neat discussion of this and related matters.

- Theorem 5.4.16 shows that the two-point function $_L\langle\Psi_\beta|O_L^\dagger(t_2)O_L(t_1)|\Psi_\beta\rangle_L$ behaves as the expectation value of a single-trace operator in the ensemble of representations (5.43). The lemma morally follows from this fact and the factorization properties of matrix models at large N. However, there are complications due to the time dependence, which make the proof more technical and are dealt with in Appendix 5.14.

- We warn the reader of some subtleties to pass from (2) to (3), which are dealt with in Appendix 5.14. The hypotheses of the planar limit and that the saddle point corresponds to a representation of large size are both crucial.

- Let us mention that it should be possible to give a Feynman diagram derivation of the factorization property. The models we consider generalize [246], and one should be able to perform a computation of the correlation functions through more standard QFT techniques, very much along the lines of [337], and show that they factorize. Such a formulation is worth to be studied in detail and is left as an open problem.

$\square$

The results so far are succinctly summarized in the statement:

> **Statement 5.4.20** (Corollary 5.4 and Theorem 5.3.5)**.** The correlation functions of the probe operators in our quantum systems are reproduced by large N von Neumann algebras of Type III_1.

The main technical achievements of this section are (5.105)-(5.107). Combining these two, we immediately get Corollary 5.4, whose assumptions are generically satisfied by the ensembles of representations (5.43). Combining this fact with Theorem 5.3.5, we have that, generically, the quantum systems constructed and studied in this section have an associated Type III_1 von Neumann algebra.

We thus state the more precise version of the qualitative Statement 5.4.20.

Theorem 5.4.21. *Consider the quantum systems of Subsection 5.4, coupled to a probe as detailed in Subsection 5.4. The Hilbert space is $\mathscr{H}_L^{\text{tot}}$ (5.71) and the Hamiltonian is H' (5.74). Assume that the parameters entering the definition (5.43) are such that the eigenvalue density of the discrete matrix model (5.59) has a saddle point approximation $\varrho_*(x)$ which coalesces to a continuum. Then, their large N algebras of operators are von Neumann algebras of Type III_1.*

Additionally, the models based on the ensembles (5.138), (5.234), (5.273), (5.284) satisfy the above hypothesis $\forall\, 0 < \beta < \infty$.

Proof. Corollary 5.4 holds by assumption. Moreover, the technical result of Lemma 5.4.19 shows that the hypotheses of Theorem 5.3.5 are satisfied. Combining the two yields the first part of the result.

For the ensembles listed in the theorem, it is known in the literature and we will show explicitly in Part 5.5 that they satisfy the hypothesis on the non-trivial saddle point in the Veneziano limit. $\qquad\square$

5.5 Systems with Hagedorn transitions
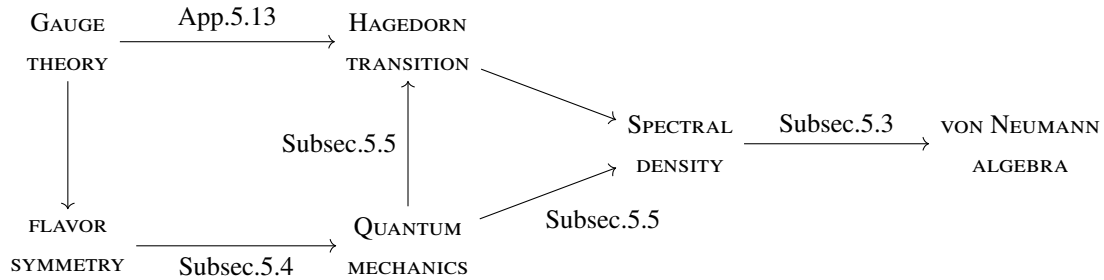
Figure 5.4: Chart of the main concepts explored in this section.

The initial inputs to derive the quantum systems of the previous section were unitary matrix integrals. Such systems generically do not exhibit a sharp Hagedorn-like behavior; rather, they tend to display a third order phase transition [211, 448, 449]. Mapping the models to a Hilbert space of states organized in representations of the flavor symmetry, these third order phase transitions crop up in the discrete matrix models and are due to the gauge constraint indexed by N. In this section, we will describe a general procedure to promote these systems to systems with a first order Hagedorn-like transition. The basic idea, presented in Subsection 5.5, is to introduce an extended Hilbert space with sectors indexed by the rank L of the flavor symmetry group.

The central result of this work is to assign a quantum system to a matrix model and determine the type of its von Neumann algebra of operators. It hinges upon three main steps:

1. Show how the type of von Neumann algebra is encoded in the Källén–Lehmann spectral density;

2. Obtain the planar limit of the quantum mechanical systems;

3. Compute the Källén–Lehmann spectral densities in the quantum systems.

In Section 5.3 we have already explained how the type of von Neumann algebra of operators is determined by looking at the Källén–Lehmann spectral density. The main outcome is (5.23). This section lies down the remaining two of the three main steps.

2. In Subsection 5.5 we discuss the phase structure of our new class of models. The outcome is summarized in (5.127).

3. In Subsection 5.5 we compute the spectral densities for our class of quantum mechanical models, obtaining (5.135).

The three steps are put together in Subsection 5.5. The web of relations between the various concepts is sketched in Figure 5.4. The take-home message of this central section is that a type III_1 algebra can only emerge above the Hagedorn temperature.

Extended quantum mechanical system

In this section we go one step beyond the unitary one-matrix models (5.42), and construct models whose partition function takes the form:

$$\mathcal{Z}(\mathfrak{q}, y) := \sum_{L \geq 0} \mathfrak{q}^{L^2} \mathcal{Z}_L^{(N)}(y). \tag{5.109}$$

We have introduced a weighted sum over the flavor symmetry rank L, with weight $\mathfrak{q}^{L^2}$ controlled by the free parameter $\mathfrak{q}$, which we will equivalently write

$$\mathfrak{q} = \exp\left(-\frac{1}{2a}\right), \qquad a > 0. \tag{5.110}$$

The idea will be to interpret (5.109) as the partition function of an extended quantum system with sectors indexed by the flavor symmetry rank, and an extra "fugacity"

$\mathfrak{q}$ associated to these sectors.[7] We stress that the sum is over the rank of the flavor symmetry of the systems, while the integer N, related to the rank of the gauge group, is not summed. Thus N remains as a genuine parameter of the extended systems.

To be precise, the convergence of (5.109) is not guaranteed in general, and a more rigorous definition requires to truncate it to a large value $L_{\max}$. Our regularization is as follows: we choose a very large number $\gamma_{\max} \gg 1$ and let $L_{\max}(N) := \lfloor \gamma_{\max} N \rfloor + 1$, and define

$$\mathcal{Z}(\mathfrak{q}, y) := \sum_{L=0}^{L_{\max}(N)} \mathfrak{q}^{L^2} \mathcal{Z}_L^{(N)}(y). \tag{5.111}$$

This implies that the sum has linearly many terms in N. We may let $\gamma_{\max}$ depend on the inverse temperature β, in a convenient way depending on the specific model of interest in each case. In practice, the idea is to wisely choose a regularization scheme $\gamma_{\max}$ so that $\mathcal{Z}$ will not miss the interesting physical phenomena for a vast range of temperatures.

It is shown in Appendix 5.13 that a common feature of the ensemble (5.109) is to promote a unitary matrix model (5.42) with third order phase transition to a model with first order, Hagedorn-like phase transition. This statement can equivalently be argued for from the perspective of a discrete matrix model, using the rewriting of $\mathcal{Z}_L^{(N)}$ from Subsection 5.4. This approach is presented in full generality in Subsection 5.5, and exemplified in Part 5.5.

Definition 5.5.1. Let $\mathcal{Z}(\mathfrak{q}, y)$ be as in (5.109). The parameter space of the model is

$$\{0 < |\mathfrak{q}| < 1, \ 0 \leq \arg(\mathfrak{q}) < 2\pi\} \times \{y > 0\}. \tag{5.112}$$

We will set $\arg(\mathfrak{q}) = 0$ throughout. The *constant-$\mathfrak{q}$ slice* of the parameter space is the region $\{y > 0\}$ at a fixed real value $0 < \mathfrak{q} < 1$.

The *Schur slice* of the parameter space is the region $\mathfrak{q} = \sqrt{y}$ and we call the partition function on the Schur slice the limit

$$\mathcal{Z}(y) := \mathcal{Z}(\sqrt{y}, y). \tag{5.113}$$

For a as in (5.110) and $y = e^{-\beta}$, we restrict the parameter space to be the positive quadrant $(a, \beta) \in \mathbb{R}_{>0} \times \mathbb{R}_{>0}$. The first kind of slice is a slice of constant $a > 0$, and the Schur slice is $a = \beta^{-1}$.

---

[7]Viewing $\mathcal{Z}_L^{(N)}$ as a statistical ensemble of representations, the importance of considering generating functions like (5.109) has been advocated for in the mathematical literature [54].

- Note that the physical interpretation of the Schur slice is particularly natural, as it amounts to adding a *vacuum energy* to each sector and considering a thermal state with no other fugacity involved.

- The nomenclature *Schur slice* is chosen in (vague) analogy with the degeneration of the Macdonald polynomials into Schur polynomials when the two fugacities are equal.

- In the constant-$\mathfrak{q}$ slice we assume that $0 < \mathfrak{q} < 1$ is a given number and describe the structure of the theory as a function of y alone.

- Finally, note that $\mathrm{Arg}(\sqrt{y})$ is not a free parameter, because it can be reabsorbed by a gauge transformation, equivalently in a change of variables in (5.42).

Now, the quantity $\mathcal{Z}(\mathfrak{q}, y)$ can be identified with the partition function of a quantum system living on the extended Hilbert space

$$\mathscr{H}^{(N)} := \bigoplus_{0 \leq L \leq L_{\max}(N)} \mathscr{H}_L^{(N)} = \bigoplus_{0 \leq L \leq L_{\max}(N)} \bigoplus_{R \in \mathfrak{R}_L^{(N)}} \mathscr{H}_L(R) \otimes \mathscr{H}_L(\phi(R)), \quad (5.114)$$

where the second equality recalls the definition of the gauge-invariant Hilbert space $\mathscr{H}_L^{(N)}$ from (5.50). More precisely, we have:

Proposition 5.5.2. *With the notation as just explained, it holds that*

$$\mathcal{Z}(\mathfrak{q}, e^{-\beta}) = \sum_{L=0}^{L_{\max}(N)} \mathfrak{q}^{L^2} \, \mathrm{Tr}_{\mathscr{H}_L^{(N)}} \left(e^{-\beta H} \right). \qquad (5.115)$$

Once again, note that in the case of the Schur slice, the new fugacity $\mathfrak{q}$ itself depends on the temperature, in such a way that (5.115) can be interpreted as the partition function of a quantum system at inverse temperature β with a vacuum energy.

Hagedorn transition and partition function

In this subsection we establish the phase structure of the extended models (5.109) at large N.

Remember that the scope of the whole construction is to derive a tractable quantum mechanical system from a gauge theory on $\mathbb{S}^{d-1} \times \mathbb{S}^1$, whenever the partition function of the latter can be expressed in the form (5.24). We now proceed to show that, passing to the extended systems introduced in Subsection 5.5, we generically obtain

models with a first order phase transition, in which the partition function stays finite at large N for $\beta^{-1} < T_H$ and diverges like $O(e^{N^2})$ when $\beta^{-1} > T_H$, where T_H is a critical temperature to be determined in each case.

Physical significance

Before diving in the analysis of the phase structure, a disclaimer is in order. In a realistic holographic model of a black hole, we expect the existence of two distinct temperatures: T_{HP} and $T_{\mathrm{breakdown}}$. At $T = T_{\mathrm{HP}}$, the thermal AdS solution and the black hole solution exchange their dominance, in a process known as Hawking–Page transition. At $T = T_{\mathrm{breakdown}} \geq T_{\mathrm{HP}}$, the perturbative expansion around the thermal AdS solution breaks down. Since the gauge theory interpretation of our matrix models holds only at very weak gauge coupling [427, 5], it is expected that $T_{\mathrm{breakdown}} \approx T_{\mathrm{HP}}$ [5, 14]. In the light of this discussion we simply refer to the transitions we observe as Hagedorn transitions [5, 14].

Hagedorn transitions from matrix models

The idea is schematically as follows. Consider the fixed-L unitary matrix model (5.42) in the planar large N limit, as a function of the Veneziano parameter γ (as introduced in Definition 5.4.15). Assume it has a third order phase transition at a critical curve $\gamma = \gamma_c(\beta)$ in the (β, γ)-plane. This phase transition is mapped to a third order phase transition in the discrete matrix model (5.59).

Passing to (5.109) with $\mathfrak{q} = e^{-1/(2a)}$, we write

$$\mathcal{Z}(e^{-\frac{1}{2a}}, e^{-\beta}) = \sum_{L=0}^{L_{\max}(N)} \exp\left[-N^2\left(\frac{\gamma^2}{2a} - \mathcal{F}(\gamma, \beta) + \cdots\right)\right] \tag{5.116}$$

where the N^2 scaling is the typical growth of matrix models, so that $\mathcal{F}(\gamma, \beta) = O(1)$, or more precisely

$$\lim_{N \to \infty} \frac{1}{N^2} \ln \mathcal{Z}_L^{(N)}(e^{-\beta})\Big|_{L=\gamma N} = \mathcal{F}(\gamma, \beta), \tag{5.117}$$

is finite and independent of N, and the ellipses indicate sub-leading contributions. Moreover, by assumption, we have

$$\mathcal{F}(\gamma, \beta) = \begin{cases} \mathcal{F}_-(\gamma, \beta) & \gamma \leq \gamma_c \\ \mathcal{F}_+(\gamma, \beta) & \gamma > \gamma_c, \end{cases} \tag{5.118}$$
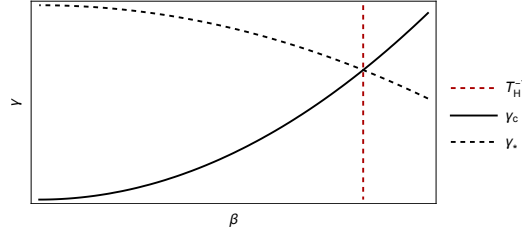
Figure 5.5: Illustration of a constant-a slice of the parameter space. The intersection of the curves γ_c and γ_* produces a phase transition. The solution γ_* to (5.119) is valid only for values of β such that $\gamma_* > \gamma_c$, on the left of the dashed vertical line.

with $\mathcal{F}_-$ and $\mathcal{F}_+$ coinciding up to the second derivative at γ_c, but distinct away from the critical curve $\gamma_c(\beta)$.[8]

At large N, the sum over L effectively enforces an average over γ. The leading planar contribution to $\mathcal{Z}$ comes from the saddle points γ_* of the quantity $\gamma^2/(2a) - \mathcal{F}(\gamma, \beta)$. We can start by looking for the saddle point in the phase $\gamma > \gamma_c$, for which γ_* is determined by

$$\frac{\partial}{\partial \gamma} \mathcal{F}_+(\gamma, \beta) \bigg|_{\gamma_*} = \frac{\gamma_*}{a}. \tag{5.119}$$

The solution is $\gamma_* = \gamma_*(\beta, a)$. In each constant-$a$ slice of the parameter space, γ_* is moved as we dial the inverse temperature, and in the Schur slice $a = \beta^{-1}$ the saddle point γ_* is uniquely determined as a function of β.

However, as we dial β, γ_* may cross γ_c. At that precise value of β, $\mathcal{F}_+$ in (5.119) is replaced by $\mathcal{F}_-$. The explicit form of the saddle point equation for γ_* changes. Therefore, the value of γ_* jumps at that critical value of β, which we denote $1/T_H$.

More precisely, in any fixed slice $a = a(\beta)$ (possibly constant) of the (a, β)-parameter space, there are two curves

$$\gamma_c(\beta) \text{ and } \gamma_*(\beta) \subset (\beta, \gamma)\text{-plane}. \tag{5.120}$$

The curve $\gamma_c(\beta)$ is independent of a and remains the same in every slice. The curve $\gamma_*(\beta)$ is fibered in the parameter space over the a-direction $\mathbb{R}_{>0}$. Assume that, in a chosen slice of the parameter space, the curve $\gamma_*(\beta)$ obtained solving (5.119) intersects $\gamma_c(\beta)$. Then, the solution is consistent only for values of β such that $\gamma_* > \gamma_c$, see Figure 5.5. Crossed that critical inverse temperature, namely $1/T_H$, the new branch of the curve $\gamma_*(\beta)$ solves a different equation.

---

[8]Abstractly, $\mathcal{F}_\pm$ are local functions on a two-dimensional manifold with local coordinates (γ, β), whose 2-jets are equal at every point of a codimension-one submanifold parametrized by the embedding $\beta \mapsto \gamma_c(\beta)$.

When β^{-1} crosses T_H a new value γ_* becomes the saddle point. This discontinuity will produce a phase transition in the ensemble (5.109) at a critical temperature T_H. The transition can in principle be first or second order. As we will show in examples and further support with a general prescription in Appendix 5.13, a widespread situation in this type of ensembles is that

$$\gamma_*(\beta) = 0 \qquad \text{if } \beta^{-1} < T_H. \tag{5.121}$$

In fact, under mild assumptions,

$$\mathcal{F}_-(\gamma, \beta) = \gamma^2 f_-(\beta) \tag{5.122}$$

for some smooth function f_- (cf. Lemma 5.13.1),[9] whence the trivial saddle (5.121) in the low temperature phase, valid for $\frac{1}{2a} > f_-(\beta)$.

The trivial saddle point kills the $O(N^2)$ growth of $\ln \mathcal{Z}$, leading to a first order[10] phase transition at T_H. When this is the case, Gaussian integration in the phase $1/\beta < T_H$ leads, near the critical point, to

$$\mathcal{Z} \sim \frac{1}{\sqrt{T_H - \beta^{-1}}}, \tag{5.123}$$

which in turn is associated with Hagedorn behavior as the critical temperature T_H is approached from below. Strictly at $N = \infty$ we have $\mathcal{Z}(\beta^{-1} < T_H) = O(1)$ and $\mathcal{Z}(\beta^{-1} > T_H) = \infty$, with $\ln \mathcal{Z}$ diverging proportionally to N^2.

More precisely, we have the following result:

Proposition 5.5.3. *Assume that if $\beta^{-1} < T_H$, there exist $c_0, K > 0$ independent of L such that for all N,*

$$q^{L^2} \mathcal{Z}_L^{(N)}(e^{-\beta}) \le K e^{-c_0 L^2}. \tag{5.124}$$

Also assume that if $\beta^{-1} > T_H$, there exist A, B, c_1, c_2 with $0 < c_1 < c_2$, $A > 0, B > 0$, such that for all N, the largest contribution to the sum is comprised in $[A e^{c_1 N^2}, B e^{c_2 N^2}]$. Then,

$$\ln \mathcal{Z}(e^{-\beta}) = \begin{cases} O(1) & \beta^{-1} < T_H \\ O(N^2) & \beta^{-1} > T_H. \end{cases} \tag{5.125}$$

---

[9] Both the presence of a third order transition and the form of $\mathcal{F}_\pm$ are consistent with and supported by [410], which studies QCD-like theories on $\mathbb{S}^{d-1} \times \mathbb{S}^1$ in the Veneziano limit.

[10] Strictly speaking, "weakly" first order, because there is no coexistence of saddles.

Proof. In the low temperature phase, the result is a simple consequence of domination by a convergent series. In the high temperature phase it suffices to bound the sum by its largest term times the number of terms, and to notice that this number of terms is very small compared to the largest contribution. Taking the logarithm on both sides yields the desired result. $\qquad\square$

To conclude, let us mention that it would be interesting to explore examples in which $\frac{\gamma^2}{2a} - \mathcal{F}_+$ develops new minima at some high temperature $1/\beta > T_H$.

Probing the Hagedorn transition with a Polyakov loop

Phase transitions are famously diagnosed by suitable order parameters. In the present case, the transition can be probed at the level of the matrix model by looking at a Polyakov loop. Inserting a Polyakov loop, it is not hard to show that is acquires a non-trivial expectation value at $\beta^{-1} > T_H$, indicating deconfinement. We state the result here and defer the details to Appendix 5.13.

At the level of the matrix model, it holds that

$$
\begin{aligned}
\langle \text{Polyakov loop} \rangle = 0 \qquad & \text{if } T < T_H \\
\langle \text{Polyakov loop} \rangle \neq 0 \qquad & \text{if } T > T_H \ .
\end{aligned}
\tag{5.126}
$$

Summary: Hagedorn transition

The bottom line of our analysis is that a wide class of extended models (5.109) undergoes a first order phase transition at a critical temperature T_H, with

$$
\begin{aligned}
\ln \mathcal{Z} = O(1) \qquad & \text{if } T < T_H \\
\ln \mathcal{Z} = O(N^2) \qquad & \text{if } T > T_H \ .
\end{aligned}
\tag{5.127}
$$

This feature of the quantum mechanical models is demonstrated explicitly in three examples in Part 5.5. The transition (5.127) is obtained summing over the parameter L, which, from the point of view of the discrete ensemble, is the maximum length of the Young diagrams R. The index N, labelling the constraint, is kept fixed. The phase transition is along a critical curve $T_H(a)$ in the (a, T)-plane, which projects onto a unique point T_H on the slice $a = T$.

It has been proposed that the algebras of single-trace operators are type I von Neumann algebras in the phase $T < T_H$, and become type III$_1$ factors at $T > T_H$.

The main result of this work is to prove this expectation rigorously in the class of models whose microscopic description has been given in Subsection 5.4. This is done next, in Subsection 5.5.

Spectral densities

Coupling the extended quantum mechanics to a probe

Akin to Subsection 5.4, we now introduce the operators of interest in the extended quantum mechanical systems of Subsection 5.5. Our take on (5.109) and the associated Hilbert space (5.114) is that each fixed-L sector describes a full-fledged quantum system, and the sum over L renders the whole ensemble closer to a holographic interpretation. Therefore, the prescription for the correlation function in the systems of Subsection 5.5 is to

  (i) couple a probe to each fixed-L system as prescribed in Subsection 5.4,

 (ii) compute the correlation function, and

(iii) take the weighted sum over L of the result.

A practical way of doing so is to promote $\mathscr{H}_L^{(N)}$ to $\mathscr{H}_L^{\text{tot}}$ as explained in Subsection 5.4, *before* summing over L and defining (5.114). That is, we work with:

$$\mathscr{H}^{\text{tot}} := \bigoplus_{L \geq 0} \mathscr{H}_L^{\text{tot}}. \tag{5.128}$$

Alternatively, one may first define $\mathscr{H}^{(N)}$ according to (5.114), and then define a probe on that space. To specify such a probe, we need in addition the choice of sector L to which it couples, and the choice must be fine-tuned to explore the regime of interest in each case. We refrain from this definition and stick to the former approach.

At this point, we promote the operators $O_L, O_L^\dagger$ of Subsection 5.4 to block-diagonal operators on $\mathscr{H}^{\text{tot}}$,

$$O, O^\dagger \in \mathcal{L}\left(\mathscr{H}^{\text{tot}}\right) \cong \mathcal{L}\left(\bigoplus_{L \geq 0} \mathscr{H}_L^{(N)} \otimes \Gamma_{\text{probe}}\right), \tag{5.129}$$

that act sector-wise as $O_L, O_L^\dagger$ for every L. Note that for each summand, the one-particle Hilbert space inside Γ_{probe} has a different dimension, equal to the flavor rank L.

Spectral densities of the extended quantum mechanics

We now sketch the adaptation of the procedure of Subsection 5.4 to the new case with the sum over L. The ingredients we need, as explained in Section 5.3, are the finite temperature Wightman functions and the associated Källén–Lehmann spectral density $\rho(\omega)$. The novelty in this section is the presence of a Hagedorn transition, highlighted in Subsection 5.5. We will pay special attention to how the properties of $\rho(\omega)$ change across the transition.

The obvious version of the Wightman function (5.90) for the ensemble (5.42) is:

Definition 5.5.4. The real-time, finite temperature Wightman function is

$$G_+(t) := \frac{1}{\mathcal{Z}} \sum_{L=0}^{L_{\max}(N)} \mathfrak{q}^{L^2} \operatorname{tr}_{\mathcal{H}_L^{\text{tot}}} \left(e^{-\beta H'} \, O^\dagger(t) O(0) \right). \tag{5.130}$$

The dependence on the parameters N, a, β is left implicit in the notation.

We need to prescribe the probe parameters in the same way as we did before. We choose the mass μ to be the same in all sectors, and large enough that the probe approximation can always be applied (so it is always large enough compared to $L_{\max}(N)$). The coupling of the interaction in a given sector is scaled in a 't Hooft way.

Once again, in the case of the Schur slice $a = \beta^{-1}$, (5.130) is interpreted simply as a thermal correlation function in an extended quantum system at inverse temperature β. The only difference between the right-hand side of (5.130) and its fixed-L counterpart (5.90) is the weighted sum over L and the overall normalization by $\mathcal{Z}$ instead of $\mathcal{Z}_L^{(N)}$. Let $\widetilde{G}_+(\omega)$ be the Fourier transform of $G_+(t)$. Once again, $\widetilde{G}_+(\omega)$ is simply related to the spectral density $\rho(\omega)$ through (5.91),

$$\widetilde{G}_+(\omega) = \frac{\rho(\omega)}{1 - e^{-\beta\omega}}. \tag{5.131}$$

We elaborate further on the properties of $\rho(\omega)$ and the probe approximation in the case of summing over sectors in Subsection 5.5.

Theorems 5.4.16 and 5.4.17 go through, with the only modification of the weighted sum over L and the normalization by $\mathcal{Z}$ outside the sum, instead of normalizing by $\mathcal{Z}_L^{(N)}$. This fact can be easily checked directly, and it does not involve any large N limit. To get an equivalent of Corollary 5.4, we will follow the extremization procedure over the Veneziano parameter γ explained in Subsection 5.5. The Corollary holds using the eigenvalue density ϱ_* evaluated at the saddle point γ_*.

In slightly more detail, for every N we can schematically write

$$\mathcal{Z} = \sum_{L=0}^{L_{\max}(N)} \exp\left[-N^2 \mathcal{S}_N(\gamma)\right], \tag{5.132}$$

where the dependence on β and $\mathfrak{q}$ is left implicit to reduce clutter, and the dependence on γ means that we replace $L \mapsto N\gamma$ everywhere. The sequence $\{\mathcal{S}_N\}_{N\in\mathbb{N}}$ admits a finite and well-defined point-wise limit $\lim_{N\to\infty} \mathcal{S}_N(\gamma) = \mathcal{S}(\gamma)$. Consider the family of functions of the form $F_N(\vec{\omega})/\mathcal{Z}$, where

$$F_N(\vec{\omega}) := \sum_{L=0}^{L_{\max}(N)} \exp\left[-N^2 \mathcal{S}_N(\gamma)\right] f_N(\vec{\omega}, \gamma), \tag{5.133}$$

and the sequence f_N is subject to the constraint

$$\lim_{N\to\infty} \frac{\ln f_N(\vec{\omega}, \gamma)}{N^2} = 0. \tag{5.134}$$

Here $\vec{\omega}$ generically indicates variables in the domain of f_N which do not appear in the definition of $\mathcal{Z}$. In the case of interest to us presently, there is just one variable $\omega \in \mathbb{C}$ and we are looking at a correlation function given by Theorem 5.4.16 or Theorem 5.4.17.

In the large N limit, the saddle points of F_N are entirely determined by $\mathcal{S}_N$, and therefore are the same as for $\mathcal{Z}$ (since the correlation functions converge to a finite value). In computing the ratios $F_N(\vec{\omega})/\mathcal{Z}$ at leading order in the large N limit, the first non-trivial contribution is given precisely by $f_N(\vec{\omega}, \gamma)|_{\text{saddle}}$, i.e., the defining function evaluated at the saddle point.

We therefore approximate $\widetilde{G}_+(\omega)$ by its value at the saddle point γ_* in the phase in which the saddle point γ_* is non-trivial, and we deduce Corollary 5.4 with the modification that we must evaluate the eigenvalue density, and in particular the endpoints of its support, at γ_*.[11]

We now explicitly relate the support of the spectral density $\rho(\omega)$ to the two phases of the matrix model, as we did in Subsection 5.4. We observe that the factorization Lemma 5.4.19 works in the high temperature phase, in which $\ln \mathcal{Z} = O(N^2)$. The proof is identical, with the large N limit being evaluated at the saddle point γ_*. Moreover, we showed that the spectral density there is continuous. In the low

---

[11]It is usual to approximate the large N expectation value of observables with a saddle point analysis, although proving a completely rigorous result here would require a study of the rate of convergence to the saddle which is beyond the scope of this chapter.

temperature phase, the assumption of a non-trivial saddle point in Lemma 5.4.19 fails. The partition function remains finite in this phase. If we scale the interaction λ between the probe and the system like $1/L$ (in a sector-dependent way), then there is no large N factorization and it does not really make sense to talk about the spectral density. However, here, unlike in Section 5.4, N and L have fundamentally inequivalent roles: only N is a free parameter, while now L is summed over. Then, if we scale the interaction like $1/N$ (in a sector-independent way), given that the partition function is finite the correlation function simply converges to its limit as $N \to \infty$ with L fixed, which is the limit in which the probe decouples from the rest of the system. In this limit, in the probe approximation, the spectral function of the probe reduces to delta functions at $\pm\mu$. Therefore, the large N Hilbert space is that of a free oscillator, and in particular the algebra of observables for the probe has type I. Hence, for the choices of scaling of λ described in this paragraph:

$$
\boxed{
\begin{aligned}
\operatorname{supp} \rho &= \bigsqcup \{ \text{ isolated pts } \} & &\text{if } \ln \mathcal{Z} = O(1) \\
\operatorname{supp} \rho &\subseteq \mathbb{R} \text{ continuous} & &\text{if } \ln \mathcal{Z} = O(N^2)
\end{aligned}
}
\tag{5.135}
$$

and in the former case $e^{-\beta|\omega|}$ is integrable on the support of ρ.

Comments on the probe approximation in the extended quantum mechanics

The probe approximation in the extended quantum mechanical systems can be defined in the analogous fashion to Definition 5.4.10. Again we expand partition functions and correlation functions as power series in the parameter $e^{-\beta\mu}$. This time the expansion is less trivial, because the probe sectors depend on L and therefore cannot be brought out of the sum over L. This does not change the strategy, and we simply retain the term independent of $e^{-\beta\mu}$ in the series expansion.

The comments about the mass of the probe in Subsection 5.4 apply identically to this case. In particular, one may express everything in terms of the shifted ω_r as in (5.98), which corresponds to neglecting the uniform shift of the energy levels given by the probe mass. The latter is a contribution due to the probe alone, not directly relevant for the quantum mechanical systems.

Summary

The three main results in the planar limit so far are:

RESULT		SECTION	CRYSTALLIZED IN
1.	von Neumann algebra type from supp ρ	Subsec. 5.3	Eq. (5.23)
2.	growth of $\ln \mathcal{Z}$ from Temperature	Subsec. 5.5	Eq. (5.127)
3.	supp ρ from growth of $\ln \mathcal{Z}$	Subsec. 5.5	Eq. (5.135)

Putting them together we arrive at the central result of our work:

Statement 5.5.5 ((5.23), (5.127) and (5.135))**.** In the saddle point approximation, the large N von Neumann algebras associated to our probe operators jump to type III_1 above the Hagedorn temperature, in accordance with the holographic picture of a Hawking–Page transition.
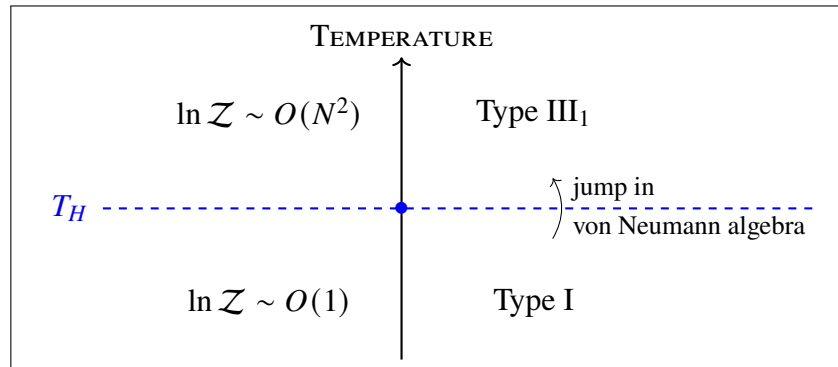
Figure 5.6: Illustration of Theorem 5.5.5. At the Hagedorn temperature T_H, the partition function starts diverging, and the von Neumann algebra experiences a sharp transition from type I to type III_1.

The content of this statement is represented pictorially in Figure 5.6. We now give a more detailed and rigorous formulation of the qualitative claim of Statement 5.5.5.

Theorem 5.5.6. *Consider a quantum mechanical system as defined in Subsection 5.5, coupled to a probe as detailed in Subsection 5.5, and such that the system at fixed L satisfies the assumptions of Theorem 5.4.21. The Hilbert space is $\mathcal{H}^{\mathrm{tot}}$ (5.128). Assume that* (5.43) *undergoes a third order phase transition, and that there exists $T_H(a) > 0$ such that* (5.109) *has the Hagedorn-like behaviour* (5.127) *in the planar limit. Then, the large N algebra of probe operators is a Type III_1 von Neumann algebra if and only if $T > T_H$.*

Additionally, the models (5.173) *or* (5.237) *satisfy the above hypotheses* $\forall\ 0 < a < \infty$.

Proof. The first part follows from combining the results of this section. As emphasized in Subsection 5.5, the construction is tailored so that, if (5.43) has a third order phase transition, it is a generic feature that (5.109) satisfies (5.127) in the planar limit.

The second part of the theorem follows from the explicit derivations in Part 5.5. □

Examples

In this second part of the work we move on to apply the general principles of Part 5.1 to selected examples. We present in detail four case studies, where all the quantities discussed in Part 5.1 are shown to display the desired properties.

5.6 Example 1: Variations on the IOP model

We begin in Subsection 5.6 by introducing a family of toy models that includes and generalizes a model of holographic relevance from [246]. In detail, we will give four equivalent characterizations of the system.

 i) It is a constrained version of a matrix model from [246, Sec.5]. We will refer to this matrix model (and not to the underlying quantum mechanics) as *IOP model*, and it will be the simplest instance of our broader family that we dub *constrained IOP model* (cIOP for short), introduced in Subsection 5.6.

 ii) It is the low energy theory of the chiral operators in four-dimensional super-symmetric QCD, or SQCD$_4$ for short. This perspective allows us to establish a direct relation with Calabi–Yau varieties in Subsection 5.6. In this framework, the Calabi–Yau attached to the original IOP model is just $\mathbb{C}^{L^2}$, whereas the cIOP model bears a connection with non-trivial Calabi–Yau varieties.

 iii) It is a toy model of two-dimensional lattice QCD with bosonic quarks (Subsection 5.6).

 iv) It is one-dimensional QCD with bosonic quarks.

To fit in the paradigm of Section 5.5, in Subsection 5.6 we consider the sum over an integer $L \in \mathbb{N}$, which has the meaning of number of flavors in all the presentations. In Subsections 5.6-5.6 and 5.6 we study the Veneziano limit of the theory without and with sum over L, respectively. The spectral density $\rho(\omega)$ is computed in Subsection 5.6.

Partition function of variations on IOP

Variations on IOP: Definition

Definition 5.6.1. Let $\beta > 0$, $y = e^{-\beta}$ and $L \in \mathbb{N}$. The IOP matrix model is

$$\mathcal{Z}_{\text{IOP}}(L, y) = \sum_R y^{|R|} (\dim R)^2, \tag{5.136}$$

with the sum running over Young diagrams of length $\ell(R) \leq L$.

The sum over Young diagrams (5.136) was derived from a quantum mechanics in [246, Sec.5], whence the nomenclature IOP. It is easy to prove that [312]

$$\mathcal{Z}_{\text{IOP}} = (1 - y)^{-L^2}. \tag{5.137}$$

The IOP matrix model does not show a phase transition and $\ln \mathcal{Z} = O(L^2)$ at all temperatures, however, it serves as inspiration for the subsequent discussion. For any $N \in \mathbb{N}$, $N \geq L$, one can embed $SU(L + 1) \hookrightarrow SU(N + 1)$. This allows for a generalization of (5.136).

Definition 5.6.2. Let $0 < y < 1$ and $L, N \in \mathbb{N}$. The *constrained* IOP matrix model (cIOP) is

$$\mathcal{Z}_{\text{cIOP}}^{(N)}(L, y) = \sum_R y^{|R|} (\dim R)^2, \tag{5.138}$$

with the sum running over Young diagrams of bounded length

$$\ell(R) \leq \min \{L, N\}. \tag{5.139}$$

Of course, for every $N \geq L$, the constraint (5.139) is immaterial and one recovers (5.136). However, the presence of the constraint plays a role in the Veneziano limit

$$L \to \infty, \quad N \to \infty, \qquad \text{with} \quad \gamma = \frac{L}{N} \text{ fixed.} \tag{5.140}$$

Indeed, the cIOP model undergoes a third order phase transition as a function of γ [29, 405].

It is convenient to adopt the change of variables $h_i = R_i - i + L$ introduced in (5.60) and then use formula (5.62). With these expressions at hand, we write

$$\mathcal{Z}_{\text{IOP}} = \frac{y^{-L^2/2}}{G(L + 2)^2} \sum_{h_1 > h_2 > \cdots > h_L \geq 0} y^{\sum_{j=1}^{L} \left(h_j + \frac{1}{2} \right)} \prod_{1 \leq i < j \leq L+1} (h_i - h_j)^2, \tag{5.141}$$

with $G(\cdot)$ being Barnes's G-function [38] and understanding $h_{L+1} \equiv -1$.

From cIOP to one-plaquette bosonic QCD$_2$

Let us now introduce a unitary matrix model equal to the cIOP partition function.

Lemma 5.6.3 ([190])**.** *For every $y \in \mathbb{C}$, $|y| \neq 1$, and $L, N \in \mathbb{N}$ it holds that*

$$\mathcal{Z}_{\text{cIOP}}^{(N)}(L, y) = \oint_{SU(N+1)} [dU] \left[\det \left(1 - \sqrt{y} U \right) \det \left(1 - \sqrt{y} U^{-1} \right) \right]^{-L}. \tag{5.142}$$

With $y = e^{-\beta}$, the right-hand side is a toy model for one-plaquette lattice QCD$_2$ with bosonic quarks, studied in [342, 406]. The interpretation of L as the flavor rank and N as the gauge rank of the gauge theory, put forward in Section 5.4, finds a neat realization here. Comparing (5.142) and [55, Eq.(3.8)], we also observe that $\mathcal{Z}_{\text{cIOP}}^{(N)}$ is the partition function of a gauged matrix quantum mechanics describing 1d QCD with L bosonic quarks, where again $y = e^{-\beta}$ (note that [55] includes an additional adjoint field).

Proof of Lemma 5.6.3. This lemma is well-known both in the mathematics and physics literature, see for instance [91, 186] for overviews and generalizations. For completeness, we provide one proof here. The so-called Cauchy identity states that [312]

$$\prod_{i=1}^{L+1}\prod_{k=1}^{N+1} \frac{1}{1 - y_i z_k} = \sum_R \chi_R(Y)\chi_R(U), \tag{5.143}$$

where on the right-hand side the sum runs over Young diagrams R with bounded length

$$\ell(R) \leq \min\{L, N\}, \tag{5.144}$$

exactly as in (5.139). Y and U are special unitary matrices with eigenvalues $\{y_i\}$ and $\{z_k\}$, respectively, and χ_R is the character of the group.

Setting $y_i = \sqrt{y}$ and using the property [312, Sec.3][12]

$$\chi_R(\text{diag}(\sqrt{y}, \ldots \sqrt{y})) = \sqrt{y}^{\sum_i R_i}\chi_R(\text{diag}(1, \ldots, 1)) = \sqrt{y}^{|R|} \dim R, \tag{5.145}$$

(5.143) implies

$$\sum_R \sqrt{y}^{|R|} \dim R \chi_R(U) = \det\left(1 - \sqrt{y}U\right)^{-L}. \tag{5.146}$$

Inserting this expression and its complex conjugate in the right-hand side of (5.142), one gets

$$\oint_{SU(N+1)} [dU] \left[\det\left(1 - \sqrt{y}U\right) \det\left(1 - \sqrt{y}U^{-1}\right)\right]^{-L}$$

$$= \sum_{R,R'} \dim(R)\dim(R')\sqrt{y}^{|R|+|R'|} \oint_{SU(N+1)} [dU]\chi_R(U)\chi_{R'}(U^{-1}). \tag{5.147}$$

---

[12]The first equality in (5.145) can be shown using the definition of χ_R as a ratio of determinants, $\chi_R(\text{diag}(y_1, \ldots, y_{L+1})) = \det_{1 \leq j < k \leq L+1}\left[y_k^{R_j+L-j+1}\right]/\det_{1 \leq j < k \leq L+1}\left[y_k^{L-j+1}\right]$. Particularizing to $y_k = \sqrt{y}$, one pulls $\sqrt{y}$ out of the determinants and simplifies between numerator and denominator to get (5.145).

Taking into account the orthogonality of characters:

$$\oint_{SU(N+1)} [dU] \chi_R(U) \chi_{R'}(U^{-1}) = \delta_{RR'}, \tag{5.148}$$

we obtain the identity (5.142). $\qquad\qquad\qquad\qquad\qquad\qquad\qquad\qquad\square$

IOP: Veneziano limit

For completeness, we now rederive the large L limit of the IOP and cIOP models, in the presentation (5.141), so to directly compute the relevant quantities in our formalism and make the chapter self-contained. However, we omit the more technical details and refer to the pertinent literature. We start with IOP, and explain how the picture gets modified in the constrained models in Subsection 5.6.

To begin with, the restriction $h_1 > \cdots > h_L$ in (5.141) can be lifted using the invariance of the summand under action of the Weyl group. This step introduces an overall factor $1/L!$.

Equation (5.141) describes a discrete ensemble of L variables with a hard wall at $h_i = 0$. It is an easy task to solve its large L limit, following for instance [148]. The summand in (5.141) is rewritten in the form $e^{-S(h_1,\ldots,h_L)}$ with

$$S(h_1, \ldots, h_L) = \beta \sum_{i=1}^{L} h_i - \sum_{i \neq j} \ln|h_i - h_j|. \tag{5.149}$$

At large L, we may assume a scaling of the eigenvalues

$$h_i = L^\eta x_i, \tag{5.150}$$

for $\{x_i\} \sim O(1)$ and a power $\eta > 0$ which we now determine. With the replacement (5.150), the first term in (5.149) has a growth $\propto L^{1+\eta}$, while the second term in (5.149) yields a piece $\eta L(L-1) \ln L$, independent of the eigenvalues and thus irrelevant for the sake of the saddle point analysis, and a piece $\propto L^2$. We only need to focus on the two terms carrying a dependence on the eigenvalue. Demanding that they compete, so to find a nontrivial equilibrium, imposes $1 + \eta = 2$, thus fixing $\eta = 1$.

It is customary to introduce the density of eigenvalues

$$\varrho(x) = \frac{1}{L} \sum_{i=1}^{L} \delta(x - x_i), \qquad x > 0, \tag{5.151}$$

which is normalized to 1 by definition. Furthermore, the discreteness of the ensemble (5.141) imposes a minimal distance among any two eigenvalues, which translates into the condition [148]

$$\varrho(x) \leq 1 \qquad \forall x > 0. \tag{5.152}$$

With these definitions, $S(h_1, \ldots, h_L)$ is a functional of ϱ and (5.149) becomes (up to x-independent terms)

$$S[\varrho] = L^2 \int dx \varrho(x) \left[\beta x - \mathrm{P}\!\!\!\int dx' \varrho(x') \ln|x - x'| \right], \tag{5.153}$$

where $\mathrm{P}\!\!\!\int$ stands for the principal value integral. We have thus expressed the summand in (5.141) as $e^{-L^2(\cdots)}$, with the dots indicating a positive $O(1)$ term. At large L, the leading contributions come from the saddle points of (5.153). The saddle point equation, also known as equilibrium equation, is

$$2\mathrm{P}\!\!\!\int dx' \frac{\varrho_*(x')}{x - x'} = \beta. \tag{5.154}$$

Here ϱ_* is the eigenvalue density that extremizes the functional (5.153). It must be looked for in the functional space subject to the constraints:

$$\int_0^\infty dx \varrho(x) = 1, \qquad 0 \leq \varrho(x) \leq 1, \qquad \mathrm{supp}\, \varrho \subseteq [0, \infty). \tag{5.155}$$

While the derivation was standard so far, the IOP matrix model has two peculiar features, encapsulated in (5.155):

- the discreteness of the ensemble, and

- the hard wall at $x = 0$.

Matrix models with a hard wall typically have an inverse square root behavior near the edge [175, 132], which in our case would produce

$$\varrho(x) \sim \frac{1}{\sqrt{x}}, \qquad x \to 0. \tag{5.156}$$

Clearly, this is incompatible with the restriction (5.152). Following the seminal work [148], we thus look for a "capped" eigenvalue density of the form

$$\varrho(x) = \begin{cases} 1 & 0 \leq x < x_- \\ \hat{\varrho}(x) & x_- \leq x \leq x_+ \\ 0 & x > x_+ \end{cases} \tag{5.157}$$
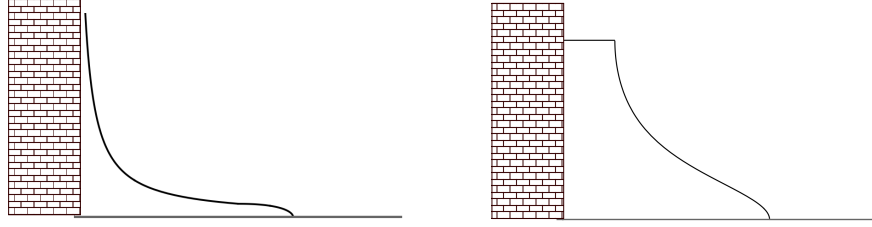
Figure 5.7: Schematic representation of the eigenvalue density in presence of a hard wall for the eigenvalues. Left: Continuous matrix models typically have a square root singularity near the hard wall. Right: Discrete matrix models have eigenvalue densities bounded above.

with $\hat{\varrho}$ a nontrivial function subject to the continuity conditions

$$\hat{\varrho}(x_-) = 1, \qquad \hat{\varrho}(x_+) = 0. \tag{5.158}$$

The values of $x_{\pm}$ will be determined by normalization. See Figure 5.7 for a sketch.

To solve the saddle point equation (5.154) with the ansatz (5.157) is a standard procedure, see, e.g., [148]. The non-trivial part to be determined lies on the domain $x_- \leq x \leq x_+$. In this region, (5.157) leads to

$$\mathrm{P}\!\int_{x_-}^{x_+} \mathrm{d}x' \frac{\hat{\varrho}_*(x')}{x - x'} = \frac{\beta}{2} + \ln\left(\frac{x}{x - x_-}\right). \tag{5.159}$$

This is the standard equilibrium equation, now for the equilibrium measure $\hat{\varrho}_*(x)\mathrm{d}x$ supported on $[x_-, x_+]$ and with a modified effective potential

$$\beta x \mapsto \beta x + 2x \ln(x) - (x - x_-) \ln(x - x_-), \tag{5.160}$$

to account for the term $\ln\left(\frac{x}{x-x_-}\right)$ on the right-hand side of (5.159). Therefore, we have effectively reduced the problem of finding an eigenvalue density with a hard wall which is bounded above, to the problem of finding the eigenvalue density $\hat{\varrho}_*$, at the price of trading the linear potential for a more complicated one. The latter problem admits a solution via a standard procedure. We skip the more technical details, and refer in particular to [115, Sec.5], where a very similar calculation is performed.

In a nutshell, the textbook prescription consists in introducing a complex function, called resolvent, supported on $\mathbb{C} \setminus [x_-, x_+]$. This function uniquely determines $\hat{\varrho}_*$ and $x_{\pm}$. Then, (5.159) is interpreted as a discontinuity equation for the resolvent, which can be solved by complex analytic methods. Once the resolvent is found, one extracts the eigenvalue density $\hat{\varrho}_*$ and its support.
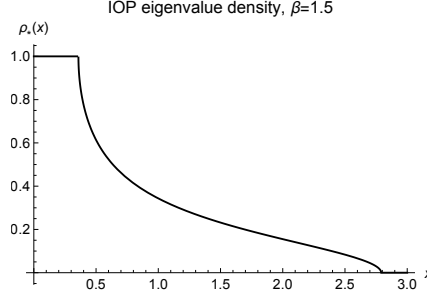
Figure 5.8: Eigenvalue density of the IOP matrix model, shown at $\beta = 1.5$.

Omitting the more technical part and jumping to the last step, we find (see also [115])

$$\hat{\varrho}_*(x) = \frac{2}{\pi} \arctan \left(\sqrt{\frac{x_-}{x_+}} \sqrt{\frac{x_+ - x}{x - x_-}} \right) \tag{5.161}$$

with supp $\hat{\varrho}_* = [x_-, x_+]$ given by

$$x_- = \tanh \left(\frac{\beta}{4} \right), \qquad x_+ = \coth \left(\frac{\beta}{4} \right). \tag{5.162}$$

The full density of eigenvalues $\varrho_*(x)$ is shown in Figure 5.8.

For completeness, we compare with the original derivation of [246, Sec.5]. There, the large L limit of $\mathcal{Z}_{\text{IOP}}$ was addressed directly in the sum over Young diagrams form (5.136). The result was encoded in a function $f(x)$ capturing the shape of the Young diagram R that dominates in the limit. Notice that our conventions are such that the flavor rank, denoted L here, corresponds to N of [246].

Comparing the definitions of $\varrho(x)$ with that of $f(x)$ using (5.60) to compare h_j and R_j, we get the relation

$$\hat{\varrho}_*(x) = \frac{1 - f'_*(x)}{2} \qquad \forall x \in \mathbb{R} \tag{5.163}$$

and our formulas agree with the existing literature using this substitution.

The remaining step is to evaluate the effective action (5.153) onto the solution ϱ_* that extremizes it. A direct computation gives

$$\ln \mathcal{Z}_{\text{IOP}} = -L^2 \log \left(1 - e^{-\beta/2} \right), \tag{5.164}$$

reproducing the closed form evaluation (5.137).

Variations on IOP: Veneziano limit

The IOP model is recovered from the constrained IOP in the region $N \geq L$, i.e., $\gamma \leq 1$ in the planar limit. In turn, the cIOP model has a third order phase transition at $\gamma = \gamma_c$, with

$$\gamma_c = \frac{1 + \sqrt{y}}{2\sqrt{y}}. \tag{5.165}$$

This can be proven along the lines of [115]. We therefore only sketch the main ideas here.

In a nutshell, the difference between IOP and cIOP is not in the summand in the discrete matrix models, but in the domain. This means that the effective matrix model action for cIOP is again (5.149), thus leading to the exact same saddle point equation (5.154) as in IOP. We can thus use the same solution for ϱ_* as long as it belongs to the constrained functional space. In cIOP, the additional constraint, yielding the additional parameter γ, implies that the IOP solution is only valid for certain values of γ (which in particular include $\gamma \leq 1$), but fails to satisfy the constraint when γ is large, leading to a phase transition.

Lemma 5.6.4. *In the cIOP model, the saddle point eigenvalue density ϱ_* is the same found in Subsection 5.6 for $\gamma \leq \left(e^{\beta/2} + 1 \right)/2$.*

Proof. The constraint in the cIOP model is formulated in the large N limit as follows.

Let $0 \leq s \leq 1$ be the limiting value of the index j/L and denote $x(s)$ the limit of h_j/L. Then, when $N \leq L$, we have that $R_j = 0$ if $j > N$, which, by the change of variables, implies $h_j = L - j$ if $j > N$. Hence, dividing both sides of the latter equation by L, we find the constraint

$$x(s) = 1 - s \quad \text{if} \quad s > \gamma^{-1}. \tag{5.166}$$

Inverting the relation using the inverse function theorem, we have $\varrho(x) = -\frac{\mathrm{d}s(x)}{\mathrm{d}x}$. Therefore, the eigenvalue density of the cIOP model must be consistent with

$$\varrho(x) = 1 \quad \text{if} \quad 0 \leq x < 1 - \gamma^{-1}. \tag{5.167}$$

Recalling (5.157), we see that the solution derived in the unconstrained case has $\varrho(x) = 1$ if and only if $0 \leq x \leq x_-$. Thus, it is inconsistent with the requirement (5.167) if $x_- < 1 - \gamma^{-1}$.

We conclude that, if $x_- < 1 - \gamma^{-1}$, we cannot simultaneously satisfy the defining constraint on cIOP and (5.155). The solution breaks down at the value of $\gamma = \gamma_c$ for which $x_- = 1 - \gamma_c^{-1}$. Substituting $x_- = \tanh(\beta/4)$ we obtain (5.165).

$\square$

Beyond the critical point, we ought to determine a new density ϱ_* that belongs to the restricted functional space (5.155) and moreover satisfies the additional constraint (5.167) in the region $\gamma > \gamma_c$. The computation is technical, but can be achieved adapting from [115, Sec.5]. However, we omit it, because the only ingredients we need to know are (i) whether supp ϱ_* is continuous, and (ii) the large N expression of the partition function.

The answer to (i) is affirmative, since the solution is a variation of the ansatz (5.157) where we additionally impose (5.167). For later reference, we note that imposing (5.167) together with the normalization of $\varrho(x)$, implies that the non-constant part of $\varrho_*(x)$ bounds an area of γ^{-1}. Thus it always have finite support, which shrinks as γ is increased at fixed temperature.

The answer to (ii) was computed in [405] by other methods, so it suffices to quote the result therein. Defining

$$\mathcal{F}_{\text{cIOP}} := \lim_{N \to \infty} \frac{1}{N^2} \ln \mathcal{Z}_{\text{cIOP}}^{(N)}, \tag{5.168}$$

where the limit is understood to be the Veneziano limit, we have:

$$\mathcal{F}_{\text{cIOP}} = \begin{cases} -\gamma^2 \ln(1 - y) & \gamma < \frac{1+\sqrt{y}}{2\sqrt{y}} \\ -(2\gamma - 1) \ln(1 - \sqrt{y}) - \frac{1}{4} \ln y + C(\gamma) & \gamma > \frac{1+\sqrt{y}}{2\sqrt{y}} \end{cases} \tag{5.169}$$

where, in the second phase, the piece $C(\gamma)$ is independent of the temperature and is explicitly given by

$$C(\gamma) = -\gamma^2 \ln \left(\frac{4\gamma(\gamma - 1)}{(2\gamma - 1)^2} \right) + (2\gamma - 1) \ln \left(\frac{2(\gamma - 1)}{2\gamma - 1} \right) - \frac{1}{2} \ln (2\gamma - 1). \tag{5.170}$$

This expression presents a discontinuity in the third derivative of $\mathcal{F}_{\text{cIOP}}$ at γ_c. Obviously, for $\gamma < \gamma_c$, the constraint is not active and (5.169) agrees with the partition function of the IOP model.

Variations on IOP: Sum over flavor symmetries

The finite temperature partition function of the IOP matrix model can be evaluated exactly. We are interested in summing over the integer L, which has the meaning of

the rank of the flavor symmetry. We let $0 < \mathfrak{q} = e^{-1/(2a)} < 1$ and consider

$$\sum_{L=0}^{\infty} \mathfrak{q}^{L^2} \mathcal{Z}_{\text{IOP}} = \sum_{L=0}^{\infty} \exp\left[-L^2\left(\frac{1}{2a} + \ln(1 - e^{-\beta})\right)\right], \qquad (5.171)$$

where the right-hand side follows from (5.137). This expression is only well-defined and convergent for low temperatures, that is, for β such that

$$\frac{1}{2a} + \ln(1 - e^{-\beta}) > 0. \qquad (5.172)$$

As it was discussed in Part 5.1, Section 5.5, to render the sum defined at every temperature, we must therefore truncate it at a large value $L_{\max}$ which, in the case of cIOP, may depend on N.

While this procedure is not especially enlightening for the IOP model, it already highlights that the behavior of the partition function summed over the rank of the flavor symmetry drastically changes at the critical temperature at which the inequality (5.172) is saturated. We now move on and consider the richer cIOP model. We will show how the interplay between the third order phase transition present in cIOP and the sum over L leads to an interesting Hagedorn-like behavior.

Variations on IOP: Flavor sum and planar limit

The cIOP model has a third order phase transition with $\ln \mathcal{Z}_{\text{cIOP}}^{(N)} = O(N^2)$ on both sides. We now proceed to promote it to a first order transition with our "sum over flavors" prescription.

Theorem 5.6.5. *With the notation as in (5.138) and $y = e^{-\beta}$, $\mathfrak{q} = e^{-1/(2a)}$, let*

$$\mathcal{Z}_{\text{Ex1}}(\mathfrak{q}, y) = \sum_{L=0}^{L_{\max}(N)} \mathfrak{q}^{L^2} \mathcal{Z}_{\text{cIOP}}^{(N)}(L, y). \qquad (5.173)$$

$\forall\, a > 0$ *there exists* $T_H > 0$ *such that, in the large N limit, (5.173) has a first order phase transition at* $1/\beta = T_H$. *Moreover,*

$$\ln \mathcal{Z}_{\text{Ex1}} = \begin{cases} O(1) & \frac{1}{\beta} < T_H \\ O(N^2) & \frac{1}{\beta} > T_H. \end{cases} \qquad (5.174)$$

The free energy $\ln \mathcal{Z}_{\text{Ex1}}$ as a function of the temperature $T = 1/\beta$ at fixed N is shown in Figure 5.9. Likewise, plotting a numerical evaluation of $\ln \mathcal{Z}_{\text{Ex1}}$ at various N, one may check that the trend is consistent with the analytic prediction that it remains small and approximately constant for $T < T_H$ and it shows a polynomial growth in N if $T > T_H$.
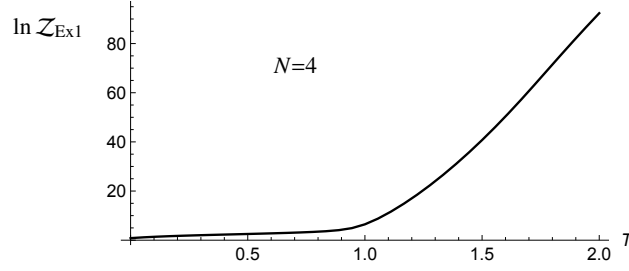
Figure 5.9: Plot of $\ln \mathcal{Z}_{\mathrm{Ex1}}(y)$ as a function of the temperature $T = -1/\ln(y)$ at $N = 4$. The sum over L in (5.173) has been truncated at $L \leq 20$. A change in behavior around $T \approx 1$ is already visible at such low value of N, although the sharp phase transition is smoothed by finite N effects. The plot is taken in the Schur slice $a = T$, but the qualitative behavior is the same in other slices.

Proof. The details of the proof of Theorem 5.6.5 are essentially identical to the calculations in Subsection 5.7 below, thus we omit them. The basic idea is that, introducing the weighted sum over L, the large N limit is taken in two steps:

(i) Extremize $\mathcal{Z}_{\mathrm{cIOP}}^{(N)}$ in the Veneziano limit as a function of γ and y;

(ii) Evaluate the resulting effective action at the saddle point $\gamma = \gamma_*$.

Step (i) has been sketched in Subsection 5.6, and the result we need is expression (5.169).

To set up step (ii), we define

$$S_{\beta,a}^{\mathrm{cIOP}}(\gamma) := \frac{1}{N^2} \ln \mathcal{Z}_{\mathrm{cIOP}}^{(N)}(L, e^{-\beta}) - \frac{\gamma^2}{2a} \tag{5.175}$$

and write

$$\mathcal{Z}_{\mathrm{Ex1}}(\mathfrak{q}, e^{-\beta}) = \sum_{L=0}^{L_{\max}(N)} \exp\left\{ N^2 S_{\beta,a}^{\mathrm{cIOP}}\left(\gamma = \frac{L}{N}\right) \right\}. \tag{5.176}$$

At large N, $S_{\beta,a}^{\mathrm{cIOP}}(\gamma)$ approaches a function of continuous variable $\gamma \geq 0$, and the leading contribution comes from its maximum, located at γ_*. The function to extremize is

$$S_{\beta,a}^{\mathrm{cIOP}}(\gamma) = \mathcal{F}_{\mathrm{cIOP}} - \frac{\gamma^2}{2a}, \tag{5.177}$$

with the first summand written explicitly in (5.169). We see that, if $\gamma < \gamma_c := \frac{1+e^{-\beta/2}}{2e^{-\beta/2}}$, then $S_{\beta,a}^{\mathrm{cIOP}}(\gamma)$ is quadratic, and moreover if

$$\frac{1}{2a} \geq -\ln(1 - e^{-\beta}), \tag{5.178}$$
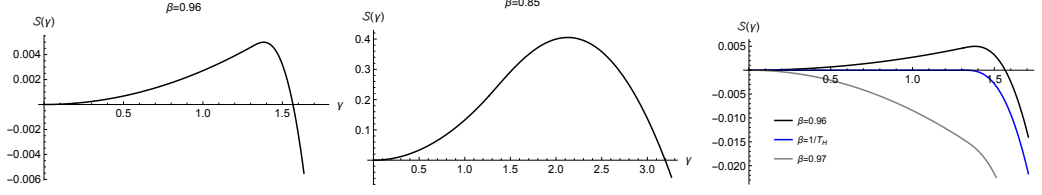
Figure 5.10: Plot of $\mathcal{S}^{\text{cIOP}}_{\beta,\beta^{-1}}(\gamma)$ as a function of γ for different values of β. Left: $\beta = 0.96$. Center: $\beta = 0.85$. Right: a comparison for β slightly above (gray), at the critical point (blue), and slightly below (black). The absolute maximum is $\gamma_* = 0$ if $\beta > 1/T_H$, while $\mathcal{S}^{\text{cIOP}}_{\beta,\beta^{-1}}(\gamma)$ attains a positive absolute maximum at $\gamma_* > 0$ if $\beta < 1/T_H$.

the partition function $\mathcal{Z}_{\text{Ex1}}$ is Gaussian and damped at $\gamma > 0$. We denote $1/T_H$ the value of β for which the inequality (5.178) is saturated and $\mathcal{S}^{\text{cIOP}}_{\beta,a}(\gamma)$ flips sign. For example, if $a = 1/\beta$, $T_H \approx 1.039$.

Step (ii) is akin to Subsection 5.7 — especially Figure 5.19, and the discussion around (5.256). Here we discuss explicitly only the case $a = 1/\beta$, but the case of constant a independent of β can be dealt with in exactly the same manner, similarly to Subsection 5.7. Studying the maximum of (5.177) as a function of γ, for different ranges of values of β, we find the following:

- $\mathcal{S}^{\text{cIOP}}_{\beta,a}$ is non-negative definite with a global maximum at $\gamma_* = 0$ if $\beta > 1/T_H$;

- $\mathcal{S}^{\text{cIOP}}_{\beta > T_H^{-1},a}(0) = 0$.

- At $\beta < 1/T_H$ we ought to look for a different saddle point;

- By direct inspection of $\mathcal{S}^{\text{cIOP}}_{\beta,a}$, we observe that it has a global maximum at a certain $\gamma_* > 0$ if $\beta < 1/T_H$; examples at fixed β are shown in Figure 5.10.

- At this value, $\mathcal{S}^{\text{cIOP}}_{\beta < T_H^{-1},a}(\gamma_*) > 0$, with strict inequality.

- The two saddle points do not coexist and exchange dominance exactly at $\beta = 1/T_H$.

Next, we have to evaluate (5.177) on the saddle point, to obtain the leading order of $\ln \mathcal{Z}_{\text{Ex1}}$. In the phase $\beta^{-1} < T_H$, we have seen that the leading term trivializes, leaving behind a $O(1)$ correction. In the high temperature phase $\beta^{-1} > T_H$, on the other hand, we have a strictly positive leading order, accompanied by the overall factor N^2. Accordingly, $\ln \mathcal{Z}_{\text{Ex1}}$ has a jump from $O(1)$ to $O(N^2)$ at T_H.

While we have performed the computation explicitly for $a = \beta^{-1}$, one can plot (5.177) for other choices, in particular on constant-a slices, and check that the same behaviour holds. We stress that

- The precise value of T_H depends on a, and in the Schur slice $a = 1/\beta$ we find $T_H \approx 1$;

- Nevertheless, the *existence* of a jump in the saddle point value γ_* holds for all $a > 0$.

Moreover, the Gaussian integration over fluctuations around the saddle point, in the low temperature phase, produces a universal factor

$$\mathcal{Z}_{\text{Ex1}} \propto \left(y - e^{-1/T_H} \right)^{-1/2}, \tag{5.179}$$

which gives rise to Hagedorn behavior of the Laplace transform of $\mathcal{Z}_{\text{Ex1}}$ as $\beta^{-1} \to T_H$ from below. The behavior of this model is analogous to the one observed in the matrix model for $\mathcal{N} = 4$ super-Yang–Mills [302, 150]. □

Spectral density of variations on IOP

We now analyze the spectral density $\rho(\omega)$ in the variations of the IOP model. As above, we construct from IOP, and eventually pass to the model summed over the number of flavors, which fits in the overarching formalism of Section 5.5. The definition of Wightman functions and their relation with $\rho(\omega)$ is taken from Subsection 5.4. We do not discuss explicitly the microscopic operators O, but take the general expressions for the Wightman functions in Subsection 5.4 as our starting point.

Intermezzo: Comparison with IOP

For the sake of comparison, let us notice that the space of states generated by the adjoint fields A_{ij} in the notation of [246] agrees with our Hilbert space. The fundamental field in [246] is the analogue of our probe, and in the SQCD$_4$ language (cf. Subsection 5.6) it is an auxiliary, massive chiral field without anti-chiral counterpart. Both our cIOP generalization and the map to SQCD$_4$ yield an embedding of the IOP model in broader setups.

To compare the Wightman functions, one should be aware of the following differences: our conventions for the Fourier transform are such that $\omega \mapsto -\omega$ with respect

to [246]; moreover, the interaction Hamiltonian differs by an overall sign, and our representations are allowed to be (R, R) or $(R, \overline{R})$, which differ by a renaming from the basis $(\overline{R}, R)$ considered in [246]. To more easily relate our expressions to the existing literature, throughout this example we fix $\phi(R) = \overline{R}$ and deform the definition of the Hamiltonian H' according to

$$H(R_1, \overline{R_2}) = |\overline{R_2}|; \tag{5.180}$$

$$H_{\text{int}}(R_1, \overline{R_2}) = \frac{g}{2} \left[Q(\overline{R_2}) - Q(\overline{R_1}) \right] ; \tag{5.181}$$

$$Q(R) = C_2(R) + (L + 1)|R|. \tag{5.182}$$

- The choice of letting (5.180)-(5.181) depend on $\overline{R}$ instead of R is adapted so that (5.185) below matches the conventions of [246, Sec.5].

- The redefinition of H does not affect the partition function, which is invariant under charge conjugation $R \mapsto \overline{R}$.

- In the definition of H_{int},

$$C_2(R) = \sum_{i=1}^{L} R_i (R_i - 2i + L) \tag{5.183}$$

is the quadratic Casimir of R, and in $Q(R)$ we use $(L + 1)|R|$ because R are representations of $SU(L + 1)$.

In this way, our explicit computations of the Wightman functions differ by [246, Sec.5] only by the shift by μ, which was removed "by hand" with a counterterm in [246, Eq.(2.2)] (be aware that L here was denoted N in [246]).

The IOP spectral density

Recall the general formula

$$\rho(\omega) = \lim_{\varepsilon \to 0^+} \left\{ \frac{i}{2} \left[{}_L \langle \Psi_\beta | \Omega(\omega + i\varepsilon) - \Omega(\omega - i\varepsilon) | \Psi_\beta \rangle_L \right] \right.$$
$$\left. - \frac{i}{2} \left[{}_L \langle \Psi_\beta | \Omega(-\omega + i\varepsilon) - \Omega(-\omega - i\varepsilon) | \Psi_\beta \rangle_L \right] \right\}, \tag{5.184}$$

derived in Corollary 5.4, where

$$\langle R, \mathsf{a}; \phi(R), \dot{\mathsf{a}} | \Omega(\omega) | R, \mathsf{a}; \phi(R), \dot{\mathsf{a}} \rangle = \frac{1}{(L+1)} \sum_{J \in \mathscr{J}_R} \frac{1}{\omega - \mu - E_J^{\text{int}}} \frac{\dim(R \sqcup \square_J)}{\dim R}. \tag{5.185}$$

Here

$$E_J^{\text{int}} = \frac{\lambda}{2(L+1)} \left[C_2(\overline{R}) - C_2(\overline{R \sqcup \square_J}) + L + 1 \right] \tag{5.186}$$

with $\lambda = g(L+1)$ the 't Hooft coupling for the interaction Hamiltonian (5.181). We henceforth set $\lambda = 1$ without loss of generality, and it can be reinserted at any point by multiplying the Wightman functions by $1/\lambda$ and replacing $\omega - \mu \mapsto (\omega - \mu)/\lambda$.
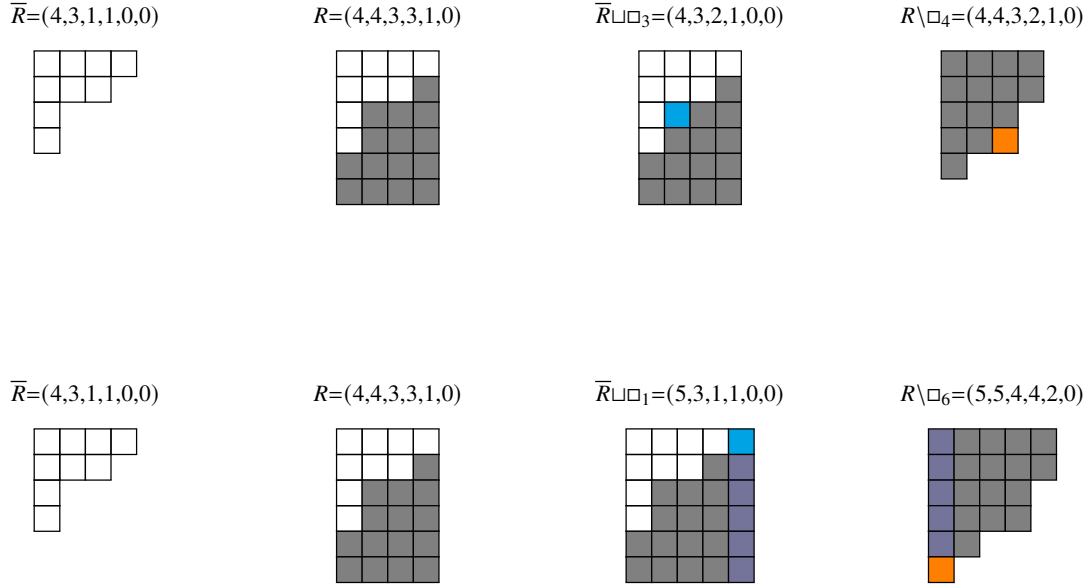
Figure 5.11: Appending a box at row J and taking the conjugate, exemplified for $SU(6)$ representations, $L = 5$. The Young diagram $\overline{R} = (4, 3, 1, 1, 0, 0)$ is shown in white, $R = (4, 4, 3, 3, 1, 0)$ in gray, the added box $\square_J$ in cyan and the removed box $\square_{L-J+2}$ in orange. Above: $J = 3$. Below: $J = 1$. In this case, R gains a whole new column at the beginning, shown is darker blue in the two rightmost diagrams.

We first change variables $R' = \overline{R}$ and use the property $\dim \overline{R} = \dim R$, and also

$$\overline{\left(\overline{R'} \sqcup \square_J \right)} = R' \setminus \square_{L-J+2}, \tag{5.187}$$

where the right-hand side is the conjugate to the Young diagram with the last box of the $(L - J + 2)^{\text{th}}$ row removed. Expression (5.187) is valid for $J = 2, \ldots, L + 1$. To address the case $J = 1$ we observe that

$$R' = (R'_1, R'_2, \ldots, R'_L, 0) \cong (R'_1 + 1, R'_2 + 1, \ldots, R'_L + 1, 1), \tag{5.188}$$

where the two expressions yield isomorphic $SU(L + 1)$ representation with same dimensions, although their $|R'|$ is shifted by L. The representation $\overline{R'} \sqcup \square_1$ is obtained

deleting the last box from the right-hand side of (5.188). We can therefore let R' run over non-empty Young diagrams with $R'_{L+1} \in \{0, 1\}$, which is equivalent to declare that the conjugate of $R = \emptyset$ is the determinant representation of $SU(L+1)$, which is trivially true representation theoretically and is most suited for dealing with Young diagrams. For instance:

$$\emptyset \sqcup \square_1 = \square = \overline{(\overline{\square})} = \overline{\underbrace{(1, \dots, 1, 0)}_{L}} = \overline{\underbrace{(1, \dots, 1)}_{L+1} \setminus \square_{L+1}}. \qquad (5.189)$$

These observations imply that we are allowed to simply use (5.187) with the understanding that R' cannot be empty but can have at most one box in its $(L + 1)^{\text{th}}$ row.[13]

Finally, we rename the summation index $I = L + 2 - J$ and use the fact that

$$\dim(R' \setminus \square_I) = 0 \qquad \text{if } -I + L + 2 \notin \mathcal{J}_{\overline{R'}} \qquad (5.190)$$

to let the sum run over $I \in \{1, \dots, L + 1\}$.

We stress that there is nothing wrong with $J = 1$, and this digression is just to explain what it means by deleting a box from the row $I = L + 1$: it means to first shift the Young diagram by one column using (5.188), and then delete the unique box in the $I^{\text{th}} = (L + 1)^{\text{th}}$ row so to get a valid $SU(L + 1)$ representation. This is manifest in Figure 5.11.

In this way we get

$$_L\langle \Psi_\beta | \Omega(\omega) | \Psi_\beta \rangle_L = \frac{1}{\mathcal{Z}_{\text{cIOP}}} \sum_{R'} e^{-\beta |R'|} (\dim R')^2 \frac{1}{(L+1)} \sum_{I=1}^{L+1} \frac{1}{\omega - \mu - E'_I} \frac{\dim(R' \setminus \square_I)}{\dim R'} \qquad (5.191)$$

where now

$$E'_I = \frac{\lambda}{(L+1)}(R'_I - I + L) \qquad (5.192)$$

descends from E_J^{int} after the various rearrangements. With the change of variables (5.60),

$$E'_I = \frac{\lambda}{(L+1)} h_I. \qquad (5.193)$$

We drop the $'$ from now on. We have thus recovered the formula of [246, Eq.(5.13)] as a particular case of the framework developed in Part 5.1.

---

[13]Strictly speaking, this would only be true if we compensate the shift in $|R'|$ with a factor $e^{\beta L \delta_{J,1}}$ in the right-hand side of (5.185). This factor does not change in any way the ensuing discussion thus we omit it.

The proof of the spectral density of the IOP model relies on the following technical result, which is a particular case of Lemma 5.4.18.

Lemma 5.6.6 ([246]). *The asymptotic behavior of $_L\langle\Psi_\beta|\Omega(\omega\pm i\varepsilon)|\Psi_\beta\rangle_L$ of the IOP model in the planar limit is*

$$_L\langle\Psi_\beta|\Omega(\omega\pm i\varepsilon)|\Psi_\beta\rangle_L \approx 1 - \exp\left(\int_0^{x_+} dx \frac{\varrho_*(x)}{x+\mu-\omega\mp i\varepsilon}\right). \tag{5.194}$$

Proof. The proof is essentially identical to Appendix 5.14 up to certain signs, and we simply sketch the main ideas here. By direct computation, the ratio of dimensions in (5.191) yields

$$\frac{\dim(R\setminus\Box_I)}{\dim R} = \prod_{j\neq I}\left(1 - \frac{1}{h_I - h_j}\right). \tag{5.195}$$

For every $(L+1)$-tuple $\vec{h} = (h_1, \ldots, h_L, -1)$ and $\xi \in \mathbb{C}$, we define the function (it slightly differs from Appendix 5.14 to make contact with the sign conventions of [246] in this example)

$$\Phi_{\vec{h}}(\xi) := \prod_{j=1}^{L+1}\left(1 - \frac{1}{\xi - h_j}\right), \tag{5.196}$$

and also denote $\Omega_{\vec{h}}$ the right-hand side of (5.185) after substituting (5.193). Thanks to the residue theorem we equate

$$\Omega_{\vec{h}}(\omega\pm i\varepsilon) = -\frac{1}{(L+1)g}\oint_C \frac{d\xi}{2\pi i}\frac{\Phi_{\vec{h}}(\xi)}{\frac{\omega\pm i\varepsilon-\mu}{g} - \xi}, \tag{5.197}$$

with the integration contour $C = C(\vec{h})$ encircling the points h_I and leaving outside the point $(\omega\pm i\varepsilon - \mu)/g$ (compared to Appendix 5.14, here the residues pick a minus sign due to the slight redefinition of $\Phi_{\vec{h}}(\xi)$, and we will see that our present computation will reproduce [246, Eq.(5.38)]). From now on we set $Lg = \lambda = 1$ without loss of generality. By contour deformation we get

$$\Omega_{\vec{h}}(\omega\pm i\varepsilon) = 1 - \Phi_{\vec{h}}\left((L+1)(\omega\pm i\varepsilon - \mu)\right), \tag{5.198}$$

see Appendix 5.14 for the details. Writing

$$\Phi_{\vec{h}}\left((L+1)(\omega\pm i\varepsilon - \mu)\right) = \exp\left[\sum_{j=1}^{L+1}\ln\left(1 - \frac{1}{(L+1)\left(\omega\pm i\varepsilon - \mu - \frac{h_j}{L+1}\right)}\right)\right] \tag{5.199}$$

and approximating at leading order in the planar limit $\ln\left(1 - \frac{c}{L+1}\right) \approx -\frac{c}{L+1}$, we get

$$\Omega_{\tilde{h}}(\omega \pm i\varepsilon)\big|_{\text{saddle point}} = 1 - \exp\left(\int dx \frac{\varrho_*(x)}{x + \mu - (\omega \pm i\varepsilon)}\right). \tag{5.200}$$

The claim follows from the usual asymptotics

$$_L\langle\Psi_\beta|\Omega(\omega \pm i\varepsilon)|\Psi_\beta\rangle_L \approx \Omega_{\tilde{h}}(\omega \pm i\varepsilon)\big|_{\text{saddle point}}. \tag{5.201}$$

□

Theorem 5.6.7. *The spectral density of the IOP model is*

$$\rho(\omega) = \frac{(1-y)}{2\omega_{\text{r}}}\left[\theta(\omega-\mu)\sqrt{(\omega_{\text{r}}-x_-)(x_+-\omega_{\text{r}})} - \theta(-\omega-\mu)\sqrt{(\omega_{\text{r}}-x_-)(x_+-\omega_{\text{r}})}\right] \tag{5.202}$$

with compact support

$$\operatorname{supp}\rho = [-x_+ - \mu, -x_- - \mu]\cup[x_- + \mu, x_+ + \mu] \subset \mathbb{R}, \qquad x_\pm = [\coth(\beta/4)]^{\pm 1}. \tag{5.203}$$

cor. *The large N correlation functions of the IOP model are described by a von Neumann algebra of type III$_1$.*

The positive branch of the square roots is taken in (5.202), and the signs in front are adjusted accordingly, and we have used the definition $\omega_{\text{r}} = |\omega| - \mu$ from (5.98) to shorten the expressions.

Proof of Theorem 5.6.7. To reduce clutter, we define the shorthand

$$\Delta\Omega(\pm\omega, i\varepsilon) := {}_L\langle\Psi_\beta|\Omega(\pm\omega + i\varepsilon) - \Omega(\pm\omega - i\varepsilon)|\Psi_\beta\rangle_L \tag{5.204}$$

and hence our ultimate goal is to compute

$$\rho(\omega) = \lim_{\varepsilon\to 0^+}\left[\frac{i}{2}\Delta\Omega(\omega, i\varepsilon) - \frac{i}{2}\Delta\Omega(-\omega, i\varepsilon)\right]. \tag{5.205}$$

We use Lemma 5.6.6 to write

$$\Delta\Omega(\omega, i\varepsilon) \approx \exp\left(\int_0^{x_+} dx \frac{\varrho_*(x)}{x + \mu - \omega + i\varepsilon}\right) - \exp\left(\int_0^{x_+} dx \frac{\varrho_*(x)}{x + \mu - \omega - i\varepsilon}\right), \tag{5.206}$$

and then plug the eigenvalue density (5.157) and integrate on the interval $[0, x_-]$, where ϱ_* is constant. We get

$$\Delta\Omega(\omega, i\varepsilon) \approx \frac{\left(\sqrt{\omega - \mu - x_- - i\varepsilon}\right)^2}{\left(\sqrt{\omega - \mu - i\varepsilon}\right)^2} \exp\left[\int_{x_-}^{x_+} dx \frac{\hat{\varrho}_*(x)}{x - \omega + \mu + i\varepsilon}\right] - (i\varepsilon \mapsto -i\varepsilon).$$

(5.207)

We use the substitution (5.163), which we recall is $\varrho_*(x)|_{[x_-, x_+]} = \frac{1}{2} - \frac{f_*'(x)}{2}$, and integrate the constant $\frac{1}{2}$ on $[x_-, x_+]$:

$$\Delta\Omega(\omega, i\varepsilon) \approx \frac{\sqrt{(\omega - \mu - x_- - i\varepsilon)}\sqrt{(\omega - \mu - x_+ - i\varepsilon)}}{\left(\sqrt{\omega - \mu - i\varepsilon}\right)^2} \exp\left[\frac{1}{2}\int_{x_-}^{x_+} dx \frac{f_*'(x)}{\omega - \mu - x - i\varepsilon}\right]$$

(5.208)

$$- (i\varepsilon \mapsto -i\varepsilon),$$

which is analogous to [246, Eq.(5.38)]. Reading the integral off from there, and denoting momentarily $\tilde{x}_\pm := x_\pm + \mu$ to lighten the expressions, one finds

$$\Delta\Omega(\omega, i\varepsilon) \approx \frac{(1-y)}{2(\omega - \mu - i\varepsilon)}\left[-1 + \sqrt{\omega - i\varepsilon - \tilde{x}_-}\sqrt{\omega - i\varepsilon - \tilde{x}_+}\right] - (i\varepsilon \mapsto -i\varepsilon).$$

(5.209)

The expression for $\Delta\Omega(-\omega, i\varepsilon)$ is obtained with the obvious replacement $\omega \mapsto -\omega$.

To evaluate the spectral density of the IOP model, we use the discontinuity equation (5.205). The pieces $\frac{(1-y)}{2(\omega - \mu \pm i\varepsilon)}$ are smooth in the limit $\varepsilon \to 0^+$, therefore they cancel in (5.205) and do not contribute to $\rho(\omega)$. The pieces

$$\sqrt{\omega \pm i\varepsilon - \tilde{x}_-}\sqrt{\omega \pm i\varepsilon - \tilde{x}_+}$$

(5.210)

in $\Delta\Omega(\omega, i\varepsilon)$ have branch cuts on $[\tilde{x}_-, \tilde{x}_+]$ in the limit $\varepsilon \to 0^+$, thus contribute non-trivially to (5.205) only if $\omega \in [\tilde{x}_-, \tilde{x}_+]$. Likewise, the corresponding pieces in $\Delta\Omega(-\omega, i\varepsilon)$ have branch cuts along $[-\tilde{x}_+, -\tilde{x}_-]$.

Formula (5.205) instructs us to assemble these building blocks into $\frac{i}{2}\Delta\Omega(\omega, i\varepsilon) - \frac{i}{2}\Delta\Omega(-\omega, i\varepsilon)$. Let us omit the smooth prefactor for a moment.

(i) Note that the signs combine to give, schematically,

$$\left[-\frac{i}{2}\left(\sqrt{-(\omega + i\varepsilon - \tilde{x}_-)(\tilde{x}_+ - \omega - i\varepsilon)} - \sqrt{-(\omega - i\varepsilon - \tilde{x}_-)(\tilde{x}_+ - \omega + i\varepsilon)}\right)\right.$$

(5.211)

$$\left.+\frac{i}{2}\left(\sqrt{-(\omega + i\varepsilon - (-\tilde{x}_+))(-\tilde{x}_- - (\omega + i\varepsilon))} - \sqrt{-(\omega - i\varepsilon - (-\tilde{x}_+))(-\tilde{x}_- - (\omega - i\varepsilon))}\right)\right],$$

where the first (respectively second) line account for the contribution from $\Delta\Omega(\omega, i\varepsilon)$ (respectively $\Delta\Omega(-\omega, i\varepsilon)$).

(ii) Note also that the first (respectively second) square root in each parenthesis approaches the branch cut from above (respectively below) as $\varepsilon \to 0^+$, see Figure 5.12.

(iii) Hence the first (respectively second) square root in each parenthesis produces a factor $e^{i\pi/2}$ (respectively $e^{-i\pi/2}$).
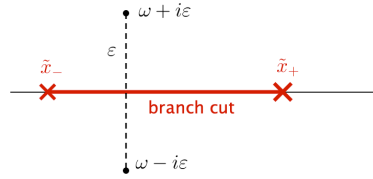
Figure 5.12: The branch cut that contributes to the spectral density of IOP. There is a second branch with ω replaced by $-\omega$.

Combining these observations we get

$$\begin{cases} -\frac{i}{2}\left(e^{i\pi/2} - e^{-i\pi/2}\right)\sqrt{(\omega - \tilde{x}_-)(\tilde{x}_+ - \omega)} & \text{if} \quad \omega \in [\tilde{x}_-, \tilde{x}_+] \\ +\frac{i}{2}\left(e^{i\pi/2} - e^{-i\pi/2}\right)\sqrt{((-\omega) - \tilde{x}_-)(\tilde{x}_+ - (-\omega))} & \text{if} \quad -\omega \in [\tilde{x}_-, \tilde{x}_+] \end{cases} \tag{5.212}$$

which, after simplifications, leaves a plus sign in front when $\omega \in [\tilde{x}_-, \tilde{x}_+]$ and a minus sign in front when $-\omega \in [\tilde{x}_-, \tilde{x}_+]$. We have observed in Subsection 5.4 that Ω is a resolvent for the density $\rho(\omega)$, and this analysis of the overall sign reproduces the standard sign conventions, with $\lim_{\varepsilon\to 0^+} i\Delta(\omega, i\varepsilon)$ giving a positive $\rho(\omega)$ if $\omega \in [\tilde{x}_-, \tilde{x}_+]$ and vanishing otherwise.

Altogether we obtain (5.202). In particular, $\rho(\omega)$ has compact support

$$\omega_r \in [x_-, x_+], \tag{5.213}$$

where recall from Subsection 5.6 that $x_\pm = [\coth(\beta/4)]^{\pm 1}$. The support thus extends to the whole real axis in the infinite temperature limit $\beta \to 0$. $\qquad\square$

Spectral density and von Neumann algebra of cIOP

Theorem 5.6.8. *The large N von Neumann algebra of the quantum mechanical system associated to the cIOP model is of type III$_1$.*

Proof. According to the prescription from Subsection 5.3, we need to show that supp ρ is continuous. On one side of the third order phase transition, namely $\gamma < \gamma_c$, the γ-dependent constraint is inactive and the proof is identical to that of Theorem 5.6.7. We remark that inverting the relation $\gamma_c(\beta)$ tells us that, for fixed γ, at low enough temperature $\beta > 2\ln(2\gamma - 1)$ we recover the IOP solution, for which we know the spectral density in closed form from Theorem 5.6.7.

At $\gamma > \gamma_c$, the eigenvalue density ϱ_* is determined as highlighted in Subsection 5.6. Even without having supp ϱ_* in closed form, we know from Subsection 5.6 that it is compact and continuous on $\mathbb{R}_{\geq 0}$. To prove this, it suffices to recall that the constraint imposes $\varrho_*(x) = 1$ for all $0 \leq x \leq 1 - \gamma^{-1}$. In particular, that part of the support extends as γ is increased for given β, while supp ϱ_* also stretches along $\mathbb{R}_{\geq 0}$ as the temperature is increased, for fixed γ.

Lemma 5.6.6 still holds but now we need to use the form of ϱ_* in the new phase. We arrive at expression (5.208), except that now f'_* will be a different function, namely the shape of the (different) representation that dominates the planar limit in the phase $\gamma > \gamma_c$. The non-trivial contribution stems from the non-constant part of ϱ_*, which, as discussed in Subsection 5.6, always exists and has compact and continuous support. The integrals are more involved, but the upshot is that they have branch cuts along $\pm$ supp ϱ_* shifted by μ. By (5.205), this is sufficient to conclude that $\rho(\omega)$ has compact support on $\mathbb{R}$. $\qquad\square$

Spectral density of cIOP with sum over flavor symmetries

Theorem 5.6.9. *The spectral density $\rho(\omega)$ associated to the matrix model $\mathcal{Z}_{\text{Ex1}}$ has compact, continuous support at $1/\beta > T_H$.*

Proof. In the high temperature phase, $1/\beta > T_H$, $\ln \mathcal{Z}_{\text{Ex1}}$ has a large N growth and the saddle point argument applies. Lemma 5.6.6 goes through, except that now $\widetilde{G}_R(\omega)$ is still given by (5.194), but with ϱ_* the eigenvalue density of the cIOP model in the planar limit, and further evaluated at the saddle point $\gamma = \gamma_*$.

Due to the lack of knowledge of γ_* as an explicit function of the inverse temperature β and the control parameter a, we did not manage to write down supp ϱ_* in closed form in the phase $\beta^{-1} > T_H$. Nevertheless, for our purposes it suffices to observe that supp $\varrho_* \subset \mathbb{R}_{\geq 0}$ is compact and non-trivial. This claim stems from the combination of the facts proven in previous subsections:

- The analysis of Subsection 5.6 shows that the eigenvalue density of cIOP in the phase $\gamma > \gamma_c > 1$ has compact and continuous support; moreover, there exists a finite compact interval on which ϱ_* is non-constant and subtends a finite area γ^{-1};

- In the high temperature phase of $\mathcal{Z}_{\text{Ex1}}$, the saddle point is an absolute maximum located at $\gamma_* > 1$, as shown in the proof of Theorem 5.6.5.

Therefore, $\operatorname{supp} \varrho_*$ at γ_* is a finite interval.

From the branch cut of $\widetilde{G}_R(\omega)$ and $\widetilde{G}_A(\omega)$ we still obtain

$$\operatorname{supp} \rho \subset \mathbb{R}_{>0} \text{ compact and continuous.} \tag{5.214}$$

This result follows from the knowledge of the branch cuts, although without a general expression in closed form.

In the low temperature phase, however, Lemma 5.6.6 fails. The δ functions in the definition of the spectral density do not coalesce in this phase, and $\rho(\omega)$ becomes trivial as the probe decouples from the rest of the system. $\qquad\square$

Temperature	$\ln \mathcal{Z}_{\text{Ex1}}$	Algebra type
$\beta^{-1} < T_H$	$O(1)$	I
$\beta^{-1} > T_H$	$O(N^2)$	III$_1$

cIOP, SQCD$_4$, and Calabi–Yau

Before moving on to the next example, we make a few comments in this independent subsection on the link between the different variants of the IOP model and the Hilbert series of some Calabi–Yau varieties appearing in the analysis of SQCD$_4$.

From bosonic QCD$_2$ to SQCD$_4$

Unitary matrix integrals such as (5.142) appear in the computation of Hilbert series of algebraic varieties [417], and play a prominent role in determining the moduli spaces of vacua of supersymmetric gauge theories [50, 210].

The basic idea is that supersymmetric gauge theories admit moduli spaces of vacua. These are complex algebraic varieties carved out by the vacuum equations modulo gauge transformations, and typically carry additional structure imposed by supersymmetry. As usual, the algebraic varieties can be specified in terms of their

generators, which are certain gauge-invariant operators, and relations among them. Physical information is encoded in these data of the moduli space of vacua, and in particular in their Hilbert series, defined below.

Lemma 5.6.10 ([210])**.** *The Hilbert series of the moduli space of vacua of four-dimensional supersymmetric QCD (SQCD$_4$) with*

$$N_{\text{colors}} = N + 1, \qquad N_{\text{flavors}} = L \tag{5.215}$$

equals (5.142)*.*

In Section 5.4 we have built quantum mechanical systems out of gauge-invariant operators. Here we are seeing this feature emerging cleanly in SQCD$_4$. Furthermore:

- The working assumption (5.25) here corresponds to demand that SQCD$_4$ is free from chiral anomalies.

- The Hilbert space $\mathcal{H}_L^{(N)}$ is constructed by the meson operators in SQCD$_4$, with the R-part and $\overline{R}$-part arising, respectively, from chiral and anti-chiral indices.

- From the SQCD$_4$ perspective, the partition function enumerates generators of the ring of gauge-invariant operators (this statement is a rephrasing of Lemma 5.6.12 below). To compare with IOP, it suffices to note that, when $L < N$, the spectrum of this ring is simply $\mathbb{C}^{L^2}$. Besides, the collection of gauge-invariant operators is identified with the span of the operators denoted A_{ij} in the quantum mechanical model of IOP [247, 246].

Calabi–Yau variations on IOP

Definition 5.6.11. Let $\mathfrak{R} = \bigoplus_{n \geq 0} \mathfrak{R}_n$ be a Noetherian graded commutative ring over $\mathbb{C}$, and denote $X = \text{Spec}(\mathfrak{R})$. The *Hilbert series* of X in the indeterminate y is

$$\text{HS}_y(X) = \sum_{n=0}^{\infty} \dim(\mathfrak{R}_n) y^n \in \mathbb{Z}[[y]]. \tag{5.216}$$

The Noetherian assumption guarantees that $\mathfrak{R}$ is finitely generated and [417]

$$\dim(\mathfrak{R}_n) < \infty \qquad \forall n \geq 0. \tag{5.217}$$

Lemma 5.6.12 ([210]). *There exists a toric Calabi–Yau manifold $X_L^{(N)}$, with*

$$\dim\left(X_L^{(N)}\right) = \begin{cases} L^2 & N \geq L \\ 2L(N+1) - N(N+2) & N < L, \end{cases} \tag{5.218}$$

such that the identity

$$\mathcal{Z}_{\text{cIOP}}^{(N)}(L, y) = \text{HS}_y\left(X_L^{(N)}\right) \tag{5.219}$$

holds. Moreover, $X_{L \leq N}^{(N)} = \mathbb{C}^{L^2}$ and $X_{N+1,N}$ is a hypersurface in $\mathbb{C}^{N^2+2N+3}$.

Proof. The statement follows from comparison with [210, Sec.4.3], with (N_c, N_f) therein replaced by $(N+1, L)$. The second part follows essentially by the definition of the Hilbert series for a freely generated complex algebraic variety, cf. also [210, Eq.(3.6)]. □

This lemma explains geometrically that the constrained IOP model carries a richer structure than the original IOP model.

Theorem 5.6.13. *The states of the IOP model are in one-to-one correspondence with elements in the ring of functions on $\mathbb{C}^{L^2}$. The states in the cIOP model are in one-to-one correspondence with elements in the ring of functions on a non-trivial Calabi–Yau variety $X_L^{(N)}$.*

The Hilbert series approach to the cIOP model allows to introduce yet another characterization, corresponding to a simple model of bosons.

Consider a square lattice of L^2 sites, labelled by $(i, j) \in \mathbb{Z}_L \times \mathbb{Z}_L$, with bosonic particles at its lattice sites. Generate a random configuration of energy levels $\left\{e_{ij} + \frac{1}{2}\right\}_{i,j} \subset (\frac{1}{2} + \mathbb{N})^{L^2}$. By taking bosons, we allow two or more particles to occupy the same energy level. See Figure 5.13 for an illustration.
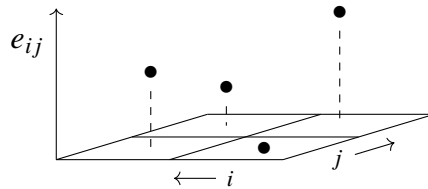
Figure 5.13: Free bosons on a square lattice. $L = 2$ in this example.

The partition function of the free system simply corresponds to summing over all such configurations, weighted by the Boltzmann factor:

$$\mathcal{Z}_B^{(\text{free})} = \prod_{(i,j)\in\mathbb{Z}_L\times\mathbb{Z}_L} \sum_{e_{ij}=0}^{\infty} e^{-\beta\left(e_{ij}+\frac{1}{2}\right)} = (2\sinh(\beta/2))^{-L^2}, \tag{5.220}$$

It is convenient to introduce $\alpha = (i,j)$ and define a lexicographic order on the set of pairs, so that $\alpha \in \mathbb{Z}_{L^2}$. To enrich the model, we impose a constraint on this system, forbidding certain energy levels. We thus define

$$\mathcal{Z}_B^{(N)} = \prod_{\alpha=0}^{L^2-1} \sum_{e_\alpha=0}^{\infty} d_{\{e_\alpha\}}^{(N)}\, e^{-\beta\sum_\alpha\left(e_\alpha+\frac{1}{2}\right)}, \qquad d_{\{e_\alpha\}}^{(N)} \in \{0,1\}. \tag{5.221}$$

Whenever a coefficient $d_{\{e_\alpha\}}^{(N)}$ is taken to vanish, the corresponding configuration $\{e_\alpha\}$ of L^2 particles is forbidden. As in Section 5.4, we are imposing a constraint indexed by $N \in \mathbb{N}$.

Proposition 5.6.14. *There exists a choice of collection*

$$\left\{ d_{\{e_\alpha\}}^{(N)},\ e_\alpha \in \mathbb{N},\ \alpha = 0, 1, \ldots, L^2 - 1 \right\} \tag{5.222}$$

such that

$$\mathcal{Z}_B^{(N)} = e^{-\frac{\beta}{2}L^2} \mathcal{Z}_{\text{cIOP}}^{(N)}. \tag{5.223}$$

Proof. We may introduce a refined Hilbert series as follows. Let $\vec{y} = (y_1, \ldots, y_L)$ and define $y_\alpha := \sqrt{y_i y_j}$, with $\alpha = (i,j)$, $\alpha \in \mathbb{Z}_{L^2}$. We have

$$\text{HS}_y(X) = \sum_{\{e_\alpha \geq 0\}} d_{\{e_\alpha\}}\left(X_L^{(N)}\right) \prod_{\alpha=0}^{L^2-1} y_\alpha^{e_\alpha}, \tag{5.224}$$

where $d_{\{e_\alpha\}}$ are non-negative integers such that

$$\dim(\mathfrak{R}_n) = \sum_{\{e_\alpha \geq 0\ |\ \sum_\alpha e_\alpha = n\}} d_{\{e_\alpha\}}\left(X_L^{(N)}\right). \tag{5.225}$$

Lemma 5.6.12 still holds, upon replacement

$$\left[\det\left(1 - \sqrt{y}U\right)\left(1 - \sqrt{y}U^{-1}\right)\right]^{-L} \longrightarrow \prod_{i=1}^{L} \det\left(1 - \sqrt{y_i}U\right)\left(1 - \sqrt{y_i}U^{-1}\right) \tag{5.226}$$

in (5.142). Unrefining the series, $y_i \to y \ \forall i = 1, \ldots, L$, we get the combinatorial identity

$$
\mathcal{Z}_{\text{cIOP}}^{(N)}(L, y) = \prod_{\alpha=0}^{L^2-1} \sum_{e_\alpha=0}^{\infty} d_{\{e_\alpha\}}\left(X_L^{(N)}\right) y^{\sum_\alpha e_\alpha}. \tag{5.227}
$$

We now use the fact that $d_{\{e_\alpha\}}\left(X_L^{(N)}\right) \in \{0, 1\}$ for $X_L^{(N)}$ a toric Calabi–Yau variety [50]. In particular, $d_{\{e_\alpha\}}\left(\mathbb{C}^{L^2}\right) = 1$ for all sets $\{e_\alpha\}_{\alpha=0,\ldots,L^2-1}$, while some of the coefficients $d_{\{e_\alpha\}}\left(X_L^{(N)}\right)$ will vanish if $L > N$, corresponding to imposing constraints, called syzygys, on the generators of the ring $\mathfrak{R}$. With this fact, multiplying (5.227) by $e^{-\beta \sum_{\alpha=0}^{L^2-1} \frac{1}{2}} = e^{-\beta L^2/2}$ proves the claim. $\qquad \square$

Flavor sum: Calabi–Yau ensembles

We finish this investigation of the relationship between the IOP matrix model and Hilbert series by looking at the sum over L through the lens of our Calabi–Yau varieties.

Proposition 5.6.15. *Let* $N \in \mathbb{N}$, $0 < y < 1$ *and* $\mathcal{Z}_{\text{Ex1}}$ *as in* (5.173). *It holds that*

$$
\mathcal{Z}_{\text{Ex1}}(\mathfrak{q} = 1, y) = 1 + \text{HS}_y\left(\bigsqcup_{L \geq 1} X_L^{(N)}\right). \tag{5.228}
$$

Proof. Let $\mathcal{O}_{X_L^{(N)}}$ be the sheaf of functions over $X_L^{(N)}$. For any $L, L' \in \mathbb{N}$ we have the short exact sequence

$$
0 \longrightarrow \mathcal{O}_{X_{L'}^{(N)}} \longrightarrow \mathcal{O}_{X_L^{(N)} \sqcup X_{L'}^{(N)}} \longrightarrow \mathcal{O}_{X_L^{(N)}} \longrightarrow 0. \tag{5.229}
$$

Additivity of the Hilbert series states that

$$
\text{HS}_y\left(X_L^{(N)}\right) + \text{HS}_y\left(X_{L'}^{(N)}\right) = \text{HS}_y\left(X_L^{(N)} \sqcup X_{L'}^{(N)}\right). \tag{5.230}
$$

Starting with $L = 1, L' = 2$ and iterating this identity in combination with Lemma 5.6.12 gives formula (5.228). The latter is understood as an inductive limit on $L_{\max}$, with the sum over L in $\mathcal{Z}_{\text{Ex1}}$ truncated at $L \leq L_{\max}$. $\qquad \square$

In summary, the cIOP model with Gaussian sum over flavors becomes a generating function of Hilbert series of Calabi–Yau varieties. It points toward a categorification, in which the structure rings of Calabi–Yau of different dimensions are assembled in a direct sum weighted by $\mathfrak{q}^{L^2}$.

As a side remark, notice that summing over moduli spaces of different dimensions is not unfamiliar in string theory. In fact, in the path integral of 2d gravity, one integrates over the moduli space of genus g surfaces, and eventually sums over $g \in \mathbb{N}$.

Summary: Calabi–Yau variations on IOP

In Theorem 5.6.13 we have pointed out a correspondence between the space of states in the cIOP model, which inherits the ring structure from the ring of representations of the flavor symmetry, and the ring of functions on a certain Calabi–Yau variety $X_L^{(N)}$. The partial dictionary so far is:

Quantum mechanics		Calabi–Yau
IOP	$\longleftrightarrow$	trivial, $\mathbb{C}^{L^2}$
cIOP	$\longleftrightarrow$	non-trivial, $X_L^{(N)}$
constraint $R \in \mathfrak{R}_L^{(N)}$	$\longleftrightarrow$	syzygys
(unweighted) flavor sum	$\longleftrightarrow$	disjoint union $\bigsqcup_L X_L^{(N)}$

The role of Calabi–Yau varieties, especially when summing over L, remains to be elucidated. We hope to report on this topic in the future.

5.7 Example 2: Matrix model of QCD$_2$

Motivated by the properties evidenced in the previous example, we introduce another similar model that illustrates the paradigm of Part 5.1. The corresponding matrix integral is an extremely streamlined low energy toy model of QCD$_2$. In Subsection 5.7 we extend the model according to Section 5.5, by including a sum over the number of flavors with Gaussian weight. Once again, the sum over flavors will promote a third order phase transition to a first order one. The corresponding spectral density is analyzed in Subsection 5.7.

Partition function of QCD$_2$ matrix model

We introduce a matrix model that captures the behaviour of thermal QCD$_2$ with $N + 1$ colors and L flavors [218] (further explored and generalized in [405, 406]). Its partition function is

$$\mathcal{Z}_{\text{QCD}_2}^{(N)}(L, y) = \oint_{SU(N+1)} [dU] \left[\det \left(1 + \sqrt{y}U \right) \det \left(1 + \sqrt{y}U^{-1} \right) \right]^L \tag{5.231}$$

with parameter $0 < y < 1$. In the QCD interpretation, $L \in \mathbb{N}$ has the meaning of the number of quarks.[14] We have the identification $y = e^{-\beta m}$, with m the quark mass. To avoid clutter, we simply redefine $m\beta \mapsto \beta$.

The matrix model (5.231) admits other interpretations:

(i) Comparing with [342], it is a simplified model of one-plaquette lattice QCD$_2$ [406].

(ii) A unitary matrix model that generalizes (5.231) was examined in [55], in the context of a black hole phase in AdS$_2$/CFT$_1$. The authors of [55] also considered correlation functions of operators similar to but distinct from our $O_L(t)$.

Lemma 5.7.1 ([190]). *For every $L, N \in \mathbb{N}$, let $\mathcal{Z}_{\mathrm{QCD}_2}^{(N)}$ be as in (5.231) with $y = e^{-\beta}$. Let also $\mathfrak{h}_L^{(N)} \subset \mathbb{N}^L$ denote the set*

$$\mathfrak{h}_L^{(N)} = \left\{ (h_1, \ldots, h_L) \in \mathbb{N}^L \ : \ N + L - 1 > h_1 > h_2 > \cdots > h_L \geq 0 \right\}. \quad (5.232)$$

It holds that

$$\mathcal{Z}_{\mathrm{QCD}_2}^{(N)}(L, e^{-\beta}) = \frac{e^{\beta L^2/2}}{G(L+1)^2} \sum_{(h_1, \ldots, h_L) \in \mathfrak{h}_L^{(N)}} \prod_{1 \leq i < j \leq L} (h_i - h_j)^2 \, e^{-\beta \sum_{j=1}^{L} \left(h_j + \frac{1}{2} \right)}. \quad (5.233)$$

Proof. The proof is very similar to the one of Lemma 5.6.3. The change of variables (5.60) rewrites the right-hand side of (5.233) as a sum over Young diagrams:

$$\sum_{R \subseteq (N)^L} y^{|R|} \, (\dim R)^2. \quad (5.234)$$

Here we have used formula (5.62) for $\dim(R)$. The sum is restricted to Young diagrams that fit inside a rectangular tableau of L rows and N columns. For instance:

$$L = 4 \text{ and } N = 4,$$
$$R = (3, 2) \subset (4, 4, 4, 4).$$
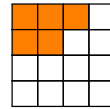
On the other hand, we apply the so-called dual Cauchy identity [312]

$$\prod_{i=1}^{L} \prod_{j=1}^{N+1} (1 + y_i z_j) = \sum_{R \subseteq (N)^L} \chi_R(Y) \chi_{R^{\mathsf{T}}}(U) \quad (5.235)$$

---

[14]For simplicity, the matrix model corresponds to the low energy limit (equivalently, it takes the approximation of large quark mass m) of the matrix model in [218], since the more general expression would not add anything new to our discussion.

and its complex conjugate to (5.231), where $R^\top$ is the transpose partition to R. We set Y to have L eigenvalues all equal to $\sqrt{y}$. Using the orthogonality of characters, as done to get (5.136), one finds (5.234). This proves the relation (5.233). □

Comparison with cIOP

The matrix model (5.231) is closely related to the cIOP matrix model (5.142), the difference residing in the plus signs in front of the fugacity $\sqrt{y}$ and in front of the power L. Because the sign in front of L appears in the exponent, it changes the geometric *series* $(1 - \sqrt{y}z_a)^{-L}$ into *polynomials* in z_a of degree L, $\{z_a\}_{a=1,\dots,N+1}$ being the eigenvalues of the random matrix U. This is reflected in the different constraints appearing in the two character expansions, where in particular $\mathcal{Z}_{\mathrm{QCD}_2}^{(N)}$ includes a sum over only a finite number of representations.

The distinction between the two models becomes starker if one compares their massless limits, which send $\sqrt{y} \to 1$. The limit is ill-posed in the cIOP model, due to the integrand developing a singularity. On the other hand, (5.231) is finite and well-defined in the limit $\sqrt{y} \to 1$. As observed in [406], these behaviors reflect the expected singularity and lack thereof in massless bosonic versus fermionic QCD$_2$. Furthermore, the latter model admits a closed form solution in the limit [76], expressed entirely with Barnes's G-functions:

$$\lim_{y \to 1} \mathcal{Z}_{\mathrm{QCD}_2}^{(N)}(L, y) = \frac{G(L+1)^2 G(N+1) G(2L+N+1)}{G(2L+1) G(L+N+1)^2}. \tag{5.236}$$

Schubert cells and quantum mechanics

From (5.234), the states of the quantum mechanical model read off from $\mathcal{Z}_{\mathrm{QCD}_2}^{(N)}$ are associated with Young diagrams that fit into the $N \times L$ rectangle $(N)^L$. In turn, these Young diagrams are in one-to-one correspondence with the Schubert cells of the decomposition of the Grassmannian $\mathrm{Gr}(L, N+L)$. Thus, while we have seen Calabi–Yau varieties emerging from the cIOP model in Subsection 5.6, the relevant algebraic geometry in the current example is that of Schubert varieties.

The appearance of the Grassmannian and its Schubert cells is of course consistent with a QCD-type interpretation of the model.

Partition function of QCD$_2$ with sum over flavor symmetries

According to our paradigm, we want to enrich the model by introducing a Gaussian weight and summing over the flavor rank in QCD$_2$.

Definition 5.7.2. Let $0 < y, \mathfrak{q} < 1$, $L, N \in \mathbb{N}$ and $\mathcal{Z}^{(N)}_{\mathrm{QCD}_2}$ as in (5.231). The QCD_2 matrix model with sum over flavors is

$$\mathcal{Z}_{\mathrm{Ex2}}(\mathfrak{q}, y) = \sum_{L=0}^{L_{\max}(N)} \mathfrak{q}^{L^2} \mathcal{Z}^{(N)}_{\mathrm{QCD}_2}(L, y). \tag{5.237}$$

Note that in the Schur slice $\mathfrak{q} = \sqrt{y}$, the factor $\mathfrak{q}^{L^2}$ in (5.237) cancels the $y^{-L^2/2}$ from (5.233).

Planar limit of QCD$_2$ with sum over flavor symmetries

Theorem 5.7.3. *Let $\mathcal{Z}_{\mathrm{Ex2}}$ be as in (5.237), with $y = e^{-\beta}$ and $\mathfrak{q} = e^{-1/(2a)}$. $\forall a > 0$, there exists $T_H > 0$ such that $\mathcal{Z}_{\mathrm{Ex2}}$ undergoes a first order phase transition in the planar limit at $\frac{1}{\beta} = T_H$, with*

$$\ln \mathcal{Z}_{\mathrm{Ex2}} = \begin{cases} O(1) & \frac{1}{\beta} < T_H \\ O(N^2) & \frac{1}{\beta} > T_H. \end{cases} \tag{5.238}$$

Moreover, in the Schur slice $a = \beta^{-1}$, $T_H \approx 1.039$.
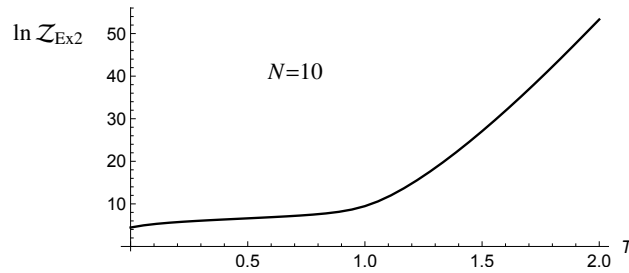
Figure 5.14: Plot of $\ln \mathcal{Z}_{\mathrm{Ex2}}(\mathfrak{q}, y)$ as a function of the temperature $T = -1/\ln(y)$ at $N = 10$. The sum over L in (5.237) has been truncated at $L \leq 20$. A change in behavior around $T \approx 1$ is already visible at small N, although the sharp phase transition is smoothed by finite N effects. The plot is taken in the Schur slice $a = T$, but the qualitative behavior is the same in all a-slices of the parameter space.

Theorem 5.7.3 argues that, passing to the ensemble (5.237), the third order phase transition experienced by $\mathcal{Z}_{\mathrm{QCD}_2}$ in the Veneziano limit is promoted to a first order one, at a critical temperature T_H. The function $\ln \mathcal{Z}_{\mathrm{Ex2}}$ at fixed N is plotted in Figure 5.14. It is also possible to evaluate numerically $\ln \mathcal{Z}_{\mathrm{Ex2}}$ at fixed T for various N, and check that the plot is consistent with an approximately constant behavior if $T < T_H$ and a polynomial shape if $T > T_H$. In Appendix 5.13 we re-derive the first order

phase transition from the unitary matrix model expression (5.231) for $\mathcal{Z}_{\mathrm{QCD}_2}^{(N)}$, and argue that it is accompanied by Hagedorn-like behavior.

In conclusion, Theorem 5.7.3 derives a first order transition with the desired holographic properties from the ingredients:

i) A simple quantum system built out of representations of the flavor symmetry;

ii) A constraint on the states descending from gauge invariance;

iii) A Gaussian sum over the number of quarks;

in accordance with the general prescription of Part 5.1.

Proof of Theorem 5.7.3. The proof is done in two steps.

(1) First we solve the planar Veneziano limit of $\mathcal{Z}_{\mathrm{QCD}_2}^{(N)}$, with

$$L \to \infty, \quad N \to \infty, \quad \gamma = \frac{L}{N} \text{ fixed.} \qquad (5.239)$$

(2) Second, we plug the result in $\mathcal{Z}_{\mathrm{Ex2}}$ and extremize over γ.

Step (1). Most of the procedure for the large L limit of (5.233) goes through exactly as in the cIOP matrix model, see Subsection 5.6. In particular, the discrete matrix models have same summand. Writing it in the form $e^{-L^2 S(\cdots)}$ and extremizing the effective action, we we get the same saddle point equation (5.154). However, the main difference here is that the discrete matrix model we deal with has two hard walls: at $h_j = 0$ and $h_j = L + N - 1$. In the large N limit, the second hard wall for the scaled eigenvalues x is placed at

$$\frac{L + N - 1}{L} \approx 1 + \gamma^{-1}. \qquad (5.240)$$

In the planar limit, the eigenvalue density $\varrho(x)$ is subject to the constraints

$$\int_0^\infty \mathrm{d}x \varrho(x) = 1, \quad \varrho(x) \le 1, \quad \mathrm{supp}\, \varrho \subseteq [0, 1 + \gamma^{-1}]. \qquad (5.241)$$

That is, compared to the cIOP model, there is an additional hard wall at $x = 1 + \gamma^{-1}$. This will play a role later. This discrete matrix model was first solved in [115]. For the explicit comparison with [115], the dictionary is:

[115]	r	s	R	α	$I_{r,s}$
here	$N + L$	L	$1 + \gamma^{-1}$	$e^{-\beta}$	$e^{-\beta L^2/2} \mathcal{Z}_{\mathrm{QCD}_2}^{(N)}$
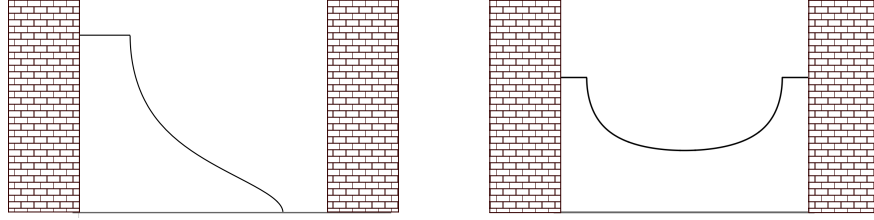
Figure 5.15: Schematic representation of the eigenvalue density in presence of two hard walls for the eigenvalues. Left: The hard wall on the right is not active, the eigenvalue density is capped only at the left edge. Right: Both hard walls are active, the eigenvalue density is capped at left and right edges.

We thus find again a solution (5.157), with the same $\varrho(x)$ as in the IOP model, as long as $x_+ < 1 + \gamma^{-1}$. When x_+ hits the hard wall, we ought to find a new solution. This takes place at

$$x_+(\gamma_c) = 1 + \frac{1}{\gamma_c} \quad \Longrightarrow \quad \gamma_c = \frac{1 - \sqrt{y}}{2\sqrt{y}}. \tag{5.242}$$

As a function of the inverse temperature, $2\gamma_c = e^{\beta/2} - 1$.

Because of the square root singularity at the second hard wall, we replace the ansatz (5.157) with an eigenvalue density "capped" both on the left and on the right edges:

$$\varrho(x) = \begin{cases} 1 & 0 \le x < x_- \\ \hat{\varrho}(x) & x_- \le x \le x_+ \\ 1 & x_+ < x \le 1 + \gamma^{-1}. \end{cases} \tag{5.243}$$

See Figure 5.15 for a schematic view. In this new scenario, the nontrivial part of the eigenvalue density is [115]

$$\hat{\varrho}_*(x) = 1 + \frac{2}{\pi} \left[\arctan\left(\sqrt{\frac{x_-}{x_+}} \sqrt{\frac{x_+ - x}{x - x_-}} \right) - \arctan\left(\sqrt{\frac{1 + \gamma^{-1} - x_-}{1 + \gamma^{-1} - x_+}} \sqrt{\frac{x_+ - x}{x - x_-}} \right) \right] \tag{5.244}$$

with

$$x_\pm = \frac{1}{2(1 + \sqrt{y})} \left[\left(2 + \gamma^{-1}\right)^{1/2} \pm y^{1/4} \gamma^{-1/2} \right]^2. \tag{5.245}$$

Computing

$$\mathcal{F}_{\mathrm{QCD}_2} = \frac{1}{N^2} \ln \mathcal{Z}_{\mathrm{QCD}_2}^{(N)} \Big|_{\text{saddle point}} \tag{5.246}$$

with this eigenvalue density we get

$$\mathcal{F}_{\mathrm{QCD}_2} = \begin{cases} -\gamma^2 \ln(1 - y) & \gamma < \frac{1 - \sqrt{y}}{2\sqrt{y}} \\ (1 + 2\gamma) \ln\left(1 + \sqrt{y}\right) - \frac{1}{4} \ln y + C(\gamma) & \gamma > \frac{1 - \sqrt{y}}{2\sqrt{y}} \end{cases} \tag{5.247}$$

where, in the second phase, $C(\gamma)$ is the y-independent term

$$C(\gamma) = -\gamma^2 \ln\left(\frac{4\gamma}{\gamma+1}\right) + 2\gamma(\gamma+1) \ln\left(\frac{1+2\gamma}{\gamma+1}\right) - \frac{1}{2} \ln\left(\frac{(\gamma+1)^2}{1+2\gamma}\right) - \gamma \ln 4 - \ln 2.$$

(5.248)

Step (2). We express the summands in $\mathcal{Z}_{\text{Ex2}}$ as functions of the Veneziano parameter $\gamma = L/N$ and approximate them for $N \gg 1$:

$$\mathcal{Z}_{\text{Ex2}}(e^{-\beta}) \approx \sum_{L=0}^{L_{\max}(N)} \exp\left\{N^2 \mathcal{S}_{\beta,a}(\gamma)\right\},$$

(5.249)

$$\mathcal{S}_{\beta,a}(\gamma) := \mathcal{F}_{\text{QCD}_2} - \frac{\gamma^2}{2a}.$$

(5.250)

In the phase $\gamma < \gamma_c$, the partition function takes the Gaussian form

$$\mathcal{Z}_{\text{Ex2}}(e^{-\beta}) \approx \sum_{L=0}^{L_{\max}(N)} \exp\left\{-N^2\gamma^2\left[\frac{1}{2a} + \ln(1 - e^{-\beta})\right]\right\}.$$

(5.251)

The saddle point is $\gamma_* = 0$, valid in the low temperature region (see Figure 5.16)

$$\frac{1}{2a} + \ln(1 - e^{-\beta}) > 0.$$

(5.252)

a) In every constant-a slice of the parameter space $\{(a, \beta) \in \mathbb{R}_{>0} \times \mathbb{R}_{>0}\}$, the trivial saddle $\gamma_* = 0$ holds if

$$\beta > \beta_c = -\ln\left(1 - e^{-1/(2a)}\right),$$

(5.253)

equivalently $0 < y < 1 - \mathfrak{q}$. For instance:

$$\beta_c\big|_{a=1/2} \approx 0.459, \qquad \beta_c\big|_{a=2} \approx 1.509.$$

(5.254)

b) In the Schur slice $a = \beta^{-1}$, i.e., $\mathfrak{q} = \sqrt{y}$, the trivial saddle $\gamma_* = 0$ holds if (Figure 5.16)

$$\frac{\beta}{2} + \ln(1 - e^{-\beta}) > 0 \quad \Longrightarrow \quad \beta > \beta_c \approx 0.962.$$

(5.255)

Notice that $0 < \beta_c < \infty$ exists and is finite $\forall a > 0$, so that the features we describe are valid for every choice of the parameter a.

Beyond this value, $\beta < \beta_c$, the exponent in (5.249) changes sign and we have to look for the maximum of $\mathcal{S}_{\beta,a}(\gamma)$. Let us start with the assumption that $\gamma > \gamma_c$. By direct inspection, we find that
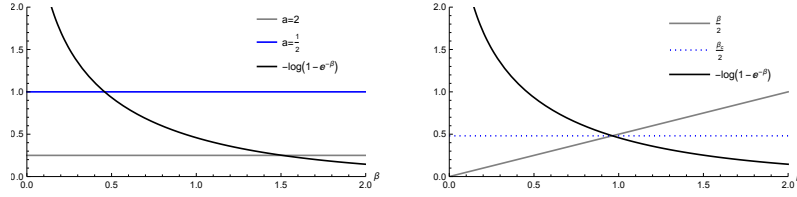
Figure 5.16: The saddle point $\gamma_* = 0$ is valid at low temperature, $\beta > \beta_c$. Left: slice of constant a. Right: Schur slice $a = \beta^{-1}$.
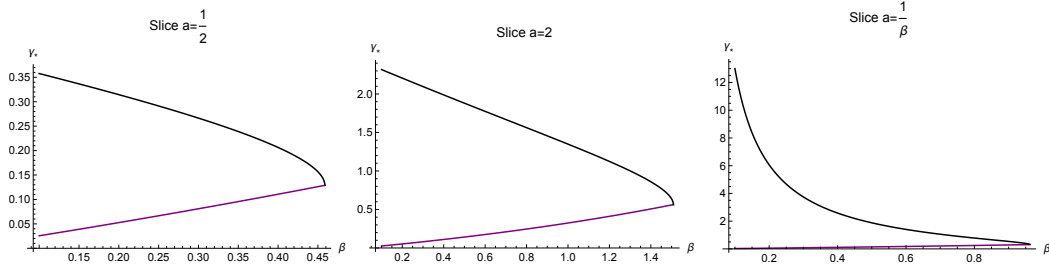
Figure 5.17: The absolute maximum γ_{peak} (black) and γ_c (purple) in the region $\beta \leq \beta_c$. Left: Slice $a = 1/2$. Center: Slice $a = 2$. Right: Schur slice $a = \beta^{-1}$.

- $\mathcal{S}_{\beta,a}$ has an absolute maximum at a value $\gamma_{\text{peak}} > 0$;

- The saddle γ_{peak} exists for all $\beta \leq \beta_c$;

- $\gamma_{\text{peak}} > \gamma_c$ for all $\beta < \beta_c$ and $\gamma_{\text{peak}}\big|_{\beta=\beta_c} = \gamma_c\big|_{\beta=\beta_c}$.

This situation is plotted in Figure 5.17. From the last point it follows that

$$\mathcal{S}_{\beta=\beta_c,a}(\gamma \leq \gamma_c) = 0, \qquad \mathcal{S}_{\beta=\beta_c,a}(\gamma > \gamma_c) < 0. \tag{5.256}$$

We thus find a positive saddle point value which is compatible with $\gamma > \gamma_c$ at all temperature above β_c^{-1}. This is thus the saddle point γ_* that we are looking for, and we set $\gamma_* = \gamma_{\text{peak}}$.

We also plot $\mathcal{S}_{\beta,a}(\gamma)$ as a function of γ at different values of β in Figure 5.18, and a zoom-in close to the transition point is in shown Figure 5.19. The behavior shown is agreement with the analytic calculation: the maximal contribution to $\mathcal{S}_{\beta,a}$ is from $\gamma_* = 0$ if $\beta > \beta_c$ (low temperature phase), whilst $\mathcal{S}_{\beta,a}$ has a global maximum at which is is strictly positive if $\beta < \beta_c$ (low temperature phase).

To conclude the proof it suffices to notice that, when $\beta < \beta_c$, $\gamma_* > 0$ and the saddle point value of $\ln \mathcal{Z}_{\text{Ex2}}$ grows with coefficient N^2, whilst at $\beta > \beta_c$ we have $\gamma_* = 0$, the $O(N^2)$ growth is cancelled and one is left with the remnant $O(1)$ contributions.
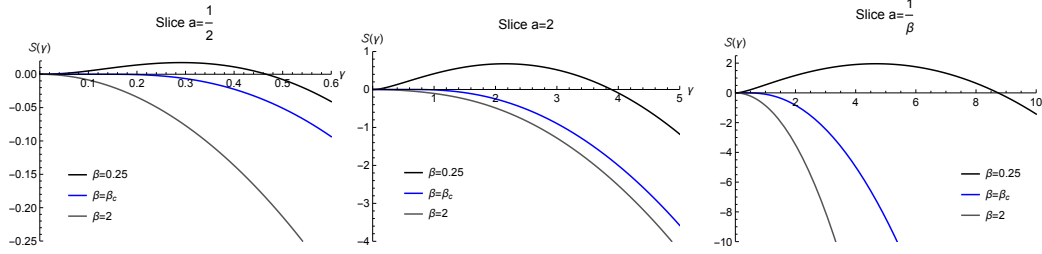
Figure 5.18: Plot of $\mathcal{S}_{\beta,a}(\gamma)$ as a function of γ for $\beta > \beta_c$ (gray), $\beta = \beta_c$ (blue) and $\beta < \beta_c$ (black). Left: Slice $a = 1/2$. Center: Slice $a = 2$. Right: Schur slice $a = \beta^{-1}$. At high temperature, $\mathcal{S}_{\beta,a}$ has a global maximum at $\gamma_* > 0$ with $\mathcal{S}_{\beta,a}(\gamma_*) > 0$ (black curve). Decreasing the temperature until the critical value (blue curve), $\mathcal{S}_{\beta,a}(\gamma_*) = 0$. Below that value, $\mathcal{S}_{\beta,a}$ is non-positive definite and vanishes at $\gamma = 0$, which is the new global maximum (gray curve).
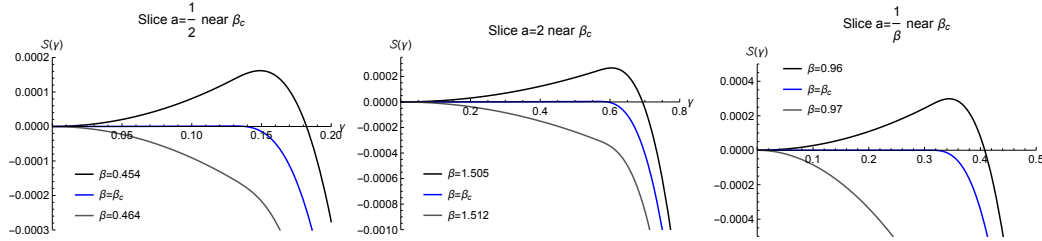
Figure 5.19: Plot of $\mathcal{S}_{\beta,a}(\gamma)$ as a function of γ for $\beta > \beta_c$ (gray), $\beta = \beta_c$ (blue) and $\beta < \beta_c$ (black). Left: Slice $a = 1/2$. Center: Slice $a = 2$. Right: Schur slice $a = \beta^{-1}$. These plots are analogous to Figure 5.18, but showing a narrow window around the critical temperature.

The exchange of dominance of saddle points at $\beta = \beta_c$ yields a first order transition at temperature

$$T_H = \beta_c^{-1}. \tag{5.257}$$

This is analogous to what happens in $\mathcal{N} = 4$ super-Yang–Mills in four dimensions at finite temperature [302].

$\square$

Spectral density of QCD$_2$ with sum over flavor symmetries

We now apply the technology of Subsection 5.5 to QCD$_2$ with the sum over flavors. The computation is essentially the same as in the model of Subsection 5.6, and the structure of the branch cuts of the Fourier transformed Wightman functions is very similar. Let us first consider the simpler case *without* summing over L, and return to the sum over flavor below.

Spectral density of QCD$_2$: no sum

Proposition 5.7.4. *Consider the quantum mechanical system with partition function given by the matrix model* $\mathcal{Z}_{\mathrm{QCD}_2}^{(N)}$ *in (5.231). The associated spectral density has compact, continuous support on* $\mathbb{R}$.

Proof. On both sides of the third order phase transition we have an explicit formula for ϱ_* and its support. In the phase in which the constraint is not active, the model behaves exactly as cIOP and IOP. In particular has the same eigenvalue density and, by Lemma 5.4.18, has the same Fourier transformed Wightman functions $\widetilde{G}_{L,R}(\omega), \widetilde{G}_{L,R}(\omega)$. It follows immediately that the spectral density $\rho(\omega)$ is the same as cIOP in that phase.

Beyond the third order transition, i.e., $\gamma > \gamma_c$, ϱ_* is supported on $[0, 1 + \gamma^{-1}]$ and is non-constant on $[x_-, x_+]$, as given in (5.245). It is clear that the open interval $x_- < x < x_+$ is non-empty if $\gamma_c < \gamma < \infty$. Applying again Lemma 5.4.18, we obtain the branch cuts of $\widetilde{G}_{L,R}(\omega), \widetilde{G}_{L,R}(\omega)$ along $[x_- + \mu, x_+ + \mu]$ if $\omega > \mu$, and along $[-x_+ - \mu, -x_- - \mu]$ if $\omega < -\mu$. In contrast, the regions $0 < x < x_-$ and $x_+ < x < 1 + \gamma^{-1}$ where ϱ_* is constant contribute to the smooth part of $\widetilde{G}_{L,R}(\omega), \widetilde{G}_{L,R}(\omega)$. Using the relation (5.105) between the spectral density $\rho(\omega)$ and the Fourier transformed Wightman functions, we conclude

$$\operatorname{supp} \rho = [-x_+ - \mu, -x_- - \mu] \cup [x_- + \mu, x_+ + \mu], \qquad (5.258)$$

explicitly known as a function of $y = e^{-\beta}$ and of the Veneziano parameter γ, cf. (5.245). $\qquad \square$

Spectral density of QCD$_2$: sum over flavor symmetries

Let us now reintroduce the sum over flavors. The argument in the high temperature phase is analogous to the one just shown. We again use

$$\rho(\omega) = \lim_{\varepsilon \to 0^+} \left[\widetilde{G}_R(\omega + i\varepsilon) - \widetilde{G}_A(\omega - i\varepsilon) \right] \qquad (5.259)$$

and the fact that, for $\beta^{-1} > T_H$, $\widetilde{G}_R(\omega), \widetilde{G}_A(\omega)$ have branch cuts along $\pm \operatorname{supp} \varrho_*$, which is the saddle point eigenvalue density obtained in (5.243) and further evaluated at $\gamma = \gamma_*$. Lacking an explicit formula for γ_* as a function of β, we are unable to provide $\rho(\omega)$ in closed form. However, computing γ_* at a given temperature, e.g., numerically, one simply needs to plug that number in (5.245).

The knowledge of the branch cuts in the high temperature phase, as well as the knowledge that the eigenvalues do not condensate in a continuum spectrum in the low temperature phase (both facts shown in Theorem 5.7.3) are sufficient to argue for the structure of $\operatorname{supp}\rho$.

Theorem 5.7.5. *The spectral density $\rho(\omega)$ associated to the matrix model $\mathcal{Z}_{\mathrm{Ex2}}$ has compact, continuous support at $1/\beta > T_H$.*

Combining this statement with the general recipe of Section 5.3, we conclude that the QCD$_2$ model summed over the number of flavors with Gaussian weight carries a type III$_1$ factor above T_H, and trivially, a type I factor below T_H.

TEMPERATURE	$\ln \mathcal{Z}_{\mathrm{Ex1}}$	ALGEBRA TYPE
$\beta^{-1} < T_H$	$O(1)$	I
$\beta^{-1} > T_H$	$O(N^2)$	III$_1$

5.8 Example 3: Conifold Donaldson–Thomas partition function

The next example we consider does not fully fit in our general discussion because it neither undergoes a phase transition, nor has a flavor symmetry indexed by L which we can sum over. It nevertheless fits in the prescription to derive a quantum mechanical system from a matrix model. It turns out that the resulting quantum system has probe correlation functions characterized by a type III$_1$ von Neumann algebra at every temperature in the large N limit.

Consider the family of matrix models

$$\mathcal{Z}^{(N)}(Q,Y) = \oint_{SU(N+1)} [dU] \, \exp\left\{ \operatorname{tr}\ln\left(1 + Y \otimes U\right) - \operatorname{tr}\ln\left(1 + QY \otimes U^\dagger\right) \right\}, \tag{5.260}$$

where $Q \in \mathbb{C}$ is a scalar parameter, Y is a square matrix, possibly of infinite size, with real eigenvalues $(y_1, y_2, \dots)$, and the trace is over both U- and Y-indices (i.e., tr in this formula means the trace in the tensor product).

Setting

$$Q = 1, \qquad y_i = \begin{cases} e^{-\beta/2} & 1 \le i \le L \\ 0 & i > L \end{cases} \tag{5.261}$$

we get a hybrid model between the two previous examples. It can be studied by the methods above and we omit this analysis.[15]

---

[15]The phase diagram of matrix models interpolating between the three cases was obtained in [406].

We consider instead the specialization

$$0 < |Q| < 1, \qquad y_i = q^{i - \frac{1}{2}} \; \forall i \geq 1 \tag{5.262}$$

for a fugacity q with $|q| < 1$. The constraint $|Q| \neq 1$ is to avoid singularities and we restrict for concreteness to the interior of the punctured unit disk without substantial loss of generality. We then define

$$\mathcal{Z}_{\text{conifold}}^{(N)}(-Q, q) := \mathcal{Z}^{(N)}(Q, Y)\Big|_{(Q,Y) \text{ as in (5.262)}}. \tag{5.263}$$

The minus sign convention in the argument $-Q$ on the left-hand side is just to reduce clutter in later expressions. The matrix model with these parameters reads

$$\mathcal{Z}_{\text{conifold}}^{(N)}(-Q, q) = \oint_{SU(N+1)} [dU] \prod_{j=1}^{\infty} \frac{\det\left(1 + q^{j - \frac{1}{2}} U\right)}{\det\left(1 + Q q^{j - \frac{1}{2}} U^\dagger\right)}, \tag{5.264}$$

with the determinant taken over $SU(N+1)$. Up to an overall factor given by $\mathcal{M}(-q)^2$, where $\mathcal{M}$ is the MacMahon function

$$\mathcal{M}(-q) := \prod_{j=1}^{\infty} \left(1 - (-q)^j\right)^{-j}, \tag{5.265}$$

the matrix model (5.264) is the generating function of Donaldson–Thomas (DT) invariants of the resolved conifold [364, 432] (here we follow [432]). More precisely, (5.264) is a truncation of the full generating function of DT invariants, which is recovered at $N \to \infty$. This is the limit we are interested in. For definition and generalities on DT invariants and their generating functions we refer to [332].

The parameter $Q \in \mathbb{C}$ is such that $-\ln Q$ is the (complexified) Kähler parameter of the exceptional rational curve in the resolution of the conifold, and $q = e^{-g_{\text{string}}}$. Therefore:

- The point $Q \to 0$ is usually referred to as large volume point, and it is possible to extract DT invariants from a Taylor expansion of (5.264) around this point;

- The singularity of the matrix model at $Q = 1 = q$ signals the singularity at the conifold point of the Kähler moduli space, where the rational curve is blown down.

Explicitly, let $\mathcal{Z}_{\text{CY3}}^{\text{DT}}(Q, q)$ denote the generating function of DT invariants of any Calabi–Yau threefold. The contribution from degree 0 sub-schemes (D0-branes in

the string theory parlance) of a Calabi–Yau with topological Euler characteristic $\chi(\text{CY3})$ is [332, 298]

$$\mathcal{Z}_{\text{CY3}}^{\text{DT}}(Q, q)\big|_{\text{degree } 0} = \mathcal{M}(-q)^{\chi(\text{CY3})}, \tag{5.266}$$

independent of Q. A reduced generating function of DT invariants was introduced and studied by Maulik–Nekrasov–Okounkov–Pandharipande [332].

Definition 5.8.1. The *reduced* generating function of DT invariants of a Calabi–Yau threefold is $\mathcal{Z}_{\text{CY3}}^{\text{DT}}$ with the generating function of degree 0 sub-schemes stripped off,

$$\mathcal{Z}_{\text{CY3}}^{\text{DT}}(Q, q) / \mathcal{Z}_{\text{CY3}}^{\text{DT}}(Q, q)\big|_{\text{degree } 0}. \tag{5.267}$$

Moreover we have [432]

$$\mathcal{Z}_{\text{conifold}}^{\text{DT}}(Q, q) = \mathcal{M}(-q)^2 \lim_{N \to \infty} \mathcal{Z}_{\text{conifold}}^{(N)}(-Q, q). \tag{5.268}$$

Comparing the expressions and using $\chi(\text{conifold}) = 2$, we conclude that

Lemma 5.8.2 ([364, 432]). $\mathcal{Z}_{\text{conifold}}^{(N)}(-Q, q)$ *is a truncation of the reduced generating function of DT invariants of the resolved conifold.*

To derive a quantum mechanical interpretation along the lines of Part 5.1, we write down the character expansion of (5.264) and set $-Q = e^{-\beta}$. That is, the Kähler parameter in the resolution of the conifold and the inverse temperature are related through

$$\text{inverse temperature } \beta \quad \longleftrightarrow \quad \text{Kähler parameter } \beta - i\pi.$$

Lemma 5.8.3. *With the notation above, the equality*

$$\mathcal{Z}_{\text{conifold}}^{(N)}(e^{-\beta}, q) = \sum_{R \,:\, \ell(R) \leq N} \left(\frac{e^{-\beta}}{q}\right)^{|R|} \chi_R\left(\text{diag}(q, q^2, q^3, \ldots)\right) \chi_{R^{\top}}\left(\text{diag}(q, q^2, q^3, \ldots)\right) \tag{5.269}$$

holds, where $R^{\top}$ denotes the transpose partition to R.

Proof. Applying the Cauchy identity (5.143) to the denominator of (5.264) gives:

$$\left[\prod_{j=1}^{\infty} \det\left(1 + Qq^{j-\frac{1}{2}}U^{\dagger}\right)\right]^{-1} = \sum_{\tilde{R} \,:\, \ell(\tilde{R}) \leq N} \chi_{\tilde{R}}\left(\text{diag}(-Qq^{\frac{1}{2}}, -Qq^{\frac{3}{2}}, -Qq^{\frac{5}{2}}, \ldots)\right) \chi_{\tilde{R}}(U^{\dagger})$$

$$= \sum_{\tilde{R} \,:\, \ell(\tilde{R}) \leq N} \left(-Qq^{-\frac{1}{2}}\right)^{|\tilde{R}|} \chi_{\tilde{R}}\left(\text{diag}(q, q^2, q^3, \ldots)\right) \chi_{\tilde{R}}(U^{\dagger}). \tag{5.270}$$

Applying the dual Cauchy identity (5.235) to the numerator of (5.264) gives:

$$
\prod_{j=1}^{\infty} \det\left(1 + q^{j-\frac{1}{2}} U\right) = \sum_{R \, : \, \ell(R^\top) \leq N} \chi_R\left(\mathrm{diag}(q^{\frac{1}{2}}, q^{\frac{3}{2}}, q^{\frac{5}{2}}, \dots)\right) \chi_{R^\top}(U)
$$

$$
= \sum_{R \, : \, R_1 \leq N} \left(q^{-\frac{1}{2}}\right)^{|R|} \chi_R\left(\mathrm{diag}(q, q^2, q^3, \dots)\right) \chi_{R^\top}(U).
$$

(5.271)

Combining the two expressions, the integration over $SU(N+1)$ yields $\delta_{R^\top, \tilde{R}}$. We thus obtain the character expansion

$$
\mathcal{Z}^{(N)}_{\mathrm{conifold}}(-Q, q) = \sum_{R \, : \, R_1 \leq N} \left(-\frac{Q}{q}\right)^{|R|} \chi_R\left(\mathrm{diag}(q, q^2, q^3, \dots)\right) \chi_{R^\top}\left(\mathrm{diag}(q, q^2, q^3, \dots)\right).
$$

(5.272)

We relabel $R' = R^\top$ (and drop the prime) to rewrite the sum over representations restricted to those of length at most N. Finally we set $-Q = e^{-\beta}$. □

The model (5.269) belongs to the family of q-ensembles and it can be shown that it possesses a single phase in the large N limit. We do not study it explicitly here, but discuss a related, albeit simpler, model in Appendix 5.13. The large N limit of $\mathcal{Z}^{(N)}_{\mathrm{conifold}}$ can be analyzed along the same lines.

Here, instead, we are interested in reading off a quantum mechanical system from the character expansion (5.269). The presence of the fugacity q prevents us from interpreting the terms χ_R as accounting for degeneracy. To overcome this difficulty, we work in the limit $q \to 1$, which in the string theory picture means $g_{\mathrm{string}} \to 0^+$.

A few technical comments:

- In this simplified regime the MacMahon function is singular, but the *reduced* generating function is well-defined.

- It is an intriguing fact that, despite our character expansion and ensuing construction need not know anything about a string theory origin of the matrix models, to have a quantum mechanical interpretation requires us to send $g_{\mathrm{string}} \to 0^+$.

- Being interested in the quantum mechanical interpretation, we stick to the limit $q \to 1$, which unrefines the DT partition function. This should not be confused with the "decategorification" limit $q \to -1$ sometimes considered in enumerative geometry.

We therefore consider

$$\mathcal{Z}_{\text{Ex3}}(e^{-\beta}) := \lim_{q \to 1} \mathcal{Z}_{\text{conifold}}^{(N)}(e^{-\beta}, q) = \sum_{R \,:\, \ell(R) \leq N} e^{-\beta|R|} \dim(R)\dim(R^{\top}). \quad (5.273)$$

Let us summarize the enumerative meaning of $\mathcal{Z}_{\text{Ex3}}$.

Proposition 5.8.4. *Let $\mathcal{Z}_{\text{Ex3}}$ be as in (5.273). The large N limit $\lim_{N \to \infty} \mathcal{Z}_{\text{Ex3}}(e^{-\beta})$ yields the reduced, unrefined generating function of Donaldson–Thomas invariants of the resolved conifold, as a function of the Kähler parameter $\beta - i\pi$.*

To emphasize the difference with the previous models, let us remind the reader that the representation $R^{\top}$ is (generically) not isomorphic to R nor to $\overline{R}$. For instance, assume $N = 4$ and $R = (3, 3, 1, 0)$, which gives $R^{\top} = (3, 2, 2, 0)$:

$$R = (3, 3, 1, 0) \quad \boxed{} \quad \Longrightarrow \quad R^{\top} = (3, 2, 2, 0) \quad \boxed{}. \quad (5.274)$$

By formula (5.62), the two have different dimensions as $SU(5)$ representations,

$$\dim(3, 3, 1, 0) = 60, \qquad \dim(3, 2, 2, 0) = 36. \quad (5.275)$$

Another well-known example is when R is the rank-k antisymmetric representation, then $R^{\top}$ is the rank-k symmetric representation,

$$R = (\underbrace{1, \ldots, 1}_{k}, 0, \ldots, 0) \quad \Longrightarrow \quad R^{\top} = (k, 0, \ldots, 0), \quad (5.276)$$

and the two are not isomorphic unless $k = 1$.

Let us focus on the quantum mechanical interpretation of (5.273), where now all the pieces are consistent with our general analysis in Section 5.4. In this example we have $\phi(R) = R^{\top}$, which requires minor edits to the interaction Hamiltonian H_{int} compared to the case $\phi(R) = \overline{R}$. We suitably adjust H_{int} so that the interaction energy E_J^{int} is as in the general discussion in Subsection 5.4, possibly up to $1/N$ terms.

To study the large N limit of $\mathcal{Z}_{\text{Ex3}}$ we adopt the method of IOP [246]. After appropriate rescaling, the Young diagram R can be represented by a piece-wise linear function as follows. One sets the (x, y)-axes rotated by $-135°$ with respect
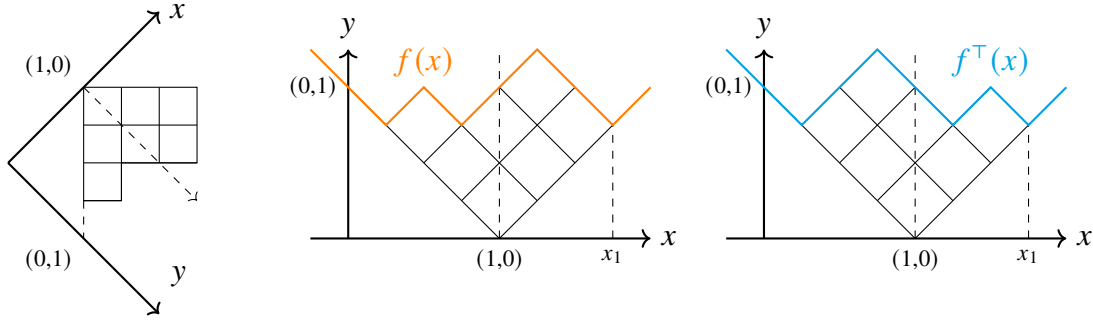
Figure 5.20: Coordinate system for Young diagrams, exemplified for $N = 4$ and $R, R^\top$ as in (5.274). Left: Orientation of the (x, y)-axes with respect to R. Center: The shape function $f(x)$ is shown in orange. Right: The shape function $f^\top(x)$ of the transposed diagram $R^\top$ is shown in cyan.

to the diagram R and with the x-axis flipped, as shown in Figure 5.20 (left). The origin of the (x, y)-plane is chosen so that the top-left corner of R has coordinates $(1, 0)$, and the length of the axis is scaled by $1/N$, so that the constraint $\ell(R) \leq N$ becomes the requirement R is entirely contained in the positive quadrant. Then the shape of R is the graph of a piece-wise linear function $f(x)$ with

$$f(x) \geq |x - 1|, \qquad f(x) = -x + 1 \text{ if } x \leq 0 \tag{5.277}$$

and there exists $x_1 \geq 1$ such that $f(x) = x - 1$ if $x > x_1$. The conventions are chosen to match with [246, Sec.5].

In this coordinate system, transposition $R \mapsto R^\top$ sends $f \mapsto f^\top$ and it acts as a reflection about the vertical axis $x = 1$. Therefore

$$f^\top(x) = f(2 - x) \tag{5.278}$$

as shown in Figure 5.20 (right).

Writing (5.273) as

$$\mathcal{Z}_{\text{Ex3}}(e^{-\beta}) = \sum_{R \,:\, \ell(R) \leq N} \exp\left\{ -\frac{1}{2} \left[\beta |R| - 2 \ln \dim(R) \right] - \frac{1}{2} \left[\beta |R^\top| - 2 \ln \dim(R^\top) \right] \right\}, \tag{5.279}$$

expressing the right-hand side in terms of the shape function f and comparing with the setup of [246, Sec.5], we have

$$\mathcal{Z}_{\text{Ex3}}(e^{-\beta}) = \sum_{R \,:\, \ell(R) \leq N} \exp\left\{ -\frac{N^2}{2} \left(\mathcal{S}_{\text{IOP}}[f] + \mathcal{S}_{\text{IOP}}[f^\top] \right) \right\} \tag{5.280}$$

where $\mathcal{S}_{\mathrm{IOP}}[f]$ is the effective action that appears in the IOP model. The saddle point equation (derived analogously to [246, Sec.5.2]) is:

$$\beta - 2\ln(x) + \int_{-\infty}^{\infty} d\xi \ln|x - \xi| \left(\frac{f''(\xi) + f''(2 - \xi)}{2} \right) = 0 \qquad (5.281)$$

for $0 < x < x_1$. While we do not solve this problem explicitly, one checks that the terms with positive and negative signs compete, exactly as in the IOP model, yielding a non-trivial saddle point. We conclude that $\ln \mathcal{Z}_{\mathrm{Ex3}} = O(N^2)$ in the large N limit.

An alternative way to argue for the same result without inspecting the details of the saddle point equation is that the typical $SU(N + 1)$ representation at large N has all rows of length $O(N)$ and $\ln \dim(R) = O(N^2)$. The only difference between this example and the IOP model of Section 5.6 is the appearance of $\dim(R)\dim(R^\top)$ instead of $\dim(R)^2$. For typical R, $\ln \dim(R^\top) = O(N^2)$ as well, and moreover there are no other negative signs that may produce cancellations. The saddle point shape f_* is thus expected to be similar to the IOP solution.

Concretely, in the low temperature limit we approximate

$$\tanh\left(\frac{\beta}{4}\right) \approx 1 - 2e^{-\beta/2}, \qquad \coth\left(\frac{\beta}{4}\right) \approx 1 + 2e^{-\beta/2}, \qquad (5.282)$$

and the IOP limit shape is supported on $[1 - 2e^{-\beta/2}, 1 + 2e^{-\beta/2}]$ and symmetric about the vertical axis $x = 1$. Therefore at low temperature, f_* in this example agrees with the IOP limit shape, and it is deformed away from the IOP shape as the temperature is increased (β is decreased), but in a continuous way, for which the property $\ln \mathcal{Z}_{\mathrm{Ex3}} = O(N^2)$ persists.

Yet another way to show that the saddle point eigenvalue density ϱ_* of this model is a continuous function, would be to study directly the unitary matrix model. In that case it is easier to work in a 't Hooft limit

$$g_{\mathrm{string}} \to 0^+, \qquad N \to \infty, \qquad \text{with } \lambda_{\mathrm{string}} := N g_{\mathrm{string}} \text{ fixed}, \qquad (5.283)$$

and take the unrefined limit $\lambda_{\mathrm{string}} \to 0$ at the end of the computation. The procedure is rather cumbersome and we do not present it here. However, one observes that it admits a solution consistent with the large N growth $\ln \mathcal{Z}_{\mathrm{Ex3}} = O(N^2)$ and moreover we have not found any phase transition as a function of β, supporting the picture advocated for using typical representations.

Constructing the Wightman functions as explained in Subsection 5.4, this observation is enough to deduce that $\rho(\omega)$, the spectral density of the quantum system coupled to a probe, has continuous support. We conclude that these correlation functions are those of a von Neumann algebra of type III_1.

TEMPERATURE	$\ln \mathcal{Z}_{\text{Ex3}}$	ALGEBRA TYPE
$\forall \beta$	$O(N^2)$	III_1

5.9   Example 4: Systems with a Casimir Hamiltonian

Consider a system with $U(L)$ global symmetry, and assume its finite temperature partition function takes the form

$$\mathcal{Z}_{\text{YM}_2}(L, e^{-\beta}) = \sum_{R \in \mathfrak{R}^{U(L)}} (\dim R)^2 \, e^{-\frac{\beta}{b} C_2(R)}, \tag{5.284}$$

where the sum is over all isomorphism classes of irreducible $U(L)$ representations, and

$$C_2(R) = \sum_{i=1}^{L} R_i (R_i - 2i + L + 1) \tag{5.285}$$

is the quadratic Casimir invariant. The number $b^{-1} > 0$ is interpreted as a coupling constant.

The inspiration to write down this system is twofold:

- Take a two-dimensional gravity system with gauge group $U(L)$, dual to an ensemble of boundary theories with global $U(L)$ symmetry. It was shown in [272] that the partition function of the random matrix ensemble with global symmetry decomposes according to (5.284).

- Take any unitary CFT in $d \geq 2$ spacetime dimensions, with $U(L)$ global symmetry, at finite temperature T. In [271] it was found that the probability of a state to be in the irreducible representation R, in the high temperature limit, is given by

$$\text{Prob}(R) = \left(\frac{4\pi}{bT^{d-1}} \right)^{\frac{L^2}{2}} (\dim R)^2 \exp\left(-\frac{1}{bT^{d-1}} C_2(R) \right). \tag{5.286}$$

The R-independent coefficient is just a normalization. Up to the overall coefficient, summing over all the states we get (5.284), with identification

$$\beta = \frac{1}{T^{d-1}}. \tag{5.287}$$

In particular, for a two-dimensional CFT, we have the identification between the quantum mechanical β and the inverse temperature T^{-1} of [271].

When (5.284) stems from a large N gauge theory, the parameter b encodes the dependence on the gauge rank N. Here we need not necessarily assume any concrete N-dependence. In order to obtain a nontrivial scaling limit, we will instead scale b with L in the following way:

Definition 5.9.1. For every $L \in \mathbb{N}, \beta > 0, b > 0$, the *planar limit* of the ensemble (5.284) is the limit $L \to \infty$ with

$$\tilde{\gamma} = \frac{L}{b} \quad \text{fixed.} \tag{5.288}$$

Regardless of the origin of (5.284), the scaling limit with $\frac{L}{b}$ fixed is necessary at the level of the matrix model, to have a non-trivial large L limit.

Quantum mechanics from ensembles with Casimir Hamiltonian

Example (5.284) slightly differs from our general discussion in Section 5.4, because we do not start from a unitary matrix model. Besides, and related, the Hamiltonian of the quantum mechanical system is quadratic in R, as opposed to the Hamiltonian linear in R considered in Section 5.4. This modification does not spoil the argument, which can be run without changes.

We henceforth take (5.284) as our starting point, and interpret it as the partition function of a system at inverse temperature β. This defines our toy model. The Hilbert space of the system decomposes into

$$\mathcal{H}_L = \bigoplus_{R \in \mathfrak{R}^{U(L)}} \mathcal{H}_L(R) \otimes \mathcal{H}_L(R), \tag{5.289}$$

and the Hamiltonian H acts diagonally on the representation basis with eigenvalues

$$H \,|R, \mathsf{a}\rangle \otimes |R, \dot{\mathsf{a}}\rangle = (C_2(R)/b) \,|R, \mathsf{a}\rangle \otimes |R, \dot{\mathsf{a}}\rangle \qquad \forall \mathsf{a}, \dot{\mathsf{a}} = 1, \ldots, \dim R. \tag{5.290}$$

We will assume the system is coupled to a probe as explained in Subsection 5.4.

Theorem 5.9.2. *Let $L \in \mathbb{N}$ and $\beta > 0$, and consider $\mathcal{Z}_{\mathrm{YM}_2}(L, e^{-\beta})$ as given in (5.284), interpreted as the partition function of a quantum mechanical system with global symmetry $U(L)$. Consider the planar limit of Definition 5.9.1. The von Neumann algebra associated to the system is of type III_1.*

Crucially, (5.284) equals the partition function of two-dimensional Yang–Mills theory on the sphere [339, 398], with $U(L)$ interpreted as a gauge group in that context. The planar limit of Definition 5.9.1 is nothing but the standard 't Hooft planar limit of 2d pure Yang–Mills. The large L planar limit of (5.284) has been addressed in [148], which lays the groundwork for Theorem 5.9.2.

Lemma 5.9.3 ([148]). *Let $\mathcal{Z}_{\mathrm{YM}_2}$ be the matrix model (5.284), at arbitrary $\beta > 0$. In the planar limit, $\ln \mathcal{Z}_{\mathrm{YM}_2} = O(L^2)$, and it undergoes a third order phase transition at $\tilde{\gamma} = \frac{\pi^2}{2\beta}$. Moreover, the density of eigenvalues has compact and continuous support on the real axis, which enhances as $\beta \to 0$.*

Proof. This lemma is part of the classical result of [148]. We briefly sketch the main ideas for completeness, and refer to [148] (and subsequent work) for the details.

The starting point is to rewrite (5.284) in a form akin to (5.59). The change of variables

$$h_i = R_i - i + \frac{L+1}{2} \tag{5.291}$$

recasts the ensemble of representations into

$$\mathcal{Z}_{\mathrm{YM}_2}(L, e^{-\beta}) = \frac{e^{\frac{\beta}{12b}L(L^2-1)}}{G(L+1)^2} \sum_{\substack{(h_1,\ldots,h_L)\in\mathbb{Z}^L \\ h_1>h_2>\cdots>h_L}} e^{-\frac{\beta}{b}\sum_{i=1}^{L} h_i^2} \prod_{1\le i<j\le L} (h_i - h_j)^2 \tag{5.292}$$

where we have used the properties of the $U(L)$ representations. Similar to the previous examples, the matrix model effective action is

$$S(h_1,\ldots,h_L) = \frac{\beta}{b} \sum_{i=1}^{L} h_i^2 - \sum_{i\neq j} \ln|h_i - h_j|. \tag{5.293}$$

Inserting the scaled variable x, defined through $h_i = L^\eta x_i$ for some $\eta > 0$ to be determined momentarily, we define the density of eigenvalues $\varrho(x)$ exactly as above. Using the definition of the parameter $\tilde{\gamma}$, we arrive at

$$S(h_1,\ldots,h_L) = L^2 \int \mathrm{d}x \varrho(x) \left[L^{2\eta-2}\beta\tilde{\gamma}x^2 - \mathrm{P}\!\!\int \mathrm{d}x' \varrho(x') \ln|x - x'| \right]. \tag{5.294}$$

In the large L limit, this action admits a non-trivial saddle point if $\eta = 1$. We arrive at the saddle point equation

$$\mathrm{P}\!\!\int \mathrm{d}x' \frac{\varrho_*(x')}{x - x'} = \beta\tilde{\gamma}x, \tag{5.295}$$

where the saddle point eigenvalue density ϱ_* is to be looked for in the restricted functional space subject to the conditions [148]

$$\int_0^\infty dx \varrho(x) = 1, \qquad 0 \le \varrho(x) \le 1. \tag{5.296}$$

So far, the derivation is analogous to Subsection 5.6, except for the quadratic dependence on x in the action. The solution to (5.295) is given by the Wigner semicircle law

$$\varrho_*(x) = \frac{\beta\tilde{\gamma}}{\pi}\sqrt{\frac{2}{\beta\tilde{\gamma}} - x^2}, \qquad \text{supp } \varrho_* = \left[-\sqrt{\frac{2}{\beta\tilde{\gamma}}}, \sqrt{\frac{2}{\beta\tilde{\gamma}}}\right]. \tag{5.297}$$

The solution satisfies $\varrho_*(x) \le 1$ on the entire support if $2\beta\tilde{\gamma} < \pi^2$. We interpret this bound as a critical value for $\tilde{\gamma}$ at arbitrary $\beta > 0$. Raising $\tilde{\gamma}$ above the threshold, one must replace the Wigner semicircle with a "capped" solution of the form [148]

$$\varrho(x) = \begin{cases} 1 & 0 \le x < x_- \\ \hat{\varrho}(x) & x_- \le x \le x_+ \\ 0 & x_+ < x \end{cases} \tag{5.298}$$

with $\hat{\varrho}$ satisfying the continuity conditions $\hat{\varrho}(x_-) = 1$, $\hat{\varrho}(x_+) = 0$. The solution in this phase is more involved, and can be found in [148].

Focusing on the high temperature regime, i.e., the Cardy limit $\beta \to 0$, the critical value for $\tilde{\gamma}$ is moved to large positive values. The system remains in the first phase for $\tilde{\gamma}$ fixed and $\beta \to 0$, and supp ϱ_* has width proportional to $\beta^{-1/2}$, thus spreads on the whole real axis in the high temperature limit. $\qquad\square$

Proof of Theorem 5.9.2. Given the saddle point eigenvalue density of [148], the result follows from it and the general result of Subsection 5.4.

It is important to note that, although the Hamiltonian H has changed, and the eigenvalues are now $C_2(R)$, we are still using the interaction Hamiltonian (5.75). The eigenvalues of H determine the eigenvalue density ϱ_*, whereas the Hamiltonian H_{int} enters in the Fourier transform of the correlation functions. For this reason, the expressions for the Wightman functions — and hence for the spectral density $\rho(\omega)$ — derived in Subsection 5.4 remain valid, as can be immediately checked walking through the same steps. What changes is the form of ϱ_* used for the evaluation of $\rho(\omega)$ at large N. $\qquad\square$

As a concluding remark, we stress once again that we are not making claims about the nature of the von Neumann algebra of the holographic CFTs considered in [271]. We find that, given the toy quantum mechanical model built out of (5.284), its correlation functions are captured by a type III$_1$ von Neumann algebra. We *do not* claim any implication for the holographic systems of [272, 271]. While the ideas developed here might prove useful, to rigorously establish the type of von Neumann algebra for those holographic systems is beyond the scope of the present work.

Ensembles with a sum over flavor symmetries

We now consider the extension of the matrix model (5.284), and of the corresponding quantum system, by introducing the sum over the rank L of the global symmetry:

$$\mathcal{Z}_{\text{Ex4}}(\mathfrak{q}, e^{-\beta}) = \sum_{L=0}^{\infty} \mathfrak{q}^{L^2} \sum_{R \in \mathfrak{R}^{U(L)}} (\dim R)^2 \, e^{-\frac{\beta}{b} C_2(R)}. \tag{5.299}$$

In this situation, the dependence on the parameter b replaces the dependence on the gauge rank N, simply because it is the only other parameter we have at hand besides β.

Proposition 5.9.4. *In the limit $b \to \infty$, the matrix model* (5.299) *behaves as*

$$\ln \mathcal{Z}_{\text{Ex4}} = O(b^2) \tag{5.300}$$

for every $\beta > 0$.

Proof. As before, we write $\mathfrak{q} = e^{-1/(2a)}$. Besides, we consider two choices of slice in the parameter space: (i) the fixed-a slice, in which a is a given number independent on the other parameters; and (ii) the Schur slice $a = \beta^{-1}$.

To begin with, we rewrite

$$\ln \mathcal{Z}_{\text{Ex4}} \approx \ln \int_0^\infty d\tilde{\gamma} \, \exp\left[-b^2 \left(\frac{\tilde{\gamma}^2}{2a} - \tilde{\gamma}^2 \mathcal{F}_{\text{YM}_2}(\beta\tilde{\gamma})\right)\right] \tag{5.301}$$

where

$$\mathcal{F}_{\text{YM}_2} = \lim_{L \to \infty} \frac{1}{L^2} \ln \mathcal{Z}_{\text{YM}_2} \tag{5.302}$$

which, by definition, only depends on the product $\beta\tilde{\gamma}$. In the limit $b \to \infty$ we ought to look for the saddle points $\tilde{\gamma}_*$ of (5.301). Assuming that the system is in the first phase, we have [148]

$$\mathcal{F}_{\text{YM}_2}\big|_{\tilde{\gamma} < \frac{\pi^2}{2\beta}} = \frac{\beta\tilde{\gamma}}{12} - \frac{1}{2}\ln(2\beta\tilde{\gamma}). \tag{5.303}$$
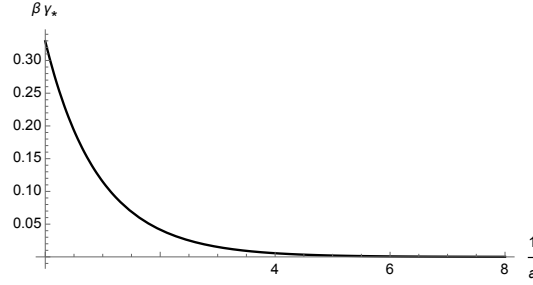
Figure 5.21: Plot of the saddle point value $\beta\tilde{\gamma}_*$ in the constant-a slice, shown as a function of a^{-1}.

In the constant-a slice, in which a is taken independent of β, the saddle point $\tilde{\gamma}_*$ of the integrand in (5.301) is

$$\beta\tilde{\gamma}_* = -4\mathsf{ProductLog}\left(-\frac{e^{-\frac{1}{2}-\frac{1}{a}}}{8}\right), \tag{5.304}$$

where $\mathsf{ProductLog}(z)$ denotes the function that gives the principal solution for w to the equation $z = we^w$. The saddle point is plotted in Figure 5.21. The most important point is that it is a positive, monotone function of $a > 0$ which satisfies

$$\lim_{a\to 0}\beta\tilde{\gamma}_* = 0, \qquad \lim_{a\to\infty}\beta\tilde{\gamma}_* \approx 0.3293. \tag{5.305}$$

That is to say,

$$0 < \beta\tilde{\gamma}_* < \frac{\pi^2}{2} \qquad \forall 0 < a < \infty. \tag{5.306}$$

On the other hand, expanding $\mathcal{F}_{\mathrm{YM}_2}$ in the phase $\tilde{\gamma} > \frac{\pi^2}{2\beta}$ near the critical point, there is no saddle point. Evaluating (5.301) at $\tilde{\gamma}_*$ we obtain $\ln \mathcal{Z}_{\mathrm{Ex4}} = O(b^2)$ at all temperatures.

Let us now consider the slice $a = \beta^{-1}$. Due to the simple way in which the dependence on a appears, it turns out that the saddle point is simply given by (5.304) with $a^{-1} = \beta$. Once again, this saddle point is positive and valid at all temperatures, thus yielding $\ln \mathcal{Z}_{\mathrm{Ex4}} = O(b^2)$ at all temperatures. $\qquad\square$

cor. *The von Neumann algebra associated to quantum system constructed from the ensemble* (5.299) *with a sum over the rank of the global symmetry is of type III$_1$ for every $\beta > 0$.*

5.10 Conclusions and outlook

In this work we obtained a general construction of large N von Neumann algebras applicable to observables satisfying large N factorization, and constructed quantum

Keyword	Result	Section
von Neumann algebra	Construction and type of large N von Neumann algebra from suppρ	Section 5.3 (Eq. (5.23))
Quantum mechanics	Quantum mechanical system with type III$_1$ algebra at large N	Section 5.4 (Thm. 5.4.21)
Hagedorn transition	Extended systems with first order type I to type III$_1$ transition	Section 5.5 (Thm. 5.5.5)

Figure 5.22: Main results in a nutshell.

systems with an emergent type III$_1$ von Neumann algebra at large N. These quantum systems, which vastly generalize the IOP model introduced in [246], are able to implement some kind of gauge constraint, and have a partition function that is expressible in terms of a matrix model. Their Hilbert space can be explicitly constructed from the character expansion of the matrix integral.

We showed that when a heavy probe is coupled to our systems, the Källén–Lehmann spectral density at finite temperature becomes continuously supported, which is a hallmark of type III$_1$ structure. Furthermore, upon introducing an extended Hilbert space with sectors carrying different flavor symmetries, we showed that our systems are generically promoted to systems with a Hagedorn transition. Upon definition of an appropriate notion of probe, we showed that below the Hagedorn temperature, the partition function is convergent, while above the Hagedorn transition, the large N algebras once again satisfy large N factorization and have type III$_1$.

Our main findings in Part 5.1 are summarized in Figure 5.22.

Our construction can be applied to a large class of examples, as was demonstrated very explicitly in the second part of this work. In particular, we introduced examples inspired from the IOP model [246], as well as from a toy model of QCD$_2$ [218]. We also analyzed a system constructed from the generating function of DT invariants of the conifold, even though a complete understanding of the possible geometric meaning of the type III$_1$ von Neumann algebra remains an open question. We have then analyzed a matrix model describing holographic systems with global symmetries [271].

The aim of this work was to lay the groundwork to explicitly set up a quantum system given any gauge theory with continuous flavor symmetry, and to assign a large N von Neumann algebra to it. There are several interesting questions that future work could address.

The most obvious and most ambitious avenue for future research is to embrace more realistic models of holography, possibly applying the techniques and results herein to the Hilbert series of these models. Maybe without studying full-fledged holographic examples, a desirable feature that the IOP model does not possess [337], nor do our models, would be that they exhibit maximal chaos. It would be interesting to see whether one can find maximally chaotic models and study their large N von Neumann algebra by extending the methods developed here to more complicated systems. Large N chaos is likely to have a nice interpretation in the language of modular flow [134, 168], and more generally, the algebraic properties of a local bulk spacetime are closely related to mathematical definitions of chaos in von Neumann algebras [191, 367].

A complementary question to ask is whether the examples presented here, which are only known to possess some of the weaker chaotic properties of [191, 367], can still have a bulk description that is geometric in some sense. In particular, the compactness of the spectral density of the models of this chapter seems to make their putative dual description very stringy. It would be interesting to understand whether for such models, one can still make sense of a notion of dual geometry that, in particular, displays some kind of connectedness between the two sides of the thermofield double. Another feature that we would like to eventually remove is the introduction of an external probe, which would be absent in a fully holographic system, where the relevant correlation functions should correspond to operators directly within the gauge theory.

Another question that remains open is a first principles understanding of the sum over flavors. Posing this question from the bulk side of the holographic correspondence, it would be very interesting to establish a connection with other recent proposals entailing averaging procedures in black hole physics.

One collateral observation (cf. Appendix 5.13) is that, for the very special case of $\mathcal{N} = 4$ super-Yang–Mills in the Cardy limit, our sum over L descends to a sum over the Riemann sheets of [95]. It remains to be seen whether there is a general lesson to be learnt from this comment.

It may also be interesting to study these systems in other states that are not thermal, like, for instance, some microcanonical versions of the thermofield double akin to the ones considered in [100]. Other types of von Neumann algebras are supposed to appear in that case, and it would be interesting to check the proposal in our matrix model context.

A related issue would be to study the crossed product of our large N algebras with their modular automorphism group, as well as perturbative $1/N$ corrections to our calculations. Moreover, including both perturbative and non-perturbative corrections to the large N correlation functions computed here is expected to give a von Neumann algebra of type I. It would be interesting to see explicitly how this happens in examples, deploying the non-perturbative techniques of, e.g., [325, 323, 327, 326].

Finally, it is also worthwhile to ask to what extent our criterion sheds light on partial deconfinement. The partial deconfinement proposal [222, 51, 223] argues for an intermediate coexistence phase in the Hagedorn transition. Passing to the micro-canonical ensemble at energies $1 \ll E \ll N^2$, the first order deconfinement transition in the gauge theory is smoothed into a phase in which only a $U(N_{\text{eff}}) \subset U(N)$ is deconfined, with $N_{\text{eff}}^2 \propto E$. On the bulk side, this supposes the identification of the small black hole phase with the long string phase [51]. A direct application of our formula would give a type III_1 von Neumann algebra also in this intermediate region, in agreement with the proposed picture. A mathematically rigorous treatment of the partially deconfined phase is a problem that we leave for future work.

5.11 Appendix: General construction of von Neumann algebras for factorizing systems

In this slightly more formal appendix, we introduce a general procedure that allows to construct von Neumann algebras associated to factorizing systems. This procedure heavily relies on the rigorous mathematical results of [137]. We comment on how this construction can be generically applied to study large N algebras in AdS/CFT.

Bosonic case: Canonical commutation relations

In order to study bosonic factorizing systems in terms of operator algebras, the right object to introduce is a *representation of the canonical commutation relations* (CCR).

Definition 5.11.1. Let Y be a real vector space and ω be an antisymmetric form on

Y. Let $\mathcal{H}$ be a Hilbert space. A map $y \mapsto W(y)$ is said to be a representation of the CCR over Y in $\mathcal{H}$ if for $y_1, y_2 \in Y$, it satisfies the relation

$$W(y_1)W(y_2) = e^{-\frac{i}{2}\omega(y_1, y_2)}W(y_1 + y_2).$$ (5.307)

In this chapter, we are interested in states that factorize in the large N limit. These states are known as *quasi-free states* in the operator-algebraic language. We now define this notion.

Definition 5.11.2. Let $y \mapsto W(y)$ be a representation of the CCR on a Hilbert space $\mathcal{H}$. A vector $|\Psi\rangle \in \mathcal{H}$ is said to be quasi-free if it is cyclic, and there exists a quadratic form η in $\mathcal{H}$ such that for all y,

$$\langle\Psi| W(y) |\Psi\rangle = e^{-\frac{1}{4}\eta(y,y)}.$$ (5.308)

As the form η is quadratic, the fields can be treated as Gaussian, which implies that the correlation functions satisfy Wick's theorem.

An alternative definition of quasi-free states can be formulated thanks to the factorization property of correlation functions. More precisely, we have the following result.

Proposition 5.11.3 ([137]). *Let $|\Psi\rangle$ be a vector in a strongly continuous representation of the CCR $W(y) = e^{i\phi(y)}$. $|\Psi\rangle$ is quasi-free if and only if for all $y_1, \dots y_n$, $|\Psi\rangle \in \mathrm{Dom}(\phi(y_1) \dots \phi(y_n))$, and*

$$\langle\Psi| \phi(y_1) \dots \phi(y_{2m-1}) |\Psi\rangle = 0,$$ (5.309)

$$\langle\Psi| \phi(y_1) \dots \phi(y_{2m}) |\Psi\rangle = \sum_{\varpi \text{Wick pairing}} \prod_{j=1}^{m} \langle\Psi| \phi(y_{\varpi(2j-1)})\phi(y_{\varpi(2j)}) |\Psi\rangle.$$ (5.310)

The theory of quasi-free states of the CCR is well-studied, and there is a generic procedure that allows for the construction of most quasi-free representations. It is formalized by the notion of Araki–Woods representation, which we now introduce.

Let Z be a Hilbert space, and let Γ be the bosonic Fock space over $Z \oplus \bar{Z}$. We equip the space $\mathrm{Re}(Z \oplus \bar{Z} \oplus \overline{(Z \oplus \bar{Z})})$ with the symplectic form

$$\omega((x, \bar{x}), (y, \bar{y})) := 2\mathrm{Im}(x, y).$$ (5.311)

Then, there is a canonical representation of the CCR given by

$$W(z_1, \bar{z}_2) := e^{i\phi(z_1, \bar{z}_2)}, \tag{5.312}$$

where

$$\phi(z_1, \bar{z}_2) = \frac{1}{\sqrt{2}}(a^\dagger(z_1, \bar{z}_2) + a(z_1, \bar{z}_2)), \tag{5.313}$$

a and $a^\dagger$ being the usual raising and lowering operators.

The Araki–Woods representations [25] of the CCR are parameterized by an operator ρ, defined by

$$\rho := \gamma(1 - \gamma)^{-1}, \tag{5.314}$$

where γ is a self-adjoint operator satisfying $0 \leq \gamma \leq 1$. Then, for $z \in \mathrm{Dom}(\rho^{\frac{1}{2}})$, we can define two unitary operators $W_{\gamma,l}$ and $W_{\gamma,r}$ on Γ by

$$W_{\gamma,l}(z) := W((\rho + 1)^{\frac{1}{2}}z, \bar{\rho}^{\frac{1}{2}}\bar{z}),$$
$$W_{\gamma,r}(\bar{z}) := W(\rho^{\frac{1}{2}}z, (\bar{\rho} + 1)^{\frac{1}{2}}\bar{z}). \tag{5.315}$$

The von Neumann algebras generated by the $W_{\gamma,l}(z)$ (resp. $W_{\gamma,r}(\bar{z})$) are called the left (resp. right) Araki–Woods algebras associated to the operator ρ. Note, in particular, that one can recover the operator ρ entirely from the two-point functions of fields and creation and annihilation operators, for example we have the identity

$$(z_2, \rho z_1) = \langle\Omega| a^\dagger_{\gamma,l}(z_1)a_{\gamma,l}(z_2) |\Omega\rangle, \tag{5.316}$$

where the creation and annihilation operators $a^\dagger_{\gamma,l}$ and $a_{\gamma,l}$ are defined by

$$a^\dagger_{\gamma,l}(z) := a^\dagger((\rho + 1)^{\frac{1}{2}}z, 0) + a(0, \bar{\rho}^{\frac{1}{2}}\bar{z}),$$
$$a_{\gamma,l}(z) := a((\rho + 1)^{\frac{1}{2}}z, 0) + a^\dagger(0, \bar{\rho}^{\frac{1}{2}}\bar{z}), \tag{5.317}$$

and $|\Omega\rangle$ is the vacuum of the Fock space of the Araki–Woods representation.

The power of Araki–Woods representations comes from the fact that, under mild assumptions, any quasi-free representation of the CCR is isomorphic to an Araki–Woods representation. In particular, the following result, due to Dereziński, holds:

Theorem 5.11.4 ([137]). *Let $y \mapsto W(y)$, $y \in Y_0$, be a quasi-free representation of the CCR in a Hilbert space $\mathscr{H}$, with a cyclic quasi-free vector $|\Psi\rangle$ satisfying $\langle\Psi| W(y) |\Psi\rangle = e^{-\frac{1}{4}\eta(y,y)}$, where η is a nondegenerate inner product. Let Y be the real Hilbert space completion of Y_0 for η, and ω be the bounded extension of the antisymmetric form associated to Y_0 to Y. Assume ω is nondegenerate on Y. Then, W is unitarily equivalent to an Araki–Woods representation of the CCR.*

The interest of knowing that most quasi-free representations of the CCR are isomorphic to Araki–Woods representations is that there exist simple sufficient conditions to determine the type of their bicommutant.

Theorem 5.11.5 ([137]). *Let M be the bicommutant of an Araki–Woods representation of the CCR, and γ the associated operator defined as above. If γ is trace-class, then M has type I. If γ has some continuous spectrum, then M has type III$_1$.*

It is this statement that, applied to our context in Section 5.3, allows us to conclude about the type of the von Neumann algebras on both sides of the Hagedorn phase transitions.

Fermionic case: Canonical anticommutation relations

We can perform an entirely analogous analysis for fermionic oscillators. The starting point is now the algebra of the *canonical anticommutation relations* (CAR).

Definition 5.11.6. Let Y be a real vector space and α be an positive inner product on Y. Let $\mathscr{H}$ be a Hilbert space. A map $y \mapsto \phi(y)$ is said to be a representation of the CAR over Y in $\mathscr{H}$ if its range only contains bounded self-adjoint operators, and for $y_1, y_2 \in Y$, it satisfies the relation

$$\{\phi(y_1), \phi(y_2)\} = 2\alpha(y_1, y_2). \tag{5.318}$$

In the same way as before, we can define the notion of quasi-free state of the CAR.

Definition 5.11.7. Let $y \mapsto W(y)$ be a representation of the CAR on a Hilbert space $\mathscr{H}$. A vector $|\Psi\rangle \in \mathscr{H}$ is said to be quasi-free if it is cyclic, and for all y_i,

$$\langle\Psi| \phi(y_1) \dots \phi(y_{2m-1}) |\Psi\rangle = 0, \tag{5.319}$$

and

$$\langle\Psi| \phi(y_1) \dots \phi(y_{2m}) |\Psi\rangle = (-1)^{\frac{m(m-1)}{2}} \sum_{\varpi \text{Wick pairing}} \text{sgn}(\varpi) \prod_{j=1}^{m} \langle\Psi| \phi(y_{\varpi(j)})\phi(y_{\varpi(j+m)}) |\Psi\rangle .$$
$$\tag{5.320}$$

Now, closely following the bosonic case, we introduce a generic procedure to construct a large class of quasi-free representations of the CAR and classify them. These representations are called Araki–Wyss representations [27].

Let Z be a Hilbert space, and let Γ be the fermionic Fock space on $Z \oplus \bar{Z}$. We see the space $\mathrm{Re}(Z \oplus \bar{Z} \oplus (\overline{Z \oplus \bar{Z}}))$ as a real Hilbert space. Then, there is a canonical representation of the CAR given by

$$\phi(z_1, \bar{z}_2) = \frac{1}{\sqrt{2}}(a^\dagger(z_1, \bar{z}_2) + a(z_1, \bar{z}_2)), \tag{5.321}$$

a and $a^\dagger$ being the usual fermionic raising and lowering operators.

Similarly to the Araki–Woods representations of the CCR, the Araki–Wyss representations of the CAR are parameterized by an operator ρ, defined by

$$\rho := \gamma(1 - \gamma)^{-1}, \tag{5.322}$$

where γ is a self-adjoint operator satisfying $0 \le \gamma \le 1$. Then, for $z \in \mathrm{Dom}(\rho^{\frac{1}{2}})$, we can define the fields $\phi_{\gamma,l}$ and $\phi_{\gamma,r}$ on Γ by

$$\begin{aligned}
\phi_{\gamma,l}(z) &:= \phi((1-\rho)^{\frac{1}{2}} z, \bar{\rho}^{\frac{1}{2}} \bar{z}), \\
\phi_{\gamma,r}(z) &:= \phi(\rho^{\frac{1}{2}} z, (1-\bar{\rho})^{\frac{1}{2}} \bar{z}).
\end{aligned} \tag{5.323}$$

The von Neumann algebras generated by the $\phi_{\gamma,l}(z)$ (resp. $\phi_{\gamma,r}(z)$) are called the left (resp. right) Araki–Wyss algebras associated to the operator ρ. Note, in particular, that one can recover the operator ρ entirely from the two-point functions of fields and creation and annihilation operators, for example we have the identity

$$(z_2, \rho z_1) = \langle \Omega | \, a^\dagger_{\gamma,l}(z_1) a_{\gamma,l}(z_2) \, | \Omega \rangle, \tag{5.324}$$

where the creation and annihilation operators $a^\dagger_{\gamma,l}$ and $a_{\gamma,l}$ are defined by

$$\begin{aligned}
a^\dagger_{\gamma,l}(z) &:= e^{\frac{i\pi}{2}N(N-1)} \left[a^\dagger(0, (1-\bar{\rho})^{\frac{1}{2}}\bar{z}) + a(\rho^{\frac{1}{2}}z, 0) \right] e^{\frac{i\pi}{2}N(N-1)}, \\
a_{\gamma,l}(z) &:= e^{\frac{i\pi}{2}N(N-1)} \left[a(0, (1-\bar{\rho})^{\frac{1}{2}}\bar{z}) + a^\dagger(\rho^{\frac{1}{2}}z, 0) \right] e^{\frac{i\pi}{2}N(N-1)},
\end{aligned} \tag{5.325}$$

where N is the number operator. Also in the fermionic case, any reasonable quasi-free representation of the CAR is isomorphic to an Araki–Wyss representation.

Theorem 5.11.8 ([137]). *Let $y \in Z_0 \mapsto \phi(y)$ be a quasi-free representation of the CAR on a Hilbert space $\mathcal{H}$, with a cyclic quasi-free vector $|\Psi\rangle$. Let ω be the antisymmetric form defined by*

$$\omega(y_1, y_2) := \frac{1}{i} \langle \Psi | \, [\phi(y_1), \phi(y_2)] \, | \Psi \rangle, \tag{5.326}$$

and suppose that the kernel of ω is even or infinite-dimensional. Then, W is unitarily equivalent to an Araki–Wyss representation of the CAR.

Sufficient results are also available to determine the type of the bicommutant of an Araki–Wyss representation of the CAR.

Theorem 5.11.9 ([137])**.** *Let M be the bicommutant of an Araki–Wyss representation of the CAR, and γ the associated defined as above. If γ is trace-class, then M has type I. If γ has some continuous spectrum, then M has type III$_1$.*

5.12 Appendix: Exotic example: Effective $\mathcal{N} = 4$ super-Yang–Mills

The model discussed in this appendix is an effective description of four-dimensional $\mathcal{N} = 4$ super-Yang–Mills theory [427, 5]. We exploit a result of [150] to cast this example in the formalism of discrete matrix models, akin to Subsection 5.4. $\mathcal{N} = 4$ super-Yang–Mills does not possess an integer L, analogous to the number of flavors, to sum over. However, a certain summation is built-in in the formulation of [150]. This model will therefore be somewhat exotic, not fully of the type introduced in Section 5.5, but it is nonetheless instructive to explore this example. We thus mostly reviews old results and rephrases them in our overarching framework.

We stress that we content ourselves with discussion on the toy quantum mechanics, and *do not* claim implications for the spectral density of full-fledged $\mathcal{N} = 4$ super-Yang–Mills.

Consider four-dimensional $SU(N+1)$ $\mathcal{N} = 4$ super-Yang–Mills theory placed on the compact Euclidean space $\mathbb{S}^3 \times \mathbb{S}^1_{\beta_{\mathrm{SYM}}}$, with radius of the thermal circle the inverse temperature β_{SYM}. Deep in the weak 't Hooft coupling regime, the partition function reduces to [427, 5]

$$\mathcal{Z}_{\mathcal{N}=4}(a) = \oint_{SU(N+1)} \mathrm{d}U \ \exp\left\{ \frac{a}{2} \operatorname{tr}(U) \operatorname{tr}\left(U^{-1}\right) \right\}, \tag{5.327}$$

with $a = a(\beta_{\mathrm{SYM}})$ a function of the inverse temperature. Here we have discarded contributions that become irrelevant near the transition point, see Appendix 5.13 for more details. This matrix model undergoes a first order phase transition at $a = 2$ [302], reviewed in Appendix 5.13.

An alternative derivation of the first order phase transition in (5.327) was given in [150]. The authors of [150] started by uncovering the equivalent description of (5.327) in a free fermion formalism. This latter approach rewrites (5.327) as a discrete matrix ensemble, of the type we have considered in Subsection 5.4.

Lemma 5.12.1 ([150]). *For every $a > 0$, let $\mathcal{Z}_{N=4}(a)$ be as in (5.327). Besides, let $\mathfrak{S}_L$ denote the symmetric group of L elements and $d_R(\mathfrak{S}_L)$ denote the dimension of the representation R of $\mathfrak{S}_L$. It holds that*

$$\mathcal{Z}_{N=4}(a) = \sum_{L=0}^{\infty} \frac{a^L}{2^L L!} \sum_{\substack{R \,:\, |R|=L \\ \ell(R) \leq N}} d_R(\mathfrak{S}_L)^2. \qquad (5.328)$$

The inner sum runs over irreducible representations R of $\mathfrak{S}_L$, which are in one-to-one correspondence with Young diagrams of L boxes, restricted to have length at most N.

Proof. The derivation of this identity is in [150, Sec.3], to which we refer for the details. The proof is conceptually very similar to the character expansion of the other examples, although slightly more involved. It is based on the character expansion of the integrand in (5.327), and applying the orthogonality of characters to remove $\oint_{SU(N+1)}$. $\qquad\square$

The inner sum in (5.328) can be rephrased as running over irreducible representations R of $SU(N + 1)$, which are in one-to-one correspondence with Young diagrams of length at most N. Namely

$$R = (R_1, R_2, \ldots, R_N) \qquad \text{with} \quad R_1 \geq R_2 \geq \cdots \geq R_N \geq 0. \qquad (5.329)$$

Importantly, the sum is restricted to diagrams consisting of $|R| = \sum_{i=1}^{N} R_i = L$ boxes.

The quantity $d_R(\mathfrak{S}_L)$ stands for the dimension of R as a representation of $\mathfrak{S}_L$. It differs from the dimension of R viewed as a $SU(N + 1)$ representation, customarily denoted by $\dim R$:

$$R \,:\, |R| = L \text{ and } \ell(R) \leq N \quad \Longrightarrow \quad R \in \{\, SU(N + 1) \text{ reps}\,\} \cap \{\,\mathfrak{S}_L \text{ reps}\,\}$$

$$\underbrace{\dim R}_{R \text{ is } SU(N+1) \text{ rep}} \neq \underbrace{d_R(\mathfrak{S}_L)}_{R \text{ is } \mathfrak{S}_L \text{ rep}}. \qquad (5.330)$$

Finally, the outer sum in (5.328) runs over all the sizes of the symmetric group.

With the customary change of variables (5.60), and using the Frobenius–Weyl formula for $d_R(\mathfrak{S}_L)$ [312], (5.328) becomes

$$\mathcal{Z}_{N=4}(a) = \sum_{L=0}^{\infty} \left(\frac{a}{2}\right)^L \sum_{h_1>\cdots>h_N\geq 0} \frac{L!}{\prod_{j=1}^{N}(h_j!)^2} \prod_{1\leq i<j\leq N}(h_i - h_j)^2 \delta\left(|\vec{h}| - L - \frac{N(N-1)}{2}\right),$$

$$(5.331)$$
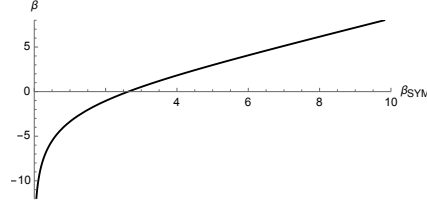
Figure 5.23: The inverse temperature β of the toy model quantum mechanics is a function of the inverse temperature β_{SYM} of $\mathcal{N} = 4$ super-Yang–Mills.

where we are using a shorthand notation $|\vec{h}| := \sum_{j=1}^{L} h_j$.

It is also possible to remove the ordering of the eigenvalues h_j and sum over unordered N-tuples $\vec{h} \in \mathbb{N}^N$, cancelling the $L!$ in the summand.

To complete the analogy with the formalism of Sections 5.4-5.5, we may write

$$a = 2 \exp(-\beta), \qquad (5.332)$$

where β is the inverse temperature of the microscopic system. This *should not* be confused with the inverse temperature β_{SYM} of $\mathcal{N} = 4$ super-Yang–Mills. $\beta = -\ln \frac{a(\beta_{\text{SYM}})}{2}$ is a monotonically increasing function of $\beta_{\text{SYM}} > 0$, as shown in Figure 5.23.

The dependence on a is then interpreted as the Boltzmann factor of the quantum system:

$$\left(\frac{a}{2}\right)^L = e^{-L\beta} = e^{-\beta\left(|\vec{h}| - \frac{N(N-1)}{2}\right)}. \qquad (5.333)$$

The partition function in this formalism reads

$$\mathcal{Z}_{\mathcal{N}=4}(2e^{-\beta}) = e^{\frac{\beta}{2}N(N-1)} \sum_{L=0}^{\infty} \sum_{h_1 > \cdots > h_N \geq 0} e^{-\beta|\vec{h}|} \frac{L!}{\prod_{j=1}^{N}(h_j!)^2} \prod_{1 \leq i < j \leq N} (h_i - h_j)^2 \qquad (5.334)$$

$$\times \delta\left(|\vec{h}| - L - \frac{N(N-1)}{2}\right).$$

We emphasize that the discrete matrix model (5.334) is closely related to but falls outside of the framework of Section 5.5.

- The identification (5.332) is really $a/2 = y$, with y a fugacity for the conserved charge H in the simplified quantum system. Let us mention that (5.331) is derived for $a > 0$, and in particular it is continuous. The resulting system is

thus defined for arbitrary real inverse temperature $\beta \in \mathbb{R}$, as a consequence of the constraint on the total energy.

- Here the roles of N and L are partly exchanged: L constrains the allowed configurations $\vec{h}$, and the total number of eigenvalues is N. Moreover, the constraint $|\vec{h}| - \frac{N(N-1)}{2} = L$ does not directly bound the allowed states, but rather fixes the total energy of the quantum mechanical system. Schematically:

	SECTION 5.4	APPENDIX 5.12
N	constraint on configurations	# of eigenvalues
L	# of eigenvalues	constraint on configurations
fixed-L	quantum system	microcanonical ensemble
weight	$\mathfrak{q}^{L^2}$	$1/L!$

Proposition 5.12.2 ([150]). *For every $a > 0$, let $\mathcal{Z}_{N=4}(a)$ be as in (5.334). In the large N limit, it undergoes a first order phase transition at $a = 2$, with*

$$\ln \mathcal{Z}_{N=4}(a) = \begin{cases} O(1) & a < 2 \\ O(N^2) & a > 2. \end{cases} \tag{5.335}$$

Proof. We only review here the salient features of [150, Sec.4] and reformulate some steps in uniformity with the rest of the work. One begins by rewriting the summand in (5.331) in the form $e^{-S(\vec{h};L)}$, where

$$S(\vec{h}; L) = 2 \sum_{i=1}^{N} \ln(h_i!) - \sum_{i \neq j} \ln |h_i - h_j| - L \ln \left(\frac{a}{2}\right) - \ln(L!). \tag{5.336}$$

In the large N limit, it is convenient to interpret the δ function as constraining the value of L, for any given configuration $(h_1, \ldots, h_N)$. Defining

$$\ell := \frac{L}{N^2}, \tag{5.337}$$

we have the constraint

$$\ell = \frac{1}{N^2} \sum_{i=1}^{N} h_i + \frac{N-1}{2N}. \tag{5.338}$$

One advantage of this approach is that, now, the configurations $\vec{h}$ are unconstrained, and hence the numbers h_j grow linearly in N.

We can in fact fix the precise scaling with N by requiring the existence of an equilibrium solution at large N. Define the scaled variables x_i through

$$h_i = N^\eta x_i, \tag{5.339}$$

for some $\eta > 0$ and x_i being $O(1)$ at large N. Introduce the eigenvalue density

$$\varrho(x) = \frac{1}{N} \sum_{i=1}^{N} \delta(x - x_i). \tag{5.340}$$

We must look for $\varrho(x)$ satisfying

$$\int \mathrm{d}x \varrho(x) = 1 \qquad \varrho(x) \le 1 \qquad \mathrm{supp}\, \varrho \subset [0, \infty). \tag{5.341}$$

At large N, we arrive at

$$\frac{S}{N^2} = 2N^{\eta-1} \int x \ln(x)\varrho(x)\mathrm{d}x - \int \varrho(x)\mathrm{d}x\, \mathrm{P}\!\!\int \mathrm{d}y \varrho(y) \ln|x-y| - \ell \ln\left(\frac{a}{2}\right) - \ell \ln(\ell) + \cdots \tag{5.342}$$

where $\mathrm{P}\!\!\int$ stands for the principal value integral and the dots include constant terms as well as terms that are sub-leading in N. We do not need them. We see that, in order to obtain a non-trivial equilibrium configuration, we must have $\eta = 1$, so that positive and negative contributions to S are of the same order in N and compete.

From here, we must find $\varrho_*(x)$, subject to (5.341), that extremizes S. The saddle point equation (i.e., equilibrium equation) reads

$$2\mathrm{P}\!\!\int \mathrm{d}y \frac{\varrho_*(y)}{x - y} = 2 \ln(x) - \ln\left(\frac{a}{2}\ell\right), \tag{5.343}$$

and the equality (5.338) fixing ℓ is

$$\ell = \int y\varrho_*(y)\mathrm{d}y - \frac{1}{2}. \tag{5.344}$$

The solution was found in [150] and reads

$$\varrho_*(x) = \frac{2}{\pi} \arccos\left(\frac{x + \xi - \frac{1}{2}}{2\sqrt{x\xi}}\right), \tag{5.345}$$

$$\mathrm{supp}\, \varrho_* = [x_-, x_+], \qquad\qquad x_\pm := \sqrt{\xi} \pm \frac{1}{\sqrt{2}}.$$

The parameter ξ is a function of a defined through

$$\xi^2 = \frac{a}{2}\ell. \tag{5.346}$$

Because ℓ depends on ϱ, and hence on ξ and a, this condition only fixes ξ implicitly.

The solution (5.345) ceases to satisfy $\varrho(x) \leq 1$ $\forall x$ at $\xi = \frac{1}{2}$. At this value, the left edge x_- hits the hard wall at $x = 0$. We then ought to look for a different solution. It was found in [150] that the solution in this case reduces to the uniform density on the interval $[0, 1]$, leading to a trivial saddle point configuration. Translated in the Young diagram language, the large N limit in this phase is dominated by the trivial representation $R = \emptyset$, and $\ln \mathcal{Z}_{\mathcal{N}=4}$ remains $O(1)$. $\qquad\qquad\qquad\qquad\square$

Double scaling of the effective $\mathcal{N} = 4$ super-Yang–Mills

A double scaling regime for the matrix model effective description of $\mathcal{N} = 4$ super-Yang–Mills on $\mathbb{S}^3 \times \mathbb{S}^1_{\beta_{\mathrm{SYM}}}$ was envisioned by Liu [302]. It consists in

$$N \to \infty, \qquad a \to 2, \qquad N^{\frac{4}{3}}\left(\frac{a}{2} - 1\right) \text{ fixed.} \qquad (5.347)$$

For the sake of completeness, we sketch here how to derive it from the discrete ensemble. Consider the high temperature phase $a > 2$. ϱ is supported on

$$x_- \leq x \leq x_+ \qquad x_\pm := \sqrt{\xi} \pm \frac{1}{\sqrt{2}} \qquad (5.348)$$

with the parameter ξ given in (5.345). We know from above that the critical regime corresponds to $a \to 2$ and $\xi \to \frac{1}{2}$. We thus define the double scaling parameters a_s and ξ_s according to

$$\frac{a}{2} - 1 = \frac{a_s}{N^{4/3}}, \qquad\qquad \xi - \frac{1}{2} = \frac{\xi_s}{N^\nu}, \qquad (5.349)$$

where the exponent of N in a was determined in (5.347), while the exponent ν will be fixed momentarily by consistency. Recall that ξ is an implicit function of a. Here we will invert the relation and dial ξ_s to go into the double scaling regime, with a_s implicitly fixed by the inverse function theorem (applied locally near $a_s \approx 0$) as a function of ξ_s.

The edges of the eigenvalue distribution become

$$x_- \approx \frac{\xi_s}{\sqrt{2}N^\nu}, \qquad x_+ \approx \sqrt{2}. \qquad (5.350)$$

In order to explore the critical regime, we zoom in close to the left edge. Stated more formally, we introduce the doubly scaled variable x_s as

$$x - x_- = \frac{x_s}{N^{\nu_2}}, \qquad (5.351)$$

for some power v_2 uniquely fixed by v. With all these substitutions into the eigen-value density (5.345), we determine the scaling exponents $2v_2 = v = \frac{2}{3}$. Using this into the condition $\xi^2 = \ell\frac{a}{2}$ and approximating $\ell = \frac{1}{4} + \frac{\ell_s}{N^{v_3}}$ we find

$$\xi_s = \sqrt{a_s} = \ell_s \tag{5.352}$$

and $v_3 = v$. Altogether we introduce the doubly scaled eigenvalue density

$$\varrho_s(x_s) := \varrho_* \left(\sqrt{\frac{a_s}{2}} N^{-2/3} + x_s N^{-1/3} \right) \approx \frac{2}{\pi} \arccos \left[\left(\frac{\xi_s}{2} \right)^{-1/4} x_s \right]$$

$$\operatorname{supp} \varrho_s = \left[\frac{a_s}{2} N^{-1/3}, \sqrt{2} N^{1/3} \right]. \tag{5.353}$$

$\operatorname{supp} \varrho_*$ tends to the positive real axis in the double scaling limit.

The double scaling limit (5.347) has been translated in the discrete matrix model to a limit probing the left edge of the distribution, where the first order transition is taking place. This is not a genuinely new result, but a consequence of mapping the result in [302] to the language of [150]. Here we have limited ourselves to perform the computation explicitly.

5.13 Appendix: Hagedorn transitions in holographic matrix models

From third to first order phase transitions in unitary matrix models

We consider a generic unitary one-matrix model, with integration domain $U(N)$:

$$\mathcal{Z}_{\mathrm{UMM}}(\sigma, \vec{g}) = \oint_{U(N)} [dU] \exp \left\{ \sigma \sum_{n=1}^{\infty} \frac{g_n}{n} \operatorname{Tr} (U^n + U^{-n}) \right\} \tag{5.354}$$

where $[dU]$ is the Haar measure and $\vec{g} = (g_n)_{n \geq 1}$ is an arbitrary collection of interaction coefficients, which satisfy the conditions [433]

$$\sum_{n=1}^{\infty} \frac{g_n}{n} < \infty, \qquad \sum_{n=1}^{\infty} \frac{g_n^2}{n} < \infty. \tag{5.355}$$

- For later convenience, we have factored out an overall coefficient $\sigma \in \mathbb{R}$. Several cases of interest in fact possess a $\mathbb{Z}_2$ symmetry $\sigma \mapsto -\sigma$, which reduces the parameter space to $\sigma \geq 0$.

- Besides, we have restricted our attention to systems that are symmetric under the involution $\mathsf{C} : U \mapsto U^{-1}$, which corresponds to charge conjugation in a $U(N)$ QFT. This assumption may be dropped, and the coefficients of $\operatorname{Tr} U^{-n}$ could be generically different from those of $\operatorname{Tr} U^n$. This generalization does

not add to the central theme of this work, thus we consider models with C-symmetry for clarity.

- We have moreover considered integration over $U(N)$, instead of $SU(N+1)$ considered in the main text. This change is to lighten the expressions and, as we are only interested in $N \to \infty$, the difference is negligible.

The unitary matrix model (5.354) belongs to the family (5.24) investigated in the main text. The exponential in the integrand is a class function, thus it admits an expansion in characters of $U(N)$. This establishes the relation with the quantum mechanics discussed in Section 5.4.

Diagonalizing the unitary matrix $U \in U(N)$, (5.354) becomes an integral over eigenvalues:

$$\mathcal{Z}_{\text{UMM}}(\sigma, \vec{g}) = \frac{1}{N!} \int_{[-\pi,\pi]^N} \prod_{1 \le a < b \le N} \left(2 \sin \left(\frac{\theta_a - \theta_b}{2} \right) \right)^2 \prod_{a=1}^{N} e^{2\sigma \sum_{n=1}^{\infty} \frac{g_n}{n} \cos(n\theta_a)} \frac{\mathrm{d}\theta_a}{2\pi}.$$
(5.356)

In the *planar* large N limit, i.e., with 't Hooft scaling

$$\sigma = N\gamma, \qquad \gamma \text{ fixed,} \tag{5.357}$$

the model (5.354) has an intricate phase structure as a function of the parameters $\gamma, \vec{g}$. This is more directly visible in the form (5.356). Typically, these phase transitions are third order. We refer to the pertinent literature, see, e.g., [396] for a review and [211, 448, 449, 266, 322, 259, 106, 407, 399, 411] for a partial list of works that address phase transitions fitting in our paradigm.

The next lemma is an extension of Szegő's theorem to the planar limit.

Lemma 5.13.1 ([433, 407]). *Let $\mathcal{Z}_{\text{UMM}}$ be as in (5.356) and*

$$\mathcal{F}_{\text{UMM}}(\gamma, \vec{g}) := \lim_{N \to \infty} \frac{1}{N^2} \ln \mathcal{Z}_{\text{UMM}}(N\gamma, \vec{g}). \tag{5.358}$$

Assume that $\{g_n\}_{n \ge 1}$ satisfy

$$\sum_{n=1}^{\infty} g_{n+1} z^n = \frac{P_{\vec{g}}(z)}{Q_{\vec{g}}(z)} \tag{5.359}$$

for some polynomials $P_{\vec{g}}, Q_{\vec{g}}$. Then, there exists $r = r(\vec{g}) > 0$ such that

$$\mathcal{F}_{\text{UMM}}(\gamma, \vec{g}) = \gamma^2 \sum_{n=1}^{\infty} \frac{1}{n} g_n^2, \qquad \forall 0 \le |\gamma| < r(\vec{g}). \tag{5.360}$$

Proof. This lemma asserts that, for γ small enough, (5.354) always admits a phase in which $\mathcal{F}_{\mathrm{UMM}}$ is quadratic in γ. This was proven by direct computation in [407], but can also be argued for by analytic continuation of Szegő's theorem [433].

The condition (5.359) guarantees that the functions appearing in the saddle point equation have at most poles. If z_p is a double zero of $Q_{\vec{g}}(z)$, it can be regularized by splitting it into simple poles at $z_p \pm i\varepsilon$, sending $\varepsilon \to 0$ at the end. We can thus assume without loss of generality that at most simple poles appear in the saddle point equation, possibly with the prescribed regularization. $\qquad\square$

In the notation of Lemma 5.13.1, $r(\vec{g})$ is the smallest value in the set of critical points. Assume that (5.354) has a phase transition at a critical curve

$$\gamma = \gamma_c(\vec{g}). \tag{5.361}$$

For concreteness, we assume the transition is third order, as is typical for unitary matrix models, but the argument works also for second order transitions.

Inspired by [302], we argue for a way to promote such third order transition to a first order one, which moreover shows Hagedorn behavior. We enforce an average over the coupling σ, with Gaussian weight of standard deviation $a > 0$. The model we consider is:

$$\mathcal{Z}_{\mathrm{holo}}(a, \vec{g}) = \int_0^\infty \mathrm{d}\sigma e^{-\frac{\sigma^2}{2a}} \, \mathcal{Z}_{\mathrm{UMM}}(\sigma, \vec{g}) \tag{5.362}$$

$$= N \int_0^\infty \mathrm{d}\gamma \, \exp\left\{-N^2\left[\frac{\gamma^2}{2a} - \mathcal{F}_{\mathrm{UMM}}(\gamma, \vec{g})\right]\right\}. \tag{5.363}$$

If (5.354) is not invariant under $\sigma \mapsto -\sigma$, the integration range is from $-\infty$ to ∞. The holographic interpretation of unitary matrix models with average over the couplings was advocated in [352], although it was implemented in a different way.

In passing, let us notice that we can refine the additional integration in (5.362) into

$$\mathcal{Z}_{\mathrm{holo}}(a, \vec{g}) = \int_0^\infty \mathrm{d}\sigma \, f(\sigma) \, e^{-\frac{\sigma^2}{2a}} \, \mathcal{Z}_{\mathrm{UMM}}(\sigma, \vec{g}) \tag{5.364}$$

for an arbitrary function $f(\sigma)$ such that

$$\lim_{N\to\infty} \frac{1}{N^2} \ln f(N\gamma) = 0. \tag{5.365}$$

This condition ensures that the refinement will not affect the phase structure of the model, and hence does not alter the ensuing discussion.

The integrand in (5.363) at large N is dominated by the saddle points in the variable γ. Consider first the region $\gamma < \gamma_c$, so that the integrand is Gaussian:

$$\exp\left\{-N^2\gamma^2\left[\frac{1}{2a} - \sum_{n=1}^{\infty}\frac{1}{n}g_n^2\right]\right\}. \tag{5.366}$$

Its maximum is located at $\gamma = 0$ if

$$a < a_c, \qquad\qquad a_c := \frac{1}{2}\left(\sum_{n=1}^{\infty}\frac{g_n^2}{n}\right)^{-1}. \tag{5.367}$$

In this case, the overall growth of (5.363) with N is cancelled, and we ought to seek an $O(1)$ solution.

However, when a is larger than the threshold a_c, the integrand (5.366) becomes exponentially large for large values of γ. We thus need to look for a new saddle point, for strictly positive γ. In the region $\gamma > \gamma_c$, the saddle point equation reads

$$\frac{\gamma}{a} = \frac{\partial}{\partial\gamma}\mathcal{F}_{\text{UMM}}(\gamma, \vec{g}). \tag{5.368}$$

If there exists a value $\gamma_* > \gamma_c$ (with $\gamma_* = \gamma_*(a, \vec{g})$ given in terms of the external parameters) that solves the equilibrium condition (5.368), then

$$\ln \mathcal{Z}_{\text{holo}}(a, \vec{g}) \approx N^2\left[\mathcal{F}_{\text{UMM}}(\gamma_*, \vec{g}) - \frac{\gamma_*^2}{2a}\right]. \tag{5.369}$$

For consistency, one should check that

$$\gamma_*(a, \vec{g}) > \gamma_c(\vec{g}). \tag{5.370}$$

This inequality is understood as defining a region in the $a > 0$ parameter space, because γ_* depends (in general) explicitly on a and $\vec{g}$, and γ_c only depends on $\vec{g}$. Let us assume the inequality is of the form $a \geq a_\star$ for some function $a_\star(\vec{g})$. Depending on the values of a_c and $a_\star$, three scenarios disclose.

(i) $a_\star < a_c$. The two phases coexists for $a_\star < a < a_c$ and a first order phase transition takes place when the dominance of the saddles is exchanged. We think of this phase transition as a function of the control parameter a at fixed couplings $\vec{g}$.

(ii) $a_\star = a_c$. There is no coexistence of phases, and a first order transition takes place at $a = a_c(= a_\star)$. This situation is sometimes referred to as a *weakly* first order transition.

(iii) $a_\star > a_c$. There is a region $a_c < a < a_\star$ which admits no saddle point. One should look for the local maxima (5.363) and check how the behavior in this intermediate region matches at the junction points $a = a_c$ and $a = a_\star$. Typically, the solution to $\ln \mathcal{Z}_{\text{holo}}$ in the intermediate region is $O(N^2)$, thus yielding a first order transition at $a = a_c$. There may or may not be an additional (second or higher order) phase transition at $a = a_\star$. The details should be checked on a case-by-case basis.

The dependence may in principle be more general than $a \geq a_\star$, for instance, restricting a to a union of intervals. The upshot of the forthcoming analysis is unchanged, although the phase structure would be more involved.

Hagedorn phase transition

In all the scenarios discussed above, the modification of the one-matrix model (5.354) into (5.362) led to a first order phase transition, in which the free energy jumps as

$$\ln \mathcal{Z}_{\text{holo}} = \begin{cases} O(1) & a < a_H \\ O(N^2) & a > a_H. \end{cases} \tag{5.371}$$

Here we are generically denoting a_H the value of a at which the transition takes place. It will be a function of the coupling $\vec{g}$ that characterize the model, and oftentimes it is $a_H = a_c$ as defined in (5.367).

Other gauge groups

While we focus on $U(N)$ matrix models, our analysis extends straightforwardly to $SO(N)$ and $Sp(N)$ gauge groups, due to the universality of the large N limit. The extension of Szegő's theorem to these groups was given by Johansson [262], from which a version of Lemma 5.13.1 is directly worked out. Our algorithm goes through unchanged, except for numerical coefficients in $\ln \mathcal{Z}_{\text{holo}}$. The result (5.371) holds. See, e.g., [380, App.S2] for explicit calculations of the large N limit of $\mathcal{Z}_{\text{UMM}}$ with gauge group $SO(N)$ or $Sp(N)$.

Polyakov loop expectation value

We have claimed in (5.126) that the expectation value of the Polyakov loop is an order parameter detecting the first order transition. We now prove the claim.

The starting point is that, in the fixed-L matrix model (5.42), the Polyakov loop corresponds to insert $\frac{1}{N}\mathrm{Tr}U$ in the matrix ensemble $\mathcal{Z}_L^{(N)}$. Our derivation based on the unitary matrix model is an extension of [5, 302].

Theorem 5.13.2. *Let $\mathcal{P}$ denote the expectation value of a Polyakov loop in the matrix model* (5.109). *Assume the matrix model has the Hagedorn transition described above. Then*

$$\begin{cases} \mathcal{P} = 0 & \text{if } \beta^{-1} < T_H, \\ \mathcal{P} \neq 0 & \text{if } \beta^{-1} > T_H, \end{cases} \tag{5.372}$$

signalling a first order phase transition at T_H.

Proof. Let $U \in SU(N+1)$ and $e^{i\theta_a}$ be its eigenvalues. Denote by $\mathrm{d}\sigma_*(\theta)$ the saddle point measure, normalized to 1. That is, $\mathrm{d}\sigma_*(\theta)$ is the equilibrium measure of the matrix model $\mathcal{Z}_L^{(N)}$ (that depends on the Veneziano parameter γ) evaluated at the saddle point γ_*. The expectation value of the Polyakov loop is

$$\mathcal{P} = \langle \frac{1}{N}\mathrm{Tr}U \rangle, \tag{5.373}$$

with $\langle \cdot \rangle$ meaning expectation value in the matrix model. A standard large N computation shows that

$$\mathcal{P} = \int_{-\pi}^{\pi} e^{i\theta} \mathrm{d}\sigma_*(\theta). \tag{5.374}$$

It automatically vanishes if the equilibrium measure is uniform on the circle, $\mathrm{d}\sigma_*(\theta) = \frac{\mathrm{d}\theta}{2\pi}$ for all $-\pi < \theta \leq \pi$, which is true in the phase $\beta^{-1} < T_H$.

In the phase $\beta^{-1} > T_H$ the unitary matrix model is, by construction, in a phase in which the eigenvalues $e^{i\theta_a}$ are not spread on the whole circle. The non-triviality of γ_* in the phase $\beta^{-1} > T_H$ guarantees that this remains true after the integration over the Veneziano parameter. More precisely, there exist $\theta_{\pm}$, with $-\pi < \theta_- < \theta_+ < \pi$ such that $\mathrm{d}\sigma_*(\theta) \neq 0$ for $\theta_- < \theta < \theta_+$ and vanishes otherwise. Measures of this type give a non-vanishing expectation value of $\mathrm{Tr}U$, thus $\mathcal{P} \neq 0$.

Before concluding the proof, we ought to comment on a subtlety in our computation. This remark is meant for experts, and is a generalization of a remark in [5].

In a deconfined phase, these models should possess a $\mathbb{Z}_{N+1}$ one-form symmetry from the center of $SU(N+1)$. We thus should obtain a collection of saddle point configurations permuted under the $\mathbb{Z}_{N+1}$ symmetry. We have only accounted for one of them, namely the one with eigenvalues centered around 0. Accounting

for all the saddle configurations, their contributions sum up to zero. Naively, the Polyakov loop would have trivial expectation value at $T > T_H$ as well. However, this is exactly the same technical issue that one would encounter when trying to compute the order parameter in the Ising model, with vanishing external field. It is well-known that one should instead do the computation of the order parameter in an external field of modulus ε, and send $\varepsilon \to 0$ at the end. In this way, one finds two different limiting values, depending on the temperature. The same resolution applies here. We implicitly assume a small perturbation of the action that breaks the $\mathbb{Z}_{N+1}$ symmetry explicitly and favours one saddle (without loss of generality, we select the one centered at 0). It is straightforward to repeat the computation at finite $\varepsilon > 0$ and, turning off the perturbation at the end, we find $\mathcal{P} \neq 0$ if $T > T_H$. □

Example 1: Variations on the IOP model

Recall the unitary matrix model cIOP partition function in (5.142), which we rewrite here:

$$\mathcal{Z}_{\text{cIOP}}^{(N)}(\sigma, y) = \oint_{U(N)} [dU] \left[\det\left(1 - \sqrt{y}U\right) \det\left(1 - \sqrt{y}U^{-1}\right) \right]^{-\sigma}. \qquad (5.375)$$

For consistency with the rest of the appendix, we have replaced the discrete number of flavors $L \in \mathbb{N}$ with a continuous parameter $\sigma > 0$. Likewise, we introduce its averaged version by integrating over σ with Gaussian weight:

$$\mathcal{Z}_{\overline{\text{cIOP}}}(y) = \int_0^\infty d\sigma \, y^{\frac{\sigma^2}{2}} \mathcal{Z}_{\text{cIOP}}^{(N)}(\sigma, y). \qquad (5.376)$$

For simplicity, we work in what we have denoted as Schur slice, in which $1/\beta = -1/\ln(y)$ plays the role of a.

Theorem 5.13.3. *Let $y = e^{-\beta}$. There exists $T_H > 0$ such that, in the large N limit,*

$$\ln \mathcal{Z}_{\overline{\text{cIOP}}} = \begin{cases} O(1) & \frac{1}{\beta} < T_H \\ O(N^2) & \frac{1}{\beta} > T_H. \end{cases} \qquad (5.377)$$

Proof. The proof is done in two steps:

   (*i*) take the large N planar limit of $\mathcal{Z}_{\text{cIOP}}^{(N)}$;

   (*ii*) insert the result in (5.376) and extremize.

The Veneziano limit of the unitary matrix model (5.375) was addressed in [29, 405] (see also [106]). The computation of step (*ii*) is almost identical to the one performed in the next subsection, thus we omit it. Suffice it here to note that (5.375) is related to (5.379) through the map

$$(\sqrt{y}, \sigma) \mapsto (-\sqrt{y}, -\sigma). \tag{5.378}$$

In particular, it also shows a third order phase transition that can be promoted to a first order one by integrating over σ. See Appendix 5.13.

$\square$

Example 2: Matrix model of QCD$_2$

The take-home lesson of this appendix is that, by introducing an extra integration with Gaussian weight, unitary one-matrix models with a third order phase transition are promoted to have a first order one, with Hagedorn behavior near the transition point.

We now exemplify this in the toy model for QCD$_2$ [218] discussed in Section 5.7. In the notation of Appendix 5.13 it reads

$$\mathcal{Z}_{\text{QCD}_2}(\sigma, y) = \oint_{U(N)} [dU] \left[\det \left(1 + \sqrt{y}U \right) \det \left(1 + \sqrt{y}U^{-1} \right) \right]^{\sigma} \tag{5.379}$$

$$= \oint_{U(N)} [dU] \exp \left\{ \sigma \text{Tr} \left[\ln \left(1 + \sqrt{y}U^{-1} \right) + \ln \left(1 + \sqrt{y}U^{-1} \right) \right] \right\}$$

$$= \oint_{U(N)} [dU] \exp \left\{ \sigma \sum_{n=1}^{\infty} \frac{y^{n/2}}{n} \text{Tr} \left(U^n + U^{-n} \right) \right\}. \tag{5.380}$$

From (5.380), the model manifestly belongs to the family (5.354) with $g_n = \sqrt{y}^n$. Here we have relaxed the QCD interpretation, replacing the number of quarks $L \in \mathbb{N}$ with $\sigma > 0$.

Lemma 5.13.4 ([218]). *The quantity*

$$\mathcal{F}_{\text{QCD}_2}(\gamma, y) := \lim_{N \to \infty} \frac{1}{N^2} \ln \mathcal{Z}_{\text{QCD}_2}(N\gamma, y) \tag{5.381}$$

shows a third order phase transition at the critical curve

$$\gamma_c(y) = \frac{1 - \sqrt{y}}{2\sqrt{y}}, \tag{5.382}$$

with

$$\mathcal{F}_{\text{QCD}_2}(\gamma, y) = \begin{cases} -\gamma^2 \ln(1 - y) & \gamma < \frac{1 - \sqrt{y}}{2\sqrt{y}} \\ -(2\gamma + 1) \ln \left(1 + \sqrt{y} \right) + \frac{1}{4} \ln y + C(\gamma) & \gamma > \frac{1 - \sqrt{y}}{2\sqrt{y}}. \end{cases} \tag{5.383}$$

In the second phase, $C(\gamma)$ is the y-independent term

$$C(\gamma) = -\gamma^2 \ln\left(\frac{4\gamma(\gamma+1)}{(2\gamma+1)^2}\right) + \frac{1}{2}\ln(1+2\gamma) + (1+2\gamma)\ln\left(\frac{2(\gamma+1)}{1+2\gamma}\right). \quad (5.384)$$

Proof. See [218] for the original proof, or [405] for a uniform treatment of this case and the model appearing in Appendix 5.13. □

According to the general discussion, we want to integrate over the external field σ, and show that this produces the Hagedorn behavior (5.371). For consistency with the rest of the appendix, here we consider:

$$\mathcal{Z}_{\overline{\text{QCD}_2}}(y) = \int_0^\infty d\sigma\, y^{\frac{\sigma^2}{2}}\, \mathcal{Z}_{\text{QCD}_2}(\sigma, y)$$

$$= \int_0^\infty d\sigma\, y^{\frac{\sigma^2}{2}} \oint_{U(N)} [dU]\, \exp\left\{\sigma\text{Tr}\left[\ln\left(1+\sqrt{y}U^{-1}\right) + \ln\left(1+\sqrt{y}U^{-1}\right)\right]\right\}.$$
$$(5.385)$$

Again we work in the analogue of the Schur slice, in which the Gaussian weight in the measure for σ is $y^{\sigma^2/2}$. We might have taken a different Gaussian weight $e^{-\sigma^2/(2a)}$, but the reader can check that the conclusions are unchanged in the more general case. Besides, in the planar limit, one can check numerically that, in this and the previous example, the difference between summing over L or integrating over σ is sub-leading in N. Hence, $\mathcal{Z}_{\overline{\text{QCD}_2}}$ and $\mathcal{Z}_{\text{Ex2}}$ of Section 5.7 will have the same properties.

Theorem 5.13.5. *Let $\mathcal{Z}_{\overline{\text{QCD}_2}}$ be as in (5.385), with $y = e^{-\beta}$. In the large N limit, it undergoes a first order phase transition at $\frac{1}{\beta} = T_H$, where $T_H \approx 1.039$. Moreover,*

$$\ln \mathcal{Z}_{\overline{\text{QCD}_2}} = \begin{cases} O(1) & \frac{1}{\beta} < T_H \\ O(N^2) & \frac{1}{\beta} > T_H. \end{cases} \quad (5.386)$$

Proof. As in the proof of Theorem 5.7.3 in Subsection 5.7, we divide the computation in two steps. Step (i) consists in maximizing the inner matrix model $\mathcal{Z}_{\text{QCD}_2}$ in the planar large N limit. The solution is in Lemma 5.13.4.

The discussion in step (ii) in the proof of Theorem 5.7.3 goes through identically at this stage. Let us recall the situation we have found in Subsection 5.7:

- There exists a trivial saddle point $\gamma = 0$, valid for $\beta > \beta_c$;

- There exists a nontrivial saddle point $\gamma_* > 0$, valid for $\beta < \beta_c$;

- There is no coexistence phase and the two saddles exchange dominance precisely at $\beta = \beta_c$.

Therefore, this case corresponds to scenario (ii). The direct inspection in the proof of Theorem 5.7.3 can be repeated here and tells us that a phase transition kicks in at $T_H = 1/\beta_c$. Putting everything together, we finally arrive at the first order, Hagedorn-like phase transition (5.386) with Hagedorn temperature

$$T_H = \frac{1}{\beta_c} \approx 1.039. \tag{5.387}$$

$\square$

Example 3: Effective $\mathcal{N} = 4$ super-Yang–Mills

The reasoning of Appendix 5.13 was inspired by and extended a result of Liu [302] on the effective description of $\mathcal{N} = 4$ super-Yang–Mills theory on $\mathbb{S}^3 \times \mathbb{S}^1_{\beta_{\mathrm{SYM}}}$, with radius of the thermal circle the inverse temperature $\beta_{\mathrm{SYM}} = 1/T$. It was shown in [427, 5] that the partition function in the weak 't Hooft coupling limit reduces to:

$$\hat{\mathcal{Z}}_{\mathcal{N}=4}(\vec{a}) = \oint_{U(N)} \mathrm{d}U \, \exp\left\{\sum_{n\geq 1} \frac{a_n}{n} \operatorname{tr}(U^n) \operatorname{tr}(U^{-n})\right\}. \tag{5.388}$$

The coefficients $(a_n)_{n\geq 1} \subset \mathbb{R}$ are functions of the inverse temperature β_{SYM}. The leading contribution at large N comes from the reduced matrix model [5, 14]

$$\mathcal{Z}_{\mathcal{N}=4}(a) = \oint_{U(N)} \mathrm{d}U \, \exp\left\{\frac{a}{2} \operatorname{tr}(U) \operatorname{tr}\left(U^{-1}\right)\right\}. \tag{5.389}$$

We have denoted

$$a := 2a_1 = \frac{4e^{-\beta_{\mathrm{SYM}}}(3 - e^{-\beta_{\mathrm{SYM}}/2})}{(1 - e^{-\beta_{\mathrm{SYM}}/2})^3}. \tag{5.390}$$

Proposition 5.13.6 ([302]). *The matrix model* (5.389) *undergoes a first order phase transition at* $\frac{1}{\beta_{\mathrm{SYM}}} = T_H$, *where*

$$T_H = \frac{1}{2\ln\left(2 + \sqrt{3}\right)}. \tag{5.391}$$

Besides, it has the behavior (5.371).

Proof. Using a Hubbard–Stratonovich transformation [302], (5.389) can be recast in the form (5.362):

$$\mathcal{Z}_{\mathcal{N}=4}(a) = \int_0^\infty \sigma \mathrm{d}\sigma \, e^{-\frac{\sigma^2}{2a}} \oint_{U(N)} \mathrm{d}U \, \exp\left\{\frac{\sigma}{2} \operatorname{tr}\left(U + U^{-1}\right)\right\}. \tag{5.392}$$

The inner integral

$$e^{N^2 \mathcal{F}_{\text{GWW}}(\sigma/N)} = \oint_{U(N)} dU \, \exp\left\{\frac{\sigma}{2} \, \text{tr}\left(U + U^{-1}\right)\right\} \tag{5.393}$$

is the famous Gross–Witten–Wadia (GWW) model [211, 448, 449], and belongs to the family (5.354) with $g_1 = \frac{1}{2}$, $g_{n>1} = 0$. In the planar limit, with scaling $\sigma = N\gamma$, it undergoes a third order phase transition at $\gamma = 1$:

$$\mathcal{F}_{\text{GWW}}(\gamma) = \begin{cases} \frac{\gamma^2}{4} & \gamma \leq 1 \\ \gamma - \frac{1}{2}\ln\gamma - \frac{3}{4} & \gamma > 1. \end{cases} \tag{5.394}$$

Plugging this result back into (5.392), the large N limit is dominated by the saddle point γ_* that solves

$$\frac{\gamma_*}{a} = \mathcal{F}'_{\text{GWW}}(\gamma_*). \tag{5.395}$$

In the region $\gamma \leq 1$, the solution is $\gamma_* = 0$, which is the absolute minimum if

$$\frac{1}{2a} - \frac{1}{4} > 0 \qquad \Longrightarrow \qquad a > 2. \tag{5.396}$$

Inspecting the region $\gamma > 1$, the solution to (5.395) is the saddle point

$$\gamma_* = \frac{1}{2}\left[a + \sqrt{a(a-2)}\right]. \tag{5.397}$$

This solution is valid in the region $a \geq 2$. Computing the free energy, one finds a first order phase transition at $a_H = 2$.

We are in the scenario (ii) described above, and the transition manifests the Hagedorn behavior (5.371), expected in this effective description of $\mathcal{N} = 4$ super-Yang–Mills [302]. Using the relation (5.390) and $\beta_{\text{SYM}} = 1/T$, one in facts finds out the expected behavior

$$\ln \mathcal{Z}_{\mathcal{N}=4}(a(T)) = \begin{cases} O(1) & T < T_H \\ O(N^2) & T > T_H, \end{cases} \tag{5.398}$$

with Hagedorn temperature

$$T_H = \frac{1}{2\ln\left(2 + \sqrt{3}\right)} \approx 0.380. \tag{5.399}$$

$\square$

Counterexample: q-ensemble and effective Chern–Simons theory

Our procedure to upgrade a third order phase transition to a first order one relies on Lemma 5.13.1. In practice, it boils down to the existence of a phase in which the eigenvalues θ_a of the random matrix in $\mathcal{Z}_{\mathrm{UMM}}$ fill the whole interval $[-\pi, \pi]$. For the sake of completeness, here we provide a counterexample to our procedure, based on violating the assumption (5.359) in Lemma 5.13.1. We will also explain that the lack of a first order phase transition in this case is expected on physical grounds.

Let $\mathcal{P}(x) = \prod_{m \geq 1}(1 - x^m)$ be the generating function of partitions and $\vartheta(z; q)$ denote the Jacobi theta function. Consider the following q-ensemble [363, 394, 432]:

$$
\mathcal{Z}_{\mathrm{CS}}(q) = \frac{1}{\mathcal{P}(q^2)N!} \int_{[-\pi,\pi]^N} \prod_{1 \leq a < b \leq N} \left(2 \sin\left(\frac{\theta_a - \theta_b}{2}\right)\right)^2 \prod_{a=1}^{N} \vartheta(e^{i\theta_a}; q) \frac{\mathrm{d}\theta_a}{2\pi}.
\tag{5.400}
$$

At $q = e^{i2\pi/k}$, $k \in \mathbb{Z}$, this unitary one-matrix model computes the partition function of topological $U(N)_k$ Chern–Simons theory on $\mathbb{S}^3$ [394], and is understood as the analytic continuation of the Chern–Simons level for $0 < |q| < 1$. Throughout, we will set

$$
q = e^{-1/2\sigma}, \qquad \sigma > 0,
\tag{5.401}
$$

which is the usual q-parameter in passing from Chern–Simons theory to the associated topological string theory. The Jacobi triple product identity implies that

$$
\begin{aligned}
\frac{\vartheta(z; q)}{\mathcal{P}(q^2)} &= \prod_{m=0}^{\infty}(1 + zq^{2m+1})(1 + z^{-1}q^{2m+1}) \\
&= \exp\left[\sum_{m=0}^{\infty}\left(\ln(1 + zq^{2m+1}) + \ln(1 + z^{-1}q^{2m+1})\right)\right] \\
&= \exp\left[\sum_{n=1}^{\infty}\frac{(z^n + z^{-n})}{n}(-1)^{n+1}\sum_{m=0}^{\infty}q^{n(2m+1)}\right] \\
&= \exp\left[\sum_{n=1}^{\infty}\frac{(z^n + z^{-n})}{n}\left((-1)^{n+1}\frac{q^n}{1 - q^{2n}}\right)\right].
\end{aligned}
\tag{5.402}
$$

Using (5.401) we immediately identify the coefficients

$$
\hat{g}_n = \frac{(-1)^{n+1}}{2 \sinh\left(\frac{n}{2\sigma}\right)}, \qquad \forall n \geq 1.
\tag{5.403}
$$

Here we are using $\hat{g}_n$ to stress that they differ from g_n in (5.354) in that they are not normalized by an overall σ. We consider the 't Hooft limit $N \to \infty$ with $\sigma = \gamma N, \gamma$

fixed. In this regime, in which (5.400) matches with the topological string partition function on $T^*\mathbb{S}^3$ [324], we have

$$\hat{g}_n \approx (-1)^{n+1}\frac{\sigma}{n}, \tag{5.404}$$

which reduces to the form (5.354). Moreover,

$$\sum_{n=1}^{\infty} \frac{\hat{g}_n}{n} z^n \approx -\sigma \mathrm{Li}_2(-z), \qquad \sum_{n=1}^{\infty} \frac{\hat{g}_n}{n} \approx \frac{\pi^2}{12}\sigma, \qquad \sum_{n=1}^{\infty} \frac{\hat{g}_n^2}{n} \approx \zeta(3)\sigma, \tag{5.405}$$

where Li_2 is the polylogarithm of order 2. Matrix models involving polylogarithmic potentials are relevant in holography and have appeared before in [15].

The relation

$$\frac{\mathrm{d}}{\mathrm{d}z}\left(-\sigma \mathrm{Li}_2(-z)\right) = -\sigma \ln(1+z) \quad \Longrightarrow \quad \sum_{n=1}^{\infty} \hat{g}_{n+1} z^n \approx -\sigma \ln(1+z) \tag{5.406}$$

implies the violation of condition (5.359). In practice, $\theta = \pi$ is a branch point for the current model, bringing a branch cut into the saddle point equation. Denoting $\varrho(\theta)$ the density of eigenvalues, a phase in which $\mathrm{supp}\,\varrho = [-\pi, \pi]$ is ruled out by the presence of the branch cut, invalidating the argument used though the rest of this appendix. The appearance of the logarithm in the saddle point equation is indeed a trademark of Chern–Simons theory on $\mathbb{S}^3$ [324].

The solution of (5.400) in the 't Hooft large N limit is a unitary matrix model version of the computation in [324]. The upshot is that only one phase exists, with eigenvalue density $\varrho(\theta)$ supported on an arc, $\mathrm{supp}\,\varrho \subset [-\pi, \pi]$, which shrinks as γ is increased. Averaging over σ with Gaussian weight,

$$\mathcal{Z}_{\overline{\mathrm{CS}}}(a) = \int_0^{\infty} \mathrm{d}\sigma \, e^{-\frac{\sigma^2}{2a}} \mathcal{Z}_{\mathrm{CS}}(e^{-1/2\sigma}), \tag{5.407}$$

we always find a non-trivial saddle point $\gamma_* > 0$, which is moved to the right as $a > 0$ is increased. This behavior is due to the higher than second order dependence of $\mathcal{Z}_{\mathrm{CS}} := \lim_{N\to\infty} \frac{1}{N^2} \ln \mathcal{Z}_{\mathrm{CS}}$ on γ, obtained by solving the saddle point equation explicitly adapting [324]. In conclusion, (5.407) is always in a phase in which $\ln \mathcal{Z}_{\overline{\mathrm{CS}}} = O(N^2)$.

Chern–Simons theory from the Cardy limit of $\mathcal{N} = 4$ super-Yang–Mills

The outcome of our analysis agrees with the physics of the problem, as we now explain.

The partition function of Chern–Simons theory on $\mathbb{S}^3$ appears in the Cardy limit of the superconformal index of $\mathcal{N} = 4$ super-Yang–Mills [22]. In particular, for q near a root of unity, one gets $U(N)_{\ell N}$ Chern–Simons theory, with ℓ specifying the root of unity [22]. Upon analytic continuation of the coupling, the factor of N matches precisely with our choice of scaling for σ, with γ playing the role of the Wick-rotated ℓ. The Cardy limit drives $\mathcal{N} = 4$ super-Yang–Mills deep in the regime in which the black hole entropy is large, thus

- no phase transition is expected, and

- the partition function should grow as e^{N^2},

consistent with our findings.

The dictionary between our computation and [22] implies that our integral over γ should correspond to a sum over $\ell \in \mathbb{N}$ in the $U(N)_{\ell N}$ Chern–Simons theory. This observation hints at an interpretation of the averaging procedure (5.407) in terms of summing over the Riemann sheets of the superconformal index of $\mathcal{N} = 4$ super-Yang–Mills, in the Cardy limit.

It would be interesting to see whether a neat holographic interpretation emerges, in connection with the work [95].

5.14 Appendix: Proofs

This appendix contains the derivation of the statements in Subsections 5.4-5.4, which build up the spine of our main result about von Neumann algebras: Theorem 5.4.21.

Throughout the main text we have worked with representations R whose Young diagram has $\ell(R) \leq L$, and interpreted them as $SU(L+1)$ representations. This has the unfortunate drawback of having all the expressions normalized by $L + 1$, rather than L. To reduce clutter throughout this (already long and technical) appendix, we adopt the shorthand notation

$$\tilde{L} := L + 1. \tag{5.408}$$

Explicit form of the Wightman functions

This appendix contains the proofs of Theorems 5.4.16 and 5.4.17.

A caveat is that we stick to the conventions of [172] for the $\pm i\varepsilon$. In particular, this entails defining the Fourier transform

$$\widetilde{f}(\omega) = \int_{-\infty}^{\infty} dt\, e^{it\omega} f(t). \tag{5.409}$$

To compare with other references, one might need to redefine $\omega \mapsto -\omega$ and some signs in intermediate expressions will be opposite. The final answers for physical quantities such as $\rho(\omega)$ are of course the same.

Proof of Theorem 5.4.16. We divide the proof of (5.102) in four steps:

(1) We decompose the problem into the evaluation of two simpler pieces;

(2) We evaluate the first piece and show that it contributes only if $\omega > 0$;

(3) We evaluate the second piece and show that it contributes only if $\omega < 0$;

(4) We sum the two pieces, being careful with the probe approximation and the factors of $e^{-\beta\mu}$.

Step (1). We plug the definition of ϕ_L into (5.90):

$$G_{L,+}(t) = \frac{1}{\mathcal{Z}_L^{(N)}} \operatorname{tr}_{\mathscr{H}_L^{(N)} \otimes \Gamma_{\text{probe}}} \left[e^{-\beta H'} \frac{1}{2} \left(e^{itH'} O_L^\dagger e^{-itH'} O_L + e^{itH'} O_L e^{-itH'} O_L^\dagger \right) \right], \tag{5.410}$$

where we have used the fact that $O_L(t)O_L(0)$ has vanishing thermal expectation value. We define

$$G_{O_L}(t) := \frac{1}{\mathcal{Z}_L^{(N)}} \operatorname{tr}_{\mathscr{H}_L^{(N)} \otimes \Gamma_{\text{probe}}} \left[e^{-\beta H'}\, e^{itH'} O_L^\dagger e^{-itH'} O_L \right], \tag{5.411}$$

so that $G_{O_L^\dagger}(t)$ is the same but with $O_L^\dagger$ and O_L exchanged, and

$$G_{L,+}(t) = \frac{G_{O_L}(t) + G_{O_L^\dagger}(t)}{2}. \tag{5.412}$$

For later convenience we also introduce the Fourier transform of this quantity,

$$\widetilde{G}_{L,+}(\omega) = \frac{\widetilde{G}_{O_L}(\omega) + \widetilde{G}_{O_L^\dagger}(\omega)}{2}. \tag{5.413}$$

Our goal is to compute

$$\rho(\omega) = \frac{(1 - e^{-\beta\omega})}{2} \left[\widetilde{G}_{O_L}(\omega) + \widetilde{G}_{O_L^\dagger}(\omega) \right]. \tag{5.414}$$

We thus need to evaluate the two terms on the right-hand side.

Step (2). We now focus on the evaluation of $\widetilde{G}_{O_L}(\omega)$.

We let the probe operators act on the system in the probe approximation $\mu \gg 1$, with μ the mass term in the probe Hamiltonian, to neglect excited states of the probe. Besides, we omit the subscript from the probe sectors to reduce clutter. We now analyze the right-hand side of (5.90). By direct computation we get

$$
\sum_{\mathsf{a},\mathsf{s},\dot{\mathsf{a}},\dot{\mathsf{s}}} \langle R, \mathsf{a}, \mathsf{s}; \phi(R), \dot{\mathsf{a}}, \dot{\mathsf{s}}| \otimes \langle 0, \ldots, 0| \, e^{-\beta H'}
$$

$$
\times \frac{1}{\tilde{L}} \sum_{p=1}^{\tilde{L}} \left[e^{itH'} (1 \otimes c_p) e^{-itH'} (1 \otimes c_p^\dagger) \right] |R, \mathsf{a}, \mathsf{s}; \phi(R), \dot{\mathsf{a}}, \dot{\mathsf{s}}\rangle \otimes |0, \ldots, 0\rangle
$$

$$
= \frac{e^{(-\beta+it)H'(R,\phi(R))}}{\tilde{L}} \mathrm{Tr}_{\bigoplus_J \mathscr{H}(R \sqcup \square_J) \otimes \mathscr{H}(\phi(R))} \left(e^{-itH'} \right) \tag{5.415}
$$

$$
= \frac{1}{\tilde{L}} \sum_{\hat{R}=R \sqcup \square} e^{-\beta H'(R,\phi(R)) - it \left[H'(\hat{R},\phi(R)) - H'(R,\phi(R)) \right]} \mathfrak{d}_R^2 \, \dim(\hat{R}) \dim(\phi(R)). \tag{5.416}
$$

The sum is over the representations $\hat{R}$ obtained in the Clebsch–Gordan expansion of the tensor product $R \otimes \square$, whose Young diagrams are obtained by adding a box to that of R in all possible consistent ways. Here and in the following we denote $H'(R_1, R_2)$ the eigenvalue of the Hamiltonian acting on a state in $\mathscr{H}_L(R_1) \otimes \mathscr{H}_L(R_2)$, and likewise for $H_{\mathrm{int}}(R_1, R_2)$.

Recall from the construction in Subsection 5.4 that the Hamiltonian H' acts on the composite system $\mathscr{H}_L^{\mathrm{tot}}$, i.e., on the quantum mechanics coupled to the external probe. The time evolved operator is $e^{itH'} (1 \otimes c_p) e^{-itH'}$. We have then used that the number operator on the probe Fock space vanishes in the state $|0, \ldots, 0\rangle$. The probe approximation is important here in discarding the contributions from the excited states of the probe.

Let us take a closer look at the sum in the last line of (5.416). Due to the ordering restriction $\hat{R}_j \geq \hat{R}_{j+1}$, not all the ways to add a box to R give an allowed Young diagram $\hat{R}$. The set of rows of R to which a box can be appended is specified by the set $\mathscr{J}_R$ in (5.94). Then, the sum over $\hat{R} = R \sqcup \square$ is more rigorously expressed as (the symbols $\delta(\cdot)$ are Kronecker delta $\delta_{\cdot,0}$)

$$
\sum_{\hat{R}=R \sqcup \square} = \sum_{J \in \mathscr{J}_R} \sum_{\hat{R} \in \mathfrak{R}^{SU(\tilde{L})}} \delta\left(\hat{R}_J - R_J - 1\right) \prod_{\substack{j=1 \\ j \neq J}}^{\tilde{L}} \delta\left(\hat{R}_j - R_j\right). \tag{5.417}
$$

We then sum (5.416) over $R \in \mathfrak{R}_L^{(N)}$ and, denoting $R \sqcup \square_J$ the Young diagram obtained by adding a box at the end of the Jth row of R, we expand the resulting expression as

$$\sum_{R \in \mathfrak{R}_L^{(N)}} \frac{1}{\tilde{L}} \sum_{J \in \mathscr{J}_R} e^{-\beta H'(R,\phi(R))-it[H'(R\sqcup\square_J,\phi(R))-H'(R,\phi(R))]} \, \mathfrak{d}_R^2 \, \dim(R \sqcup \square_J) \dim(\phi(R)).$$
(5.418)

The jth row of the diagram $R \sqcup \square_J$ has length R_j if $j \neq J$ and $R_J + 1$ if $j = J$, which only makes sense for $J \in \mathscr{J}_R$.

Recall from the definition (5.74) that we have

$$H' = H \otimes 1 + 1 \otimes H_{0,\text{probe}} + H_{\text{int}},$$
(5.419)

with, by construction, $e^{-\beta H'} |\mathsf{v}\rangle = e^{-\beta H} |\mathsf{v}\rangle$, for every $|\mathsf{v}\rangle \in \mathscr{H}_L(R) \otimes \mathscr{H}_L(\phi(R)) \otimes |0, \ldots, 0\rangle_{\text{probe}}$. The term $1 \otimes H_{0,\text{probe}}$ is simply a large mass enforcing the probe approximation. On the other hand, we restrict our attention to the interaction (5.75), which gives

$$H_{\text{int}}(R \sqcup \square_J, \phi(R)) - H_{\text{int}}(R, \phi(R)) = g(R_J + \tilde{L} - J) =: E_J^{\text{int}}$$
(5.420)

for $\phi(R) = R$ or $\overline{R}$. More general choices of $\phi(R)$ are treated analogously and yield to similar definitions of E_J^{int}. The time dependence only appears through

$$e^{-it[H'(R\sqcup\square_J,\phi(R))-H'(R,\phi(R))]} = e^{-itE_J^{\text{int}}-it\mu},$$
(5.421)

and hence, taking the Fourier transform, the dependence on ω is through

$$\delta\left(\omega - E_J^{\text{int}} - \mu\right)$$
(5.422)

in each summand. Notice that the uniform shift $E_J^{\text{int}} \mapsto E_J^{\text{int}} + \mu$ induced by the probe mass is expected, because the correlation functions we are considering are tailored to probe energies of the scale of the first excitation.

Putting all together, we obtain

$$\sum_{R \in \mathfrak{R}_L^{(N)}} \frac{1}{\tilde{L}} \sum_{J \in \mathscr{J}_R} e^{-\beta|R|} \, \delta\left(\omega - \mu - E_J^{\text{int}}\right) \, \mathfrak{d}_R^2 \dim(R \sqcup \square_J) \dim(\phi(R)).$$
(5.423)

The additional quantum numbers λ_s are not involved in our definition of probe, and this is the reason we get $\mathfrak{d}_R^2$ in the right-hand side, instead of, say, $\mathfrak{d}_R \mathfrak{d}_{R\sqcup\square_J}$.

We arrive at an expression for $\widetilde{G}_{O_L}(\omega)$ which is precisely (5.99). We also observe that

- (5.423) vanishes if $\omega < 0$, because $\mu > 0$ and $E_J^{\text{int}} > 0 \,\forall J$, and so the δ is never satisfied.

- For $\omega > 0$, expression (5.423) depends on ω_{r}.

Step (3). We repeat the procedure to evaluate $\widetilde{G}_{O_L^\dagger}(\omega)$.

Now the operator $O_L^\dagger$ acts first, thus annihilating the probe vacuum. The first non-trivial term comes from $O_L^\dagger$ acting on the first probe excited state. Namely, the lowest order in $e^{-\beta\mu}$ contribution comes from the terms schematically of the form

$$\langle \Box; \emptyset| \otimes {}_L\langle R; \phi(R)|e^{-\beta H'} e^{itH'} O_L e^{-itH'} O_L^\dagger |R; \phi(R)\rangle_L \otimes |\Box; \emptyset\rangle. \tag{5.424}$$

A computation analogous to Step (2) gives

$$\sum_{R\in\mathfrak{R}_L^{(N)}} \frac{1}{\widetilde{L}} \sum_{J\in\mathscr{J}_R} e^{-\beta H'(R\sqcup\Box_J, \phi(R))+it[H'(R\sqcup\Box_J, \phi(R))-H'(R,\phi(R))]} \, \mathfrak{d}_R^2 \, \dim(R\sqcup\Box_J) \dim(\phi(R)). \tag{5.425}$$

The difference with respect to Step (2) lies in the reflection $t \mapsto -t$ and in the fact that $\exp(-\beta H')$ acting on its left produces $\exp(-\beta H'(R \sqcup \Box_J, \phi(R)))$. Compared to the function in Step (2), the action on a probe state different from the vacuum introduces the additional factor

$$\exp\left(-\beta\mu - \beta E_J^{\text{int}}\right) \tag{5.426}$$

in each summand. Higher powers of $e^{-\beta\mu}$ are neglected by the definition of probe. Taking the Fourier transform, we are therefore led to

$$\sum_{R\in\mathfrak{R}_L^{(N)}} \frac{1}{\widetilde{L}} \sum_{J\in\mathscr{J}_R} e^{-\beta(\mu+E_J^{\text{int}})} \, e^{-\beta|R|} \, \delta\left(-\omega - \mu - E_J^{\text{int}}\right) \, \mathfrak{d}_R^2 \dim(R \sqcup \Box_J) \dim(\phi(R)). \tag{5.427}$$

This is analogous to (5.423), except for the additional weight (5.426) in front of each summand and for the reflection $\omega \mapsto -\omega$. For the same reason as above, i.e., that the energy spectrum is positive, the latter expression vanishes if $\omega > 0$. Once again, it can be written as a function of ω_{r}.

Step (4). We now wish to put the terms together. Let us take a closer look at (5.414).

(4.i) From (5.423) we know that $\widetilde{G}_{O_L}(\omega) = 0$ unless $\omega - \mu > 0$. By the probe approximation, we have

$$(1 - e^{-\beta\omega})\widetilde{G}_{O_L}(\omega) = \theta(\omega - \mu)\widetilde{G}_{O_L}(\omega) + O(e^{-\beta\mu}). \tag{5.428}$$

(4.ii) Likewise, $\widetilde{G}_{O_L^\dagger}(\omega) = 0$ unless $\omega + \mu < 0$, which in the probe approximation gives

$$(1 - e^{-\beta\omega})\widetilde{G}_{O_L^\dagger}(\omega) = -\theta(-\omega - \mu)e^{-\beta\omega}\widetilde{G}_{O_L^\dagger}(\omega) + O(e^{-\beta\mu}), \qquad (5.429)$$

where we have used $e^{-\beta\omega} \gg 1$ if $\omega < -\mu \ll 0$. By the computation in Step (3), cf. (5.427), we have that the latter expression is non-vanishing precisely when $e^{-\beta\omega}$ cancels the piece (5.426) in $\widetilde{G}_{O_L^\dagger}(\omega)$. Simplifying, we get

$$-e^{-\beta\omega}\widetilde{G}_{O_L^\dagger}(\omega) = -\widetilde{G}_{O_L}(-\omega), \qquad \text{if } \omega \leq -\mu. \qquad (5.430)$$

(4.iii) Writing $\widetilde{G}_{O_L}(\pm\omega)$ in the form (5.99) and summing the two contributions, we prove the statement.

$$\square$$

Proof of Theorem 5.4.17. Most of the details are identical to the proof of Theorem 5.4.16, so we will be sketchy. We divide the proof in various steps:

(1) We decompose the problem into the evaluation of four simpler pieces;

(2) We evaluate each piece;

(3) We take the Fourier transform;

(4) We sum the pieces, being careful with the probe approximation and the factors of $\pm i\varepsilon$.

Step (1). As in the proof of Theorem 5.4.16, we start by decomposing $\phi_L(t)$ into the operators $O_L, O_L^\dagger$. We have

$$[\phi(t), \phi(0)] = \frac{1}{2}\left(\mathcal{Y}_1(t) + \mathcal{Y}_2(t) - \mathcal{Y}_1^\dagger(t) - \mathcal{Y}_2^\dagger(t)\right) + \cdots, \qquad (5.431)$$

where the dots include all the terms that vanish when taken inside the correlation functions, and the four pieces are:

$$\mathcal{Y}_1(t) := \frac{1}{\tilde{L}} \sum_{p=1}^{\tilde{L}} e^{itH'} c_p e^{-itH'} c_p^\dagger; \tag{5.432}$$

$$\mathcal{Y}_2(t) := \frac{1}{\tilde{L}} \sum_{p=1}^{\tilde{L}} e^{itH'} c_p^\dagger e^{-itH'} c_p; \tag{5.433}$$

$$\mathcal{Y}_1^\dagger(t) := \frac{1}{\tilde{L}} \sum_{p=1}^{\tilde{L}} c_p e^{itH'} c_p^\dagger e^{-itH'}; \tag{5.434}$$

$$\mathcal{Y}_2^\dagger(t) := \frac{1}{\tilde{L}} \sum_{p=1}^{\tilde{L}} c_p^\dagger e^{itH'} c_p e^{-itH'}. \tag{5.435}$$

(recall that $\tilde{L} = L + 1 = \dim \square$).

Step (2). We compute the thermal expectation value of the four terms above. Each of them is essentially identical to Steps (2)-(3) in the proof of Theorem 5.4.16. For $\mathcal{Y}_1$ the answer was given in (5.416), and for $\mathcal{Y}_2$ in (5.425):

$$\langle \Psi_\beta | \mathcal{Y}_1(t) | \Psi_\beta \rangle = \frac{1}{\mathcal{Z}_L^{(N)}} \sum_{R \in \mathfrak{R}_L^{(N)}} e^{-\beta|R|} \mathfrak{d}_R^2 \dim(R) \dim(\phi(R)) \left[\sum_{J \in \mathscr{J}_R} e^{-itE_J(\mu)} \frac{\dim(R \sqcup \square_J)}{\tilde{L} \dim(R)} \right] \tag{5.436}$$

$$\langle \Psi_\beta | \mathcal{Y}_2(t) | \Psi_\beta \rangle = \frac{1}{\mathcal{Z}_L^{(N)}} \sum_{R \in \mathfrak{R}_L^{(N)}} e^{-\beta|R|} \mathfrak{d}_R^2 \dim(R) \dim(\phi(R)) \left[\sum_{J \in \mathscr{J}_R} e^{(-\beta+it)E_J(\mu)} \frac{\dim(R \sqcup \square_J)}{\tilde{L} \dim(R)} \right]. \tag{5.437}$$

where $E_J(\mu) := E_J^{\text{int}} + \mu$ is a shorthand notation. The analogous computation for the other two terms gives:

$$\langle \Psi_\beta | \mathcal{Y}_1^\dagger(t) | \Psi_\beta \rangle = \frac{1}{\mathcal{Z}_L^{(N)}} \sum_{R \in \mathfrak{R}_L^{(N)}} e^{-\beta|R|} \mathfrak{d}_R^2 \dim(R) \dim(\phi(R)) \left[\sum_{J \in \mathscr{J}_R} e^{itE_J(\mu)} \frac{\dim(R \sqcup \square_J)}{\tilde{L} \dim(R)} \right] \tag{5.438}$$

$$\langle \Psi_\beta | \mathcal{Y}_2^\dagger(t) | \Psi_\beta \rangle = \frac{1}{\mathcal{Z}_L^{(N)}} \sum_{R \in \mathfrak{R}_L^{(N)}} e^{-\beta|R|} \mathfrak{d}_R^2 \dim(R) \dim(\phi(R)) \left[\sum_{J \in \mathscr{J}_R} e^{(-\beta-it)E_J(\mu)} \frac{\dim(R \sqcup \square_J)}{\tilde{L} \dim(R)} \right]. \tag{5.439}$$

Step (3). We now take the Fourier transform of each term. From the definitions (5.92)-(5.93) we have

$$2G_{L,R}(t) = i\theta(t)\langle\Psi_\beta|\mathcal{Y}_1(t) + \mathcal{Y}_2(t) + \mathcal{Y}_1^\dagger(t) + \mathcal{Y}_2^\dagger(t)|\Psi_\beta\rangle, \qquad (5.440)$$

$$2G_{L,A}(t) = -i\theta(-t)\langle\Psi_\beta|\mathcal{Y}_1(t) + \mathcal{Y}_2(t) + \mathcal{Y}_1^\dagger(t) + \mathcal{Y}_2^\dagger(t)|\Psi_\beta\rangle, \qquad (5.441)$$

so that we have to compute the Fourier transform of $\pm i\theta(\pm t)\mathcal{Y}(t)$ for $\mathcal{Y} \in \left\{\mathcal{Y}_1, \mathcal{Y}_2, \mathcal{Y}_1^\dagger, \mathcal{Y}_2^\dagger\right\}$, evaluated at $\omega \pm i\varepsilon$, with the sign $\pm$ in front of $i\varepsilon$ being the same as in $\theta(\pm t)$. The only time-dependent part in $\mathcal{Y}(t)$ is the exponential $e^{\mp itE_J(\mu)}$. We thus get the contributions of $\mathcal{Y}_1, \mathcal{Y}_1^\dagger$ to $2\widetilde{G}_{L,R}(\omega + i\varepsilon)$:

$$i\theta(t)e^{-itE_J(\mu)} \mapsto -\frac{1}{\omega + i\varepsilon - E_J(\mu)} \qquad (5.442)$$

$$-i\theta(t)e^{itE_J(\mu)} \mapsto \frac{1}{\omega + i\varepsilon + E_J(\mu)} \qquad (5.443)$$

and likewise for the contributions of $\mathcal{Y}_1, \mathcal{Y}_1^\dagger$ to $2\widetilde{G}_{L,A}(\omega - i\varepsilon)$:

$$-i\theta(-t)e^{-itE_J(\mu)} \mapsto -\frac{1}{\omega - i\varepsilon - E_J(\mu)} \qquad (5.444)$$

$$+i\theta(-t)e^{itE_J(\mu)} \mapsto \frac{1}{\omega - i\varepsilon + E_J(\mu)}. \qquad (5.445)$$

The same expressions coming from $\mathcal{Y}_1$ (respectively $\mathcal{Y}_1^\dagger$) appear in the Fourier transform of $\mathcal{Y}_2^\dagger$ (respectively $\mathcal{Y}_2$).

Step (4). Denoting $\Omega(\omega)$ the operator that is diagonal in the representation basis with eigenvalues

$$\sum_{J\in\mathcal{J}_R} \frac{\dim(R \sqcup \square_J)}{\widetilde{L}\dim(R)} \frac{1}{\omega - E_J(\mu)} \qquad (5.446)$$

as defined in (5.100), we see that $2\widetilde{G}_{L,R}(\omega + i\varepsilon)$ receives contributions from

$$-\Omega(\omega + i\varepsilon) - \Omega(-\omega - i\varepsilon), \qquad (5.447)$$

while $2\widetilde{G}_{L,A}(\omega - i\varepsilon)$ receives contributions from

$$-\Omega(\omega - i\varepsilon) - \Omega(-\omega + i\varepsilon). \qquad (5.448)$$

Putting all the pieces together we arrive at:

$$\widetilde{G}_{L,R}(\omega + i\varepsilon) = -\frac{1}{2}\langle\Psi_\beta|\Omega(\omega + i\varepsilon) + \Omega(-\omega - i\varepsilon)|\Psi_\beta\rangle + O(e^{-\beta\mu}) \qquad (5.449)$$

$$\widetilde{G}_{L,A}(\omega - i\varepsilon) = -\frac{1}{2}\langle\Psi_\beta|\Omega(\omega - i\varepsilon) + \Omega(-\omega + i\varepsilon)|\Psi_\beta\rangle + O(e^{-\beta\mu}). \qquad (5.450)$$

$\square$

Wightman functions in the Veneziano limit

This appendix contains the proof of Lemma 5.4.18, which evaluates the Wightman functions in the Veneziano limit using a saddle point approximation. We still use the shorthand $\tilde{L} = L + 1$ from (5.408).

Proof of Lemma 5.4.18. Consider $\widetilde{G}_{L,R}(\omega)$ as given by Theorem 5.4.17. The change of variables (5.60) recasts the sum over R into a sum over $\tilde{L}$-tuples $\vec{h} = (h_1, \ldots, h_{\tilde{L}-1}, -1)$. The ordering $R_j \geq R_{j+1}$ becomes $h_j > h_{j+1}$, but the appearance of the Vandermonde squared factor and the total symmetry of the Hamiltonian allow us to remove this restriction. The set of indices $\mathscr{J}_R$ becomes

$$\mathscr{J}_{\vec{h}} = \left\{ J \in \{1, \ldots, \tilde{L}\} \; : \; h_J + 1 \neq h_j, \; \forall j \neq J \right\}. \tag{5.451}$$

Notice that the presence of a sum over a restricted set of indices does not spoil the total symmetry of the summand in the variables h_j, because, for those indices $j \notin \mathscr{J}_{\vec{h}}$, the Vandermonde determinant after adding a box to R vanishes. One can thus safely include them (add finitely many zeros) and sum over all indices.

With the change of variables (5.60),

$$E_J^{\text{int}} = g(h_J + 1) \tag{5.452}$$

and, subdividing

$$\prod_{1 \leq i < j \leq \tilde{L}} = \prod_{\substack{1 \leq i < j \leq \tilde{L} \\ i \neq J, \; j \neq J}} \cdot \prod_{\substack{1 \leq i \leq J-1 \\ j = J}} \cdot \prod_{\substack{J+1 \leq j \leq \tilde{L} \\ i = J}} \tag{5.453}$$

in formula (5.64), we express the ratio

$$\frac{\dim(R \sqcup \Box_J)}{\dim R} = \prod_{i=1}^{J-1} \left(1 - \frac{1}{h_i - h_J}\right) \cdot \prod_{j=J+1}^{\tilde{L}} \left(1 - \frac{1}{h_j - h_J}\right) = \prod_{j \neq J} \left(1 - \frac{1}{h_j - h_J}\right). \tag{5.454}$$

The right-hand side of (5.100) evaluated at $\omega \pm i\varepsilon$ reads

$$\frac{1}{\tilde{L}} \sum_{J \in \mathscr{J}_R} \frac{1}{\omega \pm i\varepsilon - E_J^{\text{int}} - \mu} \frac{\dim(R \sqcup \Box_J)}{\dim R} = \frac{1}{\tilde{L}} \sum_{J=1}^{\tilde{L}} \frac{1}{\omega \pm i\varepsilon - g(h_J + 1) - \mu} \prod_{j \neq J} \left(1 - \frac{1}{h_j - h_J}\right). \tag{5.455}$$

Let us repeat that, although the sum should be restricted to $J \in \mathscr{J}_{\vec{h}}$, the right-hand side of (5.455) vanishes for j such that $h_j = h_J + 1$, so that the extra contributions that we include in the sum are trivial.

Let us introduce some notation. First, we redefine

$$\tilde{\omega}_\pm = \omega \pm i\varepsilon - \mu - g. \tag{5.456}$$

We are eventually interested in the planar limit $N \to \infty$ with $g = \lambda/N$ and λ fixed, so that the shift by g drops out, whereas $\Im\tilde{\omega}_\pm = \pm\varepsilon$. We denote the expression in the right-hand side of (5.455) $\Omega_{\vec{h}}(\omega \pm \varepsilon)$ for short.

For every $\tilde{L}$-tuple $\vec{h} \in \mathbb{N}^{\tilde{L}}$ (the ones of interest to us have $h_{\tilde{L}} \equiv -1$), we define the auxiliary function

$$\Phi_{\vec{h}}(\xi) := \prod_{j=1}^{\tilde{L}} \left(1 - \frac{1}{h_j - \xi}\right), \qquad \xi \in \mathbb{C}. \tag{5.457}$$

The residue theorem instructs us that

$$\Omega_{\vec{h}}(\omega \pm i\varepsilon) = \frac{1}{\tilde{L}} \oint_C \frac{d\xi}{2\pi i} \frac{\Phi_{\vec{h}}(\xi)}{\tilde{\omega}_\pm - g\xi}, \tag{5.458}$$

with the integration contour $C = C(\vec{h})$ encircling the points h_J and leaving outside the point $\tilde{\omega}_\pm/g$. This is exemplified in Figure 5.24. Let us remark that, had we restricted the sum on $J \in \mathscr{F}_{\vec{h}}$, we could take a contour that leaves outside the points h_J for $J \notin \mathscr{F}_{\vec{h}}$. Then, deforming such contour into C, we pick the poles with vanishing residues, obtaining (5.458).
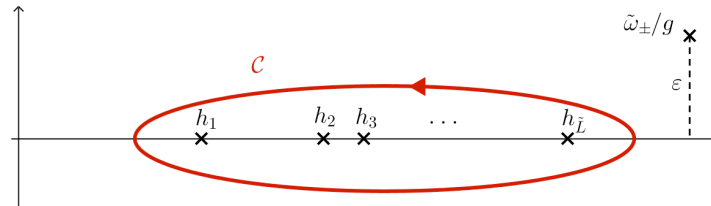
Figure 5.24: Integration contour C.

Deforming the contour C to infinity, the Cauchy integral (5.458) picks up the pole at $\xi = \tilde{\omega}_\pm/g$, and one is left with a residual integration over the circle at infinity. Using that $\Phi_{\vec{h}}(\xi) \to 1$ as $\xi \to \infty$, the residual integration evaluates to

$$\frac{1}{\tilde{L}} \oint_{|\xi| \gg 1} \frac{d\xi}{2\pi i} \frac{\Phi_{\vec{h}}(\xi)}{(-g\xi)} = -\frac{1}{\tilde{L}g}. \tag{5.459}$$

Conveniently expressing (5.458) as

$$\tilde{L}g\, \Omega_{\vec{h}}(\omega \pm i\varepsilon) = \oint_C \frac{d\xi}{2\pi i} \frac{\Phi_{\vec{h}}(\xi)}{\frac{\tilde{\omega}_\pm}{g} - \xi}, \tag{5.460}$$

we arrive at

$$\tilde{L}g\,\Omega_{\vec{h}}(\omega) = \Phi_{\vec{h}}(\tilde{\omega}_{\pm}/g) - 1. \tag{5.461}$$

We write[16] $\frac{\tilde{\omega}_{\pm}}{g} = \frac{\tilde{L}\tilde{\omega}_{\pm}}{\lambda}$ and

$$\Phi_{\vec{h}}(\tilde{\omega}_{\pm}/g) = \exp\left[\sum_{j=1}^{\tilde{L}} \ln\left(1 - \frac{1}{h_j - \frac{\tilde{L}\tilde{\omega}_{\pm}}{\lambda}}\right)\right]$$

$$= \exp\left[\frac{1}{\tilde{L}}\sum_{j=1}^{\tilde{L}} \tilde{L}\ln\left(1 + \frac{1}{\tilde{L}}\cdot\frac{1}{\frac{\tilde{\omega}_{\pm}}{\lambda} - \frac{h_j}{\tilde{L}}}\right)\right]$$

$$= \exp\left[\frac{1}{\tilde{L}}\sum_{j=1}^{\tilde{L}} \frac{1}{\frac{\tilde{\omega}_{\pm}}{\lambda} - \frac{h_j}{\tilde{L}}} + O(1/\tilde{L})\right]$$

$$\approx \exp\left[\int dx \varrho(x)\frac{1}{\frac{\tilde{\omega}}{\lambda} - x}\right] \tag{5.462}$$

with the last step holding in the planar limit. In the second-to-last step, we have expanded the logarithm in power series in $\tilde{L}^{-1}$, and in the last step we have discarded the sub-leading terms. At the same time, we have plugged the eigenvalue density $\varrho(x)$ for the matrix model (5.59), defined in the standard way

$$\varrho(x) := \frac{1}{\tilde{L}}\sum_{i=1}^{\tilde{L}} \delta\left(x - \frac{h_i}{\tilde{L}}\right), \qquad x \in \mathbb{R}. \tag{5.463}$$

No assumption on $\varrho(x)$ is made at this stage, and its definition uses the fact that $h_j/\tilde{L}$ attains a finite value in the planar limit, $\forall j$. The linear growth of h_j with L is a standard result on discrete matrix models, or equivalently on the combinatorics of the distribution of partitions of length L; it is a known result that transcends the models of interest to us. The fact that this is the leading contribution in the Veneziano limit, and does not trivialize, is encoded in the assumption of the existence of a non-trivial saddle point. Therefore, in the planar limit we find that (5.461) becomes

$$\lambda\Omega_{\vec{h}}(\omega \pm i\varepsilon) \approx -1 + \exp\left[\int dx \varrho(x)\frac{1}{\frac{\tilde{\omega}_{\pm}}{\lambda} - x}\right]. \tag{5.464}$$

At leading order, we perform a saddle point approximation and evaluate this expression at the saddle point eigenvalue density $\varrho_*(x)$. We thus arrive at

$$\Omega_{\vec{h}}(\omega \pm i\varepsilon)\Big|_{\text{saddle point}} = \frac{1}{\lambda}\left[-1 + \exp\left(\int dx \frac{\varrho_*(x)}{\frac{\omega\pm i\varepsilon-\mu}{\lambda} - x}\right)\right], \tag{5.465}$$

---

[16]In this appendix and Section 5.4 we define the 't Hooft coupling $\lambda = gL$. The procedure for 't Hooft coupling gN is identical up to rescaling $\tilde{\omega}_{\pm}$ appropriately.

where we have reinserted the appropriate variable $\tilde{\omega}_\pm = \omega \pm i\varepsilon - \mu + O(1/N)$ in the planar limit. Notice that this expression only holds under the assumption that the saddle point is non-trivial. This hypothesis is crucial, but no further assumptions are made. By the standard large N argument, under the mentioned hypothesis, the eigenvalues coalesce and form a continuum, and we get

$$_L\langle \Psi_\beta | \Omega(\omega) | \Psi_\beta \rangle_L \approx \Omega_{\bar{\hbar}}(\omega) \big|_{\text{saddle point}}, \tag{5.466}$$

which concludes the proof. □

Large N factorization lemma

This appendix contains a justification for the factorization Lemma 5.4.19. We will very explicitly show that the four-point function factorizes, and then give a general argument that extends more easily to the general case.[17] The two key hypotheses are:

(H1) The partition function admits a non-trivial saddle point for large N;

(H2) H_{int} respects the flavor symmetry.

We will work explicitly with H_{int} given in (5.75), but a direct generalization of the argument holds as long as the second assumption holds.

Step 0: Lighten the notation

The approach in this appendix is based on explicit direct calculation, which will produce cumbersome equations. To lighten the expressions, we introduce shorthand notations used throughout this subsection.

Recall from Subsection 5.4 that the representation basis is given by the vectors

$$|R, \mathsf{a}, \mathsf{s};\ \phi(R), \dot{\mathsf{a}}, \dot{\mathsf{s}}\rangle, \quad \mathsf{a} = 1, \ldots, \dim R,\ \dot{\mathsf{a}} = 1, \ldots, \dim \phi(R) \tag{5.467}$$

and $\mathsf{s}, \dot{\mathsf{s}}$ running over possible additional degeneracies. The indices $\mathsf{s}, \dot{\mathsf{s}}$ do not play any role in the ensuing discussion, thus we will mute them. Likewise, by construction the probe interacts with the R-sector, and $\phi(R)$ only appears through

---

[17]An elegant proof of large N factorization for permutation invariant observables in Hermitian matrix models with a symmetric group symmetry was given in [39], based on combinatorial techniques. While our method is based on a direct evaluation of the terms, it seems plausible that the techniques of [39, 40] can be adapted and applied to the present context to establish a proof that only relies on the symmetries of the operators, and not their explicit form.

the interaction Hamiltonian. Since the state $|\phi(R), \dot{\mathsf{a}}\rangle$ is not affected by the action of the probe operators, we will omit it from the notation as well. Every sum over a will implicitly be accompanied by a sum over $\dot{\mathsf{a}}$.

Furthermore, we will further contract the notation for tensor product with a probe state and write:

$$|R, \mathsf{a}\rangle \text{ for } |R, \mathsf{a}, \mathsf{s}; \; \phi(R), \dot{\mathsf{a}}, \dot{\mathsf{s}}\rangle \otimes |0, \ldots, 0\rangle_{\text{probe}}$$

$$|R, \mathsf{a}; j\rangle \text{ for } |R, \mathsf{a}, \mathsf{s}; \; \phi(R), \dot{\mathsf{a}}, \dot{\mathsf{s}}\rangle \otimes |0, \ldots, \underbrace{1}_{j^{\text{th}}}, \ldots, 0\rangle_{\text{probe}} \qquad (5.468)$$

and so on.

We recall that H' is the total Hamiltonian, $H' = H + H_{\text{probe}} + H_{\text{int}}$. As in the main text, we will denote by $R \sqcup \square_J$ the Young diagram obtained by appending a box at the end of the Jth row, and

$$E_J(\mu) := H'(R \sqcup \square_J, \phi(R)) - H'(R, \phi(R)). \qquad (5.469)$$

We use indices a, b to run over the generators of R, hatted indices $\hat{\mathsf{a}}, \hat{\mathsf{b}}$ to run over the generators of $R \sqcup \square$ (R with one box added), and checked indices $\check{\mathsf{c}}$ to run over the generators of $R \sqcup \square \sqcup \square$ (R with two boxes added).

We will use the symbol $\approx$ to indicate that the two sides are equal up to terms that vanish in the planar limit, and also sometimes abbreviate $t_{jk} := t_j - t_k$. Finally, we continue using the abbreviation $\tilde{L} = L + 1$ from (5.408).

Step 1: Identify the non-trivial contributions

Recall that the goal of this appendix is to compute four-point functions

$$_L\langle \Psi_\beta | \phi_L(t_3) \phi_L(t_2) \phi_L(t_1) \phi_L(t_0) | \Psi_\beta \rangle_L \qquad (5.470)$$

in the planar limit, and show that (5.470) equals

$$_L\langle \Psi_\beta | \phi_L(t_3) \phi_L(t_2) | \Psi_\beta \rangle_L \cdot {}_L\langle \Psi_\beta | \phi_L(t_1) \phi_L(t_0) | \Psi_\beta \rangle_L$$

$$+ {}_L\langle \Psi_\beta | \phi_L(t_3) \phi_L(t_1) | \Psi_\beta \rangle_L \cdot {}_L\langle \Psi_\beta | \phi_L(t_2) \phi_L(t_0) | \Psi_\beta \rangle_L \qquad (5.471)$$

$$+ {}_L\langle \Psi_\beta | \phi_L(t_3) \phi_L(t_0) | \Psi_\beta \rangle_L \cdot {}_L\langle \Psi_\beta | \phi_L(t_2) \phi_L(t_1) | \Psi_\beta \rangle_L.$$

We expand (5.470) using the definition of $\phi_L(t)$ in terms of the operators $O_L(t), O_L^\dagger(t)$. After elementary calculations, we

(i) discard all terms except those with two O_L and two $O_L^\dagger$; and then

(ii) discard all the terms in which the rightmost operator in an annihilation operator or the leftmost operator is a creation operator.

The contributions discarded in (i) vanish exactly, while those discarded in (ii) are $O(e^{-\beta\mu})$, thus negligible in the probe approximation. We are therefore left with

$$_L\langle\Psi_\beta|\phi_L(t_3)\phi_L(t_2)\phi_L(t_1)\phi_L(t_0)|\Psi_\beta\rangle_L = \frac{1}{4}\,_L\langle\Psi_\beta|O_L^\dagger(t_3)O_L(t_2)O_L^\dagger(t_1)O_L(t_0)|\Psi_\beta\rangle_L$$

(5.472)

$$+ \frac{1}{4}\,_L\langle\Psi_\beta|O_L^\dagger(t_3)O_L^\dagger(t_2)O_L(t_1)O_L(t_0)|\Psi_\beta\rangle_L.$$

We claim

Proposition 5.14.1. *The first term on the right-hand side of* (5.472) *yields the first line in* (5.471)*, and the second term on the right-hand side of* (5.472) *yields the second and third lines in* (5.471)*.*

The rest of this appendix is devoted to show this statement.

We plug the definition of O_L as a sum of probe creation operators in the right-hand side of (5.472). We also set $t_0 = 0$ without loss of generality. We are then interested in four-point functions of the form

$$G^{(1)}_{ijkl}(t_1, t_2, t_3) := \,_L\langle\Psi_\beta|c_i(t_3)c_j^\dagger(t_2)c_k(t_1)c_l^\dagger(0)|\Psi_\beta\rangle_L, \qquad (5.473)$$

$$G^{(2)}_{ijkl}(t_1, t_2, t_3) := \,_L\langle\Psi_\beta|c_i(t_3)c_j(t_2)c_k^\dagger(t_1)c_l^\dagger(0)|\Psi_\beta\rangle_L, \qquad (5.474)$$

and then sum over the flavor indices $i, j, k, l \in \{1, \ldots, \tilde{L}\}$ with the overall normalization by $1/\tilde{L}^2$. The idea is to evaluate these correlation functions in a particular sector $(R, \phi(R))$ for a fixed irreducible representation R appearing in the thermal ensemble, and then to apply a saddle point argument.

Intermezzo: Useful formulas

Throughout we will make extensive use of the Clebsch–Gordan isomorphism

$$\mathscr{H}(R \otimes \square) \cong \bigoplus_{J \in \mathscr{J}_R} \mathscr{H}(R \sqcup \square_J). \qquad (5.475)$$

The normalization of the two bases are related as follows. Consider the identities

$$\sum_{j=1}^{\tilde{L}} \sum_{\mathsf{a}=1}^{\dim R} \langle R, \mathsf{a}; j | R, \mathsf{a}; j \rangle = \tilde{L} \dim R = \sum_{J \in \mathscr{J}} \sum_{\hat{\mathsf{a}}=1}^{\dim(R \sqcup \square_J)} \langle R \sqcup \square_J, \hat{\mathsf{a}} | R \sqcup \square_J, \hat{\mathsf{a}} \rangle \quad (5.476)$$

and insert the resolution of the identity on the left-most part, expressed in the representation basis. We have the normalization:

$$\sum_{j=1}^{\tilde{L}} \sum_{a=1}^{\dim R} |\langle R \sqcup \Box_J, \hat{a}|R, a; j\rangle|^2 = 1 = \sum_{J \in \mathcal{J}} \sum_{\hat{a}=1}^{\dim(R \sqcup \Box_J)} |\langle R \sqcup \Box_J, \hat{a}|R, a; j\rangle|^2. \quad (5.477)$$

To write the result of the calculations in factorized form, we will use the properties:

$$H_{\text{int}}(R \sqcup \Box_J \sqcup \Box_K) - H_{\text{int}}(R \sqcup \Box_J) \approx H_{\text{int}}(R \sqcup \Box_K) - H_{\text{int}}(R) \quad (5.478)$$

$$\frac{\dim(R \sqcup \Box_J \sqcup \Box_K)}{\dim(R \sqcup \Box_J)} \approx \frac{\dim(R \sqcup \Box_K)}{\dim R}. \quad (5.479)$$

Step 2: First correlation function

Let us start with $G^{(1)}_{ijkl}(t_1, t_2, t_3)$, and consider the contribution to the thermal expectation value for a given representation R. By the flavor symmetry of the interaction between the probe and the system (and ignoring potential antisymmetric terms that vanish when summed over) we have

$$\sum_a \langle R, a|c_i(t_3)c_j^\dagger(t_2)c_k(t_1)c_l^\dagger(0)|R, a\rangle = \delta_{ij}\delta_{kl} \sum_a \langle R, a|c_i(t_3)c_i^\dagger(t_2)c_k(t_1)c_k^\dagger(0)|R, a\rangle$$

$$\quad (5.480)$$

$$+ \delta_{il}\delta_{jk} \sum_a \langle R, a|c_i(t_3)c_j^\dagger(t_2)c_j(t_1)c_i^\dagger(0)|R, a\rangle$$

$$- \delta_{ijkl} \sum_a \langle R, a|c_i(t_3)c_i^\dagger(t_2)c_i(t_1)c_i^\dagger(0)|R, a\rangle.$$

Averaging over i, j, k, l, in the large L limit only the third term is suppressed and we get

$$\frac{1}{\tilde{L}^2} \sum_{ijkl} \sum_a \langle R, a|c_i(t_3)c_j^\dagger(t_2)c_k(t_1)c_l^\dagger(0)|R, a\rangle \approx \frac{1}{\tilde{L}^2} \sum_{ika} \langle R, a|c_i(t_3)c_i^\dagger(t_2)c_k(t_1)c_k^\dagger(0)|R, a\rangle$$

$$\quad (5.481)$$

$$+ \frac{1}{\tilde{L}^2} \sum_{ija} \langle R, a|c_i(t_3)c_j^\dagger(t_2)c_j(t_1)c_i^\dagger(0)|R, a\rangle.$$

We now proceed to show the following:

Lemma 5.14.2. *The first term in the right-hand side of* (5.481) *factorizes into the product of two-point functions, and the second term is sub-leading.*

Proof. Inserting a resolution of the identity in the representation basis, the first term is rewritten as

$$\frac{1}{\tilde{L}^2}\sum_{ik\mathsf{a}}\langle R,\mathsf{a}|c_i(t_3)c_i^\dagger(t_2)c_k(t_1)c_k^\dagger(0)|R,\mathsf{a}\rangle = \frac{1}{\tilde{L}^2}\sum_{ik\mathsf{a}\mathsf{b}}\langle R,\mathsf{a}|c_i(t_3)c_i^\dagger(t_2)|R,\mathsf{b}\rangle\langle R,\mathsf{b}|c_k(t_1)c_k^\dagger(0)|R,\mathsf{a}\rangle$$

$$=\sum_{\mathsf{a}\mathsf{b}}\left(\langle R,\mathsf{a}|\frac{1}{\tilde{L}}\sum_i c_i(t_3)c_i^\dagger(t_2)|R,\mathsf{b}\rangle\right)\left(\langle R,\mathsf{b}|\frac{1}{\tilde{L}}\sum_k c_k(t_1)c_k^\dagger(0)|R,\mathsf{a}\rangle\right)$$

$$(5.482)$$

The inner products in the last line eventually produce $\delta_{\mathsf{a}\mathsf{b}}$, and the flavor symmetry further implies that $\langle R,\mathsf{a}|\frac{1}{\tilde{L}}\sum_i c_i(t+\delta t)c_i^\dagger(t)|R,\mathsf{a}\rangle$ is actually independent of a. The last line of (5.482) is thus equal to

$$(\dim R)\left(\frac{1}{\tilde{L}\dim R}\operatorname{tr}_{R\otimes\square}\left(e^{-it_{32}H'}\right)\right)\left(\frac{1}{\tilde{L}\dim R}\operatorname{tr}_{R\otimes\square}\left(e^{-it_1 H'}\right)\right)$$

$$=(\dim R)\left(\frac{1}{\tilde{L}\dim R}\sum_{J\in\mathscr{J}_R}\operatorname{tr}_{R\sqcup\square_J}\left(e^{-it_{32}H'}\right)\right)\left(\frac{1}{\tilde{L}\dim R}\sum_{K\in\mathscr{J}_R}\operatorname{tr}_{R\sqcup\square_K}\left(e^{-it_1 H'}\right)\right)$$

$$=(\dim R)\left(\sum_{J\in\mathscr{J}_R}e^{-i(t_3-t_2)E_J(\mu)}\frac{\dim(R\sqcup\square_J)}{\tilde{L}\dim(R)}\right)\left(\sum_{K\in\mathscr{J}_R}e^{-it_1 E_K(\mu)}\frac{\dim(R\sqcup\square_K)}{L\dim(R)}\right).$$

$$(5.483)$$

Additionally, when summing over the spectator index $\dot{\mathsf{a}}$ the expression will acquire a factor $\dim\phi(R)$. Altogether it manifestly factorizes into the desired product of two-point functions.

The second term in (5.481) is suppressed by $1/L$. Indeed, inserting successive resolutions of the identity, we obtain:

$$\frac{1}{\tilde{L}^2}\sum_{ij\mathsf{a}}\langle R,\mathsf{a}|c_i(t_3)c_j^\dagger(t_2)c_j(t_1)c_i^\dagger(0)|R,\mathsf{a}\rangle$$

$$=\frac{1}{\tilde{L}^2}\sum_{ij\mathsf{a}}\sum_{J,K\in\mathscr{J}_R}\sum_{\hat{\mathsf{a}}\hat{\mathsf{b}}}\exp\{it_3 H'(R,\phi(R))-it_{32}H'(R\sqcup\square_K,\phi(R))-it_1 H'(R\sqcup\square_J,\phi(R))\}$$

$$\times\langle R\sqcup\square_J,\hat{\mathsf{a}}|R,\mathsf{a};i\rangle\langle R,\mathsf{a};i|R\sqcup\square_K,\hat{\mathsf{b}}\rangle\langle R\sqcup\square_K,\hat{\mathsf{b}}|c_j^\dagger e^{-it_{21}H'}c_j|R\sqcup\square_J,\hat{\mathsf{a}}\rangle.$$

$$(5.484)$$

In this expression $\hat{\mathsf{a}}=1,\ldots,\dim(R\sqcup\square_J)$ and $\hat{\mathsf{b}}=1,\ldots,\dim(R\sqcup\square_K)$. In the last line, the first two inner products together impose $\delta_{JK}\delta_{\hat{\mathsf{a}}\hat{\mathsf{b}}}$. We can then use the normalization formula (5.477) and simplifying, we obtain the expression

$$\frac{1}{\tilde{L}^2}\sum_K\sum_{j\hat{\mathsf{b}}}e^{i(t_3-t_2+t_1)[H'(R,\phi(R))-H'(R\sqcup\square_K,\phi(R))]}\langle R\sqcup\square_K,\hat{\mathsf{b}}|c_j^\dagger c_j|R\sqcup\square_K,\hat{\mathsf{b}}\rangle.$$

$$(5.485)$$

The innermost sum evaluates to $\dim(R \sqcup \square_K)$, and the overall factor is $1/\tilde{L}^2$, which means that the contribution is suppressed compared to a two-point function that has an overall factor $1/\tilde{L}$. This is consistent with the fact that the two-point function $\langle c_j^\dagger(t_2) c_j(t_1) \rangle$ is zero in the probe approximation. $\qquad\square$

cor. *The first term on the right-hand side of* (5.472) *equals in the planar limit the first line in* (5.471).

Proof. By hypothesis, the correlator $G_{ijkl}^{(1)}(t_1, t_2, t_3)$ localizes on a large saddle in the large L limit, so we can use the previous computation to conclude that it factorizes. After summing terms that are identically zero, we get that the first term on the right-hand side of (5.472) reduces to $G_{ijkl}^{(1)}(t_1, t_2, t_3)$ which, by formula (5.483) in the previous lemma, yields in the planar limit the first line in (5.471), as claimed. $\quad\square$

Intermezzo: Bosonic statistic and symmetric representation

By definition, the two-particle probe state lives in the symmetric representation,

$$c_i^\dagger c_j^\dagger |0\rangle_{\text{probe}} = \frac{|i, j\rangle_{\text{probe}} + |j, i\rangle_{\text{probe}}}{\sqrt{2}} \in \square\square. \qquad (5.486)$$

For simplicity of notation, here we assume $i \neq j$, and the neglected term is suppressed by $1/L$, thus safely discarded at later steps. The state $|R, \mathsf{a}\rangle$ is tensored with the latter probe state, not with $|j, i\rangle_{\text{probe}} \in \square \otimes \square$.

Hence, we will denote

$$R \sqcup \square\square_{(JK)} \subset (R \sqcup \square_J) \sqcup \square_K \oplus (R \sqcup \square_K) \sqcup \square_J \qquad (5.487)$$

the symmetrization of the ways of appending two boxes, one at the end of the Jth row and the other at the end of the Kth row, to the Young diagram for R. This notation is to insist on the fact that the bosonic statistics of the probe forces the resulting state to live in the Hilbert space sector $\mathscr{H}(R \otimes \square\square)$, rather than generically in $\mathscr{H}(R \otimes \square \otimes \square)$. At the level of Hilbert spaces we have a generic state

$$|R \sqcup \square\square_{(JK)}, \check{\mathsf{c}}\rangle = \frac{\xi}{\sqrt{2}} \left[|(R \sqcup \square_J) \sqcup \square_K, \check{\mathsf{c}}\rangle + |((R \sqcup \square_K) \sqcup \square_J), \check{\mathsf{c}}\rangle \right], \quad (5.488)$$

for all $\check{\mathsf{c}} = 1, \ldots, \dim(R \sqcup \square_J \sqcup \square_K)$, and ξ is a phase, see around Equation (5.507) for a more detailed justification. Note that the dimension is manifestly insensitive to the order in which the boxes are appended to the rows, thus the definition is well

posed. Likewise, the Hamiltonian is insensitive to the ordering, so we can simply write $H'(R \sqcup \square_J \sqcup \square_K)$.

In the calculation of the second correlation function, we will repeatedly use the notation on the left-hand side of (5.488) to signify the result of tensoring with the symmetric probe state.

Step 3: Second correlation function

We now turn to the second expression $G^{(2)}_{ijkl}(t_1, t_2, t_3)$. Similarly, for any given representation R (ignoring potential antisymmetric terms),

$$
\sum_{\mathsf{a}} \langle R, \mathsf{a} | c_i(t_3) c_j(t_2) c_k^\dagger(t_1) c_l^\dagger(0) | R, \mathsf{a} \rangle = \delta_{ik} \delta_{jl} \sum_{\mathsf{a}} \langle R, \mathsf{a} | c_i(t_3) c_j(t_2) c_i^\dagger(t_1) c_j^\dagger(0) | R, \mathsf{a} \rangle
$$

$$(5.489)$$

$$
+ \delta_{il} \delta_{jk} \sum_{\mathsf{a}} \langle R, \mathsf{a} | c_i(t_3) c_j(t_2) c_j^\dagger(t_1) c_i^\dagger(0) | R, \mathsf{a} \rangle
$$

$$
- \delta_{ijkl} \sum_{\mathsf{a}} \langle R, \mathsf{a} | c_i(t_3) c_i(t_2) c_i^\dagger(t_1) c_i^\dagger(0) | R, \mathsf{a} \rangle.
$$

Just like before, averaging over i, j, k, l in the large L limit only the first two terms are not suppressed and we obtain

$$
\frac{1}{L^2} \sum_{ijkl} \sum_{\mathsf{a}} \langle R, \mathsf{a} | c_i(t_3) c_j(t_2) c_k^\dagger(t_1) c_l^\dagger(0) | R, \mathsf{a} \rangle \approx \frac{1}{\tilde{L}^2} \sum_{ij\mathsf{a}} \langle R, \mathsf{a} | c_i(t_3) c_j(t_2) c_i^\dagger(t_1) c_j^\dagger(0) | R, \mathsf{a} \rangle
$$

$$(5.490)$$

$$
+ \frac{1}{\tilde{L}^2} \sum_{ij\mathsf{a}} \langle R, \mathsf{a} | c_i(t_3) c_j(t_2) c_j^\dagger(t_1) c_i^\dagger(0) | R, \mathsf{a} \rangle.
$$

Unlike the previous case, both terms give a nonzero contribution in the probe approximation.

Lemma 5.14.3. *Both terms in the right-hand side of* (5.490) *factorize into the product two two-point functions.*

Proof of the first term in (5.490). Inserting successive resolutions of the identity,

the first term on the right-hand side of (5.490) gives

$$\frac{1}{\tilde{L}^2} \sum_{ija} \langle R, \mathsf{a} | c_i(t_3) c_j(t_2) c_i^\dagger(t_1) c_j^\dagger(0) | R, \mathsf{a} \rangle$$

$$= \sum_{J,K \in \mathscr{J}_R} \sum_{(MP) \in \mathscr{J}_R^{(2)}} e^{it_3 H'(R,\phi(R)) - it_{32} H'(R \sqcup \square_K, \phi(R)) - it_1 H'(R \sqcup \square_J) - it_{21} H'(R \sqcup \square_M \sqcup \square_P)}$$

$$\times \frac{1}{\tilde{L}^2} \sum_{ija} \sum_{\hat{\mathsf{a}}\hat{\mathsf{b}}} \langle R, \mathsf{a} | c_i | R \sqcup \square_K, \hat{\mathsf{b}} \rangle \langle R \sqcup \square_J, \hat{\mathsf{a}} | c_j^\dagger | R, \mathsf{a} \rangle$$

$$\times \sum_{\check{\mathsf{c}}} \langle R \sqcup \square_K, \hat{\mathsf{b}} | c_j | R \sqcup \square\square_{(MP)}, \check{\mathsf{c}} \rangle \langle R \sqcup \square\square_{(MP)}, \check{\mathsf{c}} | c_i^\dagger | R \sqcup \square_J, \hat{\mathsf{a}} \rangle,$$

$$(5.491)$$

where the indices are $\hat{\mathsf{a}} = 1, \ldots, \dim(R \sqcup \square_J)$, $\hat{\mathsf{b}} = 1, \ldots, \dim(R \sqcup \square_K)$ and $\check{\mathsf{c}} = 1, \ldots, \dim(R \sqcup \square_M \sqcup \square_P)$. In this expression, $(MP) \in \mathscr{J}_R^{(2)}$ stands for the symmetrization of the ways of appending two boxes at the end of the Mth and P^{th} rows, as explained above in Subsection 5.14 — cf. the prescription (5.488).

Letting c_j act on the right and $c_i^\dagger$ act on the left, we note that the last line of (5.491) vanishes unless $K \in \{M, P\}$ and $J \in \{M, P\}$. Moreover, as we now show in more detail, the leading contribution comes from the case in which $K = M$ and $J = P$ or $J = M$ and $K = P$, while the other cases, which require $J = K$, are sub-leading in the planar limit.

To formalize the previous sentence, let us fix J, K, M, P and introduce the projections onto $R \sqcup \square_J$ and $R \sqcup \square_K$, denoted Π_J and Π_K, respectively. The last two lines of (5.491) can be recombined in such a way to remove the sums over $\mathsf{a}, \hat{\mathsf{a}}, \hat{\mathsf{b}}$, and we get

$$\frac{1}{\tilde{L}^2} \sum_{ij} \sum_{\check{\mathsf{c}}} \langle R \sqcup \square\square_{(MP)}, \check{\mathsf{c}} | c_i^\dagger \Pi_J c_j^\dagger c_i \Pi_K c_j | R \sqcup \square\square_{(MP)}, \check{\mathsf{c}} \rangle$$

$$= \frac{1}{\tilde{L}^2} \sum_{ij} \sum_{\check{\mathsf{c}}} \Big[\langle R \sqcup \square\square_{(MP)}, \check{\mathsf{c}} | c_i^\dagger \Pi_J c_i c_j^\dagger \Pi_K c_j | R \sqcup \square\square_{(MP)}, \check{\mathsf{c}} \rangle \qquad (5.492)$$

$$- \delta_{ij} \langle R \sqcup \square\square_{(MP)}, \check{\mathsf{c}} | c_i^\dagger \Pi_J \Pi_K c_j | R \sqcup \square\square_{(MP)}, \check{\mathsf{c}} \rangle \Big].$$

If $J = K$, these two terms cancel at leading order in the large L limit and the contribution is suppressed. If $J \neq K$, then the second term vanishes, and the first term is nonzero if and only if the sets $\{M, P\}$ and $\{J, K\}$ are equal. In that case, we insert a resolution of the identity for the basis of $R \otimes \square\square$ between c_i and $c_j^\dagger$,

obtaining

$$\sum_{\check{c}} \frac{1}{\tilde{L}^2} \sum_{ij} \langle\!\langle R \sqcup \square\square_{(JK)}, \check{c}| c_i^\dagger \Pi_J c_i c_j^\dagger \Pi_K c_j | R \sqcup \square\square_{(JK)}, \check{c}\rangle\!\rangle$$

$$= \sum_{\check{c}} \sum_{(M'P')\in\mathscr{J}_R^{(2)}} \sum_{\check{d}} \langle\!\langle R \sqcup \square\square_{(JK)}, \check{c}| \frac{1}{\tilde{L}} \sum_i c_i^\dagger \Pi_J c_i | R \sqcup \square\square_{(M'P')}, \check{d}\rangle\!\rangle \quad (5.493)$$

$$\times \langle\!\langle R \sqcup \square\square_{(M'P')}, \check{d}| \frac{1}{\tilde{L}} \sum_j c_j^\dagger \Pi_K c_j | R \sqcup \square\square_{(JK)}, \check{c}\rangle\!\rangle,$$

with symmetrization over the added boxes, as explained around (5.488).

Similar to the computation in step 2, the non-vanishing contributions come from $\{M', P'\} = \{J, K\}$ and $\check{d} = \check{c}$, and all the summands have the same value. We can therefore rewrite the expression as

$$\frac{1}{\dim(R \sqcup \square_J \sqcup \square_K)} \sum_{\check{c}} \langle\!\langle R \sqcup \square\square_{(JK)}, \check{c}| \frac{1}{\tilde{L}} \sum_i c_i^\dagger \Pi_J c_i | R \sqcup \square\square_{(JK)}, \check{c}\rangle\!\rangle$$

$$\times \sum_{\check{d}} \langle\!\langle R \sqcup \square\square_{(JK)}, \check{d}| \frac{1}{\tilde{L}} \sum_j c_j^\dagger \Pi_K c_j | R \sqcup \square\square_{(JK)}, \check{d}\rangle\!\rangle$$

$$= \frac{1}{\tilde{L}^2 \dim(R \sqcup \square_J \sqcup \square_K)} \left(\sum_{i,\hat{a},\check{c}} |\langle\!\langle R \sqcup \square\square_{(JK)}, \check{c}| c_i^\dagger | R \sqcup \square_J, \hat{a}\rangle\!\rangle|^2 \right)$$

$$\times \left(\sum_{j,\hat{b},\check{d}} |\langle\!\langle R \sqcup \square\square_{(JK)}, \check{d}| c_j^\dagger | R \sqcup \square_K, \hat{b}\rangle\!\rangle|^2 \right). \quad (5.494)$$

Acting with the creation operator $c_i^\dagger$ in the first bracket we get the state $|R \sqcup \square_J, \hat{a}; i\rangle\!\rangle$, to be contracted with $\langle\!\langle R \sqcup \square\square_{(JK)}, \check{c}|$. Could we forget about the symmetrization and replace $R \sqcup \square\square_{(JK)}$ with $R \sqcup \square_J \sqcup \square_K$, then we would simply apply the left-hand side of (5.477), with R there replaced by $R \sqcup \square_J$ and labels (j, J) there replaced by (i, K). Doing the residual sum over $\check{c}$, we would conclude that the first bracket contributes $\dim(R \sqcup \square_J \sqcup \square_K)$. The same applies to $c_j^\dagger | R \sqcup \square_K, \hat{b}\rangle\!\rangle$.

Let us now track more carefully the effect of the symmetrization due to the bosonic nature of the probe.

(i) Throughout this analysis, we neglect the probe states in which the two particles are created in the same index, i.e., states $|k, l\rangle$ are assumed to have $k \neq l$. We are thus neglecting $O(1/L)$ contributions, and our claims are valid at large L.

(ii) The state in the bra (both in the first and second line of (5.494)) comes from the Clebsch–Gordan expansion of states of the form $|R, \mathsf{a}\rangle \otimes \frac{|k,l\rangle_{\text{probe}} + |l,k\rangle_{\text{probe}}}{\sqrt{2}}$.

(iii) We can now expand the state by tensoring with each of the two summands. From (5.488), we write schematically

$$|R \sqcup \square\square_{(JK)}, \check{c}\rangle = \frac{\xi}{\sqrt{2}} \left[|(R \sqcup \square_J) \sqcup \square_K, \check{c}\rangle + |((R \sqcup \square_K) \sqcup \square_J), \check{c}\rangle \right],$$

(5.495)

with ξ a phase. Here we have traded the symmetrization over the probe indices to an exchange of the order of the projectors on the boxes — see around Equation (5.507) for a rigorous justification.

We observe that the projection onto the symmetric representation $\square\square$ that appears in the Clebsch–Gordan decomposition of $\square \otimes \square$ induces a projector onto $\mathscr{H}(R \otimes \square\square)$ from $\mathscr{H}(R \otimes \square \otimes \square)$, for all R. In the following, we denote by Π_{sym} this projection acting on the Hilbert space.

(iv) The $1/\sqrt{2}$ becomes a weight $1/2$ in the sum due to the absolute value square. After contraction, it cancels against a factor of 2 produced from the ket, yielding 1.

(v) The state in the ket of the first line of (5.494) is in $(R \sqcup \square_J) \otimes \square$, indexed by the pair $(\hat{a}, i)$; likewise, the state in the ket of the second line of (5.494) is in $(R \sqcup \square_K) \otimes \square$, indexed by the pair $(\hat{b}, j)$.

(vi) Contracting with the bra, using the projectors on the ket, and the orthogonality relations for the basis of $R \otimes \square \otimes \square$, we conclude that only one of the states labelled by $(\hat{a}, i)$ (respectively $(\hat{b}, j)$) in the first (respectively second) line of (5.494) contributes non-trivially, with weight 1.

The conclusion of this argument is reliable in the saddle point approximation, in which the sum over R localizes onto a large Young diagram.

In this way, we obtain a total contribution of

$$\frac{1}{\tilde{L}^2} \dim(R \sqcup \square_J \sqcup \square_K) = \frac{1}{\tilde{L}^2} \cdot \frac{\dim(R \sqcup \square_J \sqcup \square_K)}{\dim(R \sqcup \square_K)} \cdot \frac{\dim(R \sqcup \square_K)}{\dim(R)} \cdot \dim(R)$$

$$\approx \dim R \left(\frac{\dim(R \sqcup \square_J)}{\tilde{L} \dim(R)} \right) \left(\frac{\dim(R \sqcup \square_K)}{\tilde{L} \dim(R)} \right). \qquad (5.496)$$

In the second line we have used the planar approximation (5.479) for the ratio of dimensions. The latter formula implies that (5.491) asymptotes to

$$\sum_{J,K \in \mathscr{J}_R} e^{it_3 H'(R,\phi(R)) - it_{32} H'(R \sqcup \square_K, \phi(R)) - it_1 H'(R \sqcup \square_J) - it_{21} H'(R \sqcup \square_J \sqcup \square_K)}$$

$$\times \dim R \left(\frac{\dim(R \sqcup \square_J)}{\tilde{L} \dim(R)} \right) \left(\frac{\dim(R \sqcup \square_K)}{\tilde{L} \dim(R)} \right). \tag{5.497}$$

Using (5.478) and reinserting the $\phi(R)$-dependence, that produces $\dim \phi(R)$, we obtain a term that factorizes into the product of two-point functions in the large L limit (under the assumption of a non-trivial saddle point for the ensemble of representations). $\qquad\square$

Proof of the second term in (5.490). Now we treat the second term in a similar way. In this case, we obtain an analogous formula by inserting successive resolutions of the identity:

$$\frac{1}{\tilde{L}^2} \sum_{ija} \langle R, \mathsf{a} | c_i(t_3) c_j(t_2) c_j^\dagger(t_1) c_i^\dagger(0) | R, \mathsf{a} \rangle$$

$$= \sum_{J,K \in \mathscr{J}_R} \sum_{(MP) \in \mathscr{J}_R^{(2)}} e^{it_3 H'(R,\phi(R)) - it_{32} H'(R \sqcup \square_K, \phi(R)) - it_1 H'(R \sqcup \square_J) - it_{21} H'(R \sqcup \square_M \sqcup \square_P)}$$

$$\times \frac{1}{\tilde{L}^2} \sum_{ija} \sum_{\hat{\mathsf{a}}\hat{\mathsf{b}}} \langle R, \mathsf{a} | c_i | R \sqcup \square_K, \hat{\mathsf{b}} \rangle \langle R \sqcup \square_J, \hat{\mathsf{a}} | c_i^\dagger | R, \mathsf{a} \rangle$$

$$\times \sum_{\check{\mathsf{c}}} \langle R \sqcup \square_K, \hat{\mathsf{b}} | c_j | R \sqcup \square\square_{(MP)}, \check{\mathsf{c}} \rangle \langle R \sqcup \square\square_{(MP)} \check{\mathsf{c}} | c_j^\dagger | R \sqcup \square_J, \hat{\mathsf{a}} \rangle.$$

$$\tag{5.498}$$

This is only nonzero if $K = J$. In this case, the inner sum further simplifies as

$$\sum_{j,\hat{\mathsf{a}},\check{\mathsf{c}}} |\langle R \sqcup \square\square_{(MP)}, \check{\mathsf{c}} | c_j^\dagger | R \sqcup \square_J, \hat{\mathsf{a}} \rangle|^2, \tag{5.499}$$

which is nonzero only if $M = J$ or $P = J$ (without loss of generality one can suppose $M = J$). By the same argument used after (5.494), the piece (5.499) can be approximated by $\dim(R \sqcup \square_J \sqcup \square_P)$. From here together with (5.479) we readily find that expression (5.498) asymptotes to

$$\frac{1}{\tilde{L}^2} \dim(R \sqcup \square_J) \left(\frac{\dim(R \sqcup \square_J \sqcup \square_P)}{\dim(R \sqcup \square_J)} \right) \approx \dim R \left(\frac{\dim(R \sqcup \square_J)}{\tilde{L} \dim(R)} \right) \left(\frac{\dim(R \sqcup \square_P)}{\tilde{L} \dim(R)} \right). \tag{5.500}$$

Similarly, reinserting into the sum over J, K with the various Kronecker δ_{MJ} and so on, we obtain a term that factorizes into the product of two-point functions in the planar limit. □

cor. *The second line on the right-hand side of* (5.472) *reproduce in the planar limit the second and third line on the right-hand side of* (5.471).

Proof. Upon adding to $G^{(2)}_{ijkl}(t_1, t_2, t_3)$ terms that are identically zero (correlation functions of mismatching number of creation and annihilation operators), we get the second piece on the right-hand side of (5.472). On the other hand, the explicit computation in the previous lemma shows that $G^{(2)}_{ijkl}(t_1, t_2, t_3)$ reduces in the planar limit to (5.490).

Comparing the expressions we see that the two lines on the right-hand side of (5.490) reproduce in the planar limit the second and third line on the right-hand side of (5.471). □

Final step: Summing the contributions

Corollary 5.14 equates the first term on the right-hand side of (5.472) with the first line in (5.471), and Corollary 5.14 equates the second term on the right-hand side of (5.472) with the second and third line on the right-hand side of (5.471).

Summing the two concludes the derivation of Proposition 5.14.1.

Complete argument for the large N factorization

We now show that our models have factorizing correlation functions at large N for any $2n$-point function, using a different method than extends to higher point functions more directly. For concreteness we study the four-point function here, and it should be clear how this method straightforwardly generalizes to higher point functions.

Let us focus on the term

$$\frac{1}{L^2} \sum_{ijkl\mathsf{a}} \langle R, \mathsf{a} | c_i(t_3) c_j(t_2) c_k^\dagger(t_1) c_l^\dagger(0) | R, \mathsf{a} \rangle$$

$$= \frac{1}{L^2} \sum_{\substack{J \in \mathscr{J}_R \\ K \in \mathscr{J}_R}} \sum_{(MP) \in \mathscr{J}_R^{(2)}} e^{it_3 H(R, \phi(R)) + (it_2 - it_3) H(R \sqcup \square_K, \phi(R)) - it_1 H(R \sqcup \square_J) + (it_1 - it_2) H(R \sqcup \square_M \sqcup \square_P)}$$

$$\times \sum_{\mathsf{a} ijkl} \langle R, \mathsf{a} | c_i \Pi_K c_j \Pi_{(MP)} c_k^\dagger \Pi_J c_l^\dagger | R, \mathsf{a} \rangle. \tag{5.501}$$

Here, just like above, the various Π_X denote the Young projections onto the representation R with the boxes X adjoined to it. By flavor invariance, each of the inner products in the innermost sum can be nonzero only if the representations in the projectors differ by exactly one box. This is only possible if either $K = J = M$, or if $J = M$ and $K = P$. In the first case, the inner sum on the third line of (5.501) can be rewritten as

$$\sum_{\mathsf{a}ijkl} \langle R, \mathsf{a} | c_i \Pi_K c_j \Pi_{(KP)} c_k^\dagger \Pi_K c_l^\dagger | R, \mathsf{a} \rangle. \tag{5.502}$$

For i a fundamental index, let $\alpha_i^\dagger$ be the operator that tensors a representation with a copy of the fundamental in the state i. On the n-particle bosonic Hilbert space, $c_i^\dagger$ acts as $\sqrt{n} \Pi_{\mathrm{sym}} \alpha_i^\dagger$, where Π_{sym} is the symmetrization projector, explicitly realized in accordance with (5.495). With this notation, (5.502) can be rewritten as

$$2 \sum_{\mathsf{a}ijkl} \langle R, \mathsf{a} | \alpha_i \Pi_K \alpha_j \Pi_{\mathrm{sym}} \Pi_{(KP)} \Pi_{\mathrm{sym}} \alpha_k^\dagger \Pi_K \alpha_l^\dagger | R, \mathsf{a} \rangle. \tag{5.503}$$

Now, $\Pi_{\mathrm{sym}} \Pi_{(KP)} \Pi_{\mathrm{sym}} = \Pi_{(KP)}$, so we can rewrite the expression as

$$2 \sum_{\mathsf{a}ijkl} \langle R, \mathsf{a} | \alpha_i \Pi_K \alpha_j \Pi_{(KP)} \alpha_k^\dagger \Pi_K \alpha_l^\dagger | R, \mathsf{a} \rangle. \tag{5.504}$$

Here, it is useful to pause and understand the meaning of Π_K and $\Pi_{(KP)}$ in more detail. They are projectors on the irreducible representations $R \sqcup \square_K$ and $R \sqcup \square\square_{(KP)}$, respectively. The representation $R \sqcup \square\square_{(KP)}$ is to be understood as the (unique) copy of the representation $R \sqcup \square\square_{(KP)}$ in the tensor product $R \otimes (\square\square)$. It is a linear combination of the form

$$R \sqcup \square\square_{(KP)} = \gamma_1 (R \sqcup \square_K \sqcup \square_P) \oplus \gamma_2 (R \sqcup \square_P \sqcup \square_K), \tag{5.505}$$

with $|\gamma_1|^2 + |\gamma_2|^2 = 1$. $(R \sqcup \square_K \sqcup \square_P)$ and $(R \sqcup \square_P \sqcup \square_K)$ are the respective images of $R \otimes \square \otimes \square$ by the Young projectors with the two last indices at position K then P or P then K. Note that in general, Young projectors are not mutually orthogonal when the tableau shape is the same [419], however here we have a small number of added boxes compared to the size of the tableau, so most of them actually are (for example here they always are when only two boxes are added at different nonadjacent rows to a given Young diagram), and we can neglect this subtlety.

Lemma 5.14.4. $\gamma_1 = \gamma_2$, hence $|\gamma_i|^2 = \frac{1}{2}$ for $i = 1, 2$.

Proof. We now show that the γ_i are equal. Let us consider a vector of the form

$$\frac{1}{\sqrt{2}} \left(|R, \mathsf{a}; ij\rangle + |R, \mathsf{a}; ji\rangle \right). \tag{5.506}$$

We can safely assume that the boxes are added to different rows, as in this way the neglected contributions are suppressed in the large N limit. Then, the representations $(R \sqcup \square_K) \sqcup \square_P$ and $(R \sqcup \square_P) \sqcup \square_K$ with $P \neq K$ are orthogonal to each other, and we can write:

$$\langle\!\langle R \sqcup \square\square_{(KP)}, \check{\mathsf{c}} | \frac{1}{\sqrt{2}} \left(|R, \mathsf{a}; ij\rangle + |R, \mathsf{a}; ji\rangle \right) = \frac{1}{\sqrt{2}} \langle\!\langle (R \sqcup \square_K) \sqcup \square_P, \check{\mathsf{c}} | \left(|R, \mathsf{a}; ij\rangle + |R, \mathsf{a}; ji\rangle \right)$$

$$\tag{5.507}$$

$$+ \frac{1}{\sqrt{2}} \langle\!\langle (R \sqcup \square_P) \sqcup \square_K, \check{\mathsf{c}} | \left(|R, \mathsf{a}; ij\rangle + |R, \mathsf{a}; ji\rangle \right).$$

We want to show the two terms on the right-hand side are equal. It is therefore useful to compute their difference. Multiplying by $\sqrt{2}$ and expanding it we obtain:

$$\langle\!\langle (R \sqcup \square_K) \sqcup \square_P, \check{\mathsf{c}} | \left(|R, \mathsf{a}; ij\rangle + |R, \mathsf{a}; ji\rangle \right) - \langle\!\langle (R \sqcup \square_P) \sqcup \square_K, \check{\mathsf{c}} | \left(|R, \mathsf{a}; ij\rangle + |R, \mathsf{a}; ji\rangle \right)$$

$$= \langle\!\langle (R \sqcup \square_K) \sqcup \square_P, \check{\mathsf{c}} | R, \mathsf{a}; ij\rangle - \langle\!\langle (R \sqcup \square_P) \sqcup \square_K, \check{\mathsf{c}} | R, \mathsf{a}; ji\rangle$$

$$+ \langle\!\langle (R \sqcup \square_K) \sqcup \square_P, \check{\mathsf{c}} | R, \mathsf{a}; ji\rangle - \langle\!\langle (R \sqcup \square_P) \sqcup \square_K, \check{\mathsf{c}} | R, \mathsf{a}; ij\rangle. \tag{5.508}$$

Going back to (5.501), the two terms in the second line are equal by definition of the representations $(R \sqcup \square_P) \sqcup \square_K$ and $(R \sqcup \square_K) \sqcup \square_P$, respectively, and the same goes for the two terms in the third line. Therefore, we obtain that any element of $R \otimes (\square\square)$ has equal overlap with $(R \sqcup \square_P) \sqcup \square_K$ and $(R \sqcup \square_K) \sqcup \square_P$, up to corrections negligible in the large N limit. In particular $\gamma_1 = \gamma_2$, and $|\gamma_i|^2$ is constant equal to $1/2$. $\qquad\square$

When $\alpha_j^\dagger$ acts on $R \sqcup \square_K$ in (5.504), the only nonzero term after acting with $\Pi_{(KP)}$ comes from its $R \sqcup \square_K \sqcup \square_P$ component (where K and P are not symmetrized). By the above, the previous expression then becomes

$$\frac{2}{2} \sum_{\mathsf{a}ijkl} \langle R, \mathsf{a} | \alpha_i \Pi_K \alpha_j \Pi_{KP} \alpha_k^\dagger \Pi_K \alpha_l^\dagger | R, \mathsf{a}\rangle. \tag{5.509}$$

One can then further remove the intermediate projections (since we are using Young projectors [419]) and find the large N contribution

$$\sum_{\mathsf{a}ijkl} \langle R, \mathsf{a} | \alpha_i \alpha_j \Pi_{KP} \alpha_k^\dagger \alpha_l^\dagger | R, \mathsf{a}\rangle \approx \mathrm{Tr}_{R \otimes \square \otimes \square}(\Pi_{KP}) = \dim(R \sqcup \square_K \sqcup \square_P). \tag{5.510}$$

This is consistent with the factorization shown above. The second term ($J = M, K = P$) works in a similar way: we obtain

$$\sum_{\mathsf{a}ijkl\check{\mathsf{c}}} \langle R, \mathsf{a}|\alpha_i\alpha_j|R \sqcup \Box_J \sqcup \Box_K, \check{\mathsf{c}}\rangle\langle R \sqcup \Box_K \sqcup \Box_J, \check{\mathsf{c}}|\alpha_k^\dagger\alpha_l^\dagger|R, \mathsf{a}\rangle \qquad (5.511)$$

$$= \sum_{\mathsf{a}ijkl\check{\mathsf{c}}} \langle R, \mathsf{a}|\alpha_i\alpha_j|R \sqcup \Box_J \sqcup \Box_K, \check{\mathsf{c}}\rangle\langle R \sqcup \Box_J \sqcup \Box_K, \check{\mathsf{c}}|\alpha_l^\dagger\alpha_k^\dagger|R, \mathsf{a}\rangle. \qquad (5.512)$$

We then find the contribution at large N

$$\sum_{\mathsf{a}ijkl} \langle R, \mathsf{a}|\alpha_i\alpha_j\Pi_{KP}\alpha_l^\dagger\alpha_k^\dagger|R, \mathsf{a}\rangle \approx \mathrm{Tr}_{R\otimes\Box\otimes\Box}(\Pi_{KP}) = \dim(R \sqcup \Box_K \sqcup \Box_P). \quad (5.513)$$

It is a tedious but straightforward exercise to check that this method extends to higher point functions and different orders of c_i and $c_i^\dagger$, yielding large N factorization.

Chapter 6

BOUNDS ON SPECTRAL GAPS OF HYPERBOLIC SPIN SURFACES

This chapter is based on the work [201], in collaboration with Sridip Pal, David Simmons-Duffin and Yixin Xu.

6.1 Introduction

In this chapter, we derive new upper bounds on the first nonzero eigenvalue of Laplace and Dirac operators on compact orientable hyperbolic surfaces and orbifolds with spin. Our approach is inspired by a technique known in high energy physics as the conformal bootstrap [393, 415, 282, 384, 383]. Bootstrap methods have already been successfully applied to bound the first nonzero eigenvalue of the Laplace operator on hyperbolic surfaces [283, 67, 68] and hyperbolic 3-manifolds [71], see also [70, 69]. A remarkable achievement of [283, 67] is that for several low genera, it improves on the Yang–Yau bounds [460] and its successors [248, 395, 273], as well as the bounds of [245], which collectively had been the strongest bounds available for decades. (In the large genus limit, [245] gives the optimal bound, as was recently shown in [239].)

Recently, [79] used linear programming methods and the Selberg trace formula (STF) to obtain new bounds on Laplacian eigenvalues and other geometric quantities for hyperbolic surfaces. These bounds are stronger than the ones of [283] for genus $g > 6$. However, the technique of [79] cannot immediately be extended to the Dirac operator due to a lack of positivity in the STF with spin. Furthemore, [79] treats orbifolds and manifolds on a separate footing, while [283] treats them uniformly. In this chapter, we follow the methods of [283].

The basic idea of [283] is to leverage the fact that the orthonormal frame bundle of any compact orientable hyperbolic surface or orbifold can be written as $\Gamma\backslash\mathrm{PSL}(2,\mathbb{R})$, where Γ is a cocompact Fuchsian group. Constraints on spectra come from combining the associativity of pointwise multiplication of functions on $\Gamma\backslash\mathrm{PSL}(2,\mathbb{R})$ with the representation theory of $\mathrm{PSL}(2,\mathbb{R})$. By decomposing functions into irreducible representations of $\mathrm{PSL}(2,\mathbb{R})$, and imposing associativity of their pointwise products, one obtains an infinite set of constraint equations on the eigenvalues of the

Laplace operator. Linear programming techniques applied to these equations yield bounds on the spectrum.

We adapt this method to study surfaces and orbifolds with spin structure as follows. Two operators are relevant in this context: the Laplace operator, which is insensitive to the spin structure, and the Dirac operator, which depends on the spin structure. In group-theoretic language, adding a spin structure amounts to considering a quotient of the form $\widetilde{\Gamma}\backslash\mathrm{SL}(2,\mathbb{R})$, where $\widetilde{\Gamma}$ is a lift of the cocompact Fuchsian group Γ to $\mathrm{SL}(2,\mathbb{R})$. Each lift corresponds to a spin structure. We can then study the interplay between associativity of pointwise multiplication of functions on $\widetilde{\Gamma}\backslash\mathrm{SL}(2,\mathbb{R})$ and the representation theory of $\mathrm{SL}(2,\mathbb{R})$. By decomposing functions into irreducible representations of $\mathrm{SL}(2,\mathbb{R})$, and imposing associativity of their pointwise products, we derive spectral identities, which are amenable to linear/semidefinite programming.

Our bounds depend on the number of linearly-independent modular forms of various weights possessed by a surface. For forms of weight 2 or higher, the Riemann–Roch theorem determines their number from purely topological information: the genus and the orders of orbifold points. The situation is different for weight 1 forms (which correspond to harmonic spinors): the number of weight 1 forms can be different for surfaces with the same topology but different geometries. For example, except in genus 4 and 6, a surface carries the maximal possible number of weight 1 modular forms if and only if it is hyperelliptic. This allows us to obtain stronger bounds for hyperelliptic surfaces.

Among our results, we prove the following theorems:

Theorem 6.1.1 (Universal upper bound on Laplacian eigenvalue: I)**.** *Given a compact orientable hyperbolic spin orbifold X, the first non-zero eigenvalue of the Laplacian operator, $\lambda_1^{(0)}(X)$ satisfies*

$$\lambda_1^{(0)}(X) < 12.137980\,.$$

Remark 6.1.2. The above bound is nearly saturated by $[0; 3, 3, 5]$, a genus 0 orbifold with three orbifold singularities of order 3, 3 and 5. We have $\lambda_1^{(0)}([0; 3, 3, 5]) \approx 12.13623$.[1]

---

[1]See Appendix 6.8 for the estimate of the interval $[a_1, b_1]$, which contains $\lambda_1^{(0)}([0; 3, 3, 5])$.

Theorem 6.1.3 (Universal upper bound on Laplacian eigenvalue: II). *Given a compact orientable hyperbolic spin orbifold X admitting a harmonic spinor, the first non-zero eigenvalue of the Laplacian operator, $\lambda_1^{(0)}(X)$ satisfies*

$$\lambda_1^{(0)}(X) < 4.763782\,.$$

Remark 6.1.4. The above bound is nearly saturated by the most symmetric point (see fig. 6.1) of the moduli space of $[1;3]$ i.e a torus with one orbifold singularity of order 3. Let us call the orbifold $[1;3]_{sym}$. Using `FreeFEM++`, we learn that $\lambda_1^{(0)}([1;3]_{sym}) \approx 4.7609$.
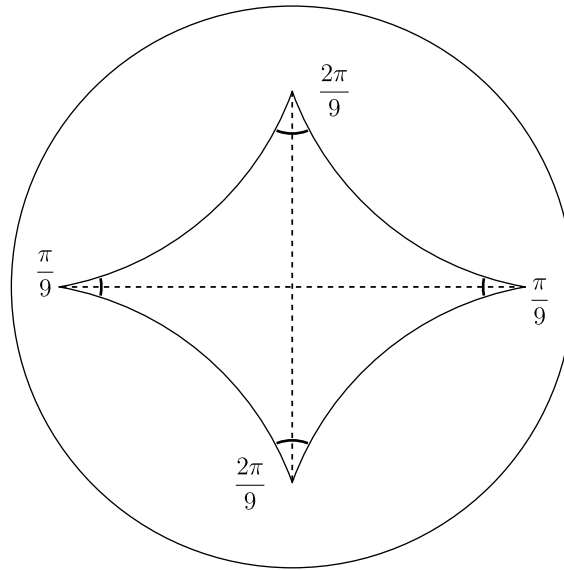
Figure 6.1: A fundamental domain of Γ drawn on the Poincaré disc where Γ is a subgroup of $\mathrm{PSL}(2,\mathbb{R})$ isomorphic to the fundamental group of the most symmetric point in the moduli space of $[1;3]$. This fundamental domain is a hyperbolic quadrilateral symmetric under reflections against the two dashed lines.

More generally, we obtain two types of bounds. The first type are *exclusion plots* in a two-dimensional parameter space, labelled by the first nonzero eigenvalues of the Laplace and Dirac operators. We use $\lambda_1^{(0)}$ to denote the first non-zero Laplacian eigenvalue. For the first non-zero Dirac eigenvalue $t_1^{(1/2)}$, we use the variable $\lambda_1^{(1/2)} := 1/4 + (t_1^{(1/2)})^2$ in the plots. Examples of such plots are given on Figures 6.2, 6.8 and 6.10. Let us focus on Figure 6.2. For any hyperbolic spin orbifold X, equipped with a spin structure such that there is no harmonic spinor, the pair $(\lambda_1^{(0)}(X), \lambda_1^{(1/2)}(X))$ must lie in the union of the pink-shaded and yellow-shaded regions. If the hyperbolic spin orbifold X has genus 1 or more and is equipped with

a spin structure admitting one or more harmonic spinors, then $(\lambda_1^{(0)}(X), \lambda_1^{(1/2)}(X))$ must lie in the pink shaded region. The yellow shaded region as well as the pink one has a kink at rightmost corner. Exclusion plots with kinks are abundant in the conformal bootstrap literature. Often, one can identify the object that lives near the kink. Here a similar phenomenon is true. Indeed, the corner point in the yellow-shaded region is very close to $(\lambda_1^{(0)}([0;3,3,5]), \lambda_1^{(1/2)}([0;3,3,5]))$. See Figure 6.7 for a zoomed-in version of the exclusion plot. For the pink shaded region, the corner point is close to $(\lambda_1^{(0)}(X), \lambda_1^{(1/2)}(X))$, where X is the most symmetric point of the moduli space of $[1;3]$, equipped with the odd spin structure. See Table 6.8 in Appendix 6.8 for the numerical estimates of the eigenvalues corresponding to these nearly saturating examples.

We can derive more specific theorems from the exclusion plot. For example, we prove

Theorem 6.1.5 (Conditional upper bound on Dirac eigenvalue). *Given any compact orientable hyperbolic spin orbifold X such that the first non-zero eigenvalue of the Laplacian operator satisfies $\lambda_1^{(0)}(X) > 1.5$, we have*

$$\lambda_1^{(1/2)}(X) < 55.9\,.$$

Here $\lambda_1^{(1/2)}(X) = 1/4 + t^2$ and $|t|$ is the lowest non-zero positive eigenvalue of Dirac operator on X.

To estimate the Laplace and Dirac eigenvalues of a given surface and compare them with our bounds, we use a numerical method based on the STF, described in [300]. Using this method, we can populate the exclusion plots as shown on Figure 6.2. We also derive more specific exclusion plots, for example Figures 6.10 and 6.11, which describe the bound applicable to all compact orientable hyperbolic genus 2 spin orbifolds. As we can see, $(\lambda_1^{(0)}(X), \lambda_1^{(1/2)}(X))$, where X is the Bolza surface with odd spin strcuture, sit very close to the boundary, see the table 6.8 in Appendix 6.8 for the numerical estimates.

The second type of bound is obtained from the first type, by noticing that the first nonzero eigenvalue of the Dirac operator corresponds to $\lambda_1^{(1/2)}(X) > 1/4$. This leads to upper bounds on the first nonzero eigenvalue of the Laplace operator for a given choice of spin structure, admitting a given number of weight 1 modular form. These upper bounds are collected in Table 6.1. Interestingly, when the spin structure allows for enough harmonic spinors, the upper bounds become more
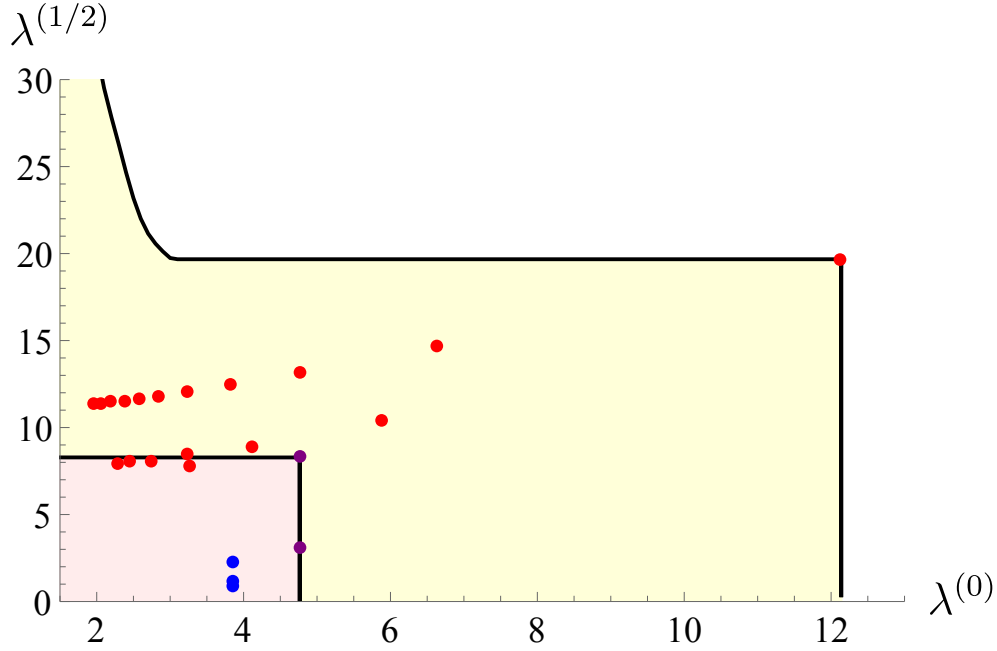
Figure 6.2: For any compact orientable hyperbolic spin orbifold X, equipped with a spin structure such that there is no harmonic spinor, $(\lambda_1^{(0)}(X), \lambda_1^{(1/2)}(X))$ must lie in the union of the pink-shaded and yellow-shaded regions. Note that, even though it is not shown explicitly, we have $\lambda_1^{1/2} > 1/4$. If the hyperbolic spin orbifold X has genus 1 or more and is equipped with a spin structure admitting one or more harmonic spinors, then $(\lambda_1^{(0)}(X), \lambda_1^{(1/2)}(X))$ must lie in the pink shaded region. The red dot in the corner corresponds to $(\lambda_1^{(0)}([0;3,3,5]), \lambda_1^{(1/2)}([0;3,3,5]))$. The other red dots come from the eigenvalues corresponding to various hyperbolic triangles while the blue dots come from the eigenvalues corresponding to the Bolza surface, equipped with various spin structures. The purple dot in the corner of the pink shaded region corresponds to $(\lambda_1^{(0)}([1;3]_{sym}), \lambda_1^{(1/2)}([1;3]_{sym}))$, where $[1;3]_{sym}$ is equipped with an odd spin structure. See the remark 6.1.4. The other purple dot lying on the boundary of the pink shaded region corresponds to $[1;3]_{sym}$, equipped with an even spin structure. See the table 6.8 in Appendix 6.8 for the numerical estimates of these eigenvalues. Here the origin is at $(1.5, 0)$.

stringent. In particular, this leads to improved upper bounds on the first Laplace eigenvalue for hyperelliptic surfaces compared to [283]. As a warmup, we can use a small number of spectral identities to derive a very simple analytical bound for genus g hyperelliptic surfaces by using the fact that they can be equipped with a spin structure, admitting $\lfloor \frac{g+1}{2} \rfloor$ harmonic spinors.

g	$\ell_{1/2}$	$\lambda_1^{(0)}(g, \ell_{1/2})$	KMP [283]	FP [79]
2	0,1	3.8388976481	3.8388976481	4.625307
3	0,1 2	2.6784823893 1.9497673318*	2.6784823893	2.816427
4	0,1 2	2.1545041334 1.9497673318*	2.1545041334	2.173806
5	0,1,2 3	1.8526509456 1.18275751*	1.8526509456	1.836766
6	0,1,2 3	1.654468363 1.386265630*	1.654468363	1.625596
7	0,1,2 3 4	1.51326783 1.38626563* 0.9160143*	1.51326783	1.480008
8	0,1,2 3 4	1.40690466 1.38626563* 1.0443114*	1.40690466	1.372804
9	0,1,2,3 4 5	1.32348160 1.148493243* 0.78690*	1.32348160	1.289024
10	0,1,2,3 4 5	1.25602193 1.148493243* 0.85292*	1.25602193	1.222189

Table 6.1: Table of upper bounds on the Scalar-Laplacian gap as a function of genus and the number of harmonic spinors. For comparison, we also tabulate the spinor-independent bounds from [283] and [79]. We note that bounds from [79] are only applicable to manifolds while the bounds from [283] and the bounds in this chapter are applicable to both manifolds and orbifolds. For $2 \leqslant g \leqslant 10$, the bounds here coincide with the ones from [283], except when, given the genus g, the surface admits a spin structure such that number of harmonic spinors is strictly more than $\lceil \ell_{Max}/2 \rceil$, where $\ell_{Max} = \lfloor (g+1)/2 \rfloor$ is the maximal number of harmonic spinors allowed for that genus. In that case, the bounds are more restrictive; we mark them with *.

Theorem 6.1.6. *Given a genus $g \geq 3$ compact hyperbolic hyperelliptic surface X, we must have*

$$\lambda_1^{(0)}(X) \leq \frac{\lfloor \frac{g+1}{2} \rfloor}{\lfloor \frac{g+1}{2} \rfloor - 1} \,. \tag{6.1}$$

Remark 6.1.7. For a given numerical value of g, it is possible to achieve a much stronger bound using computer assistance. This is evident from table 6.1, upon using the fact that the hyperelliptic surfaces can be equipped with a spin structure
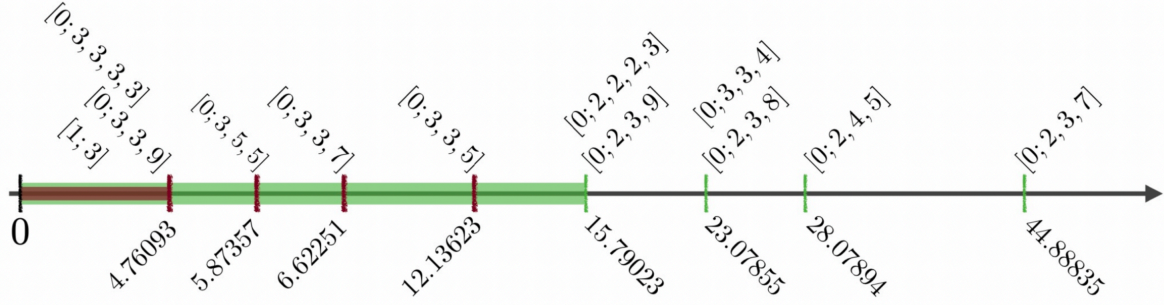
Figure 6.3: Pictorial description of Conjecture 6.1.8: The green color denotes the set of $\lambda_1^{(0)}(X)$, as X runs over all compact orientable hyperbolic orbifolds. The red color denotes the set of $\lambda_1^{(0)}(X)$, as X runs over all compact orientable hyperbolic orbifolds equipped with a spin structure. The red continuum comes from the moduli space of $[1; 3]$ and $[0; 3, 3, 3, 3]$ while the green continuum comes from the moduli space of $[0; 2, 2, 2, 3]$. This conjecture is a refinement of Conjecture 4.2 in [283] as one can see that the red continuum along with 3 discrete red points lie entirely within the green continuum.

which admits $\ell_{1/2} = \lfloor \frac{g+1}{2} \rfloor$.

Using the STF, we can compute the location of $\lambda_1^{(0)}(X)$ for many orbifolds. Combining these numerical data, we also put forward the following conjecture:

Conjecture 6.1.8. *Let $\lambda_1^{(0)}(X)$ be the first non-zero eigenvalue of the Laplacian on an hyperbolic orbifold X. Let $E_{\text{spin}} \subset \mathbb{R}_{>0}$ be the set of $\lambda_1^{(0)}(X)$ as X runs over all compact hyperbolic spin orbifolds. Then E_{spin} is the union of the interval $\left(0, \lambda_1^{[3,3,9]}\right]$ with the finite set $\left\{\lambda_1^{[3,3,5]}\right\} \cup \left\{\lambda_1^{[3,5,5]}\right\} \cup \left\{\lambda_1^{[3,3,7]}\right\}$. When X is an orbifold with signature $[0; k_1, k_2, k_3]$, we write $\lambda_1^{[k_1,k_2,k_3]}$ to denote $\lambda_1^{(0)}([0; k_1, k_2, k_3])$. See Figure 6.3.*

Remark 6.1.9. The above conjecture is a refinement of Conjecture 4.2 in [283], where the relevant set $E \subset \mathbb{R}_{>0}$ was the set of $\lambda_1^{(0)}(X)$ as X runs over all orbifolds. We believe that this conjecture can partially be proven by bootstrapping the spectral identities as done for Conjecture 4.2 in [283].

To put the above results in context, let us make some historical remarks. The Dirac operator (in particular, the twisted Dirac operator, i.e., Dirac operator in presence of a gauge connection) plays numerous interesting roles in physics. An upper bound on the spectral gap of such a twisted Dirac operator was found for the first time in the context of QCD in a chapter by Vafa and Witten [442], followed

by a chapter by Atiyah [28]. These two chapters prove a *uniform upper bound* (uniform with respect to the gauge connection) on the nth nontrivial eigenvalue of the twisted Dirac operator on a compact Riemannian spin manifold in any dimension D. Similar methods were used to arrive at further specialized bounds in [42] in terms of a smooth map from the manifold to the sphere. They further derived bounds for surfaces with positive sectional curvature. Ref.[4] derived extrinsic bounds on Dirac eigenvalues for isometrically immersed surfaces inside $\mathbb{R}^3$ in terms of mean curvature and a smooth function from the surface to $\mathbb{R}$, as well as intrinsic bounds for genus 0 and genus 1 surfaces. Finally, lower bounds for the first nonzero Dirac eigenvalue have also been studied for various kinds of spin manifolds [35], for general manifolds of positive curvature [178, 37], as well as in the case of surfaces depending on some geometric parameters including the choice of spin structure [34, 16]. For a general discussion on the spectrum of the Dirac operator on various kinds of Riemannian manifolds, we refer the readers to [179] for a review, or [36] for details on the hyperbolic case.

Our bounds have a different flavor from these results, and it is not straightforward to directly compare them. In particular, our method encodes interesting interplays between eigenvalues of Laplacian operator and eigenvalues of Dirac operator on a hyperbolic spin orbifold, for example, see Theorem 6.1.5 or Figure 6.2.

Organization of the chapter

The rest of this chapter is organized as follows. In Section 6.2, we introduce the basic notions of spectral geometry that we will need. In Section 6.3, we derive our constraint equations from associativity and harmonic analysis. In Section 6.4, we use the Selberg trace formula to develop a numerical technique to estimate the Dirac and Laplace spectra of an orbifold of interest. In Section 6.5, we derive our main bounds and exclusion plots. In Section 6.6, we discuss a few possible future directions that our results suggest. In Appendix 6.7, we relate the number of harmonic spinors a surface of low genus can carry to its geometrical properties. In Appendix 6.8 we tabulate the numerical estimates of $\lambda_1^{(0)}$ and $\lambda_1^{(1/2)}$ for various surfaces and orbifolds.

We emphasize that while the search for functionals in our linear/semidefinite programming algorithm necessitates computer assistance, the output can be rationalized in such a way that one can explicitly exhibit the required properties of the rationalized functionals leading to the bounds (such verifications of bounds coming from

linear/semidefinite programming using *rational arithmetic* appear in many contexts, for example in sphere packing [111] and in ref. [283]). Consequently, the proofs of our theorems are completely rigorous and the computer is only used as an oracle. It is only in Section 6.4 that our individual estimates, which are independent from the theorems, are numerical and not proven at a mathematical level, although it should also be possible to do so.

Technical note: Unless specified otherwise, all surfaces or orbifolds considered in this chapter are connected, compact and orientable.

6.2 Spectral geometry on a spin-surface

Dirac operator and Automorphic Laplacian

Let us consider a d-dimensional orientable connected Riemannian manifold (X, g) and the orthonormal frame bundle over X, $(Q, \pi, X; SO(d))$; here Q is the total space, $\pi : Q \to X$ is the projection map. We will often suppress π and write the shorthand $Q(X)$ to mean the orthonormal frame bundle over X. A spin structure on this principal bundle Q is a pair (P, Λ) such that P is a $\mathrm{Spin}(d)$-principal bundle and there exists a principal bundle morphism $\Lambda : P \to Q$, that is equivariant with respect to the double covering $\mathrm{Spin}(d) \to SO(d)$. A spin structure on Q exists if and only if the second Stiefel-Whitney class of the $SO(d)$ principal bundle vanishes.

To set the stage, we restrict our attention to the upper half-plane $\mathbb{H} := \{(x, y) \in \mathbb{R}^2 : y > 0\}$. The metric g is given by the Poincaré metric, i.e.,

$$ds^2 = \frac{dx^2 + dy^2}{y^2} \,. \tag{6.2}$$

There exists a unique spin structure on the orthonormal frame bundle over $\mathbb{H}$ (which is an $SO(2)$ principal bundle). The corresponding $\mathrm{Spin}(2)$ principal bundle is trivial and given by $P = \mathbb{H} \times \mathrm{Spin}(2)$. If ρ is the representation of $\mathrm{Spin}(2)$ on its Clifford module $\mathbb{C}^2$, then the bundle S associated with ρ,

$$S := P \times_\rho \mathbb{C}^2, \tag{6.3}$$

is the spinor bundle over the upper half-plane. The sections of this spinor bundle are spinor fields defined on $\mathbb{H}$. In particular, we will be interested in $\mathfrak{C}^\infty(S)$, the space of smooth sections of the spinor bundle S.

Definition 6.2.1 (Dirac operator on $\mathbb{H}$)**.** The Dirac operator $D\!\!\!/ : \mathfrak{C}^\infty(S) \to \mathfrak{C}^\infty(S)$ is given by[2]

$$D\!\!\!/ := i \begin{bmatrix} 0 & iy\partial_x + y\partial_y - \frac{1}{2} \\ -iy\partial_x + y\partial_y - \frac{1}{2} & 0 \end{bmatrix}. \tag{6.4}$$

Remark 6.2.2. By restricting the domain of $D\!\!\!/$ to $\mathfrak{C}^\infty_c(S)$, the space of smooth compactly supported sections of the spinor bundle S, one can construct a pre-Hilbert space, which can then be promoted to a Hilbert space in the standard way: first, we define the inner product of $f, g \in \mathfrak{C}^\infty_c(S)$ by

$$\langle f, g \rangle := \int_{\mathbb{H}} \langle f(z), g(z) \rangle_{\mathbb{C}^2} \, d\mu(z), \tag{6.5}$$

where μ is the hyperbolic measure on $\mathbb{H}$ and then complete $\mathfrak{C}^\infty_c(S)$ into a Hilbert space $\mathfrak{H}(S)$ using the induced norm. The space $\mathfrak{C}^\infty_c(S)$ is dense inside $\mathfrak{H}(S)$.

Remark 6.2.3. The Dirac operator is elliptic and essentially self-adjoint on $\mathfrak{C}^\infty_c(S)$, which in particular implies that its spectrum is real [66].

A compact connected orientable hyperbolic surface Σ can be thought of as $\Gamma \backslash \mathbb{H}$, where Γ is a cocompact Fuchsian group, a discrete subgroup of $\mathrm{PSL}(2, \mathbb{R})$. More precisely, the cocompact Fuchsian group Γ acts properly discontinuously on $\mathbb{H}$. If $\gamma = \pm \begin{pmatrix} a & b \\ c & d \end{pmatrix} \in \Gamma$, the action is defined by

$$\begin{array}{rcl} \Gamma \times \mathbb{H} & \longrightarrow & \mathbb{H} \\ (\gamma, z) & \longmapsto & \frac{az+b}{cz+d}. \end{array} \tag{6.6}$$

The above induces an action on the orthonormal frame bundle $Q(\mathbb{H}) \cong \mathrm{PSL}(2, \mathbb{R})$, which is simply the action by left multiplication:

$$\begin{array}{rcl} \Gamma \times \mathrm{PSL}(2, \mathbb{R}) & \longrightarrow & \mathrm{PSL}(2, \mathbb{R}) \\ (\gamma, g) & \longmapsto & \gamma \cdot g. \end{array} \tag{6.7}$$

The double cover of the bundle Q is $P(\mathbb{H}) \cong \mathrm{SL}(2, \mathbb{R})$.

Definition 6.2.4. Let $\Gamma \subset \mathrm{PSL}(2, \mathbb{R})$ be a cocompact Fuchsian group. Let $p : \mathrm{SL}(2, \mathbb{R}) \to \mathrm{PSL}(2, \mathbb{R})$ be the canonical projection. We define the $\bar{\Gamma} := p^{-1}(\Gamma)$.

---

[2]For more details on defining the Dirac operator on a d-dimensional oriented connected Riemannian manifold (X, g), see Section 3 of [44].

In order to describe spin structures more directly in terms of the action of Γ, it is convenient to apply the following result to our context:

Proposition 6.2.5 (Ref.[347]). *Spin structures on Σ are in one-to-one correspondence with lifts to $\mathrm{SL}(2, \mathbb{R})$ of the action by left multiplication of Γ on $\mathrm{PSL}(2, \mathbb{R})$. In other words, the spin structures on $\Gamma \backslash \mathbb{H}$ are in one-to-one correspondence with the possible right splittings of the short exact sequence:*

$$1 \longrightarrow \mathbb{Z}_2 \underset{\chi}{\overset{\iota}{\rightleftarrows}} \bar{\Gamma} \underset{\rho}{\overset{p}{\rightleftarrows}} \Gamma \longrightarrow 1. \tag{6.8}$$

The number of right splittings ρ (i.e., ρ for which $p \circ \rho = Id$) of this exact sequence is equal to the number of left splittings χ, for which $\chi \circ \iota = Id$, which amounts to imposing the constraint $\chi(-Id) = -1$. A natural way to establish a one-to-one correspondence between the two is to characterize χ by $\mathrm{Ker}\, \chi = \mathrm{Im}\, \rho$. As a result, we obtain:

Proposition 6.2.6. *Spin structures on a compact orientable smooth Riemann surface Σ can be labelled by homomorphisms $\chi : \bar{\Gamma} \to \mathbb{Z}_2$ satisfying $\chi(-Id) = -1$.*

Remark 6.2.7. In the language of automorphic forms, χ is a multiplier which allows the existence of nontrivial odd weight automorphic forms.

Remark 6.2.8. There is also a geometric interpretation of the morphism χ. If $\tilde{\gamma} \in \bar{\Gamma}$, $\chi(\tilde{\gamma})$ gives the holonomy of the spin bundle along the corresponding closed geodesic.

This new characterization of spin structure in terms of a homomorphism $\chi : \bar{\Gamma} \to \mathbb{Z}_2$ such that $\chi(-Id) = -1$ has the very convenient feature of easily generalizing to the case in which the cocompact Fuchsian group Γ has some elliptic elements, in particular, to the case of orbifolds which will be of particular interest to us. We hence define:

Definition 6.2.9. Let Γ be a general cocompact Fuchsian group. A spin structure on $\Gamma \backslash \mathrm{PSL}(2, \mathbb{R})$ is a group homomorphism $\chi : \bar{\Gamma} \to \mathbb{Z}_2$ such that $\chi(-Id) = -1$.

Remark 6.2.10. Unlike Riemann surfaces, not every orbifold admits a spin structure. In particular, if there exists an element of order 2 in Γ, the injectivity of ρ implies that this element must be mapped to $-\mathrm{Id} \in \bar{\Gamma}$, which lies in the image of ι, hence the kernel of p. This is inconsistent with the fact that $p \circ \rho = \mathrm{Id}$, thus there does not

exist any right splitting of the exact sequence (6.8), which, by the splitting lemma, implies that there does not exist any left splitting χ. Hence even order orbifold points are obstructions to the existence of a spin structure.

Remark 6.2.11. The geometric interpretation of χ naturally extends to the case of orbifolds. In the case of elliptic elements, it gives the holonomy around orbifold singularities.

Proposition 6.2.12 (Ref. [187], Theorem 3). *On a smooth Riemann surface of genus g, there are 2^{2g} spin structures. An orbifold admits a spin structure if and only if all its orbifold points have odd order, and then the number of spin structures is also given by 2^{2g}.*

To define the Dirac operator for Σ, we need to restrict the domain of the $D\!\!\!/$, the Dirac operator on the upper half-plane to special sets of sections (since the bundle is trivial, they are actually functions on $\mathbb{H}$ to $\mathbb{C}^2$) that satisfy the right automorphic properties under $\overline{\Gamma}$.

Definition 6.2.13 (Automorphy factor). For $\gamma = \begin{pmatrix} a & b \\ c & d \end{pmatrix} \in \overline{\Gamma}$, and $2k \in \mathbb{N}$, let us define the automorphy factor $j_\gamma : \mathbb{H} \times \frac{1}{2}\mathbb{N} \to \mathbb{C}$ and $J_\gamma : \mathbb{H} \times \frac{1}{2}\mathbb{N} \to \mathbb{C}^2$ as

$$j_\gamma(z,k) := \frac{(cz+d)^k}{(c\bar{z}+d)^k}, \qquad J_\gamma(z,k) := \begin{pmatrix} j_\gamma(z,k) & 0 \\ 0 & j_\gamma(z,k-1) \end{pmatrix}, \qquad (6.9)$$

where the choice of square roots in the definitions of the numerator and denominator of $j_\gamma(z,k)$ are chosen to be complex conjugate.

Definition 6.2.14. Let Γ be a cocompact Fuchsian group, and let χ be a multiplier of weight $2k \in \mathbb{N}$ on $\overline{\Gamma}$ ($\chi(-\mathrm{Id}) = (-1)^{2k}$). We define the space $\mathfrak{F}(\Gamma, k, \chi)$ as the space of functions $\Psi : \mathbb{H} \to \mathbb{C}^2$ that satisfy

$$\Psi(\gamma z) = \chi(\gamma)J_\gamma(z,k)\Psi(z), \quad \forall \gamma = \begin{pmatrix} a & b \\ c & d \end{pmatrix} \in \overline{\Gamma}. \qquad (6.10)$$

If these functions are asked to be smooth (resp. L^2 over the fundamental domain of Γ), the corresponding space is denoted $\mathfrak{C}^\infty(\Gamma, k, \chi)$ (resp. $\mathfrak{L}^2(\Gamma, k, \chi)$).

It can be checked that $D\!\!\!/$ leaves the space $\mathfrak{C}^\infty(\Gamma, 1/2, \chi)$ invariant and thus we have

Definition 6.2.15 (Dirac operator on Σ). The Dirac operator associated to Σ is defined to be the restriction of $D\!\!\!/$ to $\mathfrak{C}^\infty(\Gamma, 1/2, \chi)$.

Under a slight abuse of notation, we will continue calling $\not{D}$ this Dirac operator with restricted domain. $\mathfrak{C}^\infty(\Gamma, 1/2, \chi)$ is dense inside $\mathfrak{L}^2(\Gamma, 1/2, \chi)$. Compactness of the surface implies that the spectrum of $\not{D}$ is discrete.

Definition 6.2.16. Let Γ be a cocompact Fuchsian group, and let χ be a multiplier of weight $2k$ on $\bar{\Gamma}$ $(\chi(-\mathrm{Id}) = (-1)^{2k})$. We define the space $\mathcal{F}(\Gamma, k, \chi)$ as the space of functions $\psi : \mathbb{H} \to \mathbb{C}$ that satisfy

$$\psi(\gamma z) = \chi(\gamma) j_\gamma(z, k) \psi(z), \quad \forall \gamma = \begin{pmatrix} a & b \\ c & d \end{pmatrix} \in \bar{\Gamma}. \tag{6.11}$$

If these functions are asked to be smooth (resp. L^2 over the fundamental domain of Γ), the corresponding space is denoted $C^\infty(\Gamma, k, \chi)$ (resp. $L^2(\Gamma, k, \chi)$).

Definition 6.2.17. Define the weight $2k$ automorphic Laplacian $\Delta_k : C^\infty(\Gamma, k, \chi) \to C^\infty(\Gamma, k, \chi)$ as

$$\Delta_k := y^2(\partial_x^2 + \partial_y^2) - 2iky\partial_x. \tag{6.12}$$

Remark 6.2.18. The square of the Dirac operator, $\not{D}^2 : \mathfrak{C}^\infty(\Gamma, 1/2, \chi) \to \mathfrak{C}^\infty(\Gamma, 1/2, \chi)$ is given by

$$\not{D}^2 = \begin{pmatrix} -\Delta_{1/2} - \frac{1}{4} & 0 \\ 0 & -\Delta_{-1/2} - \frac{1}{4} \end{pmatrix}. \tag{6.13}$$

$\Delta_{1/2}$ is also called 1-Laplacian.

Now the following key proposition relates the spectrum of $\not{D}$ to that of $\Delta_{1/2}$.

Proposition 6.2.19. *If* $\Psi = \begin{pmatrix} \psi_1 \\ \psi_2 \end{pmatrix}$ *is an eigenform of* $-\not{D}$ *with eigenvalue t, then* ψ_1 *is an eigenform of* $-\Delta_{1/2}$ *with eigenvalue* $\lambda = 1/4 + t^2$. *Conversely, if* ψ *is an eigenform of* $-\Delta_{1/2}$ *with eigenvalue* $\lambda = 1/4 + t^2$, *then* $\Psi = \begin{pmatrix} t\psi \\ i\left(iy\partial_x - y\partial_y + \frac{1}{2}\right)\psi \end{pmatrix}$ *is an eigenform of* $-\not{D}$ *with eigenvalue t.*

Proof. See Proposition 1 of [66] and its proof. $\qquad\qquad\qquad\qquad\qquad\square$

Thus bounding the Dirac spectrum associated to a given surface Σ amounts to bounding the spectra of $\Delta_{\pm 1/2}$ on Σ. Another important feature of the Dirac spectrum is that it has two important symmetries. First, the spectrum of the Dirac operator is symmetric with respect to the origin:

Proposition 6.2.20. *If* $\begin{pmatrix} \psi_1 \\ \psi_2 \end{pmatrix}$ *is an eigenvector of* $D\!\!\!/$ *with eigenvalue t, then* $\begin{pmatrix} \psi_1 \\ -\psi_2 \end{pmatrix}$ *is an eigenvector of* $D\!\!\!/$ *with eigenvalue* $-t$. *In particular, the spectrum of* $D\!\!\!/$ *is symmetric with respect to the origin.*

The Dirac operator enjoys one more symmetry leading to what is called *Kramers degeneracy* (degeneracy is a synonym of multiplicity in the physics literature). This implies that all non-zero eigenvalues of the Dirac operator are at least doubly degenerate,

Proposition 6.2.21 (Kramers degeneracy). *Let C be the complex conjugation operator, and* $\sigma_2 := \begin{pmatrix} 0 & -i \\ i & 0 \end{pmatrix}$. *If* Ψ *is an eigenvector of* $D\!\!\!/$ *with eigenvalue t, then so is* $(i\sigma_2 C)\Psi$.

In quantum field theory, the operator implementing Kramers degeneracy is usually interpreted as the time reversal operator. In Section 6.4, we will use Kramers degeneracy in our algorithm to estimate the spectra of Dirac operator on orbifolds and surfaces. More precisely, we will note that since all the non-zero eigenvalues of the Dirac operator are degenerate, we can use Proposition 6.4.5 instead of Proposition 6.4.4, and look for the first nonzero value of t for which $I_r(\lambda) = 2$, instead of the first nonzero value of t for which $I_r(\lambda) = 1$.

Holomorphic Modular forms and spin structure

A spin structure determines the definition of holomorphic modular forms of odd weight on the surface. Let us recall that for even weights, holomorphic modular forms on a Riemann surface Σ are defined independently from any choice of spin structure. More precisely:

Definition 6.2.22. Let Γ be a cocompact Fuchsian group. A holomorphic Γ-modular form of weight $2k \in 2\mathbb{N}$ is a holomorphic function $f : \mathbb{H} \longrightarrow \mathbb{C}$, such that for all $\gamma : z \mapsto \frac{az+b}{cz+d}$ in Γ,

$$f(\gamma(z)) = (cz + d)^{2k} f(z), \tag{6.14}$$

Note that since $2k$ is an even number, $(cz+d)^{2k}$ has the same value on the two possible lifts of γ inside $\mathrm{SL}(2, \mathbb{R})$, which ensures that the above definition is unambiguous. This changes for odd powers of $cz + d$, because the automorphy factor differs by a

sign depending on the choice of lift. Instead, one must use the spin structure χ as an input to define a modular form of odd weight:

Definition 6.2.23. Let $\chi : \bar{\Gamma} \to \mathbb{Z}_2$ be a group homomorphism (or equivalently, a choice of spin structure on Σ). A holomorphic modular form of weight k for $\bar{\Gamma}$ is a holomorphic function $f : \mathbb{H} \longrightarrow \mathbb{C}$, such that for all $\gamma : z \mapsto \frac{az+b}{cz+d}$ in Γ,

$$f(\gamma(z)) = \chi(\gamma)^k (cz + d)^k f(z). \tag{6.15}$$

In the case of k even, this definition reduces to the previous one and does not depend on the choice of χ, but this is no longer true for k odd.

Our approach will use the number of linearly independent holomorphic modular forms of a given (even or odd) weight as an input to the set of consistency conditions, i.e., *bootstrap* constraints. Therefore, it is important to understand what moduli space of surfaces and orbifolds supports a given number of linearly independent holomorphic modular forms of a given (even or odd) weight. Apart from the case of modular forms of weight 1, this is determined by purely topological data, as shown by the Riemann–Roch theorem, which we now review.

The Riemann–Roch theorem comes from algebraic geometry, and allows to count the number of linearly independent holomorphic modular forms of weight $\geqslant 2$ on Σ only from the information about its topology.

Theorem 6.2.24 (Riemann–Roch for orbifolds). *Let $n \geqslant 2$ and $n \in \mathbb{Z}$. If an orbifold of genus g with elliptic points $p_1, \ldots, p_r$ of orders $k_1, \ldots, k_r$ admits a spin structure, then it possesses*

$$\ell_{n/2} = (n-1)(g-1) + \sum_{i=1}^{r} \left\lfloor \frac{n}{2} \left(1 - \frac{1}{k_i} \right) \right\rfloor + \delta_{n,2} \tag{6.16}$$

holomorphic modular forms of weight n (regardless of the choice of multiplier), and in particular g holomorphic modular forms of weight 2.

Remark 6.2.25. Note that when n is odd, there can be cases in which there is no spin structure on the space under consideration (if it is an orbifold). The Riemann–Roch theorem requires the existence of a spin structure for odd n.

Remark 6.2.26. The Riemann–Roch theorem will be the central tool that we will use in order to apply our bootstrap techniques. The number of modular forms of a certain weight will be used as an input in our symmetry constraints, and the Riemann–Roch theorem will enable us to characterize the class of Σ supporting enough modular forms in order for our constraints to apply.

Harmonic spinors

Calculating the number of modular forms of a given weight is straightforward thanks to the Riemann–Roch formula for $n \geqslant 2$: it is a topological invariant of the surfaces or orbifolds under consideration. However, the case $n = 1$ is particularly tricky. In particular, for compact orientable smooth surfaces of genus 2 or more, this number is not topologically invariant, and actually carries some nontrivial information about the surface's geometry and the spin structure on it.

Remark 6.2.27. The fact that the $n = 1$ case behaves differently is most easily understandable in terms of sheaf cohomology. In this language, the Riemann–Roch formula involves the dimension of the zeroth and first cohomology groups of the sheaf under consideration, which is a power of the canonical line bundle determined by n (see for example Theorem 16.9 of [176]). It is the dimension of the zeroth cohomology group that gives the number of linearly independent holomorphic modular forms of weight n. If $n > 1$, the first sheaf cohomology group automatically vanishes, which allows to directly compute the number of linearly independent holomorphic modular forms from the Riemann–Roch formula. It is no longer right to ignore the term coming from the first sheaf cohomology group for $n = 1$, which explains why the situation is more complicated.

What remains true in the $n = 1$ case is that the genus gives an upper bound on the number of harmonic spinors:

Proposition 6.2.28 (Ref. [240]). *The number $\ell_{1/2}$ of harmonic spinors on a compact orientable smooth Riemann surface of genus g with a spin structure satisfies*

$$\ell_{1/2} \leqslant \left\lfloor \frac{g+1}{2} \right\rfloor. \tag{6.17}$$

The natural next step is to ask when this upper bound is saturated. Here the answer is interesting, and requires the following definition:

Definition 6.2.29. Let Σ be a (smooth) Riemann surface. Σ is *hyperelliptic* if it can be realized as a branched double cover $\Sigma \rightarrow \mathbb{C}P^1$.

Remark 6.2.30. Hyperelliptic surfaces enjoy particularly nice properties, for example, they can always be described by an algebraic equation of the form

$$y^2 = F(x), \tag{6.18}$$

where *F* is a polynomial with distinct roots. At genus 1 and 2, every surface is hyperelliptic. However, at genus higher than or equal to 3, the moduli space of hyperelliptic surfaces is not the entire moduli space and hence is interesting to study.

For our purposes, the following result is relevant:

Proposition 6.2.31 (Ref. [330]). *Given* Σ, *a smooth surface of genus different from 4 or 6, there exists a spin structure on* Σ *for which the bound* (6.17) *is saturated if and only if* Σ *is hyperelliptic.*

This shows that apart from the case of genus 4 and the case of genus 6,[3] we can use the existence of a maximal number of harmonic spinors to write down the set of consistency conditions, leading to bounds on Laplacian spectra for a genus *g* hyperelliptic surface. These bounds are refined (and consequently, as we will see later, they are stronger as well), in contrast with the bounds obtained in [283], which are valid for all surfaces of genus *g*.

The upper bound on the gap of the Laplacian on some appropriately chosen moduli space of surfaces is likely to be saturated on surfaces with a large automorphism group (i.e., a locally maximal automorphism group). The classification of hyperelliptic surfaces with large automorphism groups is achieved in Table 1 of [351]. More generally, it is interesting to ask for a geometric description of the space of surfaces of a given genus that can carry a given number of harmonic spinors. As we saw, all surfaces of genus 1 and 2 are hyperelliptic so such an endeavor is trivial there, but from genus 3 onwards, the answer starts to give nontrivial information about the geometry of the surfaces. The classification of Riemann surfaces in terms of the possible dimensions of their spaces of harmonic spinors is still open in general, however, for genus $3 \leq g \leq 6$, precise results are available. In Appendix 6.7, we summarize these explicit classifications in low genus. The results collected in this appendix are condensed in Table 6.2.

6.3 Spectral identities for hyperbolic surfaces from associativity

The aim of this section is to derive the spectral identities which we will eventually *bootstrap* to bound the Laplacian and Dirac spectra on a compact connected

---

[3]It is intriguing to note that these genera are precisely the ones for which bootstrap bounds[283] for Laplace spectra are weaker than the Yang–Yau bounds [460].

g	$\ell_{1/2}^{Max}$	Moduli space	Most symmetric surface	Automorphism group
2	1	All	Bolza surface	$GL(2, \mathbb{F}_3)$
3	1	Non-hyperelliptic	Klein quartic	$PSL(2, \mathbb{F}_7)$
	2	Hyperelliptic	$y^2 = x^8 + 14x^4 + 1$	$\mathbb{Z}_2 \times S_4$
4	1	Non-hyperelliptic with smooth canonical quadric	Bring surface	S_5
	2	Hyperelliptic or non-hyperelliptic with singular canonical quadric	$z^3 y^2 = x(x^4 + y^4)$	Order 72
5	1 or 2	Non-hyperelliptic	$x_1^2 + x_2^2 + 2x_4^2 = x_4^2(x_2^2 + x_4^2) - x_3^4 = 0$	Order 192
	3	Hyperelliptic	$y^2 = x(x^{10} + 11x^5 - 1)$	$\mathbb{Z}_2 \times A_5$
6	1 or 2	Non-hyperelliptic and not a smooth quintic	Wiman sextic	S_5
	3	Hyperelliptic or smooth quintic	Fermat quintic	Order 150

Table 6.2: Table of the moduli spaces of surfaces, satisfying each genus/spin constraint, and of the most symmetric surfaces in each of these moduli spaces. Here g is the genus and $\ell_{1/2}^{Max}$ is the maximal number of harmonic spinors that a surface can carry.

orientable hyperbolic surfaces and orbifolds. A compact connected orientable hyperbolic orbifold[4] can be thought of as $\Gamma \backslash \text{PSL}(2, \mathbb{R})/PSO(2)$, where Γ is a cocompact Fuchsian group. For a spin orbifold with a given spin structure, there exists $\bar{\Gamma}$, a subgroup of $\text{SL}(2, \mathbb{R})$, such that $\Gamma \simeq \bar{\Gamma}/\mathbb{Z}_2$. This means that Γ can be consistently embedded inside $\bar{\Gamma}$ such that the embedding does not have $-Id$. We will denote this embedding as $\widetilde{\Gamma}$. As a set, we have

$$\bar{\Gamma} = \widetilde{\Gamma} \sqcup \left(-\widetilde{\Gamma}\right), \tag{6.19}$$

and $\widetilde{\Gamma}$ is isomorphic to Γ. Proposition 6.2.6 implies that $\chi(\widetilde{\gamma}) = \pm 1$ for $\widetilde{\gamma} \in \pm\widetilde{\Gamma}$, respectively. In other words, different spin structures correspond to different homomorphisms $\chi : \bar{\Gamma} \to \mathbb{Z}_2$, which amounts to saying that (6.19), and in particular $\widetilde{\Gamma}$, depends on the spin structure. We stress that even though Γ is isomorphic to $\widetilde{\Gamma}$, by choosing the embedding $\widetilde{\Gamma}$, we have already committed to a spin structure. Thus it is important to distinguish between Γ and $\widetilde{\Gamma}$ even though they are isomorphic.

---

[4]We are following the convention that the manifolds are orbifolds with no orbifold-singularity unless otherwise mentioned.

The upshot of the above is that a compact connected orientable hyperbolic spin orbifold X, with a given spin structure can be thought of as $\widetilde{\Gamma}\backslash\mathrm{SL}(2,\mathbb{R})/\mathrm{Spin}(2)$. The total space for the spin bundle, i.e. $P(X)$, is given by $\widetilde{\Gamma}\backslash\mathrm{SL}(2,\mathbb{R})$. We formulate the spectral problem for the Laplacian and Dirac operator on these hyperbolic spin orbifolds with a spin structure using the harmonic analysis on $L^2(\widetilde{\Gamma}\backslash G)$, where $G := \mathrm{SL}(2,\mathbb{R})$. Evidently, a key role is played by irreducible unitary representations of $\mathrm{SL}(2,\mathbb{R})$.

Representation theory of $\mathrm{SL}(2,\mathbb{R})$

Theorem 6.3.1 (See [279])**.** *The unitary irreducible representations of* $\mathrm{SL}(2,\mathbb{R})$ *are given up to equivalence by:*

1. *the trivial representation,*

2. *the complementary series* C_s *for* $s \in (0, \frac{1}{2})$,

3. *the principal series* $\mathcal{P}_{i\nu}^{\pm}$ *for* $\nu \in \mathbb{R}$, *except for* $\mathcal{P}_0^{-}$,

4. *the holomorphic discrete series* $\mathcal{D}_{n/2}$ *and anti-holomorphic discrete series* $\bar{\mathcal{D}}_{n/2}$, $n \geq 2$, $n \in \mathbb{Z}$,

5. *the limits of discrete series* $\mathcal{D}_{\frac{1}{2}}$, $\bar{\mathcal{D}}_{\frac{1}{2}}$.

The only equivalence between the representations listed above is the following: $\mathcal{P}_{i\nu}^{\pm} \simeq \mathcal{P}_{-i\nu}^{\pm}$.

Proposition 6.3.2. *The complexified Lie algebra* $\mathfrak{sl}_2(\mathbb{C})$ *is generated by* $L_0, L_{\pm 1}$ *and we have* $[L_m, L_n] = (m - n)L_{m+n}$. *For unitary representations, we have* $L_n^{\dagger} = L_{-n}$.

Proposition 6.3.3. *The quadratic Casimir* C_2 *takes the form*

$$C_2 := L_0^2 - \frac{1}{2}\left(L_{-1}L_1 + L_1 L_{-1}\right).$$

To explicitly construct the irreps, we find it convenient to recall that $\mathrm{SL}(2,\mathbb{R})$ can be mapped to $SU(1,1)$ by conjugation within $\mathrm{SL}(2,\mathbb{C})$. If $g = \begin{pmatrix} a & b \\ c & d \end{pmatrix} \in \mathrm{SL}(2,\mathbb{R})$, it gets mapped to $u \in SU(1,1)$; explicitly we have

$$u = \begin{pmatrix} 1 & i \\ i & 1 \end{pmatrix}^{-1} \begin{pmatrix} a & b \\ c & d \end{pmatrix} \begin{pmatrix} 1 & i \\ i & 1 \end{pmatrix} \in SU(1,1) \quad \text{if} \quad \begin{pmatrix} a & b \\ c & d \end{pmatrix} \in \mathrm{SL}(2,\mathbb{R}). \tag{6.20}$$

Under the Möbius transformation induced by the matrix,

$$\begin{pmatrix} 1 & i \\ i & 1 \end{pmatrix}^{-1} = \frac{1}{2}\begin{pmatrix} 1 & -i \\ -i & 1 \end{pmatrix}$$

the upper half-plane gets mapped to the unit disk $\mathbb{D} = \{z : |z| < 1\}$. In what follows, we denote the elements of $SU(1,1)$ by u, where

$$u := \begin{pmatrix} \alpha & \beta \\ \bar\beta & \bar\alpha \end{pmatrix}, \quad \alpha\bar\alpha - \beta\bar\beta = 1, \qquad \alpha, \beta \in \mathbb{C}. \tag{6.21}$$

Then, $SU(1,1)$ acts on $z \in \mathbb{C}$ as

$$u \cdot z := \frac{\alpha z + \beta}{\bar\beta z + \bar\alpha}, \tag{6.22}$$

Remark 6.3.4. The irreps of $PSL(2, \mathbb{R})$ are already reviewed in detail in [283]. For $n \in \mathbb{Z}$, $\mathcal{D}_n$ can be realized as antiholomorphic functions living on the unit disk $\mathbb{D} = \{z : |z| < 1\}$ or holomorphic functions on $\mathbb{D}' := \{z : |z| > 1\} \cup \{\infty\}$. $\bar{\mathcal{D}}_n$ can be realized as holomorphic functions living on the unit disk $\mathbb{D}$. The complementary series C_s and the principal series P_{iv}^+ can be realized as functions living on $\partial\mathbb{D} = \{z : |z| = 1\}$. All these functions belong to an L^2 space with respect to an appropriate G-invariant measure. The new ingredients that we are going to use are $\mathcal{P}_{iv}^-$ and $\mathcal{D}_n$, $\bar{\mathcal{D}}_n$ with $n \in 1/2 + \mathbb{Z}$. Hence, we will be brief in explaining the construction of irreps, often referring the readers to section 3 of [283] for details, and only highlight the parts that are new to this chapter.

Definition 6.3.5 (Antiholomorphic discrete series $\bar{\mathcal{D}}_{n/2}$). The explicit realization of antiholomorphic discrete series $\bar{\mathcal{D}}_{n/2}$ ($n \in \mathbb{Z}_+$) is achieved by holomorphic functions $f(z)$ on $\mathbb{D}$ such that the action of $u \in SU(1,1)$ is given by

$$u \cdot f(z) = \left(-\bar\beta z + \alpha\right)^{-n} f\left(u^{-1} \cdot z\right), \tag{6.23}$$

In particular, the nontrivial element of the center of $SL(2, \mathbb{R})$, given as in (6.21) by $\alpha = -1$, $\beta = 0$, acts nontrivially iff n is odd. The norm of a vector f inside $\bar{\mathcal{D}}_{n/2}$ is given by

$$\|f\|_{\bar{\mathcal{D}}_{1/2}} = \sup_{0 \le r < 1} \int_0^{2\pi} d\theta\, |f(re^{i\theta})|^2,$$
$$\|f\|_{\bar{\mathcal{D}}_{n/2}} = \int_{\mathbb{D}} dz\, (1 - |z|^2)^{n-1}|f(z)|^2, \quad n > 1. \tag{6.24}$$

Remark 6.3.6. We note that

$$\bar{\mathcal{D}}_{n/2} \simeq \bigoplus_{k \in -n/2 - \mathbb{Z}_{\geq 0}} V_k \,,$$

where the V_k are the one-dimensional irreducible representations of Spin(2). This amounts to saying that the L_0 spectrum of such an irrep is given by $\{-n/2 - k : k \in \mathbb{Z}_{\geq 0}\}$. The eigenvalue of the quadratic Casimir corresponding to the irrep $\bar{\mathcal{D}}_{n/2}$ is $-n/2(1 - n/2)$.

Definition 6.3.7 (Holomorphic discrete series $\mathcal{D}_{n/2}$)**.** The holomorphic discrete series $\mathcal{D}_{n/2}$ with $n \in \mathbb{Z}_+$ is realized by the space of antiholormorphic functions f on $\mathbb{D}$ such that the action of $u \in SU(1, 1)$ is given by

$$u \cdot f(\bar{z}) = (-\beta\bar{z} + \bar{\alpha})^{-n} f\left(u^{-1} \cdot \bar{z}\right) \,, \tag{6.25}$$

In particular, the nontrivial element of the center of SL$(2, \mathbb{R})$, given as in (6.21) by $\alpha = -1, \beta = 0$, acts nontrivially iff n is odd. The norm of a vector f inside $\mathcal{D}_{n/2}$ is given by

$$\begin{aligned}
||f||_{0,\mathcal{D}_{1/2}} &= \sup_{0 \leq r < 1} \int_0^{2\pi} d\theta \, |f(re^{i\theta})|^2 \,, \\
||f||_{0,\mathcal{D}_{n/2}} &= \int_{\mathbb{D}} dz \, (1 - |z|^2)^{n-1} |f(z)|^2 \,, \quad n > 1 \,.
\end{aligned} \tag{6.26}$$

However as explicitly worked out in [283], it is easier to consider another realization by holomorphic functions F on $\mathbb{D}' = \{z : |z| > 1\} \cup \{\infty\}$, where

$$F(z) := z^{-n} f(\bar{z}^{-1}) \,, \tag{6.27}$$

and the norm of F is given by

$$||F||_{\mathcal{D}_{n/2}} = ||f||_{0,\mathcal{D}_{n/2}}. \tag{6.28}$$

The functions F transform exactly in the same way as given by eq.(6.23). Again the action of the center is nontrivial iff n is odd.

Remark 6.3.8. We note that

$$\mathcal{D}_{n/2} \simeq \bigoplus_{k \in n/2 + \mathbb{Z}_{\geq 0}} V_k \,,$$

where the V_k are the one-dimensional irreducible representations of Spin(2). This amounts to saying that the L_0 spectrum of such an irrep is given by $\{n/2 + k : k \in \mathbb{Z}_{\geq 0}\}$. The eigenvalue of the quadratic Casimir corresponding to the irrep $\mathcal{D}_{n/2}$ is $-n/2(1 - n/2)$.

Definition 6.3.9 (Principal series $\mathcal{P}_{i\nu}^+$). They are realized in the space of equivalence classes of square integrable functions on $\partial\mathbb{D} = \{z : |z| = 1\}$ such that the action of $u \in SU(1,1)$ is given by

$$(u \cdot f)(z) = |-\beta\bar{z} + \bar{\alpha}|^{-1-2i\nu} f(u^{-1} \cdot z). \tag{6.29}$$

In particular, the nontrivial element of the center of $SL(2,\mathbb{R})$, given as in (6.21) by $\alpha = -1, \beta = 0$, acts trivially. The norm of f is given by

$$||f||_{\mathcal{P}_{i\nu}^+} = \int_0^{2\pi} d\theta \, |f(e^{i\theta})|^2. \tag{6.30}$$

Remark 6.3.10. We have

$$\mathcal{P}_{i\nu}^+ \simeq \bigoplus_{k \in \mathbb{Z}} V_k \,,$$

where the V_k are the one-dimensional irreducible representations of Spin(2). The spectrum of L_0 for vectors inside $\mathcal{P}_{i\nu}^+$ consists of all integers and each integer appear exactly once. A basis for functions living inside $\mathcal{P}_{i\nu}^+$ is given by $f_j(z) = z^j$ with $j \in \mathbb{Z}$. The eigenvalue of the quadratic Casimir corresponding to the irrep $\mathcal{P}_{i\nu}^+$ is $-(1/4 + \nu^2)$.

Definition 6.3.11 (Principal series $\mathcal{P}_{i\nu}^-$). They are realized in the space of equivalence classes of square integrable functions f on $\partial\mathbb{D}$ such that the action of $u \in SU(1,1)$ is given by

$$(u \cdot f)(z) = \text{sgn}\left(-\bar{\beta}z + \alpha\right) |-\beta\bar{z} + \bar{\alpha}|^{-1-2i\nu} f(u^{-1} \cdot z). \tag{6.31}$$

In particular, the nontrivial element of the center of $SL(2,\mathbb{R})$, given as in (6.21) by $\alpha = -1, \beta = 0$, acts nontrivially and gives a minus sign. The norm of f is given by $(z = e^{i\theta})$

$$||f||_{\mathcal{P}_{i\nu}^-} = \int_0^{2\pi} d\theta \, |f(e^{i\theta})|^2. \tag{6.32}$$

Remark 6.3.12. We have

$$\mathcal{P}_{i\nu}^- \simeq \bigoplus_{k \in 1/2+\mathbb{Z}} V_k \,,$$

where V_k are the one-dimensional irreducible representations of Spin(2). The spectrum of L_0 for vectors inside $\mathcal{P}_{i\nu}^-$ consists of all half-integers, and each half-integer appears exactly once. A basis for functions inside $\mathcal{P}_{i\nu}^-$ is given by $f_j(z) = z^j$ with $j \in \mathbb{Z}$ (see sections 8.2 and 8.3 of [299] for a pedagogical exposure). The eigenvalue of the quadratic Casimir corresponding to the irrep $\mathcal{P}_{i\nu}^-$ is $-(1/4 + \nu^2)$.

Definition 6.3.13 (Complementary series C_s). They are realized in the space of equivalence classes of square integrable functions on $\partial\mathbb{D}$ such that the action of $u \in SU(1,1)$ is given by

$$(u \cdot f)(z) = |-\beta\bar{z} + \bar{\alpha}|^{-1-2s} f(u^{-1} \cdot z). \tag{6.33}$$

In particular, the nontrivial element of the center of $SL(2,\mathbb{R})$, given as in (6.21) by $\alpha = -1$, $\beta = 0$, acts trivially. The norm of f is given by ($z = e^{i\theta}$)

$$||f||_{C_s} = \int_0^{2\pi} d\theta \int_0^{2\pi} d\phi \, \frac{|f(e^{i\theta})|^2}{|e^{i\theta} - e^{i\phi}|^{2-2\Delta}}, \quad \Delta = 1/2 + s. \tag{6.34}$$

Remark 6.3.14. We have

$$C_s \simeq \bigoplus_{k \in \mathbb{Z}} V_k,$$

where V_k are the one-dimensional irreducible representations of Spin(2). The spectrum of L_0 for vectors inside C_s consists of all integers and each integer appears exactly once. The eigenvalue of the quadratic Casimir corresponding to the irrep C_s is $-1/4 + s^2$.

Coherent States

We now construct the coherent states, these are functions living inside the irrep $\mathcal{D}_{n/2}$ or $\bar{\mathcal{D}}_{n/2}$. The construction of these states mimics the one presented in [283], extended in the present chapter to the case when n is an odd integer.

Definition 6.3.15. The coherent state $O_{n/2}(z)$ for $z \in \mathbb{D}$ is identified with a holomorphic function f on $\mathbb{D}'$, i.e.,

$$
\begin{aligned}
O_{1/2}(z)(w) &:= \sqrt{\frac{1}{2\pi}}(z-w)^{-1}, \\
O_{n/2}(z)(w) &= \sqrt{\frac{n-1}{\pi}}(z-w)^{-n}, \quad n > 1,
\end{aligned}
\tag{6.35}
$$

where $w \in \mathbb{D}'$.

Definition 6.3.16. The coherent state $\widetilde{O}_{n/2}(z)$ for $z \in \mathbb{D}'$ is identified with a holomorphic function f on $\mathbb{D}$. Explicitly we have, for $z \in \mathbb{D}'$ and $w \in \mathbb{D}$,

$$
\begin{aligned}
\widetilde{O}_{1/2}(z)(w) &:= \sqrt{\frac{1}{2\pi}}(z-w)^{-1}, \\
\widetilde{O}_{n/2}(z)(w) &= \sqrt{\frac{n-1}{\pi}}(z-w)^{-n}, \quad n > 1.
\end{aligned}
\tag{6.36}
$$

Proposition 6.3.17. *The inner products of coherent states are given by*

$$
\begin{aligned}
\left(O_{n/2}(z_1), O_{n/2}(z_2) \right)_{\mathcal{D}_{n/2}} &= (1 - \bar{z}_1 z_2)^{-n} \,, \\
\left(\widetilde{O}_{n/2}(z_1), \widetilde{O}_{n/2}(z_2) \right)_{\bar{\mathcal{D}}_{n/2}} &= (\bar{z}_1 z_2 - 1)^{-n} \,.
\end{aligned}
\tag{6.37}
$$

Proof. See [283] for the case when n is an even integer. The extended version for $n \in \mathbb{Z}_+$ follows from the definition of the inner product for $\mathcal{D}_{n/2}$ and $\bar{\mathcal{D}}_{n/2}$, $\qquad\square$

For a unitary representation R of G we write R^∞ for its Fréchet space of smooth vectors. We borrow the following propositions from [283], which will be useful for our purposes:

Proposition 6.3.18 (Proposition 3.3 [283])**.** *The coherent states O and $\widetilde{O}$ take values in $\mathcal{D}^\infty_{n/2}$ and $\bar{\mathcal{D}}^\infty_{n/2}$, respectively. They are holomorphic as functions $\mathbb{D} \to \mathcal{D}^\infty_{n/2}$ and $\mathbb{D}' \to \bar{\mathcal{D}}^\infty_{n/2}$. The span of the coherent states $O(z) \in \mathcal{D}_{n/2}$ for $z \in \mathbb{D}$ is dense in $\mathcal{D}_{n/2}$. The span of the coherent states $\widetilde{O}(z) \in \bar{\mathcal{D}}_{n/2}$ for $z \in \mathbb{D}'$ is dense in $\bar{\mathcal{D}}_{n/2}$.*

Remark 6.3.19. (See the proof of Proposition 3.3 of [283] and the references therein.) The reproducing kernel for $\bar{\mathcal{D}}_{n/2}$ is given by

$$
K_w(z) := \begin{cases} \frac{n-1}{\pi}(1 - \bar{w}z)^{-n} \,, & n > 1 \\ \frac{1}{2\pi}(1 - \bar{w}z)^{-1} \,, & n = 1 \end{cases} \,,
$$

i.e., for $w \in \mathbb{D}$ and $f \in \bar{\mathcal{D}}_{n/2}$, we have

$$
(K_w, f) = f(w).
$$

Thus, the coherent states are related to the reproducing kernel

$$
K_w = \begin{cases} \sqrt{\frac{n-1}{\pi}}\, (\bar{w})^{-n}\, \widetilde{O_{n/2}}((\bar{w})^{-1}) \,, & n > 1 \\ \sqrt{\frac{1}{2\pi}}\, (\bar{w})^{-1}\, \widetilde{O_{n/2}}((\bar{w})^{-1}) \,, & n = 1 \end{cases} \,,
$$

and $\bar{\mathcal{D}}_{n/2}$ is a reproducing kernel Hilbert space. Similar statements apply to $\mathcal{D}_{n/2}$.

Proposition 6.3.20 (Propostion 3.4 [283])**.** *We have $L^2(\widetilde{\Gamma}\backslash G)^\infty = C^\infty(\widetilde{\Gamma}\backslash G)$.*

Finally we define coherent states inside continuous series irreps.

Definition 6.3.21 (See section 3.4 of [283])**.** The coherent states inside R_k where $R_k = \mathcal{P}_{iv}^+$ with $\lambda_k^{(0)} = 1/4 + v^2$ or $R_k = C_s$ with $\lambda_k^{(0)} = 1/4 - s^2$ are defined as R_k^∞-valued distributions on $C^\infty(\partial\mathbb{D})$ by

$$O(f) := N_{\Delta_k}^{(0)} f, \quad f \in C^\infty(\partial\mathbb{D}), \tag{6.38}$$

where $N_{\Delta_k}^{(0)} > 0$ is chosen to ensure $N_{\Delta_k}^{(0)} ||1||_{R_k} = 1$.

Definition 6.3.22. The coherent states inside $\mathcal{P}_{iv}^-$ with $\lambda_k^{(1/2)} = 1/4 + v^2$ are defined as R_k^∞-valued distributions on $C^\infty(\partial\mathbb{D})$ by

$$O(f) = N_{\Delta_k}^{(1/2)} f, \quad f \in C^\infty(\partial\mathbb{D}), \tag{6.39}$$

where $N_{\Delta_k}^{(1/2)} > 0$ is chosen to ensure $N_{\Delta_k}^{(1/2)} ||z||_{R_k} = 1$.

Spectrum of $L^2(\widetilde{\Gamma}\backslash G)$

The space $\widetilde{\Gamma}\backslash G$ is the spin bundle over the compact orbifold X. We would like to study the space $L^2(\widetilde{\Gamma}\backslash G)$, consisting of equivalence class of square integrable functions $F : G \to \mathbb{C}$ such that $F(\widetilde{\gamma}g) = F(g)$ for all $\widetilde{\gamma} \in \widetilde{\Gamma}$ and $g \in G$. We normalize the Haar measure on G in a way such that $\mu(\widetilde{\Gamma}\backslash G) = 1$. Subsequently, we define the inner product as

$$(F_1, F_2) = \int_{\widetilde{\Gamma}\backslash G} dg\, \overline{F_1}(g)F_2(g). \tag{6.40}$$

The inner product induces the following norm on $F \in L^2(\widetilde{\Gamma}\backslash G)$:

$$||F||^2 := (F, F). \tag{6.41}$$

We can turn $L^2(\widetilde{\Gamma}\backslash G)$ into a representation of $\mathrm{SL}(2, \mathbb{R})$ by defining the following G-action: $\tilde{g} \in G$ acts on elements of $L^2(\widetilde{\Gamma}\backslash G)$ as

$$[\tilde{g} \cdot F](g) := F(g\tilde{g}). \tag{6.42}$$

It is easy to verify that the norm of F, $||F|| \equiv (F, F)$ is G invariant and thus $L^2(\widetilde{\Gamma}\backslash G)$ indeed becomes a representation of G. Recalling the NAK decomposition of $\mathrm{SL}(2, \mathbb{R})$:

$$g(x, y, \theta) = \begin{pmatrix} 1 & x \\ 0 & 1 \end{pmatrix} \begin{pmatrix} \sqrt{y} & 0 \\ 0 & \frac{1}{\sqrt{y}} \end{pmatrix} \begin{pmatrix} \cos\frac{\theta}{2} & -\sin\frac{\theta}{2} \\ \sin\frac{\theta}{2} & \cos\frac{\theta}{2} \end{pmatrix},$$

we will often write the functions $F(g)$ as $F(x, y, \theta)$.

Proposition 6.3.23. *The elements of the complexified Lie algebra corresponding to* $\mathrm{SL}(2,\mathbb{R})$ *act on* $F \in L^2(\widetilde{\Gamma}\backslash G)$ *as follows:*

$$L_0 F(x, y, \theta) = i\partial_\theta F(x, y, \theta) \,,$$
$$L_1 F(x, y, \theta) = e^{-i\theta}\left[y(\partial_x + i\partial_y) + \partial_\theta\right] F(x, y, \theta) \,, \tag{6.43}$$
$$L_{-1} F(x, y, \theta) = -e^{i\theta}\left[y(\partial_x - i\partial_y) + \partial_\theta\right] F(x, y, \theta).$$

The quadratic Casimir $C_2 := L_0^2 - \frac{1}{2}\left(L_{-1}L_1 + L_1L_{-1}\right)$ *acts as*

$$C_2 F(x, y, \theta) = \left[y^2(\partial_x^2 + \partial_y^2) - 2y\partial_x\partial_\theta\right] F(x, y, \theta) \,. \tag{6.44}$$

Proof. The above follows the transformation law, given by eq. (6.42) and *NAK* decomposition of $\mathrm{SL}(2,\mathbb{R})$. $\qquad\square$

Proposition 6.3.24. *For a cocompact* $\widetilde{\Gamma} \subset \mathrm{SL}(2,\mathbb{R})$*, such that* $-Id \notin \widetilde{\Gamma}$*, we have a discrete decomposition of* $L^2(\widetilde{\Gamma}\backslash G)$ *in terms of irreducible representations. In particular we have*

$$L^2(\widetilde{\Gamma}\backslash G) = \mathbb{C} \oplus \bigoplus_{n=1}^{\infty}\left(\mathscr{D}_{n/2} \oplus \overline{\mathscr{D}}_{n/2}\right) \oplus \bigoplus_{k=1}^{\infty}\mathscr{C}_{\lambda_k^{(0)}} \oplus \bigoplus_{k=1}^{\infty}\mathscr{P}_{\lambda_k^{(1/2)}}^{-} \,. \tag{6.45}$$

Remark 6.3.25. The group action is transitive, hence the trivial irrep $\mathbb{C}$ appears exactly once. This corresponds to the constant functions on X.

Remark 6.3.26. $\mathscr{D}_{n/2}$ is unitarily isomorphic to $\mathbb{C}^{\ell_{n/2}} \otimes \mathcal{D}_{n/2}$, where $\ell_{n/2}$ is the number of times $\mathcal{D}_{n/2}$ appears inside $L^2(\widetilde{\Gamma}\backslash G)$. The $\overline{\mathscr{D}}_{n/2}$ is unitarily isomorphic to $\mathbb{C}^{\ell_{n/2}} \otimes \bar{\mathcal{D}}_{n/2}$, where $\ell_{n/2}$ is the number of times $\bar{\mathcal{D}}_{n/2}$ appears inside $L^2(\widetilde{\Gamma}\backslash G)$.

Proposition 6.3.27. $\ell_{n/2}$ *is the number of independent normalized holomorphic modular forms of weight n. The number of independent normalized antiholomorphic modular forms of weight n is also given by* $\ell_{n/2}$.

Proof. Consider a lowest weight vector $F_{n/2,a}$ inside $\mathscr{D}_{n/2}$. Clearly, $F_{n/2,a} \in V_{n/2}$ and $e^{in\theta/2}F_{n/2,a}$ is independent of θ. Hence, one can define

$$h_{n,a}(x, y) := y^{-n/2}e^{in\theta/2}F_{n/2,a}(x, y, \theta). \tag{6.46}$$

The $\widetilde{\Gamma}$ invariance of F implies that $\tilde{h}_{n,a}(z) := h_{n,a}(\mathrm{Re}(z), \mathrm{Im}(z))$ transforms like a holomorphoic modular form of weight n for $\gamma \in \widetilde{\Gamma}$. Recalling eq. (6.19) and Proposition 6.2.6, this action can be naturally extended to $\bar{\Gamma}$ by using χ. The fact that $F_{n/2,a}$ is a lowest weight vector translates to $L_1 F_{n/2,a} = 0$, which implies $\tilde{h}_{n,a}(z)$ is holomorphic. A similar proof holds for $\overline{\mathscr{D}}_{n/2}$ by considering the highest weight vector, belonging to $V_{-n/2}$. Hence the proposition follows. $\qquad\square$

Remark 6.3.28. $\mathscr{C}_{\lambda_k^{(0)}}$ is unitarily isomorphic to

1. $\mathbb{C}^{d_k} \otimes C_s$ with $s := \sqrt{1/4 - \lambda_k^{(0)}}$ if $\lambda_k^{(0)} < 1/4$,

2. $\mathbb{C}^{d_k} \otimes \mathcal{P}_{i\nu}^+$ with $\nu := \sqrt{\lambda_k^{(0)} - 1/4}$ if $\lambda_k^{(0)} \geq 1/4$,

where d_k is the number of times C_s or $\mathcal{P}_{i\nu}^+$ appears inside $L^2(\widetilde{\Gamma}\backslash G)$.

Proposition 6.3.29. d_k *is the degeneracy of* $\lambda_k^{(0)}$, *an eigenvalue of the Laplace operator on* X.

Proof. Recall

$$\mathscr{C}_{\lambda_k^{(0)}} \simeq \mathbb{C}^{d_k} \otimes \bigoplus_{k\in\mathbb{Z}} V_k.$$

Consider a vector inside V_0, it gets mapped to a vector F inside $\mathscr{C}_{\lambda_k^{(0)}}$. Since $i\partial_\theta F = L_0 F = 0$, we can define $\phi(x, y) := F(x, y, \theta)$ and it follows $\phi(x, y)$ is a $\widetilde{\Gamma}$ invariant function on X. Furthermore, we have

$$C_2\phi(x, y) = y^2(\partial_x^2 + \partial_y^2)\phi(x, y). \tag{6.47}$$

On the other hand, C_2 of $\mathscr{C}_{\lambda_k^{(0)}}$ is $\lambda_k^{(0)}$. Hence, $\phi(x, y)$ is a $\widetilde{\Gamma}$ invariant eigenfunction of the Laplace operator, i.e., $y^2(\partial_x^2 + \partial_y^2)$, with eigenvalue $\lambda_k^{(0)}$, and the proposition follows. $\qquad\square$

Remark 6.3.30. $\mathcal{P}_{\lambda_k^{(1/2)}}^-$ is unitarily isomorphic to $\mathbb{C}^{d'_k} \otimes \mathcal{P}_{i\nu}^-$ with $\nu := \sqrt{\lambda_k^{(1/2)} - 1/4}$ and $\lambda_k^{(1/2)} > 1/4$, where d'_k is the number of times $\mathcal{P}_{i\nu}^-$ appears inside $L^2(\widetilde{\Gamma}\backslash G)$.

Proposition 6.3.31. d'_k *is the degeneracy of* $\lambda_k^{(1/2)}$, *an eigenvalue of the weight-*1 *automorphic Laplace operator (see defn. 6.2.17) on* X.

Proof. Recall

$$\mathcal{P}_{\lambda_k^{(1/2)}}^- \simeq \mathbb{C}^{d'_k} \otimes \bigoplus_{k\in 1/2+\mathbb{Z}} V_k.$$

Consider a vector inside $V_{1/2}$, it gets mapped to a vector $\Psi(x, y, \theta)$ inside $\mathcal{P}_{\lambda_k^{(1/2)}}^-$. Define $\psi(x, y) := e^{i\theta/2}\Psi(x, y, \theta)$. Since $i\partial_\theta\Psi = L_0\Psi = 1/2$, it follows that $\psi(x, y)$ is a $\widetilde{\Gamma}$-equivariant form on X. Furthermore, we have

$$C_2\psi(x, y) = \left[y^2(\partial_x^2 + \partial_y^2) - iy\partial_x\right]\psi(x, y). \tag{6.48}$$

On the other hand, C_2 of $\mathscr{P}^-_{\lambda_k^{(1/2)}}$ is $\lambda_k^{(1/2)}$. Hence, $\psi(x, y)$ is a $\widetilde{\Gamma}$-equivariant eigenform of the weight-1 automorphic Laplacian operator, i.e, $y^2(\partial_x^2 + \partial_y^2) - iy\partial_x$. Therefore, the proposition follows. $\qquad\square$

Now let us identify the coherent states inside $L^2(\widetilde{\Gamma}\backslash G)$.

Definition 6.3.32 (Coherent States inside $\mathscr{D}^\infty_{n/2}$ and $\overline{\mathscr{D}}^\infty_{n/2}$). Recall Proposition(6.3.24) and Remark 6.3.26 that $\mathscr{D}_{n/2}$ and $\overline{\mathscr{D}}_{n/2}$ are unitarily isomorphic to $\mathbb{C}^{\ell_{n/2}} \otimes \mathcal{D}_{n/2}$ and $\mathbb{C}^{\ell_{n/2}} \otimes \bar{\mathcal{D}}_{n/2}$, respectively.

Following [283], we choose an isomorphism $\tau_{n/2} : \mathbb{C}^{\ell_{n/2}} \otimes \mathcal{D}_{n/2} \to \mathscr{D}_{n/2}$ and define

$$\mathscr{O}_{n/2,a}(z) := \tau_{n/2}\left(e_a \otimes O(z)\right) \in \mathscr{D}^\infty_{n/2} \subset C^\infty(\widetilde{\Gamma}\backslash G). \qquad (6.49)$$

Here e_a for $a = 1, 2, \cdots \ell_{n/2}$ is the standard basis for $\mathbb{C}^{\ell_{n/2}}$. We further define $\bar{\tau}_{n/2} : \mathbb{C}^{\ell_{n/2}} \otimes \bar{\mathcal{D}}_{n/2} \to \overline{\mathscr{D}}_{n/2}$ as

$$\bar{\tau}_{n/2}(v \otimes f) = \overline{\tau_{n/2}(\bar{v} \otimes \widetilde{f})}, \quad \widetilde{f}(z) := z^{-n}\overline{f(\bar{z}^{-1})}, \qquad (6.50)$$

and

$$\widetilde{\mathscr{O}}_{n/2,a}(z) := \bar{\tau}_{n/2}\left(e_a \otimes \widetilde{O}(z)\right) \in \overline{\mathscr{D}}^\infty_{n/2} \subset C^\infty(\widetilde{\Gamma}\backslash G), \qquad (6.51)$$

Proposition 6.3.33 ([283]). *The generators of the complexified Lie algebra $\mathfrak{sl}_2(\mathbb{C})$ act on coherent states as follows:*

$$
\begin{aligned}
L_{-1} \cdot \mathscr{O}_{n/2,a}(z) &= \partial_z \mathscr{O}_{n/2,a}(z), & L_{-1} \cdot \widetilde{\mathscr{O}}_{n/2,a}(z) &= \partial_z \widetilde{\mathscr{O}}_{n/2,a}(z), \\
L_0 \cdot \mathscr{O}_{n/2,a}(z) &= (z\partial_z + n/2)\, \mathscr{O}_{n/2,a}(z), & L_0 \cdot \widetilde{\mathscr{O}}_{n/2,a}(z) &= (z\partial_z + n/2)\, \widetilde{\mathscr{O}}_{n/2,a}(z), \\
L_1 \cdot \mathscr{O}_{n/2,a}(z) &= \left(z^2\partial_z + nz\right) \mathscr{O}_{n/2,a}(z), & L_1 \cdot \widetilde{\mathscr{O}}_{n/2,a}(z) &= \left(z^2\partial_z + nz\right) \widetilde{\mathscr{O}}_{n/2,a}(z).
\end{aligned}
$$
$$(6.52)$$

Proposition 6.3.34 ([283]). *We have the following identity:*

$$\overline{\left(\mathscr{O}_{n/2,a}(z)\right)} = (\bar{z})^{-n}\widetilde{\mathscr{O}}_{n/2,a}\left((\bar{z})^{-1}\right).$$

Correlators of smooth functions on G

Definition 6.3.35. We consider smooth functions $F_1, F_2, \cdots F_n$ on $\widetilde{\Gamma}\backslash G$. Their correlator is defined as

$$\langle F_1 F_2 \cdots F_n \rangle := \int_{\widetilde{\Gamma}\backslash G} dg\, F_1(g) F_2(g) \cdots F_n(g). \qquad (6.53)$$

Since the functions F_i are smooth and $\widetilde{\Gamma}\backslash G$ is compact, the correlator is well-defined and finite.

Proposition 6.3.36. *The correlator* $\langle \cdot \dots \cdot \rangle : \left(C^\infty(\widetilde{\Gamma}\backslash G) \right)^N \to \mathbb{C}$ *is a G invariant functional.*

Proposition 6.3.37. *The two-function correlator is given by*

$$\langle \mathcal{O}_{m,i}(z_1)\widetilde{\mathcal{O}}_{n,j}(z_2)\rangle = \frac{\delta_{m,n}\delta_{i,j}}{(z_2 - z_1)^{2n}}, \quad where \quad 2m, 2n \in \mathbb{Z}_+ \tag{6.54}$$

Proof. Using Proposition 6.3.34 alongside with orthogonality of the decomposition given in Proposition 6.3.24, we find

$$\langle \mathcal{O}_{m,i}(z_1)\widetilde{\mathcal{O}}_{n,j}(z_2)\rangle = z_2^{-2n}\left(\mathcal{O}_{n,j}(\bar{z}_2^{-1}), \mathcal{O}_{m,i}(z_1)\right) = \delta_{m,n}\delta_{i,j}z_2^{-2n}\left(O_n(\bar{z}_2^{-1}), O_n(z_1)\right),$$

and then we use Proposition 6.3.17. □

Proposition 6.3.38. *Define $z_{ij} = z_i - z_j$. The three-function correlator between vectors inside $\mathscr{D}_k, \mathscr{D}_l$ and $\overline{\mathscr{D}}_m$ with $2k, 2l, 2m \in \mathbb{Z}_+$ is given by*

$$\left\langle \mathcal{O}_{k,a}(z_1)\,\mathcal{O}_{l,b}(z_2)\,\widetilde{\mathcal{O}}_{m,c}(z_3)\right\rangle = \frac{f^{m;c}_{(k;a)(l;b)}}{z_{21}^{k+l-m}z_{31}^{k+m-l}z_{32}^{l+m-k}}, \tag{6.55}$$

for some constants $f^{m;c}_{(k;a)(l;b)}$.

Proof. The result follows from using the same steps involving G-invariance to prove a similar result in [283] for $k, l, m \in \mathbb{Z}$. □

Remark 6.3.39. We recall that

$$\mathcal{O}_{k,a}(0) = F_{k,a}, \quad \mathcal{O}_{l,b}(0) = F_{l,b}, \quad \lim_{z\to\infty} z^{2m}\mathcal{O}_{m,c}(z) = \bar{F}_{m,c}. \tag{6.56}$$

Thus we have

$$f^{k+l,c}_{(k;a)(l;b)} = \int_{\widetilde{\Gamma}\backslash G} dg\ F_{k,a}F_{l,b}\bar{F}_{k+l,c} = \frac{1}{\mathrm{vol}(X)}\int_X dx\ dy\ y^{2(k+l-1)}h_{k,a}h_{l,b}\bar{h}_{m,c}. \tag{6.57}$$

Here the second equality follows from the definition of h, as given by eq. (6.46).

Definition 6.3.40. The G-invariant cross-ratio (denoted as z) for four points z_1, z_2, z_3, z_4 is given by

$$z := \frac{z_{12}z_{34}}{z_{13}z_{24}}, \quad z_{ij} := z_i - z_j. \tag{6.58}$$

In what follows, we will often suppress the degeneracy index a in $\mathcal{O}_{(n,a)}$ and write it as $\mathcal{O}_n$ for notational brevity.

Proposition 6.3.41. *Let* $2n_1, 2n_2, 2n_3, 2n_4 \in \mathbb{Z}_+$.

$$\langle \mathcal{O}_{n_1}(z_1)\mathcal{O}_{n_2}(z_2)\widetilde{\mathcal{O}}_{n_3}(z_3)\widetilde{\mathcal{O}}_{n_4}(z_4)\rangle = \frac{1}{z_{12}^{n_1+n_2}z_{34}^{n_3+n_4}} \left(\frac{z_{24}}{z_{14}}\right)^{n_1-n_2} \left(\frac{z_{14}}{z_{13}}\right)^{n_3-n_4} g_{\{n_1,n_2,n_3,n_4\}}(z)\,,$$

$$(6.59)$$

for some function $g_{\{n_1,n_2,n_3,n_4\}}$ *of the cross-ratio z.*

Proof. The proof mimics the one appearing in [283] for $n_1 = n_2 = n \in \mathbb{Z}$. The main idea is that G-invariance implies that the 4-function correlator can be written in terms of a single variable function of the cross-ratio z. □

Product expansion

$$F_1 F_2 = P_{\mathbb{C}}(F_1 F_2) + \sum_{n=1}^{\infty}\left[P_{\mathcal{D}_{n/2}}(F_1 F_2) + P_{\overline{\mathcal{D}}_{n/2}}(F_1 F_2)\right] + \sum_{k=1}^{\infty} P_{\mathcal{C}_{\lambda_k^{(0)}}}(F_1 F_2) + \sum_{k=1}^{\infty} P_{\mathcal{P}_{\lambda_k^{(1/2)}}^{-}}(F_1 F_2)\,.$$

$$(6.60)$$

Here P_H refers to the orthogonal projection onto the irrep H.

We choose F_i from the irrep H_i. Now the key point is that given an irrep H_m, G-invariance constrains the dependence of $P_{H_m}(F_1 F_2)$ on F_1 and F_2 upto finitely many constants. And those finitely many constants are related to triple product integrals between elements of H_1, H_2 and H_m. The spectral identities come from the associativity constriants, i.e.,

$$((F_1 F_2)F_3) = (F_1(F_2 F_3))\,. \qquad (6.61)$$

In what follows we will take $F_1 = \mathcal{O}_{n_1}$, $F_2 = \mathcal{O}_{n_2}$, $F_3 = \widetilde{\mathcal{O}}_{n_3}$. A convenient way to encode these constraints is to consider 4 point functions of the form $\langle \mathcal{O}_{n_1}\mathcal{O}_{n_2}\widetilde{\mathcal{O}}_{n_3}\widetilde{\mathcal{O}}_{n_4}\rangle$.

Now we introduce some lemmas which are relevant to the product expansion of coherent states.

Lemma 6.3.42. $P_H\left(\mathcal{O}_{n_1}(z_1)\,\mathcal{O}_{n_2}(z_2)\right) = 0$ *unless* $H = \mathcal{D}_p$ *with* $p - n_1 - n_2 \in \mathbb{Z}_{\geq 0}$. *If* $\mathcal{O}_{n_1} = \mathcal{O}_{n_2}$ *with* $n_1 = n_2$, *we further have* $p - 2n = 0(mod\ 2)$.

Proof. The proof is similar to that of Lemma 3.9 of [283] with minor modifications to include the cases when n_1 or n_2 are half-integers and possibly different. □

Proposition 6.3.43.

$$\mathcal{O}_{n_1,a_1}(z_1)\mathcal{O}_{n_2,a_2}(z_2) = \sum_{p-n_1-n_2\in\mathbb{Z}_{\geq 0}}\sum_{a=1}^{\ell_p} f^{p;a}_{(n_1;a_1)(n_2;a_2)}\tau_p\left(e_a \otimes C_p(z_1,z_2)\right). \quad (6.62)$$

Here $C_p(z_1,z_2) \in \mathcal{D}_p$ is defined as

$$C_p(z_1,z_2)(z_3) := \sqrt{\frac{2p-1}{\pi}}\frac{1}{z_{12}^{n_1+n_2-p}\, z_{13}^{n_1+p-n_2}\, z_{23}^{n_2+p-n_1}}, \quad (6.63)$$

and $f^{p;a}_{(n_1;a_1)(n_2;a_2)}$ are some constants. If $n_1 = n_2 = n$, $f^{p;a}_{(n_1;a_1)(n_2;a_2)}$ vanishes for $p = 2n + 1$.

Proof. The proof is similar to that of Lemma 3.10 of [283]. The key step is to use the fact that $\mathcal{D}_p$ is a reproducing kernel Hilbert space to relate $C_p(z_1,z_2)(z)$ with the three function correlator $\langle\mathcal{O}_{n_1,a_1}(z_1)\mathcal{O}_{n_2,a_2}(z_2)\widetilde{\mathcal{O}}_{p,a}(z)\rangle$, followed by the use of proposition 6.3.38. □

Lemma 6.3.44. $P_H\left(\mathcal{O}_n(z_1)\widetilde{\mathcal{O}}_n(z_2)\right) = 0$ *unless $H = \mathbb{C}$ or $H = \mathcal{C}_{\lambda_k^0}$.*

Proof. The proof is similar to that of Lemma 3.11 of [283] with minor modifications. $\mathscr{P}_{iv}^-$ does not appear since the center of $\mathrm{SL}(2,\mathbb{R})$ acts trivially on $\mathcal{O}_n(z_1)\widetilde{\mathcal{O}}_n(z_2)$ while the center acts nontrivially on vectors inside $\mathscr{P}_{iv}^-$. □

Lemma 6.3.45. *Let $n_1 > n_2$ such that $2(n_1+n_2) = 0 \,(mod\,2)$. $P_H\left(\mathcal{O}_{n_1}(z_1)\widetilde{\mathcal{O}}_{n_2}(z_2)\right) = 0$ unless $H = \mathcal{C}_{\lambda_k^{(0)}}$ or $H = \mathcal{D}_m$ with $1 \leq m \leq n_1 - n_2$ and $m \in \mathbb{Z}$.*

Proof. The proof is similar to that of Lemma 3.11 of [283], with minor modifications like in the previous lemma. □

Lemma 6.3.46. *Let $n_1 < n_2$ such that $2(n_1+n_2) = 0\,(mod\,2)$. $P_H\left(\mathcal{O}_{n_1}(z_1)\widetilde{\mathcal{O}}_{n_2}(z_2)\right) = 0$ unless $H = \mathcal{C}_{\lambda_k^{(0)}}$ or $H = \bar{\mathcal{D}}_m$ with $1 \leq m \leq n_2 - n_1$ and $m \in \mathbb{Z}$.*

Proof. The proof is similar to the above. □

Proposition 6.3.47 (See Lemma 3.12 of [283]). *Let $n_2 - n_1 \in \mathbb{Z}$ and $n_1 + n_2 \in \mathbb{Z}$. We have*

$$P_{\mathcal{C}_{\lambda_k^{(0)}}}\left(\mathcal{O}_{n_1,a}(z_1)\widetilde{\mathcal{O}}_{n_2,b}(z_2)\right) = \sum_{r=1}^{d_k} c^{k;r}_{(n_1;a)(n_2;b)}\kappa_k^{(0)}\left(e_r \otimes \widetilde{C}_k^{(0)}(z_1,z_2)\right), \quad (6.64)$$

for some constants $c^{k;r}_{(n_1;a)(n_2;b)}$. Here $\kappa^{(0)}_k$ is the unitary isomorphism between $\mathbb{C}^{d_k} \otimes R_k$ and $\mathscr{C}_{\lambda^{(0)}_k}$, where $R_k = \mathcal{P}^+_{iv}$ with $\lambda^{(0)}_k = 1/4 + v^2$ or $R_k = C_s$ with $\lambda^{(0)}_k = 1/4 - s^2$. Furthermore, $\widetilde{C}^{(0)}_k(z_1, z_2) \in R_k$, and is given by

$$\widetilde{C}^{(0)}_k(z_1, z_2)(z_0) := \frac{N_k z_2^{-2n_2} z_0^{n_2-n_1}}{\left(1 - z_1 z_2^{-1}\right)^{n_1+n_2-\Delta_k} \left(1 - z_1 z_0^{-1}\right)^{n_1-n_2+\Delta_k} \left(1 - z_2^{-1} z_0\right)^{n_2-n_1+\Delta_k}}, \quad |z_0| = 1.$$

Here $N_k \in \mathbb{C}$ is a constant such that the constant function equal to N_k has unit norm in R_k.

Proposition 6.3.48. *Let $n_1 > n_2$ such that $2(n_1 + n_2) = 0 (mod\ 2)$. We have for $p \leq n_1 - n_2$ and $p \in \mathbb{Z}_{\geq 0}$,*

$$P_{\mathscr{D}_p}\left(\mathcal{O}_{n_1,a_1}(z_1)\widetilde{\mathcal{O}}_{n_2,a_2}(z_2)\right) = \sum_{a=1}^{\ell_p} f^{n_2;a_2}_{(n_1;a_1)(p;a)} \tau_p\left(e_a \otimes \widetilde{C}_p(z_1, z_2)\right). \tag{6.65}$$

Here $\widetilde{C}_p(z_1, z_2) \in \mathcal{D}_p$ is defined as

$$\widetilde{C}_p(z_1, z_2)(z_3) := \sqrt{\frac{2p-1}{\pi}} \frac{1}{z_{13}^{n_1+n_2-p} z_{12}^{n_1+p-n_2} z_{32}^{n_2+p-n_1}}. \tag{6.66}$$

Remark 6.3.49. *The structure constant $f^{n_2;a_2}_{(n_1;a_1)(p;a)}$ appearing here is the same as the one appearing in $\langle \mathcal{O}_{n_1,a_1}(z_1)\mathcal{O}_{p,a}(z_3)\widetilde{\mathcal{O}}_{n_2,a_2}(z_2)\rangle$.*

Remark 6.3.50. *A similar statement can be made for $n_1 < n_2$.*

Lemma 6.3.51. *Let $n_1 \in \mathbb{N}/2$ and $n_2 \in \mathbb{N}/2$. Further assume that $n_1 < n_2$ (or $n_1 > n_2$) such that $2(n_1 + n_2) = 1 (mod\ 2)$. $P_H\left(\mathcal{O}_{n_1}(z_1)\widetilde{\mathcal{O}}_{n_2}(z_2)\right) = 0$ unless $H = \mathcal{P}^-_{\lambda^{(1/2)}_k}$ or $H = \bar{\mathcal{D}}_m (\mathcal{D}_m)$ with $1/2 \leq m \leq |n_2 - n_1|$ and $m \in 1/2 + \mathbb{Z}$.*

Proof. $\mathbb{C}$ and $\mathscr{C}_{\lambda^{(0)}_k}$ do not appear because the center acts nontrivially on $\mathcal{O}_{n_1}(z_1)\widetilde{\mathcal{O}}_{n_2}(z_2)$ for $2(n_1 + n_2) = 1 (mod\ 2)$. The rest of the proof is similar to that of Lemma 3.11 of [283]. $\square$

Proposition 6.3.52. *Let $n_1 \in \mathbb{N}/2$ and $n_2 \in \mathbb{N}/2$ be such that $2(n_1+n_2) = 1 (mod\ 2)$.*

$$P_{\mathcal{P}^-_{\lambda^{(1/2)}_k}}\left(\mathcal{O}_{n_1,a}(z_1)\widetilde{\mathcal{O}}_{n_2,b}(z_2)\right) = \sum_{r=1}^{d'_k} s^{k;r}_{(n_1;a)(n_2;b)} \kappa^{(1/2)}_k\left(e_r \otimes \widetilde{C}^{(1/2)}_k(z_1, z_2)\right), \tag{6.67}$$

for some constants $s^{k;r}_{(n_1;a)(n_2;b)}$. *Here* $\kappa_k^{(1/2)}$ *is the unitary isomorphism between* $\mathbb{C}^{d'_k} \otimes \mathcal{P}_{iv}^-$ *and* $\mathscr{P}^-_{\lambda_k^{(1/2)}}$, *where* $\lambda_k^{(1/2)} = 1/4 + v^2$ *and* $\widetilde{C}_k^{(1/2)}(z_1, z_2) \in \mathcal{P}_{iv}^-$ *is given by*

$$\widetilde{C}_k^{(1/2)}(z_1, z_2)(z_0) := \frac{N_k^{(1/2)} z_2^{-2n_2} z_0^{n_2-n_1+1/2}}{\left(1 - z_1 z_2^{-1}\right)^{n_1+n_2-\Delta_k} \left(1 - z_1 z_0^{-1}\right)^{n_1-n_2+\Delta_k} \left(1 - z_2^{-1} z_0\right)^{n_2-n_1+\Delta_k}}.$$
(6.68)

Here $N_k^{(1/2)} \in \mathbb{C}$ *is a constant such the constant function equal to* $N_k^{(1/2)}$ *has unit norm in* $\mathcal{P}_{iv}^-$.

Proof. The proof is similar to that of Lemma 3.12 of [283]: here we need to perform projections onto the $\mathcal{P}_{iv}^-$ rather than the $\mathcal{P}_{iv}^+$ and the C_s, but the techniques are exactly the same. □

Proposition 6.3.53. *Let* $n_1 > n_2$ *such that* $2(n_1 + n_2) = 1 (mod\ 2)$. *We have for* $p \leq n_1 - n_2$ *and* $p \in 1/2 + \mathbb{Z}_{\geq 0}$

$$P_{\mathscr{D}_p}\left(\mathcal{O}_{n_1,a_1}(z_1)\widetilde{\mathcal{O}}_{n_2,a_2}(z_2)\right) = \sum_{a=1}^{\ell_p} f^{n_2;a_2}_{(n_1;a_1)(p;a)}\tau_p\left(e_a \otimes \widetilde{C}_p(z_1, z_2)\right).$$
(6.69)

for some constants $f^{n_2;a_2}_{(n_1;a_1)(p;a)}$. *Here* $\widetilde{C}_p(z_1, z_2) \in \mathcal{D}_p$ *is defined as*

$$\widetilde{C}_p(z_1, z_2)(z_3) := \sqrt{\frac{2p-1}{\pi}} \frac{1}{z_{13}^{n_1+n_2-p} z_{12}^{n_1+p-n_2} z_{32}^{n_2+p-n_1}}, \quad p > 1/2$$

$$\widetilde{C}_{1/2}(z_1, z_2)(z_3) := \sqrt{\frac{1}{2\pi}} \frac{1}{z_{13}^{n_1+n_2-1/2} z_{12}^{n_1+1/2-n_2} z_{32}^{n_2+1/2-n_1}}.$$
(6.70)

Equipped with the above lemmas, we can study correlators of the form $\langle \mathcal{O}_{n_1}\mathcal{O}_{n_2}\widetilde{\mathcal{O}}_{n_2}\widetilde{\mathcal{O}}_{n_1}\rangle$. They are studied in [283] for $n \in \mathbb{Z}_+$. They can easily be extended for half-integer n_i. In particular we have

Theorem 6.3.54 (Theorem 2.3 [283]: Extended). *Let* $g_0(z) := g_{\{n_1,n_2,n_2,n_1\}}(z)$ *be as in eq.* (6.59) *and* $n_{ij} := n_i - n_j$.

1. $g_0(z)$ *has the following expansion, known as the s-channel expansion:*

$$g_0(z) = \sum_{p=n_1+n_2}^{\infty} \sum_{a=1}^{\ell_p} |f^{p,a}_{n_1,n_2}|^2 \mathcal{G}_p(n_1, n_2, n_2, n_1; z),$$
(6.71)

where

$$G_p(n_1, n_2, n_3, n_4; z) := z^p {}_2F_1(p - n_{12}, p + n_{34}, 2p, z). \qquad (6.72)$$

The s-channel sum and its derivatives converge uniformly on compact subsets of $\mathbb{C} \setminus (1, \infty)$. *Furthermore,* $f_{n_1, n_2}^{p, a} \in \mathbb{C}$ *and satisfies*

$$f_{n,n}^p = 0, \quad \text{if } p - 2n = 1 \pmod 2. \qquad (6.73)$$

2. $g_0(z)$ *has the following expansion, known as the t-channel expansion:*

$$g_0(z) = \frac{z^{n_1 + n_2}}{(1 - z)^{2n_2}} \left(1 + \sum_{k=1}^{\infty} \sum_{a=1}^{d_k} c_{n_1, n_1}^{k;a} c_{n_2, n_2}^{k;a} \mathcal{H}_{\Delta_k^{(0)}}(n_1, n_2, n_2, n_1; z) \right), \quad (6.74)$$

where

$$\mathcal{H}_\Delta(n_1, n_2, n_2, n_1; z) := {}_2F_1\left(\Delta, 1 - \Delta, 1, \frac{z}{z - 1} \right), \qquad (6.75)$$

and $c_{n_i, n_i}^{k;a} \in \mathbb{R}$, $\Delta_k^{(0)} = \frac{1}{2} + i\sqrt{\lambda_k^{(0)} - 1/4}$. *The t-channel sum and its derivatives converge uniformly on compact subsets of* $\mathbb{C} \setminus (1, \infty)$.

Proof. The proof of Theorem 6.3.54 goes exactly the same way as that of Theorem 2.3 in [283], by allowing n_1 and n_2 to take different values. □

Theorem 6.3.55 (Theorem 2.3 [283]: Extended). *Let* $g_1(z) := g_{\{n_1, n_2, n_1, n_2\}}(z)$ *be as in eq. (6.59) with* $n_1 > n_2$ *and* $n_1 \in \mathbb{Z}_+$, $2n_2 = 1 \pmod 2$. *Define* $n_{ij} := n_i - n_j$.

1. $g_1(z)$ *has the following expansion, known as the s-channel expansion:*

$$g_1(z) = \sum_{p=n_1+n_2}^{\infty} \sum_{a=1}^{\ell_p} (-1)^{p - n_1 - n_2} |f_{n_1, n_2}^{p, a}|^2 G_p(n_1, n_2, n_1, n_2; z), \qquad (6.76)$$

where $G_p(n_1, n_2, n_3, n_4; z)$ *is defined in (6.72).*

The s-channel sum and its derivatives converge uniformly on compact subsets of $\mathbb{C} \setminus (1, \infty)$. *Furthermore,* $f_{n_1, n_2}^{p, a} \in \mathbb{C}$ *and satisfies*

$$f_{n,n}^p = 0, \quad \text{if } p - 2n = 1 \pmod 2. \qquad (6.77)$$

2. $g_1(z)$ *has the following expansion, known as the t-channel expansion:*

$$g_1(z) = \frac{z^{n_1 + n_2}}{(1 - z)^{n_1 + n_2}} \left(\sum_{k=1}^{\infty} \sum_{a=1}^{d_k'} |s_{n_1, n_2}^{k;a}|^2 \mathcal{H}_{\Delta_k^{(1/2)}}(n_1, n_2, n_1, n_2; z) + \right.$$
$$\left. + \sum_{0 < m \le n_1 - n_2} \sum_{a=1}^{\ell_m} |f_{n_2, (m;a)}^{n_1}|^2 \mathcal{H}_m(n_1, n_2, n_1, n_2; z) \right), \qquad (6.78)$$

where

$$\mathcal{H}_\Delta(n_1, n_2, n_1, n_2; z) := (1-z)^{n_{12}} {}_2F_1\left(\Delta + n_{21}, 1 - \Delta + n_{21}, 1, \frac{z}{z-1}\right),$$

(6.79)

and $s_{n_1,n_2}^{k;a}, f_{n_2,(m;a)}^{n_1} \in \mathbb{C}$, $\Delta_k^{(1/2)} = \frac{1}{2} + i\sqrt{\lambda_k^{(1/2)} - 1/4}$. *The t-channel sum and its derivatives converge uniformly on compact subsets of* $\mathbb{C} \setminus (1, \infty)$.

Proof. The proof of Theorem 6.3.55 is similar to that of Theorem 2.3 in [283] with some modifications.

For the part (1), we derive

$$g_1(z) = \sum_{p=n_1+n_2}^{\infty} \sum_{a=1}^{\ell_p} f_{n_1,n_2}^{p,a} f_{n_2,n_1}^{\bar{p},a} \, \mathcal{G}_p(n_1, n_2, n_1, n_2; z),$$

in the same way we derive (6.71). In other words, we can derive the above by swapping the labels n_1 and n_2 in the discrete antiholomorphic coherent states in the correlator appearing in the theorem 6.3.54, leading to a similar swap in the R.H.S of (6.71). We then use Proposition 3.37 to deduce

$$f_{n_2,n_1}^{p,a} = (-1)^{p-n_1-n_2} f_{n_1,n_2}^{p,a},$$

to arrive at (6.76).

For the part (2), we note that the lemma 6.3.51 implies that in the R.H.S of (6.78), $\mathcal{P}_{iv}^-$ (instead of $\mathcal{P}_{iv}^+$) and the discrete series representations appear. The rest of the proof involves deriving the expression for the t channel conformal block $\mathcal{H}$, the derivation goes in a similar way as in the proof of the theorem 6.3.54 with appropriate swapping of the labels. $\square$

Spectral Identities and Linear Programming

Definition 6.3.56. Define $r := 1 - m - n_1 - n_2$, $\tilde{n}_i := 1 - n_i$, and $\Delta := 1/2 + i\sqrt{\lambda - 1/4}$. We further define

$$\mathcal{F}_m^{(n_1,n_2,n_3,n_4)}(\lambda) :=$$
$$\oint_{z=0} \frac{dz}{2\pi i} z^{-2} \mathcal{G}_r(\tilde{n}_1, \tilde{n}_2, \tilde{n}_3, \tilde{n}_4; z) \frac{z^{n_1+n_2}}{(1-z)^{n_2+n_3}} \mathcal{H}_\Delta(n_1, n_2, n_3, n_4; z).$$

(6.80)

Definition 6.3.57. We define $S_{p;(n_1,n_2)} := \sum_{a=1}^{\ell_p} |f_{n_1,n_2}^{p,a}|^2$.

Each four function correlator gives rise to a consistency condition by equating the s and t channel expansions. We can then obtain infinitely many conditions by Taylor expanding the original consistency condition around $z = 0$ and collecting the coefficient of z^m for each $m \in \mathbb{Z}_{\geqslant 0}$.

Proposition 6.3.58. *Let $m \in \mathbb{Z}_{\geq 0}$. The consistency conditions, one for each m, coming from the four function correlator, $\langle \mathcal{O}_{n_1}(z_1) \mathcal{O}_{n_2}(z_2) \widetilde{\mathcal{O}}_{n_2}(z_3) \widetilde{\mathcal{O}}_{n_1}(z_4) \rangle$ are given by*

$$S_{n_1+n_2+m;(n_1,n_2)} = \left(\mathcal{F}_m^{(n_1,n_2,n_2,n_1)}(0) + \sum_{k=1}^{\infty} \left[\sum_{a=1}^{d_k} c_{n_1,n_1}^{k;a} c_{n_2,n_2}^{k;a} \right] \mathcal{F}_m^{(n_1,n_2,n_2,n_1)}(\lambda_k^{(0)}) \right).$$
(6.81)

Proof. We recall Theorem6.3.54 and equate the s-channel and t-channel expansions and integrate against $\mathcal{G}_r$ introduced in 6.3.56, followed by exchanging the sum and integral using uniform convergence of the expansion. The proposition will follow from the orthogonality condition

$$\oint_{z=0} \frac{dz}{2\pi i} z^{-2} \mathcal{G}_{1-m_1-n_1-n_2}(\tilde{n}_1, \tilde{n}_2, \tilde{n}_3, \tilde{n}_4; z) \mathcal{G}_{m_2+n_1+n_2}(n_1, n_2, n_3, n_4) = \delta_{m_1,m_2},$$

(6.82)

where $\tilde{n}_i = 1 - n_i$. To prove (6.82), first note that $\mathcal{G}_p(n_1, n_2, n_3, n_4)$ satisfies the eigenvalue equation

$$D_{\{n_i\}} \mathcal{G}_p(n_1, n_2, n_3, n_4; z) = p(1-p) \mathcal{G}_p(n_1, n_2, n_3, n_4; z),$$
(6.83)

where the differential operator $D_{\{n_i\}}$ is given by

$$D_{\{n_i\}} = z^2(z-1) \frac{\partial^2}{\partial z^2} + (1 - n_{12} + n_{34}) z^2 \frac{\partial}{\partial z} - n_{12} n_{34} z.$$
(6.84)

By integrating by parts, one can show that $D_{\{n_i\}}$ satisfies

$$\oint_{z=0} \frac{dz}{2\pi i} z^{-2} F(z) (\mathcal{D}_{\{n_i\}} G(z)) = \oint_{z=0} \frac{dz}{2\pi i} z^{-2} (\mathcal{D}_{\{\tilde{n}_i\}} F(z)) G(z)$$
(6.85)

for any functions $F(z)$ and $G(z)$ holomorphic in an annulus around $z = 0$. Thus, for the left-hand side of (6.82) to be nonzero, the eigenvalues of $\mathcal{G}_{1-m_1-n_1-n_2}(\tilde{n}_1, \tilde{n}_2, \tilde{n}_3, \tilde{n}_4; z)$ and $\mathcal{G}_{m_2+n_1+n_2}(n_1, n_2, n_3, n_4)$ with respect to $D_{\{\tilde{n}_i\}}$ and $D_{\{n_i\}}$, respectively, must be equal, which implies $m_1 = m_2$. Finally, when $m_1 = m_2$, the left-hand side of (6.82) can be evaluated by residues, picking up the contribution of the simple pole at $z = 0$ with residue 1. □

Proposition 6.3.59. *Let $m \in \mathbb{Z}_{\geq 0}$, $n_1 \in \mathbb{N}$ and $2n_2 = 1(mod\ 2)$. The consistency condition coming from $\langle \mathcal{O}_{n_1}(z_1)\mathcal{O}_{n_2}(z_2)\widetilde{\mathcal{O}}_{n_1}(z_3)\widetilde{\mathcal{O}}_{n_2}(z_4)\rangle$ is given by*

$$
(-1)^m S_{n_1+n_2+m;(n_1,n_2)} = \left(\sum_{k=1}^{\infty} \left[\sum_{a=1}^{d_k'} |s_{n_1,n_2}^{k;a}|^2 \right] \mathcal{F}_m^{(n_1,n_2,n_1,n_2)}(\lambda_k^{(1/2)}) +
$$
$$
+ \sum_{\substack{1/2 \leq q \leq n_1-n_2 \\ q \in 1/2 + \mathbb{Z}_{\geq 0}}} \sum_{a=1}^{\ell_q} |f_{n_2,(q;a)}^{n_1}|^2 \mathcal{F}_m^{(n_1,n_2,n_1,n_2)}(q(1-q)) \right). \tag{6.86}
$$

Proof. It follows from Theorem 6.3.55. The proof is similar to that of Proposition 6.3.58. $\qquad\square$

In what follows, we consider a hyperbolic spin orbifold supporting homolomorphic modular forms of weight n and $2n$ such that $n = 1(mod\ 2)$. If $\ell_{n/2} > 1$ and/or $\ell_n > 1$, we choose a particular $\mathcal{O}_n$ and a particular $\mathcal{O}_{n/2}$ such that $f_{n/2,n/2}^n \neq 0$. One can always consider a bigger system correlator using explicitly the value of ℓ_n and $\ell_{n/2}$, however, in order to find out a universal bound irrespective of ℓ_n and $\ell_{n/2}$, we choose not to do so. This leads us to consider the system of following correlators $\langle \mathcal{O}_n\mathcal{O}_n\widetilde{\mathcal{O}}_n\widetilde{\mathcal{O}}_n\rangle$, $\langle \mathcal{O}_{\frac{n}{2}}\mathcal{O}_{\frac{n}{2}}\widetilde{\mathcal{O}}_{\frac{n}{2}}\widetilde{\mathcal{O}}_{\frac{n}{2}}\rangle$, $\langle \mathcal{O}_n\mathcal{O}_{\frac{n}{2}}\widetilde{\mathcal{O}}_{\frac{n}{2}}\widetilde{\mathcal{O}}_n\rangle$ and $\langle \mathcal{O}_n\mathcal{O}_{\frac{n}{2}}\widetilde{\mathcal{O}}_n\widetilde{\mathcal{O}}_{\frac{n}{2}}\rangle$, where we have suppressed the degeneracy index a in (n, a) and so on. The explicit crossing equations read

Proposition 6.3.60. *Let* $m \in \mathbb{Z}_{\geq 0}$, $n \in \mathbb{N}$. *We have*

$$S_{2n+2m;(n,n)} = \left(\mathcal{F}_{2m}^{(n,n,n,n)}(0) + \sum_{k=1}^{\infty} \left[\sum_{a=1}^{d_k} \left(c_{n,n}^{k;a} \right)^2 \right] \mathcal{F}_{2m}^{(n,n,n,n)}(\lambda_k^{(0)}) \right),$$

$$0 = \left(\mathcal{F}_{2m+1}^{(n,n,n,n)}(0) + \sum_{k=1}^{\infty} \left[\sum_{a=1}^{d_k} \left(c_{n,n}^{k;a} \right)^2 \right] \mathcal{F}_{2m+1}^{(n,n,n,n)}(\lambda_k^{(0)}) \right),$$

$$S_{n+2m;(n/2,n/2)} = \left(\mathcal{F}_{2m}^{(n/2,n/2,n/2,n/2)}(0) + \sum_{k=1}^{\infty} \left[\sum_{a=1}^{d_k} \left(c_{n/2,n/2}^{k;a} \right)^2 \right] \mathcal{F}_{2m}^{(n/2,n/2,n/2,n/2)}(\lambda_k^{(0)}) \right),$$

$$0 = \left(\mathcal{F}_{2m+1}^{(n/2,n/2,n/2,n/2)}(0) + \sum_{k=1}^{\infty} \left[\sum_{a=1}^{d_k} \left(c_{n/2,n/2}^{k;a} \right)^2 \right] \mathcal{F}_{2m+1}^{(n/2,n/2,n/2,n/2)}(\lambda_k^{(0)}) \right),$$

$$S_{3n/2+m;(n,n/2)} = \left(\mathcal{F}_{m}^{(n,n/2,n/2,n)}(0) + \sum_{k=1}^{\infty} \left[\sum_{a=1}^{d_k} c_{n/2,n/2}^{k;a} c_{n,n}^{k;a} \right] \mathcal{F}_{m}^{(n,n/2,n/2,n)}(\lambda_k^{(0)}) \right),$$

$$(-1)^m S_{3n/2+m;(n,n/2)} = \left(\sum_{k=1}^{\infty} \left[\sum_{a=1}^{d_k'} |s_{n,n/2}^{k;a}|^2 \right] \mathcal{F}_{m}^{(n,n/2,n,n/2)}(\lambda_k^{(1/2)}) + \right.$$

$$\left. + \sum_{0 < q \leq n/2} \sum_{a=1}^{\ell_q} |f_{n/2,(q;a)}^{n}|^2 \mathcal{F}_{m}^{(n,n/2,n,n/2)}(q(1-q)) \right).$$

Proof. This follows from Propositions 6.3.58 and 6.3.59 by choosing appropriate values of n_1 and n_2. $\qquad\square$

Based on the above crossing equations, let us formulate the following linear programming problems.

Notation: Given a hyperbolic spin orbifold X, we consider the Laplacian spectra $\{0\} \cup \{\lambda_k^{(0)}(X) : \lambda_k^{(0)}(X) > 0, \ k \in \mathbb{N}\}$, and the weight-1 automorphic Laplacian spectrum (not including the eigenvalue corresponding to a harmonic spinor if there is any) $\{\lambda_k^{(1/2)}(X) : \lambda_k^{(1/2)}(X) > 1/4, \ k \in \mathbb{N}\}$. Furthermore, without loss of generality, let us assume $\lambda_{k+1}^{(0)}(x) > \lambda_k^{(0)}(X)$ and $\lambda_{k+1}^{(1/2)}(X) > \lambda_k^{(1/2)}(X)$ for all $k \in \mathbb{N}$.

Linear Program 1 (Spectral bound on Laplacian). *Given* $\Lambda \in \mathbb{N}$, $\lambda_*^{(0)} \in \mathbb{R}_+$ *and a hyperbolic spin orbifold with a holomorphic modular form of weight n such that* $n = 1 \pmod 2$, *if there exists* $\alpha \in \mathbb{R}^{\Lambda+1}$ *with such that*

1. $\alpha_{2m} \leq 0$, $\forall m \in \mathbb{Z}_{\geq 0}$,

2. $\sum_{m=0}^{\Lambda} \alpha_m \mathcal{F}_m^{(n/2,n/2,n/2,n/2)}(0) = 1$,

3. $\forall \lambda_k^{(0)} \geq \lambda_*^{(0)}$ we have

$$\sum_{m=0}^{\Lambda} \alpha_m \mathcal{F}_m^{(n/2,n/2,n/2,n/2)}(\lambda_k^{(0)}) \geq 0, \tag{6.87}$$

we must have $\lambda_1^{(0)} < \lambda_*^{(0)}$.

Proof. We consider the third and the fourth equation of the ones appearing in the proposition 6.3.60 and write them below.

$$S_{n+2m;(n/2,n/2)} = \left(\mathcal{F}_{2m}^{(n/2,n/2,n/2,n/2)}(0) + \sum_{k=1}^{\infty} \left[\sum_{a=1}^{d_k} \left(c_{n/2,n/2}^{k;a} \right)^2 \right] \mathcal{F}_{2m}^{(n/2,n/2,n/2,n/2)}(\lambda_k^{(0)}) \right),$$

$$0 = \left(\mathcal{F}_{2p+1}^{(n/2,n/2,n/2,n/2)}(0) + \sum_{k=1}^{\infty} \left[\sum_{a=1}^{d_k} \left(c_{n/2,n/2}^{k;a} \right)^2 \right] \mathcal{F}_{2p+1}^{(n/2,n/2,n/2,n/2)}(\lambda_k^{(0)}) \right).$$

Here we renamed the variable m to p to write down the second equation.

For a given $m \in \mathbb{Z}_{\geq 0}$ and $p \in \mathbb{Z}_{\geq 0}$, we multiply the first equation above with α_{2m}, the second equation above with α_{2p+1}, and add them together. Now we sum over m and p such that $2m \leq \Lambda$ and $2p + 1 \leq \Lambda$. Then we use the trivial identity

$$\sum_{0 \leq 2m \leq \Lambda} \alpha_{2m} \mathcal{F}_{2m}^{(n/2,n/2,n/2,n/2)}(\lambda_k^{(0)}) + \sum_{0 \leq 2p+1 \leq \Lambda} \alpha_{2p+1} \mathcal{F}_{2p+1}^{(n/2,n/2,n/2,n/2)}(\lambda_k^{(0)})$$

$$= \sum_{q=0}^{\Lambda} \alpha_q \mathcal{F}_q^{(n/2,n/2,n/2,n/2)}(\lambda_k^{(0)}),$$

and the property (2) of α to finally obtain the following:

$$\sum_{k=1}^{\infty} \left(\left[\sum_{a=1}^{d_k} \left(c_{n/2,n/2}^{k;a} \right)^2 \right] \sum_{q=0}^{\Lambda} \alpha_q \mathcal{F}_q^{(n/2,n/2,n/2,n/2)}(\lambda_k^{(0)}) \right) = -1 + \sum_{m=0}^{\lfloor \frac{\Lambda}{2} \rfloor} \alpha_{2m} S_{n+2m;(n/2,n/2)}.$$

Now using the properties of α, we show that the R.H.S of the above is strictly negative. Therefore the L.H.S is strictly negative. Using (6.87), the proposition follows. □

Semidefinite Program 1 (Spectral bound on Laplacian and Dirac: I). *Let us consider a hyperbolic spin orbifold ,for which, $\exists\, n \in \mathbb{N}$ with $n = 1 (mod\ 2)$ such that the*

orbifold does not support any holomorphic modular form of weight strictly below n and does support a (at least one) holomorphic modular form of weight n.

Given $\Lambda \in \mathbb{N}$, $\lambda_*^{(0)}, \lambda_*^{(1/2)} \in \mathbb{R}_+$, if there exists $\alpha_i \in \mathbb{R}^{\Lambda+1}$ with $i = 1, 2, 3, 4$ such that

1. $\alpha_{1;2m} \leq 0$, $\forall m \in \mathbb{Z}_{\geq 0}$,

2. $\sum_{m=0}^{\Lambda} \left(\alpha_{1;m} \mathcal{F}_m^{(n,n,n,n)}(0) + \alpha_{2;m} \mathcal{F}_m^{(n/2,n/2,n/2,n/2)}(0) + \alpha_{3;m} \mathcal{F}_m^{(n,n/2,n/2,n)}(0) \right) = 1$,

3. $\alpha_{2;2m} \leq 0$, $\forall m \in \mathbb{Z}_{\geq 0}$,

4. $\alpha_{3;m} + (-1)^m \alpha_{4;m} \leq 0$, $\forall m \in \mathbb{Z}_{\geq 0}$,

5. $\sum_{m'=0}^{\Lambda} \alpha_{4;m'} \mathcal{F}_{m'}^{(n,n/2,n,n/2)} \left(\frac{n}{2}(1 - \frac{n}{2}) \right) \geq 0$, $\forall m \in \mathbb{Z}_{\geq 0}$,

6. $\forall \lambda_k^{(1/2)} \geq \lambda_*^{(1/2)}$, *we have*

$$\sum_{m=0}^{\Lambda} \alpha_{4;m} \mathcal{F}_m^{(n,n/2,n,n/2)}(\lambda_k^{(1/2)}) \geq 0, \tag{6.88}$$

7. $\forall \lambda_k^{(0)} \geq \lambda_*^{(0)}$ *we have*

$$M(\lambda_k^{(0)}) := \begin{pmatrix} \sum_{m=0}^{\Lambda} \alpha_{1;m} \mathcal{F}_m^{(n,n,n,n)}(\lambda_k^{(0)}) & \frac{1}{2} \sum_{m=0}^{\Lambda} \alpha_{3;m} \mathcal{F}_m^{(n,n/2,n/2,n)}(\lambda_k^{(0)}) \\ \frac{1}{2} \sum_{m=0}^{\Lambda} \alpha_{3;m} \mathcal{F}_m^{(n,n/2,n/2,n)}(\lambda_k^{(0)}) & \sum_{m=0}^{\Lambda} \alpha_{2;m} \mathcal{F}_m^{(n/2,n/2,n/2,n/2)}(\lambda_k^{(0)}) \end{pmatrix} \succeq 0, \tag{6.89}$$

we must have either $\lambda_1^{(0)} < \lambda_*^{(0)}$ or $\lambda_1^{(1/2)} < \lambda_*^{(1/2)}$.

Proof. The proof is similar to the proof of the Linear Program 1 and involves taking appropriate linear combination of equations appearing in (6.3.60). To be concrete, let us define

$$S_{2n+2m+1;(n,n)} = 0, \quad S_{2n+2m+1;(n/2,n/2)} = 0, \quad m \in \mathbb{Z}_{\geq 0} \tag{6.90}$$

and rewrite the equations appearing in proposition (6.3.60) in the following form:

$$S_{2n+m;(n,n)} = \left(\mathcal{F}_m^{(n,n,n,n)}(0) + \sum_{k=1}^{\infty} \left[\sum_{a=1}^{d_k} \left(c_{n,n}^{k;a} \right)^2 \right] \mathcal{F}_m^{(n,n,n,n)}(\lambda_k^{(0)}) \right),$$

$$S_{n+m;(n/2,n/2)} = \left(\mathcal{F}_m^{(n/2,n/2,n/2,n/2)}(0) + \sum_{k=1}^{\infty} \left[\sum_{a=1}^{d_k} \left(c_{n/2,n/2}^{k;a} \right)^2 \right] \mathcal{F}_m^{(n/2,n/2,n/2,n/2)}(\lambda_k^{(0)}) \right),$$

$$S_{3n/2+m;(n,n/2)} = \left(\mathcal{F}_m^{(n,n/2,n/2,n)}(0) + \sum_{k=1}^{\infty} \left[\sum_{a=1}^{d_k} c_{n/2,n/2}^{k;a} c_{n,n}^{k;a} \right] \mathcal{F}_m^{(n,n/2,n/2,n)}(\lambda_k^{(0)}) \right),$$

$$(-1)^m S_{3n/2+m;(n,n/2)} = \left(\sum_{k=1}^{\infty} \left[\sum_{a=1}^{d_k'} |s_{n,n/2}^{k;a}|^2 \right] \mathcal{F}_m^{(n,n/2,n,n/2)}(\lambda_k^{(1/2)}) + \right.$$

$$\left. + \sum_{0<q\leq n/2} \sum_{a=1}^{\ell_q} |f_{n/2,(q;a)}^n|^2 \mathcal{F}_m^{(n,n/2,n,n/2)}(q(1-q)) \right).$$

For the orbifold under consideration, there does not exist a holomorphic modular form of weight strictly below n. Hence, the sum appearing in the last line of the fourth equation appearing above collapses to a single term corresponding to $q = n/2$.

For each value of m, there are four crossing equations above. We multiply the i-th one with $\alpha_{i;m}$. Then we sum over the indices i and m such that $1 \leqslant i \leqslant 4$ and $0 \leqslant m \leqslant \Lambda$. Finally, we use (6.90) and property (2) of α to obtain:

$$\sum_{k=1}^{\infty} \sum_{a=1}^{d_k} \left(c_{n,n}^{k;a}, c_{n/2,n/2}^{k;a} \right) M(\lambda_k^{(0)}) \begin{pmatrix} c_{n,n}^{k;a} \\ c_{n/2,n/2}^{k;a} \end{pmatrix} + \sum_{k=1}^{\infty} \left[\sum_{a=1}^{d_k'} |s_{n,n/2}^{k;a}|^2 \right] \sum_{m=0}^{\Lambda} \alpha_{4;m} \mathcal{F}_m^{(n,n/2,n,n/2)}(\lambda_k^{(1/2)})$$

$$= -1 + \sum_{m=0}^{\lfloor \frac{\Lambda}{2} \rfloor} \left(\alpha_{1,2m} S_{2n+2m;(n,n)} + \alpha_{2;2m} S_{n+2m;(n/2,n/2)} \right) -$$

$$- \left[\sum_{a=1}^{\ell_{n/2}} |f_{n/2,(n/2;a)}^n|^2 \right] \sum_{m'=0}^{\Lambda} \alpha_{4;m'} \mathcal{F}_{m'}^{(n,n/2,n,n/2)} \left(\frac{n}{2} \left(1 - \frac{n}{2} \right) \right) +$$

$$+ \sum_{m'=0}^{\Lambda} \left(\alpha_{3;m'} + (-1)^{m'} \alpha_{4;m'} \right) S_{3n/2+m';(n,n/2)} .$$

Now using the properties of α, we show that the R.H.S of the above is strictly negative. Therefore the L.H.S is strictly negative. Using (6.88) and (6.89), the proposition follows. $\qquad \square$

Remark 6.3.61. When $\ell_n = \ell_{n/2} = 1$, the structure constant $\sum_{a=1}^{\ell_{n/2}} |f_{n/2,(n/2;a)}^n|^2$ appearing in the t-channel expansion in the last equation of (6.3.60) is exactly same as $S_{n;(n/2,n/2)}$. Thus we can formulate a stronger SDP problem, which we state below.

Semidefinite Program 2 (Spectral bound on Laplacian and Dirac: II). *Let us consider a hyperbolic spin orbifold , for which, $\exists\, n \in \mathbb{N}$ with $n = 1 (\mathrm{mod}\, 2)$ such that the orbifold does not support any holomorphic modular form of weight strictly below n. Finally, assume that the multiplicity of holomorphic modular forms of weight n and $2n$ are respectively given by $\ell_{n/2} = 1$ and $\ell_n = 1$.*

Given $\Lambda \in \mathbb{N}$, $\lambda_*^{(0)}, \lambda_*^{(1/2)} \in \mathbb{R}_+$, if there exists $\alpha_i \in \mathbb{R}^{\Lambda+1}$ with $i = 1, 2, 3, 4$ such that

1. $\alpha_{1;2m} \leq 0$, $\forall\, m \in \mathbb{Z}_{\geq 0}$

2. $\sum_{m=0}^{\Lambda} \left(\alpha_{1;m} \mathcal{F}_m^{(n,n,n,n)}(0) + \alpha_{2;m} \mathcal{F}_m^{(n/2,n/2,n/2,n/2)}(0) + \alpha_{3;m} \mathcal{F}_m^{(n,n/2,n/2,n)}(0) \right) = 1$

3. $\alpha_{2;2m} - \delta_{2m,0} \sum_{m'=0}^{\Lambda} \alpha_{4;m'} \mathcal{F}_{m'}^{(n,n/2,n,n/2)} \left(\frac{n}{2}(1 - \frac{n}{2}) \right) \leq 0$, $\forall\, m \in \mathbb{Z}_{\geq 0}$,

4. $\alpha_{3;m} + (-1)^m \alpha_{4;m} \leq 0$, $\forall\, m \in \mathbb{Z}_{\geq 0}$,

5. $\forall\, \lambda_k^{(1/2)} \geq \lambda_*^{(1/2)}$, *we have*
$$\sum_{m=0}^{\Lambda} \alpha_{4;m} \mathcal{F}_m^{(n,n/2,n,n/2)}(\lambda_k^{(1/2)}) \geq 0, \tag{6.91}$$

6. $\forall\, \lambda_k^{(0)} \geq \lambda_*^{(0)}$ *we have*
$$M(\lambda_k^{(0)}) := \begin{pmatrix} \sum_{m=0}^{\Lambda} \alpha_{1;m} \mathcal{F}_m^{(n,n,n,n)}(\lambda_k^{(0)}) & \frac{1}{2} \sum_{m=0}^{\Lambda} \alpha_{3;m} \mathcal{F}_m^{(n,n/2,n/2,n)}(\lambda_k^{(0)}) \\ \frac{1}{2} \sum_{m=0}^{\Lambda} \alpha_{3;m} \mathcal{F}_m^{(n,n/2,n/2,n)}(\lambda_k^{(0)}) & \sum_{m=0}^{\Lambda} \alpha_{2;m} \mathcal{F}_m^{(n/2,n/2,n/2,n/2)}(\lambda_k^{(0)}) \end{pmatrix} \succeq 0, \tag{6.92}$$

we must have either $\lambda_1^{(0)} < \lambda_*^{(0)}$ or $\lambda_1^{(1/2)} < \lambda_*^{(1/2)}$.

Proof. The proof involves taking the same linear combinations of equations appearing in (6.3.60), as done in the proof of Semidefinite Program 1 and further using the fact $\ell_{n/2} = 1$, leading to
$$\sum_{a=1}^{\ell_{n/2}} |f_{n/2,(n/2;a)}^n|^2 = S_{n;(n/2,n/2)} .$$

In this way, we obtain

$$\sum_{k=1}^{\infty}\sum_{a=1}^{d_k}\left(c_{n,n}^{k;a},\,c_{n/2,n/2}^{k;a}\right)M(\lambda_k^{(0)})\begin{pmatrix}c_{n,n}^{k;a}\\c_{n/2,n/2}^{k;a}\end{pmatrix}+\sum_{k=1}^{\infty}\sum_{a=1}^{d'_k}|s_{n,n/2}^{k;a}|^2\sum_{m=0}^{\Lambda}\alpha_{4;m}\mathcal{F}_m^{(n,n/2,n,n/2)}(\lambda_k^{(1/2)})$$

$$=-1+\sum_{m=0}^{\lfloor\Lambda/2\rfloor}\left(\alpha_{1,2m}S_{2n+2m;(n,n)}+\left(\alpha_{2;2m}-\delta_{2m,0}\sum_{m'=0}^{\Lambda}\alpha_{4;m'}\mathcal{F}_{m'}^{(n,n/2,n,n/2)}\left(\frac{n}{2}\left(1-\frac{n}{2}\right)\right)\right)\times\right.$$

$$\times\,S_{n+2m;(n/2,n/2)}\Bigg)+\sum_{m=0}^{\Lambda}\left(\alpha_{3;m}+(-1)^m\alpha_{4;m}\right)S_{3n/2+m;(n,n/2)}\,.$$

Now using the properties of α, we show that the R.H.S of the above is strictly negative. Therefore the L.H.S is strictly negative. Using (6.91) and (6.92), the proposition follows. □

In what follows, we will use $\mathcal{O}_n$ and $\mathcal{O}_{n/2}$ and assume that there is no holomorphic modular form of weight strictly below n on the orbifold under consideration. This is clearly true for $n=1$. Furthermore, we will use a clever trick introduced in [283] to reduce the size of the problem. The idea is to consider the correlators and do a Haar integral over $U(\ell_n)$ and $U(\ell_{n/2})$.

Proposition 6.3.62. *For a unitary group $U(\ell)$, we have*

$$\int_{U(\ell)}dU\,U_{a_1}^{a'_1}(\bar{U})_{a_2}^{a'_2}=\frac{1}{\ell}\delta_{a_1,a_2}\delta_{a'_1,a'_2},$$

$$\int_{U(\ell)}dU\,U_{a_1}^{a'_1}U_{a_2}^{a'_2}(\bar{U})_{a_3}^{a'_3}(\bar{U})_{a_4}^{a'_4}=\frac{1}{\ell^2-1}\left(\delta_{a_1,a_3}\delta_{a_2,a_4}\delta^{a'_1,a'_3}\delta^{a'_2,a'_4}+\delta_{a_1,a_4}\delta_{a_2,a_3}\delta^{a'_1,a'_4}\delta^{a'_2,a'_3}\right)$$

$$-\frac{1}{\ell(\ell^2-1)}\left(\delta_{a_1,a_3}\delta_{a_2,a_4}\delta^{a'_1,a'_4}\delta^{a'_2,a'_3}+\delta_{a_1,a_4}\delta_{a_2,a_3}\delta^{a'_1,a'_3}\delta^{a'_2,a'_4}\right).$$

Next the idea is to consider the symmetrized set of correlators:

Definition 6.3.63. The symmetrized correlators are defined by

$$\langle\mathcal{O}_n\mathcal{O}_n\widetilde{\mathcal{O}}_n\widetilde{\mathcal{O}}_n\rangle_{\text{SYM}}:=\int_{U(\ell_n)}dU\,U_{a_1}^{a'_1}U_{a_2}^{a'_2}(\bar{U})_{a_3}^{a'_3}(\bar{U})_{a_4}^{a'_4}\,\langle\mathcal{O}_{n,a_1}\mathcal{O}_{n,a_2}\widetilde{\mathcal{O}}_{n,a_3}\widetilde{\mathcal{O}}_{n,a_4}\rangle,$$

$$\langle\mathcal{O}_{\frac{n}{2}}\mathcal{O}_{\frac{n}{2}}\widetilde{\mathcal{O}}_{\frac{n}{2}}\widetilde{\mathcal{O}}_{\frac{n}{2}}\rangle_{\text{SYM}}:=\int_{U(\ell_{n/2})}dU\,U_{b_1}^{b'_1}U_{b_2}^{b'_2}(\bar{U})_{b_3}^{b'_3}(\bar{U})_{b_4}^{b'_4}\,\langle\mathcal{O}_{\frac{n}{2},b_1}\mathcal{O}_{\frac{n}{2},b_2}\widetilde{\mathcal{O}}_{\frac{n}{2},b_3}\widetilde{\mathcal{O}}_{\frac{n}{2},b_4}\rangle,$$

$$\langle\mathcal{O}_n\mathcal{O}_{\frac{n}{2}}\widetilde{\mathcal{O}}_{\frac{n}{2}}\widetilde{\mathcal{O}}_n\rangle_{\text{SYM}}:=\int_{U(\ell_n)}dU\,U_{a_1}^{a'_1}(\bar{U})_{a_2}^{a'_2}\int_{U(\ell_{n/2})}dU\,U_{b_1}^{b'_1}(\bar{U})_{b_2}^{b'_2}\,\langle\mathcal{O}_{n,a_1}\mathcal{O}_{\frac{n}{2},b_1}\widetilde{\mathcal{O}}_{\frac{n}{2},b_2}\widetilde{\mathcal{O}}_{n,a_2}\rangle,$$

$$\langle\mathcal{O}_n\mathcal{O}_{\frac{n}{2}}\widetilde{\mathcal{O}}_n\widetilde{\mathcal{O}}_{\frac{n}{2}}\rangle_{\text{SYM}}:=\int_{U(\ell_n)}dU\,U_{a_1}^{a'_1}(\bar{U})_{a_2}^{a'_2}\int_{U(\ell_{n/2})}dU\,U_{b_1}^{b'_1}(\bar{U})_{b_2}^{b'_2}\,\langle\mathcal{O}_{n,a_1}\mathcal{O}_{\frac{n}{2},b_1}\widetilde{\mathcal{O}}_{n,a_2}\widetilde{\mathcal{O}}_{\frac{n}{2},b_2}\rangle.$$

$$(6.93)$$

Definition 6.3.64. Let us define the following quantities:

$$\mathbf{S}_{p;n} := \frac{1}{\ell_n(\ell_n + 1)} \sum_{i=1}^{\ell_p} \sum_{a_1,a_2=1}^{\ell_n} \frac{1}{4} \left| f^{(p;i)}_{(n;a_1),(n;a_2)} + f^{(p;i)}_{(n;a_2),(n;a_1)} \right|^2,$$

$$\mathbf{A}_{p;n} := \frac{1}{\ell_n(\ell_n - 1)} \sum_{i=1}^{\ell_p} \sum_{a_1,a_2=1}^{\ell_n} \frac{1}{4} \left| f^{(p;i)}_{(n;a_1),(n;a_2)} - f^{(p;i)}_{(n;a_2),(n;a_1)} \right|^2,$$

$$\mathbf{T}_{k;n} := \frac{1}{\ell_n^2 - 1} \sum_{i=1}^{d_k} \sum_{a_1,a_2=1}^{\ell_n} \left[c^{(k;i)}_{(n;a_1),(n;a_2)} \overline{c^{(k;i)}_{(n;a_1),(n;a_2)}} - \frac{1}{\ell_n} c^{(k;i)}_{(n;a_1),(n;a_1)} \overline{c^{(k;i)}_{(n;a_2),(n;a_2)}} \right],$$

$$\mathbf{Q}_{k;n} := \frac{1}{\ell_n} \sum_{i=1}^{d_k} c^{(k;i)}_{(n;a),(n;a)},$$

$$\mathbf{B}_{p;(n_1,n_2)} := \frac{1}{\ell_{n_1}\ell_{n_2}} \sum_{i=1}^{\ell_p} \sum_{a=1}^{\ell_{n_1}} \sum_{b=1}^{\ell_{n_2}} |f^{(p;i)}_{(n_1;a),(n_2;b)}|^2,$$

$$\mathbf{P}_{k;(n_1,n_2)} := \frac{1}{\ell_{n_1}\ell_{n_2}} \sum_{i=1}^{d_k} \sum_{a=1}^{\ell_{n_1}} \sum_{b=1}^{\ell_{n_2}} |s^{(k;i)}_{(n_1;a),(n_2;b)}|^2.$$

$$(6.94)$$

Let ρ_n denote the fundamental representations of $U(\ell_n)$ and ρ_n^* its complex conjugate. The quantities $\mathbf{S}_{p;n}, \mathbf{A}_{p;n}, \mathbf{T}_{k;n}$ and $\mathbf{Q}_{k;n}$ label different trivial representations in the decomposition of $(\rho_n^{\otimes 2}) \otimes (\rho_n^*)^{\otimes 2}$. $\mathbf{S}_{p;n}$ is the element in the trivial representation which arises from $\mathrm{Sym}^2(\rho_n) \otimes \mathrm{Sym}^2(\rho_n^*)$ and $\mathbf{A}_{p;n}$ is from $\wedge^2(\rho_n) \otimes \wedge^2(\rho_n^*)$. The tensor product $\rho_n \otimes \rho_n^*$ decomposes into a symmetric traceless representation and a trivial representation. $\mathbf{T}_{k;n}$ and $(\mathbf{Q}_{k;n})^2$ come from the tensor product of these two representations, respectively. Similarly, $\mathbf{B}_{p;(n_1,n_2)}$ and $\mathbf{P}_{k;(n_1,n_2)}$ are $U(\ell_{n_1}) \times U(\ell_{n_2})$ invariants from $(\rho_{n_1} \times \rho_{n_2}) \otimes (\rho_{n_1}^* \times \rho_{n_2}^*)$

Remark 6.3.65. Except for $\mathbf{Q}_{k;n}$, all quantities defined above are positive semi-definite combinations of the OPE coefficients.

Proposition 6.3.66. *Given a hyperbolic spin orbifold, for which, $\exists\, n \in \mathbb{N}$ with $n = 1(mod\ 2)$ such that the orbifold does not support holomorphic modular forms with weight strictly smaller than n, and it supports $\ell_n \neq 0$ different holomorphic modular forms with weight 2n and $\ell_{n/2} \neq 0$ different holomorphic modular forms with weight n, the spectral identities derived from the set of symmetrized correlators defined above are given by:*

$\forall m \in \mathbb{Z}_{\geqslant 0}$:

$$\mathbf{S}_{2m+2n;n} = \sum_{k=1}^{\infty} \mathbf{T}_{k;n} \mathcal{F}_{2m}^{(n,n,n,n)}(\lambda_k^{(0)}),$$

$$-\mathbf{A}_{2m+1+2n;n} = \sum_{k=1}^{\infty} \mathbf{T}_{k;n} \mathcal{F}_{2m+1}^{(n,n,n,n)}(\lambda_k^{(0)}),$$

$$\mathbf{S}_{2m+2n;n} = \mathcal{F}_{2m}^{(n,n,n,n)}(0) + \sum_{k=1}^{\infty} \left(\mathbf{Q}_{k;n}^2 - \frac{1}{\ell_n} \mathbf{T}_{k;n} \right) \mathcal{F}_{2m}^{(n,n,n,n)}(\lambda_k^{(0)}),$$

$$\mathbf{A}_{2m+1+2n;n} = \mathcal{F}_{2m+1}^{(n,n,n,n)}(0) + \sum_{k=1}^{\infty} \left(\mathbf{Q}_{k;n}^2 - \frac{1}{\ell_n} \mathbf{T}_{k;n} \right) \mathcal{F}_{2m+1}^{(n,n,n,n)}(\lambda_k^{(0)}),$$

$$\mathbf{S}_{2m+n;n/2} = \sum_{k=1}^{\infty} \mathbf{T}_{k;n/2} \, \mathcal{F}_{2m}^{(n/2,n/2,n/2,n/2)}(\lambda_k^{(0)}),$$

$$-\mathbf{A}_{2m+1+n;n/2} = \sum_{k=1}^{\infty} \mathbf{T}_{k;n/2} \, \mathcal{F}_{2m+1}^{(n/2,n/2,n/2,n/2)}(\lambda_k^{(0)}),$$

$$\mathbf{S}_{2m+n;n/2} = \mathcal{F}_{2m}^{(n/2,n/2,n/2,n/2)}(0) + \sum_{k=1}^{\infty} \left(\mathbf{Q}_{k;n/2}^2 - \frac{1}{\ell_{n/2}} \mathbf{T}_{k;n/2} \right) \mathcal{F}_{2m}^{(n/2,n/2,n/2,n/2)}(\lambda_k^{(0)}),$$

$$\mathbf{A}_{2m+1+n;n/2} = \mathcal{F}_{2m+1}^{(n/2,n/2,n/2,n/2)}(0) + \sum_{k=1}^{\infty} \left(\mathbf{Q}_{k;n/2}^2 - \frac{1}{\ell_{n/2}} \mathbf{T}_{k;n/2} \right) \mathcal{F}_{2m+1}^{(n/2,n/2,n/2,n/2)}(\lambda_k^{(0)}),$$

$$\mathbf{B}_{m+3n/2;(n,n/2)} = \mathcal{F}_m^{(n,n/2,n/2,n)}(0) + \sum_{k=1}^{\infty} \mathbf{Q}_{k;n} \mathbf{Q}_{k;n/2} \, \mathcal{F}_m^{(n,n/2,n/2,n)}(\lambda_k^{(0)}),$$

$$(-1)^m \mathbf{B}_{m+3n/2;(n,n/2)} = \sum_{k=1}^{\infty} \mathbf{P}_{k;(n,n/2)} \, \mathcal{F}_m^{(n,n/2,n,n/2)}(\lambda_k^{(1/2)})$$
$$+ \frac{\ell_{n/2}+1}{\ell_n} \mathbf{S}_{n;n/2} \, \mathcal{F}_m^{(n,n/2,n,n/2)} \left(\frac{n}{2} \left(1 - \frac{n}{2} \right) \right).$$

Proof. The first four equations above come from $\langle \mathcal{O}_n \mathcal{O}_n \widetilde{\mathcal{O}}_n \widetilde{\mathcal{O}}_n \rangle_{\text{SYM}}$. The idea is to expand the integrand, appearing in the definition (6.93), in s and t-channel; then exchange the sum and the Haar integral, followed by performing the Haar integral using the second equation in proposition 6.3.62. These are exactly same as the ones in [283]. The 5th to the 8th equations are derived from considering $\langle \mathcal{O}_{n/2} \mathcal{O}_{n/2} \widetilde{\mathcal{O}}_{n/2} \widetilde{\mathcal{O}}_{n/2} \rangle_{\text{SYM}}$ and following similar steps. The 9th and the 10th equations are coming from considering $\langle \mathcal{O}_n \mathcal{O}_{\frac{n}{2}} \widetilde{\mathcal{O}}_{\frac{n}{2}} \widetilde{\mathcal{O}}_n \rangle_{\text{SYM}}$ and $\langle \mathcal{O}_n \mathcal{O}_{\frac{n}{2}} \widetilde{\mathcal{O}}_n \widetilde{\mathcal{O}}_{\frac{n}{2}} \rangle_{\text{SYM}}$, respectively. In short, the unsymmetrized consistency conditions imply the symmetrized consistency conditions just by averaging over all possible bases of the relevant eigenspaces. $\square$

Semidefinite Program 3 (Spectral bound on Laplacian and Dirac: III). *Let us consider a hyperbolic spin orbifold which supports $\ell_n \neq 0$ different holomorphic modular forms with weight $2n$ and $\ell_{n/2} \neq 0$ different holomorphic modular forms with weight n. Assume that the orbifold does not support any holomorphic modular form with weight strictly smaller than n.*

Given $\Lambda \in \mathbb{N}$, $\lambda_*^{(0)}, \lambda_*^{(1/2)} \in \mathbb{R}_+$, if there exist $\alpha_i \in \mathbb{R}^{\Lambda+1}$ with $i = 1, 2, 3, 4, 5, 6$ such that

1. $\sum_{m=0}^{\Lambda} \alpha_{2;m}\, \mathcal{F}_m^{(n,n,n,n)}(0) + \alpha_{4;m}\, \mathcal{F}_m^{(n/2,n/2,n/2,n/2)}(0) + \alpha_{5;m}\, \mathcal{F}_m^{(n,n/2,n/2,n)}(0) = 1,$

2. $\alpha_{1;2m} + \alpha_{2;2m} \leqslant 0, \quad \forall m \in \mathbb{Z}_{\geqslant 0}, 2m \leqslant \Lambda,$

3. $\alpha_{3;2m} + \alpha_{4;2m} - \delta_{m,0} \frac{\ell_{n/2}+1}{\ell_n} \sum_{m'=0}^{\Lambda} \alpha_{6;m'}\, \mathcal{F}_{m'}^{(n,n/2,n,n/2)}\left(\frac{n}{2}\left(1 - \frac{n}{2}\right)\right) \leqslant 0,$
   $\forall m \in \mathbb{Z}_{\geqslant 0}, 2m \leqslant \Lambda,$

4. $\alpha_{2;2m+1} - \alpha_{1;2m+1} \leqslant 0, \quad \forall m \in \mathbb{Z}_{\geqslant 0}, 2m + 1 \leqslant \Lambda,$

5. $\alpha_{4;2m+1} - \alpha_{3;2m+1} \leqslant 0, \quad \forall m \in \mathbb{Z}_{\geqslant 0}, 2m + 1 \leqslant \Lambda,$

6. $\alpha_{5;m} + (-1)^m \alpha_{6;m} \leqslant 0, \quad \forall m \in \mathbb{Z}_{\geqslant 0}, m \leqslant \Lambda,$

7.
$$\sum_{m=0}^{\Lambda} \left(\alpha_{1;m} - \frac{1}{\ell_n}\alpha_{2;m}\right) \mathcal{F}_m^{(n,n,n,n)}(\lambda_k^{(0)}) \geqslant 0, \quad \forall \lambda_k^{(0)} \geqslant \lambda_*^{(0)}, \tag{6.95}$$

8.
$$\sum_{m=0}^{\Lambda} \left(\alpha_{3;m} - \frac{1}{\ell_{n/2}}\alpha_{4;m}\right) \mathcal{F}_m^{(n/2,n/2,n/2,n/2)}(\lambda_k^{(0)}) \geqslant 0, \quad \forall \lambda_k^{(0)} \geqslant \lambda_*^{(0)}, \tag{6.96}$$

9.

$$\sum_{m=0}^{\Lambda} \alpha_{6;m} \, \mathcal{F}_m^{(n,n/2,n,n/2)}(\lambda_k^{(1/2)}) \geqslant 0, \quad \forall \lambda_k^{(1/2)} \geqslant \lambda_*^{(1/2)}, \qquad (6.97)$$

10. $\forall \lambda_k^{(0)} \geqslant \lambda_*^{(0)}$,

$$M'(\lambda_k^{(0)}) := \begin{pmatrix} \sum_{m=0}^{\Lambda} \alpha_{2;m} \mathcal{F}_m^{(n,n,n,n)}(\lambda_k^{(0)}) & \frac{1}{2} \sum_{m=0}^{\Lambda} \alpha_{5;m} \mathcal{F}_m^{(n,n/2,n/2,n)}(\lambda_k^{(0)}) \\ \frac{1}{2} \sum_{m=0}^{\Lambda} \alpha_{5;m} \mathcal{F}_m^{(n,n/2,n/2,n)}(\lambda_k^{(0)}) & \sum_{m=0}^{\Lambda} \alpha_{4;m} \mathcal{F}_m^{(n,n,n,n)}(\lambda_k^{(0)}) \end{pmatrix} \succeq 0,$$

$$(6.98)$$

then at least one of the following statements must be true:

1. $\lambda_1^{(0)} < \lambda_*^{(0)}$,

2. $\lambda_1^{(1/2)} < \lambda_*^{(1/2)}$.

Proof. The proof is similar in nature to the ones appearing before for the semidefinite linear programs. Let us define

$$V_{1;m} := \begin{cases} \mathbf{S}_{m+2n;n}, & m = 0 \,(\mathrm{mod}\ 2) \\ -\mathbf{A}_{m+2n;n}, & m = 1 \,(\mathrm{mod}\ 2) \end{cases} , \quad V_{2;m} := (-1)^m V_{1;m}$$

$$V_{3;m} := \begin{cases} \mathbf{S}_{m+2n;n/2}, & m = 0 \,(\mathrm{mod}\ 2) \\ -\mathbf{A}_{m+2n;n/2}, & m = 1 \,(\mathrm{mod}\ 2) \end{cases} , \quad V_{4;m} := (-1)^m V_{3;m}$$

$$V_{5;m} := \mathbf{B}_{m+3n/2;(n,n/2)}, \quad V_{6;m} := (-1)^m V_{5;m}.$$

$$(6.99)$$

Using these, we rewrite the equations appearing in (6.3.66):

$$V_{1;m} = \sum_{k=1}^{\infty} \mathbf{T}_{k;n} \mathcal{F}_m^{(n,n,n,n)}(\lambda_k^{(0)}),$$

$$V_{2;m} = \mathcal{F}_m^{(n,n,n,n)}(0) + \sum_{k=1}^{\infty} \left(\mathbf{Q}_{k;n}^2 - \frac{1}{\ell_n}\mathbf{T}_{k;n}\right) \mathcal{F}_m^{(n,n,n,n)}(\lambda_k^{(0)}),$$

$$V_{3;m} = \sum_{k=1}^{\infty} \mathbf{T}_{k;n/2} \, \mathcal{F}_m^{(n/2,n/2,n/2,n/2)}(\lambda_k^{(0)})$$

$$V_{4;m} = \mathcal{F}_m^{(n/2,n/2,n/2,n/2)}(0) + \sum_{k=1}^{\infty} \left(\mathbf{Q}_{k;n/2}^2 - \frac{1}{\ell_{n/2}}\mathbf{T}_{k;n/2}\right) \mathcal{F}_m^{(n/2,n/2,n/2,n/2)}(\lambda_k^{(0)}),$$

$$V_{5;m} = \mathcal{F}_m^{(n,n/2,n/2,n)}(0) + \sum_{k=1}^{\infty} \mathbf{Q}_{k;n}\mathbf{Q}_{k;n/2} \, \mathcal{F}_m^{(n,n/2,n/2,n)}(\lambda_k^{(0)}),$$

$$V_{6;m} = \sum_{k=1}^{\infty} \mathbf{P}_{k;(n,n/2)} \, \mathcal{F}_m^{(n,n/2,n,n/2)}(\lambda_k^{(1/2)})$$

$$+ \frac{\ell_{n/2}+1}{\ell_n}\mathbf{S}_{n;n/2} \, \mathcal{F}_m^{(n,n/2,n,n/2)}\left(\frac{n}{2}\left(1-\frac{n}{2}\right)\right).$$

For a given $m \in \mathbb{Z}_{\geqslant 0}$, there are six crossing equations above. We multiply the i-th equation by $\alpha_{i;m}$ and sum them up. Then we take linear combination by summing over m such that $m \leqslant \Lambda$. At this point, we write the variable V in terms of the

original variable **S**, **A**, **B** to obtain:

$$
\sum_{m=0}^{\lfloor \Lambda/2 \rfloor} \Big[(\alpha_{1;2m} + \alpha_{2;2m}) \mathbf{S}_{2m+2n;n}
$$

$$
+ \big(\alpha_{3;2m} + \alpha_{4;2m} - \delta_{2m,0} \frac{\ell_{n/2}+1}{\ell_n} \times \sum_{m'=0}^{\Lambda} \alpha_{6;m'} \mathcal{F}_{m'}^{(n,n/2,n,n/2)} \big(\frac{n}{2}(1 - \frac{n}{2}) \big) \big) \mathbf{S}_{2m+n;n/2} \Big]
$$

$$
+ \sum_{m=0}^{\lfloor \frac{\Lambda-1}{2} \rfloor} \Big[(\alpha_{2;2m+1} - \alpha_{1;2m+1}) \mathbf{A}_{2m+1+2n;n} + (\alpha_{4;2m+1} - \alpha_{3;2m+1}) \mathbf{A}_{2m+1+n;n/2} \Big]
$$

$$
+ \sum_{m=0}^{\Lambda} \big(\alpha_{5;m} + (-1)^m \alpha_{6;m} \big) \mathbf{B}_{m+3n/2;(n,n/2)}
$$

$$
- \sum_{m=0}^{\Lambda} \Big(\alpha_{2;m} \mathcal{F}_m^{(n,n,n,n)}(0) + \alpha_{4;m} \mathcal{F}_m^{(n/2,n/2,n/2,n/2)}(0) + \alpha_{5;m} \mathcal{F}_m^{(n,n/2,n/2,n)}(0) \Big)
$$

$$
= \sum_{m=0}^{\Lambda} \sum_{k=1}^{\infty} \Big[\mathbf{T}_{k,n} \big(\alpha_{1;m} - \frac{1}{\ell_n} \alpha_{2;m} \big) \mathcal{F}_m^{(n,n,n,n)}(\lambda_k^{(0)})
$$

$$
+ \mathbf{T}_{k;n/2} \Big(\alpha_{3;m} - \frac{1}{\ell_{n/2}} \alpha_{4;m} \Big) \mathcal{F}_m^{(n/2,n/2,n/2,n/2)}(\lambda_k^{(0)})
$$

$$
+ \mathbf{P}_{k;(n,n/2)} \, \alpha_{6;m} \, \mathcal{F}_m^{(n,n/2,n,n/2)}(\lambda_k^{(1/2)}) + \Big(\mathbf{Q}_{k;n} \quad \mathbf{Q}_{k;n/2} \Big) M'(\lambda_k^{(0)}) \begin{pmatrix} \mathbf{Q}_{k;n} \\ \mathbf{Q}_{k;n/2} \end{pmatrix} \Big].
$$

Now using the properties of α, the L.H.S of the above identity is strictly negative. Therefore the R.H.S is strictly negative. Using (6.95), (6.96), (6.97), (6.98), the proposition follows. $\qquad\square$

Remark 6.3.67. The Semidefinite Program 3 and its proof explicitly show that analyzing the symmetrized correlators is sufficient to derive a bound.

6.4 Estimates of spectral gaps from the Selberg trace formula

In this section, we use the Selberg trace formula to estimate the spectral gap of a given surface X. The standard approach for numerically computing the operator spectrum on a hyperbolic surface is the finite element method. Thanks to the `FreeFEM++` package, the spectrum of Laplacian operator, with periodic and twisted periodic boundary conditions (see supplementary material of [313]), is known for many surfaces. For our purposes, we look at a different approach to compute the gaps of the Laplacian and the Dirac operator of explicit orbifolds and surfaces. This will allow us to compare these spectra to the previously established bootstrap bounds. The key idea is to use the Selberg trace formula, with the geodesic spectrum

as an input, to rule out points on the real line that are not in the eigenvalue spectrum. Our algorithm can be divided into three steps:

- Find a Dirichlet domain for the surface of interest and explicit generators for the fundamental group.

- Use this Dirichlet domain to produce a complete non-redundant list of conjugacy classes of geodesics on the surface whose length is bounded by a given value L.

- Choose a compactly supported test function that yields an estimate of the first eigenvalue of the Laplace/Dirac spectrum when substituted into the Selberg trace formula.

Note that the first two steps of this algorithm work in the same way in order to produce the Laplace and Dirac spectra. Only the explicit form of the Selberg trace formula used in the last step differs.

Step 1: Constructing the Dirichlet domain

We start by reviewing some basic definitions.

Definition 6.4.1. (Dirichlet domain of a Fuchsian group) Let Γ be a Fuchsian group and let $x \in \mathbb{H}$ be a point not fixed by any element of Γ other than the identity. A *Dirichlet domain with base point x* is the set

$$D(x) := \{p \in \mathbb{H} \mid \forall \gamma \in \Gamma \backslash \{e\}, d(x, p) < d(x, \gamma p)\}. \qquad (6.100)$$

For a cocompact Fuchsian group, its Dirichlet domain is a hyperbolic polygon with finite area. The boundary of this hyperbolic polygon consists of finitely many geodesic segments. We will denote this set of geodesic segments by $S(D)$ and it satisfies the property [447] that for every $s \in S(D)$, there exists a unique $s' \in S(D)$ and a unique $\gamma_s \in \Gamma$ such that $s' = \gamma_s s$. This is known as the *side-pairing* property. The segment s is the perpendicular bisector of the geodesic between x and $\gamma_s x$. The set $G(S) := \{\gamma_s | s \in S(D)\}$ is a generating set for Γ and we will refer to its elements as *side-paring generators*. See [447] for a systematic algorithm computing $G(S)$ and its application to arithmetic Fuchsian groups.

Definition 6.4.2. (Maximin edge distance of the Dirichlet domain) Let Γ be a cocompact Fuchsian group with Dirichlet domain $D(x)$ where x is the base point.

Let $S(D)$ be the set of geodesic segments forming the boundary of $D(x)$. The *maximin edge distance $R(D)$* is defined as the maximum over all the domain's edges of the minimum distance from the edge to the base-point x:

$$R(D) := \max_{s \in S(D)} \left(\inf_{p \in s} d(x, p) \right). \tag{6.101}$$

We briefly summarize the Dirichlet domain and the corresponding side-paring generators for surfaces and orbifolds relevant to us:

1. Hyperbolic triangles:

   As shown on Figure 6.4, the Dirichlet domain of a genus-0 hyperbolic triangle $[0; p, q, r]$ consists of two geodesic triangles $\Delta(p, q, r)$ with the four vertices located at $\hat{s}(1/p, 1/q, 1/r; 0)$, $\hat{s}(1/p, 1/q, 1/r; 1)$ and $\pm\hat{s}(1/p, 1/q, 1/r; \infty)$, where $\hat{s}(1/p, 1/q, 1/r; z)$ is the rescaled Schwarz function [228]

   $$\hat{s}(\alpha, \beta, \gamma; z) = v s(\alpha, \beta, \gamma; z), \quad s(\alpha, \beta, \gamma; z) = z^\alpha \frac{{}_2F_1(a', b', c'; z)}{{}_2F_1(a, b, c; z)}, \tag{6.102}$$

   $$v = \sqrt{\frac{\cos(\pi\alpha + \pi\beta) + \cos(\pi\gamma)}{\cos(\pi\alpha - \pi\beta) + \cos(\pi\gamma)} \cdot \frac{\cos(\pi\alpha - \pi\beta - \pi\gamma) + 1}{\cos(\pi\alpha + \pi\beta + \pi\gamma) + 1}} \cdot \frac{\Gamma(a')\Gamma(b')}{\Gamma(c')} \cdot \frac{\Gamma(c)}{\Gamma(a)\Gamma(b)}, \tag{6.103}$$

   with

   $$a = \frac{1 - \alpha - \beta - \gamma}{2}, \quad b = \frac{1 - \alpha + \beta - \gamma}{2}, \quad c = 1 - \alpha, \tag{6.104}$$

   and

   $$a' = \frac{1 + \alpha - \beta - \gamma}{2}, \quad b' = \frac{1 + \alpha + \beta - \gamma}{2}, \quad c' = 1 + \alpha. \tag{6.105}$$

2. The Bolza surface:

   The Dirichlet domain of the Bolza surface is a regular octagon. The side-paring generators are $\gamma_1, \gamma_2, \gamma_3, \gamma_4, \gamma_1^{-1}, \gamma_2^{-1}, \gamma_3^{-1}, \gamma_4^{-1}$ with

   $$\gamma_k = \pm \begin{pmatrix} \cosh(l/2) & e^{\frac{i\pi k}{4}} \sinh(l/2) \\ e^{-\frac{i\pi k}{4}} \sinh(l/2) & \cosh(l/2) \end{pmatrix}, \quad l = 2\cosh^{-1}\left(\cot\left(\frac{\pi}{8}\right)\right). \tag{6.106}$$

   Here we used "$\pm$" to stress the fact that γ_k's are elements in PSU(1, 1). The sign ambiguity will be removed once the surface is given a spin structure.

3. The most symmetric point in the moduli space with signature [1;3]:

   The Dirichlet domain for the one-punctured torus is an octagon with side-paring generators being $\gamma_1, \gamma_2, \gamma_1\gamma_2, \gamma_2\gamma_1, \gamma_1^{-1}, \gamma_2^{-1}, \gamma_1^{-1}\gamma_2^{-1}, \gamma_2^{-1}\gamma_1^{-1}$ where

$$\gamma_1 = \begin{pmatrix} \dfrac{1-x^2y^2}{\sqrt{(1-x^2)(1-y^2)(x^2y^2+1)}} & \dfrac{-x(1-y^2)+i(1-x^2)y}{\sqrt{(1-x^2)(1-y^2)(x^2y^2+1)}} \\[4mm] \dfrac{-x(1-y^2)-i(1-x^2)y}{\sqrt{(1-x^2)(1-y^2)(x^2y^2+1)}} & \dfrac{1-x^2y^2}{\sqrt{(1-x^2)(1-y^2)(x^2y^2+1)}} \end{pmatrix}, \qquad (6.107)$$

$$\gamma_2 = \begin{pmatrix} \dfrac{1-x^2y^2}{\sqrt{(1-x^2)(1-y^2)(x^2y^2+1)}} & \dfrac{x(1-y^2)+i(1-x^2)y}{\sqrt{(1-x^2)(1-y^2)(x^2y^2+1)}} \\[4mm] \dfrac{x(1-y^2)-i(1-x^2)y}{\sqrt{(1-x^2)(1-y^2)(x^2y^2+1)}} & \dfrac{1-x^2y^2}{\sqrt{(1-x^2)(1-y^2)(x^2y^2+1)}} \end{pmatrix}, \qquad (6.108)$$

   with

$$x = \tanh\left[\frac{1}{2}\cosh^{-1}\left(\frac{\cos(\pi/9)}{\sin(\pi/18)}\right)\right], \quad y = \tanh\left[\frac{1}{2}\cosh^{-1}\left(\frac{\cos(\pi/18)}{\sin(\pi/9)}\right)\right]. \qquad (6.109)$$

We conclude this subsection with a few comments on generalizations to hyperbolic surfaces with higher genus. We will sketch a general method for constructing a fundamental domain and to look for explicit expressions of the generators. The surfaces or orbifolds that are most likely to saturate the numerical bounds are conjectured to always possess a large number of symmetries, as we already observed in genus 1 and genus 2. For these special surfaces, the following result holds:

Proposition 6.4.3 ([351])**.** *Let Σ be a compact hyperbolic Riemann surface of genus $g > 1$. Σ realizes a local maximum of the number of automorphisms on the moduli space of Riemann surfaces of genus g if and only if it is isomorphic to a quotient of the upper half-plane by a torsion-free normal subgroup of a cocompact Fuchsian triangle group.*

This result means that in the relevant cases for our purposes, all fundamental domains can be constructed from gluing geodesic triangles $\Delta(p, q, r)^5$ together. Hence, the very general problem of finding an explicit fundamental domain for a given Riemann surface maps to a much simpler one in our case: the problem of

---

[5]The geodesic triangles are also the fundamental domains of the triangle group $T(p, q, r) = \langle a, b, c \mid a^2 = b^2 = c^2 = (ab)^p = (bc)^q = (ca)^r = 1\rangle$. The generators a, b, c are reflections against the three edges.

1. Constructing a tiling of the hyperbolic plane by triangles of given angles, and

2. Gluing geodesic triangles to obtain fundamental domains of the surface/orbifold of interest.

(a)

(b)

(c)
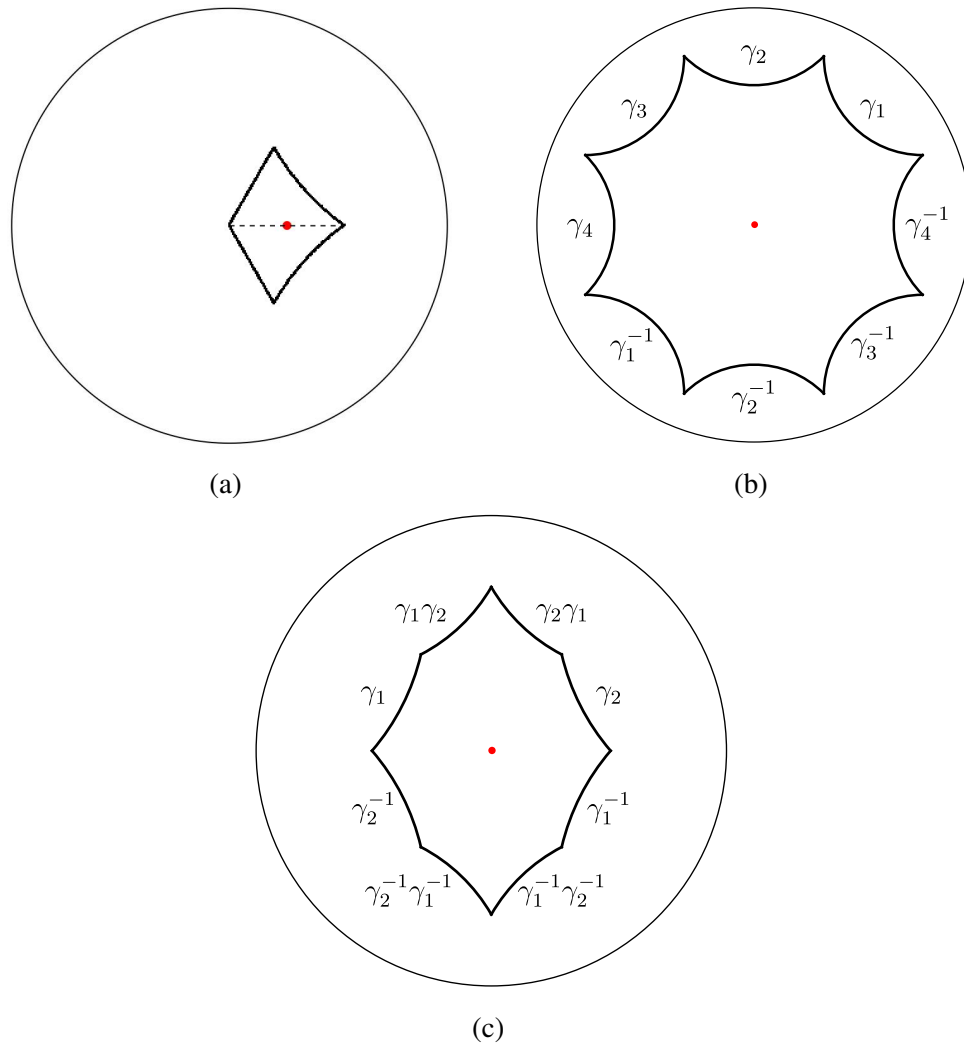
Figure 6.4: (A) The Dirichlet domain for the hyperbolic triangle $[0; 3, 3, 5]$. It consists of two geodesic triangles $\Delta(3, 3, 5)$ (B) The Dirichlet domain for the Bolza surface. Each side of the Dirichlet domain is labeled by the corresponding side-pairing generator. (C) The Dirichlet domain of the most symmetric point in the moduli space of one punctured torus with signatrue $[1;3]$. Each side of the Dirichlet domain is labeled by the corresponding side-pairing generator. The red dots in the figures are the corresponding base points.

To find explicit expressions for the generators, the simplest method would be to directly search for a presentation of a normal subgroup N of the triangle group

$T(p, q, r)$ such that

$$\text{Aut}(\Sigma) \cong T(p, q, r)/N. \tag{6.110}$$

This can in principle be done using the GAP software, although there could be cases in which there is more than one possible choice. We reserve a more careful examination of this problem to future work.

Once this subgroup is found, one can construct a fundamental domain by singling out one representative triangle per coset in T/N and taking the union of all such representatives. Note that the obtained fundamental domain is made of exactly $|\text{Aut}(\Sigma)|$ triangles.

Step 2: Enumerating the closed geodesics of length bounded by L

For this second step, we will mostly adapt the method proposed in [241] to our case. Before stating the algorithm, we first summarize the ideas behind it:

- In every hyperbolic conjugacy class, there is at least one representative whose axis[6] passes within a distance $R(D)$ of the basepoint, where $R(D)$ is the maximin edge distance of the Dirichlet domain. (See Propositions 3.2 and 3.3 from [241].)

- Working with such representatives, it is intuitive to see that we only need to tile the Poincaré disk $\mathbb{D}$ up to a certain radius in order to exhaust all hyperbolic conjugacy classes below a certain length cutoff. This radius depends both on the length cutoff and the size of the Dirichlet domain D. To be more precise, it suffices to find all translates γD such that $d(x, \gamma x) \leqslant 2 \cosh^{-1}(\cosh R(D) \cosh \frac{L}{2})$. (see Proposition 3.5 of [241].)

- If two hyperbolic elements with geodesic length L are conjugate to each other and both of their axes pass within a distance $R(D)$ from the base point, then the conjugating element γ must satisfy $d(x, \gamma x) \leqslant 2 \cosh^{-1}(\cosh R(D) \cosh \frac{L}{4})$ (see Proposition 3.7 of [241].)

With these basic ideas in mind, we state the algorithm:

1. (Initialize) Set T and T_h to be two empty lists. Given a spin structure, write all side-paring generators $\tilde{\gamma}_i$ of $\widetilde{\Gamma}$ as 2×2 matrices .

---

[6]Recall that a hyperbolic element γ can be specified by the geodesic it fixes. This geodesic is known as the axis of γ.

2. (Enumerate translates) Let T_n be the list of irreducible n-letter words formed by the $\tilde{\gamma}_i$. Remove from T_n all elements $\tilde{\tau}$ such that $d(x, \tilde{\tau}x) > 2\cosh^{-1}(\cosh R(D) \cosh \frac{L}{2})$. Here x is the base point of the Dirichilet domain. If T_n becomes an empty list, terminate this step. Otherwise append T_n to T. To generate T_{n+1}, multiply every element in T_n by side-paring generators $\tilde{\gamma}_i$ and remove the redundant matrices that are already in T.[7] This procedure terminates after a finite number of steps.

3. (Count hyperbolic conjugacy classes) Given the list T, let T_h be the subset of hyperbolic elements whose axis passes within a distance $R(D)$ from the base point. Group T_h by geodesic length (or equivalently, absolute value of the traces of the corresponding 2×2 matrices):

$$T_h = \bigsqcup_l T_h^{(l)}, \quad T_h^{(l)} = \{\tilde{\gamma} \in T_h \mid 2\cosh^{-1}(|\mathrm{Tr}\,(\tilde{\gamma})|/2) = l\}. \qquad (6.111)$$

For all sublists of T_h sharing the same geodesic length l, select all $\tilde{\tau} \in T$ such that $d(x, \tilde{\tau}x) \leqslant 2\cosh^{-1}(\cosh R(D) \cosh \frac{l}{4})$:

$$C_l := \left\{\tilde{\tau} \in T \,\middle|\, d(x, \tilde{\tau}x) \leqslant 2\cosh^{-1}\left(\cosh R \cosh \frac{l}{4}\right)\right\}, \qquad (6.112)$$

and use these elements to partition the sublist into conjugacy classes:

$$\mathrm{Orb}_l(\tilde{\gamma}) := \{\tilde{\gamma}' \in T_h^{(l)} \mid \exists \tilde{\tau} \in C_l, \tilde{\tau}\tilde{\gamma}\tilde{\tau}^{-1} = \pm\tilde{\gamma}'\}, \quad T_h^{(l)} = \bigsqcup_i \mathrm{Orb}_l(\tilde{\gamma}_i). \qquad (6.113)$$

Note that if the orbifold $\Gamma \backslash \mathbb{H}$ is spin, the traces of all matrices in the same conjugacy class should share the same sign. This sign is exactly the multiplier χ that enters the sum over hyperbolic elements in the Selberg trace formula for the 1-Laplacian.

4. (Compute the winding) Compute the winding number of each conjugacy class by checking whether it could be powers of other classes.

Step 3: Applying the Selberg trace formula to a well-chosen test function

Now that our algorithm can find all the geodesics up to a certain length, we can plug them into the geometric side of the Selberg trace formula. The Selberg trace

---

[7]The enumeration procedure would fail if there exist some translate γD such that γx is closer to x than all of its neighboring tiles, but this will not happen if we work with Dirichlet domain instead of an arbitrary fundamental domain. See Proposition 3.1 of [241].

formulae for the Laplacian and the squared Dirac operator (which is related to 1-Laplacian, see Remark 6.2.18) are respectively (see Theorem 5.1 of Chapter 3 of [233] and Equation 6.56 of Chapter 9 of [234]):

$$\sum_{n=0}^{\infty} \widehat{h}(t_n^{(0)}) = \frac{V(\Sigma)}{4\pi} \int_{-\infty}^{\infty} t\widehat{h}(t)\tanh(\pi t)dt + \sum_{\{\gamma_h\}} \frac{l(\gamma_{h;0})}{2\sinh(l(\gamma_h)/2)} h(l(\gamma_h))$$
$$+ \sum_{\{\gamma_e\}} \frac{ie^{-i\theta}}{4M_{\gamma_e}\sin\theta} \int_{-\infty}^{\infty} \frac{h(u)e^{-\frac{u}{2}}(e^u - e^{2i\theta})}{\cosh u - \cos(2\theta)} du,$$

and

$$\sum_{n=0}^{\infty} \widehat{h}(t_n^{(1/2)}) = \frac{V(\Sigma)}{4\pi} \int_{-\infty}^{\infty} t\widehat{h}(t)\frac{\sinh(2\pi t)}{\cosh(2\pi t) - 1}dt + \sum_{\{\gamma_h\},\mathrm{Tr}\,\gamma_h>2} \frac{\chi(\gamma_h)l(\gamma_{h;0})}{2\sinh(l(\gamma_h)/2)} h(l(\gamma_h))$$
$$+ \sum_{\{\gamma_e\},\pi>\theta(\gamma_e)>0} \frac{i\chi(\gamma_e)}{4M_{\gamma_e}\sin\theta} \int_{-\infty}^{\infty} \frac{h(u)(e^u - e^{2i\theta})}{\cosh u - \cos(2\theta)} du.$$

Let us explain the notations in these formulas:

- h is an acceptable even compactly supported test function such that $\widehat{h}$ is even.

- The $t_n^{(0)}$ and $t_n^{(1/2)}$ are equal to the $\sqrt{\lambda_n^{(0)} - 1/4}$ and $\sqrt{\lambda_n^{(1/2)} - 1/4}$, where the $\lambda_n^{(0)}$ and $\lambda_n^{(1/2)}$ are the eigenvalues of the Laplacian and 1-Laplacian, respectively.

- $V(\Sigma)$ is the volume of Σ.

- The sum over $\{\gamma_h\}$ is a sum over conjugacy classes of hyperbolic elements in $\pi_1(\Sigma)$, or of its double cover in $\mathrm{SL}(2,\mathbb{R})$ in the case of the 1-Laplacian.

- For a given hyperbolic element γ_h, $l(\gamma_h) = 2\cosh^{-1}(|\mathrm{Tr}\,(\gamma_h)|/2)$ is the length of the corresponding geodesic.

- For a given hyperbolic element γ_h, $\gamma_{h;0}$ denotes the primitive hyperbolic element associated with γ_h, that is, $\gamma_{h;0}$ is the element with shortest geodesic length such that γ_h can be expressed as a power of $\gamma_{h;0}$.

- The sum over $\{\gamma_e\}$ is a sum over conjugacy classes of elliptic elements in $\pi_1(\Sigma)$, or of its double cover in $\mathrm{SL}(2,\mathbb{R})$ in the case of the 1-Laplacian.

- For a given elliptic element γ_e, M_{γ_e} is the order of γ_e.

- χ is a multiplier on the double cover of $\pi_1(\Sigma)$ in $\mathrm{SL}(2, \mathbb{R})$ implementing a choice of spin structure.

- $\theta(\gamma_e)$ is the angle of the rotation matrix γ_e.

- A hat denotes a Fourier transform.

Our strategy will closely follow the reference [300]. The idea is to apply the Selberg trace formula to functions whose Fourier transform that appears on the geometric side of the Selberg trace formula has compact support – so that only a finite number of terms contribute to the sum over hyperbolic elements, and that we can find all of them using the procedure outlined in the previous subsection.

Let $h_1, \ldots, h_n$ be such test functions with support in $[-r, r]$ and λ_i be the eigenvalues of the operator of interest (it can be the Laplacian or the squared Dirac operator). It will also be useful to introduce extra parameters t_i, related to the eigenvalues through

$$\lambda_i := \frac{1}{4} + t_i^2. \tag{6.114}$$

Define a matrix A whose entries are given by

$$A_{ab} = \sum_j \widehat{h}_a(t_j)\widehat{h}_b(t_j). \tag{6.115}$$

If c_t is the column vector

$$c_t = \begin{bmatrix} \widehat{h}_1(t) \\ \vdots \\ \widehat{h}_n(t) \end{bmatrix}, \tag{6.116}$$

let

$$I_r(\lambda) := \inf_{\langle c_t, x \rangle = 1} \langle Ax, x \rangle. \tag{6.117}$$

$I_r(\lambda)$ can be calculated by introducing a Lagrange multiplier, and is equal to

$$I_r(\lambda) = \frac{1}{\langle A^{-1}c_t, c_t \rangle}. \tag{6.118}$$

This quantity can be evaluated explicitly using the geometric side of the Selberg trace formula applied to the functions $h_a * h_b$. One can then prove (see [300]):

Proposition 6.4.4. *If $I_r(\lambda) < 1$, then λ is not an eigenvalue of the operator of interest.*

Proof. A test function h with support on $[-r, r]$ is called *admissible* if $\widehat{h} \geq 0$ and the Selberg trace formula of interest can be applied to it. For $t \in [-r, r]$, define the quantity

$$I_r^\bullet(\lambda) := \inf_{\substack{h \text{ admissible} \\ \text{supp } h \subset [-r, r] \\ \widehat{h}(t) = 1}} \sum_j \widehat{h}(t_j). \tag{6.119}$$

Then, if there exists j_0 such that $t = t_{j_0}$, then for any test function $\widehat{h}$, we have

$$1 = \widehat{h}(t) \leq \sum_j \widehat{h}(t_j). \tag{6.120}$$

This is just because a sum is larger than or equal to all of its summands if the summands are non-negative. Hence,

$$I_r^\bullet(\lambda) \geqslant 1. \tag{6.121}$$

By contrapositive, we deduce that if $I_r^\bullet(\lambda) < 1$, then t cannot be one of the t_j. All that now remains to be shown is that for all t, $I_r^\bullet(\lambda) \leq I_r(\lambda)$. Now, $I_r(\lambda)$ can itself be reexpressed as an infimum: let

$$S := \left\{ h * h, \text{supp } h \subset \left[-\frac{r}{2}, \frac{r}{2} \right], h = \sum x_i h_i \text{ for } x_i \in \mathbb{R} \right\}. \tag{6.122}$$

We have

$$\inf_{\substack{H = h*h \in S \\ \widehat{h}(t) = 1}} \sum_j \widehat{H}(t_j) = I_r(\lambda). \tag{6.123}$$

But now, $I_r^\bullet(\lambda)$ is also an infimum, over a larger set of functions. We deduce

$$I_r^\bullet(\lambda) \leq I_r(\lambda), \tag{6.124}$$

which completes the proof of the proposition. $\square$

There is a straightforward generalization of the proof of the above result to the case in which the eigenvalue of the operator of interest is degenerate:

Proposition 6.4.5. *Let $k \in \mathbb{N}$. If $I_r(\lambda) < k$, then λ is not an eigenvalue of multiplicity k or higher of the operator of interest.*

These results provide a method to numerically estimate a lower bound on the gap of the Laplace and Dirac operators on a hyperbolic surface or orbifold. The method works as follows:

1. Calculate the matrix A_{ab} for some compactly supported test functions h_a and h_b using the Selberg trace formula and the geodesic spectrum generated in the previous step.

2. Deduce the value of $I_r(\lambda)$ as a function of $t = \sqrt{\lambda - \frac{1}{4}}$.

3. For Laplace operators, find the first interval $[a_1, b_1] \subset \mathbb{R}_+$ such that $I_r(\lambda) \geq 1$ when $\lambda \in [a_1, b_1]$. This interval $[a_1, b_1]$ provides an estimate for $\lambda_1^{(0)}$ of the surface or orbifold under consideration . In the case of the 1-Laplacian, all eigenvalues above $1/4$ must have even multiplicity due to Kramers degeneracy, see Proposition 6.2.21. Hence, the interval containing $\lambda_1^{(1/2)}$ is the first interval $[c_1, d_1] \in \mathbb{R}_+$ such that $I_r(\lambda) \geq 2$ when $\lambda \in [c_1, d_1]$.

The accuracy of our method is dependent on the choice of test functions h_k. In order to get a good bound, we need to slightly modify the choices of test functions made in [300]. We now explain in more detail how we choose these test functions.

For our application, we define our test functions h_a in terms of three parameters : n, m and L. Let

$$\delta = \frac{L}{2m + 2n}, \tag{6.125}$$

introduce

$$h := \left(\frac{1}{2\delta} \mathbb{1}_{[-\delta, \delta]} \right)^{*m}. \tag{6.126}$$

Then our test functions h_a are defined for $a = 1, \ldots, n$ by

$$h_a(x) := \frac{1}{2} (h(x + a\delta) + h(x - a\delta)). \tag{6.127}$$

In this formula:

- L is the length of the longest geodesic that appears on the right hand side of the Selberg trace formula. Numerically, we observe that when L gets larger, $I_r(\lambda)$ gets more and more relatively sharp peaks, that is, there are more intervals

$[a_i, b_i]$ and $[c_i, d_i]$ such that $b_i - a_i < \epsilon$, $d_i - c_i < \epsilon$ where ϵ is a parameter characterising the precision of the estimation. The more information we have on the geodesic spectrum, the more eigenvalues we can estimate with a reasonably high precision.

- n is the size of the A matrix. Numerically, we observe that increasing n makes the peaks of $I_r(\lambda)$ sharper. However, the integral following $V(\Sigma)/4\pi$ on the geometric side of the Selberg trace formulae needs to be evaluated numerically. A very large value of n produces very fast oscillations in the integrand, making the numerical integration difficult to handle.

- m is the number of convolutions. Increasing it also makes the peaks of $I_r(\lambda)$ sharper, but we face a similar problem related to fast oscillations.

Figure 6.6 shows the results given by this method when applied to the case of the $[0; 3, 3, 5]$ orbifold. In Appendix 6.8 we tabulate the numerical estimates of $\lambda_1^{(0)}$ and $\lambda_1^{(1/2)}$ for various surfaces and orbifolds.
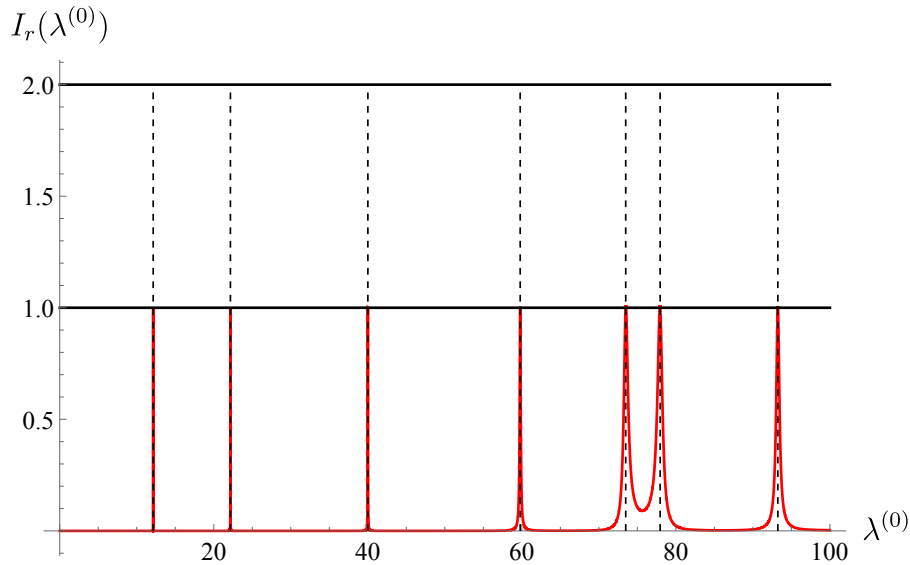
Figure 6.5: The spectral exclusion plot for the Laplacian spectrum of the hyperbolic triangle $[0;3,3,5]$ with $m = 4$, $n = 24$ and $L = 10.9$. The dashed vertical lines correspond to the first few eigenvalues computed using the finite element method.

Remark 6.4.6. The rigorous result that Figure 6.5 and similar plots can show is a *lower* bound on the first eigenvalue. $I_r(\lambda^{(0)})$ remaining lower than 1 on a certain interval starting at the origin shows rigorously that there is no eigenvalue in that interval. Our algorithm does not show rigorously that $I_r(\lambda^{(0)})$ being larger than 1
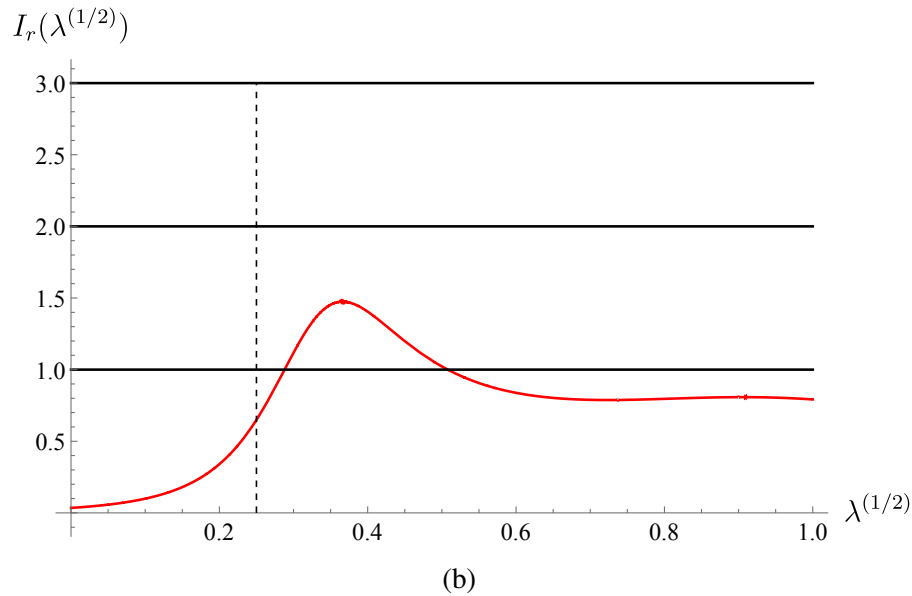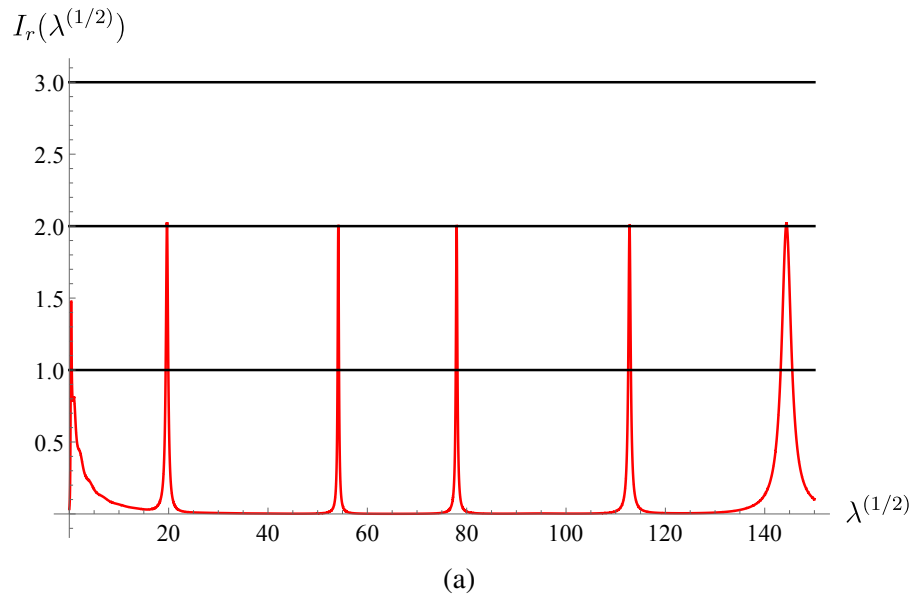
Figure 6.6: (A) Spectral exclusion plot for the 1-Laplacian spectrum of the hyperbolic triangle [0;3,3,5] with $m = 4, n = 24$ and $L = 10.9$. The leftmost peak does not imply the existence of any eigenvalues. The curve is below 1 at $\lambda^{(1/2)} = 1/4$ therefore it does not indicate the existence of a harmoinc spinor. The peak is also below 2 and by Kramers degeneracy it does not represent a non-harmonic eigenfunction. (B) Spectral exclusion plot for the 1-Laplacian spectrum of the hyperbolic triangle [0;3,3,5] zoomed into the interval from 0 to 1. The dashed vertical line is located at $\lambda^{(1/2)} = 1/4$.

implies the presence of a new eigenvalue. However, we observe that the curve in the figure 6.5 and similar plots are well converged numerically, i.e., the maximum value of $I_r(x)$ with x in that interval stays larger than 1, even with the inclusion of more geodesic-length data. This indicates that the interval should contain an eigenvalue. It is possible to make this claim completely rigorous by using a similar algorithm (see section 5.4 of [71] and the reference therein), which certifies that a given interval contains an eigenvalue. We do not pursue that here because our goal is to saturate the upper bounds that we obtain from the bootstrap equations. Therefore what matters to us is to find a lower bound for a given candidate orbifold that is close to the upper bound provided by the bootstrap. Similar statements apply to $I_r(\lambda_1^{(1/2)})$ as well.

6.5 Results: bounds from semi-definite programming

In this section we present the proofs of the theorems mentioned earlier, as well as write down further bounds that we obtain using linear and semidefinite programming.

Proofs of theorems using Semi definite programming

Proof of Theorem 6.1.1. For genus 1 or more, the above bound follows the results in [283]. For genus 0 hyperbolic spin orbifold, we use the fact $\ell_{1/2} = 0$. Since it is a spin orbifold, the orbifold orders are odd, i.e., $k_i \geq 3$ and there has to be at least 3 orbifold points for the surface to be spin. Using Riemann-Roch, we then deduce $\ell_3 \geq 1$ and $\ell_{3/2} \geq 1$. Furthermore, we have $\lambda^{(1/2)} \geq 1/4$ for all spin orbifolds. Now we leverage SDP(1) with $n = 3$ and choosing $\lambda_*^{(1/2)} = 1/4$. We have verified the bound using rational arithmetic as done in [283]. $\qquad\square$

Proof of Theorem 6.1.3. We note that for a hyperbolic spin orbifold X admitting harmonic spinor, we have $\ell_{1/2} \geq 1$ and hence $\ell_1 \geq 1$. Furthermore, we have $\lambda^{(1/2)} \geq 1/4$ for all spin orbifolds. Now we leverage SDP(1) with $n = 1$ and choosing $\lambda_*^{(1/2)} = 1/4$. We have verified the bound using rational arithmetic as done in [283]. $\qquad\square$

Proof of Theorem 6.1.5. We leverage SDP(1) with $n = 3$ and choosing $\lambda_*^{(0)} = 3/2$. $\qquad\square$

Proof of Theorem 6.1.6. Given a compact orientable hyperbolic hyperelliptic spin manifold X of genus $g > 2$, we have $\ell_{1/2} = \lfloor (g + 1)/2 \rfloor > 1$. We consider the

spectral identities derived from $\langle \mathcal{O}_{\frac{n}{2}} \mathcal{O}_{\frac{n}{2}} \widetilde{\mathcal{O}}_{\frac{n}{2}} \widetilde{\mathcal{O}}_{\frac{n}{2}} \rangle_{\text{SYM}}$ with $n = 1$. They are given by (see Proposition 6.3.66)

$$\mathbf{S}_{2m+n;n/2} = \sum_{k=1}^{\infty} \mathbf{T}_{k;n/2} \, \mathcal{F}_{2m}^{(n/2,n/2,n/2,n/2)}(\lambda_k^{(0)}),$$

$$-\mathbf{A}_{2m+1+n;n/2} = \sum_{k=1}^{\infty} \mathbf{T}_{k;n/2} \, \mathcal{F}_{2m+1}^{(n/2,n/2,n/2,n/2)}(\lambda_k^{(0)}),$$

$$\mathbf{S}_{2m+n;n/2} = \mathcal{F}_{2m}^{(n/2,n/2,n/2,n/2)}(0) + \sum_{k=1}^{\infty} \left(\mathbf{Q}_{k;n/2}^2 - \frac{1}{\ell_{n/2}} \mathbf{T}_{k;n/2} \right) \mathcal{F}_{2m}^{(n/2,n/2,n/2,n/2)}(\lambda_k^{(0)}),$$

$$\mathbf{A}_{2m+1+n;n/2} = \mathcal{F}_{2m+1}^{(n/2,n/2,n/2,n/2)}(0) + \sum_{k=1}^{\infty} \left(\mathbf{Q}_{k;n/2}^2 - \frac{1}{\ell_{n/2}} \mathbf{T}_{k;n/2} \right) \mathcal{F}_{2m+1}^{(n/2,n/2,n/2,n/2)}(\lambda_k^{(0)}),$$

$$(6.128)$$

To proceed, we consider the set of identities coming from $m = 0$, from which we can derive

$$0 = \mathcal{F}_0^{(1/2,1/2,1/2,1/2)}(0) + \sum_{k=1}^{\infty} \left(\mathbf{Q}_{k;n/2}^2 - \left(1 + \frac{1}{\ell_{1/2}} \right) \mathbf{T}_{k;1/2} \right) \mathcal{F}_0^{(1/2,1/2,1/2,1/2)}(\lambda_k^{(0)})$$

$$0 = \mathcal{F}_1^{(1/2,1/2,1/2,1/2)}(0) + \sum_{k=1}^{\infty} \left(\mathbf{Q}_{k;n/2}^2 + \left(1 - \frac{1}{\ell_{1/2}} \right) \mathbf{T}_{k;1/2} \right) \mathcal{F}_1^{(1/2,1/2,1/2,1/2)}(\lambda_k^{(0)}).$$

$$(6.129)$$

Plugging in the values of $\mathcal{F}$, we obtain from the above

$$0 = \sum_{k=1}^{\infty} \left[\lambda_k^{(0)} \mathbf{Q}_{k;n/2}^2 + \left(\lambda_k^{(0)} \frac{(\ell_{1/2} - 1)}{\ell_{1/2}} - 1 \right) \mathbf{T}_{k;1/2} \right] . \tag{6.130}$$

The above implies that

$$\lambda_1^{(0)} < \frac{\ell_{1/2}}{\ell_{1/2} - 1} . \tag{6.131}$$

Plugging in $\ell_{1/2} = \lfloor (g + 1)/2 \rfloor$, the theorem follows. $\qquad \square$

Theorem 6.5.1. *Given a compact orientable hyperbolic spin 2-orbifold X of genus g admitting $\ell_{1/2} > 0$ harmonic spinors, the first non-zero eigenvalue of the Laplacian operator, $\lambda_1^{(0)}(X)$ satisfies the bound, recorded in Table 6.1.*

Proof of theorem 6.5.1. On a hyperbolic spin orbifold X of genus g, we have $\ell_1 = g$ and $\ell_{1/2} \leq \lfloor (g + 1)/2 \rfloor$. We use the fact that $\lambda^{(1/2)} \geq 1/4$ for all spin orbifolds. We use SDP (3) with $n = 1$ and $\lambda_*^{(1/2)} = 1/4$. We have verified these bounds using rational arithmetic as done in [283]. $\qquad \square$

Exclusion plots

As mentioned in the introduction, an *exclusion plot* refers to a region $D \subset (0, \infty) \times (1/4, \infty)$ such that $(\lambda_1^{(0)}(X), \lambda_1^{(1/2)}(X)) \notin D$, where X can be any compact connected orientable hyperbolic spin surface or orbifold. We may also choose to consider choices of X with prescribed additional properties like genus, number of harmonic spinors it can carry etc. Here $\lambda_1^{(0)}(X)$ is the first nontrivial eigenvalue of the Laplace operator on the compact hyperbolic spin orbifold, while $\lambda_1^{(1/2)}(X)$ is the first nontrivial eigenvalue of the weight-1 automorphic Laplacian. In order to obtain the exclusion plots, we perform the following algorithm:

1. Use SDP (1) or (2), pick a value for $\lambda_*^{(1/2)}$ and search for a functional with the desired properties, leading to a bound $\lambda_1^{(0)} < \lambda_*^{(0)}$ subject to the condition $\lambda_1^{(1/2)} > \lambda_*^{(1/2)}$;

2. Repeat the above step for various values of $\lambda_*^{(1/2)}$;

or the following one:

1. Use SDP (1) or (2), pick a value for $\lambda_*^{(0)}$ and search for a functional with the desired properties, leading to a bound $\lambda_1^{(1/2)} < \lambda_*^{(1/2)}$ subject to the condition $\lambda_1^{(0)} > \lambda_*^{(0)}$;

2. Repeat the above step for various values of $\lambda_*^{(0)}$.

Using the aforementioned algorithm involving SDP, we find the disallowed region D, which is everything except the shaded region (yellow or pink) in the *exclusion* plots. We obtain Figure 6.2 by using SDP (1) with $n = 3$ (for the union of the pink and yellow shaded region) and $n = 1$ (for the pink shaded region). The corner point of the yellow shaded region is approximately at $(12.13629, 19.67)$, while the corner point of the pink-shaded region is at $(4.7611, 8.28)$, both these points being disallowed. Now, using the Selberg trace formula, we can compute $(\lambda_1^{(0)}(X), \lambda_1^{(1/2)}(X))$ for $X = [0; 3, 3, 5]$ (this orbifold has $\ell_{3/2} = \ell_3 = 1$). It is given by $(12.1362327 \pm 10^{-7}, 19.669 \pm 0.03)$. This point is depicted in red on Figure 6.2 and evidently, lies very close to the kink. Figure 6.7 zooms onto the kink and shows that the red dot is in the allowed region (up to uncertainty, predicted by the Selberg trace formula). Similarly, using the Selberg trace formula, we can compute $(\lambda_1^{(0)}(X), \lambda_1^{(1/2)}(X))$ for $X = [1; 3]_{sym}$, the most symmetric point in the moduli

space of $[1;3]$, equipped with an odd spin structure such that $\ell_{1/2} = \ell_1 = 1$. In particular we find that $\lambda_1^{(0)} \in (4.7609, 4.7654)$ and $\lambda_1^{(1/2)} \in (8.255, 8.298)$. See the table in Appendix 6.8 for a refined interval. For the Laplacian eigenvalue, we can use `FreeFEM++` as well, this provides the estimate $\lambda_1^{(0)}([1;3]_{sym}) \approx 4.7609$.

Figure 6.8 is obtained by using SDP (2) with $n = 3$. Here we restrict to the case where $\ell_3 = \ell_{3/2} = 1$, as opposed to using SDP (1) with $n = 3$, where $\ell_3 \geq 1, \ell_{3/2} \geq 1$. While Figure 6.8 looks almost similar to Figure 6.7, zooming near the kink reveals the differences. Figure 6.9 is Figure 6.8, zoomed in near the kink. The corner point is approximately at $(12.13623353125, 19.673)$ and disallowed.

Finally, Figure 6.10 is obtained by using a simplified version of SDP (3) with $n = 1$, $\ell_1 = 2$, but $\ell_{1/2} = 1$. The red dot here corresponds to the Bolza surface, equipped with an odd spin structure. See the table in Appendix 6.8 for the precise coordinates of the red dot. Figure 6.11 is the zoomed version of the above.
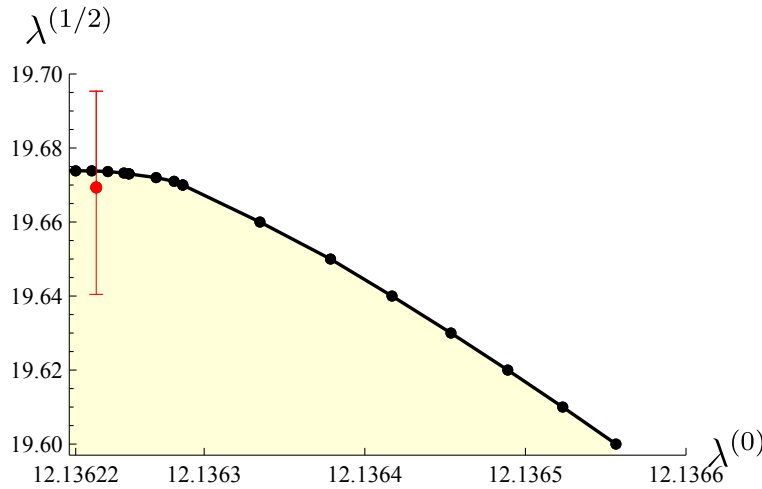
Figure 6.7: Bounds from the $\ell_{3/2} \geq 1$, $\ell_3 \geq 1$ system; zooming onto the kink. Everything except the shaded region is disallowed. The red dot near the corner corresponds to $[0; 3, 3, 5]$.

6.6 Discussion

In this chapter, we applied linear programming techniques to constrain the first nonzero eigenvalue of the Laplace and Dirac operators on a compact connected orientable hyperbolic surface or orbifold with a spin structure. The essential tool is the spectral identities coming from the associativity of the product of functions on $\Gamma \backslash \mathrm{SL}(2, \mathbb{R})$. It is the analog of the associativity of the operator product expansion in conformal field theory, which lies at the heart of the conformal bootstrap program.
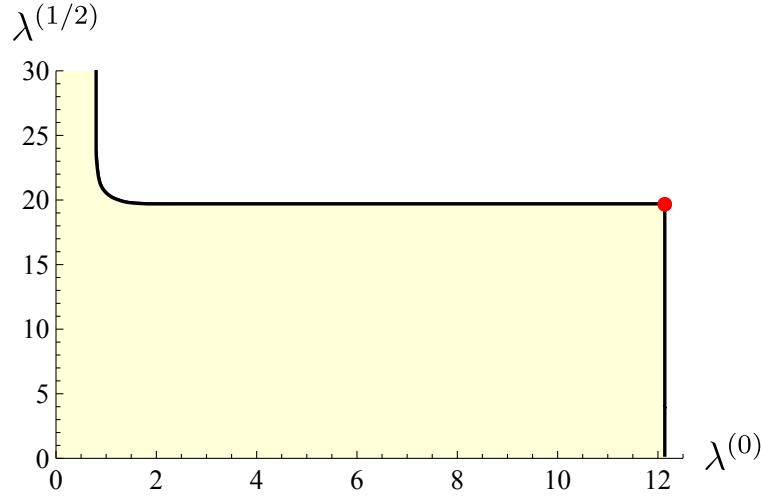
Figure 6.8: Bounds from the $\ell_{3/2} = \ell_3 = 1$ system. Everything except the yellow shaded region is disallowed for hyperbolic spin orbifolds with $\ell_{3/2} = \ell_3 = 1$. The red dot in the corner corresponds to $[0; 3, 3, 5]$.
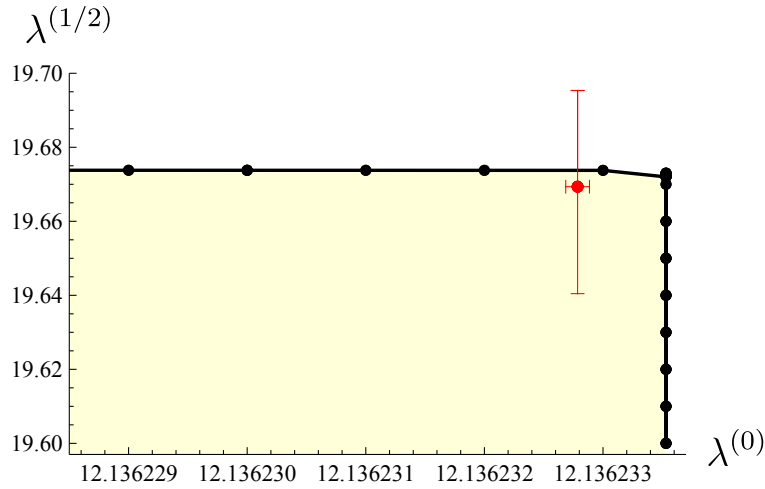
Figure 6.9: Bounds from the $\ell_{3/2} = \ell_3 = 1$ system; zooming onto the kink. Everything except the shaded region is disallowed. The red dot near the corner corresponds to $[0; 3, 3, 5]$.

Our approach is closely related to that of Bernstein and Reznikov [53], who investigated the consistency constraints arising from the spectral decomposition of integrals involving a quadruple product of functions within the principal series in $L^2(\Gamma\backslash G)$. See also [409, 338, 360]. In our current study, we have demonstrated that integrating these consistency constraints with linear programming techniques, especially when applied to the discrete series, can yield almost optimal bounds on Laplace and Dirac spectra. There is a close analogy of the above with the analytical bootstrap in CFT, in particular, the approach of Bernstein and Reznikov is akin to
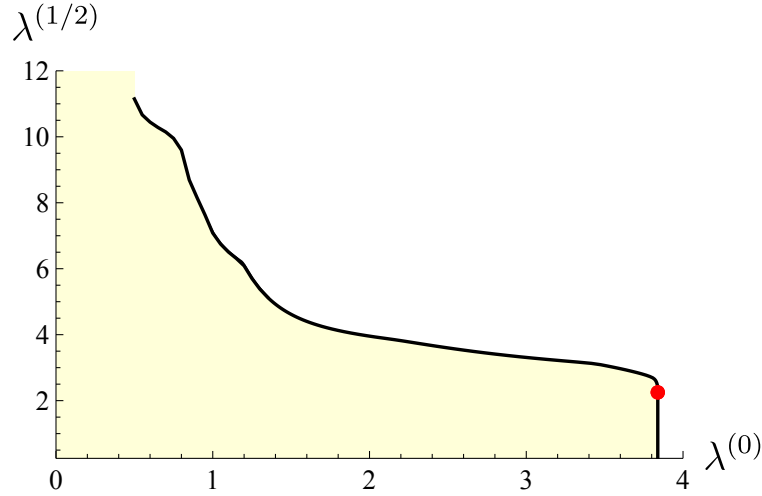
Figure 6.10: Bounds from the $\ell_{1/2} = 1, \ell_1 = 2$ system. Everything except the yellow-shaded region is disallowed. The red dot in the corner corresponds to Bolza surface with odd spin structure.
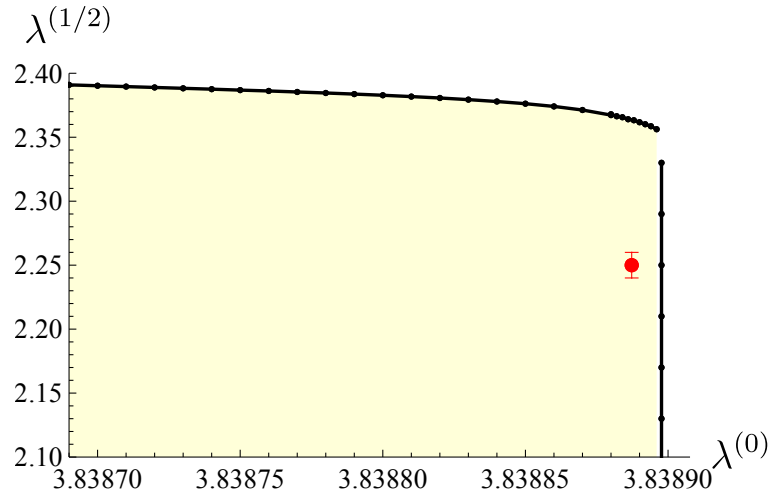
Figure 6.11: Bounds from $\ell_{1/2} = 1, \ell_1 = 2$ system, zooming onto the kink.Everything except the shaded region is disallowed.The red dot corresponds to Bolza surface with odd spin structure.

asymtptotic analysis involving Tauberian theorems, leading to universal behavior of various physical quantities in CFTs [392, 350, 349, 369].

Several points could be analysed further. In particular:

1. It is interesting to note that the bounds we obtain, for example on Laplace eigenvalues, do not always become more stringent as the number of harmonic spinors or genus increases. For example, Table 6.1 shows that the bound at genus 5 with 3 harmonic spinors is less restrictive than the bound at genus 6

with 3 harmonic spinors. We contrast this scenario with that of [283] where the bound for orbifolds with genus g_1 is not weaker compared to that of genus g_2 whenever $g_1 > g_2$. The origin of monotonicity in the context of [283] is the fact that the functional used in linear programming for genus g_2 can easily be promoted to a functional that is appropriate for genus g_1. However, unlike the spectral identities of [283], the spectral identities that we bootstrap in this chapter have discrete series irreps appearing in the t channel. This constitutes an obstruction to the previous argument. It would be interesting to understand the origin of this non-monotonicity directly and analytically at the level of the spectral identities.

2. In terms of the Dirac spectrum, it is curious that on the exclusion plot of Figure 6.8, the allowed values of $\lambda^{(1/2)}$ seem to blow up quickly as $\lambda^{(0)}$ approaches zero. This raises the question whether our methods could be improved to obtain better bounds in this region of parameter space, and maybe even a universal upper bound on $\lambda^{(1/2)}$.

3. It would also be interesting to study Dirac spectra in higher dimensions using similar spectra identities originating from associativity. In particular the three-dimensional case is quite accessible, extending the work of [71].

One can see the results of this chapter as a new contribution to an emerging program, started in [283], to apply techinques originating from conformal field theory to questions relevant to analytic number theory and hyperbolic geometry. Already in our case, as well as in the three-dimensional case [71], these techniques have been very fruitful. Natural extensions of this work on spinors would be to allow fractional spin structures, or to investigate the case of super-Riemann surfaces. More generally, it would be very interesting to push this program towards quotients of Lie groups of higher rank (for example, $SL(3, \mathbb{R})$ seems to be a natural next step), as well as the study of non-Archimedean geometries over $\mathbb{Q}_p$.

Perhaps the most striking feature of our findings is that at least in the cases displayed on Figures 6.7 and 6.10, the most symmetric surfaces (i.e., the $[0; 3, 3, 5]$ orbifold, $[1; 3]_{sym}$ and the Bolza surface, respectively) sit almost exactly at the boundary, or even the kink, of the allowed region in parameter space. The fact that hyperbolic surfaces seem to know about the boundary of the exclusion plot, which purely comes from the constraint equations, seems to suggest that the space of solutions to the constraint equations is closely related to the space of quotients of the form

$\Gamma\backslash\mathrm{SL}(2,\mathbb{R})$, where Γ is a cocompact lattice. There are well-known results establishing a one-to-one correspondence between abelian algebras and various kinds of geometric spaces. For example, the Gelfand–Naimark theorem [189] shows that each commutative C^*-algebra can be thought of as an algebra of continuous functions on a locally compact Hausdorff space. There is an analog of this theorem for von Neumann algebras and measured spaces [436, 373], and more recently, Connes showed in his reconstruction theorem [119] that for every spectral triple $(\mathcal{A}, \mathcal{H}, D)$, with $\mathcal{A}$ commutative, and a few extra conditions, one can realize $\mathcal{A}$ as $C^\infty(X)$, where X is a smooth oriented compact spin^c manifold, and that all such manifolds can be decribed by such a spectral triple. It would be interesting to see whether such reconstruction theorems hold for commutative algebras on which various Lie groups act. The existence of such theorems would likely help understand how closely the space of solutions to the constraint equations described here, and the space of 2-dimensional compact orientable spin-orbifolds, are related.

Finally, we remark on the relevance of our work in context of physics, in particular, conformal field theory. In the present chapter, the key role is played by the positivity of the measure of $\widetilde{\Gamma}\backslash\mathrm{SL}(2,\mathbb{R})$. On a similar note we expect that in the context of path integral formulation of conformal field theories, the existence of a $\mathrm{SO}(1,d)$ invariant positive measure along with associativity might lead to the discovery of new constraints on such theories. Additionally, our framework provides a systematic approach for analyzing the de Sitter bootstrap numerically as suggested recently in [426, 306, 307, 375], and for extending this program to include fermions.

6.7   Appendix: Dimension of the space of harmonic spinors in low genus

In this work, we obtained bounds on the Laplace and Dirac spectra on a surface or orbifold based on the number of modular forms of various weights on this geometric object. A particularly interesting case has been that of harmonic spinors (i.e., modular forms of weight one), as they carry more than only topological information at genus $g \geq 3$. In this appendix, we summarize the state of the art in the classification of Riemann surfaces of genus $g \geq 3$ in terms of the number of harmonic spinors they can carry. A key role is played by *hyperelliptic surfaces*, which are branched double covers of the Riemann sphere. Note that in genus up to 2, every Riemann surface is hyperelliptic, which informs why the space of harmonic spinors can only retain nontrivial geometric information at genus $g \geq 3$. This appendix cross-references the general results of [92] with explicit examples of surfaces with many automorphisms from the literature.

Genus 3

In genus 3, the situation is particularly nice: either the surface is hyperelliptic, or it admits a representation as a regular quartic in $\mathbb{CP}^2$.

The two cases are defined as follows:

- If the surface is hyperelliptic, there exists a choice of spin structure for which the upper bound of two independent harmonic spinors is saturated.

- If the surface is a regular quartic, then the maximum number of harmonic spinors is 1, and it is realized by exactly the odd spin structures on the surface.

In genus 3, the automorphism group of a hyperelliptic surface that has the largest order is $\mathbb{Z}_2 \times S_4$. The corresponding surface, given in [351], has affine equation

$$y^2 = x^8 + 14x^4 + 1. \tag{6.132}$$

The other candidate special surfaces have automorphism groups U_6, V_8 (following the notations of [412]), and $\mathbb{Z}_{14}$, see [351] for more details.

On the other hand, the automorphism group of a non-hyperelliptic surface of genus 3 can be much larger [41]. In particular, there exists a non-hyperelliptic surface of genus 3 with isometry group $\mathrm{PSL}(2, \mathbb{F}_7)$, that has 168 elements. This surface is called the *Klein quartic*, and has equation

$$z^3 x + x^3 y + y^3 z = 0. \tag{6.133}$$

The complete classification of possible automorphism groups of genus 3 surfaces is given in [41].

Genus 4

In order to understand the situation in genus 4, we need to introduce the notion of *canonical embedding*.

Definition 6.7.1. Let Σ be a Riemann surface, and let $\{\omega_1, \ldots, \omega_g\}$ be a basis of holomorphic differentials on Σ. The canonical embedding of Σ into $\mathbb{CP}^{g-1}$ is the map

$$\sigma \longmapsto [\omega_1(\sigma), \ldots, \omega_g(\sigma)]. \tag{6.134}$$

Note that the canonical embedding depends on the choice of basis of holomorphic differentials, however, a change of basis simply amounts to a projective transformation in $\mathbb{CP}^{g-1}$. We have the following general result:

Proposition 6.7.2 ([354]). *The canonical embedding of Σ is injective if and only if Σ is not hyperelliptic.*

In genus 4, we have the additional fact:

Proposition 6.7.3 ([92]). *The canonical model of a non-hyperelliptic surface of genus 4 is the intersection of a unique quadric and a cubic in $\mathbb{CP}^3$. Moreover, the quadric is either smooth or a cone.*

It turns out [92] that this classification in terms of canonical models is the right one to consider to classify the possible dimensions of harmonic spinors. More precisely:

- If the surface is hyperelliptic, there exist spin structures for which the surface admits 2 harmonic spinors.

- If the surface is not hyperelliptic and the quadric supporting its canonical embedding is a cone, then it admits a unique spin structure with 2 harmonic spinors.

- If the surface is not hyperelliptic and the quadric supporting its canonical embedding is a smooth, then the maximum number of harmonic spinors is 1, and it is realized by exactly the odd spin structures on the surface.

In genus 4, still with the notations of [412], the automorphism group of a hyperelliptic surface that has the largest order is V_{10}. The corresponding surface, given in [351], has affine equation

$$y^2 = x^{10} - 1. \tag{6.135}$$

The other candidate special surfaces have automorphism groups $\mathrm{SL}(2, \mathbb{F}_3)$, U_8, and $\mathbb{Z}_{18}$, see [351] for more details.

In a similar fashion to the case of genus 3, there exist non-hyperelliptic surfaces of genus 4 with much larger automorphism groups. These surfaces are enumerated in [139]. The surface with the largest automorphism group is *Bring's surface*, with 120 automorphisms. However, the quartic associated to Bring's surface is smooth.

If we want to impose that the canonical embedding of the surface lies on a cone, the largest possible automorphism group has order 72. The corresponding surface has equation

$$z^3 y^2 = x(x^4 + y^4). \tag{6.136}$$

A large number of other large groups (but of smaller order) arise, they are described in detail in [139].

Genus 5

In genus 5, a surface can carry a maximal number of harmonic spinors if and only if it is hyperelliptic. The automorphism group of a hyperelliptic surface that has the largest order (120) is $\mathbb{Z}_2 \times A_5$. The corresponding surface, given in [351], has affine equation

$$y^2 = x(x^{10} + 11x^5 - 1). \tag{6.137}$$

The other candidate special surfaces have automorphism groups W_2, U_{10}, V_{12} and $\mathbb{Z}_{22}$ [412], see [351] for more details.

If one drops the requirement of hyperellipticity, there is a surface that has more automorphisms: its order is 192. This surface is described in [117, 139].

Genus 6

In the case of genus 6, there are once again special surfaces with the maximal (3) number of harmonic spinors but that are not hyperelliptic. More precisely,

- If the surface is hyperelliptic, there exist spin structures for which the surface admits 3 harmonic spinors.

- If the surface is a smooth plane quintic, then it admits a unique spin structure with 3 harmonic spinors.

- If the surface is neither hyperelliptic nor a plane quintic, then there are at most 2 harmonic spinors per spin structure.

Note that the classification of the remaining cases is subtle. It is known, however [92], that trigonal surfaces cannot have more than 1 harmonic spinor per spin structure.

In genus 6, the automorphism group of a hyperelliptic surface that has the largest order is V_{14} (following the notations of [412]). The corresponding surface, given in [351], has affine equation

$$y^2 = x^{14} - 1. \tag{6.138}$$

The other candidate special surfaces have automorphism groups U_{12}, $GL(2, \mathbb{F}_3)$ and $\mathbb{Z}_{26}$, see [351] for more details.

Once again, there exist non-hyperelliptic surfaces of genus 6 with much larger automorphism groups. These surfaces are enumerated in [92]. The surface with the largest automorphism group is *Fermat's quintic* [92], with 150 automorphisms. It is a smooth plane quintic of equation

$$x^5 + y^5 = z^5, \tag{6.139}$$

so interestingly, it also can carry three harmonic spinors.

The surface of genus 6 that *cannot* carry 3 harmonic spinors and has the largest automorphism group is the Wiman sextic, described for example in [139]. Its automorphism group is isomorphic to S_5, which means that it has 120 automorphisms.

6.8 Appendix: Numerical estimate of $\lambda_1^{(0)}$ and $\lambda_1^{(1/2)}$ for various orbifolds and surfaces

In this appendix, we present the table 6.3, showing the intervals $[a_1, b_1]$ and $[c_1, d_1]$ containing the $\lambda_1^{(0)}$ and the $\lambda_1^{(1/2)}$, respectively. Note that we can rigorously only show that the intervals $[0, a_1)$ and $[0, c_1)$ does not contain $\lambda_1^{(0)}$ and $\lambda_1^{(1/2)}$, respectively. So the intervals presented in the table 6.3 are the ones, potentially containing the first eigenvalue. However, from the numerics we observe that these intervals contain the first non-trivial eigenvalue, see the remark 6.4.6.

Signature	Interval containing $\lambda_1^{(0)}$; $[a_1, b_1]$	Interval containing $\lambda_1^{(1/2)}$; $[c_1, d_1]$
[0;3,3,5]	[12.13623266082, 12.13623279684]	[19.62850299650, 19.70606979308]
[0;3,3,7]	[6.622512981830, 6.62251303689]	[14.58137931985, 14.70308279925]
[0;3,3,9]	[4.760935531772, 4.760935540974]	[13.04476106136, 13.20743304307]
[0;3,3,11]	[3.817638624612, 3.817638645376]	[12.31511817207, 12.56227388521]
[0;3,3,13]	[3.243870176473, 3.243870434758]	[11.89945757571, 12.22641050708]
[0;3,3,15]	[2.856060123567, 2.856061719363]	[11.66435497067, 12.00545171009]
[0;3,3,17]	[2.575237981382, 2.575242811203]	[11.50074150836, 11.87999680844]
[0;3,3,19]	[2.361748257939, 2.372476650392]	[11.23045200383, 11.84361592566]
[0;3,3,21]	[2.193498651071, 2.195285976813]	[11.19103656533, 11.78223049525]
[0;3,3,23]	[2.057131576807, 2.057705367329]	[11.11887135826, 11.73877352328]
[0;3,3,25]	[1.944123693427, 1.950822253982]	[11.06202801296, 11.70678314765]
[0;3,5,5]	[5.873575959007, 5.873576043568]	[10.26823286914, 10.46485970804]
[0;3,5,7]	[4.105916028717, 4.105919429281]	[8.807322253657, 9.080333571881]
[0;3,5,9]	[3.240661780680, 3.240671025102]	[8.255608604384, 8.583931161697]
[0;3,5,11]	[2.734102690099, 2.735649379604]	[7.907206673453, 8.351477142335]
[0;3,5,13]	[2.400941404204, 2.475085745560]	[7.726023042016, 8.311960209309]
[0;3,5,15]	[2.163736742483, 2.379780806385]	[7.585768436685, 8.286345064939]
[0;3,7,7]	[3.253194157760, 3.263120231408]	[7.649577360853, 8.068585239517]
$[1;3]_{\text{sym}}$	[4.760933182368, 4.765358782461]	[8.255418967910, 8.297252909660]* [3.108229958351, 3.190576244169]
Bolza surface	[3.838886940769, 3.842772834639]	[2.246498128260, 2.259880718024]* [1.188383272199, 1.192003537383] [0.8970133121437, 0.8975387540243]

Table 6.3: $\lambda_1^{(0)}$ and $\lambda_1^{(1/2)}$ for various hyperbolic spin surfaces and spin orbifolds. Orbifolds with signature [1;3] have 4 different spin structures but for the most symmetric point on the moduli space, there are only two different sets of spectra for the Dirac operator. Similarly, the Bolza surface has 16 different spin structures but there are only three different Dirac spectra. The intervals marked with * correspond to spin structures that support a harmonic spinor.

C h a p t e r 7

HOLOGRAPHIC TENSOR NETWORKS FROM HYPERBOLIC BUILDINGS

This chapter is based on the work [199], in collaboration with Matilde Marcolli and Sarthak Parikh.

7.1 Introduction

Holographic tensor networks are one of the main tools to model the emergence of spacetime in the AdS/CFT correspondence, and the associated error-correcting structure. Since the discovery of the HaPPY code [372], a plethora of examples have shown that holographic tensor networks make it possible to model numerous aspects of holography, in particular, the Ryu–Takayanagi formula [401, 167] and quantum error correction [225].

Most holographic tensor networks realize an exact or approximate quantum error-correcting code, in the sense that they (almost) isometrically map a Hilbert space of semiclassical bulk degrees of freedom, modelled by qudits associated to dangling legs, to a boundary Hilbert space, which represents the Hilbert space of the boundary conformal field theory, and is modelled by qudits on the boundary of the tensor network. For well-chosen boundary regions, the tensor network satisfies the quantum Ryu–Takayanagi formula [372]. This means that the entanglement entropy of the restriction to a given boundary region of a state in the code subspace equals the sum of the entanglement entropy of that state in the bulk and an area contribution proportional to the number of internal legs of the tensor network cut by the Ryu–Takayanagi surface of the region. The latter is defined as the surface delimiting the region attainable from the boundary by the greedy algorithm [372]. Complementary recovery is then achieved when the greedy algorithm reaches complementary bulk regions from complementary parts of the boundary.

Holographic tensor networks have an interesting geometric structure, which ranges from tesselations of the hyperbolic plane [372] or higher-dimensional spaces [280] to *p*-adic spaces [238] (see [105] for a complimentary perspective). Although it is often briefly mentioned that hyperbolic tesselations have to do with Coxeter systems [280], the interplay between holographic tensor networks and hyperbolic geometry

has been left largely unexplored.[1] The goal of this chapter is to investigate this link in more detail, and show the pertinence of the language of Gromov-hyperbolicity and building theory to talk about holographic tensor networks.

More precisely, one can ask the following questions:

- What are the geometric structures that underlie the construction of holographic tensor networks?

- How can we know when a graph makes a good holographic quantum error-correcting code?

- Can we construct tensor networks that model holographic dualities where the boundary is not homeomorphic to a sphere?

- How can we predict which boundary regions satisfy complementary recovery?

- How do we take an infinite-dimensional limit of holographic tensor networks?

- What are some insights that the geometry of holographic tensor networks can provide for studying full AdS/CFT?

In this chapter, we will provide an answer to these questions in the case of networks constructed out of perfect tensors, utilizing the framework of Gromov hyperbolicity and hyperbolic buildings. It will turn out that known examples of holographic tensor networks can all be described by the notion of hyperbolic building. Buildings, which can have different geometric structures (hyperbolic, Euclidean, spherical) are a geometric construct originally introduced by Jacques Tits [3] aimed at geometrizing some aspects of group theory. In order to do geometry on hyperbolic buildings, the right toolkit is provided by Gromov's theory of hyperbolicity, which studies metric spaces whose distance has a particular property that can be viewed as a more abstract formulation of the concept of negative curvature. On such spaces, a notion of boundary at infinity, the Gromov boundary, can be defined. In our context, holographic dualities will be between semiclassical theories living on a hyperbolic building and theories living on its Gromov boundary. Tensor networks will contain bulk dangling legs in the chambers of the buildings, and boundary legs at a certain

---

[1]However, see [58] for tensor network constructions in terms of tessellations of the hyperbolic plane inspired by Coxeter systems and [280] for a geometric condition for a tiling to define an isometry.

cutoff of the building. These boundary legs can be thought of as a coarse-grained approximation to the Gromov boundary.

One striking feature of this approach is that, unlike the case of the HaPPY code or similar tessellations, the Gromov boundary of most hyperbolic buildings is not isomorphic to a sphere – rather, it is often isomorphic to a fractal, which has a much more intricate geometric structure. Thus, our holographic dualities provide examples of dualities where the boundary theory lives on a sphere (or more generally a homology sphere) of any dimension, but also where it lives on more complicated spaces of non-integer dimension. Moreover, as we shall see, there is a close analog of conformal invariance for these theories, and it exhibits a behavior closely related to that of a CFT.

Using the more general point of view of hyperbolic buildings also allows us to reflect on some features of known holographic tensor networks, like complementary recovery. While this property is supposed to hold for arbitrary boundary regions up to nonperturbative errors in G_N in AdS/CFT [143], it does not hold for all regions of the HaPPY code [372]. While this fact may seem puzzling, it has a very natural explanation in terms of hyperbolic buildings: their global symmetry groups are smaller than the conformal group, hence only regions which are well-adapted to these symmetry groups will satisfy complementary recovery. In particular, we will provide a systematic construction of regions in the network that do satisfy complementary recovery, and applies to all networks with perfect tensors.

For these regions, we will show that a Ryu–Takayanagi formula holds, and that for ball-shaped boundary regions the number of links on the Ryu–Takayanagi surface follows a logarithmic law in the radius when the boundary time slice has dimension 1, and a power law in the radius, with exponent the *Hausdorff dimension of the boundary minus one* when the boundary time slice has dimension greater than 1. This recovers known results for the scaling of entanglement entropy in traditional conformal field theory, and introduces some new scalings that are very suggestive: the Ryu–Takayanagi surfaces see the fractal structure of the boundary! It is then of course very tempting to speculate that networks with fractal boundary simulate conformal field theories on fractal spaces.

Another interesting aspect of our approach is that the Gromov boundary lives at infinity, and makes it very natural to define an infinite-dimensional limit of holographic tensor networks. This problem has already been touched upon in [195, 196], and more generally, the question of describing holographic quantum error-correction in

the language of infinite-dimensional operator algebras is an active research program [270, 196, 164, 194]. Here we will see that there is an appropriate way to take the limit of our holographic codes such that they give a net of holographic conditional expectations. This structure has been recently shown to capture essential aspects of bulk reconstruction in AdS/CFT [164].

We now give the main results of this work:

- A general framework for the construction of holographic tensor networks with perfect tensors is given in terms of building theory and Gromov hyperbolic spaces.

- This allows us to recover all known constructions, and gives examples of holographic tensor networks in all integer dimensions.

- A lot of tensor networks fitting into that framework also have a fractal boundary, hinting at new holographic dualities where the boundary theory lives on a fractal.

- A condition for our networks to be isometric is given, as well as a construction of regions that satisfy complementary recovery. This construction can be applied to all the buildings examined in this chapter.

- A Ryu–Takayanagi formula is proven, showing that boundary entanglement entropy for ball-shaped regions follows a logarithmic law in the radius when the boundary has dimension 1, and a power law in the radius when the boundary has higher Hausdorff dimension, where the exponent is the Hausdorff dimension of the boundary minus one.

- A general technique is given to construct an infinite-dimensional limit of our networks in the language of operator algebras. This limit gives rise to a net of holographic conditional expectations.

- All our results can be applied to known examples of holographic tensor networks with perfect tensors, such as the HaPPY code.

The rest of the chapter is organized as follows: In Section 7.2, we recall the basics of the theory of Gromov-hyperbolic spaces and their boundaries, as well as the notions of hyperbolic groups and buildings. In Section 7.3, we focus for clarity on a particular case: that of Bourdon buildings, which can be understood as HaPPY codes with

branching. These buildings have a boundary homeomorphic to a fractal Menger sponge, and we show that the resulting tensor networks satisfy complementary recovery for nice regions, a Ryu–Takayanagi formula with the expected scaling in terms of the Hausdorff dimension of the boundary. We also construct an infinite-dimensional limit for these tensor networks. In Section 7.4, we extrapolate the methods of the previous section to define holographic quantum error correcting codes on a much larger class of higher-dimensional hyperbolic buildings. We give some explicit examples, including ones where the boundary is a homology-sphere of arbitrary integer dimension. In Section 7.5, we briefly comment on the results and discuss some potential future directions. In Appendix 7.6 we present an explicit example of a Bourdon building, and in the slightly more technical Appendix 7.7 we summarize relevant results from Patterson-Sullivan theory which help formalize aspects of conformal field theories on fractal spaces.

7.2 Gromov-hyperbolic spaces, hyperbolic groups and buildings

In this section, we introduce the general notion of Gromov-hyperbolic space, which will be underlying our choices of bulk spaces. We focus on two types of Gromov-hyperbolic spaces, hyperbolic groups and hyperbolic buildings, which will be the ones we will use in order to construct our examples of holographic duality.

General definitions

Gromov-hyperbolic spaces naturally generalize the setup in which one usually considers holographic dualities. We begin with a definition of the Gromov product, which is the crucial ingredient in the definition of Gromov-hyperbolic spaces (see [127]):

Definition 7.2.1. For (X, d) a metric space, the Gromov product of two points $y, z \in X$ with respect to $x \in X$ is given by

$$(y, z)_x := \frac{1}{2}(d(x, y) + d(x, z) - d(y, z)).$$

From there, a Gromov-hyperbolic space is defined by the following condition:

Definition 7.2.2. Let $\delta > 0$. (X, d) is said to be δ-hyperbolic if for all $x, y, z, w \in X$,

$$(x, z)_w \geq \min((x, y)_w, (y, z)_w) - \delta.$$

X is then Gromov-hyperbolic if it is δ-hyperbolic for some $\delta > 0$.

For our purposes, one of the main interesting features of Gromov-hyperbolic spaces is that they are endowed with a natural notion of boundary, which will make it possible for us to formulate a bulk-to-boundary correspondence. We first need to formulate a notion of geodesics in Gromov-hyperbolic spaces.

Definition 7.2.3. Fix an origin $O \in X$. A geodesic ray in X is an isometry $r : [0, +\infty) \longrightarrow X$ such that

$$r(0) = O$$

and for all $t > 0$, $r([0, t])$ is the shortest path from O to $r(t)$ in X. Two geodesic rays r_1 and r_2 are said to be equivalent if there exists $K > 0$ such that for all $t > 0$,

$$d(r_1(t), r_2(t)) \leq K.$$

The Gromov boundary ∂X of X is defined to be the set of equivalence classes of geodesic rays starting at O.

$X \cup \partial X$ is then endowed with a natural topology: a basis is given by the sets of the form

$V(p, \rho) := \{q \in \partial X, \text{there exist geodesic rays } r_1, \ r_2 \text{ ending at } p, q \text{ such that}$

$$\tag{7.1}$$

$$\lim_{t_1, t_2 \to +\infty} (r_1(t_1), r_2(t_2))_O \geq \rho.\}$$

$$\tag{7.2}$$

A convenient feature of the Gromov boundary ∂X is that one can construct a natural metric on it [126]. In what follows, we shall fix a base point O for X. For $x \in X$, define

$$|x| := d(x, O).$$

Then for $a > 1$, define

$$|x - y|_a := \inf_{r \text{ path from } x \text{ to } y} \int_r a^{-|x|} dx.$$

One can then prove [126] that there exists $a_0 > 1$ such that for $1 < a < a_0$, $X \cup \partial X$ is homeomorphic to the completion of X for the metric $|\cdot|_a$. Moreover, the metric $|\cdot|_a$ is very well-controlled by the Gromov product of X (we shall see explicit examples of this in what follows). In particular, there exists a constant λ which only depends

on δ and a such that if ξ and η are on ∂X, for x and y in small enough neighborhoods of ξ and η, we have [126]:

$$\lambda^{-1} a^{-(x,y)_O} \leq |\xi - \eta|_a \leq \lambda a^{-(x,y)_O}. \tag{7.3}$$

Hence $|\cdot|_a$ is a natural metric, called *visual metric*, on ∂X. From here on, we will consider the choices of the base point O and of a given $a > 1$ as implicit and we will drop the explicit notation unless needed.[2]

Most of the Gromov-hyperbolic spaces we will consider here can be interpreted in terms of hyperbolic groups. Here we give a general definition of a hyperbolic group, of which we will consider specific explicit examples in the subsequent sections.

Definition 7.2.4. Let G be a finitely generated group, and X be its Cayley graph. G is said to be a hyperbolic group if X, endowed with its graph metric, is Gromov-hyperbolic.

Hyperbolic buildings

In this chapter, the main setup will be that of hyperbolic buildings. We will also encounter their isometry groups, which will turn out to be hyperbolic groups. The theory of buildings is a rich and fruitful mathematical framework, first introduced by Tits [3], whose goal is to geometrize notions of group theory. Here we introduce the basic terminology associated to this theory, which will be utilized in our chapter. We will mostly follow the presentation of [439], which the interested reader can consult for a more thorough introduction.

The simplest examples of buildings are Coxeter systems:

Definition 7.2.5. A *Coxeter group* is a group W that admits a presentation of the form

$$W = \langle s \in S \,|\, (st)^{m_{st}} = 1 \text{ for } s, t \in S \rangle,$$

with S a finite set, $m_{ss} = 1$ for $s \in S$, m_{st} a (possibly infinite) integer ≥ 2 for $s \neq t$. The pair (W, S) is then called a *Coxeter system*.

A particularly nice class of Coxeter systems is given by the *right-angled* ones, which correspond to the case where the m_{st} for $s \neq t$ are either 2 or ∞.

Many interesting Coxeter systems arise from regular tessellations of n-spheres, n-Euclidean space, or n-hyperbolic spaces. In this case, the Coxeter group is

---

[2]For instance, from here on we will drop the subscript a in the metric $|\cdot|_a$.
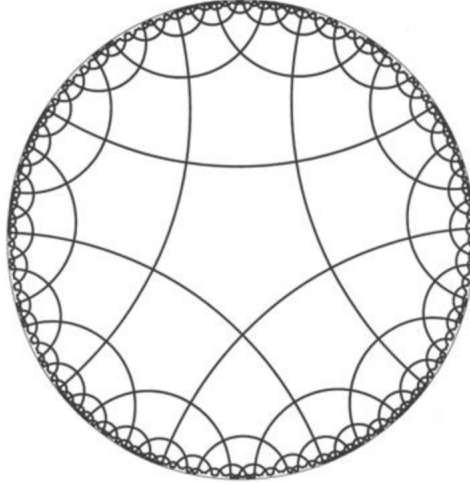
Figure 7.1: The right-angled pentagon tiling of the hyperbolic plane $\mathbb{H}^2$ used in the construction of the HaPPY code.

generated by reflections with respect to the sides of the basic polyhedron. This is for example the case for the HaPPY code, which corresponds to a right-angled Coxeter system generated by a right-angled regular pentagon in the hyperbolic plane (see Figure 7.1). More generally, a convex polyhedron in $\mathbb{X}^n$ (which can be the n-sphere, the n-Euclidean space or the n-hyperbolic space), with all dihedral angles submultiples of π is called a *Coxeter polytope*. These three possible cases for $\mathbb{X}^n$ are, respectively, referred to as *spherical*, *Euclidean*, and *hyperbolic* buildings.

Another important notion in order to define a building is that of *polyhedral complex*. Without going into too much generality, they are constructed by gluing polyhedra in spheres, Euclidean space or hyperbolic space, using isometries along the faces. The main object of interest in a polyhedral complex is its *link* at each vertex x: it is the $(n-1)$-dimensional polyhedral complex obtained by intersecting the given polyhedral complex with an n-sphere of sufficiently small radius centered at x. For example, for a 2-complex, the link at vertex x is a graph whose edges correspond to the faces adjacent to x, and whose vertices correspond to the edges incident on x.

We are now ready to define a hyperbolic building, utilizing the notions of Coxeter polytopes and polyhedral complexes.

Definition 7.2.6. Let P be a hyperbolic Coxeter polytope, and let (W, S) be the associated Coxeter system. A *hyperbolic building* of type (W, S) is a polyhedral complex Δ with a maximal family of subcomplexes, called *apartments*, such that they each are isometric to a tessellation of $\mathbb{H}^n$ by copies of P called *chambers*, and

- Any two chambers of Δ are contained in a common apartment.

- Between any two apartments, there exists an isometry that fixes their intersection.

In the case of a hyperbolic building, W, called the Weyl group of the building, is a hyperbolic discrete subgroup of the isometry group of $\mathbb{H}^n$. It is also possible to show that the link of an n-dimensional hyperbolic building at each vertex is an $(n-1)$-dimensional spherical building. The link structure of our buildings will be crucial for our proof of complementary recovery.

Remark 7.2.7. The condition that the apartments are tessellations of $\mathbb{H}^n$ can be relaxed to include a larger class of hyperbolic buildings, where the apartments are certain polyhedral complexes (Davis–Moussong complexes) with a hyperbolic structures, which are not tessellations of a single hyperbolic space. This generalization makes it possible to obtain hyperbolic buildings in arbitrary dimension, and we will discuss it in Section 7.4.

7.3 Holography on Bourdon buildings

Our first example of building holography is given by the case where the bulk space is the Bourdon building $I_{p,q}$ [77], whose boundary is a Menger sponge, which is universal among topological spaces of topological dimension 1, in the sense that all of them are homeomorphic to a subset of the Menger sponge. When interpreted as a holographic tensor network, we will see that our bulk space gives rise to the expected properties of holographic codes and states: complementary recovery, and a Ryu–Takayanagi formula involving the Patterson–Sullivan measure on the boundary.

Bourdon buildings

We start by defining the building $I_{p,q}$, for $p \geq 5$ and $q \geq 3$, closely following [77]. For the case $q = 2$ see Remark 7.3.2 below.

Definition 7.3.1. Let p, q be two integers with $p \geq 5$ and $q \geq 3$. The Bourdon building $I_{p,q}$ is the only simply connected cellular 2-complex such that its 2-cells are isometric to a regular p-gon, are attached by their edges and vertices, two 2-cells share at most one edge or one vertex, and the link of each vertex is the bipartite graph $K(q,q)$.
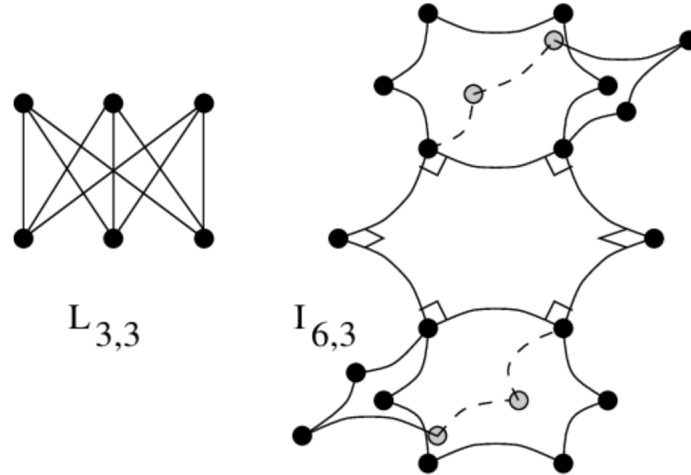
Figure 7.2: An example of a subset of a Bourdon building with the associated link, from [78].

The existence and uniqueness of such a building is proven in [77]. Let $\Gamma_{p,q}$ be the hyperbolic group defined by its presentation

$$\Gamma_{p,q} := \langle s_1, ..., s_p \mid s_i^q = 1, [s_i, s_{i+1}] = 1 \rangle.$$

Then $\Gamma_{p,q}$ acts simply transitively on the set of chambers of $I_{p,q}$. In particular, if one fixes a zero chamber in $I_{p,q}$, then the chambers of $I_{p,q}$ can be seen as the words formed by $\Gamma_{p,q}$ up to the relations in the group presentation, where each letter applies a group transformation to the chamber.

Remark 7.3.2. In the case where $q = 2$, $\Gamma_{p,q}$ is just a tesselation of the hyperbolic plane by p-gons (and the Gromov boundary is a circle). In particular, whenever this tessellation gives rise to an isometric network of perfect tensors, it can be interpreted as a form of HaPPY tiling. We refer to these tessellations as the p-gon HaPPY tilings, with $p \geq 5$.

For $q \geq 3$, the Gromov boundary changes, and becomes a Menger sponge. The Bourdon building then has branching: each tile branches out into $q - 1$ tiles at each edge. Nevertheless, the building still possesses a HaPPY-like structure, as its apartments are now tilings of the hyperbolic plane by p-gons. The $q = 2$ case corresponds to when the building only has one apartment. This nice apartment structure will greatly simplify our analysis of tensor networks on Bourdon buildings, as it will enable us to transpose a lot of useful error-correcting properties of the HaPPY code to the Bourdon case.

Bourdon tensor networks

We now define our Bourdon tensor network. The idea is to extend the HaPPY construction to the more general case of the building $I_{p,q}$. In the rest of this section, we will consider the case of holographic codes with a nontrivial code subspace, and we will hence suppose for simplicity that p is odd, in order for our bulk tensors to always have an even number of legs, independently of q.

Definition 7.3.3. The $I_{p,q}$ tensor network is constructed in the following way:

- Insert a perfect tensor in the chambers of the building.

- Perform an index contraction between every two chambers sharing an edge.

- Add $q - 1$ dangling legs for each tensor.

- Choose a central tile, and cut the building at a finite distance Λ from this central tile.

As usual for holographic quantum error correcting codes, the bulk Hilbert space is identified with the tensor product of the bulk dangling leg Hilbert spaces, while the boundary Hilbert space is identified with the tensor product of the boundary leg Hilbert spaces.

Remark 7.3.4. The existence of perfect tensors that work for any given choice of p and q in the range of Definition 7.3.1 follows from [243], see also [244].

Remark 7.3.5. We could have allowed for different types of tensor networks. In particular, when p increases, we could have introduced $k(q - 1)$ dangling legs in the bulk with $k \leq p - 4$ (as long as the total number of legs is even), while still satisfying the isometry and entanglement wedge reconstruction properties proven in the next sections.

Bulk-to-boundary isometry

We first prove that our network defines an isometry at each layer.

Theorem 7.3.6. *At each layer, the Bourdon tensor network of Definition 7.3.3 determines an isometry from the code subspace to the physical Hilbert space.*

Proof. In this proof, we will freely use the fact that the p-gon HaPPY tilings define an isometry from the bulk to the boundary. For a proof, see [372]. This being

said, our strategy will be to introduce an acyclic orientation on the edges of the network such that each tensor has at least as many outgoing links as incoming links (including bulk nodes). We will do this by induction on the layer number n. At the first layer, only the bulk node is introduced. We assign an outgoing orientation to all the edges, and the condition is clearly satisfied. Now suppose that up to layer n, the network determines an isometry. Take a chamber of the building at layer $n+1$. This chamber can be included in an apartment, which looks like a HaPPY tiling. Inside this apartment, there are more tiles touching our chamber that are part of layer $n+2$ than there are that are part of layer n or $n+1$. By symmetry of the building, for a given tile at layer $n+2$, there are $q-2$ other tiles which are also at layer $n+2$ and share the same edge with our chamber. We therefore define an orientation on the network in the following way: if two chambers share an edge, and one is in a higher layer than the other, then define the orientation of the network from the one in the lower layer to the one in the higher layer. Then collect all adjacent tiles that are in the same layer, and define any acyclic orientation on the corresponding subgraph. This gives a well-defined orientation that gives an explicit isometric interpretation to the tensor network. □

We focused here on the case where we have a nontrivial code subspace, for which the isometry condition can be stated. One can also consider similarly the case where we just have a single holographic state.

Entanglement wedges

Just like in the HaPPY code, only certain bulk regions in the Bourdon tensor network will satisfy complementary recovery, and hence the Ryu–Takayanagi formula. This has to do with the fact that the isometry group of the tensor network is not quite the whole conformal group. Here, we give a description of two nice families of such regions, thanks to the notion introduced in [77] of *tree-wall* in the bulk as well as the link structure of the Bourdon building.

Let us summarize the tree-wall construction of [77].

Definition 7.3.7. A *wall* in $I_{p,q}$ is a bi-infinite geodesic contained in the 1-skeleton of $I_{p,q}$. One can then define an equivalence relation on the 1-skeleton of $I_{p,q}$: two edges are equivalent if they share a wall. The equivalence classes are q-valent homogeneous trees: they are the *tree-walls* of the building.

In practice, in order to construct a tree-wall, one can perform the following construction.

Lemma 7.3.8. *A tree-wall is obtained by the following steps:*

- *Choose an edge in the 1-skeleton of $I_{p,q}$.*

- *Add to the tree-wall, on both sides of the chosen edge, the $q - 1$ neighboring edges (distance one in the building) that are at distance 2 from this edge in the graph of the link.*

- *Repeat the process.*

Proof. The link of $I_{p,q}$ is the bipartite graph $K(q, q)$, so in this bipartite graph, $q - 1$ vertices (which correspond to $q - 1$ edges of the building) are diametrically opposed to our edge (i.e., at distance 2 of it on the link's graph).

$\square$

Remark 7.3.9. Note that tree-walls cut the building (and hence its boundary) into q connected components. These connected components will be suitable boundary regions to study entanglement entropy, and the bulk tree-walls will be the analogues of Ryu–Takayanagi surfaces for the Bourdon building. Hence we shall call these connected components entanglement wedges.

There is another way to look at the tree-wall construction, in terms of the Coxeter system of the building.

Lemma 7.3.10. *Consider a given chamber C of the Bourdon building, and pick one of its edges, say E. The entanglement wedge with tree-wall boundary associated to the choice of C and E is obtained by considering, in all apartments containing C, the portion that is on the same side as C with respect to the hyperplane determined by E.*

Proof. In any apartment containing C, E defines a reflection with respect to a given hyperplane of this apartment. The intersection of the entanglement wedge defined by C and E with the apartment then corresponds to the portion of the apartment on the same side of the hyperplane as C. By applying this construction to all apartments containing C, we recover the same entanglement wedge, with a tree-wall boundary. $\square$

The following procedure describes another geometric method for the construction of valid entanglement wedges in $I_{p,q}$.

Lemma 7.3.11. *The following construction defines a valid entanglement wedge in $I_{p,q}$.*

- *Choose a vertex V in the building.*

- *Look at the link around the chosen vertex and pick an edge in this link, which corresponds to a chamber C in $I_{p,q}$.*

- *In a given apartment A, consider the set $S(C, V, A)$ of tiles defined by the chamber C and the vertex V as the set of tiles containing C and delimited by the two hyperplanes which are edges of the chamber and intersect at V.*

- *Define the entanglement wedge associated to C and V as the union of all $S(C, V, A)$, for A containing C.*

In this case, the entanglement wedge is delimited by two half-tree-walls attached to each other.

Figure 7.3 shows the intersection of the two types of entanglement wedges described in this section with an apartment of the Bourdon building.

Complementary recovery and a Ryu–Takayanagi formula

We now show that for an entanglement wedge defined in one of the previous manners, complementary recovery is satisfied in the Bourdon tensor network.

Proposition 7.3.12. *Complementary recovery holds for an entanglement wedge in $I_{p,q}$ constructed as in Lemmas 7.3.8 and 7.3.11.*

Proof. By symmetry, we will assume without loss of generality, both in the case defined by the intersection of two tree-walls and the case defined by a single tree-wall, that the considered entanglement wedges are on the opposite side of the tree-walls from the center of the building. These regions can be identified with regions in the network that are spanned by semi-infinite geodesics that start from the center and pass through a given chamber C (see Remark 7.3.15). As shown in [372], complementary recovery amounts to showing that the greedy algorithm reaches the surface which delimits the entanglement wedge, both starting from the boundary of
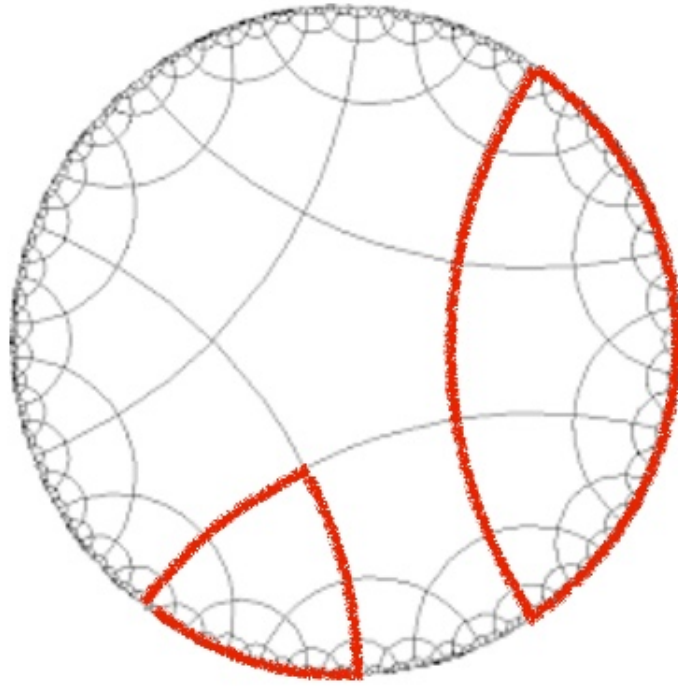
Figure 7.3: The intersections of the two types of entanglement wedges described here with an apartment of the Bourdon building. Each geodesic should be seen as a portion of a tree-wall in the full building.

the entanglement wedge (i.e., the subset of the Gromov boundary of $I_{p,q}$ that can be reached by geodesics inside the entanglement wedge), and its complement. Then, our proof amounts to showing that at layer n, the chambers inside the entanglement wedge share an edge with at least as many chambers at layer $n + 1$ as at layer n or $n - 1$. This comes from the apartment structure of the Bourdon building: each chamber can be included in an apartment which is isomorphic to a regular tiling of the hyperbolic disk, and for which each tile at layer n is in contact with at least as many at layer $n + 1$ as at layer n or $n - 1$. By symmetry of the branching, the other tiles sharing the same edge will also be at layer $n + 1$, which finishes the proof of the fact that it is possible to reconstruct the entanglement wedge on its boundary.

Now, it is also possible to reconstruct the complement of the entanglement wedge on the complementary boundary region. In the case in which the entanglement wedge corresponds to a region delimited by a tree-wall, the q connected components are symmetric with respect to the tree-wall, and thus it is possible to achieve reconstruction on the $q - 1$ connected components by symmetry.

Similarly, edges in the link (corresponding to chambers in the building) around a

given vertex have entanglement wedges that form a partition of the bulk, and satisfy recovery. Thus, the complement of the entanglement wedge defined by a given chamber and a link vertex also satisfies recovery. ☐

Proposition 7.3.13. *The Ryu–Takayanagi formula holds for entanglement wedges in $I_{p,q}$ constructed as in Lemmas 7.3.8 and 7.3.11.*

Proof. Given the previous Proposition 7.3.12, the Ryu–Takayanagi formula directly follows from the argument of [372]: since the entanglement wedge satisfies complementary recovery, the entanglement entropy of a boundary state will satisfy

$$S_{phys}(\rho) = N_{cut} \log d + S_{code}(\rho),$$

where N_{cut} is the number of links that are cut by the boundary of the entanglement wedge and d is the bond dimension. ☐

Ball entanglement wedges

We now turn our attention to entanglement wedges that correspond to ball-shaped regions on the boundary. Their construction goes as follows.

Lemma 7.3.14. *The following procedure gives an entanglement wedge construction in $I_{p,q}$.*

- *Fix a chamber C in $I_{p,q}$ and the central chamber O.*

- *The "ball entanglement wedge" defined by C and O is then given by the set of semi-infinite geodesics on the tensor network starting from C that can be extended to a semi-infinite geodesic starting from O.*

Remark 7.3.15. Note that ball entanglement wedges are particular cases of the entanglement wedges defined in Subsection 7.3, and can be defined by a chamber and either an edge or a vertex depending on where the tile is in the building. In particular, the wedges we use in the proof of Theorem 7.3.12 can be described in terms of ball entanglement wedges.

There is a nice way to estimate N_{cut} in terms of the radius of the ball which is the boundary of our entanglement wedge.

Proposition 7.3.16. *Let Λ be the layer of the network at which the code is cut off. Consider a bulk ball entanglement wedge R starting at a point z, and let g be the distance of the point z to O (note that g is the Gromov product of any two ends of the boundary of the entanglement wedge on the tensor network.) Then, if $q \geq 3$, the number of tile edges in R at layer less than Λ which are contained in ∂R equals*

$$N_{tiles} = \frac{2}{q-2}((q-1)^{\Lambda-g+1} - 1) - 1$$

if the entanglement wedge is delimited by a tree-wall, and

$$N_{tiles} = \frac{2}{q-2}((q-1)^{\Lambda-g+1} - 1)$$

if the entanglement wedge is delimited by two half-tree-walls.

Proof. This is a direct consequence of the tree structure of the boundary of the entanglement wedge. $\qquad\square$

At each of these tiles, $q - 1$ links are cut. Therefore,

$$N_{cut} = (q-1)\left(\frac{2}{q-2}((q-1)^{\Lambda-g+1} - 1) - 1\right),$$

or

$$N_{cut} = (q-1)\frac{2}{q-2}((q-1)^{\Lambda-g+1} - 1).$$

Hence,

$$N_{cut} \sim \frac{2}{q-2}\frac{(q-1)^{\Lambda+2}}{(q-1)^g}.$$

We now follow arguments of [77] to obtain a precise Ryu–Takayanagi formula for ball-shaped regions of the boundary.

Let us consider the case $q > 2$. Let $\mathrm{Hdim}\,\partial I_{p,q}$ denote the Hausdorff dimension $\mathrm{Hdim}\,\delta_x$ of Theorem 1.1 and 1.2a of [77] (see Lemma 3.1.4 of [77]).

Theorem 7.3.17. *The Ryu–Takayanagi formula holds for ball entanglement wedges in $I_{p,q}$, as in Lemma 7.3.14, with*

$$C^{-1}r^\beta \leq \frac{N_{cut}}{(q-1)^\Lambda} \leq Cr^\beta, \tag{7.4}$$

for a constant $C > 0$ (independent of the boundary region), and with

$$\beta = \mathrm{Hdim}\,\partial I_{p,q} - 1, \tag{7.5}$$

with r the radius of the boundary ball.

Proof. In [77], it is proven that there exists a visual metric δ_x of parameter $e^{\tau(p,2)}$ on the boundary of the Bourdon building, where $\tau(p, 2)$ is the growth rate of the Weyl group of the building. By definition of the distance δ_x, the radius of a boundary ball is controlled by $a^{-g} = e^{-g\tau(p,2)}$.[3] Note that then,

$$\frac{N_{cut}}{(q-1)^\Lambda} \sim \frac{1}{(q-1)^g} \sim r^\beta, \tag{7.6}$$

where

$$\beta = \frac{\log(q-1)}{\tau(p,2)}. \tag{7.7}$$

For this specific choice of $a = e^{\tau(p,2)}$, it can be shown [126] that

$$\beta = \text{Hdim}\,\delta_x - 1. \tag{7.8}$$

This is because in the case of the Bourdon building, we have [77]

$$\text{Hdim}\,\delta_x = \frac{\tau(p,q)}{\tau(p,2)}, \tag{7.9}$$

and

$$\tau(p,q) = \tau(p,2) + \log(q-1). \tag{7.10}$$

$\square$

Remark 7.3.18. This proof implies, among other things, that this choice of δ_x realizes the *conformal dimension* of the boundary of the Bourdon building [126]. This is an important result from the point of view of geometric group theory.

This result is quite striking: it tells us that entanglement entropy in our tensor network knows about the Hausdorff dimension of the boundary! It is also nice to realize that this behavior is in agreement with cases of holographic CFTs whose Cauchy slice dimension is an integer strictly larger than 1: in this case it is known that CFT entanglement entropy scales as a power law in the radius, where the exponent is dictated by the dimension of the time slice of the boundary minus one. Therefore, it seems like our tensor network is simulating a conformal field theory on a fractal! Ryu–Takayanagi surfaces in the network are given by rooted trees, and the entanglement entropy for corresponding ball-shaped regions are given by our power law.

---

[3]One can make this statement more rigorous by using Sullivan's shadow lemma, described in Appendix 7.7, to relate the geometry of the group Γ to that of the Bourdon building itself. See also Section 3.2 of [77].

The case of HaPPY-like tilings

The case $q = 2$ corresponds to a Fuchsian tiling of the hyperbolic plane, i.e., to a p-gon HaPPY tiling. In this case, it is easier to link N_{cut} with the size of the boundary ball. Indeed, we have

$$N_{tiles} = N_{cut} = 2(\Lambda - g) + 1,$$

and the size r of the boundary region satisfies

$$-g \sim \log r.$$

Hence

$$N_{cut} \sim \log \frac{r}{\varepsilon},$$

where

$$\varepsilon = e^{-\frac{\Lambda}{\alpha}}$$

for some $\alpha > 0$. This approximately reproduces the logarithmic behavior of entanglement entropy on the boundary.

The infinite-dimensional limit: Hilbert spaces and nets of local algebras

One of the advantages of our construction is that it provides us with a large family of nets of infinite-dimensional exact quantum error-correcting codes with complementary recovery. It is therefore an explicit example of nets of conditional expectations, as introduced by Faulkner in [164].

Let us first associate an infinite-dimensional code and a physical Hilbert space to our tensor network. The idea will be to take a direct limit of Hilbert spaces, both in the bulk and on the boundary.

Proposition 7.3.19. *There is an injection $\mathcal{H}_{code}^{\Lambda} \to \mathcal{H}_{code}^{\Lambda+1}$ of Hilbert spaces from the truncated network at layer Λ to level $\Lambda + 1$ compatible with the maps u^{Λ} : $\mathcal{H}_{code}^{\Lambda} \to \mathcal{H}_{phys}^{\Lambda}$ through commutative diagrams. These maps define as direct limits the infinite dimensional Hilbert spaces*

$$\mathcal{H}_{code} = \varinjlim_{\Lambda} \mathcal{H}_{code}^{\Lambda} \quad and \quad \mathcal{H}_{phys} = \varinjlim_{\Lambda} \mathcal{H}_{phys}^{\Lambda} \tag{7.11}$$

with an induced isometry $u : \mathcal{H}_{code} \to \mathcal{H}_{phys}$.

Proof. For the bulk Hilbert space, define a reference state for the dangling qudits. Let us denote it by $|ref\rangle$. If $\mathcal{H}_{code}^{\Lambda}$ denotes the code subspace of the truncated network

at layer Λ, we define an injection $\mathcal{H}^\Lambda_{code} \to \mathcal{H}^{\Lambda+1}_{code}$ by tensoring the state of $\mathcal{H}^\Lambda_{code}$ with qudits in the state $|\text{ref}\rangle$ at layer $\Lambda + 1$.[4] In order to construct a map from $\mathcal{H}^\Lambda_{phys}$ to $\mathcal{H}^{\Lambda+1}_{phys}$, we simply take the state at layer Λ, and map it through the tensor network from layer Λ to layer $\Lambda + 1$, with all dangling bulk nodes fixed in the state $|\text{ref}\rangle$. If u^Λ denotes the map from $\mathcal{H}^\Lambda_{code}$ to $\mathcal{H}^\Lambda_{phys}$, we then obtain a commutative diagram of the form

$$
\begin{array}{ccccc}
\mathcal{H}^1_{code} & \to & \mathcal{H}^2_{code} & \to & \cdots \\
\downarrow & & \downarrow & & \\
\mathcal{H}^1_{phys} & \to & \mathcal{H}^2_{phys} & \to & \cdots \quad ,
\end{array}
\tag{7.12}
$$

where the horizontal arrows denote the bulk-to-bulk maps and boundary-to-boundary maps, and the vertical arrows denote the isometries u^Λ. We can then take the direct limit of this diagram and define

$$
\mathcal{H}_{code} = \varinjlim_\Lambda \mathcal{H}^\Lambda_{code},
$$

and

$$
\mathcal{H}_{phys} = \varinjlim_\Lambda \mathcal{H}^\Lambda_{phys},
$$

as well as an isometry

$$
u : \mathcal{H}_{code} \to \mathcal{H}_{phys}
$$

as in (7.11). $\qquad \square$

Now, we are interested in studying a net of local observables on the boundary, and assigning an entanglement wedge to each of them.

Theorem 7.3.20. *For a given entanglement wedge associated to a tile T as before, there are C^*-algebras $\mathcal{A}_{code}$ and $\mathcal{A}_{phys}$, obtained as direct limits of entanglement wedge algebras $\mathcal{A}^\Lambda_{code}$ at layers Λ and their bulk-to-boundary maps. They are related by a unital isometric $\star$-homomorphism $\iota : \mathcal{A}_{code} \to \mathcal{A}_{phys}$, which is compatible with the isometry $u : \mathcal{H}_{code} \to \mathcal{H}_{phys}$ of Proposition 7.3.19 in the sense that $\iota(A)u = uA$.*

Proof. For this, consider a bulk tile T, and define an entanglement wedge associated to this tile as in Subsection 7.3. On top of each bulk qudit, we introduce a finite-dimensional algebra $\mathcal{M}_d(\mathbb{C})$. The entanglement wedge algebra $\mathcal{A}^\Lambda_{code}$ at layer Λ

---

[4]These maps have a few shortcomings, like the fact that they do not create an entangled bulk state. See [195] for another possible choice of Hilbert space maps. However, our maps here have good functorial properties at the level of operators, and will be enough for our purposes.

is given by the tensor product of all bulk dangling legs, and the map from $\mathcal{A}^\Lambda$ to $\mathcal{A}^{\Lambda+1}$ is given by tensoring with the identity on qudits at layer $\Lambda + 1$. Recall that there is a well-defined bulk-to-boundary map ι^Λ at the level of operators, by successively tensoring with the appropriate number of identities and conjugating by perfect tensor unitaries [372],[5] and that by the previous subsections, this map has a range contained on the boundary of the entanglement wedge defined by T. Moreover, one can define a map from the complement algebra to the complement boundary region, by complementary recovery. We can use the ι^Λ to define a boundary-to-boundary map at the level of algebras: just add one more layer of tensor network, and conjugate an operator by the perfect tensor isometries with identitity matrices on the new bulk nodes, following the map given by $\iota^{\Lambda+1}$. We then obtain another commutative diagram of the form

$$
\begin{array}{ccccc}
\mathcal{A}^1_{code}(T) & \to & \mathcal{A}^2_{code}(T) & \to & \cdots \\
\downarrow & & \downarrow & & \\
\mathcal{A}^1_{phys}(T) & \to & \mathcal{A}^2_{phys}(T) & \to & \cdots \quad ,
\end{array}
\tag{7.13}
$$

where the horizontal arrows are the bulk-to-bulk and boundary-to-boundary maps, and the vertical arrows are the ι^Λ. Like in the previous case, we can take the direct limit C^*-algebra, and we obtain two C^*-algebras $\mathcal{A}_{code}$ and $\mathcal{A}_{phys}$, related by a unital isometric $*$-homomorphism

$$
\iota : \mathcal{A}_{code} \to \mathcal{A}_{phys}.
$$

Moreover we can see $\mathcal{A}_{code}$ and $\mathcal{A}_{phys}$ as acting on $\mathcal{H}_{code}$ and $\mathcal{H}_{phys}$, and by construction of ι, for $A \in \mathcal{A}_{code}$,

$$
\iota(A)u = uA,
$$

and similarly for the complementary algebras. □

Note that this construction depends on our choice of map ι, which is not always unique. For example, it is not unique in the case of the pentagonal HaPPY code. This breaks the symmetry of the network, but it still gives rise to a net of holographic conditional expectations in the sense of [164] (with the difference that we left the construction here at the level of C^*-algebras).

---

[5]This map is not unique.

7.4 The general case: holographic tensor networks on hyperbolic buildings

Our construction for the case of Bourdon buildings can be generalized to a much larger class of buildings in various integer bulk dimensions and non-integer boundary Hausdorff dimension. We first give a set of sufficient conditions for our construction to easily generalize. We then introduce a few interesting examples of tensor networks that satisfy these conditions.

A class of tensor networks

We want to extend our construction to a well-chosen class of hyperbolic buildings. In order for the same method to work, we need to check the following conditions:

- The tensor network still defines an isometric map at each layer.

- Complementary recovery still works for well-chosen entanglement wedges.

- The Ryu–Takayanagi scaling of the entanglement entropy for well-chosen boundary balls still follows a power law of exponent $\beta - 1$, where β encodes the dimension of the boundary time slice, if $\beta > 1$, or a logarithmic behavior if $\beta = 1$.

First, in order to show that the tensor network defines an isometric map at each layer, we had to use the fact that, given a central chamber and a fixed apartment containing it, any chamber of that apartment is adjacent to more outgoing tiles further away from the center than tiles closer or equidistant to the center. Thus, our argument only used the apartment structure. We are therefore reduced to finding a condition of the Weyl group of our building that guarantees that it maps the bulk to the boundary Hilbert spaces isometrically. An explicit sufficient condition on the Coxeter system has been found by Kohler and Cubitt (see Section 6.1.2 of [280]), and we use it here:

Definition 7.4.1. Let B be a building of Weyl group W with Coxeter system (W, S). Let $\mathcal{F} := \{J \subset S, W_J \text{ is finite}\}$. We will say that B satisfies the *isometry condition* if for all $J \in \mathcal{F}$,
$$|J| \le \frac{t-2}{2},$$
where t is the number of indices of the perfect tensor, divided by the branching.

Lemma 7.4.2. *The isometry condition is always satisfied for a right-angled hyperbolic building.*

Proof. Indeed, in that case the Coxeter system associated to the building has matrix entries 2 and ∞. Hence, the subsets J of S for which W_J is finite can only contain elements for which the Coxeter matrix elements for each pair are 2. These must then be adjacent faces in the basic chamber of the building. Now, a hyperbolic polytope can be right angled iff it has more faces than a hypercube. This means that a maximal set of adjacent faces will always have less elements than half of the number of faces of the polytope. Identifying Coxeter generators with the faces of the polytope, and recalling that there is always at least one dangling leg inside the perfect tensors, we obtain the isometry condition. □

Remark 7.4.3. When the isometry condition is satisfied on top of our other conditions, a slight adaptation of the argument of [372] shows that our building defines an isometry from the bulk to the boundary at all layers.

The second point that needs to be confirmed is complementary recovery for well-chosen entanglement wedges.

Lemma 7.4.4. *The entanglement wedge constructions of Section 7.3 extend to arbitrary hyperbolic buildings satisfying the isometry condition and satisfy complementary recovery.*

Proof. This is guaranteed by the building structure of our networks. More precisely, consider a link in the building, and an $(n-1)$-polytope P on that link corresponding to a given tensor in the network. Embed P into a given apartment of the network. This apartment is isomorphic to a hyperbolic Coxeter system, hence we can repeat the construction of the previous section and use the link to construct a partition of the bulk into reconstructable regions. The other definition in terms of one single hyperplane (generalization of the tree-wall) is even more straightforward. □

The third and last point is probably the most subtle one: our argument on the Hausdorff dimension scaling required calculating the Hausdorff dimension of the Bourdon building for a specific visual metric. A full study is out of the scope of this chapter, but in order to be able to generalize it, we want our building chambers to each connect to the same number of edges through a wall, and to use the transitivity of the action of the isometry group of X on the set of apartments that contain it, to reproduce the proof of the Ryu–Takayanagi scaling. This requires B to contain a chamber whose fixator in the isometry group of X acts transitively on the set of apartments that contain it. We now obtain the following result:

Theorem 7.4.5. *Let B be an n-dimensional hyperbolic building such that:*

- *The Weyl group of B satisfies the isometry condition.*

- *The link at each point is the same, and each $(n-1)$-polytope of the link is q-valent (in the sense that it touches q other $(n-1)$-polytopes) for some q.*

- *B contains a chamber whose fixator in the isometry group of X acts transitively on the set of apartments that contain it.*

Then, B defines a quantum error-correcting code with complementary recovery for well-chosen bulk regions, and in a large class of these tensor networks, for these regions, the size of the Ryu–Takayanagi surface scales like $r^{\beta-1}$, where r is the radius of the associated boundary ball, and β is the scaling dimension of ∂B.

Remark 7.4.6. Note that in this theorem, the Ryu–Takayanagi formula scales like the *scaling dimension* (self-similarity dimension, see Chapter 4 of [374]) of the boundary, but not necessarily like the Hausdorff dimension of a given visual metric. This is because in order for these two dimensions to be equal, one needs to show the existence of a visual metric with such a Hausdorff dimension, and this existence property is not always guaranteed. In the case of the Bourdon building, it was shown [77] that this could be done by explicitly constructing a visual metric with parameter *a* equal to the growth rate of the Weyl group of the building, that realizes the conformal dimension. However, it is a difficult and important problem in geometric group theory to understand when such a metric can be constructed in higher dimension. In particular, we expect this question to be related to subtle rigidity properties of the buildings. Even in order to show a matching of the scaling dimensions, one needs to have some nice formula that relates the growth rates of the building and of its apartments. See for example [110], where some partial answers to these questions are given in the case of right-angled buildings, particularly in three dimensions. We leave a more precise study of the scaling properties of the RT surfaces in higher-rank buildings, as well as of these issues related to the comparison of Hausdorff, scaling and conformal dimensions, to future work.

Higher dimensional examples

We now show that our techniques can be adapted to construct holographic codes in arbitrary integer dimensions (as well as non-integer boundary Hausdorff dimensions). This will be done through an explicit construction, due to Davis–Moussong, of an

interesting class of hyperbolic buildings in any given dimension. This construction is slightly more technical than the rest of the chapter, the main takeaway being that holographic codes exist in all integer bulk dimensions, and that the Ryu–Takayanagi formula and entanglement wedge reconstruction for well-chosen regions, carry over to these more general cases.

We have focused primarily on the Bourdon buildings, which are the primary example of hyperbolic buildings. More generally, it is known that hyperbolic buildings are more difficult to obtain than Euclidean ones. Indeed, if one takes as part of the definition of buildings the requirement that they are polyhedral complexes where apartments are (in the hyperbolic case) polyhedrally isometric to a tesselation of the n-dimensional hyperbolic space, then there are strong restrictions on the dimension of hyperbolic buildings. There is a bound $n \leq 29$ on the dimension of a compact convex hyperbolic Coxeter polytope [446]. In particular, Theorem 7.4.5, as stated, only applies in this range.

In the case of the Bourdon buildings, as we have seen, a useful property is the fact that they are right-angled buildings. In general, a Coxeter system (W, S) is right-angled if all the m_{ij} with $i \neq j$ in the relations are equal to 2 or ∞. With this further requirement, it is known that right-angled Coxeter polytopes can only exist in dimension $n \leq 4$ [390]. Thus, right-angled hyperbolic buildings (with the definition as above) can only exist in dimension $n \leq 4$.

This seems to limit the range of validity of the general setting we introduced above for the construction of holographic tensor networks on hyperbolic buildings. However, it is in fact possible to relax slightly the definition of buildings in such a way that right-angled hyperbolic buildings will be available in arbitrary dimension. This was done in [260] by considering geometries where the apartments are Davis–Moussong complexes of the Coxeter group W, instead of copies of hyperbolic space tessellated by the action of W. In general, the Davis–Moussong complex associated to a Coxeter system (W, S) is a piecewise Euclidean (non-positively curved) polyhedral complex with a properly discontinuous cocompact action of W, see [133, 348].

The construction of the Davis–Moussong complex $K(W, S)$ is obtained in the following way [348]. Given a Coxeter system, the associated nerve $N(W, S)$ is the simplicial complex with one vertex for each element of S, with subset $T \subset S$ defining a simplex of $N(W, S)$ if the subgroup $W_T \subset W$ generated by T is finite. Let N' be the barycentric subdivision of $N = N(W, S)$ and let CN' be the cone of N'. For each $s \in S$ let X_s be the closed star of the vertex s in N'. The collection $M = \{X_s\}_{s \in S}$ of

closed subspaces of $X = CN'$ is called the set of panels. For $x \in X$ one also sets $S(x) := \{s \in S \mid x \in X_s\}$. There is an associated a universal W-space $U(W, X, M)$, with a CW complex structure, given by the quotient of $W \times X$ by the equivalence relation $(w, x) \sim (w'x')$ if $x = x'$ and $w^{-1}w' \in W_{S(x)}$. This space is universal with respect to maps $f : X \to Y$ with $sf(x) = f(x)$ for $x \in X_s$: each such map uniquely extends to a continuous W-equivariant map $f : U \to Y$. The Davis–Moussong complex is $K(W, S) = U(W, CN', M)$. It is contractible with $K(W, S)/W \simeq CN'$.

There is a characterization of hyperbolic Coxeter groups, in terms of the presence of a hyperbolic structure on the Davis–Moussong complex $K(W, S)$. The Coxeter group is hyperbolic iff it contains no subgroup isomorphic to $\mathbb{Z} \oplus \mathbb{Z}$. This condition is in turn equivalent to the condition that there is no subset $T \subset S$ with W_T an affine Coxeter system of rank ≥ 3 and there are no pairs T_1, T_2 of disjoint subsets of S for which W_{T_1} and W_{T_2} commute and are infinite, see Theorem 17.1 of [348]. This last condition in turn implies that $K(W, S)$ can be given a hyperbolic structure by considering for each $T \subset S$ with W_T finite a hyperbolic space $\mathbb{H}^{n_T}$ with $n_T = \#T$. The building blocks of CN' are the $CN(W_T, T)'$ for $T \subset S$ with W_T finite. Each of these building blocks is homeomorphic to a combinatorial n_T-cube $B(W_T)_\epsilon \subset \mathbb{H}^{n_T}$, for some $\epsilon > 0$ (see [348] for more details). These building blocks are glued together according to the relations of subsets $T \subset S$ into a decomposition of $K(W, S)$. The condition above on the hyperbolicity of the Coxeter group W ensures that, with this hyperbolic structure on the blocks $CN(W_T, T)'$, the complex $K(W, S)$ itself has a the structure of a hyperbolic complex.

The difference with the usual apartments of buildings in the more restrictive sense is that here the contractible manifolds $K(W, S)$ are in general not homeomorphic to Euclidean space (hence not tessellated copies of $\mathbb{H}^n$). Indeed, the boundary at infinity of $K(W, S)$ is not necessarily simply connected, but it has the topology of a generalized $(n - 1)$-dimensional homology sphere, see [133] and [260].

The construction of [260] of higher dimensional right-angled hyperbolic buildings with Davis–Moussong complexes as apartments is obtained via complexes of groups.

A complex of groups is an assignment of groups and compatible maps to a simplicial complex that reflects the properties of the orbit space of a group action on a cell complex, see [129]. It generalizes the Bass–Serre construction of graphs of groups.

A complex of groups $G(K)$ consists of combinatorial CW complex K (namely a CW complex that is either simplicial or that can be subdivided into simplicial complexes),

with a group G_{e_α} assigned to each cell e_α and monomorphisms $\phi_{\alpha,\beta} : G_{e_\alpha} \to G_{e_\beta}$ for each cell e_β in the boundary of e_α. Boundary inclusions $e_\gamma \subset e_\beta \subset e_\alpha$ give $Ad(g)\phi_{\alpha,\gamma} = \phi_{\beta,\gamma} \circ \phi_{\alpha,\beta}$, for some $g \in G_{e_\gamma}$ acting by conjugation. For our purposes we can assume that K is a polyhedral complex (or a simplicial complex after passing to barycentric subdivision).

The complex of groups associated to a simplicial action of a group on a combinatorial cell complex has finite stabilizer groups attached to the cells, with monomorphisms of stabilizers contravariantly associated to inclusions of cells. A complex of groups is developable if it is the complex of groups associated to a simplicial action of a group on a simply connected combinatorial cell complex. Not all complexes of groups are developable, but developability is implied by a non-positively curved condition [84].

The construction via complexes of groups of a right-angled building with apartments shaped as Davis–Moussong complexes $K(W, S)$ is obtained as follows. Start with a right-angled Coxeter system (W, S) that satisfies the hyperbolicity condition above, so that $K(W, S)$ has a hyperbolic structure. Take as additional datum a set $\{q_s\}_{s\in S}$ of integers $q_s \geq 2$, and let G_s be a group of order q_s. As above, vertices of CN' has type some $J \subset S$ with W_J finite. Let $G(K)$ be the complex of groups that assigns to a vertex of type J the group given by the direct product $G_J = \amalg_{s\in J} G_s$, with maps given by inclusions. This complex of groups is developable with cover a right-angled building. As above let X_s be the closed star of the vertex s in N'. Each copy of X_s is contained in q_s chambers in this building, with each chamber given by a copy of CN'.

The existence in any dimension of this type of hyperbolic buildings with Davis–Moussong apartments is then proved in [260] by showing the existence in any dimension of a right-angled Coxeter system (W, S) satisfying the hyperbolicity condition, i.e., containing no subgroup isomorphic to $\mathbb{Z} \oplus \mathbb{Z}$.

This class of buildings satisfy our conditions for tensor networks with good holographic properties.

Theorem 7.4.7. *The hyperbolic buildings built using Davis–Moussong complexes and with all the $q_s = q$, satisfy the isometry condition and have complementary recovery.*

Proof. The isometry condition is still satisfied: as shown in [348], the girth of the links is strictly greater than 2π, which means that if one fixes a vertex of a chamber

of the building, as the chamber is right-angled, more faces of the chamber will not touch that vertex than touch it, and W_J can be finite only if J only contains faces that touch the same vertex. This same argument allows us to prove complementary recovery for well-chosen regions (generalizations of either tree-walls or vertex-based entanglement wedges). The third condition formulated in Theorem 7.4.5 is satisfied by construction: the Davis–Moussong complex can be seen as the quotient of the building by the action of the group developed by the complex of stabilizers. So by acting on an apartment by all the group elements that stabilize a given cell (which makes sense because the action is simplicial), one can obtain all apartments containing that cell. □

Remark 7.4.8. In the proof, we also included a discussion of the third condition of Theorem 7.4.5, and it should also be possible to formulate a nice statement about of the area of the Ryu–Takayanagi surfaces in terms of the scaling, Hausdorff or conformal dimensions of the boundary. This question should also be interesting from the point of view of geometric group theory.

In particular, this shows the existence of tensor networks with good holographic properties in arbitrary dimension.

7.5 Discussion

In this chapter, we explained how one could construct a large class of holographic tensor networks from hyperbolic buildings. The language of buildings and Gromov-hyperbolicity allows to recover the usual properties of hyperbolic tensor networks and to describe them in a unified way. In particular, our buildings:

- Contain a large class of bulk regions that satisfy complementary recovery. These regions admit an explicit description in terms of building theory.

- Satisfy the Ryu–Takayanagi formula. For ball-shaped boundary regions of Hausdorff dimension strictly greater than 1, the entanglement entropy of holographic states follows a power law in the radius of the ball, with exponent given by the *Hausdorff dimension of the boundary minus one*, in a large number of cases including the one of Bourdon buildings. If the boundary has dimension 1, we recover the logarithmic scaling of the HaPPY code.

- Exist for boundaries of all integer dimensions, and therefore provide explicit examples of holographic codes in all integer dimensions.

- Recover all known holographic codes constructed out of networks of perfect tensors as particular cases. In particular, the HaPPY code as well as the higher-dimensional examples of [280] can be studied through the lens of our construction.

Several future directions can be envisioned. First, we only considered holographic codes made out of perfect tensors in this chapter, but it would be nice to study holographic codes made out of random tensors in our context.

It would also be interesting to understand the situation for disconnected boundary regions better. Our explicit entanglement wedge constructions all involve a connected boundary region, and it would be nice to understand whether similar descriptions based on building theory hold for disconnected boundary regions.

Another question is whether the fact that the entanglement entropy of ball-shaped regions sees the fractal dimension of the boundary means that it could be possible to define theories that resemble conformal field theory on a fractal background (see [81] for a related attempt in one dimension).

It is also interesting to ask if more general objects than hyperbolic buildings are well-adapted to the construction of holographic codes. In particular, it would be interesting to understand if quotients of our buildings can be taken in order to describe nontrivial bulk topologies in the spirit of the BTZ-like topologies constructed in [238]. We expect that the setup of latin square designs [116] might be helpful to think about this kind of problem.

Finally, this chapter showed that the theory of Gromov hyperbolicity can be very useful to show geometric results about the bulk, such as the Ryu–Takayanagi formula. One can then wonder whether the notions of Gromov product and of hyperbolicity can also be utilized in the continuum, to understand the geometric structure of the bulk in full AdS/CFT.

7.6 Appendix: An example: the building $I_{5,3}$

In this appendix, we explicitly compute the various quantities and regions described in the bulk of the chapter in the case of the simplest Bourdon building: the building $I_{5,3}$.

We first describe explicitly the structure of the building $I_{5,3}$.

- **Apartment structure:** The apartments of the building $I_{5,3}$ are HaPPY tessellations of the hyperbolic plane: regular, right-angled tessellations by pentagons. Their Schläfli symbols are $\{5, 4\}$. Their Coxeter group is generated by five reflections r_1, r_2, r_3, r_4, r_5 such that $(r_i r_{i+1})^2 = 1$ (where the index is understood modulo 5).

- **Link:** The link is the bipartite complete graph $K(3, 3)$. This means that at each vertex of the building, six edges concur. These six edges can be split into two groups of three. Each edge shares a face only with the three edges of the opposite group.

Then, we introduce the growth rates of the Weyl group and the isometry group of the building [77]:

- **Growth rate of the Weyl group:** The growth rate of the Weyl group is equal to

$$\tau(5, 2) = \text{Arccosh}\left(\frac{3}{2}\right). \tag{7.14}$$

- **Growth rate of the isometry group:** The growth rate of the isometry group is equal to

$$\tau(5, 3) = \text{Arccosh}\left(\frac{3}{2}\right) + \log 2. \tag{7.15}$$

In the case of the Bourdon building, it is possible to show [77] that there exist visual metrics on $\partial I_{5,3}$ whose Hausdorff dimension realizes the conformal dimension of the building, and is equal to the ratio of the growth rate of the isometry group by the growth rate of the Weyl group. We then have:

$$\text{Hdim}(\partial I_{p,q}) = 1 + \frac{\log 2}{\text{Arccosh}\left(\frac{3}{2}\right)}. \tag{7.16}$$

The second term on the right hand side corresponds to the exponent of the scaling of entanglement entropy.

Finally, we describe "ball entanglement wedge" bulk regions that satisfy complementary recovery in the building $I_{5,3}$. They are delimited either by a tree-wall or by the intersection of two tree-walls. In the case of $I_{5,3}$, a tree-wall divides the building into three valid entanglement wedges (see Figure 7.4).
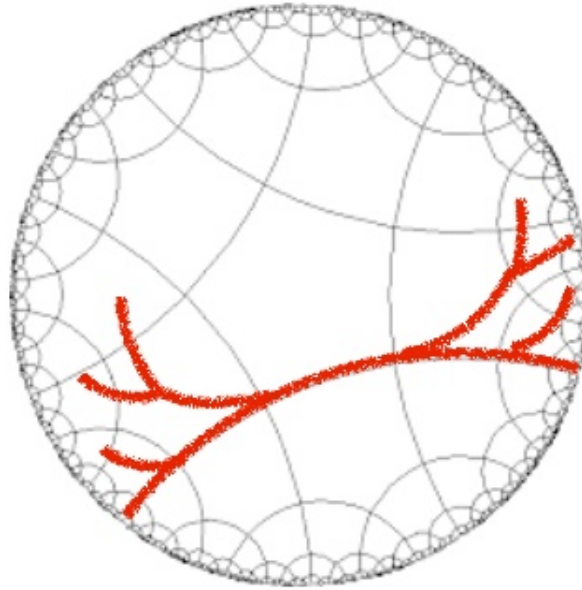
Figure 7.4: A tree-wall in $I_{5,3}$ and its intersection with an apartment. The tree-wall coincides with a geodesic in the HaPPY apartment, but at every tile, it divides into two branches due to the link structure of $I_{5,3}$. In the end, we end up with a homogeneous trivalent tree.

7.7 Appendix: Quasi-conformal measures and Patterson–Sullivan theory

In this slightly more technical appendix, we elaborate on the idea that our networks describe some features of an approximate conformal field theory on a fractal space. The idea is that for any visual metric of the boundary of a Gromov hyperbolic group (such as the isometry group of the Bourdon building, which can be identified with its chambers), one can define a privileged measure that behaves "almost conformally" under isometries. This measure is called the Patterson–Sullivan measure, and we review its construction here. We begin with a few definitions:

Definition 7.7.1. Let r be a geodesic ray in X. The Busemann function associated to r is the map

$$h : X \longrightarrow \mathbb{R}$$
$$x \longmapsto \lim_{t \to +\infty} (|x - r(t)| - t).$$

Note that this function is well-defined by the triangle inequality.

Definition 7.7.2. Let Γ be a group of isometries of X, let $\gamma \in \Gamma$. For $\xi \in \partial X$,

choose a geodesic ray arriving at ξ, let h be its Busemann function, and define

$$j_\gamma(\xi) := a^{\Delta(\xi)},$$

where

$$\Delta(\xi) = h(O) - h(\gamma^{-1}O).$$

Let μ be a regular Borel measure on ∂X, of finite nonzero total mass. Then, define

$$\gamma^*\mu := \mu \circ \gamma.$$

The measure μ is said to be Γ-quasiconformal of dimension D if all the $\gamma^*\mu$ are absolutely continuous with respect to each other[6] for $\gamma \in \Gamma$, and there exists $C \geq 1$ such that

$$C^{-1}j_\gamma^D \leq \frac{d\gamma^*\mu}{d\mu} \leq Cj_\gamma^D,$$

μ-almost everywhere.[7]

One can view a Γ-quasiconformal measure as a measure on ∂X for which Γ "behaves like a conformal group." Under a reasonable assumption on Γ, there exists a generic construction of such a Γ-quasiconformal measure, due to Patterson and Sullivan [126].

Let Y be the orbit of O under Γ. For $R \geq 0$, let $n_Y(R)$ be the number of points of Y within a distance R of O.

Definition 7.7.3. We define the *base-a critical exponent of* Γ as

$$e_a(\Gamma) := \limsup_{R\to+\infty}\frac{\log_a n_Y(R)}{R}.$$

For $s \geq 0$, we define the Poincaré series

$$g_Y(s) := \sum_{y\in Y} a^{-s|y|}.$$

One can then prove [126] that this series is divergent for $s < e_a(\Gamma)$ and convergent for $s > e_a(\Gamma)$. Then, one can construct a sequence (s_n) of limit $e_a(\Gamma)$, with $s_i > e_a(\Gamma)$. Consider the sequence of measures

$$\mu_n := \frac{1}{g_Y(s_n)}\sum_{y\in Y} a^{-s_n|y|}\delta_y,$$

---

[6]This means that they have the same zero-measure sets.

[7]That is, the inequality holds everywhere except for a set of measure zero as measured with respect to μ.

where δ_y is the Dirac measure at y. As $X \cup \partial X$ is compact, one can then extract a weakly convergent subsequence of (μ_n). The limit μ of this subsequence is called a Patterson–Sullivan measure for Γ and one can prove (up to some technical refinements on the sequence (μ_n) in the case where the Poincaré series converges at $e_a(\Gamma)$):

Proposition 7.7.4 ([126])**.** *If $e_a(\Gamma)$ is finite, then the Patterson–Sullivan measure μ is Γ-quasiconformal of exponent $e_a(\Gamma)$. Moreover, its support is the limit set of Γ, denoted Λ.*

Under the extra assumption of Γ being quasi-convex cocompact [126], more can be said about the space of Γ-quasiconformal measures on ∂X:

Proposition 7.7.5 ([126])**.** *If Γ is a quasi-convex cocompact group acting on X such that $e_a(\Gamma)$ is finite, then, Λ has Hausdorff dimension $e_a(\Gamma)$, and the associated Hausdorff measure is Γ-quasiconformal of dimension $e_a(\Gamma)$. Moreover, if μ is another Γ-quasiconformal measure whose support is contained in Λ, then it has dimension $e_a(\Gamma)$ and it is of the form $\psi \mathcal{H}$, where $\mathcal{H}$ is the Hausdorff measure of Λ and $\psi \in L_0^\infty(\mathcal{H})$. Reciprocally, all such measures are Γ-quasiconformal of dimension $e_a(\Gamma)$ with support contained in Λ.*

A lot of results in Patterson–Sullivan theory rely on Sullivan's shadow lemma. We state it here in its most general form, see also Lemma 8 of [462] for a useful variant:

Proposition 7.7.6 ([126], Proposition 6.1)**.** *Let μ be a Γ-quasiconformal measure of dimension D on ∂X. If $O(x, d)$ is the intersection with ∂X of the set of all geodesic rays starting at O and passing at a distance smaller than d of x, then there exist constants $C \geq 1$ and $d_0 \geq 0$ such that for all $d \geq d_0$ and $\gamma \in \Gamma$,*

$$C^{-1}r^D \leq \mu(O(x, d)) \leq Cr^D a^{2Dd},$$

where we have chosen $x = \gamma^{-1}O$, for the chosen base point O and $r = a^{-|x|}$. The set $O(x, d)$ is called the shadow on ∂X of the ball centered on x with radius d.

ON INFINITE TENSOR NETWORKS, COMPLEMENTARY RECOVERY AND TYPE II FACTORS

This chapter is based on the work [102], in collaboration with Wissam Chemissany, Alexander Jahn, Daniel Murphy and Leo Shaposhnik.

8.1   Motivation and setting

Tensor networks have become an ubiquitous tool in modern physics, ranging from the description of ground states of many-body quantum-mechanical systems and topological phases of matter [83, 109] to the study of quantum information aspects of holographic dualities [431, 32, 33, 31, 258, 345, 88]. Despite their success in describing physical systems, discussions of the continuum limit of finite dimensional tensor networks have usually been limited to investigations of the limiting correlation functions of local operators [381, 109] and a precise formulation of the continuum limit in terms of a concrete Hilbert space and operators acting on it is often left implicit. Although some models of continuum tensor networks, such as continuous matrix product states (cMPS), can be understood in terms of a continuum limit [443] from a lattice-based model, other more heuristic models, such as the continuous multiscale entanglement renormalization ansatz (cMERA), do not directly correspond to such a limit [217]. Based on wavelet models, the convergence to a free quantum field theory of certain lattice models was shown in [459, 423, 366], where an explicit realization of such a limit in terms of a MERA circuit was given in [459]. However, tools to analyze the limits of more general tensor networks remain limited; in particular, the operator algebras of subsystems are poorly understood.

In this work, we investigate such operator algebras in infinitely large tensor networks for a class of layered tensor networks that can be associated with quantum error-correcting codes, using tools from the theory of inductive systems and the description of the observables of the system using local algebras, borrowing the language of algebraic quantum field theory [213]. The use of inductive limits as a mathematical tool to rigorously formulate the continuum limit of tensor networks has been inspired by analogous studies in the context of Banach spaces and operator algebras [308]. This perspective has direct parallels with the layered tensor networks discussed here, particularly in how local algebras and Hilbert spaces grow iteratively to form

a limiting theory. Similar constructions were given in [365, 269, 195, 199, 196] which focused on the formulation of the limiting systems and assignment of the limiting Hilbert space but, with the exception of [269], did not discuss the type of the resulting algebras. Furthermore, in [346, 422, 423, 459] similar methods were used to prove convergence of certain lattice systems of free quantum field theories based on wavelet models. In contrast to these studies aiming to obtain quantum field theories that always have local algebras of type III_1, we focus on tensor networks on finite-dimensional Hilbert spaces that implement holographic quantum error-correcting codes that a priori do not have to converge to a quantum field theory. In particular, our goal is to determine the type of local algebra for these networks from an entanglement-based perspective. We are able to compute the type because we restrict ourselves to a very specific class of networks, namely networks that implement quantum error-correcting codes with complementary recovery, also known as holographic quantum error-correcting codes [10]. We will focus primarily on the Harlow-Pastawski-Preskill-Yoshida (HaPPY) code model, which achieves complementary recovery with a hyperbolic tensor network of *perfect tensors* [372]. As we will describe in the following, this property gives us strong control over the structure of the state of the network during the iteration process and allows for a direct mapping to the standard form of hyperfinite factors, the *Araki-Woods-Powers factors* [26, 391], a possibility that was not made manifest in earlier studies of limits of infinitely large instances of such codes [195, 199, 196].

The main result of our work concerns the appearance of *type II von Neumann algebras* associated to boundary regions of the infinitely large HaPPY code that contain infinite entanglement with their complementary region, but whose underlying entanglement pattern has the structure of maximally entangled *Einstein-Podolski-Rosen* (EPR) pairs (Fig. 8.1(a)). These algebras famously allow for the definition of a trace and reduced density matrices, notions which become ill-defined in systems with more complicated entanglement divergences, such as the type III algebras found in causally complete subregions of quantum field theories. As we shall show, type II algebras appear naturally in the scaling limits of layered tensor networks with a property known as *complementary recovery*. These were first considered in tensor networks that model holographic bulk/boundary dualities and act as encoding isometries of quantum error-correcting codes, known as *holographic codes* [10, 372, 257, 385]. As visualized in Fig. 8.1(b), holographic codes provide an isometric map from a bulk to a boundary Hilbert space, and we consider those with a layered structure such that the dimension of both Hilbert spaces diverges in the scaling
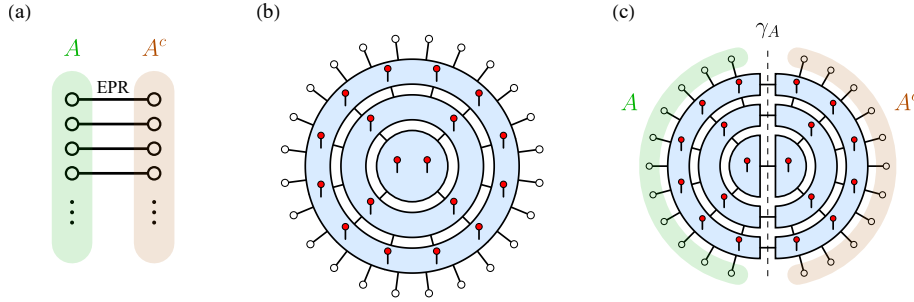
Figure 8.1: (a) The Araki–Woods construction of a type II von Neumann algebra $\mathcal{A}$. One constructs an infinite series of maximally entangled pairs of qubits (EPR pairs), one side of which constitutes a subsystem A (with complement A^c) on which operators in $\mathcal{A}$ act. (b) A layered tensor-network code forms an isometric map between bulk qubits (red) and boundary qubits (white). Layers can be added iteratively until both the number of bulk and boundary qubits become infinite. The tensor network contraction (black connecting lines) itself acts as a projection onto EPR pairs. (c) For a holographic tensor-network code with complementary recovery, a bipartition of the boundary qubits induces a clean bipartition of the bulk qubits along a Ryu-Takayanagi surface γ_A. Adding more layers increases EPR-like entanglement across γ_A, again ultimately leading to a type II von Neumann algebra for operators acting on A in the limit of infinitely many layers, provided that boundary states contain only finite bulk entanglement.

limit of infinitely many layers. Complementary recovery ensures that a bipartition of the "physical" boundary qubits into the A and A^c subregions induces a clean bipartition among the "logical" bulk qubits (Fig. 8.1(c)). Given this property, the tensor network also splits into two parts connected by a contraction (projection onto EPR pairs) that contributes to the entanglement between A and A^c. By analogy with continuum holography, this tensor network cut is commonly referred to as a (discrete) *Ryu-Takayanagi (RT) surface* [401]. An operator-algebraic formulation of complementary recovery for the finite-dimensional type I setting has already been established in [225], with the appearance of $C^\star$ and von Neumann algebras in the scaling limit studied in subsequent works [269, 196, 164, 168, 192]. The contribution of our work is to show the precise decomposition of these algebras in holographic codes in the inductive limit and how the "geometrical" entanglement in these models leads to a type II von Neumann algebra.

The starting point of our work are tensor networks with a layered structure, i.e., iterative maps

$$|\Psi^1\rangle \mapsto |\Psi^2\rangle \mapsto |\Psi^3\rangle \mapsto \ldots \tag{8.1}$$

between states of the network at different layers, each described by finite dimensional

Hilbert spaces

$$\mathcal{H}^1 \to \mathcal{H}^2 \to \mathcal{H}^3 \to \dots \tag{8.2}$$

We assume that each of these Hilbert spaces spaces at layer Λ can be written as a bipartition

$$\mathcal{H}^\Lambda = \mathcal{H}_A^\Lambda \otimes \mathcal{H}_{A^c}^\Lambda, \tag{8.3}$$

which can be thought of as a decomposition of the space into "local" subsystems. The sequences of networks are obtained by taking the network at layer Λ and contracting it with a new layer of the network, which we encode by an isometric operator $\gamma^{\Lambda,\Lambda+1} : \mathcal{H}^\Lambda \to \mathcal{H}^{\Lambda+1}$, such that

$$|\Psi^{\Lambda+1}\rangle = \gamma^{\Lambda,\Lambda+1} |\Psi^\Lambda\rangle. \tag{8.4}$$

$\gamma^{\Lambda,\Lambda+1}$ has to be isometric, so we map normalized states to normalized states. The collection of Hilbert spaces $\mathcal{H}^\Lambda$ together with the maps $\gamma^{\Lambda,\Lambda+1}$ defined by the tensor network is called an *inductive system*. As described later, this allows one to define a limiting Hilbert space $\mathcal{H}$ that can intuitively be thought of as having a vacuum described by a reference state of the infinite tensor network, together with states that arise from acting with a local operator on a subregion of the tensor network during the iteration procedure. Additionally, we demand of our network that, together with the isometry $\gamma^{\Lambda,\Lambda+1}$ that translates between states at different layers, we can identify a bounded operator $O^\Lambda \in \mathcal{B}(\mathcal{H}^\Lambda)$ at layer Λ with an operator in the next layer. We denote this identification as an operator-pushing map $\phi^{\Lambda,\Lambda+1}$

$$O^{\Lambda+1} = \phi^{\Lambda,\Lambda+1}(O^\Lambda). \tag{8.5}$$

and we demand that these are unital $*$-homomorphisms, i.e., they are linear maps mapping the identity to the identity that respect multiplication of operators and satisfy $\phi^{\Lambda,\Lambda+1}(O^\dagger) = \phi^{\Lambda,\Lambda+1}(O)^\dagger$, so that they preserve the algebraic structure. Note that one might be tempted to implement $\phi^{\Lambda,\Lambda+1}$ by a conjugation with isometry $\gamma^{\Lambda,\Lambda+1}$, which may appear natural in the tensor network but will not allow for good reconstruction properties to study the inductive limit, as we shall see below. Instead, we will define $\phi^{\Lambda,\Lambda+1}$ in the HaPPY code as a conjugation with a unitary

$$\phi^{\Lambda,\Lambda+1}(O) = U^\dagger(O \otimes \mathbb{1})U^\dagger, \tag{8.6}$$

where the unitary exists in an enlarged space on which the additional identity acts.[1] We think of a subsystem at layer Λ as given by a subset of the legs A of the tensor

---

[1]In the context of entanglement renormalization, such maps between layers are often referred to as *ascending superoperators* [445].

network state $|\Psi^\Lambda\rangle$ with decomposition (8.3) and a global algebra

$$\mathcal{B}(\mathcal{H}^\Lambda) = \mathcal{B}(\mathcal{H}^\Lambda_A) \otimes \mathcal{B}(\mathcal{H}^\Lambda_{A^c}), \tag{8.7}$$

so that the operators belonging to A are represented as elements of the local algebra

$$\mathcal{A}^\Lambda_A = \mathcal{B}(\mathcal{H}^\Lambda_A) \otimes \mathbb{1}_{\mathcal{H}^\Lambda_{A^c}}. \tag{8.8}$$

Using the operator pushing map (8.5), we can push the whole algebra $\mathcal{A}^\Lambda_A$ to the next layer, thus also obtaining an inductive system of algebras $(\mathcal{A}^\Lambda_A, \phi^{\Lambda,\Lambda+1})$. Therefore, we can define its inductive limit $\mathcal{A}_A$ which is an abstract $C^\star$-algebra that defines the operators that are associated to A in the limit $\Lambda \to \infty$. This algebra can be represented on the limiting Hilbert space $\mathcal{H}$ and the image can be completed to a von Neumann algebra. The collection of all such von Neumann algebras then defines a *net* of algebras $\mathcal{N}$. We define the limiting theory to then be given by the tuple $(\mathcal{H}, \mathcal{N}, \Psi)$, where Ψ is the state of the infinite-dimensional tensor network that, given operators O^Λ that exist at layer Λ, is defined by

$$\Psi(O) := \langle \Psi^\Lambda | O^\Lambda | \Psi^\Lambda \rangle. \tag{8.9}$$

and by a limiting procedure for more general operators.[2] Performing this construction and an analysis of the local algebras for tensor networks that represent holographic quantum error-correcting codes is the main goal of this chapter. In particular, we demonstrate that for the HaPPY code, the von Neumann algebras associated to boundary subregions that satisfy complementary recovery are type II_∞ factors. We begin by providing a recap of von Neumann algebras and inductive limits in Sec. 8.2. In Sec. 8.3, we take the inductive limit of the HaPPY code and show that II_∞ factors emerge for subregions satisfying complementary recovery. Then in Sec. 8.4 we provide a summary of our construction in the general case and explain more generally how to determine the von Neumann algebra type. In Sec. 8.5, we discuss examples and generalizations of this construction, including other tensor networks such as the MERA and those based on Majorana dimers. We end with a general discussion in Sec. 8.6.

8.2 Background and preliminaries

We begin by laying the theoretical foundations for our analysis. This includes an overview of von Neumann algebras, tensor networks, and the basics of the theory of inductive limits.

---

[2]Note that this definition only makes sense if the operator pushing map is compatible with the isometry, so that the value is independent of the layer at which one evaluates the state. We comment further on this below.

A von Neumann algebra primer

In this section, we provide a brief introduction to the key concepts of von Neumann algebras necessary to understand the following sections.

General von Neumann Algebras

To define a von Neumann algebra, one needs to first introduce $C^\star$-algebras. A $C^\star$-algebra $\mathcal{A}$ is built on a vector space over the complex numbers together with a norm $\|.\|$, a multiplication, an addition, and an involution $\dagger : a \to a^\dagger$. The algebra has to be complete for the norm, i.e., every Cauchy sequence $a_n \in \mathcal{A}$ with respect to $\|.\|$ has a limit in $\mathcal{A}$. A sequence $(a_\mu)_1^\infty$ is called a Cauchy sequence if, for every δ, there exists an $M \in \mathbb{N}$ such that for all $\mu, \nu \geq M$, $\|a_\mu - a_\nu\| < \delta$. The involution is an antilinear map that additionally satisfies

$$a = (a^\dagger)^\dagger \, , \qquad\qquad (ab)^\dagger = b^\dagger a^\dagger \, . \qquad\qquad (8.10)$$

Elements of a $C^\star$-algebra satisfy the usual rules of addition and multiplication, but additionally the norm satisfies the condition

$$\|aa^\dagger\| = \|a\|^2. \qquad\qquad (8.11)$$

The simplest example is the set of bounded linear operators $\mathcal{B}(\mathcal{H})$ acting on a Hilbert space $\mathcal{H}$.[3] In the following, we fix a Hilbert space $\mathcal{H}$ and restrict our analysis to unital algebras, i.e., those that contain the identity $\mathbb{1}$. Defining a von Neumann algebra involves introducing the commutant of a subset $S \subset \mathcal{B}(\mathcal{H})$, which is defined as the set of bounded operators that commute with all of S, i.e.,

$$S' := \{a \in \mathcal{B}(\mathcal{H}) : [a, s] = 0 \,\forall s \in S\}. \qquad\qquad (8.12)$$

A von Neumann algebra is then defined as a subalgebra of $\mathcal{B}(\mathcal{H})$ that is closed under Hermitian conjugation and equal to its double commutant, i.e.,

$$\mathcal{A} = \mathcal{A}''. \qquad\qquad (8.13)$$

Now, given a self-adjoint subset $A \subset \mathcal{B}(\mathcal{H})$, the double commutant

$$\mathcal{A} := A'' \qquad\qquad (8.14)$$

is always a von Neumann algebra, and is called the von Neumann algebra *generated* by A. Von Neumann's double commutant theorem [436, 428] establishes that this

---

[3]In general, a $C^\star$- algebra can be defined without making an explicit reference to an underlying Hilbert space.

is equivalent to the algebra $\mathcal{A}$ being closed in the *weak operator topology* (WOT). This means that for a sequence $a_n \in \mathcal{A}$, there exists a bounded operator a with

$$\lim_{n \to \infty} \langle \xi | a_n | \psi \rangle = \langle \xi | a | \psi \rangle \tag{8.15}$$

for all states $|\xi\rangle$ and $|\psi\rangle$, then $a \in \mathcal{A}$. This implies that a von Neumann algebra is automatically a $C^\star$-algebra, where the norm refers to the usual operator norm. This is because if a sequence of operators converges in the operator norm, then it also converges in the weak operator topology. Finally, a von Neumann algebra is called a factor if

$$\mathcal{A} \cap \mathcal{A}' = \mathbb{C}\mathbb{1}. \tag{8.16}$$

A simple example of a factor can be found in a bipartite system whose Hilbert space $\mathcal{H}$ takes on the form

$$\mathcal{H} = \mathcal{H}_A \otimes \mathcal{H}_B. \tag{8.17}$$

Consider the algebra

$$\mathcal{A} = \mathcal{B}(\mathcal{H}_A) \otimes \mathbb{1}, \tag{8.18}$$

whose commutant reads

$$\mathcal{A}' = \mathbb{1} \otimes \mathcal{B}(\mathcal{H}_B), \tag{8.19}$$

and is therefore clearly a factor.

Layered tensor networks

The main object of study in this chapter are limits of tensor networks that can be constructed by an iteration across layers. Roughly speaking, given a Hilbert space $\mathcal{H}$ that has the form $\mathcal{H} = \bigotimes_{i=1}^{N} \mathcal{H}_i$, a tensor network is a representation of a state $|\Psi\rangle \in \mathcal{H}$ that has a graph Γ associated to it. The graph has a set of vertices V and edges E, where E is subdivided into a set of "bond" edges B that connect two vertices and "physical" edges P that are only attached to one vertex. We associate a Hilbert space $\mathcal{H}_{(e,v)}$ to each edge $e \in E$ adjacent to a vertex $v \in V$, i.e., for each bond edge we have two Hilbert spaces, one for each vertex it connects to. We assume that for any bond b that connects vertices v_1, v_2, the Hilbert spaces $\mathcal{H}_{(b,v_1)} \cong \mathcal{H}_{(b,v_2)}$ are isomorphic, so that their dimensions match. The physical Hilbert spaces $\mathcal{H}_i$ are attached to physical edges in P. To obtain a tensor network state $|\Psi\rangle$ one associates to each vertex v a state

$$|\psi\rangle_v \in \bigotimes_{\{(e,v)\}} \mathcal{H}_{(e,v)}, \tag{8.20}$$

where the product runs over all edges connected to v. Given a collection of such states for each vertex, one obtains the tensor network state by projecting the states on the two sides of each bond edge $b \in B$ onto the maximally entangled state, which contracts the tensors characterizing the state at the vertex v along the indices associated to the bond, i.e., for any $b \in B$ we define

$$|\chi\rangle_b = \sum_k \frac{1}{\sqrt{\dim(\mathcal{H}_b)}} |k\rangle_{v_1} \otimes |k\rangle_{v_2} \in \mathcal{H}_{(b,v_1)} \otimes \mathcal{H}_{(b,v_2)}, \qquad (8.21)$$

where $|k\rangle_{v_i}$ is an orthonormal basis for $\mathcal{H}_{(b,v_i)}$. Then the tensor network state $|\Psi\rangle$ is given by

$$|\Psi\rangle = \bigotimes_{b \in B} \langle\chi|_b \left(\bigotimes_v |\psi\rangle_v \right). \qquad (8.22)$$

In a graphical representation, each of the above states lives on the node of a graph, where the edges connecting two nodes represent the maximally entangled state contracted into the states of the respective vertex and the open edges represent the information associated to the "physical" Hilbert spaces $\mathcal{H}_i$. For more details see [83]. Using the isomorphism between linear maps $O : \mathcal{H} \rightarrow \mathcal{H}'$ between finite-dimensional Hilbert spaces and states $|O\rangle \in \mathcal{H}' \otimes \mathcal{H}^*$, where $\mathcal{H}^*$ is the dual space, we can also represent linear maps as tensor networks. Here we will be interested in layered tensor networks, where we consider a sequence of tensor network states

$$|\Psi^1\rangle \rightarrow |\Psi^2\rangle \rightarrow \ldots \qquad (8.23)$$

that are connected via isometries

$$|\Psi^{\Lambda+1}\rangle = \gamma^{\Lambda,\Lambda+1} |\Psi^\Lambda\rangle, \qquad (8.24)$$

where the isometries are themselves given by tensor networks. One can think of it as a graph that is built in an iterative procedure where in each iteration the open edges of the previous step are contracted with edges of another graph. Furthermore, we consider networks where to each isometry $\gamma^{\Lambda,\Lambda+1}$ one assigns a layer-to-layer operator pushing map $\phi^{\Lambda,\Lambda+1}$ (which is a unital $\star$-homomorphism) that associates to each operator living at layer Λ an operator that lives at layer $\Lambda + 1$ such that expectation values

$$\langle\Psi^{\Lambda+1}|\phi^{\Lambda,\Lambda+1}(O^\Lambda)|\Psi^{\Lambda+1}\rangle = \langle\Psi^\Lambda|O^\Lambda|\Psi^\Lambda\rangle \qquad (8.25)$$

are preserved and the identity is mapped to the identity.

Complementary recovery

As we will explain in Sec. 8.4, we focus on layered tensor networks which satisfy an inductive version of complementary recovery, which is a fundamental property of holographic quantum error-correcting codes [225] that gives us control over the entanglement pattern in the network. Complementary recovery can be defined as follows. Let V be an isometry $V : \mathcal{H}_{\text{bulk}} \rightarrow \mathcal{H}_{\text{bdy}}$, that maps from a "bulk" to a "boundary" Hilbert space in the language of holography or from a "logical" to a "physical" Hilbert space in the language of quantum error correction. Now consider a subalgebra $\mathcal{A}_a$ of $\mathcal{B}(\mathcal{H}_{\text{bulk}})$. If the boundary has a bipartition $\mathcal{H}_{\text{bdy}} = \mathcal{H}_A \otimes \mathcal{H}_{A^c}$, we say that $\mathcal{A}_a$ is *recoverable* from A if $\forall O \in \mathcal{A}_a$ there exists an operator $\iota(O_a) \in \mathcal{B}(\mathcal{H}_A) \otimes \mathbb{1}_{A^c}$ such that for all $|\psi\rangle \in \mathcal{H}_{\text{bulk}}$ one has

$$\iota(O_a)V |\psi\rangle = V O_a |\psi\rangle . \tag{8.26}$$

We assume furthermore that the map $\iota : \mathcal{A}_a \rightarrow \mathcal{B}(\mathcal{H}_A) \otimes \mathbb{1}$ is a faithful, unital $\star$-homomorphism. We call such a map ι a bulk-to-boundary operator pushing map. Note that we have assumed that $\mathcal{H}$ manifestly factorizes into A and its complement. A slightly more general perspective is to consider instead an abstract boundary subalgebra $\mathcal{A}_A$ such that $\iota(\mathcal{A}_a) \subset \mathcal{A}_A$ and eq. (8.26) hold. This way one removes oneself from the geometric picture and in case that $\mathcal{A}_A$ is a factor recovers the geometric decomposition after a suitable isomorphism. Now we say that the code V satisfies *complementary recovery* for $\mathcal{A}_a$ in the boundary region A if $\mathcal{A}_a$ is recoverable from A and its commutant $\mathcal{A}'_a$ is recoverable from A^c. A bulk region a anchored in a boundary region A that satisfies complementary recovery is called an *entanglement wedge*. Note that the above does not assume that $\mathcal{A}_a$ is a factor but in the following we will usually restrict to factors, i.e., that $\mathcal{H} = \mathcal{H}_a \otimes \mathcal{H}_{a^c}$ and $\mathcal{A}_a = \mathcal{B}(\mathcal{H}_a) \otimes \mathbb{1}$. Now Harlow proved [225] that if V is a code with complementary recovery for $\mathcal{A}_a$ and one considers a product state $|ij\rangle$, where $|i\rangle \in \mathcal{H}_a, |j\rangle \in \mathcal{H}_{a^c}$, that there exist a pair of local unitaries U_A, U_{A^c} in A, A^c such that

$$V |ij\rangle = U_A U_{A^c} \big(|ij\rangle \otimes |\chi\rangle \big), \tag{8.27}$$

where the state $|\chi\rangle$, independent of $|ij\rangle$, determines the entanglement between A and A^c. We will refer to this statement in the following as *Harlow's theorem*. Note that we have here presented an algebraic view on operator reconstruction. This does not have to fit into a geometric picture where $\mathcal{A}_a$ is a "set of bulk qubits" and $\mathcal{A}_{a^c}$ is the complementary set of bulk qubits as in the HaPPY code. The mathematical reason is that, if one considers $\mathcal{A}_a$ to be the operators that act on a "set of bulk

qubits" it automatically is a factor. We see that if $\mathcal{A}_a$ is not a factor, such a geometric picture has to break down. An explicit example of such a situation is given in [418] where the entanglement wedges of boundary regions do not have a simple geometric picture. On the other hand, if $\mathcal{A}_a$ is a factor, one can always find a unitary U such that

$$\mathcal{H} = U(\mathcal{H}_a \otimes \mathcal{H}_{a^c}), \ \mathcal{A}_a = U\big(\mathcal{B}(\mathcal{H}_a) \otimes \mathbb{1}\big)U^\dagger, \tag{8.28}$$

so that with respect to the decomposition induced by U, the reconstruction is "geometric."

Inductive limits

Inductive limits provide a mathematical framework for constructing infinite-dimensional structures from sequences of finite-dimensional ones, which we employ to construct the limiting system of a tensor network as the inductive limit of $C^\star$-algebras and Hilbert spaces induced by the tensor network. For $C^\star$-algebras, this involves a directed system $(\mathcal{A}_n, \phi_{mn})$, where $\mathcal{A}_n$ are $C^\star$-algebras and

$$\phi_{mn}: \quad \mathcal{A}_n \to \mathcal{A}_m \tag{8.29}$$

are $\star$-homomorphism for $n \leq m$, satisfying compatibility conditions [63] defined below. The inductive limit algebra $\mathcal{A}$ is then a $C^\star$-algebra that encodes the structure of the entire sequence. Similarly, for Hilbert spaces, an inductive system consists of a sequence of Hilbert spaces $\{\mathcal{H}_n\}$ and isometric embeddings $\{\iota_{nm}\}$ [63]. In the following, we present an overview of inductive limits. We begin by describing the limits of general vector spaces, which will directly translate to the limiting Hilbert spaces generated by tensor networks, and then proceed to describe limits of algebras, laying the groundwork for our later discussion of von Neumann algebras.

Inductive Limits of Vector spaces

Here we provide an introduction to inductive limits [63, 268, 311, 89] in the category of Banach spaces, i.e., normed, complete vector spaces. $C^\star$-algebras and Hilbert spaces carry the structure of a Banach space so it serves as an example for inductive limits that illustrates the procedure. To obtain limits in the category of $C^\star$-algebras and Hilbert spaces, one has to define an additional structure such as a multiplication and adjoint for $C^\star$-algebras and an inner product for Hilbert spaces, which modify the exact construction. Since the main steps, up to the additional structure, are conceptually the same, we describe the procedure for Banach spaces here.

Assume that we have a sequence of normed vector spaces $\mathcal{V}_i$, indexed by some set Ω, such as the Hilbert spaces $\mathcal{H}_i$ in which a layered tensor network lives at each level, and linear maps $\phi^{ij} : \mathcal{V}_j \to \mathcal{V}_i$ that are contractive, i.e.,

$$\|v\|_{\mathcal{V}_i} \geq \|\phi^{ij}(v)\|_{\mathcal{V}_j}, \tag{8.30}$$

and are compatible between the indices in the sense that

$$\phi^{ij} = \phi^{kj} \circ \phi^{ik}, \forall i \leq k \leq j. \tag{8.31}$$

One can then identify vectors between the layers via their image under the maps ϕ^{ij}, i.e., we identify two vectors $v_i \in \mathcal{V}_i, v_j \in \mathcal{V}_j$, where we assumed $j \geq i$, if v_j is the image of v_i under the embeddings ϕ^{ij}:

$$v_i \sim v_j \Leftrightarrow \phi^{ij}(v_i) = v_j. \tag{8.32}$$

We denote the equivalence class of v_i as $[v_i]$. A family of examples is the actual tensor networks we consider in this chapter: The state they represent at layer i is identified with the state at layer $j \geq i$. We denote the set of such equivalence classes of vectors by V. Given V, we can define sums of its elements directly via representatives, i.e., if $j \geq i$ then we define

$$[v_i] + [v_j] := [\phi^{ij}(v_i) + v_j]. \tag{8.33}$$

and multiplication via scalars

$$\alpha[v] := [\alpha v], \ \forall \alpha \in \mathbb{C}. \tag{8.34}$$

This definition does not depend on the choice of representative and promotes the set of equivalence classes to a vector space. Because the maps ϕ^{ij} are contractive, we can define the norm of $[v_i]$ via

$$\|[v_i]\| = \lim_{j \to \infty} \|\phi^{ij}(v_i)\|. \tag{8.35}$$

This extends $(V, +, \|.\|)$ to a normed vector space. Now taking the completion with respect to this norm defines a Banach space $\mathcal{V}$. $\mathcal{V}$ is what we call the inductive limit of the inductive set $(\mathcal{V}_i, \phi^{ij})$ and we write it as

$$\mathcal{V} = \varinjlim V_i. \tag{8.36}$$

Inductive Limits of Hilbert spaces and Algebras in Layered Tensor Networks

The above discussion defines the inductive limit of Banach spaces. This already allows us to associate a limiting object with both the tensor network and the local algebras, i.e., given the isometry $\gamma^{\Lambda,\Lambda+1}$ that embeds the network at layer Λ into the network at layer $\Lambda + 1$, we define equivalence classes for states via the identification

$$\gamma^{\Lambda,\Lambda+1} |\Psi^\Lambda\rangle \sim |\Psi^\Lambda\rangle. \tag{8.37}$$

The set of equivalence classes again defines an inductive limit $\mathcal{V}$. However, we have not equipped $\mathcal{V}$ with the structure of a Hilbert space, namely a scalar product. We now explain how to do so. We first define an inner product between equivalence classes: For two equivalence classes $[\Psi^\Lambda], [\Psi^{\Lambda'}], \Lambda \leq \Lambda'$ we define the inner product as

$$\langle[\Psi^\Lambda]|[\Phi^{\Lambda'}]\rangle = \langle\gamma^{\Lambda,\Lambda'}(\Psi^\Lambda)|\Phi^{\Lambda'}\rangle, \tag{8.38}$$

where we defined the multi-layer isometry

$$\gamma^{\Lambda,\Lambda'} = \gamma^{\Lambda'-1,\Lambda'} \circ \gamma^{\Lambda'-2,\Lambda'-1} \circ \ldots \circ \gamma^{\Lambda+1,\Lambda+2} \circ \gamma^{\Lambda,\Lambda+1}. \tag{8.39}$$

This inner product is defined on a dense set of vectors in $\mathcal{V}$ and since the embeddings $\gamma^{\Lambda,\Lambda'}$ are isometries, the norm defined by the inner product coincides with the norm of the representatives. Therefore, one can extend the scalar product to all vectors in $\mathcal{V}$, which extends $\mathcal{V}$ (upon completion) to a Hilbert space $\mathcal{H}$. Having constructed the limiting Hilbert space, we want to identify operators, or more generally, operator algebras that arise from algebras at finite layers and survive the limiting procedure. Having the operator pushing map $\phi^{\Lambda,\Lambda+1}$ associated to the layered network at hand, we define equivalence classes of operators in which we identify an operator O that lives at layer Λ with its image under the pushing map

$$\phi^{\Lambda,\Lambda+1}(O) \sim O. \tag{8.40}$$

This step is why we demanded in the introduction that the operator pushing map be unital, so that the identity of a given layer will be identified with the identity of the next. Later on in Sec. 8.4 we will need the unitality of ϕ also to have a good decomposition of the Hilbert space between layers that preserves the structure of the previous layers. Similarly, we can consider a local subalgebra $\mathcal{A}_A^\Lambda = \mathcal{B}(\mathcal{H}_A^\Lambda) \otimes \mathbb{1}_{A^C}$ of $\mathcal{H}^\Lambda$ at layer Λ that corresponds to the bounded operators of a subset A of the open legs of the network at layer Λ. We can similarly identify it with its image in the next layer

$$\mathcal{A}_A^\Lambda \sim \phi^{\Lambda,\Lambda+1}(\mathcal{A}_A^\Lambda). \tag{8.41}$$

When mapping between layers, the local algebra $\mathcal{A}_A^\Lambda$ will be mapped to a subalgebra of the lightcone of A, where the lightcone $J^+(A)$ is defined as the set of qubits on which $\phi^{\Lambda,\Lambda+1}(A)$ is supported. Note that we define the lightcone through the map ϕ, which defines it in the sense of the connectivity of the underlying network rather that in a sense of time evolution. We therefore obtain a sequence of algebras $\mathcal{A}_A^\Lambda, \mathcal{A}_{J^+(A)}^{\Lambda+1}, \ldots$ that together with the operator pushing map between layers $\phi^{\Lambda,\Lambda+1}$ again form an inductive system. For this inductive system we also take the inductive limit and obtain a lightcone $C^\star$-algebra $\hat{\mathcal{A}}_A$, i.e.,

$$\hat{\mathcal{A}}_A = \varinjlim \mathcal{A}_{J^+(A)}^\Lambda. \tag{8.42}$$

This will be an abstract $C^\star$-algebra because the embedding ϕ is implemented by an isometry. We represent this algebra on the Hilbert space we just constructed by defining it on a dense set of states for each operator O^Λ that is representable at a finite layer Λ using

$$\pi([O^\Lambda])\,|[\Psi^{\Lambda'}]\rangle := \begin{cases} |[\phi^{\Lambda,\Lambda'}(O^\Lambda)\Psi^{\Lambda'}]\rangle & \text{if } \Lambda \leq \Lambda', \\ |[O^\Lambda \gamma^{\Lambda',\Lambda}(\Psi^{\Lambda'})]\rangle & \text{if } \Lambda' \leq \Lambda, \end{cases} \tag{8.43}$$

and extending the representation to all of $\hat{\mathcal{A}}_A$ by continuity. Note that for this definition to be well defined, the operator pushing map $\phi^{\Lambda,\Lambda+1}$ has to be compatible with the Hilbert space isometry $\gamma^{\Lambda,\Lambda+1}$ in the sense that if one considers an operator O^Λ at layer Λ that is also the image of an operator $O^\Lambda = \phi^{\Lambda',\Lambda}(O^{\Lambda'})$ at a lower layer Λ' and the same holds for the state, then both cases of eq. (8.43) have to coincide, i.e.,

$$O^\Lambda \gamma^{\Lambda',\Lambda}\,|\Psi^{\Lambda'}\rangle = \phi^{\Lambda',\Lambda}(O^{\Lambda'})\gamma^{\Lambda',\Lambda}\,|\Psi^{\Lambda'}\rangle \overset{!}{=} \gamma^{\Lambda',\Lambda}\,|O^{\Lambda'}\Psi^{\Lambda'}\rangle. \tag{8.44}$$

Here we have for convenience let the layer associated to the operator $O^{\Lambda'}$ be the same as for the state $\Psi^{\Lambda'}$. This requirement can be straightforwardly generalized when these differ, the main point being that operator pushing and the isometry between Hilbert spaces have to be compatible. We then define the von Neumann algebra

$$\mathcal{A}_A := \pi(\hat{\mathcal{A}}_A)''. \tag{8.45}$$

Our main objective in this chapter is to determine the type of the von Neumann algebra $\mathcal{A}_A$ for layered tensor networks. A recap of the type classification suitable for our needs is provided in Appendix 8.7. Next we will provide the main intuition behind our study on the example of the HaPPY code.
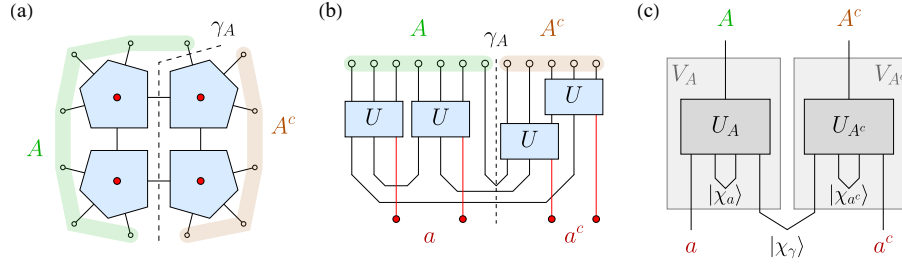
Figure 8.2: Turning a holographic tensor network into an encoding circuit. (a) We take a small HaPPY code with four contracted perfect tensors and consider a boundary bipartition into A and A^c. From each region, two logical qubits (red dots) can be recovered, forming the "bulk regions" a and a^c, separated by a cut γ_A through the tensor network. (b) Using the property that the six-leg perfect tensor acts as a unitary U from any three legs to the remaining three, we can reorganize the tensor network into a circuit from the logical qubits in a and a^c to the physical qubits in A and A^c. In this circuit, some of the tensor contractions become insertions of maximally entangled pairs into the circuit. Three of such pairs cross between A and A^c, leading to an entanglement entropy $S_A = \log 3 + S_a$. (c) The generic holographic encoding circuit in terms of two unitaries U_A and U_{A^c} (or equivalently, isometries V_A and V_{A^c}), with resource states $|\chi_a\rangle$ and $|\chi_{a^c}\rangle$ contributing only to entanglement within each subregion and $|\chi_\gamma\rangle$ contributing to the entanglement between A and A^c. For HaPPY codes, these resource states are copies of maximally entangled pairs.

8.3 Intuition from the HaPPY code

HaPPY codes at a fixed layer

In this section we provide intuition behind the direct limit construction of the previous section using holographic tensor network codes. We use the code structure of the network to identify operators between layers, allowing us to rigorously treat the inductive limit of the algebras. In particular, we demonstrate that the network can be written as a unitary map by opening contracted legs in the network, which enables us to find a decomposition of boundary subregion algebras by considering their analogous bulk decomposition. We focus on the family of HaPPY codes [372], built from perfect tensors with an even number of legs, one of which is associated with an encoded logical qubit. Such tensors mediate maximal entanglement between any bipartition into two sets of legs, thereby forming an isometry from the smaller set to the larger. In particular, any bipartition into equally many legs yields a unitary map. For the case of six-leg tensors (one bulk leg and five "planar" legs) and qubits associated with each leg (i.e., bond dimension $\chi = 2$), such a perfect tensor is given by the encoding isometry of the five-qubit *Laflamme code* [288], which can correct one single-qubit error. As we show in Fig. 8.2, one can use the perfect
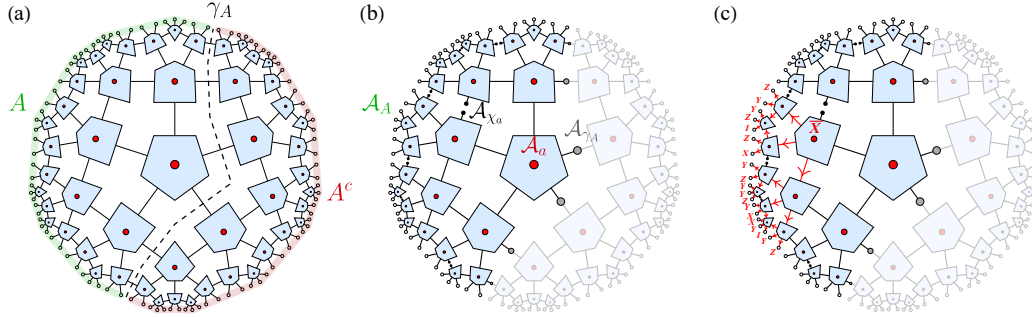
Figure 8.3: Subregion algebra reconstruction in the HaPPY model. (a) A boundary bipartition into A and A^c of the full $\{5, 4\}$ HaPPY code. The Ryu-Takayanagi cut γ_A separates the bulk into two wedges a and a^c, logical qubits (red dots) in which are reconstructable (only) on A and A^c (white dots), respectively. (b) Mapping the full boundary subregion algebra $\mathcal{A}_A$ back into the bulk: Removing a^c and bonds corresponding to (one choice of) ancillas $|\chi_a\rangle$ turns the remaining tensors into a unitary circuit (following Fig. 8.2). $\mathcal{A}_A$ is unitarily mapped to the bulk algebra $\mathcal{A}_a$ (red), the wedge ancilla algebra $\mathcal{A}_{\chi_a}$ (black), and the Ryu-Takayanagi algebra $\mathcal{A}_{\gamma_A}$ (gray). (c) With the ancilla bonds removed, operator-pushing a logical operator (here $\bar{X}$ acting on one bulk qubit) follows a unique flow towards the boundary, resulting in a unique boundary representation of the logical operator.

tensor property to decompose any bipartition (A, A^c) of the open boundary legs of the full HaPPY code into a unitary circuit that prepares the physical boundary state starting from the logical bulk state and some maximally entangled ancillary states.[4] While some of the ancillae contribute to the entanglement between A and A^c, others act only within one of the two regions. The latter type is necessary for the tensor network code to provide meaningful quantum error correction under bipartition: otherwise, the encoding unitary U_A for a subregion A (see Fig. 8.2(c) following [225]) would merely mix n logical qubits and m additional qubits that are maximally entangled with A^c into $n + m$ physical qubits. This would imply that each operator O_a acting on the logical qubits in a has only one representation on A, making it highly susceptible to errors. Introducing additional ancillae $|\chi_a\rangle$ and $|\chi_{a^c}\rangle$ into the circuit allows one to apply "gauge" operators on them, leading to different physical representations of O_a. We have two natural ways to encode a bulk operator O_{bulk} in the boundary. The first is to conjugate it with the isometries for each bulk *entanglement wedge* a and a^c: $V_A = U_A |\chi_a\rangle$, $V_{A^c} = U_{A^c} |\chi_{a^c}\rangle$, where

---

[4]As noted in Ref. [372], such a clear decomposition can fail for a small subset of boundary regions for which the bulk bipartition is not exactly complementary. Here we do not consider these cases.

U_A, U_{A^c} are the opened-up networks, so that

$$O_{\text{bdy}} = V_A V_{A^c} \, |\chi_\gamma\rangle \, O_{\text{bulk}} \, \langle\chi_\gamma| \, V_A^\dagger V_{A^c}^\dagger \,, \tag{8.46}$$

which can be checked to have the correct action on code states $V |ij\rangle$, where $V = V_A V_{A^c} |\chi_\gamma\rangle$, essentially because of the isometric property $V^\dagger V = \mathbb{1}$. However, these representations O_{bdy} act as projectors onto the codespace. Rather than including the physical identity acting on A, they only include a *logical* identity that acts as an identity on states within the codespace. For our purposes, a more suitable operator map is the natural *operator pushing map* defined by the perfect tensors, whose stabilizers allow one to replace operators acting on a subset of $k \leq 2$ physical qubits by equivalently-acting operators on the other $5 - k$ qubits [372]. In the notation where we have opened up some of the internal legs of the tensor network to extend the isometry V_A into a unitary U_A, this takes the form

$$O_{\text{bdy}} = \iota(O) := U_A U_{A^c} \, O \, U_A^\dagger U_{A^c}^\dagger \,, \tag{8.47}$$

which is the bulk-to-boundary map of Fig. 8.2(c), where one encodes an operator $O = O_{\text{bulk}} \otimes \mathbb{1}_\gamma \otimes \mathbb{1}_{\chi_a} \otimes \mathbb{1}_{\chi_{a^c}}$ (here, χ refers to ancilla degrees of freedom while γ refers to degrees of freedom on the RT surface). For a bulk operator $O_{\text{bulk}} = O_a \otimes \mathbb{1}_{a^c}$ that only has support in the entanglement wedge a of A, this further simplifies into a boundary operator O_A that only has support on A:

$$O_A = \text{tr}_{A^c} \, O_{\text{bdy}} = U_A O_a U_A^\dagger \,. \tag{8.48}$$

We thus find that the operator map $\iota(O)$ also satisfies complementary recovery. Note that our construction of U_A and U_{A^c} is non-unique [199], as one may open different pairs of contracted legs to construct such unitaries from the isometries V_A and V_{A^c}. These different choices of unitaries lead to different bulk-to-boundary maps ι, related to different logical representations that we discuss further below.

In the language of quantum error correction, O_A is a logical operator $\overline{O_{\text{bulk}}}$ that acts on a subset of the qubits of a physical state. As $\dim \mathcal{H}_a < \dim \mathcal{H}_A$, the boundary algebra generated by encoding with (8.47) every element of the wedge algebra $\mathcal{A}_a$ (operators acting on the logical qubits in a) is only a subalgebra of the full algebra $\mathcal{A}_A$ of all boundary operators. What are the other subalgebras? We find the answer by conjugating the unitary U_A, which acts on the Hilbert spaces

$$U_A^\dagger : \mathcal{H}_A \rightarrow \mathcal{H}_a \otimes \mathcal{H}_{\chi_a} \otimes \mathcal{H}_{\gamma_A} \,, \tag{8.49}$$

whose algebras are visualized in Fig. 8.3(b). Operators acting on the last piece of the tensor product form the *Ryu-Takayanagi algebra* $\mathcal{A}_{\gamma_A}$. For the standard HaPPY code where $|\chi_\gamma\rangle$ is a set of EPR pairs, these operators act equivalently on $\mathcal{H}_{\gamma_A}$ and $\mathcal{H}_{\gamma_{A^c}}$. The second piece of the tensor product is acted upon by the so-called *wedge ancilla algebra* $\mathcal{A}_{\chi_a}$. The geometric setting for this mapping of algebras in the HaPPY code is shown in Fig. 8.3. By conjugating operators belonging to these algebras by U_A, U_{A^c} we again obtain their respective boundary representations. Note that the above discussion gives a concrete realization of the bulk-to-boundary operator pushing map, usually denoted by ι, which maps logical bulk operators to a boundary operator by explicit conjugation by an unitary (8.53). Repeating the same discussion for the complementary region, we find that

$$\mathcal{H} \cong \mathcal{H}_a \otimes \mathcal{H}_{\chi_a} \otimes \mathcal{H}_{\gamma_A} \otimes \mathcal{H}_{a^c} \otimes \mathcal{H}_{\chi_{a^c}} \otimes \mathcal{H}_{\gamma_{A^c}} , \tag{8.50}$$

for the full boundary Hilbert space $\mathcal{H}$.

Ancilla algebras and stabilizers

In our construction of the operator pushing map ι, we have extended the isometric map furnished by the HaPPY tensor network into a unitary. We now briefly comment on the nonuniqueness of such an extension and its relationship to quantum error correction. In a quantum code, we map logical states to a subspace of the physical space, called *codespace*, allowing different physical operators to have equal action on states in the codespace. We call such different but logically equivalent operators *representations* of a logical operator. In a *stabilizer code* [208], we can switch between different representations of logical operators by applying stabilizer operators, the +1 eigenspace of which forms the codespace. The HaPPY code on a hyperbolic pentagon tiling is an example of a qubit stabilizer code. By opening some legs of the tensor network to extend the isometries V_A and V_{A^c} into unitaries U_A and U_{A^c}, we have effectively fixed all logical operators to a unique representation, or equivalently, fixed the operator-pushing flow from bulk to boundary (see Fig. 8.3(c)). Suppose that there are three ways to extend this construction to produce different representations:

1. Act on the fixed representation with stabilizer operators, which act as identities on codestates.

2. Open different legs of the tensor network that lead to different unitaries U_A and U_{A^c}.

3. Set a different operator-pushing flow to map bulk to boundary operators.

We now show that approach 2 and 3 are equivalent and form a special case of approach 1, in which we take a particular choice of U_A and U_{A^c} (and correspondingly opened legs), which projected onto ancilla states within each bulk region form the isometries $V_A = U_A |\chi_a\rangle$ and $V_{A^c} = U_{A^c} |\chi_{a^c}\rangle$. Any bulk state $|\psi\rangle$ in $\mathcal{H}_a \otimes \mathcal{H}_{a^c}$ is then mapped to the logical state

$$|\bar{\psi}\rangle \equiv V_A V_{A^c} |\psi\rangle |\chi_\gamma\rangle \ . \tag{8.51}$$

We now try to find an operator $O = O_a O_{\chi_a} O_{\chi_{\gamma_A}}$ (omitting identities on a^c and χ_{a^c}) that is mapped to a logical operator $\overline{O}$ with support only on A that acts as a stabilizer $\overline{\mathbb{1}}$, i.e., leaves any $|\bar{\psi}\rangle$ invariant. We find

$$
\begin{aligned}
\bar{O} |\bar{\psi}\rangle &= U_A O_a O_{\chi_a} O_{\chi_{\gamma_A}} U_A^\dagger V_A V_{A^c} |\psi\rangle |\chi_\gamma\rangle \\
&= U_A V_{A^c} (O_a |\psi\rangle)(O_{\chi_a} |\chi_a\rangle)(O_{\chi_{\gamma_A}} |\chi_\gamma\rangle) \ .
\end{aligned}
\tag{8.52}
$$

For this expression to reduce to $|\bar{\psi}\rangle$, we require three conditions

$$O_a \otimes \mathbb{1}_{a^c} |\psi\rangle = |\psi\rangle \ , \tag{8.53a}$$

$$O_{\chi_a} |\chi_a\rangle = |\chi_a\rangle \ , \tag{8.53b}$$

$$O_{\chi_{\gamma_A}} \otimes \mathbb{1}_{\gamma_{A^c}} |\chi_\gamma\rangle = |\chi_\gamma\rangle \ , \tag{8.53c}$$

where we have restored identity operators. To fulfill the first condition for a general $|\psi\rangle$, we require $O_a = \mathbb{1}_a$. For the HaPPY code, where $|\chi_a\rangle$ and $|\chi_\gamma\rangle$ are sets of EPR pairs, solutions of the second and third condition are given by $O_{\chi_{\gamma_A}} = \mathbb{1}_{\gamma_A}$ and such operators O_{χ_a} that act equivalently on both ends of each EPR pair, e.g., Paulis $X \otimes X$ for a 2-qubit EPR pair. The stabilizers with support on A are thus found by considering all such operators O_{χ_a} and unitarily mapping them to the boundary using ι. Now consider approach 2, which fixes the input operator $O = O_a \mathbb{1}_{\chi_a} \mathbb{1}_{\chi_{\gamma_A}}$ and instead changes which legs to open up to define ι, i.e., changing the sites on which $\mathcal{A}_{\chi_a}$ acts. In the operator-pushing picture, opening up the legs fixes the local stabilizer on each tensor that can be used to push an operator from one layer to the next. Changing which leg is opened up is equivalent to changing which local stabilizer to push with, which shows the equivalence between approach 2 and 3. What is the operator that maps from a boundary representation of a logical operator that is pushed along one leg rather than another? We find that this is exactly an operator that fulfills (8.53c), acting on both of the newly opened legs with a pair

of conjugate operators. An example for the Pauli stabilizers of the Laflamme code used in the HaPPY model: Here valid stabilizers are cyclic permutations of either $XZZXI$, $YXXYI$, or $ZYYZI$ (the products of elements of any one set yield the other two). If we consider the first qubit as an input (part of $\mathcal{H}_a$) and "open" the tensor leg corresponding to the last qubit (part of $\mathcal{H}_{\chi_a}$), we can operator-push an input X by applying $XZZXI$, thus mapping $XIIII \mapsto IZZXI$. More specifically, consider three pentagon tensors that jointly form a unitary map ι from three incoming physical legs, three logical legs, and a pair of legs formed by opening up a contraction. For the central pentagon, operator-pushing X can then be visualized as

$$\qquad (8.54)$$

where we used the stabilizer $XZZXI$ on the central pentagon and $IZYYZ$ on the right-most pentagon. However, we could have also turned this contraction of three pentagon tensors into a unitary map by instead opening up the contraction between the central and the right-most pentagon. In that case, operator-pushing X would take the form

$$\qquad (8.55)$$
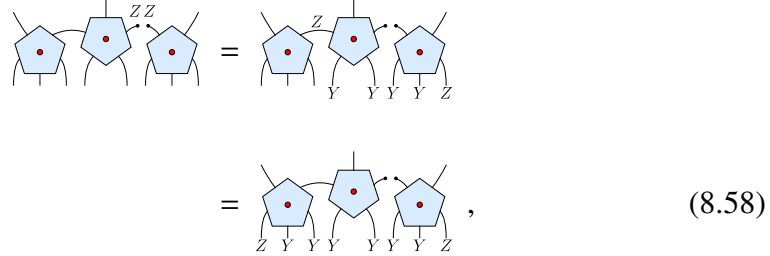
On the "boundary" (the legs on the bottom), these two representations differ by

$$(IIIXZYYZ)(ZYYZXIII) = ZYYYYYYZ\,, \qquad (8.56)$$

which acts as a stabilizer on the full code. We can see that applying this stabilizer corresponds to changing the operator-pushing flow of X from the right to the left (and vice-versa). We can also generate this stabilizer term for a fixed operator pushing map ι (and associated opened legs) by pushing the operator corresponding to the product of the two stabilizers applied to the central qubit in both situations,

$$(XZZXI)(XIXZZ) = IZYYZ\,, \qquad (8.57)$$

which is another stabilizer of the five-qubit code. It acts trivially on the first qubit, thus not performing any logical operation on $\mathcal{H}_a$. This is equivalent to operator-pushing a pair of Z operators applied on the newly-opened legs:
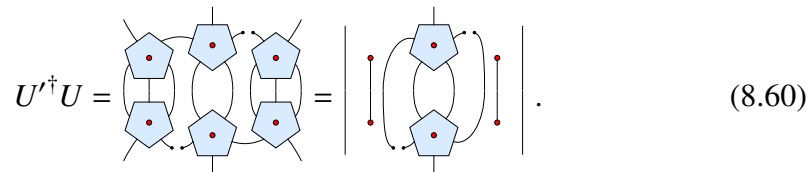
$$= \qquad , \qquad (8.58)$$

which yields the stabilizer (8.56). Note that this pair of Zs would cancel each other out if we contracted both legs (turning the unitary map into an isometry), which confirms that (8.56) acts as a logical identity under the encoding isometry of the full code. We can explicitly construct the map between the two operator pushing maps ι and ι' (given by the tensor networks in (8.54) and (8.55), respectively) from the tensor network construction. Consider a logical operator O in one configuration and O' in the other, which are assumed to map to the same boundary operator $\iota(O) = \iota'(O')$. As each operator pushing map is associated with a unitary transformation U and U', we find

$$O' = U'^{\dagger} U\, O\, U^{\dagger} U' \,, \qquad (8.59)$$

resulting in a transformation by another unitary $U'^{\dagger}U$ defining a unitary *superoperator* $\mathcal{S}(\bullet) = U'^{\dagger}U \bullet U^{\dagger}U'$ acting on bulk operators, mapping between the logical representations corresponding to different operator-pushing flows. The unitary map can again be expressed as a tensor network:

$$U'^{\dagger}U = \qquad = \qquad . \qquad (8.60)$$

Here the lower row of tensors form the adjoint $U'^{\dagger}$, which is simply a mirrored version of the original tensors of the Laflamme code (which has a real-valued tensor representation). In the last step we used the perfect tensor property to reduce two tensor pairs into products of identities (in general, the non-reducible part will consist of tensors stretching between the two choices of ancilla openings). Using operator pushing with this extended map shows how ancilla-free operators in one

configuration of opened legs get mapped to operators with nontrivial ancilla support in the other, e.g.,

$$\tag{8.61}$$

which reproduces the ZZ ancilla insertion we showed in (8.58).

Let us summarize the relationship between the three approaches discussed above. The second and third approach both amount to setting a unique operator-pushing flow that associates a unique boundary operator to a bulk operator $O_a O_{\chi_a} O_{\chi_{\gamma_A}}$ acting on a subregion a. Crucially, the resulting operator-pushing map ι is always unital, i.e.,

$$\iota(\mathbb{1}_a \mathbb{1}_{\chi_a} \mathbb{1}_{\chi_{\gamma_A}}) = \mathbb{1}_A \ . \tag{8.62}$$

Similarly, in the stabilizer code picture we consider boundary operators logically equivalent if they differ only by a product with an operator $\iota(\mathbb{1}_a O_{\chi_a} \mathbb{1}_{\chi_{\gamma_A}})$ where $O_{\chi_a} |\chi_a\rangle = |\chi_a\rangle$. However, changing the operator-pushing flow does not simply correspond to taking the product of every logical operator with a fixed stabilizer, which would not preserve $\mathbb{1}_A$. Instead, as we have seen above, the new operator pushing flow is equivalent to applying specific stabilizers on specific logical operators, which can be implemented as a tensor network map such as (8.60). Incidentally, the role of the RT algebra $\mathcal{A}_{\gamma_A}$ can be understood in a similar vein as the ancilla algebra $\mathcal{A}_{\chi_a}$: By pushing a pair of conjugate operators, such as two copies of a Pauli operator, from the RT surface γ_A to both A and A^c, we obtain the stabilizers that map between logical representations in either region. The existence of such exact stabilizers is an algebraic way of identifying EPR-like entanglement between A and A^c.

Throughout the rest of this chapter, we consider a fixed configuration of opened bulk legs in the tensor network, leading to a unique operator map ι. This simplifies the construction of the inductive limit, where we consider the image of all operators acting on the subregion, i.e., $\mathcal{H}_a \otimes \mathcal{H}_{\chi_a} \otimes \mathcal{H}_{\gamma_A}$. The algebra of operators acting on $\mathcal{H}_{\chi_a}$ then includes both the stabilizers and their conjugate error operators, i.e., those that anti-commute with at least one stabilizer. While this includes operators O_{χ_a} that do not preserve the codespace, the choice of including or excluding such operators will not affect the algebra type in our setting of finitely-entangled bulk

states. This is because we may think of the Hilbert space $\mathcal{H}_{\chi_A}$ simply as additional bulk qubits in our entanglement wedge a that encode degrees of freedom beyond the codespace.
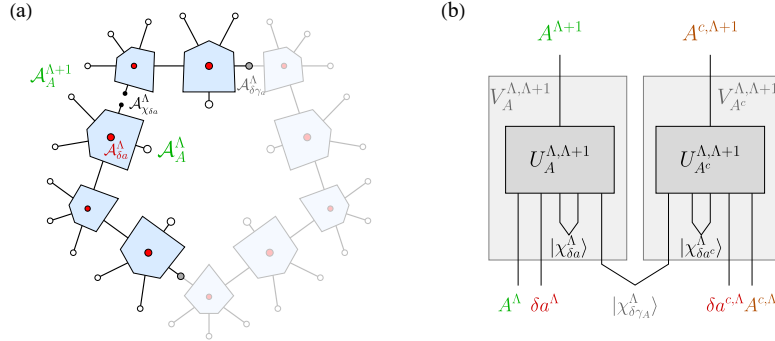
Figure 8.4: Subregion algebra mapping with one layer of the HaPPY model. (a) A single vertex inflation layer of the "opened-up" HaPPY code of Fig. 8.3, acting as a unitary map from the subregion algebra $\mathcal{A}_A^\Lambda$ at layer Λ and the algebras of the degrees of freedom of the new layer, the bulk algebra $\mathcal{A}_{\delta a}^\Lambda$ (red), wedge ancilla algebra $\mathcal{A}_{\chi_{\delta a}}^\Lambda$ (black), and Ryu-Takayanagi algebra $\mathcal{A}_{\delta\gamma_A}^\Lambda$ (gray) to the subregion algebra $\mathcal{A}_A^{\Lambda+1}$ on the next layer. (b) The generic form of a layer of the HaPPY code with ancillas, written as a circuit diagram with the two unitary subregion maps $U_A^{\Lambda,\Lambda+1}$ (highlighted in (a)) and $U_{A^c}^{\Lambda,\Lambda+1}$.

Mapping algebras layer by layer

In Sec. 8.3 we studied the HaPPY code at a fixed number of layers Λ. We found that after splitting the boundary into subsystems A, A^c, we can further divide it into three subsystems associated to the entanglement wedge algebra A_a, the RT algebra A_{γ_A} and the wedge ancilla algebra A_{χ_a}. This division is implemented by an unitary $U_A^\dagger$. Now we can grow the HaPPY code that consists of Λ layers by contracting it with another layer of the tensor network. Here we will repeat the procedure and push operators of layer Λ through to layer $\Lambda + 1$. We will from now on indicate the layer at which a given object lives by the superscript Λ. We will also refer to the process of mapping operators at layer Λ to layer $\Lambda + 1$ as operator pushing, but one should be aware that this layer-to-layer pushing, indicated by the map $\phi^{\Lambda,\Lambda+1}$, is different from the bulk-to-boundary pushing ι as it maps the whole boundary of a given layer to the next, not just the bulk operator to the boundary. We can represent the tensor network of the outermost layer again as an unitary map

$$U_A^{\Lambda,\Lambda+1} : \mathcal{H}_A^\Lambda \otimes \mathcal{H}_{\delta a}^{\Lambda+1} \otimes \mathcal{H}_{\chi_{\delta a}}^{\Lambda+1} \otimes \mathcal{H}_{\delta\gamma_A}^{\Lambda+1} \to \mathcal{H}_A^{\Lambda+1} \tag{8.63}$$

that takes the boundary $\mathcal{H}_A^\Lambda$ at layer Λ, the logical information of the next layer $\mathcal{H}_{\delta a}^{\Lambda+1}$ and further auxiliary and RT degrees of freedom $\mathcal{H}_{\chi\delta a}^{\Lambda+1} \otimes \mathcal{H}_{\delta\gamma_A}^{\Lambda+1}$ and embeds them into the next layer. This induces the isometric map $\gamma^{\Lambda,\Lambda+1}$ we discussed in the context of inductive systems. Following the discussion of the previous section, we could also consider $\gamma^{\Lambda,\Lambda+1}$ to be made from the isometry $V^{\Lambda,\Lambda+1} = U_A^{\Lambda,\Lambda+1} |\chi_{\delta a}\rangle$ as again arising from the contraction of some auxiliary entangled pairs into the unitary but keeping the unitary picture is convenient for the following discussion as it provides an direct decomposition of the boundary algebra of A at any layer. We will comment on this more in Sec. 8.4. We remind the reader that the boundary subregion A is chosen such that its successive mappings under operator pushing have a support that satisfies complementary recovery. Because of this, we will not distinguish between A, the subregion of the boundary we considered at layer Λ and its lightcone $J^+(A)$ at later layers and collectively denote the subregion as A, where the respective lightcone is implicit by the layer-label Λ. Since we rephrased the growing of the network as a unitary embedding of the old network with additional degrees of freedom corresponding to the added layer, it is clear that we have an embedding of algebras

$$U_A^{\Lambda,\Lambda+1} \mathcal{A}_A^\Lambda U_A^{\Lambda,\Lambda+1\dagger} \subset \mathcal{A}_A^{\Lambda+1}. \tag{8.64}$$

Now we have to decide how the state grows. We will suppress the layer index Λ for degrees of freedom that are added by the new layer. For the bulk, we choose that the bulk qubits are, at each layer, put in reference states where there is no entanglement between the bulk entanglement wedges a and a^c, so that at each layer the "new" bulk qubits come in product states $|i_{\delta a}\rangle$, $|j_{\delta a^c}\rangle$. We note that this is an arbitrary choice we made and one could also consider states with bulk entanglement. Then one would have to be more careful about the structure of the entanglement to compute the type. In addition, the network representing the bulk-to-boundary isometry at layer $\Lambda + 1$ is obtained by projecting additional Bell pairs $|\chi_{\delta a}\rangle |\chi_{\delta a^c}\rangle$ onto the open legs of $U_A^{\Lambda,\Lambda+1} U_{A^c}^{\Lambda,\Lambda+1}$ that were opened up to generate the unitaries, as well as additional Bell pairs $|\chi_{\delta\gamma_A}\rangle$ into the legs that extend the RT surface from layer Λ by a new bond. Therefore, the state on $\mathcal{H}^{\Lambda+1}$ is

$$|\psi\rangle_{\Lambda+1} = U_A^{\Lambda,\Lambda+1} U_{A^c}^{\Lambda,\Lambda+1} |\psi\rangle_\Lambda |i_{\delta a}\rangle |j_{\delta a^c}\rangle |\chi_{\delta a}\rangle |\chi_{\delta a^c}\rangle |\chi_{\delta\gamma_A}\rangle \tag{8.65}$$

and defines the same state on the image of $\mathcal{B}(\mathcal{H}^\Lambda)$ as the state of the previous layer, i.e., for

$$O^{\Lambda+1} = U_A^{\Lambda,\Lambda+1} O^\Lambda U_A^{\Lambda,\Lambda+1\dagger}, O^\Lambda \in \mathcal{B}(\mathcal{H}_A^\Lambda) \tag{8.66}$$

we have

$$\langle\psi|_{\Lambda+1}\, O^{\Lambda+1}\, |\psi\rangle_{\Lambda+1} = \langle\psi|_{\Lambda}\, O^{\Lambda}\, |\psi\rangle_{\Lambda}\,. \qquad (8.67)$$

This only works because $U_A^{\Lambda,\Lambda+1}$ is a unitary. Note that, because of this preservation of the state of the previous layer, as well as having a unitary embedding, the algebra of the previous layer is preserved into the next, i.e.,

$$\mathcal{A}_A^{\Lambda+1} \cong \mathcal{A}_A^{\Lambda} \otimes \delta\mathcal{A}_A^{\Lambda+1}, \qquad (8.68)$$

so the algebra of the new layer decomposes into the algebra of the previous layer together with addititional degrees of freedom $\delta\mathcal{A}_A^{\Lambda+1}$. In summary, we obtain a sequence of algebras $\{\mathcal{A}_A^{\Lambda}\}_{\Lambda\in\mathbb{N}}$ and a sequence of states on each algebra $\{|\psi\rangle_{\Lambda}\}_{\Lambda\in\mathbb{N}}$, where we have an embedding $\phi^{\Lambda,\Lambda+1}(\mathcal{A}_A^{\Lambda}) \subset \mathcal{A}_A^{\Lambda+1}$ implemented by the unitary transformation (8.66). We see that, due to the unitary nature of the embedding, we can at each layer decompose $\mathcal{A}_A^{\Lambda}$ into the tensor product

$$\mathcal{A}_A^{\Lambda} \sim \mathcal{A}_a^{\Lambda} \otimes \mathcal{A}_{\chi_a}^{\Lambda} \otimes \mathcal{A}_{\gamma_A}^{\Lambda} \otimes \mathbb{1}_{A^c} \qquad (8.69)$$

with its commutant

$$\mathcal{A}_{A^c}^{\Lambda} \sim \mathbb{1}_A \otimes \mathcal{A}_{\gamma_{A^c}}^{\Lambda} \otimes \mathcal{A}_{a^c}^{\Lambda} \otimes \mathcal{A}_{\chi_{a^c}}^{\Lambda} \qquad (8.70)$$

on which the tensor network state takes the form

$$|\Psi^{\Lambda}\rangle \sim |i\rangle_a \otimes |\chi_a\rangle \otimes |\chi_\gamma\rangle \otimes |j\rangle \otimes |\chi_{a^c}\rangle\,, \qquad (8.71)$$

where $i(j)$ is the bulk logical state in $a(a^c)$, $\chi_{a(a^c)}$ is the state of the internal auxiliary degrees of freedom in the entanglement wedge $a(a^c)$ and χ_γ is the maximal entangled state that comes from the contraction of the two sides of the tensor network along the RT surface γ. This decomposition is preserved between layers via Eq. (8.68). We note that all the entanglement entropy of the two boundary sides A, A^c comes from χ, if the bulk state $|ij\rangle_{aa^c}$ is pure. Because we rewrote the construction of the network through opening the legs associated to χ_a, χ_{a^c}, this split of the boundary state is obvious.

Limit algebras

We can now take the inductive limit of the procedure defined above. It is clear that, as we grow the network, due to the unitary nature of the embedding, the boundary state always decomposes as in 8.71 at every layer and one has essentially the same setup as in the Araki-Woods-Powers factors described in Appendix 8.7 just with tensor products between the different kinds of spin chains and that the decomposition

is manifestly true only after the application of local unitaries U_A, U_{A^c}. Note that one has unentangled logical and auxiliary degrees of freedom $|ij\rangle, |\chi_a\rangle, |\chi_{a^c}\rangle$ corresponding to the type I case and a maximally entangled state for the algebra $\mathcal{A}_\gamma$ as in the type II_1 case. We therefore expect that, as we increase the number of layers to infinity, given a pure bulk-input state $|ij\rangle$, the algebra $\mathcal{A}_A$ in the direct limit Hilbert space becomes type II_∞, because it reduces to the algebra of the form $B(\mathcal{H}) \otimes \text{II}_1$ for $\mathcal{H}$ encoding the Hilbert space built out of auxiliary and wedge degrees of freedom in a and the II_1 factor acting on the RT surface γ.

Let us now make this statement precise. We can first consider the inductive-limit algebra $\mathcal{A}_{\gamma_A}$. Let $A^\Lambda, B^\Lambda \in \mathcal{A}^\Lambda_{\gamma_A}$. The state χ_A is maximally mixed on $\mathcal{A}^\Lambda_{\gamma_A}$, so that

$$\langle \chi_A | [A^\Lambda, B^\Lambda] | \chi_A \rangle = 0. \tag{8.72}$$

Since

$$\hat{\mathcal{A}}_{\gamma_A} = \varinjlim \mathcal{A}^\Lambda_{\gamma_A}, \tag{8.73}$$

we deduce by continuity that $|[\chi^\Lambda_{\gamma_A}]\rangle$ induces a tracial state on $\hat{\mathcal{A}}_{\gamma_A}$. Now $|[\Psi^\Lambda_{\gamma_A}]\rangle$, which restricts to $|[\chi^\Lambda_{\gamma_A}]\rangle$ on $\hat{\mathcal{A}}_{\gamma_A}$, is a state on the inductive-limit Hilbert space, so it is normal on $\mathcal{A}_{\gamma_A} = \pi(\hat{A}_{\gamma_A})''$. Moreover, it is tracial on a weak-operator dense subalgebra of $\mathcal{A}_{\gamma_A}$, so it extends by continuity for the weak operator topology to a tracial normal state on $\mathcal{A}_{\gamma_A}$. From this we deduce:

Theorem 8.3.1. *The inductive-limit RT von Neumann algebra $\mathcal{A}_{\gamma_A}$ has type II_1.*

By an exactly similar reasoning, since the states $|[\chi_a]\rangle$ and $|[i]\rangle$ are pure on $\mathcal{A}_{\chi_a}$ and $\mathcal{A}_a$, we deduce

Theorem 8.3.2. *The inductive-limit ancilla and bulk von Neumann algebras $\mathcal{A}_{\chi_a}$ and $\mathcal{A}_a$ have type I.*

We can then deduce the type of full boundary algebra from the following observation (see for example [308]): the algebra $\hat{\mathcal{A}}_A$ can be decomposed as

$$\hat{\mathcal{A}}_A = \hat{\mathcal{A}}_{a,\chi_a} \otimes \hat{\mathcal{A}}_{\gamma_A}, \tag{8.74}$$

where the tensor product of C^*-algebras is unambiguously defined because all considered algebras are nuclear. We then have

$$\mathcal{A}_A = \mathcal{A}_{a,\chi_a} \overline{\otimes} \mathcal{A}_{\gamma_A}. \tag{8.75}$$

Since the first tensor factor has type I and the second tensor factor has type II_1, we deduce

Theorem 8.3.3. *The boundary subregion algebra $\mathcal{A}_A$ has type II$_\infty$.*

A useful way of seeing this result in view of the next section is that we have decomposed $\mathcal{A}_A$ (using unitary equivalence) into an infinite tensor product of finite-dimensional factors, where the tensor network state is pure on some of them (corresponding to bulk inputs and ancillas), whereas it is maximally entangled on others (the RT degrees of freedom). The Araki–Woods classification of infinite tensor products then tells us that the algebra $\mathcal{A}_A$ has type II$_\infty$. Note that the above results will also hold if the bulk state $|ij\rangle$ carries an $O(1)$ amount of entanglement, where the counting parameter is the number of layers Λ. If the bulk state carries a divergent amount of entanglement, it will be able to change the type of the resulting bulk algebra, depending on its entanglement structure. We note that the geometrical entanglement of the RT surface will always lead to a type II factor $\mathcal{A}_\gamma$ associated to the RT surface due to maximal entanglement in the state that glues the two wedges a and a^c.

In the next section we will explain how our discussion extends to a more general class of tensor networks with a layered structure that satisfy complementary recovery.

8.4 An abstract perspective

In the previous discussion, we focused on the HaPPY code that we could open up to write the operator pushing from bulk to boundary and between layers as an explicit conjugation by a unitary. In this section, we identify the mathematical barebones of our construction. In the first section, we explain, following [164, 199, 168, 192] that the structure of a holographic code with complementary recovery can be formalized as a code subspace-preserving conditional expectation. We then show that this conditional expectation structure can be leveraged to define a general notion of inductive system of codes, for which results akin to the ones derived in the previous section hold.

Codes and conditional expectations

Holographic tensor networks truncated at a finite layer number form holographic codes with complementary recovery. Throughout this section, we will denote the bulk "code" Hilbert space by $\mathcal{H}$. Specifying the local algebra and Hilbert space associated with a bulk subregion a (at a finite cutoff) will be done by the labels $\mathcal{H}_a$ and $\mathcal{A}_a$. We will label boundary "physical" Hilbert spaces with $\mathcal{K}$ and we will label the boundary algebra with $\mathcal{A}_\mathcal{K}$. Choosing a boundary subregion A, we will label

the local Hilbert space and algebra with $\mathcal{K}_A$ and $\mathcal{A}_A$. No subscripts will denote the full boundary or bulk objects.

The bulk-to-boundary isometry of a code will be labeled $V : \mathcal{H} \to \mathcal{K}$. Given a subregion A on the boundary, there exists a region a in the bulk, the entanglement wedge of A such that $\mathcal{A}_a, \mathcal{A}'_a$ are recoverable in $\mathcal{A}_A$ and $\mathcal{A}'_A$, respectively. This supplies us with operator pushing maps ι_a, ι'_a, which are faithful unital $\star$-homomorphisms $\iota_a : \mathcal{A}_a \to \mathcal{A}_A$, $\iota'_a : \mathcal{A}'_a \to \mathcal{A}'_A$. Defining $\alpha : \mathcal{A} \to \mathcal{O}$ by $\alpha(x) = V^\dagger x V$, the map $\iota_a \circ \alpha : \mathcal{A}_A \to \iota_a \mathcal{A}_a$ is a conditional expectation from $\mathcal{A}_A$ onto the image of ι_a, i.e. a linear map with $E(\mathbb{1}) = \mathbb{1}$ and

$$E(abc) = aE(b)c, \forall a, c \in \mathcal{N}, b \in \mathcal{M}. \tag{8.76}$$

Other work on the connection of error-correcting codes with conditional expectations appeared in [164, 168, 182, 192]. Similarly, the map $\iota'_a \circ \alpha$ is a conditional expectation onto $\iota'_a \mathcal{A}'_a$. Furthermore, we assume that all algebras involved are factors. The existence of a conditional expectation guarantees that $\mathcal{A}_A \cong \iota_a(\mathcal{A}_a) \otimes \iota_a(\mathcal{A}_a)^c$ [424], where we use $\cong$ to denote unitary equivalence and where the second term denotes the relative commutant in $\mathcal{A}_A$,

$$\iota_a(\mathcal{A}_a)^c := \iota(\mathcal{A}_a)' \cap \mathcal{A}_A. \tag{8.77}$$

The first term in $\mathcal{A}_A$ is the set of those operators acting on the Hilbert space of logical states, and the second term is the operators acting on $\mathcal{H}_A$ which do not affect the logical degrees of freedom. Since, in the case of finite layers, all the above algebras are Type I factors, the existence of a conditional expectation guarantess, see Sec. 9.15 in [424], that

$$\mathcal{K}_A \cong \mathcal{H}_a \otimes \mathcal{K}_c, \tag{8.78}$$

where $\mathcal{K}_c$ denotes the space on which the relative commutant acts, i.e., $\iota_a(\mathcal{A}_a)^c = \mathcal{B}(\mathcal{K}_c)$. These unitary equivalences can be seen as an algebraic version of Harlow's theorem 8.27 that appears if the operator pushing map is unital. In the language of the previous section, this isomorphism is implemented by the conjugation of operators in $\mathcal{A}_A$ with U_A. As before, we now assume that a particular isomorphism has been chosen at every layer. We can write down the subsystem decomposition for the full physical space

$$\mathcal{K} \cong \mathcal{H}_a \otimes \mathcal{H}_{\bar{a}} \otimes \mathcal{K}_c \otimes \mathcal{K}_{\bar{c}} \tag{8.79}$$

$$\mathcal{A} \cong \mathcal{A}_a \otimes \mathcal{A}_{\bar{a}} \otimes \mathcal{A}_c \otimes \mathcal{A}_{\bar{c}} \tag{8.80}$$

The conditional expectations $\iota_a \circ \alpha$, $\iota'_a \circ \alpha$ project $\mathcal{A}_A$ onto $\mathcal{A}_a$ and $\mathcal{A}'_A$ onto $\mathcal{A}'_a$, respectively. States in the code subspace are invariant under these conditional expectations, i.e., they can be written as $|\psi\rangle_{code} \otimes |\chi\rangle$, where $|\psi\rangle_{code} \in \mathcal{K}_a \otimes \mathcal{K}_{\bar{a}}$ and $|\chi\rangle$ is one, fixed reference state on $\mathcal{K}_c \otimes \mathcal{K}_{\bar{c}}$. The analog of $|\chi\rangle$ in the case of the HaPPY code at one fixed layer truncation is the tensor product of the RT state and the ancilla state.

We will now show how to study the growth of such a system once suitable inductive maps are defined.

Inductive systems of codes

We now explain how to take the inductive limit of a family of exact holographic codes. The data we want are:

1. A sequence of logical Hilbert spaces $\mathcal{H}_\Lambda$, which should be seen as the Hilbert spaces of bulk logical legs for a network truncated at layer Λ.

2. A sequence of physical Hilbert spaces $\mathcal{K}_\Lambda$, which should be seen as the Hilbert spaces of boundary legs for a network truncated at layer Λ.

3. Bulk-to-boundary isometries V_Λ for each truncation at layer Λ. They are the usual holographic maps defined by holographic tensor networks.

4. Bulk-to-bulk isometries $\gamma_{\mathcal{H}}^{\Lambda, \Lambda+1}$. They correspond to enlarging the bulk Hilbert spaces with more bulk qubits put in a (usually disentangled) reference state.

5. Boundary-to-boundary isometries $\gamma_{\mathcal{K}}^{\Lambda, \Lambda+1}$. They correspond to enlarging the boundary Hilbert spaces by acting with one layer of the tensor network, the bulk qubits being each put in the same reference state as the one chosen for the bulk-to-bulk maps.

6. A sequence of logical algebras $\mathcal{A}_a^\Lambda$, $\mathcal{A}_a'^\Lambda$ which should be seen as the operators acting on of bulk logical legs on either side of the RT surface for a network truncated at layer Λ.

7. A sequence of physical algebras $\mathcal{A}_A^\Lambda$, $\mathcal{A}_A'^\Lambda$, which should be seen as the operators acting on the boundary on either side of the RT surface for a network truncated at layer Λ.

8. Bulk-to-boundary $\star$-homomorphisms ι_Λ for each truncation at layer Λ. They are the usual operator pushing maps defined by holographic tensor networks.

9. Bulk-to-bulk $\star$-homomorphisms $\phi_{\mathcal{H}}^{\Lambda,\Lambda+1}$ and $\phi_{\mathcal{H}}'^{\Lambda,\Lambda+1}$ for each truncation at layer Λ. They correspond to tensoring bulk operators with identities on the next layer on either side of the RT surface.

10. Boundary-to-boundary $\star$-homomorphisms $\phi_{\mathcal{K}}^{\Lambda,\Lambda+1}$ and $\phi_{\mathcal{K}}'^{\Lambda,\Lambda+1}$ for each truncation at layer Λ. They correspond to pushing boundary operators at layer Λ through one layer of the tensor network on either side of the RT surface, the bulk qubits being each put in the same reference state as the one chosen for the bulk-to-bulk maps.

We also require compatibility of the operator reconstruction maps with the bulk-to-boundary isometries, and of the layer-to-layer isometries and operator pushing maps between each other, i.e., for $O \in \mathcal{A}_{\mathcal{H}}^{\Lambda}, O' \in \mathcal{A}_{\mathcal{H}}'^{\Lambda}$,

$$V_{\Lambda} O = \iota_{\Lambda}(O) V_{\Lambda}, \quad V_{\Lambda} O' = \iota'_{\Lambda}(O') V_{\Lambda}, \tag{8.81}$$

and for $O \in \mathcal{A}_{\mathcal{H},\mathcal{K}}^{\Lambda}, O' \in \mathcal{A}_{\mathcal{H},\mathcal{K}}'^{\Lambda}$,[5]

$$\gamma_{\mathcal{H},\mathcal{K}}^{\Lambda,\Lambda+1} O = \phi_{\mathcal{H},\mathcal{K}}^{\Lambda,\Lambda+1}(O) V_{\Lambda}, \quad \gamma_{\mathcal{H},\mathcal{K}}^{\Lambda,\Lambda+1} O' = \phi_{\mathcal{H},\mathcal{K}}'^{\Lambda,\Lambda+1}(O') V_{\Lambda}. \tag{8.82}$$

The above structure is summarized by the commutative diagram in Figure 8.5. All these operator equations are also assumed to hold on commutant algebras. First, Equation (8.81) implies that

$$V^{\Lambda} |\varphi\rangle \cong |\varphi\rangle \otimes |\Psi^{\Lambda}\rangle, \tag{8.83}$$

where Ψ_{Λ} is a reference state which is identified in the case of the HaPPY code with the RT and auxiliary Bell pair degrees of freedom at layer Λ. Second, Equation (8.82) implies that the layer-to-layer maps *also* implement error-correcting codes with complementary recovery, both at the level of the bulk and at the level of the boundary. We therefore deduce from the inherited conditional expectation structure that in the bulk,

$$\mathcal{H}^{\Lambda+1} \cong \mathcal{H}^{\Lambda} \otimes \delta\mathcal{H}^{\Lambda}, \tag{8.84}$$

and

$$\gamma_{\mathcal{H}}^{\Lambda,\Lambda+1} |\psi\rangle \cong |\psi\rangle \otimes |\Omega^{\Lambda}\rangle \in \mathcal{H}^{\Lambda+1}, \tag{8.85}$$

with $|\Omega^{\Lambda}\rangle$ fixed. Similarly on the boundary,

$$\mathcal{K}^{\Lambda+1} \cong \mathcal{K}^{\Lambda} \otimes \delta\mathcal{K}^{\Lambda},$$
$$\gamma_{\mathcal{K}}^{\Lambda,\Lambda+1} |\psi\rangle \cong |\psi\rangle \otimes |\Theta^{\Lambda}\rangle \in \mathcal{K}^{\Lambda+1}. \tag{8.86}$$

---

[5]Strictly speaking, this last equation is not required to have a well-defined inductive limit code, but it allows to keep track of the RT and auxiliary Bell pair degrees of freedom added at each step.

This choice fits the structure of the HaPPY code, where $|\Theta^\Lambda\rangle$ corresponds to the extra bulk qubits and $|\Theta^\Lambda\rangle$ corresponds to the extra RT- and auxiliary Bell pairs. We can say more about this structure by recognizing that because of the compatibility of operator pushing between layers and bulk-to boundary operator pushing combined with the compatibility of operator pushing with the layer-to-layer Hilbert space isometries (8.81),(8.44) we also have a conditional expectation that decomposes

$$\delta\mathcal{K}^\Lambda \cong \delta\mathcal{H}^\Lambda \otimes \delta\bar{\mathcal{K}}^\Lambda \tag{8.87}$$

such that

$$|\Theta^\Lambda\rangle \cong |\Omega^\Lambda\rangle \otimes |\Psi^\Lambda\rangle, \tag{8.88}$$

where $|\Psi\rangle$ are all "new" degrees of freedom that come from growing the code, such as the extra RT-pairs and auxiliary degrees of freedom in the HaPPY code.

Limit algebras

With this structure, we define the inductive sequence of bulk and boundary Hilbert spaces $\{\mathcal{H}^\Lambda, \gamma_\mathcal{H}^{\Lambda,\Lambda+1}\}$, $\{\mathcal{K}^\Lambda, \gamma_\mathcal{K}^{\Lambda,\Lambda+1}\}$, and algebras $\{\mathcal{A}_a^\Lambda, \phi_\mathcal{H}^{\Lambda,\Lambda+1}\}, \{\mathcal{A}_A^\Lambda, \phi_\mathcal{K}^{\Lambda,\Lambda+1}\}, \{\mathcal{A}_a'^\Lambda, \phi_\mathcal{H}'^{\Lambda,\Lambda+1}\}, \{\mathcal{A}_A'^\Lambda, \phi_\mathcal{K}'^{\Lambda,\Lambda+1}\}$. The choice of how to grow the inductive system is fully contained in the choice of $|\Omega^\Lambda\rangle, |\Theta^\Lambda\rangle$. For example, if we consider the HaPPY code and choose the $|\Omega^\Lambda\rangle$ to be just the $|0\rangle$ state on the additional bulk legs, one can think of the inductive limit of the bulk as the Hilbert space of bulk states which are asymptotically in the $|0\rangle$ state. To construct the inductive limit bulk and boundary Hilbert spaces and algebras from the Λ-layer Hilbert spaces, we now take the direct limit accordingly:

$$\mathcal{H} \equiv \varinjlim \mathcal{H}^\Lambda, \qquad \mathcal{K} \equiv \varinjlim \mathcal{K}^\Lambda, \tag{8.89}$$

and similarly for the algebras of observables. The above compatibility relations ensure that these algebras of observables have a valid representation on the inductive limit Hilbert space, so that one can take their bicommutant and construct an inductive limit von Neumann algebra. Moreover, the bulk-to-boundary maps ι_Λ and ι_Λ' also extend to the inductive limit, and can be extended by continuity to unital normal $\star$-homomorphisms, so that the conditional expectation structure is preserved in the limit. If the states $|\Theta^\Lambda\rangle$ and $|\Omega\rangle^\Lambda$ have a similar structure to the HaPPY code, we can compute the types of the various algebras appearing in this section in a similar way, by essentially reducing the calculation of the type to an Araki–Woods-like situation, where the $|\Omega^\Lambda\rangle$ and $|\Theta^\Lambda\rangle$ lead to a decomposition into an infinite tensor product of finite density matrices. In the case of the HaPPY code, we found that the $|\Omega^\Lambda\rangle$

were pure, while the $|\Theta^\Lambda\rangle$ had a maximally entangled part, which led to the type II_∞ structure. In more general cases, the entanglement properties of the $|\Omega^\Lambda\rangle$ and $|\Theta^\Lambda\rangle$ similarly lead to the type of the algebra through the Araki–Woods classification.
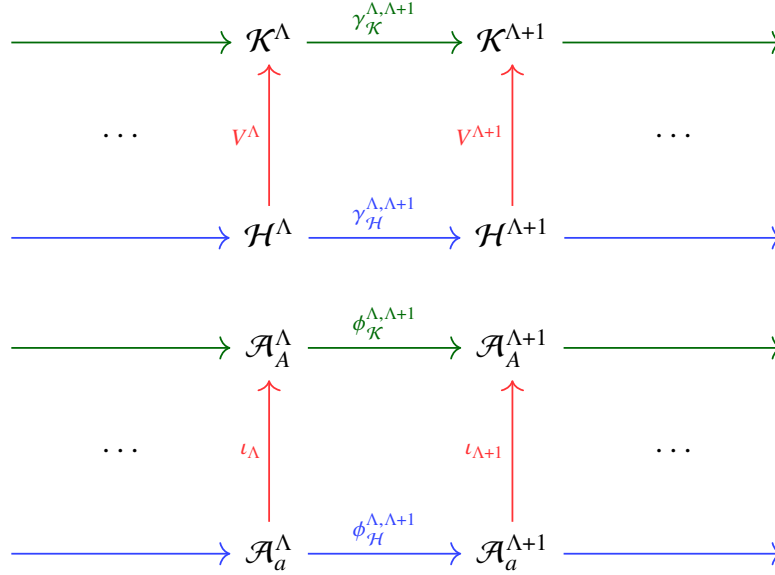
Figure 8.5: Commutative diagram summarizing the structure required for an inductive limit of codes. The sequence of logical Hilbert spaces and their isometries is shown on the top diagram, while the sequence of algebras and their operator pushing maps is shown on the bottom diagram. We ask that the arrows of the same color on the commutative diagram satisfy the compatibility conditions (8.81) (for the red ones), and (8.82) (for the blue and green ones). A similar diagram to the bottom one must also hold for commutant algebras and maps.

8.5 Examples

HaPPY code from Majorana dimers

Here we describe a specific instance of the HaPPY code in terms of Majorana dimers as described in [256]. Although it does not add any new conclusions to the type of boundary algebras in the HaPPY code, we develop techniques that can be applied to analyze the algebras of other networks that are not based on perfect tensors but arise from the contraction of dimer states. Additionally, this provides us with a graphical understanding of the codespace and local algebras on the boundary of the HaPPY code. In short, Majorana dimer states are states in qubit systems that have a graphical representation in terms of graphs, where each edge corresponds to a single qubit and has two nodes on it, which represent Majorana operators. Each node is connected to a different node by a *dimer*, which indicates that a fermionic annihilation operator build of the Majorana operators associated to the two nodes

annihilates the state. As we demonstrate below, one can associate a single qubit to such a pair of nodes connected by a dimer. A review of Majorana dimers is given in Appendix 8.8. We use the following encoded representation of logical states as dimer states

$$|\bar{0}\rangle_5 \quad = \qquad\qquad\qquad\qquad (8.90)$$

$$|\bar{1}\rangle_5 \quad = \qquad\qquad\qquad\qquad (8.91)$$

In the following, we will describe how one can interpret the previous considerations explicitly in the dimer picture of the HaPPY code by giving a graphical interpretation of the unitaries U_A, U_{A^c} of Harlow's theorem (8.27).

Disentangling the bulk

As a first step in the explicit construction of U_A of equation (8.49), we need to identify how the bulk logical information is encoded in the boundary state. For this we note that each dimer originates originally from some bulk qubit. For each bulk qubit of a, we will have some dimers coming from the local tensor that pierce the RT surface and some dimers that stay in the subregion, thus they begin and end in A. We want to associate some particular dimer that stays in A with the information carried by this bulk qubit. To do so, we note the following.

Theorem 8.5.1. *In the HaPPY code represented by Majorana dimers on a $\{5, 4\}$ tiling of the hyperbolic plane, there exists a collection of dimers beginning and ending in A of which the parities are different between any two basis states of the codespace, that differ only in bulk qubits in the entanglement wedge of our subregion, independent of the state in the complementary wedge.*

This theorem is proven in Appendix 8.8. Note that we do not mean that given just the parities of the logical dimers, the bulk logical state can be trivially read of, i.e.,

we do not mean that if a particular bulk is in state $|1\rangle$ that the associated logical dimer will have its parity inverted compared to the state $|0\rangle$ but that the collection of parities of logical dimers is in one-to-one correspondence with the logical state. This theorem states that there is a collection of dimers that stand in one-to-one correspondence with the logical state of the entanglement wedge, independent of what the state is in the complementary wedge, an example of a collection of such logical dimers is shown in Fig. 8.6 (a).
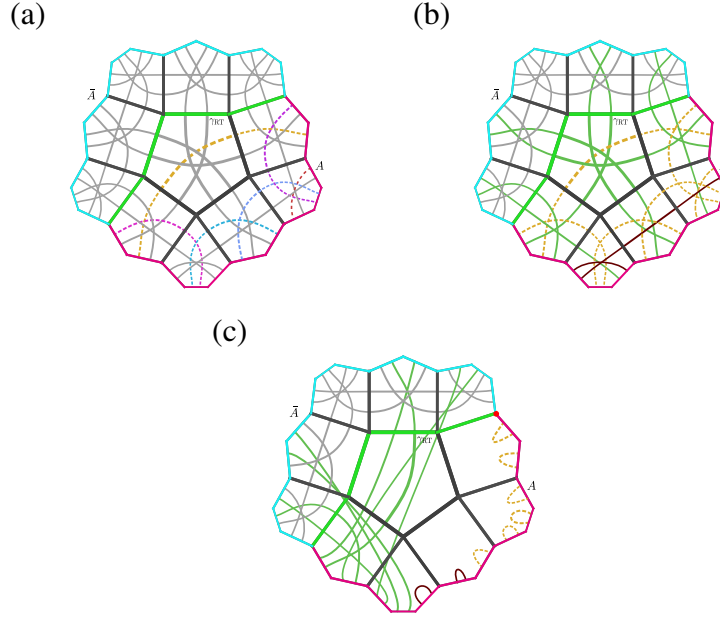
Figure 8.6: (a) Two boundary regions A, A^c with their respective entanglement wedges and RT surface γ_{RT} and dimers carrying logical information drawn with colored dashed lines. Note that there is one dimer for each bulk qubit. (b) HaPPY code with different dimers in region A colored. Green are dimers belonging to D_γ, red are dimers that belong to D_a^A and and dashed yellow are the logical dimers in D_l^A. The parity of the dimers was neglected in this figure. (c) Dimers in A after disentangling logical and auxiliary dimers by applying local swap operations.

Following Theorem 8.5.1 we have a set of dimers which we can associate with information in the entanglement wedge. What we want to do now is to construct a unitary C_i^A that distills this information from the codespace state $|i\bar{j}\rangle$, where i is the logical state in a and j the logical state in a^c. To achieve this, we use the following corollary.

Lemma 8.5.2. *Given the above setup, there exists a local unitary $\tilde{U}_A \otimes \mathbb{1} : \mathcal{H}_A \otimes \mathcal{H}_{A^c} \to \mathcal{H}_A \otimes \mathcal{H}_{A^c}$ such that for any bulk input $|j\rangle \in \mathcal{H}_{a^c}$:*

$$\tilde{U}_A |i\bar{j}\rangle = |i\rangle |\chi_a\rangle |\chi_{\gamma,j}\rangle, \tag{8.92}$$

where i is the logical state written out in a set of qubits that are associated to the logical dimers in theorem 8.5.1, χ_j is a j- dependent state that carries the entanglement that comes from the dimers associated to the RT surface and the complementary and $|\chi_a\rangle$ is an arbitrary fixed state of an additional set of qubits that come from dimers that do not belong to either the logical or RT dimers. Furthermore, there exists a local unitary in A^c that satisfies Eq. (8.92) if one swaps i with j and a with a^c on the r.h.s. Their combined action satisfies Harlow's theorem (8.27)

$$\tilde{U}_{A^c}\tilde{U}_A |\bar{i}\bar{j}\rangle = |i\rangle |j\rangle |\chi_a\rangle |c_{a^c}\rangle |\chi_\gamma\rangle, \tag{8.93}$$

where now $|j\rangle$ is associated to logical dimers of the complementary region, $|\chi_{a^c}\rangle$ comes from auxilliary dimers in the complementary region and $|\chi_\gamma\rangle$ is a maximally entangled state made up from all the dimers that cross the RT surface and connected region A with A^c.

Sketch of Proof. The full proof can be found in 8.8. We give a sketch of it since it conveys the conceptual action of the unitaries U_A. One begins by grouping all dimers ending in region A into groups D_l^A of logical dimers, dimers D_γ that cross the RT surface and the remaining dimers D_a, as illustrated in Fig. 8.6(b). Then, independently of the bulk input, one can perform swap operations S_A that are local unitaries in A and move the logical and auxiliary dimers so that after the swaps, each dimer will start and end at the same edge, as illustrated in Fig. 8.6 (c). As shown in [256], whenever a dimer starts and ends at the first edge after the pivot, the state factorizes as illustrated in Fig. 8.7, where the parity of the dimer that factorizes can be directly translated into whether ψ is in the state $|0\rangle$ or $|1\rangle$.

Figure 8.7: Illustration that a dimer state in which an edge is connected to itself next to the pivot can be factorized into a qubit system and the remaining dimer state.

By aligning all the logical and auxiliary information on the edges directly following the pivot, one ends up with a state that has the form

$$S_A |\bar{i}\bar{j}\rangle = |\psi_i\rangle_a |\chi_{i,a}\rangle_{\chi_a} |\chi_j\rangle_\gamma, \tag{8.94}$$

where $\psi_i, \chi_{i,a}$ are states in qubit Hilbert spaces that depend only on the bulk state in α and $|\chi_j\rangle_\gamma$ is the part of the state associated to the dimers in the complementary

entanglement wedge and the RT dimers. Now we can apply state dependent unitaries $\mathcal{X}_i^A$ made out of X-operators acting on the factorized qubits[6] via

$$\mathcal{X}_i^A \ket{\psi_i}_a \ket{\chi_{i,a}}_{\chi_a} = \ket{i} \ket{\chi_a}, \tag{8.95}$$

i.e., they extract the original bulk state i in a and safe it in the qubits associated to logical dimers and set the qubits associated to auxiliary dimers into a fixed reference χ_a. This state dependent unitaries can be combined into a fixed unitary $\tilde{U}_A$ that applies the correct transformation depending on the bulk input. A similar transformation can be applied in the complementary region, which can be made local by first shifting the pivot as described in the appendix to the leftmost edge of the complementary region A^c and repeating the same logic of disentangling via swaps, factorization of logical and auxiliary dimers and subsequent state dependent flipping via a unitary $\mathcal{X}_j^{A^c}$. This will also comprise a unitary $\tilde{U}_{A^c}$ that acts analogous as $\tilde{U}_A$. The combined action of $\tilde{U}_a \tilde{U}_{A^c}$ will result in a state

$$\tilde{U}_A \tilde{U}_{A^c} \ket{\bar{i}\bar{j}} = \ket{i} \ket{j} \ket{\chi_a} \ket{\chi_{a^c}} \ket{\chi'}, \tag{8.96}$$

where χ' is a fixed maximally entangled state between A and A^c made from dimers that cross the RT surface. □

In the last step χ' is just a maximally entangled state and it is a priori unclear that the associated algebra of operators acting on it factorizes into a simple tensor product. However, all the operators acting on this state originate, as discussed above, from operators that can act on the edges of the tensor network that cross the RT surface and were mapped unitarily to the boundary. The preceding arguments can be summarized in

cor. *In the Majorana dimer version of the HaPPY code, there exist local unitaries U_A, U_{A^c} such that the full boundary algebra $B(\mathcal{H}_A) \otimes \mathbb{1}$ is mapped to*

$$U_A U_{A^c} \left(B(\mathcal{H}_A) \otimes \mathbb{1}_{A^c} \right) \left(U_A U_{A^c} \right)^\dagger =$$
$$B(\mathcal{H}_a) \otimes B(\mathcal{H}_{\chi_a}) \otimes B(\mathcal{H}_{a,\gamma}) \otimes \mathbb{1}_{A^c}, \tag{8.97}$$

---

[6]At this stage we treat dimers and qubits in a hybrid setting, where we relabeled the Jordan-Wigner transformation in such a way that only the qubits that did not factorize in the previous steps, i.e., the dimers associated to the RT surface and the complementary wedge a^c, participate in the Jordan-Wigner transformation and the factorized ones are excluded and we treat them as regular qubits with Pauli operators acting on them. However, a single factorized dimer represents a qubit, so we can think of the factorized qubits graphically also in terms of dimers having each their own Jordan-Wigner transformation associated to them.

where $\mathcal{H}_a$ is a Hilbert space made out of qubits that are formed from dimers that are the logical dimers from Thm. 8.5.1, $\mathcal{H}_{\chi_a}$ are the auxiliary dimers and $\mathcal{H}_{a,\gamma}$ are the qubits associated to Bell-pairs that originate from dimers that cross the RT surface and in particular each of the $B(\mathcal{H}_i)$ can be written as a tensor product of algebras that act on tensor products of $\mathbb{C}^2$ or, as in the case of $B(\mathcal{H}_{a,\gamma})$, it can be written as the tensor product of algebras that act on the tensor product of Bell-pairs that originate from dimers that cross the RT surface.

The preceding theorem makes it clear that in the case of the Majorana dimer version of the HaPPY code, all one has to keep track of, when growing the network to understand how the algebras are mapped between layers, is what happens to the logical, RT and auxiliary dimers. Furthermore the fact that growing the network corresponds to feeding the network at layer Λ into a unitary together with extra Bell-pairs now becomes evident from the fact that a logical dimer at layer Λ still is a logical dimer at layer $\Lambda + 1$ and the same holds for auxiliary and RT dimers. Accordingly the operators that correspond to operators acting on the logical, auxiliary and RT dimers stay of this kind, when embedding them in the next layer, because the unitaries $U_A^{\Lambda+1}, U_{A^c}^{\Lambda+1}$ will again disentangle them in such a way that their image acts on a qubit that is associated to the same dimer as in the previous layer.

Dimerized networks

We now consider general tensor networks built out of contraction of dimer states that have a similar structure as the HaPPY code: In the HaPPY code, we considered sequences of subregions $A, J^+(A), \ldots$ with their associated algebra $\mathcal{A}_A^1, \mathcal{A}_{J^+(A)}^2, \ldots$ where the full algebra $\mathcal{A}_A$ was mapped completely to a subalgebra of $\mathcal{A}_2$ when growing the network. This is most evident from the circuit picture (c) 8.2, where all that connects the two subsystems is the maximally entangled state $|\chi_\gamma\rangle$ of the RT surface whose one-sided algebra gets completely mapped to A. In the dimer picture, this was visible by the fact that all dimers that ended in A at layer Λ were extended to $J^+(A)$ when growing the network and all that changed was that additional dimers were added, i.e., no dimers left the region A. We saw that we could then decompose the full algebra into operators that act on pairs of dimers that connect A with its complement A^c and dimers that remain completely in A and that this decomposition is respected by the embedding because under growing the network, dimers just get extended to the larger region and do not leave it. This is the dimer version of complementary recovery. We can repeat the analysis of the previous section for any

network generated by contracting dimer states that has this property and find that the total algebra decomposes into

$$\mathcal{B}(\mathcal{H}^\Lambda) = \mathcal{B}(\mathcal{H}_A^\Lambda) \otimes (\mathcal{B}(\mathcal{H}_{A,\gamma}^\Lambda) \otimes \mathcal{B}(\mathcal{H}_{A^c,\gamma}^\Lambda)) \otimes \mathcal{B}(\mathcal{H}_{A^c}^\Lambda), \qquad (8.98)$$

where $\mathcal{H}_{A(A^c)}^\Lambda$ denotes the Hilbert space of dimers that begin and end in $A(A^c)$ and $\mathcal{H}_{A,\gamma}^\Lambda$ the Hilbert space of dimers that connect A with A^c. By an analogous derivation as in the previous section, we can then construct disentangling unitaries $U_A, U_{A^c}^\Lambda$ that decompose the total state $|\Psi^\Lambda\rangle$ of the network at layer Λ into

$$U_A^\Lambda U_{A^c}^\Lambda \, |\Psi^\Lambda\rangle = |\xi_A\rangle \, |\chi_\gamma\rangle \, |\xi_{A^c}\rangle \,, \qquad (8.99)$$

where χ_γ is maximally entangled and ξ_A, ξ_{A^c} are the states of the dimers building $\mathcal{H}_{A(A^c)}^\Lambda$. Since we assume that the network does not make dimers leave the subregion under growing of the network, each additional layer will again just add maximal entangled pairs to χ_γ or dimers that remain in A, so that again, growing a layer just amounts to the addition of Bell pairs to γ or unentangled reference states to ξ_A. We can therefore conclude again that the inductive limit of the algebra of A decomposes into

$$\mathcal{A}_A = \mathcal{B}(\mathcal{H}_\xi) \otimes \mathcal{A}_{A,\gamma} \otimes \mathbb{1}_{A^c}, \qquad (8.100)$$

where $\mathcal{A}_{A,\gamma}$ is the hyperfinite type II$_1$ factor. Depending on, whether $\mathcal{H}_\xi$ is finite or infinite dimensional, we see again that the resulting algebra either has type II$_1$ or type II$_\infty$.

Type II factors and the absence of magic

Dimer states, as well as the image of bulk states $|ij\rangle$ in the boundary of the HaPPY code built out of perfect tensors, are called stabilizer states, which are states that can be obtained from a unitary circuit U applied to $|0\rangle$, where the circuit U is made out of Clifford gates. This is a subset of all unitary gates that can be efficiently simulated by a classical computer using the Gottesman-Knill theorem [209]. Clifford gates are defined as the stabilizer of the Pauli group, i.e., all unitaries that map Pauli operators to Pauli operators under conjugation. States that are prepared by circuits containing gates that do not belong to the Clifford group are said to have *magic* and their properties are tightly linked to the efficiency of quantum compared to classical computation. We saw above several examples of inductive limits of stabilizer states that lead to type II factors. We suspect that this is a general feature of stabilizer circuits and subregions that with respect to the circuit satisfy complementary recovery, that is, that the state prepared by a layered Clifford circuit

will generate local algebras that are at most type II, but never type III. An intuitive reason for that is that a generating set for Clifford circuits is given by the Pauli group together with the CNOT and Hadamard gate, of which the latter two satisfy

$$CNOT(H \otimes \mathbb{1}) \, |00\rangle = \frac{1}{\sqrt{2}}(|11\rangle + |00\rangle), \tag{8.101}$$

i.e., they naturally generate maximally entangled states. One can more generally argue that the bipartite entanglement spectrum of stabilizer states only contains inverse powers of 2, so that one can decompose the state into maximally entangled pairs and unentangled states and one cannot achieve the submaximal entanglement spectrum necessary for a type III factor. It is tempting to conjecture that the requirement for complementary recovery causes the possible circuits to be of the form 8.2 so that again all the entanglement comes from gluing the two halves together by maximal entangled pairs. In light of this, we formulate the heuristic *Magic is necessary for type III algebras* which appears to provide a different point of view on recent observations concerning magic in quantum field theory [452, 94] as local algebras in quantum field theory are type III_1 factors. In a system with complementary recovery, the information of both halves does not get mixed under the induction step, and one can hope to provide an analogous decomposition into entangled pairs and unentangled local pieces as in the dimer picture. A more precise form of our conjecture is *The inductive limits of local algebras of tensor networks that are prepared by Clifford circuits and are associated with regions that satisfy complementary recovery are never type III.* A detailed investigation of this claim is left for future work [61].

MERA

The multi-scale entanglement renormalization ansatz (MERA) is a tensor network ansatz for the discretized renormalization group flow of critical, gapless theories. As shown in Fig. 8.8, it can map operators and states between coarse-grained "infrared" (IR) and fine-grained "ultraviolet" (UV) degrees of freedom. This ansatz has been shown to include good approximations of grounds state correlation functions of simple critical theories and the spectrum of their primary operators [381, 464]. Its geometry also mimics the path integral of a conformal field theory [341, 464], which appear in the continuum limit of certain discrete critical models. Assuming that the MERA, given instances with suitable input parameters on their two types of tensors, can well-approximate states of a (conformal) field theory in its infinite scaling limit, it should then be expected that the local subregion algebra of such instances is
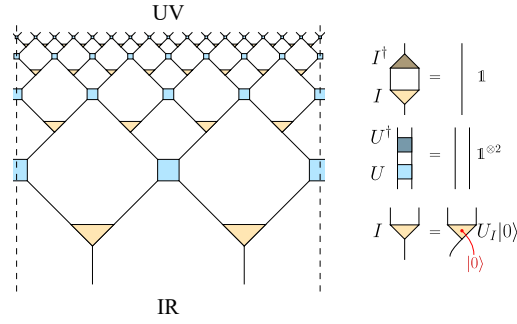
Figure 8.8: The multi-scale entanglement renormalization ansatz (MERA) with four layers. The MERA is a tensor network that maps coarse-grained (IR) degrees of freedom to fine-grained (UV) ones, designed to describe the renormalization group flow of critical, gapless theories. It is constructed from isometries I (triangles) and unitary *disentanglers* U (squares). As shown in the legend, I can be rewritten as a unitary map U_I postselected onto a reference state $|0\rangle$. Here we show the MERA with periodic boundary conditions, denoted by dashed lines.

described by a type III von Neumann algebra. Like the HaPPY code, the MERA has been proposed as a model of a holographic bulk-to-boundary map [431]; if it leads to type III instead of type II algebras, then the MERA must possess qualitative features that deviate from our discussion of holographic codes so far. As we will briefly show now, this is due to a breakdown of complementary recovery, which allows for nontrivial entanglement spectra between two sides of a bipartition to appear. To understand the algebras of half-infinite systems associated with the MERA, it is convenient to extend the isometry tensors into unitaries by adding a bulk leg to each tensor, with a projection of this leg onto a reference state $|0\rangle$ recovering the initial isometry (see legend in Fig. 8.8). This extension is always possible and allows us to turn the entire tensor network into a unitary map and consider the pre-image of any boundary subalgebra. Now we want to determine the type of the algebra associated to half-infinite systems in this network. For this we have essentially two choices: At a given layer, one can either split the systems between two disentanglers as in Fig. 8.9(a), or at a disentangler as in Fig. 8.9(c). Both choices for the subregion A have the property that adding a new layer to the network results in a nontrivial overlap of the lightcones of A and A^c, thus breaking complementary recovery. For concreteness, let us now fix the choice to (a). The effect of the breaking of complementary recovery is that for operators in $\mathcal{A}_A$ that are in the image of operators that act on the RT surface γ_A, the state prepared by the tensor network is not necessarily maximally entangled anymore. This is visible in the circuit picture 8.9(b) from the fact that the state $|\chi_{\gamma_A}\rangle$ does not merely connect to the input legs of the unitaries U_A, U_{A^c}, and
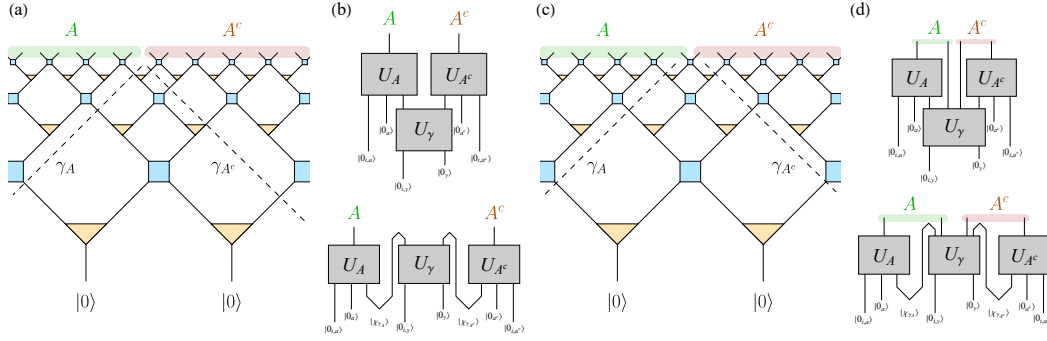
Figure 8.9: Bipartitions of MERA boundary sites. (a) A choice of a half-infinite system A that only contains both legs of any disentangler in its support. The boundary of its preimage is marked as γ_A. If one grows the network by an additional layer, this algebra is completely embedded into a set of bulk legs at the next layer but its image does have spatial overlap with the image of A^c, so that it breaks complementary recovery. The bulk separates into three regions a (between A and γ_A), a^c (between A^c and γ_{A^c}), and the "thick" RT region γ (between γ_A and γ_{A^c}). (b) A circuit representation of the previous setup. Here $|0_a\rangle, |0_{a^c}\rangle, |0_\gamma\rangle$ are the auxiliary bulk states that are fed into each unitary defining an isometry tensor in each bulk region, and $|0_{i,a}\rangle, |0_{i,a^c}\rangle, |0_{i,\gamma}\rangle$ are the input states at the bottom layer. The bottom circuit shows a parallel implementation with maximally entangled input pairs $|\chi_{\gamma_A}\rangle$ and $|\chi_{\gamma_{A^c}}\rangle$, along with post-selection, highlighting the difference from the holographic encoding circuit in Fig. 8.2(c). (c) Another choice of bi-partitioning the MERA into half-infinite subsystems that splits the output qubits of a disentangler, also breaking complementary recovery. (d) Circuit representations of (c).

U_γ but connects input and output legs. This gives rise to a "thick" Ryu-Takayanagi (RT) surface γ in Fig. 8.9(a) that consists of several tensors between the cuts γ_A and γ_{A^c} that bound the causal past of A and A^c. While the algebras $\mathcal{A}_a$ and $\mathcal{A}_{a^c}$ of each bulk region above these cuts are unitarily mapped to A and A^c, respectively, the algebra $\mathcal{A}_\gamma$ of bulk operators in γ (acting on the extended isometries) is shared between both boundary regions. In contrast to the HaPPY code, where γ_A and γ_{A^c} typically coincide and $\mathcal{A}_\gamma$ lives in the center of $\mathcal{A}_A$ and $\mathcal{A}_{A^c}$, complementary recovery is therefore not a feature of a general MERA. Even asymptotically, there is generally no complementary recovery, as each iterative step of growing the tensor network adds more tensors and algebra elements to γ. The choice of subregions in Fig. 8.9(a) leads to a further complication that the cut γ_{A^c} is not stable under such an iteration, as tensors near the boundary that belonged to a^c become part of γ in the next iteration step. This can be ameliorated by the subregion choice of Fig. 8.9(c), but does not solve the problem that operators with support entirely on A or A^c in one step can have overlapping support on both in the next. In terms of

entanglement between A and A^c, the breakdown of complementary recovery then allows for complicated non-bipartite entanglement, potentially approximating the entanglement spectra of QFT subregions. In the scaling limit, one may then recover the type III factors expected from such a QFT [177]. We note that we can still associate type I sub-factors to each of the half-infinite systems that arise from the operators acting on bulk and input legs for which MERA network just prepares the state $|0_a\rangle \otimes |0_{i,a}\rangle$ which has no intrinsic entanglement.

There is an additional issue in any one of the above algebras that makes them unsuitable to fit into the structure of a quantum field theory. By the Reeh-Schlieder Theorem [456], for any local algebra the vacuum state $|\Omega\rangle$ is cyclic and separating, where cyclic means that every state in the Hilbert space can be approximated by states of the form $O|\Omega\rangle$, where O is an operator in the local algebra and separating means that $|\Omega\rangle$ is not annihilated by any operator in the local algebras that is not identically zero. That the state prepared by MERA is not separating for the local algebra can be seen as follows: One can push the operator $|1\rangle\langle1|$ that acts on any of the input states $|0\rangle$ through the network and obtain an operator that is localized in the region A or A^c and thus belongs to the local algebra, but this operator by construction annihilates the state of the MERA. We see that each of the local algebras has a large set of operators that annihilates the state represented by the MERA, breaking the separability. This feature is also true in the HaPPY code, where bulk projections pushed to the boundary can annihilate the boundary state but here it is essential to deal with it, if one wants to recover a quantum field theory. It thus seems evident that to recover a quantum field theory, one has to make further restrictions on the allowed operators.

8.6 Discussion

Our exploration of infinite, layered tensor networks has revealed a link between features of quantum error-correcting codes implemented by such tensor networks, in particular the property of complementary recovery, and the classification of hyperfinite factors as introduced by Araki-Woods and Powers [26, 391]. A particular focus and practical example of our studies has been the HaPPY code [372], a tensor network model of holographic quantum error correction in which complementary recovery naturally appears. Generalizing to layered tensor network codes, we showed that these lead to the emergence of von Neumann algebras associated to boundary subregions, with complementary recovery further restricting these algebras to type II factors.

Summary

Employing the theory of inductive limits of Hilbert spaces and $C^\star$-algebras, we developed a framework that enables us to identify local algebras in infinitely large tensor networks. This binds together tensor network states and operator algebras, allowing for a systematic examination of emergent features. A major finding is that the subregion algebras in the HaPPY code form the unique hyperfinite type II_∞ factor, a conclusion that extends to any exact quantum error-correcting tensor network with complementary recovery between layers and between the Ryu-Takayanagi (RT) surfaces that glue the complementary regions of the network together. This stems from the unitary equivalence between the network state, the Araki-Woods-Powers construction, and the subregion algebra. The type II nature is inherited from maximal entanglement across the bulk RT surface.

In addition to the HaPPY code, we studied networks under a spin-to-fermion equivalence via the Jordan-Wigner transformation, finding that those built from a contraction of Majorana dimer tensors [256] also generically lead to type II factors, provided the network satisfies complementary recovery. We commented on similar observations for algebras for subsystems of Clifford circuits that appear to be fixed to type II or type I factors. We discussed how the MERA network [444], due to the appearance of a "thick" RT surface, breaks complementary recovery, thus allowing for more complicated entanglement patterns than in the simple Araki-Woods-Powers factors. We conjectured that the type III algebras that are associated with half-infinite subsystems in quantum field theory, which is a widely expected limit of the MERA for a suitable choice of tensors, might arise from this thick RT surface. We also argued that it appears reasonable that our usage of all operators is too relaxed and that one should employ the possibility in the MERA to define an operator pushing map using the superoperator. This would allow for the restriction to operators made of primary fields as already suggested in [381]. Based on this, the approach of [346] of using the GNS construction and focus on more complicated inductive maps seems like a better avenue to study the limit of the MERA. The presumably most useful observation stemming from our work concerns the connection between the notion of complementary recovery and the Araki-Woods-Powers factors, which allows for strong control of the entanglement structure of the state of the network as it is grown layer by layer.

Outlook

Multiple open directions emerge. First, our analysis centers upon networks with maximal entanglement in link states, intrinsically favoring type II factors. Examining networks with submaximal entanglement [107] may result in type III algebras. In particular, random tensor networks [232] in the limit of large bond dimension are made out of approximately perfect tensors. So, an extension of our method to random networks might be a fruitful next step to understand operator algebras in holographic systems, at least in a probabilistic or average sense. The absence of complementary recovery in MERA networks suggests that its "RT algebra" allows for more complicated entanglement patterns that might lead to type III algebras. A better understanding of the thick RT surfaces could deepen our understanding of the role of tensor networks in approximating CFTs. Furthermore, our conjecture on the appearance of type II factors from systems prepared by Clifford circuits provides a new perspective on the interplay of operator algebras with quantum computation. Understanding the relation of this line of thought to recent work [310, 309] on von Neumann algebras in many-body quantum systems and the operational perspective on the type classification that the authors provide seems like a natural extension of our work. From the perspective of holography, it seems interesting that the type II nature of HaPPY code subregions arises from maximal entanglement across the RT surface, as observed in fixed-area states in quantum gravity [141]. We want to mention a direct parallel to the construction by Soni [416] which considered a similar system based on the notion of holographic codes or gauge-invariant Hilbert spaces in lattice gauge theories that also carry maximal entanglement across the subsystem boundary [146, 147, 21]. However, in contrast to our choice of fixing the bulk of the HaPPY code to finitely-entangled states so that the associated algebras are type I, Soni considered a limit where the bulk logical algebras are type III and the resulting limit mimics the gravitational crossed product that was used in [457, 101] in the context of perturbative quantum gravity to obtain local algebras of type II, which has been studied extensively in recent years [100, 261, 278, 286, 103, 207, 287, 135, 9] motivated by the discovery of type transitions in holographic dualities [294]l. A more concrete realization of this limit within our framework might be useful to gain intuition on the appearance of the crossed product. It would be interesting to understand whether this entanglement-induced structure of the algebra underlies type II factors in gravity, as could be made possible by thinking of the RT degrees of freedom as gravitational edge modes that contribute to the area operator, which in turn contributes to the entropy. The idea to connect edge modes with black

hole entropy can be found at several places in the literature [225, 278, 216]. In [182] a framework for connecting error-correcting codes and conditional expectations to the real-space version of the renormalization group were made and it would appear as a natural consideration to apply our results in this context. By exploring these questions, future work can further clarify the interplay between tensor networks, operator algebras and their role in quantum field theory and quantum gravity.

8.7 Appendix: The type classification and entanglement

In this section, we summarize the classification of types of von Neumann algebras through the lens of spin systems, drawing on the description by Witten [456]. This presents a physicist's perspective on the factors introduced by Powers [391] and later expanded upon by Araki and Woods [26]. Consider a system consisting of an infinite collection of pairs of qubits; formally, we have the infinite tensor product [361]

$$\hat{\mathcal{H}} = \bigotimes_{i=1}^{\infty} \mathbb{C}^2 \otimes \mathbb{C}^2. \tag{8.102}$$

This space is non-separable, and care needs to be taken to determine which vectors actually belong to it. To compute inner products, one must consider infinite products of numbers, which introduces complications. As a result, this space falls outside the typical scope of physics [361]. To obtain a separable Hilbert space, i.e., a space with a countable basis, we have to choose a vacuum or reference state within this large Hilbert space and consider finite excitations placed on top of it. This will provide a toy example of layered tensor networks. We consider the sequence of Hilbert spaces

$$\mathbb{C}^2 \otimes \mathbb{C}^2 \rightarrow (\mathbb{C}^2 \otimes \mathbb{C}^2)^{\otimes 2} \rightarrow (\mathbb{C}^2 \otimes \mathbb{C}^2)^{\otimes 3} \rightarrow \dots, \tag{8.103}$$

where each step adds a pair of qubits. The layered tensor network is replaced by a sequence of states

$$|\psi^{(0)}\rangle \rightarrow |\psi^{(0)}\rangle \otimes |\psi^{(1)}\rangle \rightarrow \dots, \tag{8.104}$$

where, at each level, a new state of a qubit-pair is tensored in. In the language of the main body of the text, this is equivalent to a layered tensor network with the isometry

$$|\Psi^{\Lambda+1}\rangle = \gamma^{\Lambda,\Lambda+1} |\Psi^{\Lambda}\rangle = |\Psi^{\Lambda}\rangle \otimes |\psi^{(\Lambda+1)}\rangle. \tag{8.105}$$

Similarly, the operator pushing map between layers is then

$$\phi^{\Lambda,\Lambda+1}(O) = O \otimes \mathbb{1} \tag{8.106}$$

so that the operator becomes the identity on the additional qubits. Following the inductive limit procedure described in Sec. 8.2, we consider the sequence of states Ψ^{Λ} and Hilbert spaces with the isometries $\gamma^{\Lambda,\Lambda+1}$ as an inductive system with an limiting Hilbert space $\mathcal{H}_{\Psi}$ that contains a reference vacuum state $|\Psi\rangle$ that represents the state

$$|\Psi\rangle = \bigotimes_{\Lambda=1}^{\infty} |\psi^{\Lambda}\rangle. \tag{8.107}$$

As a subregion, we consider the algebra of operators that act only on one qubit of each qubit pair [7]. These algebras again form an inductive system with inductive limit $\mathcal{A}$ that can be represented on the limiting Hilbert space $\mathcal{H}_\Psi$ induced by the sequence $|\Psi^\Lambda\rangle$ and define a von Neumann algebra $\mathcal{A}_\Psi$. Note that the Hilbert space isometries and the operator pushing maps are compatible in the sense of eq. (8.44). Now consider the specific states

$$|\psi_\lambda^{(i)}\rangle := |\psi_\lambda\rangle = \frac{1}{\sqrt{1+\lambda^2}}(|\uparrow\uparrow\rangle + \lambda\,|\downarrow\downarrow\rangle). \tag{8.108}$$

so that the chain of states is homogeneous between the levels. We denote the resulting one-sided von Neumann algebras by $\mathcal{A}_\lambda$ and the Hilbert spaces by $\mathcal{H}_\lambda$. With this setup one has

(I) If $\lambda = 0$, the underlying state is unentangled, and one can show that the resulting Hilbert space takes the form

$$\mathcal{H}_0 = \mathcal{H}_A \otimes \mathcal{H}_B, \tag{8.109}$$

where $\mathcal{H}_A$ and $\mathcal{H}_B$ are separable, infinite-dimensional Hilbert spaces. In particular, one has

$$\mathcal{A}_0 = \mathcal{B}(\mathcal{H}_A) \otimes \mathbb{1}. \tag{8.110}$$

This is a particular case of a more general situation: a von Neumann algebra that can be represented as the bounded operators of a Hilbert space is called a *type I_∞ factor*, with the subscript ∞ denoting the infinite dimensionality of the Hilbert space. If the Hilbert space is finite dimensional they are called *type I_n factors*.

(II) If $\lambda = 1$, the state $|\psi_1\rangle$ is a maximally entangled Bell pair. As a result, the reference state $|\Psi\rangle \in \mathcal{H}_\Psi$ satisfies

$$\langle\Psi|ab|\Psi\rangle = \langle\Psi|ba|\Psi\rangle, \quad \forall a, b \in \mathcal{A}_1. \tag{8.111}$$

This is the defining property of a tracial state. In particular, since equivalence classes $[a]$ in the inductive limit algebra that come from finite-level operators act only on finitely many qubit-pairs, the number 8.111 has a finite value on each $[a]$, and by extension, on each element of $\mathcal{A}_1$. Therefore, $\mathcal{A}_1$ allows

---

[7]Because the locality here is ambiguous, we just make an arbitrary choice which of the two qubits we consider at each layer, since due to the embedding (8.105) both choices are valid to consider as lightcones.

for a normal[8] state that is tracial on each element of $\mathcal{A}_1$. This is the defining property of a von Neumann algebra of *type II$_1$*.

(III) For $0 < \lambda < 1$, one can show that none of the above holds, so $\mathcal{A}_\lambda$ can not be represented as $\mathcal{B}(\mathcal{H})$ for some Hilbert space, and it does not allow for a finite trace. Specifically, every function that could be cyclic on $\mathcal{A}_\lambda$ must take the values 0 or ∞, a property usually referred to as $\mathcal{A}_\lambda$ being a properly infinite factor[9]. Such an algebra is said to have *type III$_\lambda$*.

(IV) As a generalization, one can consider, instead of a fixed Ψ_λ, an alternating sequence

$$|\Psi_{\lambda_1}\rangle \rightarrow |\Psi_{\lambda_1}\rangle |\Psi_{\lambda_2}\rangle \rightarrow |\Psi_{\lambda_1}\rangle |\Psi_{\lambda_2}\rangle |\Psi_{\lambda_1}\rangle, \tag{8.112}$$

where $\frac{\lambda_1}{\lambda_2}$ is not a rational number. This leads to an entanglement spectrum between the two sides which becomes continuous in the limit of infinitely many levels. The one-sided von Neumann algebra $\mathcal{A}$ then has *type III$_1$* and neither admits representations as $\mathcal{B}(\mathcal{H})$ nor a tracial state. These algebras describe causally complete subregions in quantum field theory [177].

All of the von Neumann algebras listed above are referred to as *hyperfinite* factors, meaning that they are the weak operator closure of an increasing union of finite-dimensional subalgebras. Another type of algebra that is relevant to us in the following is the hyperfinite factor of *type II$_\infty$*, which can be shown to be isomorphic to an algebra acting on a Hilbert space of the form

$$\mathcal{H} = \mathcal{H}_A \otimes \mathcal{H}_B, \tag{8.113}$$

and the algebra being of the form

$$\mathcal{A} = \mathcal{B}(\mathcal{H}_A) \otimes \mathrm{II}_1, \tag{8.114}$$

where the notation indicates that it is a II$_1$ factor on $\mathcal{H}_B$ multiplied with $\mathcal{B}(\mathcal{H}_A)$, where $\mathcal{H}_A$ is a separable, infinite dimensional Hilbert space. These algebras do allow for a trace but are not finite, as the trace of $\mathcal{H}_1$ maps the identity to ∞.

---

[8]Normal means that the state behaves well with limits of sequences of operators.
[9]In contrast to case (II) which is a finite factor.

8.8 Appendix: Majorana dimers

Here we introduce a basic description of states represented by Majorana dimers, which are heavily used in Sec. 8.5. This can be applied whenever one has a Hilbert space of the form

$$\mathcal{H} = \bigotimes_{i=1}^{N} \mathbb{C}^2. \tag{8.115}$$

Instead of considering the Hilbert space in this "spin picture" as a tensor product of local qubit Hilbert spaces, one performs a Jordan-Wigner transformation [264] to obtain a "Majorana picture" of the Hilbert space and operators. In particular, we define

$$\gamma_{2k-1} = Z_1 Z_2 \ldots Z_{k-1} X_k , \tag{8.116}$$

$$\gamma_{2k} = Z_1 Z_2 \ldots Z_{k-1} Y_k , \tag{8.117}$$

where $k \in \{1, \ldots N\}$, N being the number of spins, and Z_i, X_i denoting the respective Pauli operator acting on the i-th spin. These represent Majorana operators that satisfy $\{\gamma_l, \gamma_m\} = 2\delta_{l,m}$. We can then define fermionic creation and annihilation operators via

$$f_k^\dagger := \frac{1}{2}(\gamma_{2k-1} - i\gamma_{2k}). \tag{8.118}$$

Given any state

$$|\psi\rangle = \sum_{i_1,\ldots,i_N=0}^{1} T_{i_1\ldots i_N} |i_1 \ldots i_N\rangle , \tag{8.119}$$

we can associate a fermionic representation of ψ via

$$|\psi\rangle_f = \sum_{i_1,\ldots,i_L=0}^{1} T_{i_1\ldots i_N} (f_1^\dagger)^{i_1} \ldots (f_N^\dagger)^{i_N} |\Omega\rangle , \tag{8.120}$$

where $|\Omega\rangle$ is the fermionic vacuum, which coincides with the $|0\rangle^{\otimes N}$ state in the spin/qubit picture. The fermionic vacuum satisfies

$$f_i |\Omega\rangle = \frac{1}{2}(\gamma_{2i-1} + i\gamma_{2i}) |\Omega\rangle = 0, i \in \{1, \ldots, N\}. \tag{8.121}$$

This provides N conditions of the form

$$(\gamma_k + i p_{k,l}\gamma_l) |\psi\rangle = 0, \tag{8.122}$$

where for the vacuum state $\psi = \Omega$, $p_{k,l} = 1$, $l = k+1$, $k = 2m$, $m \in \{1, \ldots, N\}$. A state satisfying (8.122) for L pairs that are mutually exclusive is called a *Majorana*

dimer state and the numbers $p_{k,l}$ are the *dimer parities*. The contraction of two states ψ, ϕ along the say third and fourth index is then a new state in a bigger system, i.e., we define

$$|C(\psi, 3, \phi, 4)\rangle := \sum_{i_k, j_m} (T^{\psi}_{i_1 i_2 0 i_3 i_4 i_5} T^{\phi}_{j_1 j_2 j_3 0 j_5} \tag{8.123}$$

$$+ T^{\psi}_{i_1 i_2 1 i_3 i_4 i_5} T^{\phi}_{j_1 j_2 j_3 1 j_5}) |i_1 i_2 i_3 i_5 j_1 j_2 j_3 j_5\rangle. \tag{8.124}$$

It was shown in [256] that if the individual tensors T^{ϕ}, T^{ψ} give a dimer state in the dimer representation, the contracted tensor does so as well. Since the logical basis states $\bar{0}$ and $\bar{1}$ of the five-qubit Laflamme code are themselves represented by dimer states, the encoding of a bulk basis state via the full HaPPY code is itself a dimer state on the boundary.

Dimer calculus

Given a dimer state, we can represent it using a simple graphical representation, as for the following two logical basis states of the five-qubit code (each qubit represented as the edge of a pentagon):

$$|\bar{0}\rangle_5 = \quad \tag{8.125}$$

$$|\bar{1}\rangle_5 = \quad \tag{8.126}$$

Here a blue arrow from e.g. 1 to 6 in $|\bar{0}\rangle$ indicates that the state is annihilated by the operator $\gamma_1 + i \gamma_6$. The orange arrow from 1 to 6 in $|\bar{1}\rangle$ indicates that the corresponding state is annihilated by $\gamma_1 - i \gamma_6$ and so on. One can check that application of a Majorana operator γ_i has the effect of flipping the parity of the dimer associated to γ_i, i.e., if

$$\gamma_j + i \gamma_i |\psi\rangle = 0, \tag{8.127}$$

then

$$(\gamma_j - \mathrm{i}\,\gamma_i)\gamma_i \,|\psi\rangle = \gamma_i(-\gamma_j - \mathrm{i}\,\gamma_i)\,|\psi\rangle$$
$$= -\gamma_i(\gamma_j + \mathrm{i}\,\gamma_i)\,|\psi\rangle$$
$$= 0\,. \tag{8.128}$$

Therefore, we can think of the application of a Majorana operator on a dimer state in the pictorial representation as a flip of the respective color of the dimer. Also we can swap dimers by applying the swap operator

$$P_{j,k} = \frac{\mathcal{P}_{\text{tot}}}{\sqrt{2}}(\gamma_j - \gamma_k), \tag{8.129}$$

the effect of which is just the exchange of the dimer connected to the point j to become connected to the point k and vice-versa. Here $\mathcal{P}_{\text{tot}}$ is the total parity operator

$$\mathcal{P}_{\text{tot}} = \prod_{i=1} Z_i. \tag{8.130}$$

An example is given in Fig. 8.10. Given two such states, we can contract the corresponding tensors to a new state as in the following picture

$$\| \tag{8.131}$$
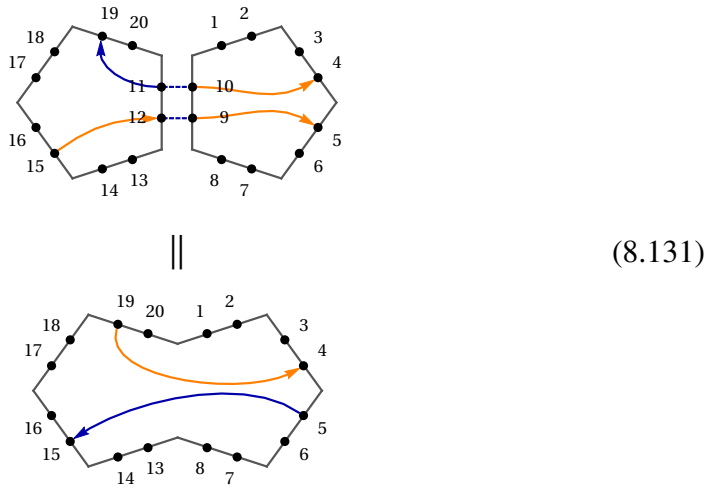
i.e, if neighboring edges (here edge 5 and 6) are contracted, the neighboring dimers are extended and the resulting dimer parities are the product of the dimer parities of the dimers that were contracted. Here it is important that one contracts neighboring edges. In particular if one wants to contract the HaPPY code, one has to first choose an orientation of the local pentagons. This comes with choosing a *pivot*, i.e., an edge at which one starts counting the dimers and that implicitly defines the starting point of the Jordan-Wigner transformation. To be able to contract neighboring edges with

non-consecutive indices, one first has to rotate the local dimers so that their pivots align upon contraction. As explained in [256], for parity-even states[10] a rotation does not do anything except changing the order. For parity-odd states, the rotation of a dimer amounts to the insertion of a Z string along the path of the pivot, which has the effect of flipping all dimer parities that are traversed by the pivot when moving from the old position to the new one. These Z strings have to be taken into account when performing the full contraction.
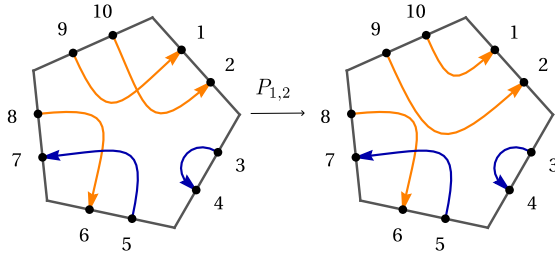
Figure 8.10: Representation of swap operation between node 1 and 2.

Z strings

Here we describe the use of Z strings in the proof of theorem 8.5.1. The Z strings appear when one changes the Jordan-Wigner transformation by a cyclic permutation of the spin indices when performing the transformation (8.116), which visually corresponds to "rotating the pivot." This is used when one wants to align the edges during the contraction of two dimer states such that the edges contracted are consecutive edges $k, k + 1$, for which the rules for contracting dimer states from the previous section apply. As described in [256], if the dimer state has even total parity, a cyclic permutation does not generate any change in the individual dimer parities, but if the state has odd total parity, then the parity of every dimer whose endpoint is passed by the pivot is flipped (if the pivot passed over both endpoints, the dimer parity is preserved). An example of the logical state $\bar{1}$ for a single pentagon is given in Fig. 8.11 where the pivot is rotated over one edge. When contracting the whole network for the HaPPY code the appearance of Z strings can be thought of as follows: If one starts out with the bulk vacuum $|\bar{0}\,\bar{0}\ldots\bar{0}\rangle$ no Z strings appear during the contraction since the total state is parity-even and all dimers in the resulting state have positive parity. If a single bulk qubit is instead in the $\bar{1}$ state, the corresponding pentagon has to be rotated during contraction, and this rotation will produce a Z

---

[10]Parity-even dimer states are those where the number of parity-odd dimers times $(-1)^{N_c}$, N_c being the number of dimer crossing points, is even
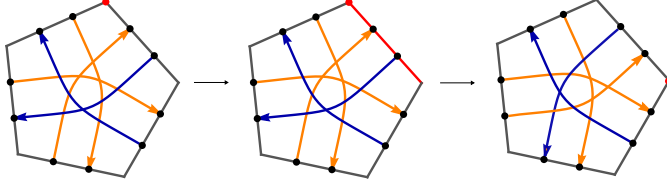
Figure 8.11: Demonstration of the generation of a Z string as an effect of rotating the Pivot by one edge.

string. As described in [256], the Z string will stretch from the initial pivot of the pentagon to the pivot of the complete state representing the fully contracted network, as demonstrated in Fig. 8.12 (b) and (c). In the following, we place the pivot of the contracted network at the end of the rightmost edge of the RT surface of a boundary subregion, as indicated in Fig. 8.12.(a). In this situation, any Z string that arises when flipping a bulk qubit in layer n can be located only on the edges that connect the layer n with the layer $n-1$ until it hits the RT surface as demonstrated in Fig. 8.12(c). Thinking of Z strings in this way makes it clear that the effect of flipping any qubit in layer n will flip only dimers that state $\bar{1}$ from state $\bar{0}$ or dimers that connect layer n with layer $n-1$ or with the complementary entanglement wedge via the RT surface. For this reason, in the proof of Theorem 8.5.1 we can focus on dimers that connect the layer n to itself, since all other dimers were considered in the previous layers.
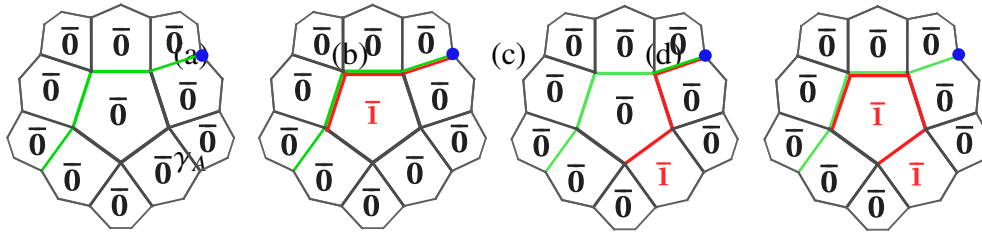
Figure 8.12: Illustration of Z strings that appear when exciting bulk qubits from $|0\rangle$ to $|1\rangle$. (a) The RT surface γ_A is indicated by green edges and the pivot at the rightmost edge of the RT surface by a blue dot. (b) Only the central qubit gets excited and a Z string, indicated by a red edge, stretches from its pivot to the global pivot located on the boundary. (c) A qubit in the second layer gets excited and the corresponding Z string goes along the edge that connects the first with the second layer. (d) A qubit in the first and second layer get excited. Both Z strings from (b) and (c) appear such that a edge is contained in two individual Z strings that cancels out, leading to a Z string connecting the pivots of the individual pentagons.

Proof of Theorem 4

Proof. We will prove the theorem for every layer individually, where we count the layers according to how the tensor network is grown, i.e., some pentagons directly at the RT surface are the deepest in the bulk and come from the same layer of growing the tensor network, such as the central pentagon in Fig. 8.6. These pentagons comprise the layer $n = 1$. The pentagons immediately surrounding the $n = 1$ pentagons form the layer $n = 2$ and so on. We will now show that for any n we can make a consistent choice of logical dimers that does not depend on the choice of the previous layer. In our setup, we assume that the pivot is located at the rightmost edge of our subregion, so the node nearest to the RT surface is node 1. If we now perform a logical operation in the layer n on a single bulk qubit, we will flip 3 dimers that distinguish the logical 0 from the logical 1 state. Additionally, as explained in Appendix 8.8, there will be a Z string stretching from the pivot of the bulk qubit to the pivot of the subregion A. This Z string only passes edges that lie between layer n and $n + 1$, therefore only flipping dimers that existed at layer n. Therefore, if we can make a consistent choice for logical dimers in layer n that do not arise from the previous layer, we can make this selection at each layer separately. For the code on the $\{5, 4\}$ tiling, one can see a consistent choice considering a corner, as illustrated in Fig. 8.13(a). Each layer consists of a chain of tensors like T_1, T_2 aligned along a chain.
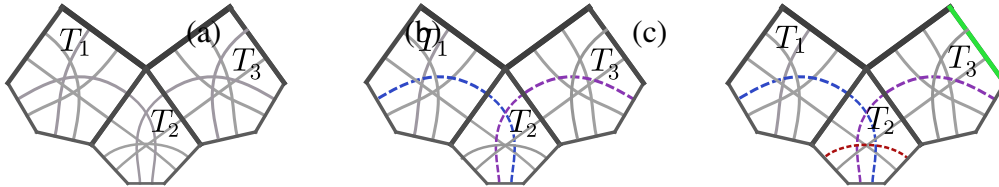
Figure 8.13: (a) A corner piece which illustrates all situations that can occur in the $\{5, 4\}$ tiling of the hyperbolic plane. The lower three pentagons are representing layer n. Every layer consists of pentagons contracted as the bottom three pentagon. (b) Logical dimers of the two leftmost pentagons in dashed lines if the rightmost pentagon does not border the RT surface. (c) Logical dimers of T_1, T_2, T_3 in dashed lines if the T_3 does border the RT surface indicated by a green edge.

Regardless of whether T_1 borders the RT surface, as long as T_3 does not border the RT surface, logical dimers can be chosen as in Fig. 8.13(b) for the pentagons T_1, T_2. This choice can be repeated as one goes to the right through the layer. Note that these dimers are flipped independently of where the pivot of T_1 or T_2 is located, as can be seen from the representation of the logical states in dimer form (8.91).

If T_3 borders the RT surface, then logical dimers can be chosen as in Fig. 8.13(c). The only difference between these two configurations is that in the case that the RT surface borders the rightmost pentagon, one cannot choose the dimers as in Fig. 8.13(b) because this would make the logical dimers cross the RT surface. If however, the RT surface borders the corner Pentagon that is not connected with the previous layer, then one can go for the logical dimers as in 8.13(c) by not coloring the logical dimer of the neighboring pentagon that lies in the complementary entanglement wedge. □

Proof of Lemma 1

Proof. As established previously, we divide the dimers that end in region A into three sets: Logical dimers D_l^A as established by Thm. 8.5.1, dimers that cross the RT surface D_γ and the remaining dimers that are not logical but start and end in region A as the auxilliary dimers D_a. We think of the state $|\bar{i}\bar{j}\rangle$ as a state where all the bulk qubits which are in the $|1\rangle$ state as the result of applying the respective logical X operators on the bulk state in which all qubits are in the $|0\rangle$ state. Furthermore, we locate the pivot on the rightmost edge of the RT surface as indicated in Fig. 8.12. We will construct U_A by defining a *state-dependent* unitary C_i^A for each logical state $|i\rangle$ in the entanglement wedge a that implements the action of U_A just on this state and then combine each of the C_i^A together to the unitary U_A. For a fixed state $|i\rangle$ in the entanglement wedge a, C_i^A will have the action

$$C_i^A |\bar{i}\bar{j}\rangle = |i\rangle |\chi_a\rangle |\chi_{\gamma,j}\rangle, \tag{8.132}$$

so that $|\chi_a\rangle$ is a fixed reference state of the auxilliary dimers D_a and $|\chi_{\gamma,j}\rangle$ is a state such that if $|j\rangle = |0\rangle$, the RT dimers have a fixed parity. Given the state $|\bar{i}\bar{j}\rangle$ we explicitly construct C_i^A as follows: First, we recall [256] that a state that has a dimer connecting the same edge factorizes with the rest, as demonstrated in Fig. 8.7. If the dimer has positive parity $|\psi\rangle = |0\rangle$, if it has negative parity $|\psi\rangle = |1\rangle$. The first action that we want to implement is to achieve the factorization of 8.132 by applying swaps on the logical and auxilliary dimers, so that the resulting state factorizes between the respective qubits. A selection of logical, RT and auxilliary dimers is illustrated in Fig. 8.6(b). We will now apply swap operations (For more information on swaps, see Appendix 8.8).

$$P_{j,k} = \frac{\mathcal{P}_{tot}}{\sqrt{2}} (\gamma_j - \gamma_k), \tag{8.133}$$

to the dimers in D_l^A, D_a, D_γ to put them in a configuration that can be used with the rule illustrated in Fig. 8.7 to obtain a logical and auxiliary system that factorizes

with the rest. The swap $P_{j,k}$ has the effect of swapping the dimers beginning or ending at j, k to now begin or end at k, j. We produce the desired state by swapping the position of the endpoint of any dimer in D_l^A, D_a so that it is located on the same edge as it begins, thus providing a factorizing state. This disentangling procedure is illustrated in Fig. 8.14.
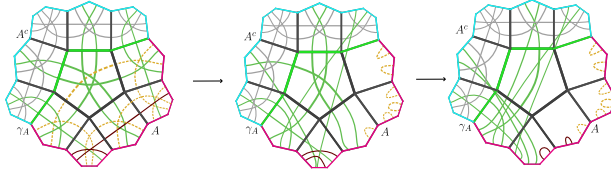
Figure 8.14: Illustration of a sequence of swap operations that disentangles the logical from the RT and the auxiliary degrees of freedom. Between each step a set of swap operations was applied. Note that the parity of dimers was neglected. The colors are used to show the logical affiliation of each dimer, dashed and yellow being in D_l^A, red being in D_a and green dimers are in D_γ. The boundary region A is indicated in pink and its complement A^c in blue. The RT surface γ_A is also drawn in green to fit the respective dimers.

In addition, we will swap the RT dimers so that dimers that cross the RT surface at the same edge also end at the same edge in A. After we have done this, we will end up only with RT dimers connecting A to the edges of A^c and a piece that factorizes with the rest. In total, we get a system that, after applying the factorization rule of Fig. 8.7, has the form $\mathcal{H} = \mathcal{H}_a \otimes \mathcal{H}_{\chi_a} \otimes \mathcal{H}_{\gamma,A^c}$ as in Eq. (8.92), so we have a product state between the three Hilbert spaces that has the form

$$S_A \, |\bar{ij}\rangle = |\psi_i\rangle \, |\phi_{i,a}\rangle \, |\chi_{ij}\rangle \tag{8.134}$$

where χ_{ij} is the state of the dimers in D_γ, $|\psi_i\rangle$ the state of the logical dimers and $|\phi_{i,a}\rangle$ the state of the auxilliary dimers. Here, we have denoted the sequence of swap operations by S_A. This map is independent of $|i\rangle$ because the dimers of the logical 0 and 1 state differ only in parity, not in connectivity as provided by Thm. 8.5.1. Therefore, to get to the factorized form we have to apply the same swaps for any bulk input. This swap can be made unitary because one has $P_{i,j}^\dagger = P_{i,j}^{-1} = -P_{i,j}$. So if we needed to apply an odd number of swaps to get to the factorizing state, we can just apply an additional swap on an edge carrying a logical or auxiliary dimer which will only change its parity. We end up with an even number of swaps S_A that is a local unitary operation. We will now abuse notation and go into a hybrid between dimer and qubit language, where we will talk about operators that act on $\mathcal{H}_{\gamma,A^c}$ in dimer language and we will talk about operators that act on the, now disentangled

dimers, in qubits language because the set of disentangled dimers is just a system of qubits, where each dimer represents a single qubit. Another way of thinking about it is that we define a Jordan-Wigner transformation only on the Hilbert space $\mathcal{H}_{\gamma,A^c}$ without involving the disentangled dimers.

In Eq. (8.134) the state of the dimers of D_a, D_γ is still i-dependent. To remove this dependence, we define a local unitary $\mathcal{X}_i^A$ that will remove the i-dependence. First, the state $\phi_{i,a}$ is a state described by zeros and ones because it comes from disentangled dimers in D_a. We can apply X operators to put them into the $|0\rangle$ state. This sequence of X's forms a unitary $\mathcal{X}_{i,a}$. Furthermore, if the state in the complementary wedge is $|j\rangle = |0\rangle$, the parity of the RT dimers only depends on the state i. We will now apply a product of majorana operators γ that act on these RT dimers and set all their parities to be positive, if $|j\rangle = |0\rangle$. This comprises a local unitary $\mathcal{X}_{i,\gamma}$. At last, we can apply X operators on the logical dimers to transform the sequence of zeros and once in ψ_i into the state $|i\rangle$ where the logical dimer associated to each bulk qubit in a is in the state the corresponding bulk qubit is in. This last step is not necessary, we could just continue to work with ψ_i but for concreteness sake we will also perform such an respective application of X's via a unitary $\mathcal{X}_{i,l}$. We then define

$$\mathcal{X}_i^A = \mathcal{X}_{i,l}\mathcal{X}_{i,a}\mathcal{X}_{i,\gamma}. \tag{8.135}$$

We now define

$$C_i^A = \mathcal{X}_i^A \mathcal{S}_A. \tag{8.136}$$

This unitary will satisfy (8.132) by construction where $|\phi_a\rangle = |0\rangle$. We can repeat the same construction for the complementary region to obtain a unitary $C_j^{A^c}$. [11] The connectivity of the state $C_i^A C_j^{A^c} |\bar{i}\bar{j}\rangle$ is represented graphically in Fig. 8.15. Note that we constructed $\mathcal{S}_A, \mathcal{S}_{A^c}$ such that pairs of RT dimers that crossed the same edge on the RT surface also begin and end on the same edge. We can also choose them such that the dimers associated to one RT edge do not cross each other. As was shown in [256], such dimer pairs give maximally entangled states. We defined $\mathcal{X}_{i,\gamma}$ such that if $|j\rangle = |0\rangle$ all the RT dimers have positive parity in $C_i^A |\bar{i}0\rangle$. Because of this, all the maximally entangled pairs associated to each edge will be in the same state with the same parities for any bulk state $|ij\rangle$, because if going from $|\bar{0}\bar{0}\rangle$ to $|i0\rangle$ a pair of RT dimers flipped their parities, then $\mathcal{X}_{i,\gamma}$ will reverse this parity change. The same parity-flip reversal takes place from $|\mathcal{X}_{j,\gamma}\rangle$ when the dimers change their parity when going from $|\bar{0}\bar{0}\rangle$ to $|\bar{0}j\rangle$, so that the combined action $\mathcal{X}_{j,\gamma}\mathcal{X}_{i,\gamma}$ will flip

---

[11]Note that we have to move the pivot to the rightmost edge of the complementary region A^c so that the swap operators one has to apply are local unitaries.

the parity of these RT dimers twice, so that their parity is the same as in the $|\bar{0}\bar{0}\rangle$ state, namely positive.
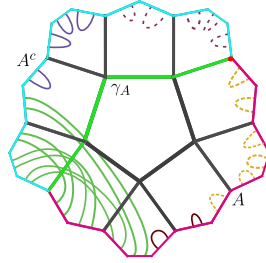
Figure 8.15: Dimers after full disentangling. All RT dimers begin and end in pairs at the same edge to form maximally entangled pairs.

Figure 8.16: Fully disentangled codestate without indication of parities.

By construction we then have

$$C_i^A C_j^{A^c} |\bar{i}\bar{j}\rangle = |i\rangle |j\rangle |\chi_a\rangle |\chi_{a^c}\rangle |\chi\rangle, \tag{8.137}$$

where $|\chi_a\rangle = |0\rangle$, $|\chi_{a^c}\rangle = |0\rangle$ and $|\chi\rangle$ is a collection of maximally entangled pairs between A and A^c, one for each edge in the RT surface and that is independent of the bulk logical state $|\bar{i}\bar{j}\rangle$ Now that we can disentangle each state $|\bar{i}\bar{j}\rangle$ individually, we construct the unitaries U_A, U_{A^c}. We can now define projectors

$$\begin{aligned} P_i^A &= (C_i^A)^\dagger |i\rangle \langle i| C_i^A \\ P_j^{A^c} &= (C_j^{A^c})^\dagger |j\rangle \langle j| C_j^{A^c}, \end{aligned} \tag{8.138}$$

where $|i\rangle \langle i| = |i\rangle \langle i| \otimes \mathbb{1}_{\mathcal{H}_{\chi_a}} \otimes \mathbb{1}_{\mathcal{H}_{\gamma,A}} \otimes \mathbb{1}_{A^c}$, so that the identities act on the space of auxilliary, RT dimers and the complementary region A^c. In the following we will omit these identities. The projction P_i^A projects on the dimer states in which the logical dimers of region A have the same parity as they have in the codestate $|i\rangle$ but independent of what parities the other dimers have. These are mutually orthogonal because in their product

$$P_i^A P_j^A = (C_i^A)^\dagger |i\rangle \langle i| C_i^A (C_j^A)^\dagger |j\rangle \langle j| C_j^A, \tag{8.139}$$

we have

$$C_i^A (C_j^A)^\dagger = \mathcal{X}_i^A \mathcal{S}_a \mathcal{S}_a^\dagger (\mathcal{X}_j^A)^\dagger = \mathcal{X}_i^A (\mathcal{X}_j^A)^\dagger \tag{8.140}$$

in (8.139) we will thus end up with $\mathcal{X}_j^\dagger$ flipping the spins in $|j\rangle$ to the parities that the corresponding dimers have in the original dimer picture and a analogous operation will be done by $\langle i| \mathcal{X}_i^A$. Here it is that Thm. 8.5.1 is important, namely it forces the operator $|i\rangle \langle i| \mathcal{X}_i^A$ to multiply to zero with $\mathcal{X}_j^\dagger (|j\rangle \langle j|$ if $i \neq j$ because the application of $\mathcal{X}_i^A$ on $|i\rangle \langle i|$ will flip the spins in such a way that the parities are the same as one had in the initial HaPPY state for the dimers that built up the logical $|i\rangle$. These parities (or effectively this collection of ones and zeros) will differ at least in one spin from the state one gets by computing $\mathcal{X}_j^\dagger (|j\rangle \langle j| \otimes \mathbb{1})$ exactly because this is the content of proposition 8.5.1 – the parities of logical dimers differ between any two distinct codestates. Therefore we have

$$
\begin{aligned}
&P_i^A P_j^A \\
&= \delta_{ij} (C_i^A)^\dagger |i\rangle \langle i| \mathcal{X}_i^A (\mathcal{X}_i^A)^\dagger |i\rangle \langle i| C_i^A \\
&= \delta_{ij} (C_i^A)^\dagger |i\rangle \langle i| C_i^A = P_i \delta_{ij},
\end{aligned}
\tag{8.141}
$$

Furthermore, P_i^A is by construction local in A and thus commutes with all $P_i^{A^c}$. We now define the operators

$$
\begin{aligned}
U_A &:= \sum_i C_i^A P_i^A = \sum_i |i\rangle \langle i| \mathcal{X}_i^A \mathcal{S}_A, \\
U_{A^c} &:= \sum_j C_j^{A^c} P_j^{A^c} = \sum_i |i\rangle \langle i| \mathcal{X}_i^{A^c} \mathcal{S}_{A^c}.
\end{aligned}
\tag{8.142}
$$

Lastly, we want to show that these are unitaries. We compute

$$
\begin{aligned}
U_A U_A^\dagger &= \sum_{ij} |i\rangle \langle i| \mathcal{X}_i^A \mathcal{S}_A \mathcal{S}_A^\dagger \mathcal{X}_j^\dagger (|j\rangle \langle j| \\
&= \sum_{ij} |i\rangle \langle i| \mathcal{X}_i^A (\mathcal{X}_j^A)^\dagger (|j\rangle \langle j| \\
&= \sum_i |i\rangle \langle i| \mathcal{X}_i^A (\mathcal{X}_i^A)^\dagger |i\rangle \langle i| \\
&= \sum_i |i\rangle \langle i| = \mathbb{1}.
\end{aligned}
\tag{8.143}
$$

Here we used the unitarity of $\mathcal{S}_A$ in the second line, the argument of orthogonality following from proposition 8.5.1 as in the proof of the pairwise orthogonality of P_i^A and in the end that $|i\rangle \langle i|$ is an orthonormal basis for the logical Hilbert space. Similarly, we have

$$
\begin{aligned}
U_A^\dagger U_A &= \sum_{ij} \mathcal{S}_A^\dagger (\mathcal{X}_j^A)^\dagger |j\rangle \langle j| |i\rangle \langle i| \mathcal{X}_i^A \mathcal{S}_A \\
&= \sum_i \mathcal{S}_A^\dagger (\mathcal{X}_i^A)^\dagger |i\rangle \langle i| \mathcal{X}_i^A \mathcal{S}_A = \sum_i P_i = \mathbb{1}.
\end{aligned}
\tag{8.144}
$$

Here, we used the fact that P_i is summing to the identity, which follows from a dimension-counting argument. The P_i's are mutually orthogonal and there are as many of them as we have bulk qubit states. Each of them projects onto a subspace that has the dimensionality $\text{Dim}(\mathcal{H})/2^{n_{bulk}}$, where n_{bulk} is the number of bulk qubits and $\mathcal{H}$ is the full boundary Hilbert space. Since we have $2^{n_{bulk}}$ of those orthogonal subspaces, the sum of them must be the total Hilbert space, so the projections must sum to the identity. $\qquad\square$

Chapter 9

NONPERTURBATIVE GRAVITY CORRECTIONS TO BULK RECONSTRUCTION

This chapter is based on the work [194], in collaboration with Monica Jinwoo Kang.

9.1 Introduction

Understanding the holographic principle and the theory of quantum gravity has been a constant focus and desire in modern theoretical physics, and much progress has been achieved within the last decade utilizing the framework of quantum error correction. In the context of the AdS/CFT correspondence, the semi-classical limit can be interpreted as a quantum error correcting code and this perspective has provided new tools to understand the emergence of spacetime [142, 224, 193] and the Page curve analysis [368, 13, 379].

The first hint of the error correcting structure of the semiclassical limit of AdS/CFT lies within the Ryu–Takayanagi formula [401, 400]. More precisely, each region *A* of the boundary CFT in a given state that possesses a semiclassical dual corresponds to a bulk region called the *entanglement wedge*, whose geometry and field content are encoded solely in *A*. Given the bulk geometry, the entanglement wedge for a given boundary region is determined through a minimization procedure: it is delimited by a *quantum extremal surface* homologous to the boundary region, and has the property of being an extremum of the generalized entropy of the boundary state. More formally, it is the bulk surface (*a*) homologous to the boundary region that extremizes the quantity

$$S_{gen} := \frac{1}{4G_N}\text{Area}(a) + S_a(\rho_{bulk}), \tag{9.1}$$

where ρ_{bulk} is the state that describes the system in the semiclassical theory (i.e., the code subspace).

It is important to note that the entanglement wedge can be much larger than the causal wedge, which is the bulk region that is reconstructible through the Hamilton–Kabat–Lifschytz–Lowe protocol [220, 219]. For example, this is possible in the case of disconnected subregions of the boundary. In this aspect, entanglement wedge

reconstruction is a highly nontrivial and unexpected property of the semiclassical limit of AdS/CFT.

The validity of the Ryu–Takayanagi formula is equivalent to several other claims including complementary recovery [142]. If the boundary theory is in a pure state and a is the entanglement wedge of a boundary region A, then semiclassical operators in a can be reconstructed from operators in A and semiclassical operators in the bulk complement $\overline{a}$ can be reconstructed from the boundary complement $\overline{A}$. This is the key ingredient needed for establishing the connection between entanglement wedge reconstruction and the Ryu–Takayanagi formula in the context of finite-dimensional Hilbert spaces. In this setting, together with the relative entropy equivalence between bulk and boundary derived by Jafferis–Lewkowycz–Maldacena–Suh (JLMS) [254], it has been proven that entanglement wedge reconstruction, the Ryu–Takayanagi formula, and the JLMS formula are all equivalent [225].

Formulating a rigorous analog of the Ryu–Takayanagi formula in the context of infinite-dimensional Hilbert spaces is hard, as it needs to be regulated, and the absence of tracial states on certain von Neumann algebras makes it particularly tricky to even define von Neumann entropy. However, its equivalent counterparts, namely, complementary recovery and the conservation of relative entropy (and modular flow) between the bulk and the boundary, can still be formulated in the context of infinite-dimensional Hilbert spaces, and are shown to be equivalent under some assumptions in [270]. The required assumptions for this exact relation to hold have been extended to more settings in [196, 164]. It is important to note that this exact relation between entanglement wedge reconstruction and the relative entropy equivalence between bulk and boundary in infinite-dimensional Hilbert spaces is relevant for the case of an actual boundary conformal field theory, utilizing an operator-algebraic perspective.

The analysis in [270] relies on von Neumann algebras acting on Hilbert spaces. The code subspace and the physical Hilbert space are embedded into one another via an isometry. The fundamental objects of the theory then become the algebra of CFT observables in a certain boundary region M_{phys} acting on the physical Hilbert space, and an algebra of effective field theory observables M_{code} acting on the code subspace. It has recently been shown that the underlying structure associated to exact entanglement wedge reconstruction was that of a net of conditional expectations between boundary and bulk local algebras [164]. In this context, the equivalence between the conservation of modular flows and complementary recovery for a state

in the code subspace naturally arises as a consequence of Takesaki's theorem.

A striking feature of the entanglement wedge is that it is a state-dependent object. This is due to the presence of the bulk entropy term in the quantum extremal surface formula. In the case of two almost equally contributing local extrema of the generalized entropy [6], or of a large amount of semiclassical entanglement in the bulk [231], this bulk entropy term may become dominant and create large variations of the entanglement wedge, even within the same code subspace. This can happen in situations when the bulk contains a black hole such that there exist enough bulk entropy giving rise to such entanglement wedge jumps. In such cases, the JLMS formula [254] has to be corrected to include the difference in generalized entropies of the two bulk states in their relative entanglement wedges [142].

There is an important subtlety in studying some crucial features of the emergence of the bulk in AdS/CFT: the quantum extremal surface formula can only be approximate, albeit to nonperturbative order in G_N [231]. This subtlety is essential for resolving some apparent paradoxes in AdS/CFT, such as aspects of the information paradox [379] and non-additivity of entanglement wedges [276]. For studying black holes in the $G_N \to 0$ limit, we allow the code subspace to have an arbitrarily large dimension. In this setting, given a boundary region, a code subspace operator can only be reconstructed in a state-independent manner if it is in its entanglement wedge for both pure and mixed states in the code subspace [231]. The intersection of all these entanglement wedges is called the *reconstruction wedge*. In particular, the black hole interior, which lies outside of the reconstruction wedge, can only be reconstructed in a state-dependent manner.

Subtleties about approximate recovery that include non-perturbative gravitational errors have thus far only been considered in finite-dimensional toy models [231]; however, we eventually need to deal with the case of local algebras on an infinite-dimensional boundary Hilbert space. Here, we intend to formulate an approximate version of infinite-dimensional holographic recovery. We first focus on the case of the reconstruction wedge. More specifically, we prove that if a quantum extremal surface formula with an inclusion of non-pertubative gravitational errors can be true in all entanglement wedges, then the bulk algebra of the reconstruction wedge is reconstructable from the boundary up to small nonperturbative gravitational corrections. Putting everything together, we present Theorem 9.1.1 that captures the precise result. We note that we use a *modified-JLMS formula* that adapts the statement of relative entropy conservation to the case in which the quantum extremal

surface jumps, by adding generalized entropy terms. Here $\mathcal{B}(\mathcal{H})$ denotes bounded operators on a Hilbert space, $S_{\rho,\omega}(M)$ denotes the relative entropy of the states ρ and ω on the algebra M, and R is interpreted a reference system.

Theorem 9.1.1. *Let $\mathcal{H}_{code}$ and $\mathcal{H}_{phys}$ be two Hilbert spaces, $V : \mathcal{H}_{code} \to \mathcal{H}_{phys}$ be an isometry, and $\mathcal{H}^*_{code}$ be any finite-dimensional Hilbert space of dimension smaller or equal to the one of $\mathcal{H}_{code}$. Let M_A be a von Neumann algebra on $\mathcal{H}_{phys}$. To each normal state ω in $\mathcal{B}(\mathcal{H}_{code} \otimes \mathcal{H}^*_{code})_*$, we associate two entanglement wedge von Neumann algebras $M_{EW(\omega,A)}$ and $M_{EW(\omega,\overline{A}\cup R)}$ of operators on $\mathcal{H}_{code} \otimes \mathcal{H}^*_{code}$ such that $M_{EW(\omega,\overline{A}\cup R)} \subset M'_{EW(\omega,A)}$. Let*

$$M_a := \bigcap_{\omega} M_{EW(\omega,A)} \subset \mathcal{B}(\mathcal{H}_{code})$$

be the reconstruction wedge von Neumann algebra on $\mathcal{H}_{code}$, and suppose that $M_{a'}$, the commutant of M_a in $\mathcal{B}(\mathcal{H}_{code})$, is a product of type I factors. Suppose that for all choices of $\mathcal{H}^*_{code}$ and all pairs of states ρ, ω in $\mathcal{B}(\mathcal{H}_{code} \otimes \mathcal{H}^*_{code})_*$ such that $S_{\rho,\omega}(M_{EW(\omega,\overline{A}\cup R)})$ is finite, we have the following modified-JLMS condition:

$$|S_{\rho\circ(\mathcal{E}^c\otimes Id),\omega\circ(\mathcal{E}^c\otimes Id)}(M'_A \otimes \mathcal{B}(\mathcal{H}^*_{code})) - S_{\rho,\omega}(M_{EW(\omega,\overline{A}\cup R)})$$
$$+ S_{gen}(\rho, EW(\rho, \overline{A} \cup R)) - S_{gen}(\rho, EW(\omega, \overline{A} \cup R))| \leq \varepsilon,$$

where $\mathcal{E}$ and $\mathcal{E}^c$ refer to the respective restrictions of $A \mapsto V^\dagger AV$ to M_A and M'_A, and the function $S_{gen}(\rho, EW(\omega, \overline{A} \cup R))$ depends only on the restrictions of ρ and ω to $M_{a'} \otimes \mathcal{B}(\mathcal{H}^*_{code})$. Then, there exists a quantum channel $\mathcal{R} : M_a \to M_A$ such that

$$\|\mathcal{E} \circ \mathcal{R} - Id_{M_a}\|_{cb} \leq 2(2\varepsilon)^{\frac{1}{4}}.$$

We then move on to the state-dependent case, and explain how to extend the state-dependent α-bit reconstruction of the black hole interior [231] to the infinite-dimensional case. We also compare our approach through complementary recovery to the recent extension [170] of the twirled Petz map [130] to the infinite-dimensional case. While the twirled Petz map provides an explicit recovery channel, the approximate recovery it gives is only controlled by a bound involving the operator norm, rather than the completely bounded norm that we get from our approach. Moreover, it is unclear whether the twirled Petz map still provides a valid reconstruction at subleading order in G_N, whereas the error in our approach is nonperturbative.

Building on this operator algebraic framework [270, 269, 164, 170, 165, 225, 196, 193, 195, 456] on understanding bulk reconstruction, modular structure, and relative entropy equivalence between bulk and boundary, our results expand the dictionary between holography and operator algebras. We summarize this in Table 9.1, which also captures the emerging quantum error correcting structure.

At the end of the chapter, we expand on how our algebraic approach enables us to capture nontrivial features of the bulk, and propose some future research directions. In particular, we comment on the possibility of bridging the quantum error correction approach to the semiclassical limit of the bulk, with the recent advances involving averaged theories and gravitational path integrals. We further analyze the modified-JLMS condition required for our theorem in more detail and show how our result can be relevant to the case of an evaporating black hole.

The remaining parts of the chapter are organized as follows. In Section 9.2, we first provide a toolkit of relevant mathematical concepts for the purpose of this chapter, including conditional expectations, modular flow, relative entropy from Araki's perspective, the Petz map, and basic Tomita–Takesaki theory. In Section 3, we provide background on existing results for exact entanglement wedge reconstruction in infinite dimensions. In Section 4, we introduce the notions of approximate privacy and correctability for quantum channels, as well as a fundamental result that relates them. In Section 5, we utilize this result to prove that an approximate modified-JLMS formula implies approximate complementary recovery in the reconstruction wedge. In Section 6, we move on to the state-dependent case, beyond the reconstruction wedge. We describe the properties of black hole α-bits in the case of an infinite-dimensional boundary Hilbert space, and we study the fundamental differences between our framework and the use of a universal recovery channel. In particular, we find that our framework, although non-constructive, is more robust, and valid up to nonperturbative errors in G_N. In Section 7, we explain how this perspective can help understanding various physical settings from our result, and provide some promising research directions. In particular, we explain how to connect our algebraic approach with the gravitational path integral and probing averages over theories. We study in detail the modified-JLMS condition, which we utilized as an assumption to our main theorem, and show the relevance of our framework in the case of an evaporating black hole.

9.2 Preliminaries: algebraic perspective

In this section, we describe various mathematical objects that are used in this chapter for studying entanglement wedge reconstruction. We also give some important properties of these objects.

Conditional expectations

For holographic theories, the algebra of observables of quantum field theory on a fixed spacetime geometry is usually described as a von Neumann algebra acting on a Hilbert space, which is then isometrically embedded in a bigger Hilbert space onto which a bigger von Neumann algebra acts.

Motivated by this picture, we want to have an appropriate way to project any element of a von Neumann algebra onto a smaller one. The right object to consider for such an operation is a *conditional expectation*, which can be defined as the following.

Definition 9.2.1. Let M be a von Neumann algebra and N be a von Neumann subalgebra of M. A conditional expectation from M to N is a positive linear map

$$E : M \to N$$

satisfying, for $A \in M$ and $B, C \in N$,

$$E(Id) = Id, \quad E(BAC) = BE(A)C.$$

One should think of a conditional expectation as the abstract equivalent of "tracing out degrees of freedom." It takes into account the fact that an observer may only have an access to part of the information contained in a quantum system - in our case, the code subalgebra.

The properties of conditional expectations, and how they interact with the states of the theory, will be at the heart of our discussion on entanglement wedge reconstruction. Indeed, as we will shortly see, in the exact picture, the holographic map can be identified with a conditional expectation [164].

Tomita–Takesaki theory and modular flow

Tomita–Takesaki theory is fundamental in the theory of von Neumann algebras. We briefly define the main objects appearing in this theory, and state the Tomita–Takesaki theorem. We utilize these concepts for our purposes to study relative entropies and the modular flow.

Definition 9.2.2. A vector $|\Psi\rangle \in \mathcal{H}$ is *cyclic* with respect to a von Neumann algebra M acting on a Hilbert space $\mathcal{H}$ when the vectors $O |\Psi\rangle$ for $O \in M$ form a dense set in $\mathcal{H}$.

Definition 9.2.3. A vector $|\Psi\rangle \in \mathcal{H}$ is *separating* with respect to a von Neumann algebra M when $O |\Psi\rangle = 0 \implies O = 0$ for $O \in M$.

It is important to note that a cyclic and separating state can be interpreted as a state that sufficiently entangles the observables of the algebra M with the rest of the system. In finite-dimensions, a state being cyclic and separating for a given algebra boils down to its restriction to the algebra being a thermal density matrix.

We remind the reader that states on von Neumann algebras can be defined as norm-continuous positive linear functionals of norm 1 directly.

Definition 9.2.4. A state ω on a von Neumann algebra M is *normal* if for any uniformly bounded, monotone, increasing net of positive operators $H_\alpha \in M$,

$$\omega(\sup_\alpha H_\alpha) = \sup_\alpha \omega(H_\alpha).$$

The predual M_* of the von Neumann algebra M is then spanned by the normal states.

Definition 9.2.5. A state ω on a von Neumann algebra M is *faithful* if for $A \in M$,

$$\omega(A^*A) = 0 \implies A = 0.$$

It is easy to see that a separating vector for the von Neumann algebra M induces a faithful state on M.

With these refined properties of states formulated in an algebraic manner, we now further define (relative) modular operators, first on a certain subset of the Hilbert space.

Definition 9.2.6. Let $|\Psi\rangle, |\Phi\rangle \in \mathcal{H}$ and M be a von Neumann algebra. The *relative Tomita operator* is the closure of the operator $S_{\Psi|\Phi}$ defined by

$$S_{\Psi|\Phi} O |\Psi\rangle := O^\dagger |\Phi\rangle$$

for $O \in M$.

If $|\Psi\rangle$ is cyclic and separating with respect to the von Neumann algebra M, the relative Tomita operator can be defined on a dense subset of the Hilbert space.

Theorem 9.2.7 ([263], p.94). *Let* $|\Psi\rangle, |\Phi\rangle \in \mathcal{H}$ *be cyclic and separating vectors with respect to a von Neumann algebra M. Let* $S_{\Psi|\Phi}$ *and* $S'_{\Psi|\Phi}$ *be the relative Tomita operators respectively defined with respect to M and its commutant M'. Then*

$$S^\dagger_{\Psi|\Phi} = S'_{\Psi|\Phi}, \quad S'^\dagger_{\Psi|\Phi} = S_{\Psi|\Phi}. \tag{9.2}$$

Definition 9.2.8. Let $S_{\Psi|\Phi}$ be the relative Tomita operator for two vectors $|\Psi\rangle, |\Phi\rangle \in \mathcal{H}$, which are cyclic and separating with respect to a von Neumann algebra M. The *relative modular operator* is

$$\Delta_{\Psi|\Phi} := S^\dagger_{\Psi|\Phi} S_{\Psi|\Phi}.$$

When $|\Psi\rangle$ and $|\Phi\rangle$ are the same vector, the relative Tomita operator specializes into a Tomita operator as follows.

Definition 9.2.9. Let M be a von Neumann algebra on $\mathcal{H}$ and $|\Psi\rangle$ be a cyclic and separating vector for M. The *Tomita operator* S_Ψ is

$$S_\Psi := S_{\Psi|\Psi},$$

where $S_{\Psi|\Psi}$ is the relative modular operator defined with respect to M. The *modular operator* $\Delta_\Psi = S^\dagger_\Psi S_\Psi$ and the *modular conjugation* J_Ψ are the operators that appear in the polar decomposition of S_Ψ such that

$$S_\Psi = J_\Psi \Delta_\Psi^{1/2}.$$

We note that the modular operator given by a state defined by a thermal density matrix in finite-dimensions has a simple expression: it is just the thermal density matrix itself. In particular, its logarithm coincides with the familiar notion of modular Hamiltonian.

The Tomita–Takesaki theorem is a powerful tool to study properties of von Neumann algebras, which is given as the following.

Theorem 9.2.10 (Tomita–Takesaki [434]). *Let M be a von Neumann algebra on* $\mathcal{H}$ *and let* $|\Psi\rangle$ *be a cyclic and separating vector for M. Then*

- $J_\Psi M J_\Psi = M'$.

- $\Delta_\Psi^{it} M \Delta_\Psi^{-it} = M \quad \forall t \in \mathbb{R}$.

This theorem shows that, associated to each cyclic separating state, there is a canonical "time evolution" given by the modular flow. This flow can be defined through conjugating an algebra element by imaginary powers of the modular operator, and its physical interpretation is that the restriction of the state $|\psi\rangle$ to M is at thermal equilibrium with respect to its modular flow [118]. In quantum field theory, the Bisognano–Wichmann theorem [213] shows that the modular flow of the vacuum generates boosts for Rindler wedges. The fact that the vacuum is at thermal equilibrium with respect to these boosts is then related to the Unruh effect.

We do not require any additional structure in our main results. However, our setup can be applied to more structured particular cases as well where there exists a more general definition of modular objects for non-cyclic and non-separating vectors; see for example [96].

The Connes cocycle and Araki's relative entropy

Based on the notion of modular flow, we can now define the Connes cocycle of two states ψ and φ, with φ faithful and normal.

Definition 9.2.11. Let ψ and φ be two states on a von Neumann algebra M, with φ faithful and normal. The Connes cocycle of ψ and φ is defined as

$$[D\psi : D\varphi]_t := \Delta_{\psi|\varphi}^{it} \Delta_{\varphi}^{-it}.$$

It is a highly nontrivial result that the Connes cocycle of two states on M is always in M. In other words, the difference between modular flows of two states is always an inner automorphism. The Connes cocycle has a nice geometric interpretation in AdS/CFT [80], and it would be nice to understand it in more detail in the context of our framework.

Another useful quantity to define from Tomita–Takesaki theory is Araki's relative entropy, which is provided in Definition 9.2.12.

Definition 9.2.12 (Araki [24])**.** Let $|\Psi\rangle, |\Phi\rangle \in \mathcal{H}$ and $|\Psi\rangle$ be cyclic and separating with respect to a von Neumann algebra M. Let $\Delta_{\Psi|\Phi}$ be the relative modular operator. The *relative entropy* with respect to M of $|\Psi\rangle$ is

$$S_{\Psi|\Phi}(M) = -\langle\Psi| \log \Delta_{\Psi|\Phi} |\Psi\rangle.$$

It is important to note that Araki's relative entropy can be obtained from the Connes cocycle by the following formula:

$$S(\omega, \varphi) = i \lim_{t \to 0^+} t^{-1} (\omega([D\varphi : D\omega]_t) - 1). \tag{9.3}$$

This formula shows that Araki's relative entropy can be thought of as a sort of derivative of an expectation value of the Connes cocycle flow.

Araki's notion of relative entropy will be the main tool coming from Tomita–Takesaki theory that we will require in this chapter. Indeed, the equivalence of relative entropies between the bulk and the boundary is one of the equivalent characterizations of exact entanglement wedge reconstruction, as well as the starting point of our theorem, which tackles approximate recovery settings that include nonperturbative gravity corrections.

It is important to remind the readers that there exists a generalization of the notion of relative entropy that allows to define it even for non-cyclic and non-separating states, and satisfies the Pinsker inequality. The details can be found in [362].

The Petz map from Tomita–Takesaki theory

A map that is often used in the context of entanglement wedge reconstruction is the Petz map [130, 104]. This map has a particularly nice property as a natural map between a von Neumann algebra and a von Neumann subalgebra leaving a given state φ invariant.

Definition 9.2.13. Let $M_{code} \subset M_{phys}$ be two von Neumann algebras acting on a Hilbert space $\mathcal{H}$. Let $|\Phi\rangle$ be a cyclic separating vector for M_{phys}, and J the associated modular conjugation. Similarly, let J_0 be the modular conjugation for M_{code} acting on $\overline{M_{code} |\Phi\rangle}$. Let P be the orthogonal projection onto $\overline{M_{code} |\Phi\rangle}$. Then, the Petz map E_φ associated to $|\Phi\rangle$ is given by

$$E_\varphi(A) := J_0 P J A J P J_0,$$

and can be seen as the dual of the von Neumann algebra embedding.

It is important to note that this E_φ is a map from M_{phys} to M_{code} and satisfies

$$\varphi \circ E_\varphi = \varphi. \tag{9.4}$$

However, nothing tells us that the Petz map will follow the axioms of a conditional expectation![1] In fact, we explain a necessary and sufficient condition for it to be a conditional expectation in Section 9.3 via a theorem of Takesaki. We want to emphasize this aspect as the cases where the Petz map is a conditional expectation will coincide with the cases of exact entanglement wedge reconstruction in our discussion. When taking into account corrections from gravitational effects that are nonperturbative in G_N, the "exact" entanglement wedge reconstruction breaks down. In this scenario with gravitational corrections, the situation will be much more subtle and the Petz map will no longer be a good description of entanglement wedge reconstruction in general, although we will briefly comment on the efficacy of the twirled version of the Petz dual of a noisy channel in Section 9.6.

9.3 Exact infinite-dimensional entanglement wedge reconstruction

We review the code subspace formalism for the exact correspondence between entanglement wedge reconstruction and relative entropy equivalence. This perspective is first introduced in [225], later extended to infinite-dimensional settings in [270, 269, 164], and this technology has even been further expanded to state-dependent contexts in [196]. Combining these results together in our setting, we provide a summarizing theorem that describes the mathematical structure underlying this formalism, including conditional expectations, the Petz map, and Takesaki's theorem.

Entanglement wedge reconstruction in the code subspace formalism

The Ryu–Takayanagi formula, which relates the generalized entropy of a semiclassical bulk state of AdS/CFT to the entanglement entropy of the corresponding boundary state, is equivalent to relative entropy conservation between bulk and boundary [254] and the quantum error correcting structure of the semiclassical limit of AdS/CFT, which allows us to see the space of states that represent effective field theory on a fixed curved background in the bulk as a code subspace of the space of boundary states.

In the modern information-theoretic formalism, this code subspace of the theory is seen as a vector space isometrically embedded into the physical Hilbert space of quantum gravity. In this setup, bulk reconstruction is seen as the existence of operators acting on the physical Hilbert space that reproduce the action of operators acting on the code subspace. The equivalence between complementary recovery and

---

[1]One should approach with caution the misleading terminology "φ-conditional expectation" for the Petz map, which is often used in the mathematical literature.

the conservation of relative entropy (in the context of infinite-dimensions) has been proven in increasingly general cases [270, 269, 196, 164]. Here, we give a summary theorem that combines these results in the context of von Neumann algebras.

Theorem 9.3.1. *Let $u : \mathcal{H}_{code} \to \mathcal{H}_{phys}$ be an isometric map of Hilbert spaces, let M_{phys} be a von Neumann algebra on $\mathcal{H}_{phys}$ and M_{code} be a von Neumann algebra on $\mathcal{H}_{code}$. Suppose that there exists $|\psi\rangle \in \mathcal{H}_{code}$ such that $u |\psi\rangle$ is cyclic and separating with respect to M_{phys}. Consider two following statements:*

(i) There exist unital normal injective *-homomorphisms $\iota : M_{code} \to M_{phys}$ and $\iota' : M'_{code} \to M'_{phys}$ such that for $O, O' \in M_{code}, M'_{code}$,

$$uO = \iota(O)u, \ uO' = \iota'(O')u.$$

(ii) If $|\varphi\rangle$ and $|\psi\rangle$ are two vectors in $\mathcal{H}_{code}$, then

$$S_{\psi,\varphi}(M_{code}) = S_{u\psi,u\varphi}(M_{phys}), \quad S_{\psi,\varphi}(M'_{code}) = S_{u\psi,u\varphi}(M'_{phys}). \tag{9.5}$$

Then, $(i) \Rightarrow (ii)$.

If we further assume that the set of cyclic and separating vectors with respect to M_{code} is dense in $\mathcal{H}_{code}$ and u maps cyclic and separating states for M_{code} to cyclic and separating states for M_{phys}, then $(i) \Leftrightarrow (ii)$.

Note that in [270], it is not explicitly shown that ι and ι' define unital, normal, injective *-homomorphisms. However, it is a straightforward consequence of the fact that $u |\psi\rangle$ is cyclic and separating with respect to M_{phys} and M'_{phys}: the separating property directly implies homomorphism properties as well as unitality and injectivity, while normality follows from Proposition 2.5.11 of [17].

In the next subsection, we show how Theorem 9.3.1 is deeply related to some well-explored concepts in the theory of von Neumann algebras, such as conditional expectations and an important theorem of Takesaki [435].

Link to conditional expectations and Takesaki's theorem

Under the assumptions Theorem 9.3.1, we can infer that the reconstruction operators $\iota(O)$ form a von Neumann subalgebra of M_{phys}. We suppose that the assumptions of Theorem 9.3.1 are satisfied. Utilizing this setup, we now turn to constructing a conditional expectation from M_{phys} onto $\iota(M_{code})$.

In the proofs of the various results available on exact entanglement wedge reconstruction in infinite-dimensions [270, 164], a crucial lemma showed that if $O \in M_{phys}$, then $u^\dagger O u \in M_{code}$. It follows that the map

$$E : O \longmapsto \iota(u^\dagger O u) \tag{9.6}$$

is well-defined from M_{phys} to $\iota(M_{code})$ and satisfies the conditional expectation property. Indeed, we see that the identity is preserved under this map,

$$E(Id) = \iota(u^\dagger u) = Id, \tag{9.7}$$

and if $A \in M_{phys}$ and $B, C \in M_{code}$,

$$E(\iota(B)A\iota(C)) = \iota(u^\dagger \iota(B)A\iota(C)u) = \iota(Bu^\dagger AuC) = \iota(B)\iota(u^\dagger Au)\iota(C) = \iota(B)E(A)\iota(C). \tag{9.8}$$

Moreover, E leaves any state of the form $u\,|\varphi\rangle$ invariant, if $|\varphi\rangle$ is cyclic and separating for M_{code}. For such cases, we see that $u\,|\varphi\rangle$ is cyclic and separating for M_{phys} and, for $A \in M_{phys}$,

$$\langle\varphi|\,u^\dagger E(A)u\,|\varphi\rangle = \langle\varphi|\,u^\dagger uu^\dagger Au\,|\varphi\rangle = \langle\varphi|\,u^\dagger Au\,|\varphi\rangle. \tag{9.9}$$

This remark directs us towards a more conceptual understanding of entanglement wedge reconstruction. Indeed, the isometry u provides us with a conditional expectation, that projects M_{phys} onto $\iota(M_{code})$ and preserves the states in the code subspace. This is the definition of a *sufficient* von Neumann algebra inclusion, which is the cornerstone of the framework of exact entanglement wedge reconstruction.

Interestingly, this structure can be interpreted as a theorem of Takesaki in [435]. In fact, this theorem shows the equivalence between the existence of a state-preserving conditional expectation, from a von Neumann algebra onto one of its subalgebras, and the stabilization of this subalgebra under the modular flow of the state. We rephrase this theorem as Theorem 9.3.2.

Theorem 9.3.2 (Takesaki [435])**.** *Let φ be a faithful normal state on a von Neumann algebra M, and let N be a von Neumann subalgebra of M. Then, there exists a faithful normal conditional expectation $E : M \to N$ such that $\varphi \circ E = \varphi$ if and only if $\sigma_t(N) \subset N$, where σ_t is the modular flow associated to φ for the von Neumann algebra M. Moreover, the conditional expectation E which realizes the sufficiency condition is unique, and coincides with the Petz map of φ.*

From this perspective, in the code subspace formalism, all states of the form $u |\psi\rangle$, with $\psi \in \mathcal{H}_{code}$, are preserved under the conditional expectation E. Then, in particular, E corresponds to the Petz map of these states, and the algebra $\iota(M_{code})$ is preserved under modular flow. Under the conditions of Takesaki's theorem, it is then possible to prove the following: for all faithful normal states ω, φ on M_{phys} induced by vectors of the form $u |\omega\rangle, u |\varphi\rangle \in \mathcal{H}_{phys}$ with $|\omega\rangle, |\varphi\rangle \in \mathcal{H}_{code}$ [362],

(i) Connes cocycles are conserved:

$$[D\omega : D\varphi]_t = [D\omega|_{\iota(M_{code})} : D\varphi|_{\iota(M_{code})}]_t. \tag{9.10}$$

(ii) Relative entropies are conserved:

$$S_{\omega,\varphi}(M_{phys}) = S_{\omega|_{\iota(M_{code})},\varphi|_{\iota(M_{code})}}(\iota(M_{code})). \tag{9.11}$$

(iii) Petz maps coincide:

$$E_\varphi = E_\omega. \tag{9.12}$$

Limitations of the exact approach

We briefly comment on how the exact approach is insufficient to capture some crucial aspects of entanglement wedge reconstruction in AdS/CFT. First, one has to bear in mind that the AdS/CFT duality is a large N statement from a CFT perspective: as N is taken to be large but finite, there will be quantum corrections obstructing the ideal picture of a reconstruction through a conditional expectation, and this will make the picture break down. In other words, making Newton's constant G_N finite breaks the exact quantum error correcting code structure. This is not a mere technicality and it has been pointed out in [276, 231, 379] that handling approximation is crucial for understanding the semiclassical limit of AdS/CFT and accounts for important physical aspects of the correspondence. In particular,

- The redundancy in the bulk-to-boundary encoding can only be consistent with the Reeh-Schlieder theorem on the boundary if entanglement wedge reconstruction is approximate (with an error that may be nonperturbative in G_N) [276].

- For a state-independent recovery to be possible in the approximate setting, a local bulk operator has to be in the entanglement wedge of *all pure and mixed states* of the corresponding boundary region (this is called the *reconstruction wedge*) [231]. This feature cannot be seen through an exact approach.

- The presence of nonperturbative errors in bulk reconstruction is crucial to the resolution of the black hole information paradox [379].

Our goal is then to generalize, to an approximate setting, the relation between entanglement wedge reconstruction and the relative entropy equivalence between bulk and boundary. In turn, this requires borrowing and extending the concept of approximate complementary recovery, introduced in the context of AdS/CFT in [231]. In the remainder of the chapter, we combine this toolkit and the operator-algebraic perspective to extend the results from [270, 269, 196] to an approximate setting.

In order to reach this objective, we first need to introduce some vocabulary regarding correctability and privacy for infinite-dimensional von Neumann algebras, as well as an important result due to Crann–Kribs–Levene–Todorov [131], which will be at the heart of our proof, and can be seen as an infinite-dimensional generalization of the information-disturbance tradeoff theorem [285]. We will present and utilize this machinery to derive an approximate relation between entanglement wedge reconstruction and relative entropy conservation between bulk and boundary.

9.4 Private and correctable algebras and complementary recovery

The strongest argument for entanglement wedge reconstruction is the argument of Dong–Harlow–Wall in [142], which derives entanglement wedge reconstruction from the modified-JLMS formula. As demonstrated in [231], there are many subtleties related to the problem of generalizing the argument of [142] to the approximate case; in particular, an operator can be reconstructed on the boundary in a state-independent way only if it is in the entanglement wedge of all pure and mixed states in the code subspace. If indeed this is the case, then the main ingredient for proving that the modified-JLMS formula implies approximate reconstruction is the information-disturbance tradeoff [285].

Here, we introduce a framework which will allow us to generalize this notion to the case of an infinite-dimensional boundary Hilbert space for the CFT, as expected in any quantum field theoretic setting. The main ingredients for constructing this Hilbert space setting involve the notions of completely bounded norm, (approximately) private and correctable algebras, as well as a theorem by Crann, Kribs, Levene, and Todorov [131]. In particular, we take the norm to be the completely bounded norm, as it is the one appropriate for state-independent recovery. In fact, the completely bounded norm takes into account an extra tensor factor representing

an auxiliary system, and that is crucial for recreating all pure and mixed states on the code subspace. As such, a completely bounded norm bound will quantify the quality of a recovery quantum channel with respect to all states at the same time. We expect the completely bounded norm to be bounded whenever the we can perform a recovery in a state-independent fashion. We utilize a region called *reconstruction wedge* to describe the appropriate geometric region of the semi-classical gravitational dual where state-independent recovery is possible.

The completely bounded norm, privacy, and correctability

In order to utilize a von Neumann algebra construction for our setup, we need to introduce a new norm for bounded linear maps, which is called *completely bounded norm*.

Definition 9.4.1. Let $\varphi : M \to N$ be a bounded linear map between two von Neumann algebras. We define the *completely bounded norm* of φ as

$$\|\varphi\|_{cb} := \sup_{k \in \mathbb{N}} \|\varphi \otimes Id_{\mathcal{M}_k(\mathbb{C})}\|.$$

If this quantity is finite, then we say that φ is *completely bounded*.

In particular, one can prove that a quantum channel (i.e., a normal, unital, completely positive map) is always completely bounded. Another nice property (called Smith's lemma) is that if N is of the form $\mathcal{M}_n(\mathbb{C})$, then the supremum in the definition can be only taken for $k \leq n$.

The completely bounded norm is the "Heisenberg picture" equivalent of the notion of diamond norm, which appears more often in the quantum information literature. However, the completely bounded norm is more natural in our operator-algebraic setting, and also reacts better with the conditional expectation-like structure we will use.

We now give the definition of a private algebra with respect to a quantum channel (i.e., a normal, unital, completely positive map).

Definition 9.4.2. Let $\mathcal{H}$ be a Hilbert space, M be a von Neumann algebra, and $\mathcal{E} : M \to \mathcal{B}(\mathcal{H})$ a quantum channel. A von Neumann algebra $N \subset \mathcal{B}(\mathcal{H})$ is said to be *private* for $\mathcal{E}$ if $\mathcal{E}(M) \subset N'$. For $\varepsilon > 0$, N is said to be *ε-private* for $\mathcal{E}$ if there exists another quantum channel $\mathcal{P} : M \to \mathcal{B}(\mathcal{H})$ such that N is private for $\mathcal{P}$ and $\|\mathcal{E} - \mathcal{P}\|_{cb} \leq \varepsilon$.

The interpretation of a private algebra for a given quantum channel is that none of the information it contains is accessible from the domain of the quantum channel. For instance, in an exact idealization of AdS/CFT, if A is a boundary region with entanglement wedge a, then the bulk algebra of a is private with respect to the complement of A for the usual boundary to bulk map. We will show that a similar statement holds in the approximate case, in a somewhat smaller region called the *reconstruction wedge*.

The "dual" notion of privacy is that of correctability, which is given by the following definition:

Definition 9.4.3. Let $\mathcal{H}$ be a Hilbert space, M be a von Neumann algebra, and $\mathcal{E} : M \to \mathcal{B}(\mathcal{H})$ a quantum channel. A von Neumann algebra $N \subset \mathcal{B}(\mathcal{H})$ is said to be *correctable* for $\mathcal{E}$ if there exists a quantum channel $\mathcal{R} : N \to M$ such that $\mathcal{E} \circ \mathcal{R} = Id_N$. For $\varepsilon > 0$, N is said to be *ε-correctable* for $\mathcal{E}$ if there exists a quantum channel $\mathcal{R} : N \to M$ such that $\|\mathcal{E} \circ \mathcal{R} - Id_N\|_{cb} \leq \varepsilon$.

In the exact setting, correctability of the entanglement wedge a of region A corresponds to the existence of the *-homomorphism ι between the algebra M_{code} and M_{phys}, respectively, corresponding to a and A.

Note that both in the definition of a private algebra and in the definition of a correctable algebra, we have resorted to the completely bounded norm, rather than the usual operator norm. Such a distinction is crucial in order for the next theorem to work, and can be traced back to the fact that state-independent reconstruction of a bulk operator is only possible if it is in the entanglement wedge of *both pure and mixed* states in the code subspace.

A duality between privacy and correctability

If $\mathcal{H}$ is a Hilbert space, M a von Neumann algebra, and $\mathcal{E} : M \to \mathcal{B}(\mathcal{H})$ a quantum channel, recall that by the Stinespring dilation theorem [421], there exist a Hilbert space $\mathcal{K}$, a representation π of M on $\mathcal{K}$ and an isometry $V : \mathcal{H} \to \mathcal{K}$ such that for $A \in M$,

$$\mathcal{E}(A) = V^{\dagger}\pi(A)V. \tag{9.13}$$

Following [131], we call the datum $(\pi, V, \mathcal{K})$ a Stinespring triple for $\mathcal{E}$. Given a Stinespring triple, it is natural to define the complementary channel of a channel $\mathcal{E}$ on the commutant of $\pi(M)$, which we give below as Definition 9.4.4.

Definition 9.4.4. Let $\mathcal{H}$ be a Hilbert space, M be a von Neumann algebra, and $\mathcal{E} : M \to \mathcal{B}(\mathcal{H})$ a quantum channel. Let $(\pi, V, \mathcal{K})$ be a Stinespring triple for $\mathcal{E}$. We define the complementary channel for the triple $(\pi, V, \mathcal{K})$, $\mathcal{E}^c : \pi(M)' \to \mathcal{B}(\mathcal{H})$, by

$$\mathcal{E}^c(A) := V^\dagger A V.$$

With this definition in hand, we now have the tools to describe the main theorem of this section, which is the crucial ingredient of our discussion of approximate recovery in the reconstruction wedge, by Crann, Kribs, Levene, and Todorov:

Theorem 9.4.5 (Crann–Kribs–Levene–Todorov[131])**.** *Let $\mathcal{H}$ be a Hilbert space, M be a von Neumann algebra on a Hilbert space $\mathcal{K}$, and $\mathcal{E} : M \to \mathcal{B}(\mathcal{H})$ a quantum channel. If a von Neumann subalgebra $N \subset \mathcal{B}(\mathcal{H})$ is ε-private (resp. ε-correctable) for $\mathcal{E}$, then it is $2\sqrt{\varepsilon}$-correctable (resp. $8\sqrt{\varepsilon}$-private) for any complementary channel to $\mathcal{E}$.*

This result is far from trivial, and states that there is an equivalence between being approximately private (i.e., almost no information in the bulk region is accessible from the boundary region), and having an approximately correctable commutant (i.e., almost all information in the bulk region can be reconstructed in the complementary boundary region), in a Stinespring representation.

We now pause for a moment to consider the specific case of $\varepsilon = 0$, before moving on to the approximate case. The case $\varepsilon = 0$ shows that being *exactly* private for a given quantum channel implies being *exactly* correctable for any complementary channel. In holographic settings, we retrieve the result of Dong–Harlow–Wall for the case of finite-dimensional Hilbert spaces [142]. This provides a check on our infinite-dimensional construction as a natural generalization of the gravitational recovery.

Indeed, in the code subspace formalism, consider a von Neumann algebra M_A acting on $\mathcal{H}_{phys}$, and its commutant M'_A. Introduce the code subspace injection $V : \mathcal{H}_{code} \to \mathcal{H}_{phys}$. Then we denote M_a and M'_a as the bulk entanglement wedge algebras that correspond to A and its complement. Since relative entropy has to be conserved, for any two normal states ρ and φ with finite relative entropy in the code subspace,

$$S_{\rho \circ \mathcal{E}^c, \, \varphi \circ \mathcal{E}^c}(M'_A) = S_{\rho, \varphi}(M'_a). \tag{9.14}$$

Now suppose that there exists a normal norm-one projection $\mathcal{P}_{a'}$ from $\mathcal{B}(\mathcal{H}_{code})$ onto M'_a. In particular, for $\varphi = \rho \circ \mathcal{P}_{a'}$, the relative entropy conservation formula gives

$$S_{\rho \circ \mathcal{E}^c, \, \rho \circ \mathcal{P}_{a'} \circ \mathcal{E}^c}(M'_A) = 0. \tag{9.15}$$

This implies that for all normal states ρ,

$$\rho \circ \mathcal{E}^c = \rho \circ \mathcal{P}_{a'} \circ \mathcal{E}^c. \tag{9.16}$$

This being true independently of the choice of ρ, we deduce

$$\mathcal{E}^c = \mathcal{P}_{a'} \circ \mathcal{E}^c. \tag{9.17}$$

This implies that the algebra M_a is private for the quantum channel $\mathcal{E}^c$, so it is correctable for the quantum channel $\mathcal{E}$. The same argument holds for M'_a as long as there exists a normal norm one projection $\mathcal{P}_a$ onto M_a.[2] Thus, we have proven complementary recovery, in an operator-algebraic way that closely echoes the Dong–Harlow–Wall argument [142]. We thus obtain an exact result on exact holographic recovery in Theorem 9.4.6. This new exact theorem is similar to Theorem 9.3.1 but now it is in a setting that can be naturally generalized to include nonperturbative gravity corrections to give rise to Theorem 9.1.1.

Theorem 9.4.6. *Let $V : \mathcal{H}_{code} \to \mathcal{H}_{phys}$ be an isometry, let M_{code} be a von Neumann algebra on $\mathcal{H}_{code}$ and M_{phys} be a von Neumann algebra on $\mathcal{H}_{phys}$. Let $\mathcal{E}$ be the quantum channel $V^\dagger(\cdot)V$ on M_{phys}. Suppose that there exists a normal norm one projection $\mathcal{P}_{code} : \mathcal{B}(\mathcal{H}_{code}) \to M'_{code}$, and that for all normal states ρ and φ on M'_{code},*

$$S_{\rho \circ \mathcal{E}^c, \, \varphi \circ \mathcal{E}^c}(M'_{phys}) = S_{\rho, \varphi}(M'_{code}).$$

Then M_{code} is exactly correctable from M_{phys}.

In particular, when conservation of relative entropy and the existence of a normal norm one projection are satisfied for both M_{phys} and M'_{phys}, exact complementary recovery can be realized.

---

[2]We will see that this is equivalent to M'_a being a product of type I factors.

9.5 State-independent approximate recovery in the reconstruction wedge

With the theorems and results of Section 9.4 at hand, we have all the ingredients needed to derive a new result incorporating nonperturbative gravitational effects to the recovery. This requires the setting of *approximate recovery* with respect to reconstruction of bulk operators in the *reconstruction wedge*. This can be viewed both as a direct extension of infinite-dimensional exact recovery [196] to a precise approximate recovery setup, that includes nonperturbative gravitational errors, and an infinite-dimensional generalization of finite-dimensional approximate recovery [231].

Setup

We consider a time slice of a CFT on the boundary of some asymptotically AdS spacetime, which we divide into two subregions A and $\overline{A}$. We associate to A and $\overline{A}$ von Neumann algebras M_A and $M_{\overline{A}}$ acting on the CFT Hilbert space $\mathcal{H}_{phys}$, and we suppose that Haag duality [213] is valid on the boundary:

$$M_{\overline{A}} = M'_A. \tag{9.18}$$

We consider a bulk Hilbert space $\mathcal{H}_{code}$, as well as an isometry

$$V : \mathcal{H}_{code} \to \mathcal{H}_{phys}. \tag{9.19}$$

In what follows, we are interested in the quantum channel $\mathcal{E}$ given by

$$\begin{aligned} \mathcal{E} : M_A &\longrightarrow \mathcal{B}(\mathcal{H}_{code}), \\ A &\longmapsto V^\dagger A V, \end{aligned} \tag{9.20}$$

for this isometry V, as well as its complementary channel $\mathcal{E}^c$ for the same isometry V as

$$\begin{aligned} \mathcal{E}^c : M'_A &\longrightarrow \mathcal{B}(\mathcal{H}_{code}), \\ A &\longmapsto V^\dagger A V. \end{aligned} \tag{9.21}$$

Note that in the exact setting, these maps composed with their recovery channels would correspond to the holographic conditional expectation, and they would exactly map M_A to the bulk algebra M_a of its entanglement wedge, and $M_{\overline{A}}$ to the bulk algebra $M_{\overline{a}}$ of its entanglement wedge.

In our new setup, the situation will be slightly more complicated; however, one can still associate a bulk algebra M_a to the *reconstruction wedge* of A, which corresponds

to the intersection of the entanglement wedges of *A* with respect to all *mixed* states in the code subspace, i.e., mixed with respect to $\mathcal{B}(\mathcal{H}_{code})$.[3] In order to take these mixed states into account (and to give them a physical interpretation), the easiest resolution is to introduce a copy of the code subspace $\mathcal{H}^*_{code}$ and consider the doubled Hilbert space $\mathcal{H}_{code} \otimes \mathcal{H}^*_{code}$. This doubled Hilbert space can be obtained from the GNS representation of any faithful normal (i.e., KMS) state on $\mathcal{B}(\mathcal{H}_{code})$, and it is also often identified with the standard form Hilbert space of $\mathcal{B}(\mathcal{H}_{code})$.[4] The maps $\mathcal{E}$ and $\mathcal{E}^c$ can then be canonically extended such that

$$\mathcal{E} \longrightarrow \mathcal{E} \otimes Id \quad \text{on} \quad M_A \otimes \mathcal{B}(\mathcal{H}^*_{code}), \tag{9.22a}$$

$$\mathcal{E}^c \longrightarrow \mathcal{E}^c \otimes Id \quad \text{on} \quad M'_A \otimes \mathcal{B}(\mathcal{H}^*_{code}). \tag{9.22b}$$

Furthermore, any normal mixed state on $\mathcal{B}(\mathcal{H}_{code})$ has a vector purification on $\mathcal{H}_{code} \otimes \mathcal{H}^*_{code}$. For technical reasons associated to the definition of the completely bounded norm and subtleties regarding tensor products of operator algebras in infinite-dimensions, in the case in which $\mathcal{H}_{code}$ is infinite-dimensional, we will choose $\mathcal{H}^*_{code}$ to be finite-dimensional of arbitrarily large dimension. This will not change the physics: being able to adjoin an arbitrarily large reference system to $\mathcal{H}_{code}$ will be enough to guarantee state-independent approximate recovery. In fact, this amounts to giving an arbitrarily precise approximation to an infinite-dimensional copy of $\mathcal{H}_{code}$.

Main result

Utilizing the setup of Section 9.5, we now prove our main theorem regarding approximate recovery in the reconstruction wedge for infinite-dimensional Hilbert spaces, which will be coming from the correctability and privacy correspondence. We start by applying the modified-JLMS formula (which we assume here) to two well-chosen code states. Let *a* denote the reconstruction wedge of *A* and *a'* denote its complement in the bulk. Let $\mathcal{P}_{a'}$ denote a normal projection of norm one from $\mathcal{B}(\mathcal{H}_{code})$ onto $M_{a'}$. Before we set up further structures, it is important to note that such a projection will not exist for all possible types of von Neumann algebras. While we do not need further restrictions on the boundary von Neumann algebra, the bulk algebra cannot be completely general. The right assumption to guarantee the existence of such a projection is to suppose that

$$M_{a'} \text{ is } purely \; atomic,$$

---

[3]The necessity to resort to the reconstruction wedge rather than the entanglement wedge in order to obtain a state-independent reconstruction was first pointed out by Hayden and Penington in [231].

[4]For more on this technology, please see [196].

i.e., a product of type I factors [62]. This is slightly more restrictive than just asking for $M_{a'}$ to have type I, as not every direct integral of type I factors can be written as a product. However, finite-dimensional von Neumann algebras, as well as every finite or countable direct sum of type I factors, will satisfy this property. We expect this to be enough to model the bulk algebras in physically relevant situations.

Let ρ be a normal state on $\mathcal{B}(\mathcal{H}_{code} \otimes \mathcal{H}_{code}^*)$. Then, we note that $\rho \circ (\mathcal{E}^c \otimes Id)$ is a state on $M_{\overline{A}} \otimes \mathcal{B}(\mathcal{H}_{code}^*) = M_A' \otimes \mathcal{B}(\mathcal{H}_{code}^*)$.[5] We will apply the modified-JLMS formula for relative entropy to the two states ρ and $\rho \circ (\mathcal{P}_{a'} \otimes Id)$:

$$
\begin{aligned}
|S_{\rho \circ (\mathcal{E}^c \otimes Id), \rho \circ (\mathcal{P}_{a'} \otimes Id) \circ (\mathcal{E}^c \otimes Id)}(M_A' \otimes \mathcal{B}(\mathcal{H}_{code}^*)) - S_{\rho, \rho \circ (\mathcal{P}_{a'} \otimes Id)}(M_{EW(\rho \circ (\mathcal{P}_{a'} \otimes Id), \overline{A} \cup R)}) \\
+ S_{gen}(\rho, EW(\rho, \overline{A} \cup R)) - S_{gen}(\rho, EW(\rho \circ (\mathcal{P}_{a'} \otimes Id), \overline{A} \cup R))| \quad \leq \varepsilon,
\end{aligned}
\tag{9.23}
$$

where ε is nonperturbatively small in G_N. Indeed, while we can naively assume that the highest order correction to this inequality is of order G_N, the quantum extremal surface prescription ensures that only strictly non-zero nonperturbative gravitational errors persist in entanglement wedge reconstruction, with a lower bound [231]

$$
\varepsilon \sim e^{-\kappa/G_N}, \quad \kappa > 0.
\tag{9.24}
$$

These nonperturbative gravitational errors share their origin with the derivation of the Page curve [379]: saddles with nontrivial topologies can only appear when nonperturbative effects are taken into account in the gravitational path integral. This is in contrast with the (H)RT prescription, which is only valid up to $O(1)$.

As we shall show, the second term of the left hand side of equation (9.23) is zero; henceforth, this term is finite, which allows us to apply this formula. Now we analyze the second, third, and fourth terms of this equation (9.23). In the second term, $EW(\rho \circ (\mathcal{P}_{a'} \otimes Id), \overline{A} \cup R)$ denotes the entanglement wedge of the boundary region $\overline{A}$ and the reference system R in the bulk state $\rho \circ (\mathcal{P}_{a'} \otimes Id)$. Recall that the region a' in the bulk is the complement of the intersection of all entanglement wedges in pure and mixed states for A. It follows that no matter how ρ is chosen, $EW(\rho \circ (\mathcal{P}_{a'} \otimes Id), \overline{A} \cup R)$ is always contained in $a' \cup R$. Hence, the states ρ and $\rho \circ (\mathcal{P}_{a'} \otimes Id)$ coincide on it. Thus, we can conclude that the second term is zero.

The third and fourth terms correspond to the generalized entropies, i.e., the sum of the area term and the bulk correction, for the two states ρ and $\rho \circ (\mathcal{P}_{a'} \otimes Id)$.

---

[5]Note that defining the tensor product of von Neumann algebras is subtle, and that there are a lot of different ways to do so. Here, we do not expand on these subtleties, as $\mathcal{H}_{code}^*$ is finite-dimensional, and all definitions coincide in this case.

This may naively pose a problem as we do not know yet how to define a suitable regularization for these generalized entropies in the infinite-dimensional setting. Luckily, however, it does not matter here: as the states ρ and $\rho \circ (\mathcal{P}_{a'} \otimes Id)$ always coincide on the entanglement wedge of $\overline{A} \cup R$ for all states, they give rise to the same quantum extremal surface, and the third and last terms of the equation (9.23) cancel out.

Incorporating these results into the equation (9.23), we obtain a much simpler identity:

$$|S_{\rho \circ (\mathcal{E}^c \otimes Id), \rho \circ (\mathcal{P}_{a'} \otimes Id) \circ (\mathcal{E}^c \otimes Id)}(M'_A \otimes \mathcal{B}(\mathcal{H}^*_{code}))| \leq \varepsilon. \tag{9.25}$$

By Pinsker's inequality [362, Proposition 5.23], this yields

$$\|\rho \circ (\mathcal{E}^c \otimes Id) - \rho \circ (\mathcal{P}_{a'} \otimes Id) \circ (\mathcal{E}^c \otimes Id)\| \leq \sqrt{2\varepsilon}. \tag{9.26}$$

For convenience, we define the difference in the quantum channel $\mathcal{E}^c$ and its projected quantum channel $\mathcal{P}_{a'} \circ \mathcal{E}^c$ as

$$\mathcal{E}^{diff} \equiv \mathcal{E}^c - \mathcal{P}_{a'} \circ \mathcal{E}^c \tag{9.27}$$

such that equation (9.26) can be rewritten as

$$\|\rho \circ (\mathcal{E}^{diff} \otimes Id)\| \leq \sqrt{2\varepsilon}. \tag{9.28}$$

We now utilize the following proposition, which we come back to and prove after the main theorem: Theorem 9.1.1.

Proposition 9.5.1. *Let M and N be two von Neumann algebras and let $\Phi : M \to N$ be a $*$-preserving normal map. Then,*

$$\|\Phi\|_{cb} = \sup_{n \in \mathbb{N}} \sup_{\rho_n} \|\rho_n \circ (\Phi \otimes Id_{M_n})\|, \tag{9.29}$$

where ρ_n varies over normal states on $N \otimes M_n(\mathbb{C})$.

Given that $\mathcal{H}^*_{code}$ can be chosen to have an arbitrarily high dimension if $\mathcal{H}_{code}$ is infinite-dimensional, in that case this can be rewritten using the completely bounded norm:

$$\|\mathcal{E}^{diff}\|_{cb} = \|\mathcal{E}^c - \mathcal{P}_{a'} \circ \mathcal{E}^c\|_{cb} \leq \sqrt{2\varepsilon}. \tag{9.30}$$

This is exactly what we want! By definition of $\mathcal{P}_{a'}$, the von Neumann algebra M_a is private for the quantum channel $\mathcal{P}_{a'} \circ \mathcal{E}^c$, so in turn, it is $\sqrt{2\varepsilon}$-private for $\mathcal{E}^c$.

As the last step, by the correctability and privacy duality as presented in Theorem 9.4.5, it follows that the von Neumann algebra M_a is $2(2\varepsilon)^{\frac{1}{4}}$-correctable for the quantum channel $\mathcal{E}$. In other words, there exists a channel $\mathcal{R} : M_a \to M_A$ such that

$$\|\mathcal{E} \circ \mathcal{R} - Id_{M_a}\|_{cb} \le 2(2\varepsilon)^{\frac{1}{4}}. \tag{9.31}$$

Note that the precise statement of Proposition 9.5.1 cannot be used in the case where $\mathcal{H}_{code}$ is finite-dimensional, as $\mathcal{H}^*_{code}$ is only allowed to have dimension up to that of $\mathcal{H}_{code}$, which means that the supremum can only be taken over $n \le \dim\mathcal{H}_{code}$. After the proof of 9.5.1, we will show that this assumption can actually be made in the case of a finite-dimensional $\mathcal{H}_{code}$.

We can then likewise utilize the privacy-correctability correspondence for the finite-dimensional case, and we conclude that this setup gives rise to approximate recovery. More formally, our result can be summed up and presented as Theorem 9.1.1 below.

Theorem 9.1.1. Let $\mathcal{H}_{code}$ and $\mathcal{H}_{phys}$ be two Hilbert spaces, $V : \mathcal{H}_{code} \to \mathcal{H}_{phys}$ be an isometry, and $\mathcal{H}^*_{code}$ be any finite-dimensional Hilbert space of dimension smaller or equal to the one of $\mathcal{H}_{code}$. Let M_A be a von Neumann algebra on $\mathcal{H}_{phys}$. To each normal state ω in $\mathcal{B}(\mathcal{H}_{code} \otimes \mathcal{H}^*_{code})_*$, we associate two entanglement wedge von Neumann algebras $M_{EW(\omega,A)}$ and $M_{EW(\omega,\overline{A}\cup R)}$ of operators on $\mathcal{H}_{code} \otimes \mathcal{H}^*_{code}$ such that $M_{EW(\omega,\overline{A}\cup R)} \subset M'_{EW(\omega,A)}$. Let

$$M_a := \bigcap_\omega M_{EW(\omega,A)} \subset \mathcal{B}(\mathcal{H}_{code})$$

be the reconstruction wedge von Neumann algebra on $\mathcal{H}_{code}$, and suppose that $M_{a'}$, the commutant of M_a in $\mathcal{B}(\mathcal{H}_{code})$, is a product of type I factors. Suppose that for all choices of $\mathcal{H}^*_{code}$ and all pairs of states ρ, ω in $\mathcal{B}(\mathcal{H}_{code} \otimes \mathcal{H}^*_{code})_*$ such that $S_{\rho,\omega}(M_{EW(\omega,\overline{A}\cup R)})$ is finite, we have the following modified-JLMS condition:

$$|S_{\rho\circ(\mathcal{E}^c\otimes Id),\omega\circ(\mathcal{E}^c\otimes Id)}(M'_A \otimes \mathcal{B}(\mathcal{H}^*_{code})) - S_{\rho,\omega}(M_{EW(\omega,\overline{A}\cup R)})$$
$$+S_{gen}(\rho, EW(\rho, \overline{A} \cup R)) - S_{gen}(\rho, EW(\omega, \overline{A} \cup R))| \ \le \ \varepsilon,$$

where $\mathcal{E}$ and $\mathcal{E}^c$ refer to the respective restrictions of $A \mapsto V^\dagger AV$ to M_A and M'_A, and the function $S_{gen}(\rho, EW(\omega, \overline{A} \cup R))$ depends only on the restrictions of ρ and

ω to $M_{a'} \otimes \mathcal{B}(\mathcal{H}^*_{code})$.[6] Then, there exists a quantum channel $\mathcal{R} : M_a \to M_A$ such that

$$\|\mathcal{E} \circ \mathcal{R} - Id_{M_a}\|_{cb} \leq 2(2\varepsilon)^{\frac{1}{4}}.$$

In Theorem 9.1.1, the von Neumann algebra M_a corresponds to the observables in the reconstruction wedge of the boundary region A. Depending on this boundary region A, we defined the reconstruction wedge, as the notion required for nonperturbative gravitational effects, to be the intersection of all entanglement wedges of pure and mixed states on A. Then, what this theorem entails physically is that utilizing this new reconstruction wedge we can guarantee state-independent reconstruction. On the contrary, observables that are outside the reconstruction wedge but inside a specific entanglement wedge, cannot be reconstructed on this region A in a state-independent manner.

There often exists a macroscopic difference between a fixed entanglement wedge in a code subspace and the reconstruction wedge associated to this code subspace, due to the bulk term in the quantum extremal surface formula that relates the boundary entanglement entropy to the bulk generalized entropy of the entanglement wedge. This bulk term can sometimes be dominant in the presence of a large amount of bulk entropy. This shows the importance of jumps of the entanglement wedge in the presence of gravity; it further suggests that the reconstruction wedge is an important object in the holographic dictionary.

We want to emphasize that this remains true in a generic Hilbert space formalism, both finite and infinite dimensional cases, for the bulk and boundary construction. As the reconstruction wedge is a natural object to consider in the context of quantum extremal surfaces, it would be interesting to determine the boundary dual of the area of the reconstruction wedge.

We further note that the proof of Theorem 9.1.1 remains unchanged if we consider some von Neumann algebra N' containing $M_{a'}$, instead of $M_{a'}$. Even if $M_{a'}$ itself is not purely atomic, any purely atomic algebra N' containing $M_{a'}$ will have a reconstructable commutant. This loosens the assumptions of Theorem 9.1.1, but this particular algebra N would not necessarily correspond to a geometric region in the bulk. If we consider a finite-dimensional code subspace, all algebras are purely atomic, but if the code subspace becomes infinite-dimensional, we expect

---

[6]We note that this assumption summarizes restriction conditions associated to any specific entanglement wedge, of the form $M_{EW(\omega,\overline{A}\cup R)}$, into one single condition.

the existence of such relevant subalgebras to be related to whether or not something like the split property is valid in the bulk. Indeed, the split property [213] provides us with type I factors that approximate local regions in the bulk. Whether the split property is valid in the bulk effective theory is not entirely clear at this stage, as it can sometimes fail for generalized free field theories due to violations of nuclearity bounds. It is an important question to understand better whether something like the split property can be valid in the bulk effective field theory, or perhaps some version of it with perturbative gravity implemented.

We now prove Proposition 9.5.1, which is essential to complete the proof of Theorem 9.1.1.[7] We first recall Proposition 9.5.1.

Proposition 9.5.1. Let M and N be two von Neumann algebras and let Φ be a $*$-preserving normal map. Then,

$$\|\Phi\|_{cb} = \sup_{n \in \mathbb{N}} \sup_{\rho_n} \|\rho_n \circ (\Phi \otimes Id_{M_n})\|, \tag{9.32}$$

where ρ_n varies over normal states on $N \otimes M_n(\mathbb{C})$.

We first prove the two following lemmas that lead to proving this propostition.

Lemma 9.5.2. *Let M be a von Neumann algebra and ω be a normal $*$-preserving linear functional on M. Then, ω attains its norm on a self-adjoint element.*

Proof. Let $A \in M$ on which ω attains its norm. A exists by the Hahn–Banach theorem because M is the dual of M_*. Let ξ a complex number of modulus 1 such that

$$|\omega(A)| = \xi \omega(A). \tag{9.33}$$

Now let

$$H := \frac{\xi A + \bar{\xi} A^\dagger}{2}. \tag{9.34}$$

By the triangle inequality, H is Hermitian of norm smaller or equal to that of A. Moreover, as ω is $*$-preserving,

$$\omega(H) = |\omega(A)|. \tag{9.35}$$

This concludes the proof that ω attains its norm on self-adjoint elements. □

---

[7] We thank Vern Paulsen for communicating ideas of this proof.

Lemma 9.5.3. *Let* $\Phi : M \longrightarrow N$ *be a normal map between von Neumann algebras. Then,*

$$\|\Phi\|_{cb} = \sup_{n\in\mathbb{N}} \|\Phi \otimes Id_{M_n}\|_{sa},$$

where $\|\cdot\|_{sa}$ *means that the supremum in the definition of the norm is restricted to self-adjoint elements of* $M \otimes M_n(\mathbb{C})$.

Proof. Let $A \in M$, and define

$$B := \begin{pmatrix} 0 & A \\ A^\dagger & 0 \end{pmatrix} \in M \otimes M_2(\mathbb{C}). \tag{9.36}$$

Then, B is self-adjoint and $\|B\| = \|A\|$. Moreover,

$$\|(\Phi \otimes Id_{M_2})(B)\| = \max(\|\Phi(A)\|, \|\Phi(A^\dagger)\|). \tag{9.37}$$

This last equality shows that we have the upper and lower bounds

$$\|\Phi\| \leq \|\Phi \otimes Id_{M_2}\|_{sa} \leq \|\Phi \otimes Id_{M_2}\|. \tag{9.38}$$

Iterating the tensor product with Id_{M_2} and taking the supremum, we get

$$\|\Phi\|_{cb} = \sup_{n\in\mathbb{N}} \|\Phi \otimes Id_{M_n}\|_{sa}. \tag{9.39}$$

$\square$

With these two lemmas in hand, we are ready to prove Proposition 9.5.1. By Lemma 9.5.3, for $n \in \mathbb{N}$, we have that

$$\|\Phi\|_{cb} = \sup_{n\in\mathbb{N}} \sup_{A_n \text{ self-adjoint, } \|A_n\|=1} \|(\Phi \otimes Id_{M_n})(A_n)\|. \tag{9.40}$$

We note that the $(\Phi \otimes Id_{M_n})(A_n)$ are all self-adjoint (as Φ is $*$-preserving), and that the norm of a self-adjoint operator in a von Neumann algebra can be obtained by taking the supremum of its values against normal states. Hence, we have

$$\|\Phi\|_{cb} = \sup_{n\in\mathbb{N}} \sup_{A_n \text{ self-adjoint, } \|A_n\|=1} \sup_{\rho_n} |\rho_n((\Phi \otimes Id_{M_n})(A_n))|. \tag{9.41}$$

This precisely yields

$$\|\Phi\|_{cb} = \sup_{n\in\mathbb{N}} \sup_{\rho_n} \|\rho_n \circ (\Phi \otimes Id_{M_n})\|_{sa}. \tag{9.42}$$

We now use Lemma 9.5.2 to drop the self-adjoint condition on the right hand side:

$$\|\Phi\|_{cb} = \sup_{n \in \mathbb{N}} \sup_{\rho_n} \|\rho_n \circ (\Phi \otimes Id_{M_n})\|, \tag{9.43}$$

which concludes the proof of Proposition 9.5.1.

Note that in the case in which $\mathcal{H}_{code}$ is finite-dimensional, this proof only allows us to take the supremum over $n \leq 2 \dim \mathcal{H}_{code}$, which is slightly more restrictive than the assumption $\dim \mathcal{H}^*_{code} \leq \dim \mathcal{H}_{code}$. Here we adapt an argument from [251] to our setting to show that the factor of 2 can in fact be removed: it is enough to take the supremum over

$$n \leq \dim \mathcal{H}_{code}. \tag{9.44}$$

In the case of $\mathcal{H}_{code}$ finite-dimensional, the previous proof shows that there exists a state ρ on $\mathcal{B}(\mathcal{H}_{code}) \otimes \mathcal{B}(K)$, with $\dim K = 2 \dim \mathcal{H}_{code}$, such that

$$\|\Phi\|_{cb} = \|\rho \circ (\Phi \otimes Id_{\mathcal{B}(K)})\|. \tag{9.45}$$

By the triangle inequality, we can assume without loss of generality that ρ is a pure state, i.e., that there exists a vector $|y\rangle \in \mathcal{H}_{code} \otimes K$ such that

$$\rho(A) = \langle y| A |y\rangle. \tag{9.46}$$

We let $\mathcal{H}^*_{code}$ be isomorphic to $\mathcal{H}_{code}$. We can consider an orthogonal projection $\Pi \in \mathcal{B}(K)$ such that

$$\mathrm{rk}\Pi = \dim(\mathcal{H}^*_{code}), \quad |y\rangle = Id_{\mathcal{H}_{code}} \otimes \Pi |y\rangle. \tag{9.47}$$

Then, there exists a linear isometric map $\sigma : \mathcal{H}^*_{code} \to K$ such that $|y\rangle = Id_{\mathcal{H}_{code}} \otimes \sigma\sigma^* |y\rangle$. We are now able to introduce a state

$$|x\rangle := Id_{\mathcal{H}_{code}} \otimes \sigma^* |y\rangle. \tag{9.48}$$

Then we can show that $|x\rangle$ realizes the completely bounded norm:

$$\|\rho \circ (\Phi \otimes Id_{\mathcal{B}(K)})\| = \sup_{\|A\|=1} \langle y| (\Phi \otimes Id_{\mathcal{B}(K)})(A) |y\rangle$$
$$= \sup_{\|A\|=1} \langle x| (Id_{\mathcal{H}_{code}} \otimes \sigma^*)(\Phi \otimes Id_{\mathcal{B}(K)})(A)(Id_{\mathcal{H}_{code}} \otimes \sigma) |x\rangle$$
$$= \sup_{\|A\|=1} \langle x| (\Phi \otimes Id_{\mathcal{B}(\mathcal{H}^*_{code})})(A) |x\rangle = \|(|x\rangle \langle x|) \circ (\Phi \otimes Id_{\mathcal{B}(\mathcal{H}^*_{code})})\|. \tag{9.49}$$

We then deduce that there exists a state φ on $\mathcal{B}(\mathcal{H}_{code} \otimes \mathcal{H}^*_{code})$ such that

$$\|\Phi\|_{cb} = \|\varphi \circ (\Phi \otimes Id_{\mathcal{B}(\mathcal{H}^*_{code})})\|. \tag{9.50}$$

This proves that it is actually enough to consider a reference system $\mathcal{H}^*_{code}$ of dimension smaller or equal to that of $\mathcal{H}_{code}$ in the finite-dimensional case.

9.6 State-dependent recovery beyond the reconstruction wedge

The reconstruction result we derived thus far is completely state-independent: operators inside the reconstruction wedge are inside the entanglement wedge of any pure or mixed state, and we saw that infinite-dimensional privacy/correctability duality allowed to derive state-independent bounds on correctability from a modified version of the JLMS formula.

However, some observables that reach deeper than the reconstruction wedge (for example, the black hole interior), cannot be reconstructed in such a state-independent fashion [370, 371]. Instead, their boundary representatives are *state-dependent*, and this feature has been at the center of many discussions, including understandings of finite [231] to infinite-dimensional [196] Hilbert space settings. In particular, it provides a lot of tools for the resolution of the information paradox [379].

α-bits

Discussions on state-dependence are rooted in the works of Papadodimas–Raju [370, 371], but here we will focus on the modern approach to the problem by Hayden–Penington, through the notion of α-bits [231]. The main idea is that only subspaces whose dimension grows like a certain power of the dimension of the whole code subspace can be recovered inside a black hole.

We first recall the setup of [231], and show how the arguments can be generalized to infinite-dimensions. The idea is to consider a finite-dimensional code subspace, that factorizes into a black hole and an exterior piece

$$\mathcal{H} = \mathcal{H}_{BH} \otimes \mathcal{H}_{ext}, \tag{9.51}$$

with the area-dependence given by

$$\lim_{G_N \to 0} G_N \log d_{BH} = \frac{\mathcal{A}_0}{4}, \tag{9.52}$$

where $\mathcal{A}_0$ is the black hole area. Then, two bulk regions are considered, both anchored in the same boundary region A, of respective areas $\mathcal{A}_1$ and $\mathcal{A}_2$. The region $\mathcal{A}_1$ corresponds to the entanglement wedge of A for a pure boundary state and contains the black hole, whereas the region $\mathcal{A}_2$ corresponds to the entanglement wedge of a thermal boundary state and does not contain the black hole. We then assume that

$$\alpha := \frac{\mathcal{A}_2 - \mathcal{A}_1}{\mathcal{A}_0} \tag{9.53}$$

is strictly smaller than 1. We also assume that the geometric and matter contributions are small outside of the black hole, then it is argued in [231] that there are only 2 possible quantum extremal surfaces for the entanglement wedge, of respective areas $\mathcal{A}_1$ and $\mathcal{A}_2$. In order to be able to get a state-independent recovery for the black hole, one then needs the quantum extremal surface containing the black hole to always be dominant: this is the case when the dimension of the subspace we wish to decode satisfies

$$d \leq e^{\alpha \frac{\mathcal{A}_0}{4G_N}}, \tag{9.54}$$

which is strictly less than the dimension of the black hole Hilbert space. Hence, the previous reasoning only shows that the black hole interior reconstruction is only possible in a state-dependent way. It turns out this $d \leq e^{\alpha \frac{\mathcal{A}_0}{4G_N}}$ is the best possible bound for the dimension of a subspace whose reconstruction can be achieved in a state-independent manner [231].

Let us generalize this argument to the case of an infinite-dimensional boundary Hilbert space. Suppose that the black hole Hilbert space is entangled with a Hilbert space $\mathcal{H}_r$ of dimension d' given by

$$d' = e^{\alpha' \frac{\mathcal{A}_0}{4G_N}}, \quad \text{for} \quad \alpha' > \alpha. \tag{9.55}$$

This Hilbert space $\mathcal{H}_r$ corresponds to a reference system that takes into account all the degrees of freedom the black hole can be entangled to - for example, Hawking radiation. We can then, by our previous reasoning, construct a subspace

$$\mathcal{H}_S \subset \mathcal{H}_{code} \otimes \mathcal{H}_r \tag{9.56}$$

such that the algebra M_b of observables on $\mathcal{H}_S$ located in a region b that contains the black hole, can be reconstructed from $M'_A \otimes \mathcal{B}(\mathcal{H}_r)$ up to nonperturbative error. Indeed, perturbing outside of the black hole but still between the two candidate quantum extremal surfaces cannot change the quantum extremal surface, so it suffices to perturb in such a way around a state which is maximally entangled between the black hole and the reference system in order to construct a subspace of states whose entanglement wedge contains the black hole. Note that if the dimension of $\mathcal{H}_S$ is chosen to be small enough, this is still true even for states that are entangled with a second reference system whose dimension equals the one of $\mathcal{H}_S$. In other words, following the proof of Theorem 5.1, M_b is δ-correctable for $M'_A \otimes \mathcal{B}(\mathcal{H}_r)$ for some nonperturbatively small $\delta > 0$, and also δ'-private for $M_A \otimes Id$ for some nonperturbatively small $\delta' > 0$ by privacy/correctability duality. This shows the impossibility to recover the black hole interior for any $\alpha' > \alpha$.

Universal recovery channel

It is proven in a finite-dimensional context that a universal recovery channel, known as the *twirled Petz map*, can be used to recover any state in a subspace for which the JLMS formula is satisfied [130]. This statement was later extended to the infinite-dimensional case by Faulkner, Hollands, Swingle, and Wang [170, 165]. We use their ideas and rephrase it in the following form for our purposes.

Theorem 9.6.1. *Let $\mathcal{E} : M \longrightarrow N$ be a unital quantum channel between two von Neumann algebras M and N. Let ρ, ω be two normal states on N such that ω is faithful. Then, there exists a channel $\alpha : N \longrightarrow M$, that just depends on ω and $\mathcal{E}$ such that*

$$S_{\rho,\omega}(N) - S_{\rho\circ\mathcal{E},\omega\circ\mathcal{E}}(M) \geq \frac{1}{4}\|\rho \circ \mathcal{E} \circ \alpha - \rho\|^2. \tag{9.57}$$

We first explain how this Theorem 9.6.1 is relevant to our context, without going into details. For our setup, the von Neumann algebras M and N act respectively on the boundary Hilbert space and on the code subspace, and $\mathcal{E}$ represents a boundary-to-bulk map for operators. Note that the analog of a key step in [130] is that if the left hand side of this inequality is small, then it means that the twirled Petz map α is a good choice of recovery channel. This is true when the JLMS condition is satisfied; we emphasize a crucial subtlety that this is different from the modified-JLMS condition. Hence, the twirled Petz map will be a good choice of recovery map only for states that have the same entanglement wedge, for example when the entanglement wedge does not jump and coincides with the reconstruction wedge, or in α-bit spaces.

Hence, Theorem 9.6.1 shows that we may be able to use the twirled Petz map to decode bulk operators in AdS/CFT, both for the reconstruction wedge (with an appropriate choice of ω), and for α-bit subspaces of the code subspace. However, it is important to emphasize that while the privacy/correctability duality provides a robust proof of bulk reconstruction with nonperturbatively small error in G_N in the reconstruction wedge, it is still unclear whether an argument based on the twirled Petz map will be exact at all orders in perturbation theory [231]. Moreover, the bound we get is only in terms of the operator norm, and not in terms of the completely bounded norm. Thus, this type of approximate reconstruction is much weaker than the one we derived through privacy/correctability duality.

9.7 Discussion

We developed in this chapter an operator algebraic framework that includes nonperturbative gravity corrections to entanglement wedge reconstruction. We described it by first formulating the *exact* entanglement wedge reconstruction via Theorem 9.3.1 that summarizes known results, and investigated the conditional expectation structure of the exact holographic map before introducing the *approximate* setting of entanglement wedge reconstruction.

While the exact setting has multiple shortcomings due to gravitational aspects, the approximate nature of bulk reconstruction has many important implications. It is therefore crucial to generalize the infinite-dimensional picture [269, 196, 164] to the approximate setting. We achieve this as portrayed in Theorem 9.1.1, which shows that under a modified-JLMS assumption for the code subspace tensored with a reference system, the local algebra of the *reconstruction wedge* of a boundary region can be approximately reconstructed in a state-independent and dimension-independent manner, as long as its bulk complement is a product of type *I* factors. In particular, this is the case for finite-dimensional code subspaces.

Within this framework, we considered situations beyond the state-independent settings, which requires going beyond the reconstruction wedge. As shown in [231], reconstruction beyond the reconstruction wedge may only be state-dependent, as only the α-bits of the black hole can be reconstructed on the boundary. We showed that our formalism is still enough to account for state-dependent reconstructions with an infinite-dimensional boundary, by resorting to privacy/correctability duality and our main theorem. Furthermore, we pointed out that the universal recovery channel known as the 'twirled Petz map' achieves approximate recovery whenever the (original) JLMS formula is valid, but only at the order G_N^0 and in the sense of the operator norm rather than the completely bounded norm.

On top of formulating new approximation results both in the state-dependent and in the state-independent case for an arbitrary boundary Hilbert space, this chapter can also be seen as containing most known results on exact and approximate entanglement wedge reconstruction as particular cases. Here, we intended to present their most general formulation, which would be useful in the case of an actual CFT on the boundary. This allowed us to construct an exhaustive dictionary between physical notions relevant to holography and operator-algebraic concepts.

We expect our results to be physically relevant at least whenever the boundary theory can be reasonably well-described in terms of algebraic quantum field theory (AQFT).

This approach, based on the Haag–Kastler axioms [214], has several shortcomings, but has proven to be quite useful, in particular for modelling 2d Lorentzian conformal field theories, thanks to the framework of conformal nets [274]. In examples of AdS$_3$/CFT$_2$ where the boundary is described by conformal nets, our results should in particular apply. We also expect that in higher-dimensional examples of holography, at least some of the structures and basic mechanisms uncovered here should survive. We hope to make these statements more precise in the future.

Another interesting place to test out this operator algebraic formulation would be in (limits of) random tensor networks, where error-correction becomes approximate. This, however, would require extending our theorem to the case of non-isometric maps, which we leave to future research.

We emphasize that proving entanglement wedge reconstruction results in AdS/CFT within this operator-algebraic framework would increase the level of rigor of current derivations, which rely on the Euclidean gravitational path integral. In low dimensions, the Euclidean path integral is surprisingly powerful in capturing a lot of the UV physics of the CFT, and proving results such as the quantum extremal surface formula or the island prescription. However, this path integral is thought to capture the physics of an average of gravitational theories, rather than a single one. Hence, if we want to rigorously show entanglement wedge reconstruction for a single boundary theory, we will need to tackle the problem directly within this operator-algebraic setup. Moreover, in dimension 4 or higher, it is unclear whether the gravitational path integral will be a good enough tool to capture the effects described in this chapter. Even more so in that context, it is a very important problem to understand the relation between the semiclassical effective field theory and the UV complete one directly at the level of the operator algebras describing the CFT.

Further, we hope to draw a precise link between our operator-algebraic framework and geometry, and to maybe be able to derive the bulk Einstein equation in the spirit of [297]. In particular, recent work [80] has shown that the Connes cocycle, a purely operator-algebraic quantity on the boundary, has a precise geometric interpretation in the bulk as a kink transform. Given that in the exact framework, the Connes cocycle is preserved under the holographic conditional expectation, it would be interesting to study it in our approximate setting, and try to formulate a more precise correspondence between operator algebraic quantities on the boundary and geometric data in the bulk. In particular, this could allow one to understand the bulk dynamics and the bulk Lorentzian structure.

Another interesting research direction is to try to study in detail how some apparent paradoxes raised by the framework of exact entanglement wedge reconstruction are resolved by going to the approximate case. This was done in finite-dimensions by Penington [379] in the case of the information paradox, but for instance, the tension between the lack of additivity of entanglement wedges and the boundary Reeh-Schlieder theorem, first uncovered by Kelly [276] and precisely stated in the operator-algebraic context by Faulkner [164], still seems quite mysterious, and can only be treated in an infinite-dimensional setting. Ultimately, we hope that our approximate statements for infinite-dimensional boundary Hilbert spaces will be a first step towards a fully consistent formulation of the emergence of the bulk from the entanglement structure of the CFT.

We now conclude our analysis by giving a more detailed interpretation of our modified-JLMS condition, and explaining how our results are related to the recent progress on the information paradox.

Generalized entropies for quantum extremal islands

Considering two states in the same code subspace, we know that their entanglement wedges may be different [142]. In other words, there is a difference in the term regarding generalized entropy which effectively imposes changes in the original JLMS formula, that corresponds to the reconstruction of a single entanglement wedge. To take these contributions into account, we consider instead the modified-JLMS condition.

For the modified-JLMS formula, not only did we have to assume the relative entropy conservation between the bulk and the boundary, but we also needed the formula to hold for the states supported on the reference system $\mathcal{H}^*_{code}$. In fact, this is because we had to define the map $\mathcal{E}^c \otimes Id$ in our proof. We use the privacy and correctability duality theorem in our proof which can only hold for the completely bounded norm, whose use requires adding an extra reference system.

Due to this setup with an extra reference system, we can apply our framework to various different physical settings. The entanglement wedge of $\mathcal{H}^*_{code}$ can be nontrivial and significantly change our description of bulk reconstruction. In some cases, though not always, this auxiliary system can be identified with the space of semiclassical states of the Hawking radiation or of another boundary.

The idea that black hole interior degrees of freedom can be encoded in an auxiliary system traces back to the identification between wormholes and thermofield double

states [317], which is a well suited model to think about holographic entanglement. In this setup with the auxiliary system, the black hole interior simply becomes the other side of a Lorentzian wormhole. It follows that the entanglement wedge of the second boundary corresponds to what would be the black hole interior from the viewpoint of the first boundary. In particular, the modified-JLMS formula will be valid for states, in the code subspace, supported on both boundaries.

The necessity to consider the reconstruction wedge and state-dependence only appears when nonperturbative gravitational corrections to entanglement wedge reconstruction are taken into account. These nonperturbative corrections, although individually insignificant, may pile up in the presence of a nontrivial amount of gravitational corrections until they significantly alter the encoding of bulk information. This is, for example, what happens for black hole interior reconstruction from the Hawking radiation after the Page time. Taking into account a conformal field theory bath, it is possible to have nontrivial nonperturbative effects from replica wormholes form quantum extremal islands in the semiclassical bulk. Then, the interior of an island is encoded in the early Hawking radiation of the black hole and the entropy of the radiation is computed from the quantum island formula, which generalizes the quantum extremal surface prescription. Applying this formula leads to a coherent semiclassical derivation of the Page curve.

Replica wormhole calculations [11, 377] considerably strengthen the evidence for the validity of such an island formula. It would be very interesting to derive a justification for it directly within the boundary theory, without resorting to the gravitational path integral.

Application to the information paradox

In this chapter, we explained how to formulate approximate entanglement wedge reconstruction for an infinite-dimensional boundary Hilbert space in the case where the boundary is divided into two regions A and $\overline{A}$. We obtained that in the case where there is a black hole in the bulk, the quantum extremal surface associated to the boundary region A experiences jumps between pure and mixed states. This allows a state-dependent reconstruction of the interior.

As outlined in [379], one can perform a similar analysis in the case of an evaporating black hole, whose semiclassical description is encoded in part in the CFT and in part in a bath of Hawking radiation collected during evaporation. In order to do this, one must be able to collect Hawking radiation by imposing transparent boundary

conditions on the AdS boundary.

In this case, the whole boundary plays the role of the boundary region A, while the Hawking radiation plays the role of $\overline{A}$. It can be shown that after the Page time, the radiation bath contains enough information so that a quantum extremal surface that contains most of the black hole interior appears, allowing the interior to be inside the entanglement wedge of the bath. However, the reconstruction of interior operators is state-dependent for a sufficiently later time after the Page time, as the quantum extremal surface disappears when the bulk system is in an overall mixed state. It would be interesting to apply our framework to the setting where the UV-complete dual contains a bath of Hawking radiation in addition to the CFT. We expect the difficulty comes from the fact that the bulk-to-boundary map is only approximately an isometry after the Page time.

The gravitational path integral and quantum error-correction

The most convincing argument for the Page curve in holographic theories in the literature has been derived through the use of the Euclidean gravitational path integral, by including contributions coming from nontrivial topologies [11, 377]. Even for the regular quantum extremal surface formula, the Euclidean path integral is our best justification [143]. However, it is still not completely understood why the Euclidean path integral knows so much about the UV degrees of freedom of the theory. Recent calculations in two and three dimensions have put forward a possible interpretation, which can be made rigorous in the case of Jackiw–Teitelboim gravity [403] or Narain CFTs [321]: the Euclidean path integral would only allow to calculate *averaged* quantities over a moduli space of dual theories, rather than quantities in a single unitary theory. For example, this interpretation may provide a resolution to the factorization problem.

However, it is still very important to understand how semiclassical calculations work in a single unitary holographic theory. Indeed, if we are to describe a non-self-averaging observable in the bulk, it will be sensitive to the specific features of individual theories that compose the ensemble of boundary theories; importantly, calculating the gravitational path integral will not likely suffice. Moreover, in four or higher dimensions, it is unclear whether the gravitational path integral will be as successful, and even if it is possible to think of an ensemble of boundary theories at all. For instance, $\mathcal{N} = 4$ super Yang–Mills is thought to be a unique boundary theory.

The operator algebraic approach does not a priori rely on any kind of averaging procedure or any explicit path integral formula, but on a bulk-to-boundary map between the code subspace and the boundary Hilbert space. In that sense, it allows for an understanding of the semiclassical limit of a single unitary holographic theory. With our approximation theorem in hand, this approach can also handle the nonperturbative corrections that appear through nontrivial topologies in the gravitational path integral. In particular, we showed that even in infinite dimensions, which is the relevant setting for quantum field theories, approximate recovery is possible inside the reconstruction wedge. For local operators that are in the entanglement wedge of a given state, but not contained in all entanglement wedges of pure and mixed states, reconstruction can only be performed in a state-dependent manner. The fact that this reconstruction wedge is strictly smaller than some entanglement wedges shows that gravity affects some large region of the bulk that we tackle in our operator-algebraic framework.

The relationship between the gravitational path integral and ensembles has recently been investigated in detail, and given a new interpretation through the notion of Hilbert space of closed universes. This is relevant to considering the bulk with multi-boundaries. This Hilbert space describes possible nucleations of baby universes in the bulk, which correspond to new asymptotic boundaries [328, 193]. In this approach, the Euclidean path integral becomes dependent on the state of these baby universes, which are described by a commutative algebra of observables at infinity. In the Hartle–Hawking state of baby universes, the Euclidean path integral is dual to an ensemble of boundary theories, while in some very specific baby universe states, known as α-states, which correspond to the basic superselection sectors of the theory, it actually computes observables in a single member of the dual ensemble.

It is then interesting to ask whether this distinction between α-states and ensemble averaging can be understood within the operator-algebraic framework of quantum error-correction, and more generally, how the notion of ensemble averaging can be encoded within our approach. Such a result would clarify the link between the Euclidean path integral and unitary theories, and explain why the Euclidean path integral works so well to understand some subtle features of gravity. Moreover, it should shed light on the Lorentzian structure of the bulk, as the operator-algebraic framework can be well-adapted to Lorentzian signature. We hope to return to these questions in future work.

Holography	**Operator Algebras**
Physical operators	Von Neumann algebras M_{phys}
Logical operators	Von Neumann algebra M_{code}
Projection onto the logical operators	Conditional expectation
Exact bulk reconstruction	Invariance under conditional expectation
JLMS formula	Takesaki theorem
Petz map	Generalized conditional expectation
State-independent bound	Completely bounded norm bound
(Approximate) complementary recovery	(ε-) privacy/correctability duality
Twirled Petz map	Faulkner–Hollands map

Table 9.1: A dictionary between concepts in holography and their operator algebraic counterparts. This chapter extends the dictionary to the approximate case, which is covered by the last three entries.

WORMHOLE RENORMALIZATION: THE GRAVITATIONAL PATH INTEGRAL, HOLOGRAPHY, AND A GAUGE GROUP FOR TOPOLOGY CHANGE

This chapter is based on the work [198], in collaboration with Matilde Marcolli and Jacob McNamara.

10.1 Introduction

Should the path integral of quantum gravity include a sum over topologies? There are good reasons to think it must: quantum mechanics instructs us to sum the amplitudes for all allowed processes, and gravity is supposed to be a theory of dynamical spacetime manifolds of arbitrary topology. However, it has been known for quite some time that the sum over topologies leads to deep structural issues [420, 1, 114, 204, 203]. These issues have been sharpened into the Factorization Paradox [458, 320], a direct conflict between the holographic principle and a gravitational path integral over topologies. The holographic principle asserts that quantum gravity defines a local quantum field theory (QFT) living on the boundary of spacetime.[1] However, the space of configurations in the gravitational path integral, given by the set of bulk spacetimes with fixed boundary, is not local to the boundary.[2] In particular, while the holographic principle requires that correlation functions defined with a disconnected boundary must factorize, there are non-factorizing configurations in the gravitational path integral, otherwise known as spacetime wormholes.

There is essentially only one possible resolution to the Factorization Paradox: in a complete, holographic theory of quantum gravity, the net sum of all wormholes in the gravitational path integral must exactly vanish [328, 335, 404, 402, 64].[3]

---

[1]Strictly speaking, this is likely only exactly true in the context of AdS/CFT. While some much more general form of holography is expected to be true, the details are still far from clear.

[2]Mathematically, the Factorization Paradox is the fact that the configuration space in the gravitational path integral, given by the set of spacetime manifolds, does not define a sheaf over the space of boundaries.

[3]A trivial way to achieve factorization would be give a description of the theory that manifestly factorizes. For example, we could attempt to excludes wormholes by fiat, as envisioned in [420, 1]. Alternatively, we could retreat to the holographically dual description in terms of a local path integral on the boundary. The puzzle of the Factorization Paradox is to understand how a holographic

This cancelation of all wormholes has been demonstrated in a few very specialized corners of string theory, such as a particular tensionless limit [151] or when computing supersymmetric indices [249].[4] Importantly, these examples involve supersymmetric localization, and the necessary cancelations occur simply, between nearby wormhole configurations related by the action of supersymmetry. In more generic contexts, we should not expect any simple cancelation between wormholes beyond what is required by holography. Thus, even if we know the final answer must vanish, it is not obviously clear how to organize the sum over wormholes in the absence of a complete theory of quantum gravity.

In [404, 402, 64], a useful organizing principle has been proposed. The idea is to view the Factorization Paradox through the lens of effective field theory (EFT), and group all non-factorizating configurations in our complete theory into two collections: those which can be described in the EFT as smooth, geometric wormholes, and those which cannot. We will refer to the second class as *stringy wormholes*, which could be Planckian, non-geometric, or something even wilder. While the net sum of all geometric and stringy wormholes vanishes by assumption, the sum over geometric wormholes on its own need not vanish. Thus, in order to define an effective gravitational path integral that matches the microscopics, we must include additional non-localities beyond the geometric wormholes in order to parametrize the effects of stringy wormholes that have been excluded from our effective description.

In this chapter, we propose a tight formal analogy between these additional non-localities, which we dub *counter-wormholes*, and the counterterms needed to cancel ultraviolet (UV) divergences in the perturbative calculation of QFT observables.[5] If we attempted to use finite, effective coupling constants to directly evaluate Feynman graphs, we would obtain physically unreasonable answers involving UV divergences from the integration over high-energy modes of our EFT fields. Analogously, if we attempted to define a gravitational path integral including only those wormholes visible in the EFT, we would obtain physically unreasonable answers involving non-factorization or ensembles arising from wormhole contruibutions in our effective

---

theory could still admit a description in terms of a gravitational path integral which seems to include wormholes and does not manifestly factorize.

[4]See also [49] for a related mechanism involving the gauging of a bulk global symmetry.

[5]Our original motivation for this analogy was the observation that loop divergences arise from shrinking a loop to zero size, and thus inherently involve topology change on the particle worldline. See also, e.g., [18, 389] for recent discussions of a possible analogy between topology change and perturbative quantum field theory.

gravitational path integral.

In both cases, these physically unreasonable answers should not be taken too seriously. They are not an inconsistency of the theory, but rather signal the importance of some UV effects we have incorrectly ignored in our effective description.[6] In the case of perturbation theory, the resolution is to modify our naive action by the addition of UV divergent counterterms which precisely cancel against the UV divergences in Feynman graphs. If we then calculate using a renormalized perturbation theory that includes the counterterms, we obtain finite answers for physically observable quantities which can be matched to our effective description. Analogously, we view the prescriptions of [404, 402, 64] as instances of a *renormalized gravitational path integral*, where we have modified the naive sum over smooth spacetimes by the addition of counter-wormholes in order to obtain physically reasonable, factorizing answers for disconnected correlation functions.

This approach to the Factorization Paradox has mainly been studied on a case-by-case basis. Our goal in proposing an analogy with perturbative renormalization is to look for precise gravitational analogs of well-known structures that control the systematics of renormalization. In particular, the perturbative calculation of counterterms is controlled by an algebraic structure, the Connes-Kreimer Hopf algebra $\mathcal{H}_{\mathrm{CK}}$ [121, 122, 123], which formalizes the recursive Bogoliubov-Parasiuk-Hepp-Zimmermann (BPHZ) procedure [65, 235, 463].[7] This Hopf algebra efficiently encodes the combinatorial structure of divergences in Feynman graphs, taking into account the possibility of sub-divergences: sub-graphs of a given graph which are independently divergent, and which are already renormalized by a local counterterm at an earlier stage of the recursive procedure.

In an extremely simple gravitational path integral [328], we explain how the calculation of counter-wormholes is controlled by an analogous Hopf algebra, which turns out to be the well-known Faà di Bruno Hopf algebra $\mathcal{H}_{\mathrm{FdB}}$. We show how $\mathcal{H}_{\mathrm{FdB}}$ efficiently encodes the combinatorics of multi-boundary wormholes and systematizes the construction of a factorizing renormalized gravitational path integral. The analogs of sub-divergences are sub-wormholes: embedded submanifolds of a given spacetime which are themselves wormholes, and which might already be canceled by counter-wormholes at an earlier stage of the gravitational analog of the

---

[6]See [237] for further comments on the relationship between spacetime wormholes and the coarse-graining of UV-complete theories.

[7]See Section 10.2 or [124] for a review.

BPHZ procedure.[8] While the toy model we consider is quite simple, our hope is to identify algebraic structures that might serve as useful organizing structures for understanding factorization in more realistic theories.

One immediate upshot of this result is the existence of a symmetry group of the renormalized gravitational path integral. In the case of perturbative renormalization, the group $G_{CK} = \text{Spec}(\mathcal{H}_{CK})$ dual to the Connes-Kreimer Hopf algebra acts as a group of symmetries of renormalized perturbation theory, reorganizing the sum over Feynman diagrams and counterterms.[9] Analogously, the group $G_{FdB} = \text{Spec}(\mathcal{H}_{FdB})$ acts as a symmetry of the gravitational path integral, reorganizing the sum over spacetime manifolds and counter-wormholes. One instance of this group action is the integration out of microscopic wormholes into non-local effects as desribed by Coleman, Giddings, and Strominger [114, 204, 203]. Another is the cancelation of microscopic, stringy wormholes against smooth, geometric wormholes, which can be interpreted as a form of ER = EPR [317].[10]

More generally, we view the action of G_{FdB} as realizing the gravitational gauge redundancies of [255, 328] in our toy model, illustrating explicitly that the different gauge fixings described in [328] are related by the action of G_{FdB}. These gravitational gauge redundancies between spacetimes of distinct topology go hand in hand with the cancelation of non-factorizing contributions,[11] and seem to be essential to the resolution of the Factorization Paradox.[12] In most cases, these gravitational gauge redundancies have been described rather abstractly via the existence of null states. We find it intriguing that in a toy model these gauge redundancies are realized concretely by a group action, and hope this structure persists in general.

The rest of this chapter is organized as follows. In Section 10.2, we review the BPHZ approach to perturbative renormalization and its formalization in terms of the Connes-Kreimer Hopf algebra, highlighting the physical and mathematical structures relevant for our analogy. In Section 10.3, we describe the very simple toy model

---

[8]A very similar recursive algorithm was used in [64] in order to achieve all-order factorization.

[9]Recall that the spectrum $\text{Spec}(A)$ of a commutative $\mathbb{C}$-algebra A is the set of algebra homomorphisms $A \to \mathbb{C}$. See 10.5.2 for the definition of the group structure on $\text{Spec}(\mathcal{H})$ for a commutative Hopf algebra $\mathcal{H}$.

[10]See [333] for further comments on the meaning of ER = EPR in spacetime, as opposed to merely in space, and its role in gauge fixing the sum over topologies.

[11]In general, gauge redundancies and detailed cancelations are closely related: a gauge redundancy implies the cancelation of anything non-gauge-invariant, and conversely, a cancelation suggests the existence of a gauge fixed description in which the cancelations are made manifest.

[12]These gauge redundancies also plays a key role in understanding how bulk EFT could remain valid in a restricted sense behind old black hole horizons [7].

of [328] and explicitly carry out the gravitational analog of the BPHZ procedure. We also show that the algebraic structure of this gravitational BPHZ is captured by the Faà di Bruno Hopf algebra $\mathcal{H}_{\text{FdB}}$ and its dual group G_{FdB}. Finally in Section 10.4, we comment on the lessons that may be drawn from our results, and discuss some possible extensions and applications.

The analogy drawn in this chapter between the gravitational path integral and perturbative renormalization is summarized in Table 10.1.

Gravity	Renormalization
Multiboundary partition functions	1PI effective action
Semiclassical wormholes	Divergent Feynman diagrams
Sub-wormholes	Sub-divergences
Stringy wormholes	Counterterms
Faà di Bruno Hopf algebra	Connes–Kreimer Hopf algebra

Table 10.1: The analogy between the gravitational path integral and perturbative renormalization.

10.2 Review of perturbative renormalization

In this section, we briefly review the BPHZ approach to perturbative renormalization [65, 235, 463] and its algebraic formalization [121, 124] in terms of the Connes-Kreimer Hopf algebra, with an eye towards our analogy with the gravitational path integral.[13] First, in Section 10.2, we recall the basic idea of renormalization. Next, in Section 10.2, we review the BPHZ procedure for handling sub-divergences. Finally, in Section 10.2, we review the formalization of perturbative renormalization in terms of the Connes-Kreimer Hopf algebra.

Divergences and counterterms

The starting point of perturbative renormalization is a D-dimensional local action functional of some dynamical fields ϕ:

$$S(\phi) = \int \mathrm{d}^D x \, \mathcal{L}(\phi). \tag{10.1}$$

---

[13]We assume the reader is somewhat familiar with the basics of perturbative renormalization. For a comprehensive review, see [124].

For notational simplicity we consider a single scalar field ϕ. We take the Lagrangian $\mathcal{L}(\phi)$ to be of the form

$$\mathcal{L}(\phi) = \frac{1}{2}(\partial\phi)^2 - \frac{1}{2}m^2\phi^2 + \mathcal{L}_{\text{int}}(\phi). \tag{10.2}$$

The interaction Lagrangian $\mathcal{L}_{\text{int}}(\phi)$ is assumed to be a polynomial (or power series) in ϕ and its derivatives. For example, we might consider ϕ^3 theory, defined by

$$\mathcal{L}_{\text{int}}(\phi) = \frac{1}{3!}g\phi^3. \tag{10.3}$$

Each possible monomial in the interaction Lagrangian comes with a coupling constant, such g above, which we view as tunable parameters defining the theory.[14]

The action functional $S(\phi)$ defines a (Euclidean) QFT through the formal path integral

$$\mathcal{Z} = \int \mathcal{D}\phi \, e^{-S(\phi)/\hbar}. \tag{10.4}$$

Physical observables are computed perturbatively in $\hbar$ via a sum over Feynman graphs Γ, whose edges are labeled by particle species and whose vertices are labeled by monomials in the interaction Lagrangian $\mathcal{L}_{\text{int}}$. Each Feynman graph Γ defines an integral

$$U(\Gamma)(p_1, \ldots, p_N) = \int \frac{\mathrm{d}^D k_1}{(2\pi)^D} \cdots \frac{\mathrm{d}^D k_L}{(2\pi)^D} \, I_\Gamma(p_1, \ldots, p_N, k_1, \ldots, k_L), \tag{10.5}$$

over unconstrained loop momenta k_i, refered to as the *unrenormalized Feynman integral* of the graph Γ. Here N is the number of external legs of Γ and L is the loop number (first Betti number) of Γ. The integrand I_Γ is computed via truncated *Feynman rules*, which assign a propagator to each internal edge and an interaction term to each vertex. Our convention is that the powers of $\hbar$ and the couplings g_i are excluded from the integrals $U(\Gamma)$, for reasons that will be important later; to recover the more standard values assigned to a Feynman graph Γ, we must multiply $U(\Gamma)$ by appropriate powers of the $\hbar$ and the couplings, as in (10.7) below. For example, in ϕ^3 theory (10.3), the Feynman graph Γ illustrated in Figure 10.1 represents the integral

$$U(\Gamma)(p) = \int \frac{\mathrm{d}^D k}{(2\pi)^D} \left(\frac{1}{k^2 + m^2}\right)\left(\frac{1}{(p+k)^2 + m^2}\right). \tag{10.6}$$

---

[14]For field strength and mass renormalization, we must include the possibility of quadratic terms in $\mathcal{L}_{\text{int}}(\phi)$.
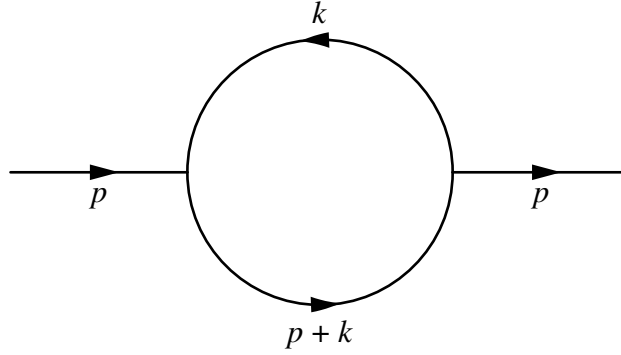
Figure 10.1: A simple Feynman diagram Γ in ϕ^3 theory presented in [124], whose unrenormalized Feynman integral $U(\Gamma)$ is given by (10.6). The integration is over the internal momentum k that runs through the loop.

An efficient way to encode all physical observables of our QFT at once is through the *effective action* $S_{\text{eff}}(\phi)$, computed via a sum over all *one-particle irriducible* (1PI) Feynman graphs as

$$S_{\text{eff}}(\phi) = S(\phi) - \sum_{\Gamma \in 1\text{PI}} \hbar^L (-g_I)^{n_I} \frac{U(\Gamma)(\phi)}{\sigma(\Gamma)}. \tag{10.7}$$

There are various things to explain in this equation. First of all, for a given graph Γ, L is the loop number and $n_I = (n_1, n_2, \dots)$ are the numbers of vertices associated to couplings g_i. We have further abbreviated $(-g_I)^{n_I} = \prod_i (-g_i)^{n_i}$ for the product of all couplings associated to vertices in Γ. The minus signs in (10.7) arise from the minus sign in the path integral (10.4). The symmetry factor $\sigma(\Gamma)$ is the order of $\text{Aut}(\Gamma)$ defined holding external legs fixed. Finally, the functional $U(\Gamma)(\phi)$ is defined in terms of the momentum-space fields $\phi(p)$ by

$$U(\Gamma)(\phi) = \frac{1}{N!} \int_{\sum p_i = 0} \frac{d^D p_1}{(2\pi)^D} \cdots \frac{d^D p_N}{(2\pi)^D} \, \phi(p_1) \cdots \phi(p_N) \, U(\Gamma)(p_1, \dots, p_N). \tag{10.8}$$

An important note is that the relevant notion of 1PI Feynman graph for the sum in (10.7) excludes trees, since the first term $S(\phi)$ can be interpreted as the contribution of tree graphs to the effective action $S_{\text{eff}}(\phi)$. The benefit of the effective action is that it reproduces, at tree-level, the full perturbative expansion of physical observables computed from $S(\phi)$ at all loops.

Famously, if we naively take our coupling constants in the action $S(\phi)$ to be finite numbers, the integrals $U(\Gamma)$ will contain UV divergences from the integration over large values of the loop momenta k_i. These UV divergences will show up in the calculation of the effective action $S_{\text{eff}}(\phi)$, producing unreasonable answers for physical

observables. The basic idea of renormalization is that the bare coupling constants appearing in the path integral are not directly observable. Thus, demanding that they be finite is a mis-application of the relevant physical condition: the couplings that need to be finite are the effective couplings in $S_{\text{eff}}(\phi)$, not the bare couplings. We are free to take the bare couplings to be divergent, if doing so allows us to produce finite answers to physically meaningful questions.

Suppose, then, that we are given an action functional $S(\phi)$ with finite couplings, and we seek to use it to produce a physically sensible theory. Rather than directly using $S(\phi)$ to define a path integral as in (10.4), we must first modify our action by the addition of UV divergent *counterterms* to define a *bare action* $S_{\text{bare}}(\phi)$.[15] These counterterms must be precisely tuned so that the UV divergences they produce exactly cancel against every UV divergence arising from loops. Once appropriate counterterms are chosen, we may then define a path integral using the bare action, and derive a finite effective action as in (10.7) by using the Feynman rules of $S_{\text{bare}}(\phi)$.

Practically speaking, to compute appropriate counterterms, one must first choose a regularization scheme, say dimensional regularization (dimreg), in order to regulate the divergences in loop integrals. This yields finite values for the unrenormalized Feynman integrals $U(\Gamma)$ at the cost of dependence on an unphysical cutoff parameter ε, which must be taken to zero at the end of the calculation. The counterterms are also taken to be functions of ε, and the goal is to choose counterterms such that the physical observables computed with counterterms included yield finite values in the limit $\varepsilon \to 0$. To make this choice of counterterms, we must first choose a subtraction scheme, such as minimal subtraction (MS), that specifies the "divergent part" of any regulated loop integral.

Sub-divergences and the BPHZ procedure

The essential insight of the BPHZ procedure is that counterterms, like physical observables, can be computed perturbatively via a sum over Feynman graphs. To each 1PI Feynman graph Γ, we associate a counterterm $C(\Gamma)$ which is chosen in

---

[15]A possible point of contention is whether the counterterms are something to be added or whether they were always there in the first place. As discussed in the introduction, the physically meaningful answer is that they must have always been there, as the counterterms represent unknown UV physics needed to render the theory sensible. However, our starting point here is more formal, given by the problem of defining a sensible physical theory out of an action principle with finite couplings. This will be analogous to the formal problem of defining a physically sensible theory out of a given gravitational path integral.
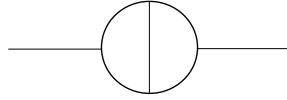
Figure 10.2: A simple example of diagram with sub-divergences in ϕ^3 theory. This diagram has loops nested inside other loops, which is the source of the recursive nature of the BPHZ procedure.

order to precisely cancel UV divergences in $U(\Gamma)$.[16] Each counterterm defines a functional $C(\Gamma)(\phi)$, which is normally required to be local. The bare action is then defined via the addition of the counterterms for every 1PI graph Γ, as follows.

$$S_{\text{bare}}(\phi) = S(\phi) - \sum_{\Gamma \in 1\text{PI}} \hbar^L (-g_I)^{n_I} \frac{C(\Gamma)(\phi)}{\sigma(\Gamma)}. \tag{10.9}$$

Note the similarity to the calculation of the effection action (10.7).

An essential complication is the possibility of sub-divergences: sub-graphs $\gamma \subset \Gamma$ of a given Feynman graph which are divergent on their own. Figure 10.2 presents a simple example of Feynman graph with a sub-divergence. While the divergent subgraph γ will certainly contribute to the divergences in $U(\Gamma)$,[17] these divergences will already be taken into account by the counterterm $C(\gamma)$ we have chosen to cancel the divergence in $U(\gamma)$. If we were to include this divergence when computing $C(\Gamma)$, we would overcount the divergences, and fail in defining finite physical observables. Thus, even in dimreg with minimal subtraction, the counterterm $C(\Gamma)$ will not merely be given by the divergent piece of $U(\Gamma)$ when Γ contains a divergent subgraph.

Instead, to compute the counterterm for any given Feynman graph Γ, we must follow the *BPHZ procedure* [65, 235, 463], a recursive algorithm for computing counterterms while taking sub-divergences into account. To compute $C(\Gamma)$, we first identify all divergent subgraphs $\gamma \subset \Gamma$,[18] and recursively compute their counterterms $C(\gamma)$ via the BPHZ procedure. Then, we compute a *prepared Feynman integral*

---

[16]As with the unrenormalized Feynman integrals $U(\Gamma)$, our convention is that $C(\Gamma)$ excludes powers of $\hbar$ and the couplings, which must be reintroduced to obtain the more conventional values of the counterterms.

[17]In fact, it will contribute in a severe way: the divergent piece will be a non-local functional of the external momenta in Γ which could not be canceled by any local counterterm $C(\Gamma)(\phi)$.

[18]The subgraph γ is assumed to be a non-empty, proper subgraph. However, γ can be disconnected. If this happens, we define $U(\gamma)$ and $C(\gamma)$ to be the product of their values on each connected component of γ.

$\overline{R}(\Gamma)$ by summing all relevant contracted graphs Γ/γ weighted by the previously computed counterterms.[19]

$$\overline{R}(\Gamma) = U(\Gamma) + \sum_{\gamma \subset \Gamma} C(\gamma) U(\Gamma/\gamma). \qquad (10.10)$$

The prepared Feynman integral $\overline{R}(\Gamma)$ may still be divergent, but will only include those divergences in Γ that do not arise from any subgraph. We may then compute the counterterm $C(\Gamma)$ to be the divergent piece of $\overline{R}(\Gamma)$, as determined by our subtraction scheme, so that the *renormalized Feynman integral*

$$R(\Gamma) = \overline{R}(\Gamma) + C(\Gamma) = C(\Gamma) + U(\Gamma) + \sum_{\gamma \subset \Gamma} C(\gamma) U(\Gamma/\gamma), \qquad (10.11)$$

is finite.

Once we have computed counterterms via the BPHZ procedure, we now have three distinct yet equivalent ways to incorporate them into the calculation of physical observables.

First approach: The first, most direct approach is to replace the unrenormalized Feynman integrals $U(\Gamma)$ with the renormalized ones $R(\Gamma)$ when calculating physical observables. In particular, we can replace $U(\Gamma)$ with $R(\Gamma)$ in (10.7), in order to compute a physically reasonable effective action directly from $S(\phi)$:

$$S_{\text{eff}}(\phi) = S(\phi) - \sum_{\Gamma \in 1\text{PI}} \hbar^L (-g_I)^{n_I} \frac{R(\Gamma)(\phi)}{\sigma(\Gamma)}. \qquad (10.12)$$

This approach has the benefit of making the cancelation of UV divergences manifest, since each renormalized value $R(\Gamma)$ is independently finite. However, it has the downside of seeming a bit arbitrary. We have modified the way we evaluate Feynman diagrams, only including some finite piece of the Feynman integrals in our calculation.

Second approach: The second approach is to add the counterterms $C(\Gamma)$ to the action, in order to define a bare action as in (10.9). We then forget where the bare action came from, and recompute physical observables using the "unrenormalized Feynman integrals" $U(\Gamma)$ computed with the Feynman rules derived from S_{bare}. Graph by graph, we will encounter UV divergences which will cancel out of any

---

[19]In (10.10), each connected Feynman graph with N external legs should be equipped with the data of a specific monomial of degree N in the fields ϕ, and the sum over subgraphs includes a sum over this data. The vertices in the contracted graph Γ/γ obtained by contracting a component of γ are labeled by the monomial chosen for γ.

physical observable, seemingly miraculously. While this approach obscures the cancelation of UV divergences, it makes manifest that we are playing the same sort of game as before: our theory is defined via the path integral by some local action functional, which simply happens to have UV divergent couplings. Notably in this approach, the cancelation occurs between Feynman diagrams of different loop orders.

Third approach: The third approach is somewhere between the first two, and consists of enlarging the set of Feynman graphs we include in our perturbative expansion. In addition to vertices labeled by interaction terms in $S(\phi)$, we now have additional vertices labeled by the counterterms. Now, each Feynman diagram will still be individually divergent, but the combinatorics of formula (10.11) will be more readily visible, since we can keep track of the contributions of each counterterm.

Crucially, while these three approaches organize the perturbative expansion differently, they produce exactly equal answers for physical observables. The only difference is whether to group the counterterms $C(\Gamma)$ with the graphs Γ from which they arise, add them all to the action, or leave them as an explicit, additional type of contribution to the perturbative expansion. This redundancy in how we organize the perturbative expansion is a form of gauge redundancy (or duality): we have multiple, exactly equivalent descriptions of the same physics. To see this redundancy more explicitly, we turn now to the algebraic formalization of renormalized perturbation theory.

The Connes–Kreimer Hopf algebra

In the algebraic formalization of renormalization, the BPHZ procedure described above is efficiently packaged in terms of the Connes-Kreimer Hopf algebra $\mathcal{H}_{\mathrm{CK}}$, a commutative Hopf algebra over $\mathbb{C}$. As reviewed in Appendix 10.5, a commutative Hopf algebra $\mathcal{H}$ defines a dual group $G = \mathrm{Spec}(\mathcal{H})$, whose group law $\star : G \times G \rightarrow G$ is defined in terms of the coproduct on $\mathcal{H}$. The group $G_{\mathrm{CK}} = \mathrm{Spec}(\mathcal{H}_{\mathrm{CK}})$ is precisely the group underlying the multiple descriptions of renormalized perturbation theory described in the previous section, and allows one to effortlessly pass between them.

In order to motivate the definition of $\mathcal{H}_{\mathrm{CK}}$, let us examine a formula that appeared at multiple points in the discussion above. In (10.7), (10.9), and (10.12), we have

seen transformations of the form

$$S(\phi) \to S(\phi) - \sum_{\Gamma \in 1\mathrm{PI}} \hbar^L (-g_I^S)^{n_I} \frac{F(\Gamma)(\phi)}{\sigma(\Gamma)}, \tag{10.13}$$

where $F(\Gamma)$ is some functional on the set of 1PI graphs and the couplings g_I^S are those in the action S. The goal of this section is to interpret (10.13) as the action of $F \in G_{\mathrm{CK}}$ on the space of action functionals. In terms of this group action, the results of the previous section can be summarized via a commutative diagram:

$$\begin{array}{ccc}
S & \xrightarrow{\;\;C\;\;} & S_{\mathrm{bare}} \\
& \diagdown_R & \downarrow U \\
& & S_{\mathrm{eff}}
\end{array} \tag{10.14}$$

In other words, as described above, we can obtain S_{eff} in three ways: by acting on S with R, by acting on S_{bare} by U, or by acting on S first with C and then with U.

Our goal, then, is to define $\mathcal{H}_{\mathrm{CK}}$ such that R, C, and U are elements of the dual group G_{CK} of algebra homomorphisms out of $\mathcal{H}_{\mathrm{CK}}$, and further such that we have

$$R = C \star U, \tag{10.15}$$

under the group law of G_{CK}.[20] We have already seen how R, C and U are related in (10.11): in order to evaluate R on a Feynman graph Γ, we extract all possible subgraphs $\gamma \subset \Gamma$, and evaluate C and U on the subgraphs and quotient graphs, respectively. This motivates the following definition.

Definition 10.2.1. For a given QFT, the *Connes–Kreimer Hopf algebra* $\mathcal{H}_{\mathrm{CK}}$ is the free commutative algebra over $\mathbb{C}$ generated by the set of 1PI Feynman graphs Γ (excluding trees),[21] equipped with counit $\varepsilon : \mathcal{H}_{\mathrm{CK}} \to \mathbb{C}$ and coproduct $\Delta : \mathcal{H}_{\mathrm{CK}} \to \mathcal{H}_{\mathrm{CK}} \otimes \mathcal{H}_{\mathrm{CK}}$ defined on algebra generators Γ by $\varepsilon(\Gamma) = 0$ and

$$\Delta(\Gamma) = \Gamma \otimes 1 + 1 \otimes \Gamma + \sum_{\gamma \subset \Gamma} \gamma \otimes \Gamma/\gamma, \tag{10.16}$$

and extended multiplicatively.

Proposition 10.2.2 ([122])**.** *As defined above, $\mathcal{H}_{\mathrm{CK}}$ is a Hopf algebra.*

---

[20]The order of multiplication is chosen so that the action of G_{CK} on the space of action functionals (10.13) is a *right* action.

[21]As in Footnote 19, each Feynman graph Γ with N external legs must be equipped with a choice of a monomial of degree N in the fields ϕ. This data is summed over in (10.16). We will not keep careful track of this data in our exposition; for details, see [124].

Proof. We follow the proof of [124, Theorem 1.27]. By definition, ε and Δ are algebra homomorphisms, and it is immediate from equation (10.16) that ε is a two sided counit for Δ. For coassociativity, observe that both $(\Delta \otimes \mathrm{Id})(\Delta(\Gamma))$ and $(\mathrm{Id} \otimes \Delta)(\Delta(\Gamma))$ can be written as a sum over nested subgraphs,

$$\Delta^2(\Gamma) = \sum_{\gamma \subset \gamma' \subset \Gamma} \gamma \otimes \gamma'/\gamma \otimes \Gamma/\gamma', \tag{10.17}$$

where now the sum includes both empty and improper subgraphs and we interpret the empty graph as the unit $1 \in \mathcal{H}_{\mathrm{CK}}$.

We have shown that $\mathcal{H}_{\mathrm{CK}}$ is a bialgebra. The existence of an antipode follows from Proposition 10.5.3 upon noting that $\mathcal{H}_{\mathrm{CK}}$ is a connected graded bialgebra, where the grading of a generator Γ is its loop number. $\qquad\square$

Definition 10.2.3. The *Connes–Kreimer group* G_{CK} is the spectrum $\mathrm{Spec}(\mathcal{H}_{\mathrm{CK}})$ (see [121, 124]). The multiplication of two elements $F, G \in G_{\mathrm{CK}}$ (given by arbitrary maps from the set of 1PI Feynman graphs to $\mathbb{C}$) is defined by

$$(F \star G)(\Gamma) = F(\Gamma) + G(\Gamma) + \sum_{\gamma \subset \Gamma} F(\gamma)G(\Gamma/\gamma), \tag{10.18}$$

as in (10.11) for the product $R = C \star U$.

Proposition 10.2.4 ([123]). *The formula* (10.13) *defines a right action of G_{CK} on the space of action functions $S(\phi)$.*

Proof. Clearly, the identity element $1 \in G_{\mathrm{CK}}$ given by the counit $\varepsilon : \mathcal{H}_{\mathrm{CK}} \to \mathbb{C}$ acts trivially, since $\varepsilon(\Gamma) = 0$ for all 1PI graphs Γ. Now, for $F, G \in G_{\mathrm{CK}}$, we have that

$$(S \cdot (F \star G))(\phi) = S(\phi) - \sum_{\Gamma \in \mathrm{1PI}} \hbar^L (-g_I^S)^{n_I} \frac{(F \star G)(\Gamma)(\phi)}{\sigma(\Gamma)}. \tag{10.19}$$

Expanding $F \star G$, we obtain

$$(S \cdot (F \star G))(\phi) = S(\phi) - \sum_{\Gamma \in \mathrm{1PI}} \sum_{\gamma \subset \Gamma} \hbar^L (-g_I^S)^{n_I} \frac{F(\gamma)(\phi)G(\Gamma/\gamma)(\phi)}{\sigma(\Gamma)}, \tag{10.20}$$

where to alleviate notations compared to Equation (10.18), we have included the cases $\gamma = \emptyset$ and $\gamma = \Gamma$ in the sum. This sum can be rewritten as

$$(S \cdot (F \star G))(\phi) = S(\phi) - \sum_{\Gamma' \in \mathrm{1PI}} \hbar^L (-g_I^{S \cdot F})^{n_I} \frac{G(\Gamma')(\phi)}{\sigma(\Gamma')}, \tag{10.21}$$

where

$$g_I^{S \cdot F} = g_I - \sum_{\gamma \in 1\mathrm{PI}} \hbar^L (-g_I^S)^{n_I} \frac{F(\gamma)(\phi)}{\sigma(\gamma)}, \tag{10.22}$$

are the coupling constants appearing in $S \cdot F$. But (10.21) is simply the expression for $((S \cdot F) \cdot G)(\phi)$. $\qquad\qquad\square$

Note that in the proof of Proposition 10.2.4, it was important that the action of G on $S \cdot F$ involved the shifted coupling constants $g_I^{S \cdot F}$ appearing in the action functional $S \cdot F$. This is the reason why we excluded the coupling constants from our definitions of the functionals $U, C, R \in G_{\mathrm{CK}}$ above, as elements of G_{CK} must be defined independently from the coupling constants in the action functionals on which they act.

10.3   A gravitational BPHZ procedure

In the previous section, we summarized the BPHZ procedure underlying perturbative renormalization, and described the underlying Hopf algebraic structure discovered by Connes and Kreimer. We now turn to formulating an analogous procedure to systematically restore factorization in simple two-dimensional topological theories of gravity by the addition of *counter-wormholes*, explicit non-localities in the bulk action.

We will first review a topological theory based on a gravitational path integral due to Marolf and Maxfield [328] which fails to factorize due to the presence of spacetime wormholes. We will then show that this theory can be systematically corrected into a factorizing theory by introducing counter-wormholes, following a precise analog of the BPHZ procedure underlying perturbative renormalization. This procedure is quite similar to that considered in [64]; our goal here is to illuminate the algebraic structures controlling this approach to resolving the Factorization Paradox.

Marolf–Maxfield theory

In [328], Marolf and Maxfield introduced an exactly solvable topological theory of gravity in two dimensions. The observables of this theory are the n-boundary correlation functions $\langle Z^n \rangle$, defined via a discrete path integral over the set $\mathcal{V}_n$ of (diffeomorphism classes of) oriented smooth surfaces Σ with n labeled circular boundaries:

$$\langle Z^n \rangle = \mathfrak{Z}^{-1} \sum_{\Sigma \in \mathcal{V}_n} \mu(\Sigma) e^{S_0 \tilde{\chi}(\Sigma)}. \tag{10.23}$$

Here, $\mathfrak{Z}$ is a normalizing factor, $\tilde{\chi}(\Sigma) = \chi(\Sigma) + n$ is a modified Euler characteristic of Σ, and $\mu(\Sigma)$ is a symmetry factor, defined by

$$\mu(\Sigma) = \frac{1}{\prod_g m_g!}, \tag{10.24}$$

where the m_g are the numbers of *closed universes* (connected components of Σ with no boundary) of genus g. The modified Euler characteristic $\tilde{\chi}(\Sigma)$ is independent of the number of boundaries of Σ, since adding a boundary decreases $\chi(\Sigma)$ by one while increasing n by one.

Following [328], we may simplify (10.23) by integrating out all higher genus surfaces and closed universes. For a given connected component of Σ, summing over genus gives a contribution λ to the path integral, where

$$\lambda = \sum_{g=0}^{\infty} e^{-S_0(2-2g)} = \frac{e^{2S_0}}{1 - e^{-2S_0}}. \tag{10.25}$$

Moreover, the sum over closed universes exponentiates into an overall prefactor e^λ, which can be absorbed by choosing $\mathfrak{Z} = e^\lambda$. All that remains is to sum over the possible genus zero surfaces Σ connected to the boundary. Let $\mathcal{W}_n$ denote the subset of $\mathcal{V}_n$ consisting of genus zero surfaces with n boundaries with no closed components. We have

$$\langle Z^n \rangle = \sum_{\Sigma \in \mathcal{W}_n} \lambda^{k_\Sigma}, \tag{10.26}$$

where k_Σ is the number of connected components of Σ. Note that an element of $\mathcal{W}_n$ is uniquely specified by a partition of the set of boundary components, so we may equivalently write (10.26) as a sum over partitions of n.

Evaluating (10.26) as in [328] gives

$$\langle Z^n \rangle = B_n(\lambda), \tag{10.27}$$

where B_n is the Bell polynomial of order n. See Figure 10.3 for an illustration of the computation of $\langle Z^3 \rangle$ in a Marolf–Maxfield theory. Notably, Marolf–Maxfield theory is not factorizing, and we do not have $\langle Z^n \rangle = \langle Z \rangle^n$. This is unsurprising, as Marolf–Maxfield theory contains spacetime wormholes that contribute nonzero amplitudes to the multi-boundary correlation functions $\langle Z^n \rangle$, with no stringy wormholes to possibly cancel against. The interpretation given in [328] is that (10.26) does not define a single quantum theory of gravity, but instead an ensemble of theories, where Z defines a Poisson random variable of mean λ, whose moments are given by (10.27).

$$\langle Z^3 \rangle = \quad \text{[figure]} \quad +3 \quad \text{[figure]} \quad + \quad \text{[figure]}$$

Figure 10.3: The computation of the spacetime amplitude $\langle Z^3 \rangle$ in a Marolf–Maxfield theory. The first topology has 1 connected component so it contributes λ, the second topology has 2 connected components so it contributes λ^2 with multiplicity 3, and the last topology has 3 connected component so it contributes λ^3. We then recover the $n = 3$ case of Equation (10.27).

In this chapter, we pursue a complementary interpretation motivated by perturbative renormalization, in which we view (10.26) as defining only a low energy gravitational EFT. This EFT is good for answering some questions, but breaks down when pushed to answer more detailed questions like the factorization of multi-boundary correlation functions. We assume that this EFT correctly computes the single boundary partition function $\langle Z \rangle = \lambda,$[22] which can be interpreted as the partition function of a holographically dual topological quantum mechanics. However, we will modify the calculation of multi-boundary correlation functions by adding additional *counter-wormholes* which parameterize the unknown stringy wormholes needed to guarantee factorization.

Note that the single boundary partition function $\langle Z \rangle$ already includes contributions from wormholes in the form of higher-genus surfaces in the sum (10.25), which can be understood as a renormalization of the parameter e^{2S_0} to $\lambda = e^{2S_0}(1 + O(e^{-2S_0}))$. In a more complete treatment, we should also modify the calculation of the single-boundary partition function by counter-wormholes, leading to the simultaneous consideration of the renormalization of e^{2S_0} and the breakdown of factorization. We will ignore this issue in our treatment to simplify the algebra, taking (10.26) to be the definition of Marolf–Maxfield theory and considering only genus zero surfaces and their associated counter-wormholes. See [64] for a complete treatment of wormholes and higher-genus surfaces at the same time.

Renormalizing Marolf–Maxfield

Now that the stage is set for Marolf–Maxfield theory, we would like to use the intuition gained in Section 10.2 to introduce and motivate an analogy between the Factorization Paradox and perturbative renormalization.

---

[22] We do not require $\lambda \in \mathbb{N}$. We will comment on this further in Sections 10.3 and 10.4.

The first step in making our analogy is to identify the gravitational analogs of tree-level and loop-level Feynman diagrams in the Marolf–Maxfield theory (10.26). As stated above, we assume that (10.26) correctly computes the single boundary partition function $\langle Z \rangle = \lambda$, arising from the bulk manifold Σ given by a single disk. In any correlation function $\langle Z^n \rangle$, we always have a term λ^n arising from n disks, and we may rewrite (10.26) as

$$\langle Z^n \rangle = \lambda^n + \sum_{\Sigma \in \mathcal{W}_n^{\text{wh}}} \lambda^{k_\Sigma}, \qquad (10.28)$$

where $\mathcal{W}_n^{\text{wh}}$ is the subset of $\mathcal{W}_n$ such that at least one component of Σ is a wormhole, i.e., has more than one boundary. We view the first term in (10.28) as "tree-level," requiring no renormalization, and the rest as "loop-level," requiring renormalization due to their failure to factorize. Thus, the analog of loop-level Feynman diagrams are spacetimes that include wormholes.

In the case of perturbative renormalization, we saw that the physically meaningful observables can be efficiently summarized via effective coupling constants, computed perturbatively from the tree-level couplings via (10.7). Analogously, we view (10.28) as defining an effective bulk action functional arising from integrating out wormholes. In particular, the observables of Marolf–Maxfield theory can reproduced from a "tree-level" calculation involving only spacetimes without wormholes, provided we assign the value $B_{k_\Sigma}(\lambda)$ to a spacetime consisting of k_Σ disconnected disks rather than merely λ^{k_Σ}. In the case of perturbative renormalization, the effective coupling constants differ from the bare coupling constants only by terms subleading in $\hbar$, the loop-counting parameter. Here, we see that the role of $\hbar$ is being played by λ^{-1}, as $B_{k_\Sigma}(\lambda)$ agrees with λ^{k_Σ} up to terms subleading in λ^{-1} arising from spacetime wormholes.

In perturbative renormalization, we know that if we naively take the microscopic coupling constants defining our QFT to be finite numbers, then the physically observable effective couplings constants will suffer UV divergences from loops. Here, we see a direct analog: if we take the bulk action functional $e^{-S(\Sigma)} = \lambda^{k_\Sigma}$ to factorize on disconnected bulk spacetimes, then the physically observable multi-boundary correlation functions $\langle Z^n \rangle = B_n(\lambda)$, analogous to the effective coupling constants, will fail to factorize due to wormholes.

Motivated by [64], we claim that factorization can be restored if we modify the bulk action functional $e^{-S(\Sigma)} = \lambda^{k_\Sigma}$ of Marolf–Maxfield theory, allowing it to become a

non-local functional of Σ which we denote $e^{-S_{\text{bare}}(\Sigma)}$. This is the analog of passing to a bare action in perturbative renormalization, where we allow coupling constants to be divergent. Schematically, we expect this "bare bulk action" to take the form

$$e^{-S_{\text{bare}}(\Sigma)} = \lambda^{k_\Sigma} + \text{Non-local corrections}. \qquad (10.29)$$

These non-local corrections should be precisely tuned such that the modified gravitational path integral

$$\langle Z^n \rangle = e^{-S_{\text{bare}}(n \text{ disks})} + \sum_{\Sigma \in \mathcal{W}_n^{\text{wh}}} e^{-S_{\text{bare}}(\Sigma)}, \qquad (10.30)$$

produces factorizing answers, i.e., $\langle Z^n \rangle = \lambda^n$, due to cancellations between non-localities in the first, "tree-level" term, and non-factorizations arising from the sum over wormhole contributions. As in the unmodified Marolf–Maxfield theory (10.26), we make the simplifying assumption that $e^{-S_{\text{bare}}(\Sigma)}$ is independent of the number of boundaries of Σ and depends only on the number k_Σ of connected components.[23]

As described in the Introduction, we view the non-local corrections in (10.29) as arising from having already integrated out microscopic, stringy wormholes in a UV complete theory, whose role is to cancel against the geometric wormholes described by the EFT. With this expectation in mind, we will make the ansatz

$$e^{-S_{\text{bare}}(n \text{ disks})} = \lambda^n + \sum_{\Sigma \in \mathcal{W}_n^{\text{wh}}} \lambda^{k_\Sigma} C(\Sigma), \qquad (10.31)$$

where $C(\Sigma)$ is some functional of the set of spacetime manifolds, defined to be multiplicative on connected components.[24] Each term $\lambda^{k_\Sigma} C(\Sigma)$ in (10.31) represents the contribution of a *counter-wormhole* (see Figure 10.4) associated to the wormhole Σ. The factors $C(\Sigma)$ must be chosen to precisely cancel the non-factorization arising from Σ in the gravitational path integral. Crucially, the wormhole contributions in (10.30) are computed using the modified action functional $e^{-S_{\text{bare}}(\Sigma)}$, rather than the unmodified Marolf–Maxfield action, which themselves include counter-wormhole contributions. Thus, the problem of choosing appropriate counter-wormhole factors $C(\Sigma)$ in order to guarantee factorization is inherently recursive. Now, due to the simplicity of Marolf–Maxfield theory, we could directly solve this recursive problem by hand, in order to obtain $e^{-S_{\text{bare}}(\Sigma)}$. However, as our goal is to highlight algebraic

---

[23]This assumption is merely for convenience: relaxing it would not change anything of conceptual consequence but would require keeping track of much more data.

[24]Note that $e^{-S_{\text{bare}}(\Sigma)}$ for more general Σ is defined to be equal to $e^{-S_{\text{bare}}(k_\Sigma \text{ disks})}$, by our assumption that $e^{-S_{\text{bare}}(\Sigma)}$ depends only on the number of components k_Σ of Σ.
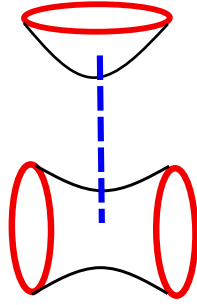
Figure 10.4: A schematic notation for a contribution including a counter-wormhole, represented as a dashed blue line, going between two connected components of spacetime.
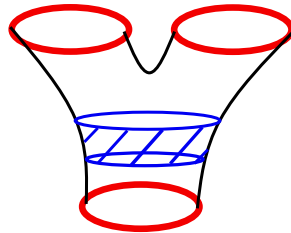
Figure 10.5: An example of sub-wormhole. The pair of pants Σ has an embedded cylinder $\sigma \subset \Sigma$ which itself leads to a wormhole contribution.

structures that may exist in more general gravitational theories, let us instead describe the conceptual root of this recursive subtlety.

In the case of perturbative renormalization, we saw that the BPHZ procedure was needed in order to handle the possibility of divergent subgraphs $\gamma \subset \Gamma$. What are the gravitational analogs of subd-ivergences? Inside a given spacetime manifold Σ defining a wormhole contribution to the gravitational path integral, we might have embedded submanifolds $\sigma \subset \Sigma$ which are, themselves, spacetime wormholes (see Figure 10.5).

Presumably, at an earlier stage of the recursive procedure, we would have chosen a counter-wormhole factor $C(\sigma)$ to cancel against the non-factorizations arising from
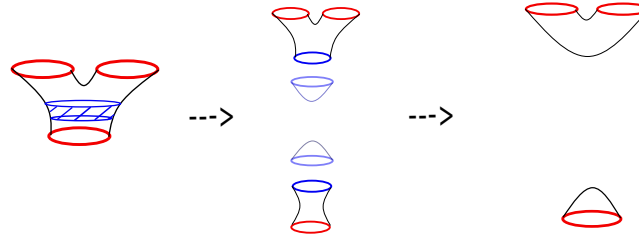
Figure 10.6: The construction of the manifold Σ/σ, when Σ is a pair of pants and σ an embedded cylinder. We excise the embedded cylinder and fill each hole with a disk, so that we are left with the disjoint union of a disk and a cylinder.

σ. Thus, not all of the non-factorization in the unmodified contribution of Σ to the gravitational path integral is new: some of it must be ascribed to the *sub-wormhole* $\sigma \subset \Sigma$. As a result, $C(\Sigma)$ should not be chosen merely to cancel the contribution of Σ to the gravitational path integral, but only the part of its contribution which cannot be ascribed to any sub-wormhole.[25]

To handle the possibility of sub-wormholes, we would like to construct a gravitational analog of the BPHZ formula (10.11). We first need to determine what the analog of the unrenormalized Feynman integrals $U(\Gamma)$ are. These will be given by *unrenormalized wormhole factors* $U(\Sigma)$, defined to be equal to 1 for all Σ, so that we may rewrite the Marolf–Maxfield path integral (10.28) as

$$\langle Z^n \rangle = \lambda^n + \sum_{\Sigma \in \mathcal{W}_n^{\mathrm{wh}}} \lambda^{k_\Sigma} U(\Sigma). \tag{10.32}$$

With the somewhat trivial functional $U(\Sigma)$ defined, we can now define a *prepared wormhole factor* for a connected surface Σ via an analog of (10.10)

$$\overline{R}(\Sigma) = U(\Sigma) + \sum_{\sigma \subset \Sigma} C(\sigma) U(\Sigma/\sigma), \tag{10.33}$$

where Σ/σ denotes the surface obtained by excising σ from Σ and gluing in disks along the new boundaries (see Figure 10.6).

---

[25]If our theory were not topological, we might want to especially focus on the contribution of metrics on Σ where the sub-wormhole $\sigma \subset \Sigma$ is becoming very small. An interesting point of comparison is the definition of n-point interaction vertices in closed string field theory: the n-point vertex is not merely the n-point string amplitude, but involves subtracting off some part corresponding to the sewing of lower-point interaction vertices with propagators arising from a neighborhood of the degeneration limits in moduli space [465].

We extend $\overline{R}(\Sigma)$ to disconnected Σ multiplicatively. The intuition behind (10.33) is that for each sub-wormhole $\sigma \subset \Sigma$, we subtract off the counter-wormhole factors associated to σ, in order to quantify the non-factorization arising from Σ that cannot be ascribed to a sub-wormhole. A precise definition of the set of (proper, non-empty) sub-wormholes $\sigma \subset \Sigma$ over which we sum in (10.33) is as follows.

Definition 10.3.1. Let Σ_n denote a connected genus zero surface with n circular boundaries. The set of proper, non-empty sub-wormholes over which we sum in (10.33) is the set of (mapping class group equivalence classes of) connected[26] embedded submanifolds $\sigma \subset \Sigma_n$ such that $\sigma \cong \Sigma_k$ for some $2 \leq k < n$ and such that the surface $\Sigma_n/\sigma \cong \Sigma_{n_1} \sqcup \cdots \sqcup \Sigma_{n_k}$ for some partition $n = n_1 + \cdots + n_k$ of the set of boundaries of Σ_n into k non-empty parts. Note that a sub-wormhole $\sigma \subset \Sigma_n$ is uniquely specified (up to the action of the mapping class group) by the partition it induces on the set of n boundaries.

With the prepared wormhole factors $\overline{R}(\Sigma)$ defined, we now define the counter-wormhole factors $C(\Sigma)$ recursively by $C(\Sigma) = -\overline{R}(\Sigma)$ for all wormholes Σ, so that the *renormalized wormhole factors*

$$R(\Sigma) = C(\Sigma) + \overline{R}(\Sigma) = C(\Sigma) + U(\Sigma) + \sum_{\sigma \subset \Sigma} C(\sigma)U(\Sigma/\sigma) \tag{10.34}$$

vanish for all wormholes, $R(\Sigma) = 0$. As $\overline{R}(\Sigma_n)$ only involves wormhole factors $C(\Sigma_k)$ for $k < n$, this recursive process terminates. We will refer to this recursive definition of $C(\Sigma)$ as the *gravitational BPHZ procedure*.

Now that we have defined the counter-wormhole factors $C(\Sigma)$ for all wormholes Σ, we can use them to construct a renormalized, factorizing gravitational path integral in three different ways, directly analogous to the three approaches to defining renormalized perturbation theory described in Section 10.2:

First approach: The first, most direct approach is to replace the unrenormalized wormhole factors $U(\Sigma)$ with the renormalized ones $R(\Sigma)$ in the gravitational path integral (10.32), obtaining

$$\langle Z^n \rangle = \lambda^n + \sum_{\Sigma \in \mathcal{W}_n^{\text{wh}}} \lambda^{k_\Sigma} R(\Sigma). \tag{10.35}$$

---

[26]The requirement that the sub-wormholes $\sigma \subset \Sigma_n$ be connected is a bit artificial, and is chosen only to simplify the algebraic structure. As with the case of higher-genus surfaces, see [64] for a treatment that does not make this restriction.

Since we have set $R(\Sigma) = 0$ for all wormholes Σ, this reduces to removing all wormholes by hand in the sum over topologies, and we are left with

$$\langle Z^n \rangle = \lambda^n, \tag{10.36}$$

a factorizing result. While somewhat tautological, excluding wormholes by hand does have the benefit of making factorization manifest, just as the first approach to defining renormalized perturbation theory in Section 10.2 makes the cancelation of UV divergences manifest. However, this approach involves dramatically changing the rules of the game by hand, which obscures the meaning of the many useful semiclassical computations that include summing over wormholes.

Second approach: The second approach is to use $C(\Sigma)$ to define a non-local bare action functional $e^{-S_{\text{bare}}(\Sigma)}$ as in (10.31). We then forget where this bare action functional came from, and compute using the unrenormalized wormhole factors $U(\Sigma) = 1$, but now with the contribution of a surface Σ being given by $e^{-S_{\text{bare}}(\Sigma)}$ rather than λ^{k_Σ}, obtaining (10.30), which we can rewrite here as

$$\langle Z^n \rangle = e^{-S_{\text{bare}}(n \text{ disks})} + \sum_{\Sigma \in \mathcal{W}_n^{\text{wh}}} e^{-S_{\text{bare}}(\Sigma)} U(\Sigma). \tag{10.37}$$

While it may not be obvious yet, if the counter-wormhole factors $C(\Sigma)$ are chosen recursively through the gravitational BPHZ procedure, then this second approach will agree with the first, and yield $\langle Z^n \rangle = \lambda^n$, as desired. In this approach, we perform a nontrivial sum over wormhole contributions, but the non-localities in the bare action functional will conspire to cancel against the wormholes and lead to factorization. While this approach obscures factorization, it makes manifest that we are still performing a sum over the same topologies as in the semiclassical Marolf–Maxfield theory, with non-local rules for the contribution of a spacetime depending on its number of connected components. It is worth pointing out that the non-localities in $e^{-S_{\text{bare}}(\Sigma)}$ are all subleading in λ^{-1}, so we may view these as non-local corrections to the Marolf–Maxfield EFT, suppressed by λ^{-1}.

Third approach: The third approach consists of enlarging the set of topologies we include in our gravitational path integral, by explicitly including counter-wormhole topologies. In this approach, each wormhole or counter-wormhole contribution will still be individually non-factorizing, but the combinatorics of formula (10.34) will be more readily visible, since we can keep track of the contributions of each counter-wormhole individually.
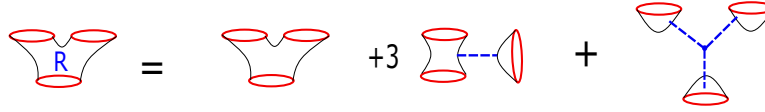
Figure 10.7: A graphical representation of the counter-wormholes contributing to the renormalized value of a pair of pants. In order to restore factorization, we derive the contributions of the counter-wormholes recursively by asking that the renormalized values of all nontrivial wormholes are zero.

A few explicit examples

We now show how the gravitational BPHZ procedure implemented by (10.34) implements factorization for the first few correlation functions $\langle Z^2 \rangle$, $\langle Z^3 \rangle$. In addition, we will show explicitly that the three approaches for incorporating the counter-wormhole factors $C(\Sigma)$ discussed above are equivalent.

Before being able to apply any of these approaches, we first need to compute the factors $C(\Sigma_2)$, $C(\Sigma_3)$ associated to the cylinder Σ_2 and the pair of pants Σ_3. For the cylinder Σ_2, there are two terms in Equation (10.34), which reads

$$R(\Sigma_2) = C(\Sigma_2) + U(\Sigma_2). \tag{10.38}$$

Since we want to impose $R(\Sigma_2) = 0$, and we have that $U(\Sigma_2) = 1$, we learn that

$$C(\Sigma_2) = -1. \tag{10.39}$$

In other words, the counter-wormhole associated to the cylinder exactly compensates the contribution of the cylinder, as there are no nontrivial sub-wormholes to consider.

Let us move on to the next order. For the pair of pants Σ_3, Equation (10.34) reads

$$R(\Sigma_3) = C(\Sigma_3) + U(\Sigma_3) + 3C(\Sigma_2)U(\Sigma_2 \sqcup \Sigma_1), \tag{10.40}$$

arising from the three topologically distinct sub-wormholes $\Sigma_2 \subset \Sigma_3$ associated to the three partitions of the set $\{1, 2, 3\}$ into two non-empty parts. By imposing $R(\Sigma_3) = 0$ and inserting the previously computed value $C(\Sigma_2) = -1$, we obtain:

$$C(\Sigma_3) = -U(\Sigma_3) - 3C(\Sigma_2)U(\Sigma_2 \sqcup \Sigma_1) = -1 - 3(-1) = 2. \tag{10.41}$$

This last computation is illustrated on Figure 10.7.

Let us now implement the three methods described above to these first two steps of the gravitational BPHZ procedure.
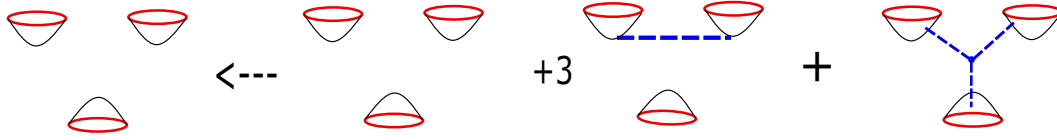
Figure 10.8: A graphical representation of all the counter-wormholes getting re-summed into the contribution $e^{-S_{\text{bare}}(3 \text{ disks})}$ of a spacetime with three connected components (here taken to be three disks). After resumming the counter-wormholes, this contribution is no longer λ^3: the counter-wormholes introduce non-localities.

First approach: The above computations of the counterterms guarantee that $R(\Sigma_2) = R(\Sigma_3) = 0$. Therefore all wormholes become excluded from the gravitational path integral by hand, and we simply calculate

$$\langle Z^2 \rangle = \lambda^2, \qquad \langle Z^3 \rangle = \lambda^3, \tag{10.42}$$

which is of course consistent with factorization.

Second approach: We first compute $e^{-S_{\text{bare}}(\Sigma)}$ for $k_\Sigma = 2, 3$, using (10.31). For $k_\Sigma = 2$ we obtain:

$$e^{-S_{\text{bare}}(2 \text{ disks})} = \lambda^2 + \lambda^{k_{\Sigma_2}} C(\Sigma) = \lambda^2 - \lambda, \tag{10.43}$$

and for $k_\Sigma = 3$ we obtain

$$e^{-S_{\text{bare}}(3 \text{ disks})} = \lambda^3 + 3\lambda^{k_{\Sigma_2 \sqcup \Sigma_1}} C(\Sigma_2) + \lambda^{k_{\Sigma_3}} C(\Sigma_3) = \lambda^3 - 3\lambda^2 + 2\lambda. \tag{10.44}$$

As an explicit illustration, the computation of $e^{-S_{\text{bare}}(3 \text{ disks})}$ is represented on Figure 10.8.

Now we can compute the values of $\langle Z^2 \rangle$ and $\langle Z^3 \rangle$ using Equation (10.30):

$$\langle Z^2 \rangle = e^{-S_{\text{bare}}(\Sigma_1 \sqcup \Sigma_1)} + e^{-S_{\text{bare}}(\Sigma_2)} = (\lambda^2 - \lambda) + \lambda = \lambda^2, \tag{10.45}$$

and

$$\langle Z^3 \rangle = e^{-S_{\text{bare}}(\Sigma_1 \sqcup \Sigma_1 \sqcup \Sigma_1)} + 3e^{-S_{\text{bare}}(\Sigma_2 \sqcup \Sigma_1)} + e^{-S_{\text{bare}}(\Sigma_3)} \tag{10.46}$$

$$= (\lambda^3 - 3\lambda^2 + 2\lambda) + 3(\lambda^2 - \lambda) + \lambda = \lambda^3, \tag{10.47}$$

which explicitly shows that once again, factorization is restored.

$$\langle Z^2 \rangle =$$

Figure 10.9: The systematic expansion of the gravitational path integral with two boundaries, including the counterterm $C(\Sigma_2)$ represented here with a dashed line.

$$\langle Z^3 \rangle =$$

Figure 10.10: The sum of all wormholes and counter-wormholes contributing to the spacetime amplitude $\langle Z^3 \rangle$. The way we constructed counter-wormhole contributions recursively ensures that this sum leads to a factorizing answer.

Third approach: In this method, we represent each term of the expanded forms of Equations (10.45) and (10.47) as a topology of its own, including counter-wormholes explicitly, as shown on Figures 10.9 and 10.10. This corresponds to adding more topologies to the gravitational path integral, which make it explicit that we have included additional wormhole-like contributions to the gravitational path integral.

The Faà di Bruno Hopf Algebra

Now that we have gained some intuition on how the gravitational BPHZ procedure leads to factorization for the first few multi-boundary correlation functions, we are ready to describe the abstract algebraic structure controlling this recursive process. We will define a Hopf algebra $\mathcal{H}_{\text{FdB}}$ that underlies the gravitational BPHZ algorithm, analogous to the Connes-Kreimer Hopf algebra $\mathcal{H}_{\text{CK}}$ that underlies the BPHZ algorithm in perturbative renormalization. In addition, we will be able to interpret the group of characters G_{FdB} of this Hopf algebra as a group of gauge

equivalences or dualities which interpolate between equivalent prescriptions for the gravitational path integral, and in particular, between the first, second, and third approaches described above.

In the case of perturbative renormalization, we saw that many transformations of the form (10.13). In the case of gravity, many of the key equations (such as (10.31), (10.32), (10.35), or (10.37)) were of the form

$$B_n = A_n + \sum_{\Sigma \in \mathcal{W}_n^{\text{wh}}} A_{k_\Sigma} F(\Sigma).,$$

(10.48)

where A_n, B_n are sequences of values assigned to spacetimes with $n \geq 1$ components (for instance, λ^n, $B_n(\lambda)$, or $e^{-S_{\text{bare}}(n \text{ disks})}$), and $F(\Sigma)$ some functional on the set of wormholes that is multiplicative on disjoint connected components.

We wish to interpret the transformation (10.48) as the right action of a group G_{FdB}. Functionals $F(\Sigma)$ will define elemnts of G_{FdB}, and we aim to summarize the discussion in Section 10.3 in terms of a commutative diagram

$$
\begin{array}{ccc}
\lambda^n & \xrightarrow{\quad C \quad} & e^{-S_{\text{bare}}(n \text{ disks})} \\
\downarrow{\scriptstyle U} & \searrow{\scriptstyle R} & \downarrow{\scriptstyle U} \\
\langle Z^n \rangle = B_n(\lambda) & & \langle Z^n \rangle = \lambda^n
\end{array}
.
$$

(10.49)

In this diagram, the vertical arrows U use a sequence A_n to compute an unrenormalized gravitational path integral

$$\langle Z^n \rangle = A_n + \sum_{\Sigma \in \mathcal{W}_n^{\text{wh}}} A_{k_\Sigma},$$

(10.50)

the diagonal arrow R computes a tautological "renormalized gravitational path integral"

$$\langle Z^n \rangle = A_n + \sum_{\Sigma \in \mathcal{W}_n^{\text{wh}}} A_{k_\Sigma} R(\Sigma) = A_n,$$

(10.51)

and the horizontal arrow C sums over counter-wormhole contributions according to the ansatz (10.31). The three approaches to the gravitational BPHZ procedure correspond to different ways of reaching the lower right hand corner, and result in equivalent physical theories.

As in the case of Connes-Kreimer, we can motivate the group law $\star$ on G_{FdB} by observing that we should have $R = C \star U$, and extrapolating from (10.34) to define:

$$(F \star G)(\Sigma) = F(\Sigma) + G(\Sigma) + \sum_{\sigma \subset \Sigma} F(\sigma) G(\Sigma/\sigma),$$

(10.52)

Figure 10.11: The coproduct of a pair of pants wormhole. In the second line we have made it manifest that disks get identified with the unit of the Faà di Bruno algebra.

where σ runs over the set of sub-wormholes $\sigma \subset \Sigma$ specified in Definition 10.3.1. Dually, we can define the Hopf algebra $\mathcal{H}_{\text{FdB}}$ dual to G_{FdB}, which turns out to be isomorphic to a well-known Hopf algebra called the Faà di Bruno Hopf algebra (as proven below in Proposition 10.3.4):

Definition 10.3.2. The *Faà di Bruno algebra* $\mathcal{H}_{\text{FdB}}$ is the free commutative algebra $\mathbb{C}[\Sigma_2, \Sigma_3, \dots]$ generated by the set of (diffeomorphism classes of) connected genus zero surfaces Σ with $n \geq 2$ circular boundaries, equipped with counit $\varepsilon : \mathcal{H}_{\text{FdB}} \to \mathbb{C}$ and coproduct $\Delta : \mathcal{H}_{\text{FdB}} \to \mathcal{H}_{\text{FdB}} \otimes \mathcal{H}_{\text{FdB}}$ defined on algebra generators Σ by $\varepsilon(\Sigma) = 0$ and

$$\Delta(\Sigma) = \Sigma \otimes 1 + 1 \otimes \Sigma + \sum_{\sigma \subset \Sigma} \sigma \otimes \Sigma/\sigma, \tag{10.53}$$

and extended multiplicatively. The sum in (10.53) runs over all sub-wormholes $\sigma \subset \Sigma$ as specified in Definition 10.3.1 (see Figure 10.11), and we identify the disjoint union of surfaces with the free algebra structure on $\mathcal{H}_{\text{FdB}}$. We further define G_{FdB} to be the spectrum $\text{Spec}(\mathcal{H}_{\text{FdB}})$, consisting of algebra homomorphisms $F : \mathcal{H}_{\text{FdB}} \to \mathbb{C}$. The coproduct Δ defines a multiplication law $\star : G_{\text{FdB}} \times G_{\text{FdB}} \to G_{\text{FdB}}$ given by (10.52).

Proposition 10.3.3. *The coproduct Δ equips $\mathcal{H}_{\text{FdB}}$ with the structure of a Hopf algebra.*

Proof. This proof could be circumvented by using the following Proposition 10.3.4 that G_{FdB} is isomorphic to a well-known group. Nevertheless, we present a more direct proof along the lines of the proof of Proposition 10.2.2 because it is valuable for intuition.

By definition, ε and Δ are algebra homomorphisms, and it is immediate that ε is a two sided counit for Δ. For coassociativity, observe that for connected surface Σ, both $(\Delta \otimes \mathrm{Id})(\Delta(\Sigma))$ and $(\mathrm{Id} \otimes \Delta)(\Delta(\Sigma))$ can be written as

$$\Delta^2(\Sigma) = \sum_{\sigma \subset \sigma' \subset \Sigma} \sigma \otimes \sigma'/\sigma \otimes \Sigma/\sigma', \tag{10.54}$$

where the sum runs of nested subwormholes $\sigma \subset \sigma' \subset \Sigma$ and further includes empty and improper subwormholes, where we identify the disk Σ_1 with the unit $1 \in \mathcal{H}_{\mathrm{FdB}}$.

This shows that $\mathcal{H}_{\mathrm{FdB}}$ is a bialgebra. Equipped with the grading $|\Sigma_n| = n - 1$, we see that $\mathcal{H}_{\mathrm{FdB}}$ is connected graded, so it a Hopf algebra by Proposition 10.5.3, with the antipode defined recursively through the formula

$$S(\Sigma) = 1 - \Sigma - \sum_{\sigma \subset \Sigma} S(\sigma)\Sigma/\sigma. \tag{10.55}$$

$\square$

cor. $(G_{\mathrm{FdB}}, \star)$ *is a group.*

Proof. This follows from Proposition 10.5.2. $\square$

We now introduce another presentation of G_{FdB} that makes some of its algebraic structure more manifest, and will greatly simplify the calculations in a lot of cases. Indeed, while the presentations of the Faà di Bruno Hopf algebra and its associated group given above are the most natural ones from the point of view of the gravitational theories at hand, they are isomorphic to objects that may look more familiar to the reader. In particular, the group G_{FdB} can be identified with the group of formal power series with zero constant term and unit linear term, equipped with a much more familiar law: the law $\circ$ of composition. More precisely, we have:

Proposition 10.3.4. *The map*

$$\begin{array}{rcl} (G_{\mathrm{FdB}}, \star) & \longrightarrow & (t + t^2 \mathbb{C}[[t]], \circ) \\ F & \longmapsto & \hat{F}(t) = t + \sum_{k \geq 2} F(\Sigma_k)\frac{t^k}{k!}, \end{array} \tag{10.56}$$

where Σ_k denotes the genus zero topological surface with k boundaries, is an isomorphism of groups.

Proof. Let $F, G \in G_{\mathrm{FdB}}$. We have that

$$\widehat{(F \star G)}^{(n)}(t) = (F \star G)(\Sigma_n) = \sum_{k_1 + \cdots + k_p = n} F(\Sigma_p)\left(\prod_{i=1}^{p} G(\Sigma_{k_i})\right) = (\hat{F} \circ \hat{G})^{(n)}(t),$$

$$\tag{10.57}$$

by Faà di Bruno's formula for the nth derivative of the composition of two formal power series. Thus, $F \mapsto \hat{F}$ is a group homomorphism. Moreover it admits an inverse, defined by setting $F(\Sigma_k) = \hat{F}^{(k)}$, so it defines an isomorphism of groups. $\qquad\square$

Remark 10.3.5. Proposition 10.3.4 justifies the name of the Faà di Bruno Hopf algebra: the combinatorics underlying our gravitational path integral are the same as the ones underlying the composition of formal power series (as is already evident in [328]), which leads to the Faà di Bruno formula for the nth derivative of a composite function. Both cases involve a sum over partitions of n, which in our case correspond to all the possible wormhole configurations between n boundaries.

Remark 10.3.6. The inverse law of the group $t + t^2\mathbb{C}[[t]]$ under composition is given by the well-known Lagrange inversion formula:

$$\hat{F}^{-1}(t) = \sum_{n=1}^{\infty} \frac{1}{n!} \frac{\mathrm{d}^{n-1}}{\mathrm{d}s^{n-1}} \left(\frac{\hat{F}(s)}{s} \right)^{-n} \Bigg|_{s=0} t^n. \tag{10.58}$$

To define the action of G_{FdB} on the space of possible gravitational action functionals, we make the following definition.

Definition 10.3.7. The space of *bulk action functionals* is the space of formal power series

$$A(t) = 1 + \sum_{k>0} A_k \frac{t^k}{k!}, \tag{10.59}$$

with constant term 1. We interpret the power series $A(t)$ as the gravitational action functional that assigns the value $e^{-S(\Sigma)} = A_{k_\Sigma}$ to any spacetime manifold Σ with k_Σ connected components.

Example 10.3.8. The bulk action functional for Marolf–Maxfield theory is

$$A_{\mathrm{MM}}(t) = \sum_{k \geq 0} \lambda^k \frac{t^k}{k!} = e^{\lambda t}, \tag{10.60}$$

while the effective bulk action functional after integrating out wormholes is

$$A_{\mathrm{MM}}^{\mathrm{eff}}(t) = \sum_{k \geq 0} B_k(\lambda) \frac{t^k}{k!} = e^{\lambda(e^t - 1)}, \tag{10.61}$$

to be compared with [328, Section 3.2].

Proposition 10.3.9. *Equation* (10.48) *defines a right action of the group* G_{FdB} *on the set of bulk action functionals* $A(t) = 1 + \sum_{k \geq 1} A_n t^k / k!$.

Proof. For $F \in G_{\text{FdB}}$, define the right action

$$(A \cdot F)(t) = A(t) + \sum_{\Sigma \in \mathcal{W}^{\text{wh}}} A_{k_\Sigma} F(\Sigma) \frac{t^{n_\Sigma}}{(n_\Sigma)!}, \tag{10.62}$$

where the sum runs over the set $\mathcal{W}^{\text{wh}} = \coprod_n \mathcal{W}_n^{\text{wh}}$ of wormhole spacetimes Σ with any number of boundaries n_Σ. Note that the nth component $(A \cdot F)^{(n)}(t)$ of (10.62) is precisely given by (10.48). Applying Faà di Bruno's formula to (10.62), we have that

$$(A \cdot F)(t) = (A \circ \hat{F})(t), \tag{10.63}$$

using the isomorphism constructed in Proposition 10.3.4. Acting by precomposition is manifestly a right action. $\qquad \square$

Factorization at all orders

Leveraging the algebraic framework developed in the previous section, we can now compute appropriate counter-wormhole factors $C(\Sigma_n)$ to restore factorization in the Marolf–Maxfield path integral at all orders. In particular, the constraint that $R(\Sigma) = 0$ for all Σ ensures that $R = \varepsilon$, and so R is simply the unit of G_{FdB}. Thus, the equation $R = C \star U$ tells us that C is simply given by the inverse of U under the group law: we have $C = U \circ S$, where S is the antipode on $\mathcal{H}_{\text{FdB}}$.

The easiest way to compute C is through the isomorphic presentation of G_{FdB} as a group of formal power series under composition provided by Proposition 10.3.4. Note that the image of U under this isomorphism is the formal power series

$$\hat{U}(t) = t + \sum_{k \geq 2} \frac{t^k}{k!} = e^t - 1. \tag{10.64}$$

Thus, it is straightforward to compute $\hat{C}(t)$ as the compositional inverse of $\hat{U}(t)$, given by

$$\hat{C}(t) = \log(1 + t). \tag{10.65}$$

By Taylor expanding this expression, we obtain:

Proposition 10.3.10. *The counter-wormhole factors for Marolf–Maxfield theory to all orders are given by*

$$C(\Sigma_n) = (-1)^{n+1}(n - 1)! \tag{10.66}$$

We can now recast the three approaches to defining a renormalized gravitational path integral in terms of the identity

$$e^{\lambda t} = (A_{\text{MM}} \cdot C \cdot U)(t), \tag{10.67}$$

where the left hand side is the exponential generating function of the factorizing multi-boundary correlation functions $\langle Z^n \rangle = \lambda^n$. More precisely, the three approaches to incorporating counter-wormholes differ in the order in which we perform the operations and the subsequent simplifications performed.

First approach: First perform the group multiplication $R = C \star U$, so that we obtain

$$e^{\lambda t} = (A_{\mathrm{MM}} \cdot R)(t), \tag{10.68}$$

where $\hat{R}(t) = t$. This amounts to giving a zero contribution to all spacetimes with wormholes inside the gravitational path integral, and simply reading off spacetime amplitudes by evaluating the Marolf–Maxfield action on only disconnected spacetimes.

Second approach: First act with C to define

$$A_{\mathrm{MM}}^{\mathrm{bare}}(t) = (A_{\mathrm{MM}} \cdot C)(t) = 1 + \sum_{k \geq 1} e^{-S_{\mathrm{bare}}(k \text{ disks})} \frac{t^k}{k!}. \tag{10.69}$$

to define a bare action, leaving us with

$$e^{\lambda t} = (A_{\mathrm{MM}}^{\mathrm{bare}} \cdot U)(t). \tag{10.70}$$

This approach corresponds to resumming the counter-wormholes into non-local spacetime actions $e^{-S_{\mathrm{bare}}(\Sigma)}$ for the contribution of a spacetime Σ with multiple connected components, and then doing an ordinary sum over topologies with this new action functional. In particular, we can easily compute

$$A_{\mathrm{MM}}^{\mathrm{bare}}(t) = (A_{\mathrm{MM}} \circ \hat{C})(t) = (1 + t)^{\lambda}. \tag{10.71}$$

Expanding in powers of t and extracting coefficients, we deduce that a factorizing bare action functional for Marolf–Maxfield theory is given by

$$e^{-S_{\mathrm{bare}}(\Sigma)} = \lambda(\lambda - 1) \ldots (\lambda - k_{\Sigma} + 1). \tag{10.72}$$

As described in [328], something special happens when $\lambda \in \mathbb{N}$: the Taylor expansion of (10.71) terminates, and $e^{-S_{\mathrm{bare}}(\Sigma_n)} = 0$ whenever $n > \lambda$. This means that the sum over counter-wormholes for Marolf–Maxfield theory for $\lambda \in \mathbb{N}$ enforces the non-local constraint that only topologies with λ connected components or fewer may contribute! The difference between this description and the one given in [328] for

an α-sector with $\alpha = \lambda \in \mathbb{N}$ is that they fix the number of connected components to be exactly α, while we have not allowed for closed universes so can only set an upper bound on the number of connected components. In our presentation, there is nothing to stop us from taking $\lambda \notin \mathbb{N}$, as we have not imposed reflection positivity or the existence of a well defined Hilbert space.

The formula (10.72) also has the interpretation as a gravitational "exclusion rule" as described in [404, 402]. To see this, imagine that in the first approach (where wormholes are excluded by hand), the path integral counts λ many microstates of the bulk quantum gravity theory on each disk (which could be interpreted as states of half-wormholes or end-of-the-world branes). Then, to reintroduce wormholes, we take any configuration where multiple connected components are in the same microstate, and glue them into a connected topology (this is the "diagonal = wormhole" principle of [404, 402]). Thus, if one takes this second approach, and sums both disconnected topologies and wormholes in the gravitational path integral, states where distinct connected components lie in the same microstate need to be subtracted by hand in order to avoid double counting, leading to the formula (10.72).

Third approach: Perform none of the compositions in (10.67), and merely expand out all three terms A_{MM}, C, and U. This amounts to adding more topologies into the gravitational path integral, which corresponds to all the counter-wormholes being explicitly spelled out.

Remark 10.3.11. The identity (10.67) makes it very clear that the Faà di Bruno group G_{FdB} has an interpretation as a group of gauge transformations (or dualities) involving topology change inside the gravitational path integral. Indeed, we can choose arbitrary elements $\theta_1, \theta_2 \in G_{\mathrm{FdB}}$ and insert a product $1 = \theta_i^{-1} \theta_i$ in between two operations of (10.67). We obtain:

$$e^{\lambda t} = (A_{\mathrm{MM}} \cdot \theta_1^{-1} \cdot \theta_1 \cdot C \cdot \theta_2^{-1} \cdot \theta_2 \cdot U)(t). \tag{10.73}$$

The interpretation of θ_1 is that it trades counter-wormhole contributions for non-localities in the rules for sums over topologies. This can be understood as an instance of the phenemenon described by Coleman, Giddings, and Strominger [114, 204, 203], whereby we integrate out wormholes into non-local effects. The difference is that here, we are integrating out not the geometric wormholes visible in the EFT, but instead integrating out microscopic, stringy wormholes as parametrized by the counter-wormholes. In contrast, the interpretation of θ_2 is that it implements the cancelation of counter-wormholes against geometric wormholes, which can be

viewed as an example of ER = EPR for spacetime wormholes [317, 333]. In general, the gauge transformations (10.73) allow us to interpolate between infinitely many equivalent ways of organizing the gravitational path integral, including but not limited to the three approaches described above. For example, choosing $\theta_1 = C^{-1}$ allows us to switch between the second and third approaches.

10.4 Discussion

Despite the (extreme) simplicity of the toy model considered here, we believe that the structures outlined in this chapter are likely to exist in some form in much more general gravitational path integrals. In this last section, we mention several natural possible extensions of our work, and reflect on the lessons that might be drawn from our analogy between the gravitational path integral and perturbative renormalization.

More complicated toy models

This work focused on the simplest possible example that allowed us to make a precise analogy: a topological theory of gravity on surfaces of genus zero with nonempty boundary, even simpler than the model of [328]. In this context, the Hopf algebra underlying the gauge redundancies of the sum over topologies is the Faà di Bruno Hopf algebra. It would obviously be interesting to consider more complicated sums over topologies. In particular, finding a similar algebraic structure to incorporate genus insertions and end of the world branes seems to be a natural extension, in order to formalize the full analysis of [64]. In higher dimension, an interesting case study could be to try to restore factorization in the tensor models of [45, 253].

The mathematics of more complicated algebraic objects associated to topology change is likely to also contain some extra features that are absent in our model. For example, our gravitational path integrals only contain finitely many terms. In renormalization, the sums over Feynman diagrams are usually infinite due to the possibility of nesting arbitrarily many loops, and this is one of the reasons why the Connes–Kreimer Hopf algebra has a richer structure than the Faà di Bruno Hopf algebra. Such infinite sums are usually handled through combinatorial Dyson–Schwinger equations (see for example [461]), which have a rich interplay with the Hochschild cohomology of the algebra. We expect such structures to play a key role in more complete gravitational path integrals.

In our simple model, the renormalized wormhole factor $R(\Sigma)$ was given by the counit of the Hopf algebra, which sets $R(\Sigma) = 0$ for all wormholes Σ, so that the

first approach to defining a renormalized path integral was to simply exclude all wormholes. In perturbative renormalization, we only aim to subtract off the divergent part of loop integrals, leaving behind a finite piece. We would like to understand whether there is a possibility for an analogous "factorizing piece" of the wormhole contribution, so that the first approach is less tautological. Mathematically, the way that the finite piece is extracted from the divergent loop integral is through a Rota–Baxter structure and the associated Birkhoff factorization [121, 124]. It would be interesting to see whether a nontrivial Rota–Baxter structure could control the extraction of a factorizing piece of the wormhole contribution in a more complicated toy model.

Geometric models and interplay with bulk EFT

Another obvious generalization would be to go beyond topology and include geometry and dynamical fields in our bulk gravitational theory. In such a context, a crucial possibility is that the introduction of counter-wormholes and ordinary bulk EFT counterterms may not be completely independent. In particular, the effect of including counter-wormholes would likely be to introduce multi-local terms in our bulk effective action, which could be viewed as multi-local counterterms that supplement the ordinary local counterterms included to regulate bulk loop integrals.

In addition, a geometric theory contains a natural hierarchy of wormhole configurations, organized according to their geometric size. In our simple topological toy model, the integration over geometric wormholes was done in a single step. In more realistic, geometric theories, it might be more reasonable to consider integrating out all wormholes smaller than a given scale. In this way, the counter-wormholes at each scale would only be chosen to cancel against the remaining geometric wormholes larger than our cutoff, and so the counter-wormholes factors would be scale-dependent. This would lead to a natural modification of the rules of bulk effective field theory and renormalization group flow.

Bootstrapping a UV complete theory

On a more ambitious note, we might hope to find the gravitational analog of a UV complete QFT, wherein we are allowed to take the cutoff to be arbitrarily high. In a UV complete QFT, as opposed to an EFT, we no longer view the counterterms as placeholders for unknown UV physics, and instead view them as part of the fundamental definition of a complete theory. In the gravitational context, this would mean defining a UV complete, factorizing gravitational path integral by introducing

appropriate counter-wormholes at arbitrarily high scales. These counter-wormholes would no longer be viewed as a substitute for the "stringy" physics that resolves factorization; they would be that stringy physics.

For one example of this idea, the giant graviton expansion of supersymmetric gauge theories [184, 292] describes the giant graviton branes required in the bulk theory in order to correctly match the trace relations present at finite N. These giant graviton brane contributions have a similar algebraic structure to the counter-wormholes discussed in this chapter, and it would be very interesting to this connection more precise.

Factorization in higher codimension

Another interesting question is that of factorization in higher codimension. The only observable quantities we considered in this chapter were multi-boundary partition functions $\langle Z^n \rangle$, as we only considered manifolds with boundary and no corners. However, a theory of quantum gravity contains more data than just partition functions, which are associated to asymptotic boundary conditions of higher codimension. For example, it should be possible to associate Hilbert spaces to spatial slices of the boundary.[27] The locality of the holographic dual requires not only that partition functions factorize, but that these Hilbert spaces (as well as higher-codimension data) factorize as well.[28] In particular, factorization of Hilbert spaces is the original context in which gauge equivalences like ER = EPR wre originally considered, in order to explain how a spatial wormhole state could fit inside a tensor-factorized Hilbert space [318, 317].

In order to incorporate factorization of Hilbert spaces into our setup, one would need to formulate an analog of the Hopf algebraic approach presented here for a space of topological surfaces with corners.[29] We expect that the appropriate analog of a Hopf algebra in order to study factorization of Hilbert spaces would be an algebra of a higher-categorical nature, since the data of a Hilbert space can

---

[27]For a definition of these Hilbert spaces given only a reflection positive partition function, see for example [112, 113].

[28]See e.g. [226, 112, 113, 73]. This has been dubbed the "factorisation" paradox [376] (note the spelling), as suggested by Henry Maxfield. We avoid this naming convention, as there are additional factorization paradoxes in higher codimension as well (for instance, the factorization of the category of boundary conditions), and we would quickly run out of letters!

[29]The Hilbert spaces associated to manifolds with corners in the toy model we consider were discussed in [328]. The existence of such a Hilbert space is one way to see that the partition function $\langle Z \rangle$ assigned to a single boundary circle must be a natural number, as it is the dimension of a finite-dimensional vector space.

be understood as the categorification of the data of a partition function. It would be interesting to determine the appropriate higher-categorical algebra required to introduce appropriate counter-wormholes in order to guarantee factorization in all codimensions.

The resolution of these higher factorization paradoxes would also likely require the introduction of additional tools from algebraic topology. In particular, the Swampland Cobordism Conjecture [336, 335] was originally introduced in order to address these failures of factorization [334], and suggests that one should always be able to get rid of the sum over topologies in string theory by performing successive surgeries via ER = EPR [333]. It seems promising to try to use the framework described in this chapter to understand what such a procedure could look like.

One quick guess as to the possible answer is that the counter-wormholes needed to guarantee factorization in higher codimension would likely induce non-localities of a more general form, such as integrals over higher dimensional cycles as opposed to merely multi-local contact interactions. The reason is that these counter-wormholes would be needed to cancel against spacetime topologies with handles of higher dimension, which attach along higher dimensional cycles as opposed to a discrete set of points. These non-local contributions could potentially arise from the response of the worldvolume QFTs living on higher-dimensional branes which have been integrated out. These branes can be viewed as providing the microstates of the higher-dimensional handles via geometric transition.

A cosmic Galois group for quantum gravity?

As a final speculation, note that in this chapter, note that we studied *one* very simple gravitational theory with wormholes, and showed that the gravitational BPHZ procedure was described by a particular Hopf algebra $\mathcal{H}_{\text{FdB}}$, as well as its dual group G_{FdB}. In the case of perturbative renormalization, there is one Connes-Kreimer group G_{CK} per quantum field theory. However the story does not end there. Indeed, it was shown in [125] that there is a *unique* theory-independent group $\mathbb{U}$ which acts on the space of couplings of *all* QFTs and can be seen as a universal group of symmetries for perturbative quantum field theory. This group also allows to systematically implement the renormalization group flow [125]. The group $\mathbb{U}$ has very interesting number theoretic properties and is related to motivic Galois theory (see [124] for a review). In reference to Pierre Cartier's conjecture that the renormalization group is closely related to the absolute Galois group $\text{Gal}(\overline{\mathbb{Q}}/\mathbb{Q})$, the

group $\mathbb{U}$ has been referred to as a "cosmic Galois group."

Thus, it is tantalizing to ask whether a similar picture holds when it comes to the sum over topologies in quantum gravity. We put forward the following conjecture:

Conjecture 10.4.1. *There exists a gravitational cosmic Galois group that underlies the gauge redundancies associated with topology change in all quantum gravity theories.*

The existence of a gravitational cosmic Galois group underlying topology change in *all* quantum gravity theories fits very nicely with the conjectural uniqueness of UV complete quantum gravity [336]. We look forward to applying our setup to more complex models, and searching for a unified algebraic description of topology change in quantum gravity.

10.5   Appendix: Basic facts about Hopf algebras

The main mathematical result in this text is that there is a Hopf algebra structure underlying the sum over topologies in the gravitational path integral. In this appendix, we review a few standard facts about Hopf algebras that have been useful in the main text.

Definition 10.5.1. A *bialgebra* $(\mathcal{H}, \mu, \Delta, \eta, \varepsilon)$ over a field k is a k-algebra $\mathcal{H}$ (with multiplication operation $\mu : \mathcal{H} \otimes \mathcal{H} \to \mathcal{H}$ and unit $\eta : k \to \mathcal{H}$) equipped with additional algebra homomorphisms $\Delta : \mathcal{H} \to \mathcal{H} \otimes \mathcal{H}$, called the *coproduct*, and $\varepsilon : H \to k$, called the *counit*, which are coassociative and counital, i.e., such that the following diagrams commute:

$$
\begin{array}{ccc}
\mathcal{H} & \xrightarrow{\;\;\Delta\;\;} & \mathcal{H} \otimes \mathcal{H} \\
{\scriptstyle \Delta}\downarrow & & \downarrow{\scriptstyle \mathrm{Id}\otimes\Delta} \\
\mathcal{H} \otimes \mathcal{H} & \xrightarrow{\;\;\Delta\otimes\mathrm{Id}\;\;} & \mathcal{H} \otimes \mathcal{H} \otimes \mathcal{H}
\end{array}
$$

$$
\begin{array}{ccc}
\mathcal{H} & \xrightarrow{\;\;\Delta\;\;} & \mathcal{H} \otimes \mathcal{H} \\
{\scriptstyle \Delta}\downarrow & {\scriptstyle \mathrm{Id}} & \downarrow{\scriptstyle \mathrm{Id}\otimes\varepsilon} \\
\mathcal{H} \otimes \mathcal{H} & \xrightarrow{\;\;\varepsilon\otimes\mathrm{Id}\;\;} & \mathcal{H}
\end{array}
$$

Intuitively, one can think of the coproduct Δ as a decomposition operation, just as one may think of the product μ as a composition operation. In the case of Feynman

diagrams, the coproduct (10.16) on the $\mathcal{H}_{CK}$ extracts all possible sub-divergences; in the case of wormholes, the coproduct (10.53) on $\mathcal{H}_{FdB}$ extracts all possible sub-wormholes.

A *Hopf algebra* $(\mathcal{H}, \mu, \Delta, \eta, \varepsilon)$ is a bialgebra equipped with an additional k-linear map $S : \mathcal{H} \to \mathcal{H}$ called the *antipode* such that the following diagram commutes:

$$
\begin{array}{ccc}
\mathcal{H} \otimes \mathcal{H} & \xrightarrow{\;S \otimes \mathrm{Id}\;} & \mathcal{H} \otimes \mathcal{H} \\
{\scriptstyle \Delta}\nearrow & & \searrow{\scriptstyle \mu} \\
\mathcal{H} \xrightarrow{\;\;\varepsilon\;\;} & k \xrightarrow{\;\;\eta\;\;} & \mathcal{H} \\
{\scriptstyle \Delta}\searrow & & \nearrow{\scriptstyle \mu} \\
\mathcal{H} \otimes \mathcal{H} & \xrightarrow{\;\mathrm{Id} \otimes S\;} & \mathcal{H} \otimes \mathcal{H}
\end{array}
$$

When it exists, the antipode is uniquely determined by the bialgebra structure on $\mathcal{H}$.

In this chapter, all Hopf algebras considered are commutative but not co-commutative. Under the standard duality between commutative rings and their spectra, commutative Hopf algebras are dual to groups:

Proposition 10.5.2. *Let $(\mathcal{H}, \mu, \eta)$ be a commutative algebra over a field k. Then the structure of a coproduct Δ, a counit ε, and an antipode S making $\mathcal{H}$ into a Hopf algebra endows the spectrum $G = \mathrm{Spec}(\mathcal{H})$ with a group structure, called the dual group of $\mathcal{H}$. Under this equivalence, the unit $1 \in G$ is defined to be the counit ε, the group law $\star : G \times G \to G$ is defined in terms of the coproduct Δ by*

$$(g_1 \star g_2)(X) = (g_1 \otimes g_2)(\Delta(X)), \tag{10.74}$$

and the inverse map $(\cdot)^{-1} : G \to G$ is defined in terms of the antipode S by

$$g^{-1}(X) = g(S(X)). \tag{10.75}$$

In both of these formulas, X represents a Hopf algebra element $x \in \mathcal{H}$, and group elements g, g_1, g_2 are defined to be algebra homomorphisms $\mathcal{H} \to k$.

In the main text, G_{CK} and G_{FdB} are the dual groups of the Hopf algebras $\mathcal{H}_{CK}$ and $\mathcal{H}_{FdB}$, respectively. In both cases, it is essential that G_{CK} and G_{FdB} are *groups*, in which every element is invertible, due to the existence of antipodes on $\mathcal{H}_{CK}$ and $\mathcal{H}_{FdB}$. In the case of perturbative renormalization, the antipode relates the divergences to the counterterms, and in the case of gravity the antipode relates the

wormholes to the counter-wormholes. In both cases, the antipode can be defined recursively through one or the other version of the BPHZ procedure. Mathematically, such a recursive construction is possible whenever we have a *connected graded bialgebra*:

Proposition 10.5.3 ([438]). *Let $\mathcal{H}$ be a connected graded bialgebra over a field k: i.e., a bialgebra $\mathcal{H} = \bigoplus_{n \geq 0} \mathcal{H}_n$ such that μ, Δ, η and ε respect the grading, and such that $\mathcal{H}_0 = k$. Then $\mathcal{H}$ admits an antipode S, so it is a Hopf algebra.*

Proof. From the axioms for S, we must have $S(1) = 1$. Now, for $n > 0$, let $X \in \mathcal{H}_n$ be a homogenous element of degree n. Noting that ε is the projection onto $\mathcal{H}_0$ and applying counitality, we must have

$$\Delta(X) = X \otimes 1 + 1 \otimes X + \sum X' \otimes X'', \tag{10.76}$$

where X', X'' are elements of strictly lower degree than n. We define $S(X)$ recursively by the formula

$$S(X) = -X - \sum S(X')X''. \tag{10.77}$$

This formula defines an abstract version of the BPHZ procedure. $\square$

FURTHER EVIDENCE AGAINST A SEMICLASSICAL BABY UNIVERSE IN ADS/CFT

This chapter is based on the work [154], in collaboration with Netta Engelhardt.

11.1   Introduction

Recent work on black hole information starting with the calculations of the Page curve [12, 378] has clearly demonstrated that the entanglement wedge of the radiation of an old black hole includes a spatially large compact region in the black hole interior. As the black hole shrinks, the holographic encoding map becomes non-isometric [7], taking a large Hilbert space in the effective description of the system into a much smaller Hilbert space of the fundamental theory. In the limit that the black hole evaporates fully, the interior resembles a closed baby universe with a singularity that pinches off. The most natural extension of the holographic map into this regime suggests that this singular closed universe has a one-dimensional Hilbert space [13, 377].

This is a radical implication: without some additional degrees of freedom (as suggested in, e.g., [227, 2]), a one-dimensional Hilbert space results in large fluctuations in observables, inconsistent with the local physics experienced in the universe: the baby universe cannot admit a semiclassical description. While it is tempting to dismiss the original argument due to potential failure of the QES prescription [162] at the evaporation point, other arguments against semiclassicality of the baby universe, using different tools, have appeared in [328, 335, 145, 440, 441, 227]. For instance, Ref. [441] argued that if a CFT dual to the Euclidean preparation of a state via the Maldacena-Maoz wormhole [320] exists in Lorentzian time, the resulting boundary-less geometry cannot be semiclassical. This approach does not suffer from the black hole singularity endpoint issue, but it does involve an unconventional application of the AdS/CFT map to a spacetime that in Lorentzian signature has no AdS boundary. Other arguments have used the QES formula in a smooth baby universe to argue that the Hilbert space of the baby universe must be one-dimensional [13]. This approach requires an application of the QES formula to a setting in which the latter has not traditionally been applied.

Within the context of the AdS/CFT correspondence, there is a sense, spelled out in a tensor network toy model in [144], in which a closed universe must have a one-dimensional Hilbert space: the CFT Hilbert space is defined via the boundary conditions, and in the absence of a boundary, the CFT Hilbert space must be one-dimensional. This was explored in the general context of the swampland program in [335].

However, an important subtlety must be pointed out at this stage. Indeed, it may be that even though in the *fundamental description* of quantum gravity there are no closed universe degrees of freedom, *effective* semiclassical physics in a closed universe connected component could still somehow be encoded, via some unusual map, into a UV-complete theory that sits at an asymptotic boundary that is disconnected from the closed universe (see, e.g., [144] for a discussion in a tensor network toy model). This would be in some sense the most extreme possible version of nonlocality, where the physics of a connected component of spacetime would be encoded in a *different* component of spacetime disconnected from the former. However, the holographic map can be indeed be extremely nonlocal: the entanglement wedge of a boundary region can reach much deeper into the bulk than its causal wedge and even be disconnected from it[1], a feature that was crucial for the holographic realization of the Page curve [12, 379]. It is therefore not inconceivable in principle that the entanglement wedge of a boundary subregion could reach so far out that it includes a disconnected manifold.

In this article, we show, without making use of toy models or assumptions about AdS/CFT behind horizons, that at least in many cases, including a semiclassical closed universe in the entanglement wedge of a boundary region is too nonlocal, even for the holographic map. In particular, we construct an $O(1)$ complexity boundary operator whose expectation value has the power to determine whether a semiclassical baby universe exists or not. Using this operator, we find that in a large class of semiclassical geometries, the most fundamental features of AdS/CFT force the Hilbert space of a closed universe to be one-dimensional *even in the semiclassical description*. Our construction requires nothing more than the AdS/CFT extrapolate dictionary applied to the standard causal wedge of an asymptotically AdS region with $O(1)$ energy. This argument uses the baby universe state preparation of Antonini-Rath (AR) [19, 20], which we review in detail Sec. 11.2. We also provide a generalization beyond the AR construction to a class of high energy states at the

---

[1]Here we mean as a region rather than as a manifold.

cost of some additional assumptions about the AdS/CFT correspondence.

Let us briefly explain the gist of the argument. In the AR construction, a two-boundary CFT state $|\Psi\rangle_{AB}$ is prepared in a partially entangled state at some temperature below the Hawking-Page transition[20]. AR show that the path integral preparation of this state results in two disconnected asymptotically AdS regions with no horizons and a baby universe. AR then argue that this state can also be represented by an $O(1)$ number of operators of low conformal dimension acting on the vacuum; such states are of course simply dual to low energy perturbations of pure AdS [30]. The AR puzzle arises from the fact that there are now two apparent bulk geometries – one with a baby universe and one without – which are dual to the same CFT state. They propose three possible resolutions: (1) ensemble averaging; (2) invalidity of AdS/CFT: that CFT is not, in fact, dual to AdS;[2] (3) that the baby universe is not semiclassical. Another possible resolution would be that the two descriptions are somehow "gauge-equivalent," although it is not exactly clear in what sense such a statement could be made.

Here we find that (3) is the correct option. Using *only* the extrapolate dictionary in the causal wedge, we construct the aforementioned simple boundary operator $\mathcal{S}_{\partial}$ whose expectation value $\langle\mathcal{S}_{\partial}\rangle$ conclusively distinguishes between a bulk that has the baby universe

$$\langle\mathcal{S}_{\partial}\rangle_{\text{if bulk dual has baby universe}} \approx e^{-\log\dim\mathcal{H}_{\text{baby universe}}} \qquad (11.1)$$

and a bulk that does not

$$\langle\mathcal{S}_{\partial}\rangle_{\text{if bulk dual has no baby universe}} = 1. \qquad (11.2)$$

We compute the expectation value of this operator and find that it agrees exactly with the case in which the baby universe is absent. The only way in which it can *also* agree with the path integral preparation of the state that includes the baby universe is if the latter has an effective Hilbert space of dimension one. This provides a new argument that uses only the oldest and most conventional aspect of the AdS/CFT correspondence to conclude that the baby universe must have a one-dimensional Hilbert space. Any modification of AdS/CFT which would include a larger Hilbert space for the baby universe would need to give up on the extrapolate dictionary.

---

[2]In v3 of [19], this was changed to "beyond AdS/CFT," suggesting that the CFT would need to be supplemented with extra information. This essentially reduces to the statement that, on its own, the CFT is not dual to a unique bulk.

This argument can be extended to a more general setup than the precise AR construction: it clearly applies to any spacetime with a baby universe in which the fine-grained entropy is bounded from above by $O(1)$ and which can be approximately truncated to a microcanonical window of energy $O(1)$. To generalize even further to states with energy that scales with N, we consider states that have (1) no nontrivial QESs in the bulk that are homologous to the complete asymptotic boundary[3] and (2) can be represented as an $O(1)$ number of local but possibly heavy operators acting on a state of $O(1)$ energy. We show that any such CFT state with a putative baby universe in its entanglement wedge can effectively be reduced to the AR setup: thus in all such constructions, which include AR as a special case, the baby universe is not semiclassically emergent from the CFT.

To summarize:

1. We give a concrete proof that the semiclassical baby universe in AR is inconsistent with the extrapolate dictionary. We do this by showing that there must exist operators with duals localized *in the causal wedge* whose expectation values are inconsistent with the existence of more than one semiclassical baby universe state. In particular we explicitly exhibit one such operator S_∂. This also manifestly excludes the possibility of equivalence of semiclassical descriptions 1 and 2.

2. We prove that the baby universe can only be consistent with the extrapolate dictionary if it has a one-dimensional Hilbert space.

3. We give a test for any putative supplementation of AdS/CFT to include a semiclassical baby universe: it would have to correctly match the operator S_∂.

4. We generalize all of these arguments to arbitrary states with the structure described above.

The chapter is structured as follows. In Sec. 11.1 we state some global assumptions and conventions; assumptions that are necessary in only part of the chapter will be stated when needed. Sec. 11.2 reviews in the AR puzzle in a convenient framework. Sec. 11.3 constructs the operator S_∂ and proves that the AR baby universe cannot

---

[3]A sufficient (but not necessary) condition that guarantees this from the CFT side is that the simple entropy [160, 159] is $O(1)$.

be semiclassical. We extend our argument to more general states with no nontrivial QESs in Sec. 11.4 and conclude in Sec. 11.5.

Assumptions and Conventions

We will make only the following assumptions about the AdS/CFT correspondence:

1. **The extrapolate dictionary.** The algebra of boundary operators $\mathcal{A}_{\partial M}$ obtained as limits (or via the timelike tube theorem) of bulk operators in M is contained in the algebra of operators of the dual CFT in the large-N limit.

2. **Isometric Encoding in the Causal Wedge:** In the simple setting in which there are no event horizons in the bulk, the low energy EFT states and operators are encoded into the dual CFT via a map that is an application of the HKLL map [220, 219, 221] followed by the extrapolate dictionary. We assume that the HKLL map works (up to small corrections in N) as a reconstruction map at sufficiently large but finite-N, as explained in [10]; in particular, that the HKLL map is approximately identical at large but finite N on bulks that limit to the same complete causal wedge large-N geometry. In discretizations of the bulk (e.g., tensor networks) the algebra of any subregion is type I, and the encoding map $W : \mathcal{H}_{\text{bulk}} \rightarrow \mathcal{H}_{\text{CFT}}$ is an isometry [225]. In the continuum limit, the encoding map is asymptotically isometric [168]: its action on states $|\phi\rangle$ and $|\psi\rangle$ in the code subspace of low energy perturbations limits to an isometry in the infinite-N limit:

$$\lim_{N \to \infty} \langle \psi | W_N^\dagger W_N | \phi \rangle = \langle \psi | \phi \rangle . \tag{11.3}$$

   A similar statement holds for operators in the causal wedge. We refer readers looking for additional details on asymptotic encoding to [168, 192]. The encoding map W without a subscript N is the limiting operator of the sequence of operators described above.

Other assumptions that are not required throughout the chapter will only be stated when needed.

11.2 The Antonini-Rath Puzzle

We now review the Antonini-Rath (AR) puzzle in language that will be convenient for our subsequent argument. AR consider the setup of [20], which takes two CFTs
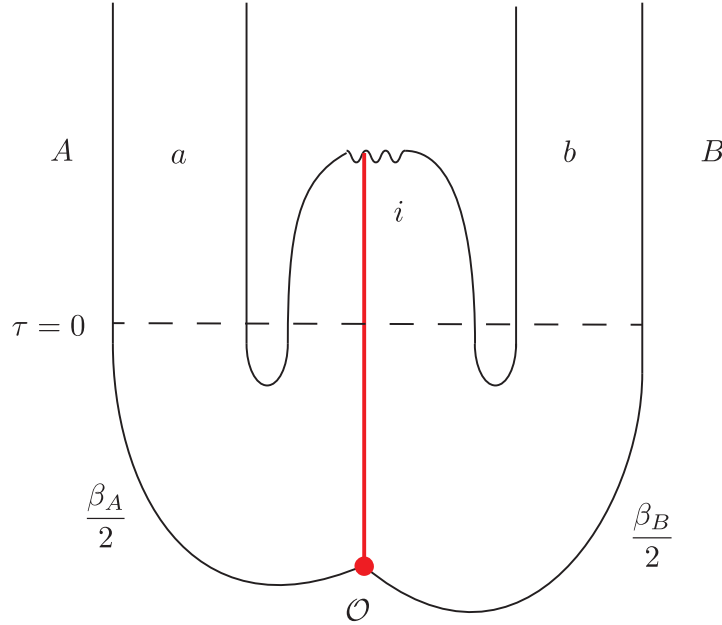
Figure 11.1: Ref. [20]'s path integral preparation of the baby universe, as used by AR in their presentation of the puzzle. There are two asymptotic boundaries A and B at different temperatures, both below Hawking-Page, and a heavy operator insertion $\mathcal{O}$ in Euclidean time. In Lorentzian time there are three disconnected bulk regions: a, i, b.

in a thermal state at a temperature below the Hawking-Page transition and inserts a heavy operator in Euclidean time:

$$|\Psi\rangle_{AB} = \frac{1}{\sqrt{Z}} \sum_{m,n} e^{-\frac{1}{2}(\beta_A E_n + \beta_B E_m)} O_{m,n} |E_n\rangle |E_m\rangle . \tag{11.4}$$

To maintain control over tails and fringe effects, AR truncate to a large but $O(1)$ microcanonical energy window; we will comment on any possible errors that this may introduce in the next section. At $\beta_A, \beta_B > \beta_{Hawking-Page}$ in this microcanonical window where black holes are very atypical, the entropy of Ψ_A (and correspondingly of Ψ_B) is large but $O(1)$.[4] The Euclidean preparation and Lorentzian continuation are illustrated in Fig. 11.1.

Let $|\psi^{(1)}\rangle_{aib}$ be the state of the bulk quantum fields prepared via the Euclidean path integral as in Fig. 11.1. By construction:

$$S_{vN}[\psi_i^{(1)}] = S_{vN}[\psi_{ab}^{(1)}] = \alpha, \tag{11.5}$$

for some large α that does not scale with N.

---

[4]This is the low temperature version of the partially entangled state construction of [205].

AR now consider a rewriting of the CFT state $|\Psi\rangle_{AB}$ in a different basis. For simplicity they consider a bulk theory with a single scalar ϕ whose boundary dual is just a single trace operator Φ. Via the state-operator correspondence in the CFT, AR write down a decomposition of $|\Psi\rangle_{AB}$ in terms of local operators of low conformal dimension acting on the vacuum:

$$|\Psi\rangle_{AB} = \sum_{A_i B_j} c_{A_i B_j} \Phi_{A_i} \Phi_{B_j} |0\rangle_A |0\rangle_B \equiv \sum_{A_i B_j} c_{A_i B_j} |A_i\rangle |B_j\rangle . \tag{11.6}$$

Let us now introduce some notation for the holographic encoding map. Define:

$$\begin{aligned}
W_a &: \mathcal{H}_a \to \mathcal{H}_A \\
W_b &: \mathcal{H}_b \to \mathcal{H}_B \\
V &: \mathcal{H}_{ab} \to \mathcal{H}_{AB}
\end{aligned} \tag{11.7}$$

so that $V = W_a \otimes W_b$. These are the holographic encoding maps from a, b, and ab into A, B, and AB. These in particular are the limiting operators in a sequence of operators in N that, when acting on states in the code subspace, asymptotically preserve inner products, expectation values, etc.

Recall now that as initially shown in [30], there is a bijection between the states $|A_i\rangle$, $|B_j\rangle$ obtained by acting with the primaries and descendants of the single trace operator Φ and the states obtained by acting with our local bulk quantum field ϕ on the AdS vacuum. AR use this to rewrite:

$$|\Psi\rangle_{AB} = \sum_{i,j} c_{A_i B_j} W_a(|a_i(A_i)\rangle) W_b(|b_j(B_j)\rangle) \tag{11.8}$$

$$= V\left(\sum_{i,j} c_{A_i B_j} |a_i\rangle |b_j\rangle \right) . \tag{11.9}$$

This shows that under the standard holographic encoding map, $|\Psi\rangle_{AB}$ is dual to a single pure state on ab which we shall call $\psi_{ab}^{(2)}$, in apparent contradiction with the fact that it was obtained by Euclidean path integral construction from a bulk that has a mixed state (with large but $O(1)$ entropy) on ab. AR float several possibilities as possible explanations of this apparent puzzle:[5]

---

[5]It is tempting to suggest that there is some problem with the path integral preparation itself, but [205] showed that such states above the Hawking-Page transition are completely conventional and reasonable states in AdS/CFT. It is difficult to see why lowering the temperature to be just below the Hawking-Page transition should all of a sudden make the state illegal.

1. Ensemble averaging. We will not consider this option here as it cannot resolve the tension in higher dimensions (and it is not clear that it can resolve the tension even in 1+1 dimensions).

2. AdS $\neq$ CFT, or equivalently, additional information is needed to determine which asymptotically AdS spacetime is semiclassically emergent from the CFT.

3. i is not semiclassical.[6] The extent of the semiclassical spacetime that is described by the CFT is just the causal wedge $a \cup b$. For example, this is the case if the emergent baby universe Hilbert space is one-dimensional.

We now give an argument that there is a definitive dual to the CFT, and that the baby universe can only be part of that dual if it has a trivial Hilbert space. We will do this by finding a concrete operator *localized in the causal wedge* that diagnoses the presence of the baby universe. Any putative supplementation of AdS/CFT to include a semiclassical baby universe must pass the test of correctly computing the expectation value of this operator. Once we give the argument in the AR setup, we will generalize it to a larger class of baby universes.

11.3 Swapping Causal Wedges

Our main tool will be the bulk swap operator.[7] Let us briefly review the definition of this operator. In a quantum system with Hilbert space $\mathcal{H}$, the swap operator $\mathcal{S}$ is a map on pairs of states:

$$\mathcal{S} : \mathcal{H} \otimes \mathcal{H} \to \mathcal{H} \otimes \mathcal{H}$$
$$|\psi\rangle \otimes |\phi\rangle \to |\phi\rangle \otimes |\psi\rangle \,.$$

Similarly, when applied to density matrices on $\mathcal{B}(\mathcal{H})$, $\mathcal{S}$ maps $\rho \otimes \sigma$ to $\sigma \otimes \rho$. Since in the AR setup none of the bulk quantities scale with N, this is an $O(1)$ complexity operator in the bulk effective field theory, whose expectation value can used as a distinguisher between states. That is, if ρ and σ are density matrices, then

$$\langle \mathcal{S} \rangle = \text{tr} \left[\rho \sigma \right] . \tag{11.10}$$

So, in particular, if $\rho = \sigma$ are identical states $\langle \mathcal{S} \rangle = \text{tr}[\rho^2]$.

---

[6]By semiclassical, we would mean that bulk effective field theory is valid up to small corrections in G.

[7]Not to be confused with the boundary swap operator, which was studied in the holographic context in [163].
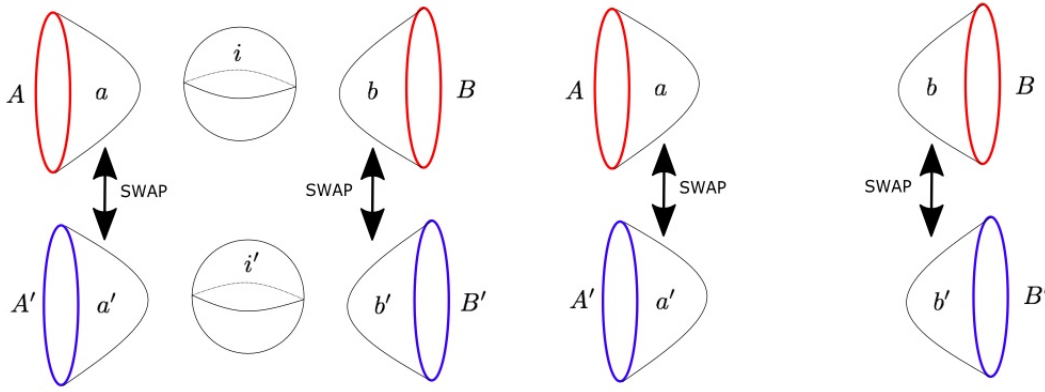
Figure 11.2: The action of the swap operator $\mathcal{S}$ on the semiclassical states $\psi^{(1)} \otimes \psi^{(1)}$ (left panel) and $\psi^{(2)} \otimes \psi^{(2)}$ (right panel). This figure represents a time slice of the doubled semiclassical geometries. In both cases the original boundary system is the red system, and the doubled system is the blue system. On the left panel, $\mathcal{S}$ swaps ab with $a'b'$, but *not* i with i'. On the right panel, there is no closed universe so $\mathcal{S}$ swaps the whole bulk ab with the whole bulk $a'b'$.

To apply $\mathcal{S}$ to our setup, we consider two copies of the ab system, which we shall label as ab and $a'b'$. We shall similarly consider two copies of our boundary system AB, which we shall label as AB and $A'B'$.

We define $\mathcal{S}$ to be the swap operator that swaps ab with $a'b'$: thus $\mathcal{S}$ has support *exclusively* in the causal wedge of $ABA'B'$. It has no support on the baby universe. The action of $\mathcal{S}$ on $\psi^{(1)} \otimes \psi^{(1)}$ and $\psi^{(2)} \otimes \psi^{(2)}$ is represented on Figure 11.2. We can compute the expectation value of $\mathcal{S}$ in both $\psi_{ab}^{(1)}$ and $\psi_{ab}^{(2)}$:[8]

$$\langle \mathcal{S} \rangle_{\psi_{ab}^{(1)} \otimes \psi_{a'b'}^{(1)}} = \text{tr}\left[\left(\psi_{ab}^{(1)} \right)^2 \right] \sim e^{-S[\psi_i^{(1)}]} \tag{11.11}$$

$$\langle \mathcal{S} \rangle_{\psi_{ab}^{(2)} \otimes \psi_{a'b'}^{(2)}} = \text{tr}\left[\left(\psi_{ab}^{(2)} \right)^2 \right] = 1, \tag{11.12}$$

where in the first equation we have used the fact that $\psi_{ab}^{(1)}$ is highly entangled with i over the code subspace.

Thus we find that *there exists an $O(1)$ complexity bulk EFT operator localized purely in the causal wedge, which can distinguish between $\psi_{ab}^{(1)}$ and $\psi_{ab}^{(2)}$*. One may attempt to argue that perhaps $\mathcal{S}$ breaks entanglement in a way that results in large energy gradients and that it thus cannot be an EFT operator; however, there is only

---

[8]Restricting the action of $\mathcal{S}$ to ab does not change its expectation value as it only acts nontrivially on the causal wedge.

at most $O(1)$ entanglement between ab and i, and this entanglement is not UV entanglement: we are only ever swapping complete disconnected universes.

Since $\mathcal{S}$ is localized to the causal wedge $aba'b'$, there is no ambiguity on whether it admits a boundary dual or not: it does. In addition, there is no ambiguity about how to represent $\mathcal{S}$ on the boundary: since $\mathcal{S}$ is a causal wedge operator of $O(1)$ complexity, it can be represented on the boundary using the standard causal wedge encoding map. Here we leave open the possibility that the encoding map is somehow unusual or different for the baby universe: because $\mathcal{S}$ is a causal wedge operator, that possibility is irrelevant to our argument; this is why in Sec. 11.1 our assumptions about the encoding map were exclusively about its action on the causal wedge. The encoding map $V \otimes V$ yields a representation $\mathcal{S}_\partial$ of $\mathcal{S}$ in the CFT on $ABA'B'$ such that [9]

$$\mathcal{S}_\partial(V \otimes V) = (V \otimes V)\mathcal{S}. \qquad (11.13)$$

We now compute the expectation value of $\mathcal{S}_\partial$ in $|\Psi\rangle_{AB}$. Because V is an isometry, if $\langle \mathcal{S}_\partial \rangle = 1$, $|\Psi\rangle_{AB}$ must be dual to description 2, whereas if $\langle \mathcal{S}_\partial \rangle \ll 1$, the dual must be description 1.

Recall now that during our review of AR's work, we established that

$$\Psi_{AB} = V\psi_{ab}^{(2)}V^\dagger. \qquad (11.14)$$

Thus

$$\langle \mathcal{S}_\partial \rangle_{\Psi_{AB}\otimes\Psi_{A'B'}} = \langle \mathcal{S}_\partial \rangle_{V\psi_{ab}^{(2)}V^\dagger\otimes V\psi_{a'b'}^{(2)}V^\dagger} = \langle \mathcal{S} \rangle_{\psi_{ab}^{(2)}\otimes\psi_{a'b'}^{(2)}} = 1, \qquad (11.15)$$

where we have used the fact that the encoding of the causal wedge is isometric, and isometries preserve expectation values. We remind the reader that $\mathcal{S}_\partial$ is *not* the boundary swap operator, so Eq. 11.15 does not just follow from purity of $|\Psi\rangle_{AB}$ but rather from the purity of $\psi_{ab}^{(2)}$.

There is thus *no* ambiguity in the dual of $|\Psi\rangle_{AB}$. We found a boundary operator $\mathcal{S}_\partial$ whose dual operator $\mathcal{S}$ is localized in the causal wedge, and this $\mathcal{S}$ definitively distinguishes between the bulk state with the baby universe and the bulk state without it. We have computed the expectation value of the corresponding CFT operator $\mathcal{S}_\partial$ and found that it conclusively agrees with the state in which the baby universe is absent.

---

[9] Note that the resulting boundary operator is *not* identical to the boundary swap operator.

We thus find that AdS/CFT has a definitive answer about the dual, assuming (a) the extrapolate dictionary, and (b) isometricity of the encoding map localized to the causal wedge in the absence of horizons. These two aspects of AdS/CFT are arguably the most well-established aspects of the duality.

How, then, are we to understand $\psi_{aib}^{(1)}$ and consistency of the gravitational path integral picture? If we insist on validity of the path integral approach, we must have

$$e^{-S[\psi_i^{(1)}]} \sim \langle \mathcal{S} \rangle_{\psi_{ab}^{(1)} \otimes \psi_{a'b'}^{(1)}} = \langle \mathcal{S} \rangle_{\psi_{ab}^{(2)} \otimes \psi_{a'b'}^{(2)}} = 1, \tag{11.16}$$

which is only possible if $|\mathcal{H}_i| = 1$. If we were to apply an encoding map to aib, the only way in which we could obtain an answer that is consistent with $\langle \mathcal{S}_\partial \rangle = 1$ is if the baby universe is not semiclassical: that is, the holographic encoding map must throw out the baby with the bathwater. In particular, our results show that any attempts to create an emergent semiclassical baby universe by modifying or altering AdS/CFT would need to find a way of matching the expectation value of $\mathcal{S}_\partial$ without destroying the extrapolate dictionary or the isometric encoding map of the causal wedge.

It is tempting to try to find a loophole in this argument by recalling that the state in Eq. 11.4 required a truncation of the tails to a microcanonical window. This suggests a potential way out: that in computing $\langle \mathcal{S} \rangle_{\psi_{ab}^{(1)}}$ from the boundary, we would find the correct answer of $e^{-S_{\text{vN}}[\psi_i^{(1)}]}$ if we had just included the tail. However, this cannot be the case: recall the exact expression of the finite N state prepared by the gravitational path integral in Eq. 11.4:

$$|\Psi\rangle_{AB} = \frac{1}{\sqrt{Z}} \sum_{m,n} e^{-\frac{1}{2}(\beta_A E_n + \beta_B E_m)} O_{m,n} |E_n\rangle |E_m\rangle. \tag{11.17}$$

The energy $\mathcal{E} = E_L + E_R$ of the two-sided state is then described by a random variable of expectation value $E_0 = O(1)$. Let us choose $\Delta_0 \gg E_0$ but still $O(1)$. By Markov's inequality,

$$\mathbb{P}(\mathcal{E} > \Delta_0) \leq \frac{E_0}{\Delta_0}. \tag{11.18}$$

This means that

$$\frac{1}{Z} \sum_{E_n + E_m > \Delta_0} e^{-(\beta_A E_n + \beta_B E_m)} |O_{m,n}|^2 \leq \frac{E_0}{\Delta_0}, \tag{11.19}$$

and so we deduce

$$\frac{1}{Z} \sum_{E_n > \Delta_0 \text{ or } E_m > \Delta_0} e^{-(\beta_A E_n + \beta_B E_m)} |O_{m,n}|^2 \leq \frac{E_0}{\Delta_0}. \tag{11.20}$$

If we denote, like in [19], by $P_{\Delta_0,(L,R)}$ the projections onto the microcanonical windows of size Δ_0 on the left and on the right, respectively, we obtain that

$$\| \, |\Psi_{AB}\rangle - P_{\Delta_0,L}P_{\Delta_0,R} \, |\Psi_{AB}\rangle \, \|^2 \leq \frac{E_0}{\Delta_0}, \tag{11.21}$$

and can therefore be made arbitrarily small since we are free to choose Δ_0 as large as we want as long as it is $O(1)$. Now, by the triangle inequality and the Cauchy–Schwarz inequality, if X is a two-sided boundary observable,

$$|\text{tr}((\Psi_{AB} - P_{\Delta_0,L}P_{\Delta_0,R}\Psi_{AB}P_{\Delta_0,L}P_{\Delta_0,R})X)| \leq 2\| \, |\Psi_{AB}\rangle - P_{\Delta_0,L}P_{\Delta_0,R} \, |\Psi_{AB}\rangle \, \|\|X\|$$

$$\tag{11.22}$$

$$\leq 2\sqrt{\frac{E_0}{\Delta_0}}\|X\|. \tag{11.23}$$

This shows that for Δ_0 chosen large enough (but $O(1)$),

$$\|\Psi_{AB} - P_{\Delta_0,L}P_{\Delta_0,R}\Psi_{AB}P_{\Delta_0,L}P_{\Delta_0,R}\|_1 \ll 1. \tag{11.24}$$

Thus the untruncated and truncated states are close in 1-norm. Since reconstruction of the causal wedge is isometric, and the 1-norm cannot grow on the preimage of an isometry, this means that if the states corresponding to the untruncated and truncated boundary states are $\psi_{ab}^{(1)}$ and $\psi_{ab}^{(2)}$, they must also be close in 1-norm:

$$||\psi_{ab}^{(1)} - \psi_{ab}^{(2)}||_1 \ll 1. \tag{11.25}$$

We now prove that this is not possible given the expectation value of the swap operator in the two different states. By Holder's Inequality:

$$|\text{tr}\left[(\rho - \sigma)\,\mathcal{S}\right]| \leq ||\rho - \sigma||_1||\mathcal{S}||_\infty, \tag{11.26}$$

where $|| \cdot ||_\infty$ refers to the operator norm, which is 1 for $\mathcal{S}$, $\rho = \psi_{ab}^{(1)} \otimes \psi_{ab}^{(1)}$, and $\sigma = \psi_{ab}^{(2)} \otimes \psi_{ab}^{(2)}$. This shows:

$$|\langle \mathcal{S}\rangle_{\psi_{ab}^{(1)}\otimes\psi_{ab}^{(1)}} - \langle \mathcal{S}\rangle_{\psi_{ab}^{(2)}\otimes\psi_{ab}^{(2)}}| \leq ||\rho - \sigma||_1. \tag{11.27}$$

We thus find:

$$||\psi_{ab}^{(1)} \otimes \psi_{ab}^{(1)} - \psi_{ab}^{(2)} \otimes \psi_{ab}^{(2)}||_1 \gtrsim 1 - e^{-S_{vN}[\psi_i^{(1)}]}. \tag{11.28}$$

The triangle inequality, together with the fact that the 1-norm is a cross norm, then yields the necessary result:

$$||\psi_{ab}^{(1)} - \psi_{ab}^{(2)}||_1 \geq \frac{1}{2}||\psi_{ab}^{(1)} \otimes \psi_{ab}^{(1)} - \psi_{ab}^{(2)} \otimes \psi_{ab}^{(2)}||_1 \gtrsim \frac{1}{2}(1 - e^{-S_{vN}[\psi_i^{(1)}]}). \tag{11.29}$$

Therefore it is not possible that any small differences between the state in Eq. 11.4 prior to truncation to the microcanonical window and the state in Eq. 11.6 could account for the large discrepancy in the expectation values of the swap operator. For both $\psi^{(1)}$ and $\psi^{(2)}$ to have CFT duals, there are only two options: (1) the duals are nearly orthogonal, or (2) the entropy of the baby universe is bounded from above by 0. Since the duals are the same state up to a truncation of the thermal tails, we conclude option (2): if it is to be encoded into the CFT, the baby universe cannot be semiclassical.

We note here that while our operator $\langle S_\partial \rangle$ acts on two copies of the state $|\Psi\rangle_{AB} \otimes |\Psi\rangle_{A'B'}$, it must be the case that there exists another operator with the same ability to distinguish $\psi_{ab}^{(1)}$ from $\psi_{ab}^{(2)}$ but which only acts on a single copy. To see this, we use Fannes' Inequality:

$$|S(\psi_{ab}^{(1)}) - S(\psi_{ab}^{(2)})| \leq \frac{1}{2}||\psi_{ab}^{(1)} - \psi_{ab}^{(2)}||_1 \log \Delta_0 + \frac{1}{e} \qquad (11.30)$$

where Δ_0 sets the dimension of the code subspace. Since $\psi_{ab}^{(1)}$ is by construction approximately maximally entangled within this code subspace, $S(\psi_{ab}^{(1)}) \sim \log \Delta_0$. We thus find that

$$||\psi_{ab}^{(1)} - \psi_{ab}^{(2)}||_1 \geq 2 - O(1/\log \Delta_0), \qquad (11.31)$$

Recall now that:

$$||\psi_{ab}^{(1)} - \psi_{ab}^{(2)}||_1 = \sup_{||X||=1} \left| \text{tr}\left[X(\psi_{ab}^{(1)} - \psi_{ab}^{(2)}) \right] \right|. \qquad (11.32)$$

Thus we find that there is an operator that can definitively distinguish between $\psi_{ab}^{(1)}$ and $\psi_{ab}^{(2)}$ even given just one copy of the system. Since this operator is localized to ab – i.e., the causal wedge – it can be encoded into the CFT via an isometry, which will preserve expectation values. Thus there exists an operator on AB that can conclusively ascertain if the state $|\Psi\rangle_{AB}$ is dual to $\psi_{aib}^{(1)}$ or $\psi_{ab}^{(2)}$. This does not, however, provide a construction of such an operator, and one could worry that this operator somehow destroys the EFT. Moreover, finding an explicit causal wedge operator whose expectation values drastically differ in the two descriptions is valuable in the sense that one can then precisely ask how to restore a consistent expectation value for this operator in the presence of a semiclassical baby universe. We will further comment on this in Section 11.5. For this reason we have opted to present our arguments in terms of the explicit operator S_∂. Let us briefly note an additional consequence of Eq. 11.32: there is a distinguishing operator if $S_{\text{vN}}[\psi_{ab}^{(1)}] > 0$ can

be made to scale like log Δ_0. On the other hand, if the baby universe Hilbert space is one-dimensional, there is no distinguisher.

This concludes our argument for the baby universe in the AR construction. We now proceed to a more general picture that does not rely on a path integral construction.

11.4 Baby universes simply cannot result from simple black holes

Our argument in the previous section relied very essentially on the absence of a QES homologous to the complete asymptotic boundary with generalized entropy larger than $O(G^0)$. It turns out that at the cost of one additional standard AdS/CFT assumption, we obtain the same result in any putative AdS/CFT baby universe construction in which there is no QES with generalized entropy larger than $O(G^0)$. We now provide the argument, starting with the following assumption:

Assumption: the simple entropy construction [161, 159, 156], which iteratively removes all sources that result in non-stationarity of horizons, applies when the horizon changes topology to the empty set. For readers unfamiliar with the simple entropy, we now briefly review this result. The primary observation is that horizons are only non-stationary due to matter (or gravitational radiation) falling across them from the asymptotic region. Thus if we can turn off the appropriate sources at $\mathscr{I}$, we would remove the infalling or outgoing matter, resulting in a stationary horizon. In a spacetime with no nontrivial QESs homologous to the complete asymptotic boundary, this removes horizons altogether. The work of [156] proved this in the absence of such topological transitions, but asserted that the result should continue to hold under such topological transitions. We will operate under the assumption that it does indeed continue to hold. This is certainly true in, e.g., Vaidya thin-shell collapse: turning off the heavy operator sourcing the shell restores the spacetime to pure AdS. We could also act on the AR state with heavy operators in Lorentzian time; that would also satisfy this assumption.

Note that we did not need to make this assumption in the AR setup as we had started with a horizonless geometry and an explicit state.

We now proceed to state the argument. Consider a bulk spacetime with the following properties:

1. A connected asymptotically AdS piece, which we shall call a. We are agnostic about how many asymptotic boundaries a has. (In the previous section, we denoted each complete connected bulk region with its own letter, e.g., a, b
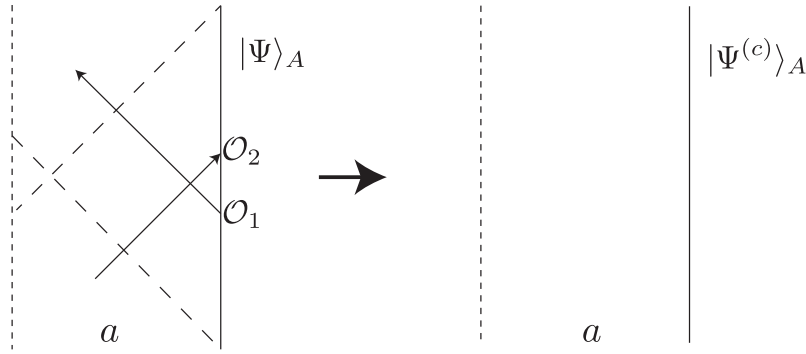
Figure 11.3: The state $|\Psi\rangle_A = O_1 O_2 |\Psi^{(c)}\rangle_A$. Turning off the sources removes the event horizon.

etc; here to maintain full generality we will use a to refer to all regions with an asymptotic boundary.)

2. A disconnected, boundaryless baby universe, which we shall call i.

3. No nonempty QESs that are homologous to the asymptotic boundary(ies) A.

Let $|\Psi\rangle_A$ be a CFT state dual to this geometry with some bulk state on it. We make one further assumption, which is that $|\Psi\rangle_A$ can be represented as an $O(1)$ number of simple (but possibly heavy) operators acting on a state of $O(1)$ energy. This is always true for a black hole formed from fast collapse. Even though the minimal QES is always the empty set, the entanglement wedge of $|\Psi\rangle_A$ depends on the entanglement of the bulk state: if the bulk state has entanglement between a and i, the entanglement wedge of the pure state $|\Psi\rangle_A$ includes i. Otherwise, we will argue that it does not.

If a has event horizons, we will remove them using the protocol of [156]: we turn on sources that (on some timefold) propagate locally from the AdS boundary and push any event horizons to the outermost QES. Since there are no nonempty QESs, this protocol removes all horizons from a.[10] We will denote by $|\Psi^{(c)}\rangle_A$ the CFT state that has been acted on in this way to reveal all of the AdS region as a causal wedge. See Fig. 11.3. We emphasize that the sources involved propagate causally from the boundary: they cannot act on the baby universe or change its state.

By our assumption on $|\Psi\rangle_A$, $|\Psi^{(c)}\rangle_A$ has $O(1)$ energy. Now we use our proof from Sec. 11.3 that the truncation of a state with $O(1)$ energy to a microcanonical window

---

[10]In the language of [197], this turns a state with an infinite causal depth parameter into a state with finite causal depth parameter.

of size $O(1)$ cannot result in a new state that has a large trace distance from the untruncated state, at least in the infinite-N limit. This means that $|\Psi^{(c)}\rangle_A$ is well approximated by a state in microcanonical window of $O(1)$, which we shall call $|\Psi^{(c)'}\rangle_A$.

Thus far our discussion has been independent of the exact state of the bulk. We now consider a low energy bulk state $|\psi\rangle_{ai}$, where there is entanglement between the AdS region and the baby universe.

Let us now introduce a second copy of a, which we shall term a'. We define, as in the previous section, the bulk swap operator $\mathcal{S}$ to swap bulk states on a and a'. It immediately follows from Sec. 11.3 that

$$\langle \mathcal{S} \rangle_{\psi_a^{(1)} \otimes \psi_{a'}^{(1)}} \sim e^{-S_{\text{vN}}[\psi_a^{(1)}]}. \tag{11.33}$$

We recall that a CFT state at large-N in an $O(1)$ microcanonical window admits a decomposition in terms of operators of low conformal dimension acting on the vacuum. Once again invoking [30], the dual of such a state is simply a low energy perturbation of AdS: no baby universe included. The expectation value $\langle \mathcal{S}_\partial \rangle = 1$, and we find that the entanglement wedge of $|\Psi^{(c)'}\rangle_A$ does not contain the baby universe unless $|\mathcal{H}_i| = 1$, and then the baby universe cannot be semiclassical.

Can $|\Psi^{(c)}\rangle_A$ contain the baby universe in its entanglement wedge? The answer is no: because $|\Psi^{(c)'}\rangle_A$ and $|\Psi^{(c)}\rangle_A$ are close in trace distance, $\langle \mathcal{S}_\partial \rangle$ must be approximately the same for the two states.

Can the original state prior to turning on simple sources, $|\Psi\rangle_A$, contain a semi-classical baby universe in its entanglement wedge? Once again, no: the locally propagating sources in question do not act on the baby universe and do not modify bulk entanglement of the state in the causal wedge. We thus arrive at the same conclusion as we did in the previous section: if there are no nontrivial QESs homologous to A, then under the stated assumptions the CFT definitively picks the state without a baby universe – unless the baby universe is contentless: $|\mathcal{H}_i| = 1$, and i is not semiclassical.

11.5   Discussion

In this chapter, we constructed a simple boundary operator whose bulk dual has support exclusively in the causal wedge, which can conclusively diagnose if a semiclassical baby universe is encoded in the CFT. In a large class of semiclassical

geometries with a closed universe, including the one of [19], the verdict is definitive: the closed universe cannot emerge in the AdS/CFT correspondence. Our argument only relies on the most basic features of the holographic dictionary: the extrapolate dictionary and the (asymptotically) isometric encoding of the causal wedge. While it is reassuring that as decades of research have shown, AdS does indeed equal CFT, failure of semiclassicality of closed universes is of course a very embarrassing state of affairs, given that we may well live in a closed cosmology. Even without worrying about our own world, this conclusion makes it very challenging to think about the interior of small black holes in the bulk of AdS at late times from the point of view of the CFT.

Recent developments [2, 227] have suggested that one way to recover semiclassical physics in a closed universe is to explicitly include an observer in the range of the holographic map [227, 2]. It would be very interesting to understand how the calculation performed in this chapter, and in particular the expectation value we found for the swap operator $\mathcal{S}_\partial$, is affected by conditioning on the presence of an observer inside the closed universe. It would also be interesting to understand what happens to these arguments in the presence of a Python's Lunch [88, 156, 157, 158], which violates the assumptions of Sec. 11.4. We leave further investigations of the implications of the bulk swap operator's encoding on the boundary to future work.

BIBLIOGRAPHY

[1] Gerard 't Hooft. "Dimensional reduction in quantum gravity". In: *Conf. Proc. C* 930308 (1993), pp. 284–296. arXiv: `gr-qc/9310026`.

[2] Ahmed I. Abdalla et al. "The gravitational path integral from an observer's point of view". In: (Jan. 2025). arXiv: `2501.02632 [hep-th]`.

[3] Peter Abramenko and Kenneth Brown. *Buildings: Theory and Applications*. Vol. 248. Jan. 2008. ISBN: 978-0-387-78834-0. DOI: `10.1007/978-0-387-78835-7`.

[4] Ilka Agricola and Thomas Friedrich. "Upper bounds for the first eigenvalue of the Dirac operator on surfaces". In: *Journal of Geometry and Physics* 30.1 (1999), pp. 1–22. ISSN: 0393-0440. DOI: `https://doi.org/10.1016/S0393-0440(98)00032-1`. URL: `https://www.sciencedirect.com/science/article/pii/S0393044098000321`.

[5] Ofer Aharony et al. "The Hagedorn - deconfinement phase transition in weakly coupled large N gauge theories". In: *Adv. Theor. Math. Phys.* 8 (2004). Ed. by H. D. Doebner and V. K. Dobrev, pp. 603–696. DOI: `10.4310/ATMP.2004.v8.n4.a1`. arXiv: `hep-th/0310285`.

[6] Chris Akers, Stefan Leichenauer, and Adam Levine. "Large Breakdowns of Entanglement Wedge Reconstruction". In: *Phys. Rev. D* 100.12 (2019), p. 126006. DOI: `10.1103/PhysRevD.100.126006`. arXiv: `1908.03975 [hep-th]`.

[7] Chris Akers et al. "The black hole interior from non-isometric codes and complexity". In: (July 2022). arXiv: `2207.06536 [hep-th]`.

[8] Christopher Akers and Geoff Penington. "Quantum minimal surfaces from quantum error correction". In: *SciPost Physics* 12.5 (May 2022). DOI: `10.21468/scipostphys.12.5.157`. URL: `https://doi.org/10.21468%2Fscipostphys.12.5.157`.

[9] Shadi Ali Ahmad and Marc S. Klinger. *Emergent Geometry from Quantum Probability*. Nov. 2024. arXiv: `2411.07288 [hep-th]`.

[10] Ahmed Almheiri, Xi Dong, and Daniel Harlow. "Bulk Locality and Quantum Error Correction in AdS/CFT". In: *JHEP* 04 (2015), p. 163. DOI: `10.1007/JHEP04(2015)163`. arXiv: `1411.7041 [hep-th]`.

[11] Ahmed Almheiri et al. "Replica Wormholes and the Entropy of Hawking Radiation". In: *JHEP* 05 (2020), p. 013. DOI: `10.1007/JHEP05(2020)013`. arXiv: `1911.12333 [hep-th]`.

[12] Ahmed Almheiri et al. "The entropy of bulk quantum fields and the entanglement wedge of an evaporating black hole". In: *JHEP* 12 (2019), p. 063. DOI: `10.1007/JHEP12(2019)063`. arXiv: `1905.08762 [hep-th]`.

[13] Ahmed Almheiri et al. "The Page curve of Hawking radiation from semiclassical geometry". In: *JHEP* 03 (2020), p. 149. DOI: `10.1007/JHEP03(2020)149`. arXiv: `1908.10996 [hep-th]`.

[14] Luis Alvarez-Gaume et al. "Finite temperature effective action, AdS(5) black holes, and 1/N expansion". In: *Phys. Rev. D* 71 (2005), p. 124023. DOI: `10.1103/PhysRevD.71.124023`. arXiv: `hep-th/0502227`.

[15] Irene Amado et al. "Probing emergent geometry through phase transitions in free vector and matrix models". In: *JHEP* 02 (2017), p. 005. DOI: `10.1007/JHEP02(2017)005`. arXiv: `1612.03009 [hep-th]`.

[16] Bernd Ammann and Christian Bär. "Dirac eigenvalue estimates on surfaces". In: *Mathematische Zeitschrift* 240.2 (2002), pp. 423–449.

[17] Claire Anantharaman and Sorin Popa. *An introduction to II$_1$ factors*. URL: `https://www.math.ucla.edu/~popa/Books/IIun.pdf`.

[18] Tarek Anous, Jorrit Kruthoff, and Raghu Mahajan. "Density matrices in quantum gravity". In: *SciPost Phys.* 9.4 (2020), p. 045. DOI: `10.21468/SciPostPhys.9.4.045`. arXiv: `2006.17000 [hep-th]`.

[19] Stefano Antonini and Pratik Rath. "Do holographic CFT states have unique semiclassical bulk duals?" In: (Aug. 2024). arXiv: `2408.02720 [hep-th]`.

[20] Stefano Antonini, Martin Sasieta, and Brian Swingle. "Cosmology from random entanglement". In: *JHEP* 11 (2023), p. 188. DOI: `10.1007/JHEP11(2023)188`. arXiv: `2307.14416 [hep-th]`.

[21] Sinya Aoki et al. "On the definition of entanglement entropy in lattice gauge theories". In: *JHEP* 06.187 (2015). DOI: `10.1007/JHEP06(2015)187`. arXiv: `1502.04267 [hep-th]`.

[22] Arash Arabi Ardehali and Sameer Murthy. "The 4d superconformal index near roots of unity and 3d Chern-Simons theory". In: *JHEP* 10 (2021), p. 207. DOI: `10.1007/JHEP10(2021)207`. arXiv: `2104.02051 [hep-th]`.

[23] Huzihiro Araki. "A lattice of von neumann algebras associated with the quantum theory of a free Bose Field". In: *Journal of Mathematical Physics* 4.11 (Nov. 1963), pp. 1343–1362. DOI: `10.1063/1.1703912`.

[24] Huzihiro Araki. "Relative Entropy of States of von Neumann Algebras". In: *Publications of The Research Institute for Mathematical Sciences* 11 (1975), pp. 809–833. URL: `https://api.semanticscholar.org/CorpusID:55415180`.

[25] Huzihiro Araki and E. J. Woods. "Representations of the Canonical Commutation Relations Describing a Nonrelativistic Infinite Free Bose Gas". In: *J. Math. Phys.* 4.5 (1963), pp. 637–662. DOI: `10.1063/1.1704002`.

[26]   Huzihiro Araki and Edward J. Woods. "A Classification of Factors". In: *Publications of The Research Institute for Mathematical Sciences* 4 (1968), pp. 51–130. URL: `https://api.semanticscholar.org/CorpusID:54930318`.

[27]   Huzihiro Araki and Walter Wyss. "Representations of canonical anticommutation relations". In: *Helvetica Physica Acta* 37 (1964), p. 136. DOI: `10.5169/SEALS-113476`.

[28]   Michael Atiyah. "Eigenvalues of the dirac operator". In: *Arbeitstagung Bonn 1984*. Ed. by Friedrich Hirzebruch, Joachim Schwermer, and Silke Suter. Berlin, Heidelberg: Springer Berlin Heidelberg, 1985, pp. 251–260. ISBN: 978-3-540-39298-9.

[29]   J. Baik. "Random vicious walks and random matrices". In: *Comm. Pure Appl. Math.* 53.11 (2000), pp. 1385–1410. DOI: `10.1002/1097-0312(200011)53:11<1385::AID-CPA3>3.0.CO;2-T`. arXiv: `math/0001022 [math.PR]`.

[30]   Tom Banks et al. "AdS dynamics from conformal field theory". In: (1998). arXiv: `hep-th/9808016 [hep-th]`.

[31]   Ning Bao et al. "Consistency conditions for an AdS multiscale entanglement renormalization ansatz correspondence". In: *Phys. Rev. D* 91.12 (2015), p. 125036. DOI: `10.1103/PhysRevD.91.125036`. arXiv: `1504.06632 [hep-th]`.

[32]   Ning Bao et al. "De Sitter space as a tensor network: cosmic no-hair, complementarity, and complexity". In: *Physical Review D* 96.12 (2017), p. 123536.

[33]   Ning Bao et al. *Holographic Tensor Networks in Full AdS/CFT*. Feb. 2019. arXiv: `1902.10157 [hep-th]`.

[34]   Christian Bär. "Dependence of the Dirac spectrum on the Spin structure". In: *Smin. Congr* 4 (Jan. 1999), pp. 17–33.

[35]   Christian Bär. "Lower eigenvalue estimates for Dirac operators". In: *Mathematische Annalen* 293.1 (1992), pp. 39–46. DOI: `10.1007/BF01444701`. URL: `https://doi.org/10.1007/BF01444701`.

[36]   Christian Bär. "The Dirac operator on hyperbolic manifolds of finite volume". In: *Journal of Differential Geometry* 54.3 (2000), pp. 439–488.

[37]   Christian Bär and Mattias Dahl. "The first Dirac eigenvalues on manifolds with positive scalar curvature". In: *Proceedings of the American Mathematical Society* 132.11 (2004), pp. 3337–3344.

[38]   E.W. Barnes. "The theory of the G-function". In: *Quart. J. Math.* 31 (1899), pp. 264–314.

[39] George Barnes, Adrian Padellaro, and Sanjaye Ramgoolam. "Hidden symmetries and large N factorisation for permutation invariant matrix observables". In: *JHEP* 08 (2022), p. 090. DOI: `10.1007/JHEP08(2022)090`. arXiv: `2112.00498 [hep-th]`.

[40] George Barnes, Adrian Padellaro, and Sanjaye Ramgoolam. "Permutation symmetry in large-N matrix quantum mechanics and partition algebras". In: *Phys. Rev. D* 106.10 (2022), p. 106020. DOI: `10.1103/PhysRevD.106.106020`. arXiv: `2207.02166 [hep-th]`.

[41] Francesc Bars. "On the automorphisms groups of genus 3 curves". In: *Barcelona* (Feb. 2005). URL: `https://mat.uab.cat/~francesc/mates/autgen3.pdf`.

[42] Helga Baum. "An upper bound for the first eigenvalue of the Dirac operator on compact spin manifolds". In: *Mathematische Zeitschrift* 206.1 (1991), pp. 409–422. DOI: `10.1007/BF02571352`. URL: `https://doi.org/10.1007/BF02571352`.

[43] Jacob D. Bekenstein. "Black Holes and Entropy". In: *Phys. Rev. D* 7 (8 Apr. 1973), pp. 2333–2346. DOI: `10.1103/PhysRevD.7.2333`. URL: `https://link.aps.org/doi/10.1103/PhysRevD.7.2333`.

[44] Florin Alexandru Belgun, Nicolas Ginoux, and Hans-Bert Rademacher. "A singularity theorem for twistor spinors". In: *Annales de l'institut Fourier*. Vol. 57. 4. 2007, pp. 1135–1159.

[45] Alexandre Belin et al. "Approximate CFTs and Random Tensor Models". In: (Aug. 2023). arXiv: `2308.03829 [hep-th]`.

[46] Alexandre Belin et al. "Symmetric Product Orbifold Universality and the Mirage of an Emergent Spacetime". In: (Feb. 2025). arXiv: `2502.01734 [hep-th]`.

[47] Michael Benedicks. "On Fourier transforms of functions supported on sets of finite Lebesgue measure". In: *Journal of Mathematical Analysis and Applications* 106.1 (1985), pp. 180–183. ISSN: 0022-247X. DOI: `https://doi.org/10.1016/0022-247X(85)90140-4`. URL: `https://www.sciencedirect.com/science/article/pii/0022247X85901404`.

[48] Michael Benedicks. "THE SUPPORT OF FUNCTIONS AND DISTRIBUTIONS WITH A SPECTRAL GAP". In: *Mathematica Scandinavica* 55.1 (1984), pp. 285–309. ISSN: 00255521, 19031807. URL: `http://www.jstor.org/stable/24491536` (visited on 07/08/2024).

[49] Francesco Benini, Christian Copetti, and Lorenzo Di Pietro. "Factorization and global symmetries in holography". In: *SciPost Phys.* 14.2 (2023), p. 019. DOI: `10.21468/SciPostPhys.14.2.019`. arXiv: `2203.09537 [hep-th]`.

[50] Sergio Benvenuti et al. "Counting BPS Operators in Gauge Theories: Quivers, Syzygies and Plethystics". In: *JHEP* 11 (2007), p. 050. DOI: `10.1088/1126-6708/2007/11/050`. arXiv: `hep-th/0608050`.

[51] David Berenstein. "Submatrix deconfinement and small black holes in AdS". In: *JHEP* 09 (2018), p. 054. DOI: `10.1007/JHEP09(2018)054`. arXiv: `1806.05729 [hep-th]`.

[52] Joseph Berkovitz, Roman Frigg, and Fred Kronz. "The ergodic hierarchy, randomness and Hamiltonian chaos". In: *Studies in History and Philosophy of Science Part B: Studies in History and Philosophy of Modern Physics* 37.4 (2006), pp. 661–691. ISSN: 1355-2198. DOI: `https://doi.org/10.1016/j.shpsb.2006.02.003`. URL: `https://www.sciencedirect.com/science/article/pii/S1355219806000700`.

[53] Joseph Bernstein and Andre Reznikov. "Subconvexity bounds for triple *L*-functions and representation theory". In: *Ann. of Math. (2)* 172.3 (2010), pp. 1679–1718. ISSN: 0003-486X. DOI: `10.4007/annals.2010.172.1679`. URL: `https://doi.org/10.4007/annals.2010.172.1679`.

[54] Dan Betea and Jérémie Bouttier. "The periodic Schur process and free fermions at finite temperature". In: *Math. Phys. Anal. Geom.* 22.3 (2019). DOI: `10.1007/s11040-018-9299-8`. arXiv: `1807.09022 [math-ph]`.

[55] Panagiotis Betzios and Olga Papadoulaki. "FZZT branes and non-singlets of matrix quantum mechanics". In: *JHEP* 07 (2020), p. 157. DOI: `10.1007/JHEP07(2020)157`. arXiv: `1711.04369 [hep-th]`.

[56] Panos Betzios and Olga Papadoulaki. "Microstates of a 2d Black Hole in string theory". In: *JHEP* 01 (2023), p. 028. DOI: `10.1007/JHEP01(2023)028`. arXiv: `2210.11484 [hep-th]`.

[57] Arne Beurling. "On quasianalyticity and general distributions". In: *Multigraphed Lectures, Stanford* (1961), p. 505.

[58] Arpan Bhattacharyya et al. "Exploring the Tensor Networks/AdS Correspondence". In: *JHEP* 08 (2016), p. 086. DOI: `10.1007/JHEP08(2016)086`. arXiv: `1606.00621 [hep-th]`.

[59] Arpan Bhattacharyya et al. "Towards the web of quantum chaos diagnostics". In: *Eur. Phys. J. C* 82.1 (2022), p. 87. DOI: `10.1140/epjc/s10052-022-10035-3`. arXiv: `1909.01894 [hep-th]`.

[60] J. J Bisognano and E. H. Wichmann. "On the Duality Condition for Quantum Fields". In: *J. Math. Phys.* 17 (1976), pp. 303–321. DOI: `10.1063/1.522898`.

[61] Lennart Bittel et al. "On the absence of magic in type II factors". in preparation. 2025.

[62] Bruce Blackadar. *Operator algebras: Theory of c*-algebras and von neumann algebras*. Springer, 2011.

[63]   Bruce Blackadar. *Operator algebras: theory of C*-algebras and von Neumann algebras*. Vol. 122. Springer Science & Business Media, 2006.

[64]   Andreas Blommaert, Luca V. Iliesiu, and Jorrit Kruthoff. "Gravity factorized". In: *JHEP* 09 (2022), p. 080. DOI: `10.1007/JHEP09(2022)080`. arXiv: `2111.07863 [hep-th]`.

[65]   N. N. Bogoliubow and O. S. Parasiuk. "Über die multiplikation der Kausalfunktionen in der Quantentheorie der Felder". In: *Acta Mathematica* 97.0 (1957), pp. 227–266. DOI: `10.1007/bf02392399`.

[66]   Jens Bolte and Hans-Michael Stiepan. "The Selberg trace formula for Dirac operators". In: *Journal of mathematical physics* 47.11 (2006), p. 112104.

[67]   James Bonifacio. "Bootstrap bounds on closed hyperbolic manifolds". In: *JHEP* 02 (2022), p. 025. DOI: `10.1007/JHEP02(2022)025`. arXiv: `2107.09674 [hep-th]`.

[68]   James Bonifacio. "Bootstrapping closed hyperbolic surfaces". In: *JHEP* 03 (2022), p. 093. DOI: `10.1007/JHEP03(2022)093`. arXiv: `2111.13215 [hep-th]`.

[69]   James Bonifacio and Kurt Hinterbichler. "Bootstrap Bounds on Closed Einstein Manifolds". In: *JHEP* 10 (2020), p. 069. DOI: `10.1007/JHEP10(2020)069`. arXiv: `2007.10337 [hep-th]`.

[70]   James Bonifacio and Kurt Hinterbichler. "Unitarization from Geometry". In: *JHEP* 12 (2019), p. 165. DOI: `10.1007/JHEP12(2019)165`. arXiv: `1910.04767 [hep-th]`.

[71]   James Bonifacio, Dalimil Mazac, and Sridip Pal. "Spectral Bounds on Hyperbolic 3-Manifolds: Associativity and the Trace Formula". In: (Aug. 2023). arXiv: `2308.11174 [math.SP]`.

[72]   Alexei Borodin and Ivan Corwin. "Macdonald processes". In: *Probab. Theory Relat. Fields* 158.1 (2014), pp. 225–400. DOI: `10.1007/s00440-013-0482-3`. arXiv: `1111.4408 [math.PR]`.

[73]   Jan Boruch et al. "How the Hilbert space of two-sided black holes factorises". In: (June 2024). arXiv: `2406.04396 [hep-th]`.

[74]   Jean-Benoît Bost and Alain Connes. "Hecke algebras, type III factors and phase transitions with spontaneous symmetry breaking in number theory". In: *Selecta Mathematica* 1 (1995), pp. 411–457. URL: `https://api.semanticscholar.org/CorpusID:116418599`.

[75]   Henning Bostelmann, Daniela Cadamuro, and Simone Del Vecchio. "Relative Entropy of Coherent States on General CCR Algebras". In: *Communications in Mathematical Physics* 389.1 (Dec. 2021), pp. 661–691. ISSN: 1432-0916. DOI: `10.1007/s00220-021-04249-x`. URL: `http://dx.doi.org/10.1007/s00220-021-04249-x`.

[76] A. Böttcher and B. Silbermann. "Toeplitz matrices and determinants with Fisher-Hartwig symbols". In: *J. Funct. Anal.* 63.2 (1985), pp. 178–214. DOI: `10.1016/0022-1236(85)90085-0`.

[77] Marc Bourdon. "Immeubles hyperboliques, dimension conforme et rigidité de Mostow". In: *Geometric & Functional Analysis GAFA* 7 (1997), pp. 245–268. URL: `https://api.semanticscholar.org/CorpusID:119749499`.

[78] Marc Bourdon and Hervé Pajot. "Poincaré inequalities and quasiconformal structure on the boundary of some hyperbolic buildings". In: 1997. URL: `https://api.semanticscholar.org/CorpusID:14071808`.

[79] Maxime Fortier Bourque and Bram Petri. "Linear programming bounds for hyperbolic surfaces". In: *arXiv preprint arXiv:2302.02540* (2023).

[80] Raphael Bousso et al. "Gravity dual of Connes cocycle flow". In: *Phys. Rev. D* 102.6 (2020), p. 066008. DOI: `10.1103/PhysRevD.102.066008`. arXiv: `2007.00230 [hep-th]`.

[81] Latham Boyle, Madeline Dickens, and Felix Flicker. "Conformal Quasicrystals and Holography". In: *Phys. Rev. X* 10.1 (2020), p. 011009. DOI: `10.1103/PhysRevX.10.011009`. arXiv: `1805.02665 [hep-th]`.

[82] Louis De Branges. "Some Hilbert Spaces of Entire Functions". In: *Proceedings of the American Mathematical Society* 10.5 (1959), pp. 840–846. ISSN: 00029939, 10886826. URL: `http://www.jstor.org/stable/2033484` (visited on 06/07/2024).

[83] Jacob C. Bridgeman and Christopher T. Chubb. "Hand-waving and Interpretive Dance: An Introductory Course on Tensor Networks". In: *J. Phys. A* 50.22 (2017), p. 223001. DOI: `10.1088/1751-8121/aa6dc3`. arXiv: `1603.03039 [quant-ph]`.

[84] Martin Bridson and Andr'e Haefliger. *Metric Spaces of Non-Positive Curvature*. Vol. 319. Jan. 2009. ISBN: 978-3-642-08399-0. DOI: `10.1007/978-3-662-12494-9`.

[85] Mauro Brigante, Guido Festuccia, and Hong Liu. "Inheritance principle and non-renormalization theorems at finite temperature". In: *Phys. Lett. B* 638 (2006), pp. 538–545. DOI: `10.1016/j.physletb.2006.05.025`. arXiv: `hep-th/0509117`.

[86] Mauro Brigante et al. "Viscosity Bound Violation in Higher Derivative Gravity". In: *Phys. Rev. D* 77 (2008), p. 126006. DOI: `10.1103/PhysRevD.77.126006`. arXiv: `0712.0805 [hep-th]`.

[87] Theodor Bröcker and Tammo tom Dieck. "Ch.2. Elementary Representation Theory". In: *Representations of Compact Lie Groups*. Berlin, Heidelberg: Springer Berlin Heidelberg, 1985, pp. 64–122. DOI: `10.1007/978-3-662-12918-0`.

[88] Adam R. Brown et al. "The Python's Lunch: geometric obstructions to decoding Hawking radiation". In: *JHEP* 08.121 (2020). DOI: 10.1007/JHEP08(2020)121. arXiv: 1912.00228 [hep-th].

[89] Nathanial Brown and Narutaka Ozawa. *C*-Algebras and Finite-Dimensional Approximations*. Vol. 88. Graduate Studies in Mathematics. Providence, Rhode Island: American Mathematical Society, Mar. 2008. ISBN: 978-0-8218-4381-9 978-1-4704-2118-2. DOI: 10.1090/gsm/088. URL: http://www.ams.org/gsm/088 (visited on 12/17/2024).

[90] Detlev Buchholz and Gandalf Lechner. "Modular nuclearity and localization". In: *Annales Henri Poincaré*. Vol. 5. Springer. 2004, pp. 1065–1080.

[91] Daniel Bump and Persi Diaconis. "Toeplitz Minors". In: *J. Comb. Theory A* 97.2 (2002), pp. 252–271. DOI: 10.1006/jcta.2001.3214.

[92] Jarolím Bureš. "Spin Structures and Harmonic Spinors on Nonhyperelliptic Riemann Surfaces of Small Genera". In: *Clifford Algebras and Their Application in Mathematical Physics: Aachen 1996*. Ed. by Volker Dietrich, Klaus Habetha, and Gerhard Jank. Dordrecht: Springer Netherlands, 1998, pp. 31–43. ISBN: 978-94-011-5036-1. DOI: 10.1007/978-94-011-5036-1{_}4. URL: https://doi.org/10.1007/978-94-011-5036-1%7B%5C_%7D4.

[93] Keith Burns, Charles Pugh, and Amie Wilkinson. "Stable ergodicity and Anosov flows". In: *Topology* 39.1 (2000), pp. 149–159. ISSN: 0040-9383. DOI: https://doi.org/10.1016/S0040-9383(98)00064-0. URL: https://www.sciencedirect.com/science/article/pii/S0040938398000640.

[94] ChunJun Cao. *Non-trivial area operators require non-local magic*. 2024. DOI: 10.1007/JHEP11(2024)105. arXiv: 2306.14996 [hep-th].

[95] Davide Cassani and Zohar Komargodski. "EFT and the SUSY Index on the 2nd Sheet". In: *SciPost Phys.* 11 (2021), p. 004. DOI: 10.21468/SciPostPhys.11.1.004. arXiv: 2104.01464 [hep-th].

[96] Fikret Ceyhan and Thomas Faulkner. "Recovering the QNEC from the ANEC". In: *Commun. Math. Phys.* 377.2 (2020), pp. 999–1045. DOI: 10.1007/s00220-020-03751-y. arXiv: 1812.04683 [hep-th].

[97] Venkatesa Chandrasekaran, Thomas Faulkner, and Adam Levine. "Scattering strings off quantum extremal surfaces". In: *JHEP* 08 (2022), p. 143. DOI: 10.1007/JHEP08(2022)143. arXiv: 2108.01093 [hep-th].

[98] Venkatesa Chandrasekaran and Adam Levine. "Quantum error correction in SYK and bulk emergence". In: *JHEP* 06 (2022), p. 039. DOI: 10.1007/JHEP06(2022)039. arXiv: 2203.05058 [hep-th].

[99] Venkatesa Chandrasekaran, Geoff Penington, and Edward Witten. "Large N algebras and generalized entropy". In: (Sept. 2022). arXiv: 2209.10454 [hep-th].

[100] Venkatesa Chandrasekaran, Geoff Penington, and Edward Witten. "Large N algebras and generalized entropy". In: (Sept. 2022). arXiv: `2209.10454` [`hep-th`].

[101] Venkatesa Chandrasekaran et al. "An algebra of observables for de Sitter space". In: *JHEP* 02 (2023), p. 082. DOI: `10.1007/JHEP02(2023)082`. arXiv: `2206.10780` [`hep-th`].

[102] Wissam Chemissany et al. "On Infinite Tensor Networks, Complementary Recovery and Type II Factors". In: (Mar. 2025). arXiv: `2504.00096` [`hep-th`].

[103] Chang-Han Chen and Geoff Penington. *A clock is just a way to tell the time: gravitational algebras in cosmological spacetimes*. June 2024. arXiv: `2406.02116` [`hep-th`].

[104] Chi-Fang Chen, Geoffrey Penington, and Grant Salton. "Entanglement Wedge Reconstruction using the Petz Map". In: *JHEP* 01 (2020), p. 168. DOI: `10.1007/JHEP01(2020)168`. arXiv: `1902.02844` [`hep-th`].

[105] Lin Chen, Xirong Liu, and Ling-Yan Hung. "Emergent Einstein Equation in p-adic Conformal Field Theory Tensor Networks". In: *Phys. Rev. Lett.* 127.22 (2021), p. 221602. DOI: `10.1103/PhysRevLett.127.221602`. arXiv: `2102.12022` [`hep-th`].

[106] Yang Chen et al. "Moduli space of supersymmetric QCD in the Veneziano limit". In: *JHEP* 09 (2013), p. 131. DOI: `10.1007/JHEP09(2013)131`. arXiv: `1303.6289` [`hep-th`].

[107] Newton Cheng et al. "Random Tensor Networks with Non-trivial Links". In: *Annales Henri Poincare* 25.4 (2024), pp. 2107–2212. DOI: `10.1007/s00023-023-01358-2`. arXiv: `2206.10482` [`quant-ph`].

[108] Fabio Ciolli, Roberto Longo, and Giuseppe Ruzzi. "The information in a wave". In: *Commun. Math. Phys.* 379.3 (2019), pp. 979–1000. DOI: `10.1007/s00220-019-03593-3`. arXiv: `1906.01707` [`math-ph`].

[109] J Ignacio Cirac and Frank Verstraete. "Renormalization and tensor product states in spin chains and lattices". In: *Journal of physics a: mathematical and theoretical* 42.50 (2009), p. 504004.

[110] Antoine Clais. "Conformal dimension on boundary of right-angled hyperbolic buildings". In: *Comptes Rendus Mathematique* 355.7 (2017), pp. 819–823. ISSN: 1631-073X. DOI: `https://doi.org/10.1016/j.crma.2017.06.006`. URL: `https://www.sciencedirect.com/science/article/pii/S1631073X17301747`.

[111] Henry Cohn and Noam Elkies. "New upper bounds on sphere packings I". In: *Annals of mathematics* (2003), pp. 689–714.

[112] Eugenia Colafranceschi, Donald Marolf, and Zhencheng Wang. "A trace inequality for Euclidean gravitational path integrals (and a new positive action conjecture)". In: (Sept. 2023). arXiv: 2309.02497 [hep-th].

[113] Eugenia Colafranceschi et al. "Algebras and Hilbert spaces from gravitational path integrals: Understanding Ryu-Takayanagi/HRT as entropy without invoking holography". In: (Oct. 2023). arXiv: 2310.02189 [hep-th].

[114] Sidney R. Coleman. "Black holes as red herrings: Topological fluctuations and the loss of quantum coherence". In: *Nucl. Phys. B* 307 (1988), pp. 867–882. DOI: 10.1016/0550-3213(88)90110-1.

[115] F. Colomo and A. G. Pronko. "Third-order phase transition in random tilings". In: *Phys. Rev.* E88 (2013), p. 042125. DOI: 10.1103/PhysRevE.88.042125. arXiv: 1306.6207 [math-ph].

[116] Noemie Combe, Yuri Manin, and Matilde Marcolli. *Moufang Patterns and Geometry of Information*. July 2021. DOI: 10.48550/arXiv.2107.07486.

[117] Marston D. E. Conder et al. "Equations of Riemann surfaces of genus 4 , 5 , and 6 with large automorphism groups". In: 2011.

[118] A. Connes and Carlo Rovelli. "Von Neumann algebra automorphisms and time thermodynamics relation in general covariant quantum theories". In: *Class. Quant. Grav.* 11 (1994), pp. 2899–2918. DOI: 10.1088/0264-9381/11/12/007. arXiv: gr-qc/9406019.

[119] Alain Connes. "On the spectral characterization of manifolds". In: *J. Noncommut. Geom.* 7.1 (2013), pp. 1–82. DOI: 10.4171/jncg/108. arXiv: 0810.2088 [math.OA].

[120] Alain Connes. "Une classification des facteurs de type III". fr. In: *Annales scientifiques de l'École Normale Supérieure* 4e série, 6.2 (1973), pp. 133–252. DOI: 10.24033/asens.1247. URL: http://www.numdam.org/articles/10.24033/asens.1247/.

[121] Alain Connes and Dirk Kreimer. "Hopf algebras, renormalization and noncommutative geometry". In: *Quantum field theory: perspective and prospective*. Springer, 1999, pp. 59–109.

[122] Alain Connes and Dirk Kreimer. "Renormalization in quantum field theory and the Riemann-Hilbert problem. 1. The Hopf algebra structure of graphs and the main theorem". In: *Commun. Math. Phys.* 210 (2000), pp. 249–273. DOI: 10.1007/s002200050779. arXiv: hep-th/9912092.

[123] Alain Connes and Dirk Kreimer. "Renormalization in quantum field theory and the Riemann-Hilbert problem. 2. The beta function, diffeomorphisms and the renormalization group". In: *Commun. Math. Phys.* 216 (2001), pp. 215–241. DOI: 10.1007/PL00005547. arXiv: hep-th/0003188.

[124] Alain Connes and Matilde Marcolli. *Noncommutative geometry, quantum fields and motives*. Vol. 55. American Mathematical Soc., 2019.

[125] Alain Connes and Matilde Marcolli. "Renormalization and motivic galois theory". In: (Sept. 2004). arXiv: math/0409306.

[126] Michel Coornaert. "Mesures de Patterson-Sullivan sur le bord d'un espace hyperbolique au sens de Gromov." In: *Pacific Journal of Mathematics* 159 (1993), pp. 241–270. URL: https://api.semanticscholar.org/CorpusID:119896973.

[127] Michel Coornaert, Thomas Delzant, and Athanase Papadopoulos. "Géométrie et théorie des groupes". In: 1990. URL: https://api.semanticscholar.org/CorpusID:117599675.

[128] Ricardo Correa da Silva and Gandalf Lechner. "Modular structure and inclusions of twisted Araki-Woods algebras". In: *Communications in Mathematical Physics* 402.3 (2023), pp. 2339–2386.

[129] Jon Michael Corson. "Complexes of groups". In: 1990. URL: https://doi.org/10.1112/plms/s3-65.1.199.

[130] Jordan Cotler et al. "Entanglement Wedge Reconstruction via Universal Recovery Channels". In: *Phys. Rev. X* 9.3 (2019), p. 031011. DOI: 10.1103/PhysRevX.9.031011. arXiv: 1704.05839 [hep-th].

[131] Jason Crann et al. "Private algebras in quantum information and infinite-dimensional complementarity". In: *arXiv: Quantum Physics* (2015). URL: https://api.semanticscholar.org/CorpusID:55235655.

[132] F. D. Cunden et al. "Third-order phase transition: random matrices and screened Coulomb gas with hard walls". In: *J. Stat. Phys.* 175.6 (2019), pp. 1262–1297. DOI: 10.1007/s10955-019-02281-9. arXiv: 1810.12593 [math-ph].

[133] Michael W. Davis. "Groups Generated by reflections and aspherical manifolds not covered by Euclidean space". In: *Annals of Mathematics* 117.2 (1983), pp. 293–324. ISSN: 0003486X, 19398980. URL: http://www.jstor.org/stable/2007079 (visited on 05/04/2025).

[134] Jan De Boer and Lampros Lamprou. "Holographic Order from Modular Chaos". In: *JHEP* 06 (2020), p. 024. DOI: 10.1007/JHEP06(2020)024. arXiv: 1912.02810 [hep-th].

[135] Julian De Vuyst et al. *Crossed products and quantum reference frames: on the observer-dependence of gravitational entropy*. Dec. 2024. arXiv: 2412.15502 [hep-th].

[136] Jean-Guy Demers, Rene Lafrance, and Robert C. Myers. "Black hole entropy without brick walls". In: *Phys. Rev. D* 52 (1995), pp. 2245–2253. DOI: 10.1103/PhysRevD.52.2245. arXiv: gr-qc/9503003.

[137] J. Dereziński. "Introduction to Representations of the Canonical Commutation and Anticommutation Relations". In: *Large Coulomb systems*. Vol. 695. Lecture Notes in Physics. Springer Berlin Heidelberg, 2006, pp. 63–143. DOI: `10.1007/3-540-32579-4_3`.

[138] Bryce S. DeWitt. "Quantum Theory of Gravity. I. The Canonical Theory". In: *Phys. Rev.* 160 (5 Aug. 1967), pp. 1113–1148. DOI: `10.1103/PhysRev.160.1113`. URL: `https://link.aps.org/doi/10.1103/PhysRev.160.1113`.

[139] Linden Disney-Hogg, Andrew Beckett, and Isabella Deutsch. "An English translation of A. Wiman's "On the algebraic curves of genus $p = 4, 5$ and 6, which posses unambiguous transformations into themselves"". In: (2022). DOI: `10.48550/ARXIV.2204.01656`. URL: `https://arxiv.org/abs/2204.01656`.

[140] Matthew Dodelson. "Ringdown in the SYK model". In: (Aug. 2024). arXiv: `2408.05790 [hep-th]`.

[141] Xi Dong, Daniel Harlow, and Donald Marolf. "Flat entanglement spectra in fixed-area states of quantum gravity". In: *JHEP* 10.240 (2019). DOI: `10.1007/JHEP10(2019)240`. arXiv: `1811.05382 [hep-th]`.

[142] Xi Dong, Daniel Harlow, and Aron C. Wall. "Reconstruction of Bulk Operators within the Entanglement Wedge in Gauge-Gravity Duality". In: *Phys. Rev. Lett.* 117.2 (2016), p. 021601. DOI: `10.1103/PhysRevLett.117.021601`. arXiv: `1601.05416 [hep-th]`.

[143] Xi Dong and Aitor Lewkowycz. "Entropy, Extremality, Euclidean Variations, and the Equations of Motion". In: *JHEP* 01 (2018), p. 081. DOI: `10.1007/JHEP01(2018)081`. arXiv: `1705.08453 [hep-th]`.

[144] Xi Dong et al. "Effective entropy of quantum fields coupled with gravity". In: *JHEP* 10 (2020), p. 052. DOI: `10.1007/JHEP10(2020)052`. arXiv: `2007.02987 [hep-th]`.

[145] Xi Dong et al. "Null states and time evolution in a toy model of black hole dynamics". In: *JHEP* 08 (2024), p. 199. DOI: `10.1007/JHEP08(2024)199`. arXiv: `2405.04571 [hep-th]`.

[146] William Donnelly. "Decomposition of entanglement entropy in lattice gauge theory". In: *Phys. Rev. D* 85 (2012), p. 085004. DOI: `10.1103/PhysRevD.85.085004`. arXiv: `1109.0036 [hep-th]`.

[147] William Donnelly. "Entanglement entropy and nonabelian gauge symmetry". In: *Class. Quant. Grav.* 31.21 (2014), p. 214003. DOI: `10.1088/0264-9381/31/21/214003`. arXiv: `1406.7304 [hep-th]`.

[148] Michael R. Douglas and Vladimir A. Kazakov. "Large N phase transition in continuum QCD in two-dimensions". In: *Phys. Lett. B* 319 (1993), pp. 219–230. DOI: `10.1016/0370-2693(93)90806-S`. arXiv: `hep-th/9305047`.

[149] Souvik Dutta and Thomas Faulkner. "A canonical purification for the entanglement wedge cross-section". In: *JHEP* 03 (2021), p. 178. DOI: 10.1007/JHEP03(2021)178. arXiv: 1905.00577 [hep-th].

[150] Suvankar Dutta and Rajesh Gopakumar. "Free fermions and thermal AdS/CFT". In: *JHEP* 03 (2008), p. 011. DOI: 10.1088/1126-6708/2008/03/011. arXiv: 0711.0133 [hep-th].

[151] Lorenz Eberhardt. "Summing over Geometries in String Theory". In: *JHEP* 05 (2021), p. 233. DOI: 10.1007/JHEP05(2021)233. arXiv: 2102.12355 [hep-th].

[152] G. G. Emch et al. "Anosov actions on noncommutative algebras". In: *J. Math. Phys.* 35 (1994), pp. 5582–5599. DOI: 10.1063/1.530766.

[153] Netta Engelhardt. "Into the Bulk: A Covariant Approach". In: *Phys. Rev. D* 95.6 (2017), p. 066005. DOI: 10.1103/PhysRevD.95.066005. arXiv: 1610.08516 [hep-th].

[154] Netta Engelhardt and Elliott Gesteau. "Further Evidence Against a Semiclassical Baby Universe in AdS/CFT". In: (Apr. 2025). arXiv: 2504.14586 [hep-th].

[155] Netta Engelhardt and Hong Liu. "Algebraic ER=EPR and Complexity Transfer". In: (Nov. 2023). arXiv: 2311.04281 [hep-th].

[156] Netta Engelhardt, Geoff Penington, and Arvin Shahbazi-Moghaddam. "A world without pythons would be so simple". In: *Class. Quant. Grav.* 38.23 (2021), p. 234001. DOI: 10.1088/1361-6382/ac2de5. arXiv: 2102.07774 [hep-th].

[157] Netta Engelhardt, Geoff Penington, and Arvin Shahbazi-Moghaddam. "Finding pythons in unexpected places". In: *Class. Quant. Grav.* 39.9 (2022), p. 094002. DOI: 10.1088/1361-6382/ac3e75. arXiv: 2105.09316 [hep-th].

[158] Netta Engelhardt, Geoff Penington, and Arvin Shahbazi-Moghaddam. "Twice Upon a Time: Timelike-Separated Quantum Extremal Surfaces". In: *JHEP* 01 (2024), p. 033. DOI: 10.1007/JHEP01(2024)033. arXiv: 2308.16226 [hep-th].

[159] Netta Engelhardt and Aron C. Wall. "Coarse Graining Holographic Black Holes". In: *JHEP* 05 (2019), p. 160. DOI: 10.1007/JHEP05(2019)160. arXiv: 1806.01281 [hep-th].

[160] Netta Engelhardt and Aron C. Wall. "Decoding the Apparent Horizon: Coarse-Grained Holographic Entropy". In: *Phys. Rev. Lett.* 121.21 (2018), p. 211301. DOI: 10.1103/PhysRevLett.121.211301. arXiv: 1706.02038 [hep-th].

[161] Netta Engelhardt and Aron C. Wall. "No Simple Dual to the Causal Holographic Information?" In: *JHEP* 04 (2017), p. 134. DOI: `10.1007/JHEP04(2017)134`. arXiv: `1702.01748 [hep-th]`.

[162] Netta Engelhardt and Aron C. Wall. "Quantum Extremal Surfaces: Holographic Entanglement Entropy beyond the Classical Regime". In: *JHEP* 01 (2015), p. 073. DOI: `10.1007/JHEP01(2015)073`. arXiv: `1408.3203 [hep-th]`.

[163] Netta Engelhardt et al. "Spoofing Entanglement in Holography". In: (July 2024). eprint: `2407.14589`. URL: `https://arxiv.org/pdf/2407.14589.pdf`.

[164] Thomas Faulkner. "The holographic map as a conditional expectation". In: (Aug. 2020). arXiv: `2008.04810 [hep-th]`.

[165] Thomas Faulkner and Stefan Hollands. "Approximate recoverability and relative entropy II: 2-positive channels of general von Neumann algebras". In: *Lett. Math. Phys.* 112.2 (2022), p. 26. DOI: `10.1007/s11005-022-01510-9`. arXiv: `2010.05513 [quant-ph]`.

[166] Thomas Faulkner and Aitor Lewkowycz. "Bulk locality from modular flow". In: *JHEP* 07 (2017), p. 151. DOI: `10.1007/JHEP07(2017)151`. arXiv: `1704.05464 [hep-th]`.

[167] Thomas Faulkner, Aitor Lewkowycz, and Juan Maldacena. "Quantum corrections to holographic entanglement entropy". In: *JHEP* 11 (2013), p. 074. DOI: `10.1007/JHEP11(2013)074`. arXiv: `1307.2892 [hep-th]`.

[168] Thomas Faulkner and Min Li. "Asymptotically isometric codes for holography". In: (Nov. 2022). arXiv: `2211.12439 [hep-th]`.

[169] Thomas Faulkner, Min Li, and Huajia Wang. "A modular toolkit for bulk reconstruction". In: *JHEP* 04 (2019), p. 119. DOI: `10.1007/JHEP04(2019)119`. arXiv: `1806.10560 [hep-th]`.

[170] Thomas Faulkner et al. "Approximate Recovery and Relative Entropy I: General von Neumann Subalgebras". In: *Commun. Math. Phys.* 389.1 (2022), pp. 349–397. DOI: `10.1007/s00220-021-04143-6`. arXiv: `2006.08002 [quant-ph]`.

[171] Guido Festuccia and Hong Liu. "Excursions beyond the horizon: Black hole singularities in Yang-Mills theories. I." In: *JHEP* 04 (2006), p. 044. DOI: `10.1088/1126-6708/2006/04/044`. arXiv: `hep-th/0506202`.

[172] Guido Festuccia and Hong Liu. "The Arrow of time, black holes, and quantum mixing of large N Yang-Mills theories". In: *JHEP* 12 (2007), p. 027. DOI: `10.1088/1126-6708/2007/12/027`. arXiv: `hep-th/0611098`.

[173]   Christopher J. Fewster and Kasia Rejzner. "Algebraic Quantum Field Theory". In: *Progress and Visions in Quantum Theory in View of Gravity*. Ed. by F Finster et al. Switzerland AG: Birkhäuser Cham, 2020. DOI: 10.1007/978-3-030-38941-3. arXiv: 1904.04051 [hep-th].

[174]   Franca Figliolini and Daniele Guido. "On the type of second quantization factors". In: *J. Operator Theory* 31.2 (1994), pp. 229–252. ISSN: 03794024, 18417744. URL: http://www.jstor.org/stable/24714460.

[175]   Peter J. Forrester. "The spectrum edge of random matrix ensembles". In: *Nucl. Phys. B* 402.3 (1993), pp. 709–728. ISSN: 0550-3213. DOI: https://doi.org/10.1016/0550-3213(93)90126-A.

[176]   Otto Forster and Bruce Gilligan. *Lectures on Riemann surfaces*. Springer, 1999.

[177]   Klaus Fredenhagen. "On the Modular Structure of Local Algebras of Observables". In: *Commun. Math. Phys.* 97 (1985), p. 79. DOI: 10.1007/BF01206179.

[178]   Th. Friedrich. "Der erste Eigenwert des Dirac-operators Einer Kompakten, Riemannschen Mannigfaltigkeit nichtnegativer Skalarkrümmung". In: *Mathematische Nachrichten* 97.1 (1980), pp. 117–146. DOI: 10.1002/mana.19800970111.

[179]   Thomas Friedrich and Andreas Nestke. *Dirac operators in Riemannian geometry*. American Mathematical Society, 2012.

[180]   Roman Frigg, Joseph Berkovitz, and Fred Kronz. "The Ergodic Hierarchy". In: *The Stanford Encyclopedia of Philosophy*. Ed. by Edward N. Zalta. Fall 2020. Metaphysics Research Lab, Stanford University, 2020.

[181]   Dmitri V. Fursaev and Sergei N. Solodukhin. "On one loop renormalization of black hole entropy". In: *Phys. Lett. B* 365 (1996), pp. 51–55. DOI: 10.1016/0370-2693(95)01290-7. arXiv: hep-th/9412020.

[182]   Keiichiro Furuya, Nima Lashkari, and Shoy Ouseph. "Real-space RG, error correction and Petz map". In: *JHEP* 01 (2022), p. 170. DOI: 10.1007/JHEP01(2022)170. arXiv: 2012.14001 [hep-th].

[183]   Keiichiro Furuya et al. "Information loss, mixing and emergent type III_1 factors". In: *JHEP* 08 (2023), p. 111. DOI: 10.1007/JHEP08(2023)111. arXiv: 2305.16028 [hep-th].

[184]   Davide Gaiotto and Ji Hoon Lee. "The Giant Graviton Expansion". In: (Sept. 2021). arXiv: 2109.02545 [hep-th].

[185]   Wolf-Dieter Garber. "The connexion of duality and causal properties for generalized free fields". In: *Commun. Math. Phys.* 42.3 (1975), pp. 195–208. DOI: cmp/1103899044.

[186] D. García-García and M. Tierz. "Toeplitz minors and specializations of skew Schur polynomials". In: *J. Comb. Theory A* 172 (May 2020), p. 105201. DOI: `10.1016/j.jcta.2019.105201`. arXiv: `1706.02574 [math.CO]`.

[187] Hansjörg Geiges and Jesus Gonzalo Perez. "Generalised spin structures on 2-dimensional orbifolds". In: (2012).

[188] Izrail Moiseevich Gel'fand and Boris Moiseevich Levitan. "On the determination of a differential equation from its spectral function". In: 1955. URL: `https://api.semanticscholar.org/CorpusID:124078768`.

[189] Israel Gelfand and Mark Naimark. "On the imbedding of normed rings into the ring of operators in Hilbert space". eng. In: *Matematiceskij sbornik* 54.2 (1943), pp. 197–217. URL: `http://eudml.org/doc/65219`.

[190] Ira M Gessel. "Symmetric functions and P-recursiveness". In: *J. Comb. Theory, Ser. A* 53.2 (1990), pp. 257–285. ISSN: 0097-3165. DOI: `10.1016/0097-3165(90)90060-A`.

[191] Elliott Gesteau. "Emergent spacetime and the ergodic hierarchy". In: (Oct. 2023). arXiv: `2310.13733 [hep-th]`.

[192] Elliott Gesteau. "Large N von Neumann algebras and the renormalization of Newton's constant". In: (Feb. 2023). arXiv: `2302.01938 [hep-th]`.

[193] Elliott Gesteau and Monica Jinwoo Kang. "Holographic baby universes: an observable story". In: (June 2020). arXiv: `2006.14620 [hep-th]`.

[194] Elliott Gesteau and Monica Jinwoo Kang. "Nonperturbative gravity corrections to bulk reconstruction". In: (Dec. 2021). arXiv: `2112.12789 [hep-th]`.

[195] Elliott Gesteau and Monica Jinwoo Kang. *The infinite-dimensional HaPPY code: entanglement wedge reconstruction and dynamics*. May 2020. arXiv: `2005.05971 [hep-th]`.

[196] Elliott Gesteau and Monica Jinwoo Kang. "Thermal states are vital: Entanglement Wedge Reconstruction from Operator-Pushing". In: (May 2020). arXiv: `2005.07189 [hep-th]`.

[197] Elliott Gesteau and Hong Liu. "Toward stringy horizons". In: (Aug. 2024). arXiv: `2408.12642 [hep-th]`.

[198] Elliott Gesteau, Matilde Marcolli, and Jacob McNamara. "Wormhole Renormalization: The gravitational path integral, holography, and a gauge group for topology change". In: (July 2024). arXiv: `2407.20324 [hep-th]`.

[199] Elliott Gesteau, Matilde Marcolli, and Sarthak Parikh. "Holographic tensor networks from hyperbolic buildings". In: *JHEP* 10.169 (2022). DOI: `10.1007/JHEP10(2022)169`. arXiv: `2202.01788 [hep-th]`.

[200] Elliott Gesteau and Leonardo Santilli. "Explicit large N von Neumann algebras from matrix models". In: (Feb. 2024). arXiv: `2402.10262 [hep-th]`.

[201] Elliott Gesteau et al. "Bounds on spectral gaps of Hyperbolic spin surfaces". In: *J. Assoc. Math. Res.* 3.1 (2025), pp. 72–139. DOI: `10.56994/JAMR.003.001.003`. arXiv: `2311.13330` [math.SP].

[202] Sudip Ghosh and Suvrat Raju. "Quantum information measures for restricted sets of observables". In: *Physical Review D* 98.4 (Aug. 2018). DOI: `10.1103/physrevd.98.046005`. URL: `https://doi.org/10.1103%2Fphysrevd.98.046005`.

[203] Steven B. Giddings and Andrew Strominger. "Baby Universes, Third Quantization and the Cosmological Constant". In: *Nucl. Phys. B* 321 (1989), pp. 481–508. DOI: `10.1016/0550-3213(89)90353-2`.

[204] Steven B. Giddings and Andrew Strominger. "Loss of incoherence and determination of coupling constants in quantum gravity". In: *Nucl. Phys. B* 307 (1988), pp. 854–866. DOI: `10.1016/0550-3213(88)90109-5`.

[205] Akash Goel et al. "Expanding the Black Hole Interior: Partially Entangled Thermal States in SYK". In: *JHEP* 02 (2019), p. 156. DOI: `10.1007/JHEP02(2019)156`. arXiv: `1807.03916` [hep-th].

[206] Valentin Y. Golodets and Sergey V. Neshveyev. "Non-Bernoullian Quantum K-Systems". In: *Commun. Math. Phys.* 195.1 (1998), pp. 213–232. DOI: `10.1007/s002200050386`.

[207] Cesar Gomez. *Cosmology as a Crossed Product*. July 2022. arXiv: `2207.06704` [hep-th].

[208] Daniel Gottesman. *Stabilizer codes and quantum error correction*. May 1997. arXiv: `quant-ph/9705052`.

[209] Daniel Gottesman. *The Heisenberg Representation of Quantum Computers*. 1998. arXiv: `quant-ph/9807006` [quant-ph]. URL: `https://arxiv.org/abs/quant-ph/9807006`.

[210] James Gray et al. "SQCD: A Geometric Apercu". In: *JHEP* 05 (2008), p. 099. DOI: `10.1088/1126-6708/2008/05/099`. arXiv: `0803.4257` [hep-th].

[211] D. J. Gross and Edward Witten. "Possible Third Order Phase Transition in the Large N Lattice Gauge Theory". In: *Phys. Rev. D* 21 (1980), pp. 446–453. DOI: `10.1103/PhysRevD.21.446`.

[212] Rudolf Haag. *Local Quantum Physics*. Theoretical and Mathematical Physics. Berlin: Springer, 1996. ISBN: 978-3-540-61049-6, 978-3-642-61458-3. DOI: `10.1007/978-3-642-61458-3`.

[213] Rudolf Haag. *Local Quantum Physics: Fields, Particles, Algebras*. Springer, 1996.

[214] Rudolf Haag and Daniel Kastler. "An Algebraic approach to quantum field theory". In: *J. Math. Phys.* 5 (1964), pp. 848–861. DOI: 10.1063/1.1704187.

[215] Uffe Haagerup. "Connes' bicentralizer problem and uniqueness of the injective factor of type III1". In: *Acta Mathematica* 158.none (1987), pp. 95–148. DOI: 10.1007/BF02392257. URL: https://doi.org/10.1007/BF02392257.

[216] Sasha Haco et al. "Black Hole Entropy and Soft Hair". In: *JHEP* 12.098 (2018). DOI: 10.1007/JHEP12(2018)098. arXiv: 1810.01847 [hep-th].

[217] Jutho Haegeman et al. "Entanglement Renormalization for Quantum Fields in Real Space". In: *Phys. Rev. Lett.* 110.10 (2013), p. 100402. DOI: 10.1103/PhysRevLett.110.100402. arXiv: 1102.5524 [hep-th].

[218] Joakim Hallin and David Persson. "Thermal phase transition in weakly interacting, large N(C) QCD". In: *Phys. Lett. B* 429 (1998), pp. 232–238. DOI: 10.1016/S0370-2693(98)00478-X. arXiv: hep-ph/9803234.

[219] Alex Hamilton et al. "Holographic representation of local bulk operators". In: *Phys.Rev.* D74 (2006), p. 066009. DOI: 10.1103/PhysRevD.74.066009. arXiv: hep-th/0606141 [hep-th].

[220] Alex Hamilton et al. "Local bulk operators in AdS/CFT: A Boundary view of horizons and locality". In: *Phys. Rev. D* 73 (2006), p. 086003. DOI: 10.1103/PhysRevD.73.086003. arXiv: hep-th/0506118.

[221] Alex Hamilton et al. "Local bulk operators in AdS/CFT: A Holographic description of the black hole interior". In: *Phys. Rev.* D75 (2007). [Erratum: Phys. Rev.D75,129902(2007)], p. 106001. DOI: 10.1103/PhysRevD.75.106001, 10.1103/PhysRevD.75.129902. arXiv: hep-th/0612053 [hep-th].

[222] Masanori Hanada and Jonathan Maltz. "A proposal of the gauge theory description of the small Schwarzschild black hole in $AdS_5 \times S^5$". In: *JHEP* 02 (2017), p. 012. DOI: 10.1007/JHEP02(2017)012. arXiv: 1608.03276 [hep-th].

[223] Masanori Hanada and Brandon Robinson. "Partial-Symmetry-Breaking Phase Transitions". In: *Phys. Rev. D* 102.9 (2020), p. 096013. DOI: 10.1103/PhysRevD.102.096013. arXiv: 1911.06223 [hep-th].

[224] Daniel Harlow. "TASI Lectures on the Emergence of Bulk Physics in AdS/CFT". In: *PoS* TASI2017 (2018), p. 002. DOI: 10.22323/1.305.0002. arXiv: 1802.01040 [hep-th].

[225] Daniel Harlow. "The Ryu–Takayanagi Formula from Quantum Error Correction". In: *Commun. Math. Phys.* 354.3 (2017), pp. 865–912. DOI: 10.1007/s00220-017-2904-z. arXiv: 1607.03901 [hep-th].

[226] Daniel Harlow and Daniel Jafferis. "The Factorization Problem in Jackiw-Teitelboim Gravity". In: *JHEP* 02 (2020), p. 177. DOI: 10.1007/JHEP02(2020)177. arXiv: 1804.01081 [hep-th].

[227] Daniel Harlow, Mykhaylo Usatyuk, and Ying Zhao. "Quantum mechanics and observers for gravity in a closed universe". In: (Jan. 2025). arXiv: 2501.02359 [hep-th].

[228] Mark Harmer. "Note on the Schwarz triangle functions". In: *Bulletin of the Australian Mathematical Society* 72.3 (2005), pp. 385–389. DOI: 10.1017/S0004972700035218.

[229] Sean A. Hartnoll and S. Prem Kumar. "AdS black holes and thermal Yang-Mills correlators". In: *JHEP* 12 (2005), p. 036. DOI: 10.1088/1126-6708/2005/12/036. arXiv: hep-th/0508092.

[230] S. W. Hawking and Don N. Page. "Thermodynamics of Black Holes in anti-De Sitter Space". In: *Commun. Math. Phys.* 87 (1983), p. 577. DOI: 10.1007/BF01208266.

[231] Patrick Hayden and Geoffrey Penington. "Learning the Alpha-bits of Black Holes". In: *JHEP* 12 (2019), p. 007. DOI: 10.1007/JHEP12(2019)007. arXiv: 1807.06041 [hep-th].

[232] Patrick Hayden et al. "Holographic duality from random tensor networks". In: *JHEP* 11.009 (2016). DOI: 10.1007/JHEP11(2016)009. arXiv: 1601.01694 [hep-th].

[233] D.A. Hejhal. *The Selberg Trace Formula for PSL (2,R): Volume 1*. Lecture Notes in Mathematics. Springer Berlin Heidelberg, 2006. ISBN: 9783540379799. URL: https://books.google.com/books?id=WoJ8CwAAQBAJ.

[234] D.A. Hejhal. *The Selberg Trace Formula for PSL (2,R): Volume 2*. Lecture Notes in Mathematics. Springer Berlin Heidelberg, 2006. ISBN: 9783540409144. URL: https://books.google.com/books?id=ylF8CwAAQBAJ.

[235] Klaus Hepp. "Proof of the Bogolyubov-Parasiuk theorem on renormalization". In: *Commun. Math. Phys.* 2 (1966), pp. 301–326. DOI: 10.1007/BF01773358.

[236] Richard H. Herman and Masamichi Takesaki. "States and automorphism groups of operator algebras". In: *Communications in Mathematical Physics* 19.2 (1970), pp. 142–160. DOI: 10.1007/bf01646631.

[237] Sergio Hernández-Cuenca. "Wormholes and Factorization in Exact Effective Theory". In: (Apr. 2024). arXiv: 2404.10035 [hep-th].

[238] Matthew Heydeman et al. "Nonarchimedean holographic entropy from networks of perfect tensors". In: *Adv. Theor. Math. Phys.* 25.3 (2021), pp. 591–721. DOI: 10.4310/ATMP.2021.v25.n3.a2. arXiv: 1812.04057 [hep-th].

[239]   Will Hide and Michael Magee. "Near optimal spectral gaps for hyperbolic surfaces". In: *Annals of Mathematics* 198.2 (2023), pp. 791–824.

[240]   Nigel Hitchin. "Harmonic Spinors". In: *Advances in Mathematics* 14.1 (1974), pp. 1–55. ISSN: 0001-8708. DOI: `https://doi.org/10.1016/0001-8708(74)90021-8`. URL: `https://www.sciencedirect.com/science/article/pii/0001870874900218`.

[241]   Craig D. Hodgson and Jeffrey R. Weeks. "Symmetries, isometries and length spectra of closed hyperbolic three-manifolds". In: *Experimental Mathematics* 3.4 (1994), pp. 261–274.

[242]   Veronika E. Hubeny, Mukund Rangamani, and Tadashi Takayanagi. "A Covariant holographic entanglement entropy proposal". In: *JHEP* 07 (2007), p. 062. DOI: `10.1088/1126-6708/2007/07/062`. arXiv: `0705.0016` [hep-th].

[243]   F. Huber and N. Wyderka. *Table of AME states*.

[244]   Felix Huber et al. "Bounds on absolutely maximally entangled states from shadow inequalities, and the quantum MacWilliams identity". In: *J. Phys. A* A 51.17 (2018), p. 175301. DOI: `10.1088/1751-8121/aaade5`.

[245]   Heinz Huber. "On the spectrum of the laplace operator on compact Riemann surfaces". In: *Geometry of the Laplace Operator* (1980), pp. 181–184. DOI: `10.1090/pspum/036/573433`.

[246]   Norihiro Iizuka, Takuya Okuda, and Joseph Polchinski. "Matrix Models for the Black Hole Information Paradox". In: *JHEP* 02 (2010), p. 073. DOI: `10.1007/JHEP02(2010)073`. arXiv: `0808.0530` [hep-th].

[247]   Norihiro Iizuka and Joseph Polchinski. "A Matrix Model for Black Hole Thermalization". In: *JHEP* 10 (2008), p. 028. DOI: `10.1088/1126-6708/2008/10/028`. arXiv: `0801.3657` [hep-th].

[248]   Said Ilias and Ahmad EL SOUFI. "Le volume conforme et ses applications d'après Li et Yau". In: *Séminaire de théorie spectrale (Grenoble)* 1 (Jan. 1983), 15 pages. DOI: `10.5802/tsg.11`.

[249]   Luca V. Iliesiu, Murat Kologlu, and Gustavo J. Turiaci. "Supersymmetric indices factorize". In: *JHEP* 05 (2023), p. 032. DOI: `10.1007/JHEP05(2023)032`. arXiv: `2107.09062` [hep-th].

[250]   A. E. Ingham. "A note on Fourier transforms". In: *Journal of the London Mathematical Society* s1-9.1 (Jan. 1934), pp. 29–32. DOI: `10.1112/jlms/s1-9.1.29`.

[251]   J. Watrous. *Lecture notes on theory of quantum information, Lecture 20, Theorem 20.5*. URL: `https://cs.uwaterloo.ca/~watrous/TQI-notes/TQI-notes.20.pdf`.

[252] Ted Jacobson. "Black hole entropy and induced gravity". In: (Apr. 1994). arXiv: `gr-qc/9404039`.

[253] Daniel L. Jafferis, Liza Rozenberg, and Gabriel Wong. "3d Gravity as a random ensemble". In: (July 2024). arXiv: `2407.02649 [hep-th]`.

[254] Daniel L. Jafferis et al. "Relative entropy equals bulk relative entropy". In: *JHEP* 06 (2016), p. 004. DOI: `10.1007/JHEP06(2016)004`. arXiv: `1512.06431 [hep-th]`.

[255] Daniel Louis Jafferis. "Bulk reconstruction and the Hartle-Hawking wavefunction". In: (Mar. 2017). arXiv: `1703.01519 [hep-th]`.

[256] A. Jahn et al. "Majorana dimers and holographic quantum error-correcting codes". In: *Phys. Rev. Research.* 1 (2019), p. 033079. DOI: `10.1103/PhysRevResearch.1.033079`. arXiv: `1905.03268 [hep-th]`.

[257] Alexander Jahn and Jens Eisert. "Holographic tensor network models and quantum error correction: a topical review". In: *Quantum Sci. Technol.* 6.3 (2021), p. 033002. DOI: `10.1088/2058-9565/ac0293`. arXiv: `2102.02619 [quant-ph]`.

[258] Alexander Jahn, Zoltán Zimborás, and Jens Eisert. "Tensor network models of AdS/qCFT". In: *Quantum* 6 (2022), p. 643. DOI: `10.22331/q-2022-02-03-643`. arXiv: `2004.04173 [quant-ph]`.

[259] Sachin Jain et al. "Phases of large N vector Chern-Simons theories on $S^2 \times S^1$". In: *JHEP* 09 (2013), p. 009. DOI: `10.1007/JHEP09(2013)009`. arXiv: `1301.6169 [hep-th]`.

[260] Tadeusz Januszkiewicz and Jacek Swiatkowski. "Hyperbolic Coxeter groups of large dimension". In: *Commentarii Mathematici Helvetici* 78 (July 2003), pp. 555–583. DOI: `10.1007/s00014-003-0763-z`.

[261] Kristan Jensen, Jonathan Sorce, and Antony J. Speranza. "Generalized entropy for general subregions in quantum gravity". In: *JHEP* 12 (2023), p. 020. DOI: `10.1007/JHEP12(2023)020`. arXiv: `2306.01837 [hep-th]`.

[262] Kurt Johansson. "On Random Matrices from the Compact Classical Groups". In: *Annals Math.* 145.3 (1997), pp. 519–545. DOI: `10.2307/2951843`.

[263] Vaughan Jones. *Von Neumann Algebras.* URL: `https://math.vanderbilt.edu/jonesvf/`.

[264] P. Jordan and E. Wigner. "Über das Paulische Äquivalenzverbot". In: *Zeitschrift für Physik* 47.9 (Sept. 1928), pp. 631–651. ISSN: 0044-3328. DOI: `10.1007/BF01331938`. URL: `https://doi.org/10.1007/BF01331938` (visited on 03/04/2025).

[265] B. Julia. "Statistical theory of numbers". In: *Springer Proceedings in Physics* (1990), pp. 276–293. DOI: `10.1007/978-3-642-75405-0_30`.

[266] J. Jurkiewicz and K. Zalewski. "Vacuum Structure of the U($N \to$ Infinity) Gauge Theory on a Two-dimensional Lattice for a Broad Class of Variant Actions". In: *Nucl. Phys. B* 220 (1983), pp. 167–184. DOI: `10.1016/0550-3213(83)90221-3`.

[267] Daniel N. Kabat. "Black hole entropy and entropy of entanglement". In: *Nucl. Phys. B* 453 (1995), pp. 281–299. DOI: `10.1016/0550-3213(95)00443-V`. arXiv: `hep-th/9503016`.

[268] Richard V Kadison and John R Ringrose. *Fundamentals of the theory of operator algebras. Volume II: Advanced theory*. Academic press New York, 1986.

[269] Monica Jinwoo Kang and David K. Kolchmeyer. "Entanglement wedge reconstruction of infinite-dimensional von Neumann algebras using tensor networks". In: *Phys. Rev. D* 103.12 (2021), p. 126018. DOI: `10.1103/PhysRevD.103.126018`. arXiv: `1910.06328 [hep-th]`.

[270] Monica Jinwoo Kang and David K. Kolchmeyer. "Holographic Relative Entropy in Infinite-dimensional Hilbert Spaces". In: (Nov. 2018). arXiv: `1811.05482 [hep-th]`.

[271] Monica Jinwoo Kang, Jaeha Lee, and Hirosi Ooguri. "Universal formula for the density of states with continuous symmetry". In: *Phys. Rev. D* 107.2 (2023), p. 026021. DOI: `10.1103/PhysRevD.107.026021`. arXiv: `2206.14814 [hep-th]`.

[272] Daniel Kapec, Raghu Mahajan, and Douglas Stanford. "Matrix ensembles with global symmetries and 't Hooft anomalies from 2d gauge theory". In: *JHEP* 04 (2020), p. 186. DOI: `10.1007/JHEP04(2020)186`. arXiv: `1912.12285 [hep-th]`.

[273] Mikhail Karpukhin and Denis Vinokurov. "The first eigenvalue of the Laplacian on orientable surfaces". In: *Mathematische Zeitschrift* 301.3 (2022), pp. 2733–2746.

[274] Yasuyuki Kawahigashi and Roberto Longo. "Classification of two-dimensional local conformal nets with c less than 1 and 2 cohomology vanishing for tensor categories". In: *Commun. Math. Phys.* 244 (2004), pp. 63–97. DOI: `10.1007/s00220-003-0979-1`. arXiv: `math-ph/0304022`.

[275] Vladimir A. Kazakov, Matthias Staudacher, and Thomas Wynter. "Character expansion methods for matrix models of dually weighted graphs". In: *Commun. Math. Phys.* 177 (1996), pp. 451–468. DOI: `10.1007/BF02101902`. arXiv: `hep-th/9502132`.

[276] William R. Kelly. "Bulk Locality and Entanglement Swapping in AdS/CFT". In: *JHEP* 03 (2017), p. 153. DOI: `10.1007/JHEP03(2017)153`. arXiv: `1610.00669 [hep-th]`.

[277] Taro Kimura and Edward A. Mazenc. "The Schur Expansion of Characteristic Polynomials and Random Matrices". In: (Nov. 2021). arXiv: `2111.02365` `[hep-th]`.

[278] Marc S. Klinger and Robert G. Leigh. "Crossed products, extended phase spaces and the resolution of entanglement singularities". In: *Nucl. Phys. B* 999 (2024), p. 116453. DOI: `10.1016/j.nuclphysb.2024.116453`. arXiv: `2306.09314 [hep-th]`.

[279] Anthony W. Knapp. *Representation theory of semisimple groups*. Princeton Landmarks in Mathematics. An overview based on examples, Reprint of the 1986 original. Princeton University Press, Princeton, NJ, 2001, pp. xx+773. ISBN: 0-691-09089-0.

[280] Tamara Kohler and Toby Cubitt. "Toy Models of Holographic Duality between local Hamiltonians". In: *JHEP* 08 (2019), p. 017. DOI: `10.1007/JHEP08(2019)017`. arXiv: `1810.08992 [hep-th]`.

[281] Kazuhiko Koike and Itaru Terada. "Young diagrammatic methods for the restriction of representations of complex classical Lie groups to reductive subgroups of maximal rank". In: *Adv. Math.* 79.1 (1990), pp. 104–135. ISSN: 0001-8708. DOI: `https://doi.org/10.1016/0001-8708(90)90059-V`.

[282] Filip Kos et al. "Precision islands in the Ising and O(N) models". In: *Journal of High Energy Physics* 2016.8 (Aug. 2016). DOI: `10.1007/jhep08(2016)036`. URL: `https://doi.org/10.1007%2Fjhep08%282016%29036`.

[283] Petr Kravchuk, Dalimil Mazac, and Sridip Pal. "Automorphic Spectra and the Conformal Bootstrap". In: *Commun. Am. Math. Soc.* 4 (2024), pp. 1–63. DOI: `10.1090/cams/26`. arXiv: `2111.12716 [hep-th]`.

[284] M.G. Krein. "On a problem of extrapolation of A.N. Kolmogorov". In: *Dokl. Akadl. Vauk SSSR* 46 (1945), pp. 306–309.

[285] Dennis Kretschmann, Dirk Schlingemann, and Reinhard F. Werner. "The Information-Disturbance Tradeoff and the Continuity of Stinespring's Representation". In: *IEEE Transactions on Information Theory* 54 (2006), pp. 1708–1717. URL: `https://api.semanticscholar.org/CorpusID:3061691`.

[286] Jonah Kudler-Flam, Samuel Leutheusser, and Gautam Satishchandran. "Generalized Black Hole Entropy is von Neumann Entropy". In: (Sept. 2023). arXiv: `2309.15897 [hep-th]`.

[287] Jonah Kudler-Flam et al. *A covariant regulator for entanglement entropy: proofs of the Bekenstein bound and QNEC*. Dec. 2023. arXiv: `2312.07646` `[hep-th]`.

[288] Raymond Laflamme et al. "Perfect Quantum Error Correcting Code". In: *Phys. Rev. Lett.* 77.1 (1996), p. 198. DOI: `10.1103/PhysRevLett.77.198`. arXiv: `quant-ph/9602019`.

[289] Finn Larsen and Frank Wilczek. "Renormalization of black hole entropy and of the gravitational coupling constant". In: *Nucl. Phys. B* 458 (1996), pp. 249–266. DOI: `10.1016/0550-3213(95)00548-X`. arXiv: `hep-th/9506066`.

[290] Gandalf Lechner and Charley Scotford. "Deformations of half-sided modular inclusions and non-local chiral field theories". In: *Communications in Mathematical Physics* 391.1 (2022), pp. 269–291.

[291] Ji Hoon Lee. "Exact stringy microstates from gauge theories". In: *JHEP* 11 (2022), p. 137. DOI: `10.1007/JHEP11(2022)137`. arXiv: `2204.09286 [hep-th]`.

[292] Ji Hoon Lee. "Trace relations and open string vacua". In: (Nov. 2023). arXiv: `2312.00242 [hep-th]`.

[293] Samuel Leutheusser and Hong Liu. "Causal connectability between quantum systems and the black hole interior in holographic duality". In: (Oct. 2021). arXiv: `2110.05497 [hep-th]`.

[294] Samuel Leutheusser and Hong Liu. "Emergent times in holographic duality". In: (Dec. 2021). arXiv: `2112.12156 [hep-th]`.

[295] Samuel Leutheusser and Hong Liu. "Subalgebra-subregion duality: emergence of space and time in holography". In: (Dec. 2022). arXiv: `2212.13266 [hep-th]`.

[296] Aitor Lewkowycz and Juan Maldacena. "Generalized gravitational entropy". In: *JHEP* 08 (2013), p. 090. DOI: `10.1007/JHEP08(2013)090`. arXiv: `1304.4926 [hep-th]`.

[297] Aitor Lewkowycz and Onkar Parrikar. "The holographic shape of entanglement and Einstein's equations". In: *JHEP* 05 (2018), p. 147. DOI: `10.1007/JHEP05(2018)147`. arXiv: `1802.10103 [hep-th]`.

[298] Jun Li. "Zero dimensional Donaldson–Thomas invariants of threefolds". In: *Geometry & Topology* 10.4 (2006), pp. 2117–2171.

[299] Matvei Libine. "Introduction to representations of real semisimple Lie groups". In: *arXiv preprint arXiv:1212.2578* (2012).

[300] Francesco Lin and Michael Lipnowski. "The Seiberg-Witten equations and the length spectrum of hyperbolic three-manifolds". In: *Journal of the American Mathematical Society* 35.1 (2022), pp. 233–293.

[301] Hai Lin, Oleg Lunin, and Juan Martin Maldacena. "Bubbling AdS space and 1/2 BPS geometries". In: *JHEP* 10 (2004), p. 025. DOI: `10.1088/1126-6708/2004/10/025`. arXiv: `hep-th/0409174`.

[302] Hong Liu. "Fine structure of Hagedorn transitions". In: (Aug. 2004). arXiv: `hep-th/0408001`.

[303] Roberto Longo. "Modular Structure of the Weyl Algebra". In: *Commun. Math. Phys.* 392.1 (2022), pp. 145–183. DOI: `10.1007/s00220-022-04344-7`. arXiv: `2111.11266 [math-ph]`.

[304] Roberto Longo, Yoh Tanimoto, and Yoshimichi Ueda. "Free products in AQFT". In: *Annales Inst. Fourier* 69.3 (2019), pp. 1229–1258. DOI: `10.5802/aif.3269`. arXiv: `1706.06070 [math-ph]`.

[305] Roberto Longo and Edward Witten. "A note on continuous entropy". In: (Feb. 2022). arXiv: `2202.03357 [math-ph]`.

[306] Manuel Loparco, Jiaxin Qiao, and Zimo Sun. "A radial variable for de Sitter two-point functions". In: (Oct. 2023). arXiv: `2310.15944 [hep-th]`.

[307] Manuel Loparco et al. "The Källén-Lehmann representation in de Sitter spacetime". In: (May 2023). arXiv: `2306.00090 [hep-th]`.

[308] Lauritz van Luijk, Alexander Stottmeister, and Reinhard F Werner. "Convergence of dynamics on inductive systems of Banach spaces". In: *Annales Henri Poincaré*. Springer. 2024, pp. 1–56.

[309] Lauritz van Luijk, Alexander Stottmeister, and Henrik Wilming. *The Large-Scale Structure of Entanglement in Quantum Many-body Systems*. Mar. 2025. arXiv: `2503.03833 [quant-ph]`.

[310] Lauritz van Luijk et al. *Embezzlement of entanglement, quantum fields, and the classification of von Neumann algebras*. Jan. 2024. arXiv: `2401.07299 [math-ph]`.

[311] N. Laustsen) M. Rørdam F. Larsen. *An Introduction to K-Theory for C*-Algebras*. Cambridge University Press, 2000.

[312] Ian G. Macdonald. *Symmetric Functions and Hall Polynomials*. Oxford Mathematical Monographs. Walton Street, Oxford, UK: Oxford University Press, 1995, p. 488.

[313] Joseph Maciejko and Steven Rayan. "Hyperbolic band theory". In: *Science Advances* 7.36 (2021), eabe9170. DOI: `10.1126/sciadv.abe9170`. eprint: `https://www.science.org/doi/pdf/10.1126/sciadv.abe9170`. URL: `https://www.science.org/doi/abs/10.1126/sciadv.abe9170`.

[314] J. Maldacena and L. Susskind. "Cool horizons for entangled black holes". In: *Fortschritte der Physik* 61.9 (Aug. 2013), pp. 781–811. DOI: `10.1002/prop.201300020`. URL: `https://doi.org/10.1002%2Fprop.201300020`.

[315] Juan Maldacena, Stephen H. Shenker, and Douglas Stanford. "A bound on chaos". In: *JHEP* 08 (2016), p. 106. DOI: `10.1007/JHEP08(2016)106`. arXiv: `1503.01409 [hep-th]`.

[316] Juan Maldacena and Douglas Stanford. "Remarks on the Sachdev-Ye-Kitaev model". In: *Phys. Rev. D* 94.10 (2016), p. 106002. DOI: `10.1103/PhysRevD.94.106002`. arXiv: `1604.07818 [hep-th]`.

[317] Juan Maldacena and Leonard Susskind. "Cool horizons for entangled black holes". In: *Fortsch. Phys.* 61 (2013), pp. 781–811. DOI: `10.1002/prop.201300020`. arXiv: `1306.0533 [hep-th]`.

[318] Juan Martin Maldacena. "Eternal black holes in anti-de Sitter". In: *JHEP* 04 (2003), p. 021. DOI: `10.1088/1126-6708/2003/04/021`. arXiv: `hep-th/0106112`.

[319] Juan Martin Maldacena. "The Large N limit of superconformal field theories and supergravity". In: *Adv. Theor. Math. Phys.* 2 (1998), pp. 231–252. DOI: `10.4310/ATMP.1998.v2.n2.a1`. arXiv: `hep-th/9711200`.

[320] Juan Martin Maldacena and Liat Maoz. "Wormholes in AdS". In: *JHEP* 02 (2004), p. 053. DOI: `10.1088/1126-6708/2004/02/053`. arXiv: `hep-th/0401024`.

[321] Alexander Maloney and Edward Witten. "Averaging over Narain moduli space". In: *JHEP* 10 (2020), p. 187. DOI: `10.1007/JHEP10(2020)187`. arXiv: `2006.04855 [hep-th]`.

[322] Gautam Mandal. "Phase Structure of Unitary Matrix Models". In: *Mod. Phys. Lett. A* 5 (1990), pp. 1147–1158. DOI: `10.1142/S0217732390001281`.

[323] Marcos Mariño. "Lectures on non-perturbative effects in large N gauge theories, matrix models and strings". In: *Fortsch. Phys.* 62 (2014), pp. 455–540. DOI: `10.1002/prop.201400005`. arXiv: `1206.6272 [hep-th]`.

[324] Marcos Mariño. "Les Houches lectures on matrix models and topological strings". In: (Oct. 2004). arXiv: `hep-th/0410165`.

[325] Marcos Mariño. "Nonperturbative effects and nonperturbative definitions in matrix models and topological strings". In: *JHEP* 12 (2008), p. 114. DOI: `10.1088/1126-6708/2008/12/114`. arXiv: `0805.3033 [hep-th]`.

[326] Marcos Mariño, Ricardo Schiappa, and Maximilian Schwick. "New Instantons for Matrix Models". In: (Oct. 2022). arXiv: `2210.13479 [hep-th]`.

[327] Marcos Mariño, Ricardo Schiappa, and Marlene Weiss. "Nonperturbative Effects and the Large-Order Behavior of Matrix Models and Topological Strings". In: *Commun. Num. Theor. Phys.* 2 (2008), pp. 349–419. DOI: `10.4310/CNTP.2008.v2.n2.a3`. arXiv: `0711.1954 [hep-th]`.

[328] Donald Marolf and Henry Maxfield. "Transcending the ensemble: baby universes, spacetime wormholes, and the order and disorder of black hole information". In: *JHEP* 08 (2020), p. 044. DOI: `10.1007/JHEP08(2020)044`. arXiv: `2002.08950 [hep-th]`.

[329] Donald Marolf and Aron C. Wall. "Eternal Black Holes and Superselection in AdS/CFT". In: *Class. Quant. Grav.* 30 (2013), p. 025001. DOI: `10.1088/0264-9381/30/2/025001`. arXiv: `1210.3590 [hep-th]`.

[330] Henrik H. Martens. "Varieties of special divisors on a curve. II." In: *Journal für die reine und angewandte Mathematik* 233 (1968), pp. 89–100. URL: `http://eudml.org/doc/150887`.

[331] Taku Matsui. "Boundedness of entanglement entropy and split property of quantum spin chains". In: *Reviews in Mathematical Physics* 25.09 (2013), p. 1350017.

[332] D. Maulik et al. "Gromov–Witten theory and Donaldson–Thomas theory, I". In: *Compos. Math.* 142.05 (2006), pp. 1263–1285. DOI: `10.1112/S0010437X06002302`. arXiv: `math/0312059`.

[333] Jacob McNamara. "Cobordism, ER = EPR, and the Sum Over Topologies". Spacetime and String Theory, Kavli Institute for Theoretical Physics. 2024.

[334] Jacob McNamara. "The Kinematics of Quantum Gravity". PhD thesis. Harvard University, 2022.

[335] Jacob McNamara and Cumrun Vafa. "Baby Universes, Holography, and the Swampland". In: (Apr. 2020). arXiv: `2004.06738 [hep-th]`.

[336] Jacob McNamara and Cumrun Vafa. "Cobordism Classes and the Swampland". In: (Sept. 2019). arXiv: `1909.10355 [hep-th]`.

[337] Ben Michel et al. "Four-point function in the IOP matrix model". In: *JHEP* 05 (2016), p. 048. DOI: `10.1007/JHEP05(2016)048`. arXiv: `1602.06422 [hep-th]`.

[338] Philippe Michel and Akshay Venkatesh. "The subconvexity problem for GL2". en. In: *Publications Mathématiques de l'IHÉS* 111 (2010), pp. 171–271. DOI: `10.1007/s10240-010-0025-8`. URL: `http://www.numdam.org/articles/10.1007/s10240-010-0025-8/`.

[339] A. A. Migdal. "Recursion Equations in Gauge Theories". In: *Sov. Phys. JETP* 42 (1975). [,114(1975)], p. 413.

[340] Alexey Milekhin. "Quantum error correction and large N". In: *SciPost Phys.* 11 (2021), p. 094. DOI: `10.21468/SciPostPhys.11.5.094`. arXiv: `2008.12869 [hep-th]`.

[341] Ashley Milsted and Guifre Vidal. *Geometric interpretation of the multiscale entanglement renormalization ansatz.* Dec. 2018. arXiv: `1812.00529 [hep-th]`.

[342] Joseph A. Minahan. "Matrix models with boundary terms and the generalized Painleve II equation". In: *Phys. Lett. B* 268 (1991), pp. 29–34. DOI: `10.1016/0370-2693(91)90917-F`.

[343] A. Mironov and A. Morozov. "Superintegrability summary". In: *Phys. Lett. B* 835 (2022), p. 137573. DOI: 10.1016/j.physletb.2022.137573. arXiv: 2201.12917 [hep-th].

[344] A. Mironov, A. Morozov, and Z. Zakirova. "New insights into superintegrability from unitary matrix models". In: *Phys. Lett. B* 831 (2022), p. 137178. DOI: 10.1016/j.physletb.2022.137178. arXiv: 2203.03869 [hep-th].

[345] Masamichi Miyaji, Tadashi Takayanagi, and Kento Watanabe. "From path integrals to tensor networks for the AdS/CFT correspondence". In: *Phys. Rev. D* 95.6 (2017), p. 066004. DOI: 10.1103/PhysRevD.95.066004. arXiv: 1609.04645 [hep-th].

[346] Vincenzo Morinelli et al. "Scaling Limits of Lattice Quantum Fields by Wavelets". In: *Commun. Math. Phys.* 387.1 (2021), pp. 299–360. DOI: 10.1007/s00220-021-04152-5. arXiv: 2010.11121 [math-ph].

[347] Andrei Moroianu. "Kähler manifolds with small eigenvalues of the Dirac operator and a conjecture of Lichnerowicz". en. In: *Annales de l'Institut Fourier* 49.5 (1999), pp. 1637–1659. DOI: 10.5802/aif.1732. URL: http://www.numdam.org/articles/10.5802/aif.1732/.

[348] Gabor Moussong. "Hyperbolic coxeter groups". PhD thesis. Ohio State University, 1988.

[349] Baur Mukhametzhanov and Sridip Pal. "Beurling-Selberg Extremization and Modular Bootstrap at High Energies". In: *SciPost Phys.* 8.6 (2020), p. 088. DOI: 10.21468/SciPostPhys.8.6.088. arXiv: 2003.14316 [hep-th].

[350] Baur Mukhametzhanov and Alexander Zhiboedov. "Modular invariance, tauberian theorems and microcanonical entropy". In: *JHEP* 10 (2019), p. 261. DOI: 10.1007/JHEP10(2019)261. arXiv: 1904.06359 [hep-th].

[351] Nicolas Müller and Richard Pink. *Hyperelliptic Curves with Many Automorphisms*. 2017. DOI: 10.48550/ARXIV.1711.06599. URL: https://arxiv.org/abs/1711.06599.

[352] Sameer Murthy. "Unitary matrix models, free fermions, and the giant graviton expansion". In: *Pure Appl. Math. Quart.* 19.1 (2023), pp. 299–340. DOI: 10.4310/PAMQ.2023.v19.n1.a12. arXiv: 2202.06897 [hep-th].

[353] Pieter Naaijkens and Yoshiko Ogata. "The Split and Approximate Split Property in 2D Systems: Stability and Absence of Superselection Sectors". In: *Communications in Mathematical Physics* 392.3 (Mar. 2022), pp. 921–950. DOI: 10.1007/s00220-022-04356-3. URL: https://doi.org/10.1007%2Fs00220-022-04356-3.

[354] Raghavan Narasimhan. "Hyperelliptic Curves and the Canonical Map". In: *Compact Riemann Surfaces*. Basel: Birkhäuser Basel, 1992, pp. 63–65. ISBN: 978-3-0348-8617-8. DOI: `10.1007/978-3-0348-8617-8{\_}12`. URL: `https://doi.org/10.1007/978-3-0348-8617-8%7B%5C_%7D12`.

[355] H. Narnhofer. "KOLMOGOROV SYSTEMS AND ANOSOV SYSTEMS IN QUANTUM THEORY". In: *Infinite Dimensional Analysis, Quantum Probability and Related Topics* 04.01 (2001), pp. 85–119. DOI: `10.1142/S0219025701000401`. eprint: `https://doi.org/10.1142/S0219025701000401`. URL: `https://doi.org/10.1142/S0219025701000401`.

[356] H. Narnhofer and W. Thirring. "Equivalence of modular K and Anosov Dynamical Systems". In: *Reviews in Mathematical Physics* 12.03 (2000), pp. 445–459. DOI: `10.1142/s0129055x00000150`.

[357] H. Narnhofer and W. Thirring. "Quantum K-systems". In: *Communications in Mathematical Physics* 125.4 (1989), pp. 565–577.

[358] Heide Narnhofer. "Quantum Anosov Systems". In: *Rigorous Quantum Field Theory: A Festschrift for Jacques Bros*. Ed. by Anne Boutet de Monvel et al. Basel: Birkhäuser Basel, 2007, pp. 213–223. ISBN: 978-3-7643-7434-1. DOI: `10.1007/978-3-7643-7434-1_15`. URL: `https://doi.org/10.1007/978-3-7643-7434-1%7B%5C_%7D15`.

[359] Tamra M. Nebabu and Xiaoliang Qi. "Bulk Reconstruction from Generalized Free Fields". In: (June 2023). arXiv: `2306.16687 [hep-th]`.

[360] Paul D. Nelson. "Bounds for standard L-functions". In: (Sept. 2021). arXiv: `2109.15230 [math.NT]`.

[361] J. von Neumann. "On infinite direct products". In: *Compositio Mathematica* 6 (1939), pp. 1–77.

[362] M. Ohya and Dénes Petz. "Quantum Entropy and Its Use". In: 1993. URL: `https://api.semanticscholar.org/CorpusID:118044922`.

[363] Takuya Okuda. "Derivation of Calabi-Yau crystals from Chern-Simons gauge theory". In: *JHEP* 03 (2005), p. 047. DOI: `10.1088/1126-6708/2005/03/047`. arXiv: `hep-th/0409270`.

[364] Hirosi Ooguri, Piotr Sulkowski, and Masahito Yamazaki. "Wall Crossing As Seen By Matrix Models". In: *Commun. Math. Phys.* 307 (2011), pp. 429–462. DOI: `10.1007/s00220-011-1330-x`. arXiv: `1005.1293 [hep-th]`.

[365] Tobias J. Osborne and Deniz E. Stiegemann. "Dynamics for holographic codes". In: *JHEP* 04.154 (2020). DOI: `10.1007/JHEP04(2020)154`. arXiv: `1706.08823 [quant-ph]`.

[366] Tobias J. Osborne and Alexander Stottmeister. "Conformal Field Theory from Lattice Fermions". In: *Commun. Math. Phys.* 398.1 (2023), pp. 219–289. DOI: `10.1007/s00220-022-04521-8`. arXiv: `2107.13834 [math-ph]`.

[367] Shoy Ouseph et al. "Local Poincaré algebra from quantum chaos". In: *JHEP* 01 (2024), p. 112. DOI: 10.1007/JHEP01(2024)112. arXiv: 2310.13736 [hep-th].

[368] Don N. Page. "Average entropy of a subsystem". In: *Phys. Rev. Lett.* 71 (1993), pp. 1291–1294. DOI: 10.1103/PhysRevLett.71.1291. arXiv: gr-qc/9305007.

[369] Sridip Pal and Jiaxin Qiao. "Lightcone Modular Bootstrap and Tauberian Theory: A Cardy-like Formula for Near-extremal Black Holes". In: (July 2023). arXiv: 2307.02587 [hep-th].

[370] Kyriakos Papadodimas and Suvrat Raju. "An Infalling Observer in AdS/CFT". In: *JHEP* 10 (2013), p. 212. DOI: 10.1007/JHEP10(2013)212. arXiv: 1211.6767 [hep-th].

[371] Kyriakos Papadodimas and Suvrat Raju. "State-Dependent Bulk-Boundary Maps and Black Hole Complementarity". In: *Phys. Rev. D* 89.8 (2014), p. 086010. DOI: 10.1103/PhysRevD.89.086010. arXiv: 1310.6335 [hep-th].

[372] Fernando Pastawski et al. "Holographic quantum error-correcting codes: Toy models for the bulk/boundary correspondence". In: *JHEP* 06.149 (2015). DOI: 10.1007/JHEP06(2015)149. arXiv: 1503.06237 [hep-th].

[373] Dmitri Pavlov. "Gelfand-type duality for commutative von Neumann algebras". In: *Journal of Pure and Applied Algebra* 226.4 (2022), p. 106884.

[374] Heinz-Otto Peitgen, Hartmut Jürgens, and Dietmar Saupe. "Chaos and Fractals". In: 2004. URL: https://api.semanticscholar.org/CorpusID:12756214.

[375] Joao Penedones, Kamran Salehi Vaziri, and Zimo Sun. "Hilbert space of Quantum Field Theory in de Sitter spacetime". In: (Jan. 2023). arXiv: 2301.04146 [hep-th].

[376] Geoff Penington and Edward Witten. "Algebras and States in JT Gravity". In: (Jan. 2023). arXiv: 2301.07257 [hep-th].

[377] Geoff Penington et al. "Replica wormholes and the black hole interior". In: *JHEP* 03 (2022), p. 205. DOI: 10.1007/JHEP03(2022)205. arXiv: 1911.11977 [hep-th].

[378] Geoffrey Penington. "Entanglement Wedge Reconstruction and the Information Paradox". In: (May 2019). arXiv: 1905.08255 [hep-th].

[379] Geoffrey Penington. "Entanglement Wedge Reconstruction and the Information Paradox". In: *JHEP* 09 (2020), p. 002. DOI: 10.1007/JHEP09(2020)002. arXiv: 1905.08255 [hep-th].

[380] David Pérez-García, Leonardo Santilli, and Miguel Tierz. "Dynamical quantum phase transitions from random matrix theory". In: (Aug. 2022). arXiv: 2208.01659 [quant-ph].

[381] Robert N. C. Pfeifer, Glen Evenbly, and Guifre Vidal. "Entanglement renormalization, scale invariance, and quantum criticality". In: *Phys. Rev. A* 79 (2009), p. 040301. DOI: 10.1103/PhysRevA.79.040301. arXiv: 0810.0580 [cond-mat.str-el].

[382] Joseph F. Plante. "Anosov Flows". In: *American Journal of Mathematics* 94.3 (1972), pp. 729–754. ISSN: 00029327, 10806377. URL: http://www.jstor.org/stable/2373755 (visited on 10/11/2023).

[383] David Poland, Slava Rychkov, and Alessandro Vichi. "The Conformal Bootstrap: Theory, Numerical Techniques, and Applications". In: *Rev. Mod. Phys.* 91 (2019), p. 015002. DOI: 10.1103/RevModPhys.91.015002. arXiv: 1805.04405 [hep-th].

[384] David Poland and David Simmons-Duffin. "The conformal bootstrap". In: *Nature Physics* 12.6 (2016), pp. 535–539. DOI: 10.1038/nphys3761. URL: https://doi.org/10.1038/nphys3761.

[385] Jason Pollack, Patrick Rall, and Andrea Rocchetto. "Understanding holographic error correction via unique algebras and atomic examples". In: *JHEP* 06.056 (2022). DOI: 10.1007/JHEP06(2022)056. arXiv: 2110.14691 [quant-ph].

[386] A. Poltoratski. "Type alternative for Frostman measures". In: *Advances in Mathematics* 349 (2019), pp. 348–366. ISSN: 0001-8708. DOI: https://doi.org/10.1016/j.aim.2019.04.018. URL: https://www.sciencedirect.com/science/article/pii/S0001870819301793.

[387] Alexei Poltoratski. "A problem on completeness of exponentials". In: *Annals of Mathematics* (2013), pp. 983–1016.

[388] Alexei Poltoratski. "Private communication". In: 4 (). DOI: 10.1063/1.1703912.

[389] Boris Post, Jeremy van der Heijden, and Erik Verlinde. "A universe field theory for JT gravity". In: *JHEP* 05 (2022), p. 118. DOI: 10.1007/JHEP05(2022)118. arXiv: 2201.08859 [hep-th].

[390] Leonid Potyagailo and Ernest Vinberg. "On right-angled reflection groups in hyperbolic spaces". In: *Commentarii Mathematici Helvetici - COMMENT MATH HELV* 80 (Mar. 2005), pp. 63–73. DOI: 10.4171/CMH/4.

[391] Robert T. Powers. "Representations of Uniformly Hyperfinite Algebras and Their Associated von Neumann Rings". In: *Annals of Mathematics* 86 (1967), p. 138. URL: https://api.semanticscholar.org/CorpusID:124896803.

[392] Jiaxin Qiao and Slava Rychkov. "A tauberian theorem for the conformal bootstrap". In: *JHEP* 12 (2017), p. 119. DOI: 10.1007/JHEP12(2017)119. arXiv: 1709.00008 [hep-th].

[393] Riccardo Rattazzi et al. "Bounding scalar operator dimensions in 4D CFT". In: *JHEP* 12 (2008), p. 031. DOI: 10.1088/1126-6708/2008/12/031. arXiv: 0807.0004 [hep-th].

[394] Mauricio Romo and Miguel Tierz. "Unitary Chern-Simons matrix model and the Villain lattice action". In: *Phys. Rev. D* 86 (2012), p. 045027. DOI: 10.1103/PhysRevD.86.045027. arXiv: 1103.2421 [hep-th].

[395] Antonio ROS. "On the first eigenvalue of the Laplacian on compact surfaces of genus three". In: *Journal of the Mathematical Society of Japan* 74.3 (2022), pp. 813–828. DOI: 10.2969/jmsj/85898589. URL: https://doi.org/10.2969/jmsj/85898589.

[396] Paolo Rossi, Massimo Campostrini, and Ettore Vicari. "The Large N expansion of unitary matrix models". In: *Phys. Rept.* 302 (1998), pp. 143–209. DOI: 10.1016/S0370-1573(98)00003-9. arXiv: hep-lat/9609003.

[397] B. Rusakov. "Large N quantum gauge theories in two-dimensions". In: *Phys. Lett. B* 303 (1993), pp. 95–98. DOI: 10.1016/0370-2693(93)90049-N. arXiv: hep-th/9212090.

[398] B. E. Rusakov. "Loop averages and partition functions in U(N) gauge theory on two-dimensional manifolds". In: *Mod. Phys. Lett. A* 5 (1990), pp. 693–703. DOI: 10.1142/S0217732390000780.

[399] Jorge G. Russo and Miguel Tierz. "Multiple phases in a generalized Gross-Witten-Wadia matrix model". In: *JHEP* 09 (2020), p. 081. DOI: 10.1007/JHEP09(2020)081. arXiv: 2007.08515 [hep-th].

[400] Shinsei Ryu and Tadashi Takayanagi. "Aspects of Holographic Entanglement Entropy". In: *JHEP* 08 (2006), p. 045. DOI: 10.1088/1126-6708/2006/08/045. arXiv: hep-th/0605073.

[401] Shinsei Ryu and Tadashi Takayanagi. "Holographic derivation of entanglement entropy from AdS/CFT". In: *Phys. Rev. Lett.* 96 (2006), p. 181602. DOI: 10.1103/PhysRevLett.96.181602. arXiv: hep-th/0603001.

[402] Phil Saad, Stephen Shenker, and Shunyu Yao. "Comments on wormholes and factorization". In: (July 2021). arXiv: 2107.13130 [hep-th].

[403] Phil Saad, Stephen H. Shenker, and Douglas Stanford. "JT gravity as a matrix integral". In: (Mar. 2019). arXiv: 1903.11115 [hep-th].

[404] Phil Saad et al. "Wormholes without averaging". In: (Mar. 2021). arXiv: 2103.16754 [hep-th].

[405] Leonardo Santilli and Miguel Tierz. "Exact equivalences and phase discrepancies between random matrix ensembles". In: *J. Stat. Mech.* 2008 (2020), p. 083107. DOI: 10.1088/1742-5468/aba594. arXiv: 2003.10475 [math-ph].

[406] Leonardo Santilli and Miguel Tierz. "Multiple phases and meromorphic deformations of unitary matrix models". In: *Nucl. Phys. B* 976 (2022), p. 115694. DOI: 10.1016/j.nuclphysb.2022.115694. arXiv: 2102.11305 [hep-th].

[407] Leonardo Santilli and Miguel Tierz. "Phase transition in complex-time Loschmidt echo of short and long range spin chain". In: *J. Stat. Mech.* 2006 (2020), p. 063102. DOI: 10.1088/1742-5468/ab837b. arXiv: 1902.06649 [cond-mat.stat-mech].

[408] Leonardo Santilli and Miguel Tierz. "Schur expansion of random-matrix reproducing kernels". In: *J. Phys. A* 54.43 (2021), p. 435202. DOI: 10.1088/1751-8121/ac2754. arXiv: 2106.04168 [math-ph].

[409] Peter Sarnak. "Integrals of products of eigenfunctions". In: *International Mathematics Research Notices* 1994.6 (Mar. 1994), pp. 251–260. ISSN: 1073-7928. DOI: 10.1155/S1073792894000280. URL: https://doi.org/10.1155/S1073792894000280.

[410] Howard J. Schnitzer. "Confinement/deconfinement transition of large N gauge theories with N(f) fundamentals: N(f)/N finite". In: *Nucl. Phys. B* 695 (2004), pp. 267–282. DOI: 10.1016/j.nuclphysb.2004.06.057. arXiv: hep-th/0402219.

[411] Matias N. Sempe and Guillermo A. Silva. "Fermionic matrix models and bosonization". In: *Phys. Rev. D* 106.10 (2022), p. 106005. DOI: 10.1103/PhysRevD.106.106005. arXiv: 2112.14270 [hep-th].

[412] Tony Shaska. "Subvarieties of the hyperelliptic moduli determined by group actions". In: *arXiv preprint arXiv:1302.3974* (2013).

[413] Stephen H. Shenker and Douglas Stanford. "Black holes and the butterfly effect". In: *JHEP* 03 (2014), p. 067. DOI: 10.1007/JHEP03(2014)067. arXiv: 1306.0622 [hep-th].

[414] Stephen H. Shenker and Douglas Stanford. "Stringy effects in scrambling". In: *JHEP* 05 (2015), p. 132. DOI: 10.1007/JHEP05(2015)132. arXiv: 1412.6087 [hep-th].

[415] David Simmons-Duffin. "The Conformal Bootstrap". In: *Theoretical Advanced Study Institute in Elementary Particle Physics: New Frontiers in Fields and Strings*. 2017, pp. 1–74. DOI: 10.1142/9789813149441_0001. arXiv: 1602.07982 [hep-th].

[416] Ronak M. Soni. "A type I approximation of the crossed product". In: *JHEP* 01.123 (2024). DOI: `10.1007/JHEP01(2024)123`. arXiv: `2307.12481 [hep-th]`.

[417] Richard P Stanley. "Hilbert functions of graded algebras". In: *Adv. Math.* 28.1 (1978), pp. 57–83. DOI: `https://doi.org/10.1016/0001-8708(78)90045-2`.

[418] Matthew Steinberg, Sebastian Feld, and Alexander Jahn. "Holographic codes from hyperinvariant tensor networks". In: *Nature Commun.* 14.1 (2023), p. 7314. DOI: `10.1038/s41467-023-42743-z`. arXiv: `2304.02732 [quant-ph]`.

[419] John R. Stembridge. "Orthogonal sets of Young symmetrizers". In: *Advances Appl. Math.* 46.1 (2011). Special issue in honor of Dennis Stanton, pp. 576–582. DOI: `https://doi.org/10.1016/j.aam.2009.08.004`.

[420] Christopher R. Stephens, Gerard 't Hooft, and Bernard F. Whiting. "Black hole evaporation without information loss". In: *Class. Quant. Grav.* 11 (1994), pp. 621–648. DOI: `10.1088/0264-9381/11/3/014`. arXiv: `gr-qc/9310006`.

[421] William F. Stinespring. "Positive functions on *-algebras". In: 1955. URL: `https://api.semanticscholar.org/CorpusID:119642419`.

[422] Alexander Stottmeister. *Anyon braiding and the renormalization group*. Jan. 2022. arXiv: `2201.11562 [quant-ph]`.

[423] Alexander Stottmeister et al. "Operator-Algebraic Renormalization and Wavelets". In: *Phys. Rev. Lett.* 127.23 (2021), p. 230601. DOI: `10.1103/PhysRevLett.127.230601`. arXiv: `2002.01442 [math-ph]`.

[424] Serban Valentin Stratila. *Modular Theory in Operator Algebras*. Oct. 2020. DOI: `10.1017/9781108489607`. URL: `http://dx.doi.org/10.1017/9781108489607`.

[425] Andrew Strominger and Cumrun Vafa. "Microscopic origin of the Bekenstein-Hawking entropy". In: *Phys. Lett. B* 379 (1996), pp. 99–104. DOI: `10.1016/0370-2693(96)00345-0`. arXiv: `hep-th/9601029`.

[426] Zimo Sun. "A note on the representations of $SO(1, d+1)$". In: (Nov. 2021). arXiv: `2111.04591 [hep-th]`.

[427] Bo Sundborg. "The Hagedorn transition, deconfinement and N=4 SYM theory". In: *Nucl. Phys. B* 573 (2000), pp. 349–363. DOI: `10.1016/S0550-3213(00)00044-4`. arXiv: `hep-th/9908001`.

[428] V. S. Sunder. *An Invitation to von Neumann Algebras*. Ed. by F. W. Gehring and P. R. Halmos. Universitext. New York, NY: Springer, 1987. ISBN: 978-0-387-96356-3 978-1-4613-8669-8. DOI: `10.1007/978-1-4613-8669-8`. URL: `http://link.springer.com/10.1007/978-1-4613-8669-8` (visited on 06/04/2024).

[429] Leonard Susskind. "The World as a hologram". In: *J. Math. Phys.* 36 (1995), pp. 6377–6396. DOI: `10.1063/1.531249`. arXiv: `hep-th/9409089`.

[430] Leonard Susskind and John Uglum. "Black hole entropy in canonical quantum gravity and superstring theory". In: *Phys. Rev. D* 50 (1994), pp. 2700–2711. DOI: `10.1103/PhysRevD.50.2700`. arXiv: `hep-th/9401070`.

[431] Brian Swingle. "Entanglement Renormalization and Holography". In: *Phys. Rev. D* 86 (2012), p. 065007. DOI: `10.1103/PhysRevD.86.065007`. arXiv: `0905.1317 [cond-mat.str-el]`.

[432] Richard J. Szabo and Miguel Tierz. "Matrix models and stochastic growth in Donaldson-Thomas theory". In: *J. Math. Phys.* 53 (2012), p. 103502. DOI: `10.1063/1.4748525`. arXiv: `1005.5643 [hep-th]`.

[433] Gabor Szegő. "On certain Hermitian forms associated with the Fourier series of a positive function". In: *Comm. Sém. Math. Univ. Lund* Tome Supplémentaire (1952), pp. 228–238.

[434] M. Takesaki. *Tomita's Theory of Modular Hilbert Algebras and its Applications*. Lecture Notes in Mathematics. Springer-Verlag, 1970. DOI: `10.1007/bfb0065832`.

[435] Masamichi Takesaki. "Conditional expectations in von Neumann algebras". In: *Journal of Functional Analysis* 9.3 (1972), pp. 306–321. ISSN: 0022-1236. DOI: `https://doi.org/10.1016/0022-1236(72)90004-3`. URL: `https://www.sciencedirect.com/science/article/pii/0022123672900043`.

[436] Masamichi Takesaki. *Theory of Operator Algebras I*. Springer New York, 1979. DOI: `10.1007/978-1-4612-6188-9`.

[437] Masamichi Takesaki. *Theory of operator Algebras II*. Vol. 125. EMS. Springer Berlin, Heidelberg, 2010. DOI: `10.1007/978-3-662-10451-4`.

[438] Mitsuhiro Takeuchi. "Free Hopf algebras generated by coalgebras". In: *Journal of The Mathematical Society of Japan* 23 (1971), pp. 561–582. URL: `https://api.semanticscholar.org/CorpusID:122558362`.

[439] Anne Thomas. "Lattices in hyperbolic buildings". In: *arXiv: Group Theory* (2012). URL: `https://api.semanticscholar.org/CorpusID:25841608`.

[440] Mykhaylo Usatyuk, Zi-Yue Wang, and Ying Zhao. "Closed universes in two dimensional gravity". In: *SciPost Phys.* 17.2 (2024), p. 051. DOI: `10.21468/SciPostPhys.17.2.051`. arXiv: `2402.00098 [hep-th]`.

[441] Mykhaylo Usatyuk and Ying Zhao. "Closed universes, factorization, and ensemble averaging". In: *JHEP* 02 (2025), p. 052. DOI: `10.1007/JHEP02(2025)052`. arXiv: `2403.13047 [hep-th]`.

[442] Cumrun Vafa and Edward Witten. "Eigenvalue inequalities for fermions in gauge theories". In: *Communications in Mathematical Physics* 95.3 (1984), pp. 257–276. DOI: 10.1007/BF01212397. URL: https://doi.org/10.1007/BF01212397.

[443] F. Verstraete and J. I. Cirac. "Continuous Matrix Product States for Quantum Fields". In: *Phys. Rev. Lett.* 104 (2010), p. 190405. DOI: 10.1103/PhysRevLett.104.190405. arXiv: 1002.1824 [cond-mat.str-el].

[444] G. Vidal. "Class of Quantum Many-Body States That Can Be Efficiently Simulated". In: *Phys. Rev. Lett.* 101 (2008), p. 110501. DOI: 10.1103/PhysRevLett.101.110501. arXiv: quant-ph/0610099.

[445] Guifre Vidal. *Entanglement renormalization: An introduction*. Ed. by Lincoln D. Carr. 2010.

[446] Ernest Borisovich Vinberg. "Absence of crystallographic groups of reflections in Lobachevskii spaces of large dimension". In: *Functional Analysis and Its Applications* 15 (1981), pp. 128–130. URL: https://api.semanticscholar.org/CorpusID:122063142.

[447] John Voight. *Computing fundamental domains for Fuchsian groups*. 2009. arXiv: 0802.0196 [math.NT].

[448] Spenta R. Wadia. "N = Infinity Phase Transition in a Class of Exactly Soluble Model Lattice Gauge Theories". In: *Phys. Lett. B* 93 (1980), pp. 403–410. DOI: 10.1016/0370-2693(80)90353-6.

[449] Spenta R. Wadia. "A Study of U(N) Lattice Gauge Theory in 2-dimensions". In: (Dec. 2012). arXiv: 1212.2906 [hep-th].

[450] Aron C. Wall. "A proof of the generalized second law for rapidly changing fields and arbitrary horizon slices". In: *Phys. Rev. D* 85 (2012). [Erratum: Phys.Rev.D 87, 069904 (2013)], p. 104049. DOI: 10.1103/PhysRevD.85.104049. arXiv: 1105.3445 [gr-qc].

[451] Peter Walters. *An introduction to ergodic theory*. Springer, 1982.

[452] Christopher David White, ChunJun Cao, and Brian Swingle. "Conformal field theories are magical". In: *Phys. Rev. B* 103.7 (2021), p. 075145. DOI: 10.1103/PhysRevB.103.075145. arXiv: 2007.01303 [quant-ph].

[453] Hans-Werner Wiesbrock. "Half-sided modular inclusions of von-Neumann-algebras". In: *Commun. Math. Phys.* 157.1 (1993), pp. 83–92. DOI: cmp/1104253848.

[454] Andreas Winter. "Tight Uniform Continuity Bounds for Quantum Entropies: Conditional Entropy, Relative Entropy Distance and Energy Constraints". In: *Communications in Mathematical Physics* 347.1 (Mar. 2016), pp. 291–313. DOI: 10.1007/s00220-016-2609-8. URL: https://doi.org/10.1007%2Fs00220-016-2609-8.

[455] Edward Witten. "Anti-de Sitter space, thermal phase transition, and confinement in gauge theories". In: *Adv. Theor. Math. Phys.* 2 (1998). Ed. by L. Bergstrom and U. Lindstrom, pp. 505–532. DOI: `10.4310/ATMP.1998.v2.n3.a3`. arXiv: `hep-th/9803131`.

[456] Edward Witten. "APS Medal for Exceptional Achievement in Research: Invited article on entanglement properties of quantum field theory". In: *Rev. Mod. Phys.* 90.4 (2018), p. 045003. DOI: `10.1103/RevModPhys.90.045003`. arXiv: `1803.04993 [hep-th]`.

[457] Edward Witten. "Gravity and the crossed product". In: *JHEP* 10 (2022), p. 008. DOI: `10.1007/JHEP10(2022)008`. arXiv: `2112.12828 [hep-th]`.

[458] Edward Witten and Shing-Tung Yau. "Connectedness of the boundary in the AdS / CFT correspondence". In: *Adv. Theor. Math. Phys.* 3 (1999). Ed. by Erik D'Hoker, Duong Phong, and Shing-Tung Yau, pp. 1635–1655. DOI: `10.4310/ATMP.1999.v3.n6.a1`. arXiv: `hep-th/9910245`.

[459] Freek Witteveen et al. "Quantum Circuit Approximations and Entanglement Renormalization for the Dirac Field in 1+1 Dimensions". In: *Commun. Math. Phys.* 389.1 (2022), pp. 75–120. DOI: `10.1007/s00220-021-04274-w`. arXiv: `1905.08821 [quant-ph]`.

[460] Paul C. Yang and Shing Tung Yau. "Eigenvalues of the Laplacian of compact Riemann surfaces and minimal submanifolds". In: *Ann. Scuola Norm. Sup. Pisa Cl. Sci. (4)* 7.1 (1980), pp. 55–63. ISSN: 0391-173X. URL: `http://www.numdam.org/item?id=ASNSP_1980_4_7_1_55_0`.

[461] Karen Yeats. *Rearranging Dyson-Schwinger equations*. Vol. 211. 995. American Mathematical Society, 2011.

[462] Feng Zhu. "Ergodicity and equidistribution in Hilbert geometry". In: 2020. URL: `https://api.semanticscholar.org/CorpusID:220936086`.

[463] W. Zimmermann. "Convergence of Bogolyubov's method of renormalization in momentum space". In: *Commun. Math. Phys.* 15 (1969), pp. 208–234. DOI: `10.1007/BF01645676`.

[464] Yijian Zou, Ashley Milsted, and Guifre Vidal. "Conformal fields and operator product expansion in critical quantum spin chains". In: *Phys. Rev. Lett.* 124.4 (2020), p. 040604. DOI: `10.1103/PhysRevLett.124.040604`. arXiv: `1901.06439 [cond-mat.str-el]`.

[465] Barton Zwiebach. "Closed string field theory: Quantum action and the B-V master equation". In: *Nucl. Phys. B* 390 (1993), pp. 33–152. DOI: `10.1016/0550-3213(93)90388-6`. arXiv: `hep-th/9206084`.